

NO-A187 859 UNITED STATES AIR FORCE RESEARCH INITIATION PROGRAM

01/10

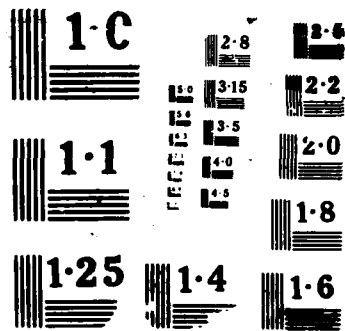
1984 RESEARCH REPORTS (U) SOUTHEASTERN CENTER FOR
ELECTRICAL ENGINEERING EDUCATION INC S M D PEELE

UNCLASSIFIED MAY 86 AFOSR-TR-87-1722 FF9620-82-C-0035 F/G 7/2

MAY 86 AFOSR-TR-87-1722 FF9620-82-C-0035 F/G 772

F/G 7/2

ML



DTIC FILE COPY

1

AFCSSR

SCITE

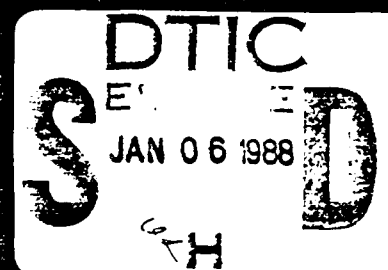
AD-A187 359

USAF RESEARCH INITIATION PROGRAM

1984

RESEARCH REPORTS

VOLUME III



CONDUCTED BY
THE SOUTHEASTERN CENTER FOR
ELECTRICAL ENGINEERING EDUCATION

PROF. WARREN D. BEILE
PROGRAM DIRECTOR

MAJ. AMOS OTIS
PROGRAM MANAGER, AFCSSR

DISTRIBUTION STATEMENT A

Approved for public release;
Distribution unlimited

AFOSR-TR. 87-1722

Page 1050;
1051.

1984 USAF/SCEEE RESEARCH INITIATION PROGRAM

Conducted by
Southeastern Center for
Electrical Engineering Education
under

USAF Contract Number F49620-82-C-0035

RESEARCH REPORTS

Volume III of IV

submitted to
Air Force Office of Scientific Research
Bolling Air Force Base
Washington, DC

BY
Southeastern Center for
Electrical Engineering Education

May 1986

DTIC
ELECTE
JAN 06 1988
S H D

DISTRIBUTION STATEMENT A

Approved for public release;
Distribution Unlimited

Accession For	
NTIS GRA&I	<input checked="checked" type="checkbox"/>
DTIC TAB	<input type="checkbox"/>
Unannounced	<input type="checkbox"/>
Justification	
By	
Distribution/	
Availability Codes	
Avail and/or	
Dist	Special
A-1	

UNCLASSIFIED

SECURITY CLASSIFICATION OF THIS PAGE

REPORT DOCUMENTATION PAGE

Form Approved
OMB No. 0704-0188

1a. REPORT SECURITY CLASSIFICATION UNCLASSIFIED			1b. RESTRICTIVE MARKINGS HD-4187 859		
2a. SECURITY CLASSIFICATION AUTHORITY			3. DISTRIBUTION/AVAILABILITY OF REPORT Approved for public release; distribution unlimited.		
2b. DECLASSIFICATION/DOWNGRADING SCHEDULE					
4. PERFORMING ORGANIZATION REPORT NUMBER(S)			5. MONITORING ORGANIZATION REPORT NUMBER(S) AFOSR-TR- 87-1722		
6a. NAME OF PERFORMING ORGANIZATION The Southeastern Center for Electrical Engineering Education		6b. OFFICE SYMBOL (if applicable)		7a. NAME OF MONITORING ORGANIZATION Air Force Office of Scientific Research/XOT	
6c. ADDRESS (City, State, and ZIP Code) 11th & Massachusetts Ave. St. Cloud, Florida 32769		7b. ADDRESS (City, State, and ZIP Code) Building 410 Bolling AFB, DC 20332			
8a. NAME OF FUNDING/SPONSORING ORGANIZATION AFOSR		8b. OFFICE SYMBOL (if applicable) XOT		9. PROCUREMENT INSTRUMENT IDENTIFICATION NUMBER F49620-82-C-0035	
8c. ADDRESS (City, State, and ZIP Code) Building 410 Bolling AFB, DC 20332		10. SOURCE OF FUNDING NUMBERS			
		PROGRAM ELEMENT NO. 61102F	PROJECT NO. 2301	TASK NO. D5	WORK UNIT ACCESSION NO.
11. TITLE (Include Security Classification) USAF Research Initiation Program - Volume 3					
12. PERSONAL AUTHOR(S) Prof. Warren D. Peele					
13a. TYPE OF REPORT Interim		13b. TIME COVERED FROM _____ TO _____		14. DATE OF REPORT (Year, Month, Day) May 86	
15. PAGE COUNT					
15. SUPPLEMENTARY NOTATION					
17. COSATI CODES			18. SUBJECT TERMS (Continue on reverse if necessary and identify by block number)		
FIELD	GROUP	SUB-GROUP			
19. ABSTRACT (Continue on reverse if necessary and identify by block number) (SEE REVERSE)					
20. DISTRIBUTION/AVAILABILITY OF ABSTRACT <input checked="" type="checkbox"/> UNCLASSIFIED/UNLIMITED <input type="checkbox"/> SAME AS RPT <input type="checkbox"/> DTIC USERS			21. ABSTRACT SECURITY CLASSIFICATION UNCLASSIFIED		
22a. NAME OF RESPONSIBLE INDIVIDUAL Amos Otis, Major, Program Manager			22b. TELEPHONE (Include Area Code) (202) 767-4971		22c. OFFICE SYMBOL XOT

INTRODUCTION.

Research Initiation Program - 1984

For several years prior to 1983, AFOSR conducted a special follow-on funding program for Summer Faculty Research Program (SFRP) participants; this was popularly known as the AFOSR Minigrant Program. That program was superseded in 1983 by the Research Initiation Program conducted by SCEE.

To compete for a 1984 Research Initiation Program award, SFRP participants must submit a complete proposal and proposed budget either during or promptly after their SFRP appointment periods. Awards to the 1984 participants may extend through 15 December 1985.

Each proposal was evaluated for technical excellence, with special emphasis on relevance to continuation of the SFRP effort, as determined by the Air Force laboratory/center. The final selection of awards was the responsibility of AFOSR.

The most effective proposals were those which were closely coordinated with the SFRP Effort Focal Point and which followed the SFRP effort with proposed research having strong prospects for later sustained funding by the Air Force laboratory/center.

The maximum award under the Research Initiation Program is \$12,000 plus cost-sharing up to a matching total amount.

The mechanics of applying for a Research Initiation Program award are as follows:

- (1) Research Initiation Program proposals of \$12,000 plus cost-sharing were to be submitted after August 1, 1984 but no later than November 1, 1984.
- (2) Proposals were evaluated and the final award decision was the responsibility of AFOSR after consultation with the Air Force Laboratory/center.
- (3) The total available funding limited the number of awards to approximately half the number of 1984 SFRP participants.
- (4) Subcontracts were negotiated with the employing institution, designating the SFRP participant as Principal Investigator, with the period of award having a start date no earlier than September 1, 1984 and a completion date no later than December 15, 1985.

Employing institutions were encouraged to cost-share since the program was designed as a research initiation procedure. Budgets included, where applicable, Principal Investigator time, graduate assistant and support effort, equipment and expendable supplies, travel and per diem costs, conference fees, indirect costs, and computer charges.

Volumes I, II, III, and IV of the 1984 Research Initiation Program Report contain copies of reports on the 89 subcontract efforts awarded under this program.

RESEARCH REPORTS
1984 USAF-SCEEE RESEARCH INITIATION PROGRAM

VOLUME I
REPORT NO.

TITLE

RESEARCH ASSOCIATE

- | | | |
|-----|--|--------------------------|
| 1. | AN ANALYTICAL STUDY OF TWO-STAGE
LIGHT GAS GUN PERFORMANCE | Dr. Robert W. Courter |
| 2. | A LOW-COST LOCAL-AREA NETWORK for
DESKTOP COMPUTERS | Dr. Myron A. Calhoun |
| 3. | DEVELOPMENT of PREDICTION MODELS for
HUMAN TORQUE STRENGTH | Dr. S. Deivanayagam |
| 4. | THE ROLE of ANTIOXIDANT NUTRIENTS in
PREVENTING HYPERBARIC OXYGEN DAMAGE to
the RETINA | Dr. William L. Stone |
| 5. | THE INFULUENCE of MELTING and REACTANT
COMSUMPTION on TEMPERATURE TRANSIENTS in
SPHERICAL and CYLINDRICAL CHARGES of EAK | Dr. John W. Sheldon |
| 6. | GEOSTROPHIC ADJUSTMENT in a THREE-
DIMENSIONAL MESOSCALE NUMERICAL MODEL of
the ATMOSPHERE | Dr. Keith L. Seitter |
| 7. | Report not received on time. Will be
provided when available. | Dr. William Czelen |
| 8. | EFFECTS of TEMPERATURE and REACTANT
SOLVATION UPON the RATES of GAS-PHASE
ION-MOLECULE REACTIONS | Dr. Peter M. Hierl |
| 9. | EFFECTS of NUCLEAR RADIATION on the
OPTICAL CHARACTERISTICS of LASER COMPONENTS | Dr. Herрман Donnert |
| 10. | A REVIEW of COMPUTER SIMULATIONS for
AIRCRAFT-SURFACE DYNAMICS | Dr. George R. Doyle, Jr. |
| 11. | COMPUTATIN OF TRANSONIC PROJECTILE
AERODYNAMICS | Dr. Chen-Chi Hsu |
| 12. | DEVELOPMENT of an ADAPTIVE GRID
GENERATION TECHNIQUE for TRANSONIC
PROJECTILE BASE FLOW PROBLEMS | Dr. Chris Reed |
| 13. | Report not received on time. Will be
provided when available. | Dr. Kendall Nygard |

INTRODUCTION

Research Initiation Program - 1984

For several years prior to 1983, AFOSR conducted a special follow-on funding program for Summer Faculty Research Program (SFRP) participants; this was popularly known as the AFOSR Minigrant Program. That program was superseded in 1983 by the Research Initiation Program conducted by SCEEE.

To compete for a 1984 Research Initiation Program award, SFRP participants must submit a complete proposal and proposed budget either during or promptly after their SFRP appointment periods. Awards to the 1984 participants may extend through 15 December 1985.

Each proposal was evaluated for technical excellence, with special emphasis on relevance to continuation of the SFRP effort, as determined by the Air Force laboratory/center. The final selection of awards was the responsibility of AFOSR.

The most effective proposals were those which were closely coordinated with the SFRP Effort Focal Point and which followed the SFRP effort with proposed research having strong prospects for later sustained funding by the Air Force laboratory/center.

The maximum award under the Research Initiation Program is \$12,000 plus cost-sharing up to a matching total amount.

The mechanics of applying for a Research Initiation Program award are as follows:

- (1) Research Initiation Program proposals of \$12,000 plus cost-sharing were to be submitted after August 1, 1984 but no later than November 1, 1984.
- (2) Proposals were evaluated and the final award decision was the responsibility of AFOSR after consultation with the Air Force Laboratory/center.
- (3) The total available funding limited the number of awards to approximately half the number of 1984 SFRP participants.
- (4) Subcontracts were negotiated with the employing institution, designating the SFRP participant as Principal Investigator, with the period of award having a start date no earlier than September 1, 1984 and a completion date no later than December 15, 1985.

Employing institutions were encouraged to cost-share since the program was designed as a research initiation procedure. Budgets included, where applicable, Principal Investigator time, graduate assistant and support effort, equipment and expendable supplies, travel and per diem costs, conference fees, indirect costs, and computer charges.

Volumes I, II, III, and IV of the 1984 Research Initiation Program Report contain copies of reports on the 89 subcontract efforts awarded under this program.



SCEEE
©
1986

RESEARCH REPORTS
1984 USAF-SCEEE RESEARCH INITIATION PROGRAM

VOLUME I
REPORT NO.

TITLE

RESEARCH ASSOCIATE

- | | | |
|-----|---|--------------------------|
| 14. | USE of BAYESIAN DECISION THEORY in
ASSESSING the POTABILITY of GROUND
WATER BASED DRINKING WATER SUPPLIES | Dr. Stephan J. Nix |
| 15. | DESIGN of a DIGITAL EW PASSIVE
RECEIVER | Dr. William S. McCormick |
| 16. | DUAL CHANNEL FFT SYSTEM ANALYSIS
FACILITY for EVALUATING INTEGRATED
COMMUNICATION SYSTEMS | Dr. Paul B. Griesacker |
| 17. | FAR-INFRARED ABSORPTION PROFILES for
DISTRIBUTED SHALLOW DONORS in GaAs-GaAlAs
HETEROSTRUCTURES | Dr. Ronald L. Greene |
| 18. | EFFECT of POLE PIECES on the AXIAL
MAGNETIC FIELD in TRAVELING WAVE TUBES | Dr. James D. Patterson |
| 19. | ENHANCING MPC-DSS to INCLUDE AUTOMATIC
RESCHEDULING and ADAPTIVE PERFORMANCE
MEASURES | Dr. Philip S. Chong |

Volume II

- | | | |
|-----|--|------------------------------|
| 20. | PARAMETRIC STABILITY in COST ESTIMATING
MODELS | Dr. Thomas R. Gullledge, Jr. |
| 21. | ANALYSIS of AIR FORCE VEHICLE CONDITION
RATINGS FROM HISTORICAL DATA | Dr. Bruce N. Janson |
| 22. | THE DEVELOPMENT of COMPUTATIONAL
EFFICIENCIES in CONTINUUM FINITE ELEMENT
CODES USING MATRIX DIFFERENCE EQUATIONS | Dr. Harold C. Sorensen |
| 23. | CENTRIFUGE MODEL STUDY and FINITE ELEMENT
ANALYSIS OF BURIED CONCRETE BOX CULVERTS | Dr. Yong S. Kim |
| 24. | EFFECTS of FLUID SHIFTS and HYPOVOLEMIA
in INDIVIDUALS with DIFFERENT WORKING
CAPACITIES WHILE RESTING at a FIVE DEGREE
DECLINATION | Dr. William G. Squires |
| 25. | STRUCTURE OF MOLTEN IMIDAZOLIUM CHLORIDE | Dr. R.D. Murphy |

RESEARCH REPORTS
1984 USAF-SCEEE RESEARCH INITIATION PROGRAM

<u>VOLUME II</u> <u>REPORT NO.</u>	<u>TITLE</u>	<u>RESEARCH ASSOCIATE</u>
26.	ALTERNATIVE COMPUTATIONAL METHODS for SEPARATED FLOWS about PITCHED FLAT SURFACES	Dr. Larry A. Glasgow
27.	NO TITLE	Dr. Hendrik F. Hameka
28.	FUNCTIONAL ROLE of SEROTONIN in the CEREBELLAR GLOMERULAR SYNAPSE	Dr. Deborah Armstrong
29.	CHOLINE and ETHANOLAMINE PHOSPHOTRANS- FERASE ACTIVITIES in GLOMERULAR PARTICLES ISOLATED FROM BOVINE CEREBELLAR CORTEX	Dr. Robert V. Dorman
30.	DYNAMICS OF LARGE SCALE VORTEX STRUCTURES and QUASI-LARGE SCALE STRUCTURES in the WAKE of a SPLITTER PLATE	Dr. Paul H. Chiu
31.	FLOW PHYSICS THROUGH A PIERCED MEMBRANE	Dr. Louis C. Chow
32.	COMPUTATIONAL STUDIES of RAMJET COMBUSTOR FLOW FIELDS	Dr. K.M. Isaac
33.	FREE STREAM TURBULENCE EFFECTS on TURBULENT HEAT and MOMENTUM TRANSFER	Dr. Paavo Sepri
34.	STUDY of COLD REACTING and COMBUSTING FLOWS AROUND BLUFF-BODY COMBUSTORS	Dr. Richard S. Tankin
35.	NUMERICAL MODELING of MULTIPHASE TURBULENT RECIRCULATING FLOWS in SUDDEN-EXPANSION RAMJET GEOMETRY	Dr. Albert Tong
36.	SiC FIBER REINFORCED GLASS-CERAMIC COMPOSITES in the ZIRCONIA/MAGNESIUM ALUMINOSILICATE SYSTEM	Dr. Charles H. Drummond, III
<u>Volume III</u>		
37.	ARYLOXY SUBSTITUTED PYROMELLITIC DIANHYDRIDES	Dr. William F. Feld
38.	ANGLE RESOLVED ION-SCATTERING STUDY of GaAs SURFACES the EXPERIMENT DESIGN	Dr. Thomas P. Graham

RESEARCH REPORTS
1984 USAF-SCEEE RESEARCH INITIATION PROGRAM

<u>VOLUME III</u> <u>REPORT NO.</u>	<u>TITLE</u>	<u>RESEARCH ASSOCIATE</u>
39.	THERMAL DECOMPOSITION STUDIES of SOME SILAHYDROCARBONS	Dr. Vijay K. Gupta
40.	SILANE-TREATED SILICA FILLERS for USE in FULRORSILICONE ELASTOMERS	Dr. Larry M. Ludwick
41.	RAMAN SPECTROSCOPIC STUDIES in EXTRINSIC P-TYPE SILICON	Dr. James Schneider
42.	GRAIN SIZE CONTROL in META STABLE BETA TITANIUM ALLOYS	Dr. Isaac Weiss
43.	THE IMPACT of EXPERT SYSTEMS on PERFORMANCE and COGNITIVE STRATEGIES in DIAGNOSTIC INFERENCE	Dr. Sallie E. Gordon
44.	EFFECTS of ENRICHING a COMPUTER-INSTRUCTED PROCEDURALIZED TASK with EXPLANATORY INFORMATION	Dr. Krystine B. Yaworsky
45.	SPECIFICATION SEARCHES in COVARIANCE STRUCTURE MODELING	Dr. Robert MacCallum
46.	A COMPUTATIONAL MODEL of the HUMAN CARDIOPULMONARY SYSTEM	Dr. David Reynolds
47.	DEVELOPMENT of an OPTIMAL TESTING PROTOCOL for the USAF CRITERION TASK SET (CTS)	Dr. Robert E. Schlegel
48.	CONSTRUCTION of CONCEPT-ATOMS.	Dr. Yin-Min Wei
49.	DEVELOPMENT of a HIGH-FREQUENCY LUNG VENTILATION MODEL for TESTING UNDER HYPOBARIC CONDITIONS.	Dr. Mukul R. Banerjee
50.	BRILLOUIN SPECTROSCOPY in SYSTEMS of BIOLOGICAL SIGNIFICANCE	Dr. Raj M. Krishnan
51.	STABILIZATION of MODE-LOCKED LASERS	Dr. Odis P. McDuff
52.	RAMAN SPECTROSCOPY of CAROTENOIDS and OTHER MOLECULES in UNSTIMULATED and STIMULATED, CULTURED Y-1 MOUSE ADRENAL TUMOR CELLS	Dr. James J. Mrotek

RESEARCH REPORTS
1984 USAF-SCEEE RESEARCH INITIATION PROGRAM

<u>VOLUME III</u> <u>REPORT NO.</u>	<u>TITLE</u>	<u>RESEARCH ASSOCIATE</u>
53.	MILITARY FAMILY STRESS and JOB PERFORMANCE	Dr. Lena Wright Myers
54.	Report not received on time. Will be provided when available	Dr. Walter Salter
55.	Report not received on time. Will be provided when available	Dr. William Thomas
56.	EVALUATION and VALIDATION of ADA PROGRAMMING SUPPORT ENVIRONMENTS	Dr. Mike Burlakoff
57.	KINETICS of HOMOGENEOUS GAS PHASE OXIDATION of HYDRAZINE in AIR	Dr. Datta V. Naik
58.	SOFTWARE CORRECTIONS and EXTENSIONS for an INTEGRATED PARTICLE SIZING SYSTEM	Dr. Arthur M. Sterling

Volume IV

59.	PREDICTING GASEOUS PHASE ADSORPTION of ORGANIC VAPORS by MICROPOROUS ADSORBENTS	Dr. Martin D. Werner
60.	NO TITLE	Dr. Frank P. Colby, Jr.
61.	SOLAR HARD X-RAY BURSTS and TYPE-II RADIO EMISSIONS	Dr. Gabriel Kojoian
62.	THE PASSIVE MODE LOCKING of an Nd ³⁺ : YAG LASER WITH a TWO-PHOTON ABSORBER	Dr. Nabil M. Lawandy
63.	PLASMA GENERATION and DIAGNOSTICS for IONOSPHERIC PLASMA SIMULATION	Dr. Bernard McIntyre
64.	STUDY of UNIFIED COMPLEX SUSCEPTIBILITY OVER MILLIMETER and INFRARED REGIONS VIA KRAMERS-KRONIG RELATIONSHIP	Dr. Ken Tomiyama
65.	DETERMINATION of PROFESSIONAL LITERATURE RESOURCES RELATING to USAF FAMILY and LIFE STYLE ATTRIBUTES AND ATTITUDES: SUPPORT for INTERPRETING AFSS DATA	Dr. L.W. Buckalew

RESEARCH REPORTS
1984 USAF-SCEEE RESEARCH INITIATION PROGRAM

<u>VOLUME IV</u> <u>REPORT NO.</u>	<u>TITLE</u>	<u>RESEARCH ASSOCIATE</u>
66.	DIFFERENT CAREER STAGES: DIFFERENT DEGREES of COMMITMENT	Dr. Jan Leeman Brooks
67.	A MULTILEVEL EXAMINATION of LEADERSHIP EFFECTS WITH THE ORGANIZATIONAL ASSESSMENT PACKAGE	Dr. Kevin W. Mossholder
68.	FUSE and SURFACE TRACKING SWITCH MODELS for the SHIVA STAR INDUCTIVE PULSE COMPRESSION SYSTEM	Dr. R. Gerald Colclaser
69.	MODELING the THERMAL LAYER	Dr. Arthur A. Kovitz
70.	DIGITAL INTERPOLATION BASED on FUNCTIONAL ITERATION	Dr. Aldy T. Fam
71.	Report not received on time. Will be provided when available.	Dr. Brian Holmes
72.	NUMERICAL CHARACTERIZATION of MICROSTRIP DISCONTINUITIES on THICK SUBSTRATES	Dr. Robert W. Jackson
73.	A SUBOPTIMUM EXTRAPOLATOR for IMPROVED SPECTRAL ESTIMATION	Dr. Lonnie C. Ludeman
74.	HANDLING FACTS with NON-CONSTANT GROUND TERMS in a KNOWLEDGE-BASED SYSTEM	Dr. John T. Minor
75.	STRUCTURAL MODIFICATION to ENHANCE the ACTIVE VIBRATION CONTROL of LARGE SPACE STRUCTURES	Dr. Franklin E. Eastep
76.	CONSISTENT SHEAR LAG MODELING of DAMAGE in UNIDIRECTIONAL COMPOSITE LAMINATES	Dr. Walter F. Jones
77.	NUMERICAL SIMULATION of a SUPERSONIC INLET FLOW	Dr. Meng-Sing Liou
78.	RECONFIGURATION of FLIGHT CONTROL SYSTEM of UNMANNED RESEARCH VEHICLE	Dr. Kuldip S. Rattan
79.	ANALYSIS of ARMOR BRACKETRY	Dr. Hemen Ray

RESEARCH REPORTS
1984 USAF-SCEEE RESEARCH INITIATION PROGRAM

<u>VOLUME IV</u> <u>REPORT NO.</u>	<u>TITLE</u>	<u>RESEARCH ASSOCIATE</u>
80.	ESTIMATING SPEED of MENTAL ROTATION THROUGH ITEM PACING	Dr. David F. Lohman
81.	DEVELOPMENT and IMPLEMENTATION of COST-EFFECTIVENESS and UTILITY METHODOLOGIES for the AF PERFORMANCE MEASUREMENT PROJECT	Dr. Robert Vance
82.	A SCANNING ELECTRON MICROSCOPICAL STUDY of PERIOSTEUM from SUBHUMAN PRIMATES	Dr. Gwendolyn B. Howze
83.	AN INVESTIGATION of TEST BIAS on the ARMED SERVICES VOCATIONAL APTITUDE BATTERY (ASVAB) FOR MALES and FEMALES.	Dr. Cynthia A. Ford
84.	MODERNIZATION of AGING HIGH-ALTITUDE ENGINE TEST CELLS	Dr. Doyle E. Hasty
85.	EFFECTS of PYRIDOSTIGMINE in the DIET UPON SIMPLE and COMPLEX BEHAVIORS in the MONGOLIAN GERBIL (MERIONES UNGUICULATUS)	Dr. Arthur Harriman
86.	SYNTHESIS of TRIFLATE and CHLORIDE SALTS of ALKYL N,N BIS (2,2,2-TRIFLUOROETHYL) AMINES	Dr. Gloria L. Anderson
87.	LIQUID ROCKET INSTABILITY MODEL DEVELOPMENT	Dr. Charles E. Mitchell
88.	LAMINARIZATION in HIGHLY ACCELERATED FLOW	Dr. Brian Vick
89.	FUTURE TACTICAL AIR CONTROL SYSTEM DATABASE DESIGN	Dr. William Perrizo

INTRODUCTION

Investigation of high-strength, light-weight thermally-stable polymers has been pursued since 1960 for applications as composite matrix materials in electronic and aerospace industries. TGA analysis of these early polymers demonstrated a high thermo-oxidative stability, but utility as matrix resins for advanced composites failed or was not economically feasible.

Development of a high temperature class of polymers known as polyimides in 1972-1974 rekindled interest.

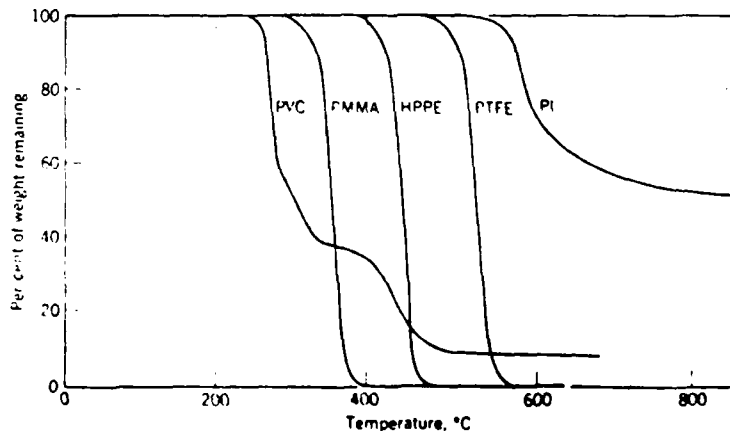


FIGURE 1. THERMOGRAVIMETRIC ANALYSIS OF PVC, PMMA, HPPE, PTFE, AND PI

Figure 1¹ shows the comparison of polyimides with PVC, PMMA, HPPE and PTFE in a thermogravimetric analysis at 5°C/min. in nitrogen. Polyimides clearly have the highest thermal stability of the group.

Polymers with aromatic structural units are superior in thermal stability to phenolics and epoxies because the aromatic units contain a minimum of oxidizable hydrogen atoms and are able to absorb thermal energy. Of the major classes of polymers that possess these structural units, polyimides are the least expensive to produce. At the present time polyimide-advanced fiber composites are being used in a variety of high-temperature structural applications. In the next ten years, approximately 40% of aircraft will be of composite construction.² Aromatic polyimides have an outstanding thermal stability and consequently are useful in applications requiring high heat resistance such as adhesives, laminates, moldings, wire and structural coatings, and insulators.³⁻¹¹

A traditional composite is composed of a polymer resin in which fibers of alumina, glass or graphite are imbedded. One disadvantage of this approach is the poor adhesion of the resin to the reinforcing material. Good adhesion and lack of voids are required to insure strength for long-term, high temperature applications. Molecular composites in which molecules act as the reinforcing material should enhance current properties and have prompted research into wholly

polymeric composites.

Aromatic polyimides can form linear rigid-rod molecules which can be imbedded in matrix resins to add internal strength. One of the problems encountered in the formation of the polyimides is their low solubility in common solvents, due to the high amount of polarity and aromaticity. This, coupled with their high transition temperatures, has made them difficult to fabricate and the subject of many research studies directed toward the preparation of soluble polyimides.¹²⁻⁴²

Polyimides are generally fabricated in the polyamic acid stage, since it has increased solubility and can be molded and closed to the imide at high temperatures. However, this practice leaves voids in the material caused by the solvent and water evolved in the imidization process. The synthesis of rigid-rod polyimides which are soluble in common solvents would circumvent these undesirable processing results, and is the basis for this research effort.

Polyimides with no pendent groups show low solubility in common solvents. Solubility can be increased by addition of bulky substituent groups on the polymer backbone.^{33,43,44} The increased solubility and compatibility should allow rigid-rods to be easily incorporated in composites. Pyromellitic dianhydride is an ideal monomer for the formation of rigid-rod polyimides because it is highly symmetrical. Polyimides generated from pyromellitic

dianhydride suffer, however, from a lack of solubility due to unhindered intermolecular interactions. Of the two monomers involved in forming a polyimide, a dianhydride and a diamine, previous studies suggest that the dianhydride structure has a greater effect on the solubility than the structure of the diamine.^{37,38}

The objectives of this research, then, were to synthesize pyromellitic dianhydrides with pendent functions to decrease intermolecular interactions, and to investigate their polymerization with common diamines to establish the conditions required for polymerization.

HISTORICAL

Rigid-rod Polymer Composites

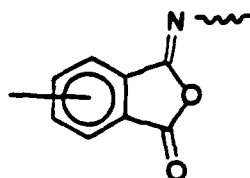
Linear polymers that have only single bonds allow rapid conformational changes due to the ease of rotation around the single bond. Cyclic structures in the backbone of the chain can drastically inhibit conformational changes and increase the rigidity of the structure. Para oriented units produce a "rigid-rod" structure that is linear with no kinks or bends in the main chain. Condensed systems, such as aromatic polyimides, show a more pronounced chain stiffening and possess a unique combination of physical properties. These linear polymers have relatively high melting points, low solubility, very high T_gs, increased hardness and heat resistance.⁴⁵ Thermal stability is complemented by an excellent radiation and solvent resistance and other favorable properties such as mechanical and electrical stability over a wide temperature range of 300 - 500°C.⁴⁶⁻⁵⁰

These physical properties make aromatic polyimides an excellent choice for the self-reinforcing component in polymer composites. The rigid-rod polymers can be imbedded in the polymer matrix to add internal strength, thus yielding a superior polymer composite in which voids are minimized

due to the lack of water or solvent in the composite. Additionally, thermal stability is increased and the overall mechanical properties could be enhanced.

Polyimides and Isoimides

In general, polyimides tend to be insoluble and intractable. An isomeric form of an imide, commonly known as an isoimide 1 can be used to enhance processibility without compromising the ultimate thermal and thermo-oxidative stability.

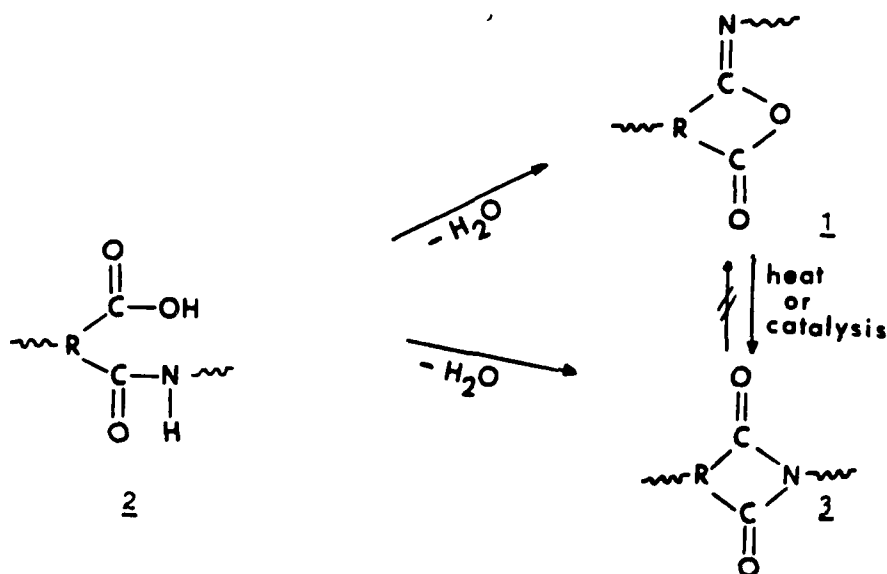


1

The isoimide, when compared to the imide, was generally found to have a much lower melting point and was much more soluble in a variety of solvents. The isoimide can readily be converted irreversibly to the imide form, either thermally or chemically.⁵¹ Catalysts include dehydrating agents such as acetic anhydride and numerous other anhydrides or basic catalysts such as pyridine, quinoline, isoquinoline, or triethylamine.⁵²⁻⁵⁴

Formation of the cyclic isoimide structure occurs by cyclodehydration of the amic acid precursor by selected chemical reagents. Generally, chemical dehydration of N-substituted amic acids 2 gives varying ratios of isoimide 1

and imide 3, depending on the reaction conditions employed, the nature of the amic acid and the chemical reagent used.^{55,56}



Thermal cyclodehydration invariably yields the imide structure. The conversion can be followed by the disappearance of the infrared NH-band at 3247 cm^{-1} and the appearance of the cyclic imide bands at 1776 , 1613 and 722 cm^{-1} as seen in Figures 2 and 3.^{57,58,59}

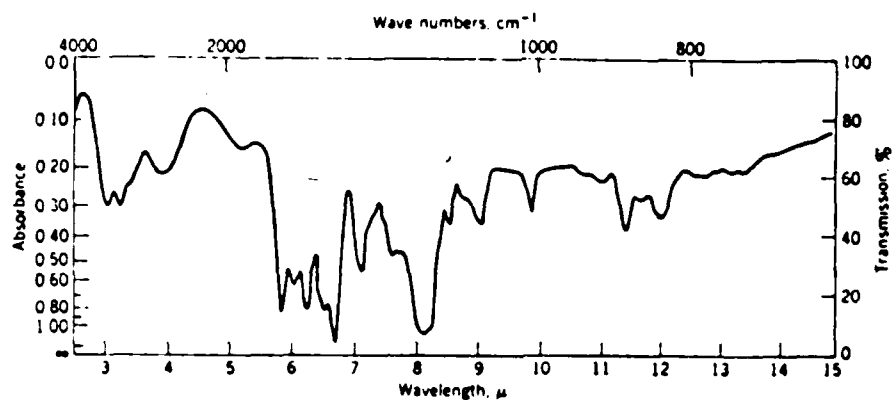


FIGURE 2. INFRARED SPECTRUM OF POLYMER H POLYAMIC ACID FILM

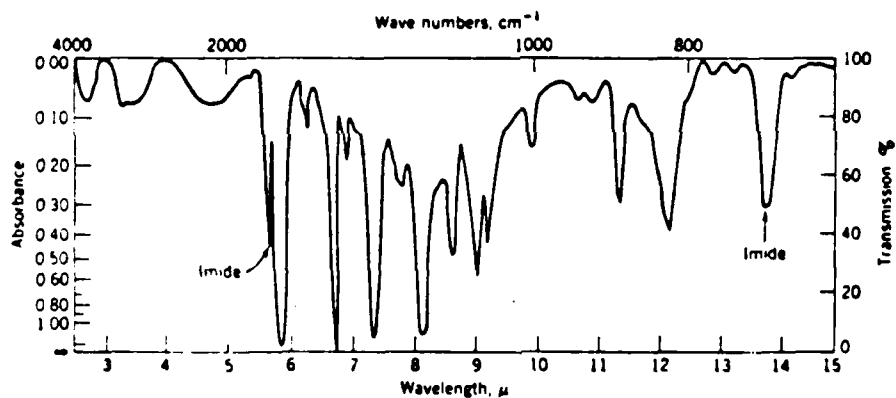
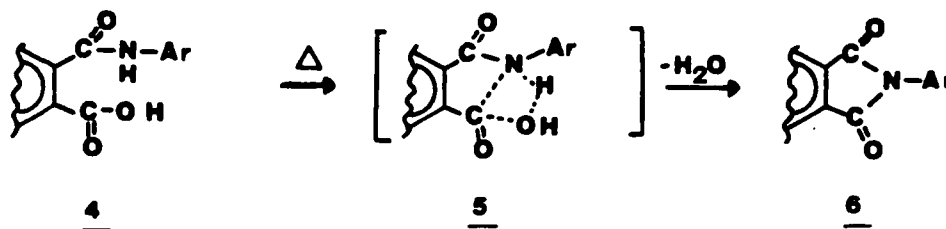


FIGURE 3. INFRARED SPECTRUM OF POLYMER H POLYIMIDE FILM

The most common method of thermal imidization of the polyamic acid involves heating the film at elevated temperatures in vacuo or an inert atmosphere. The time and temperatures vary for each polyamic acid. The heating cycle

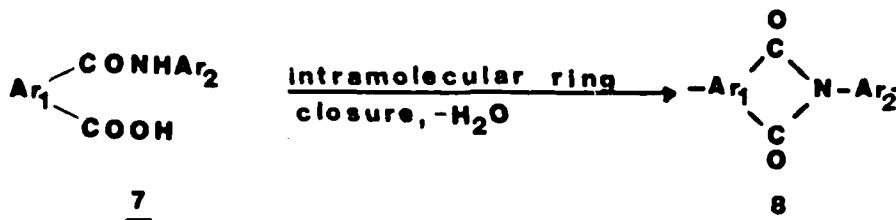
can last from 30 seconds to one half hour at 300-350°C or for several hours at 150°C followed by 30 seconds at 350°C.⁶⁰

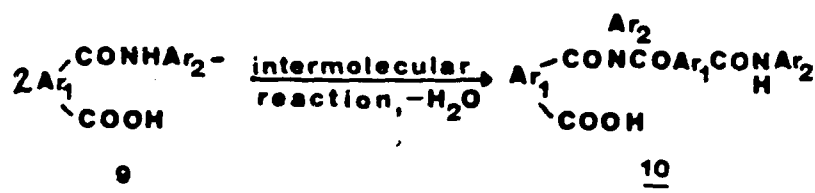
The basic scheme for thermal imidization involves conversion of the amic acid 4 via the intermediate 5 with partial formation of bonds and loss of water to the imide 6.



The processes by which thermal imidization takes place are dependent on polyamic acid characteristics and reaction conditions.⁶¹

The dehydration reaction usually takes place intramolecularly 7→8, but intermolecular reaction 9→10 can also occur leading to branched or crosslinked polymers.

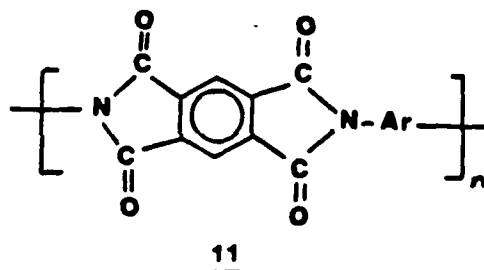




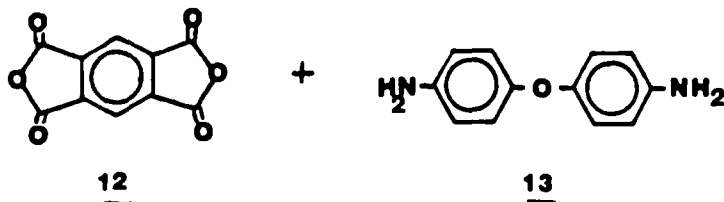
In one instance the activation energy of the intramolecular process was higher than that of the intermolecular process, and high dehydration temperatures were recommended in order to obtain a linear polymer.⁴² Other thermal imidization techniques include dehydration by refluxing the polyamic acid solution to drive off water followed by complete devolatilization at elevated temperatures. Polyamic acids can also be imidized by compression molding at high temperature. Various combinations of the above techniques are used to fit particular requirements and properties of a given polymer.

Pyromellitic Dianhydride Polymers

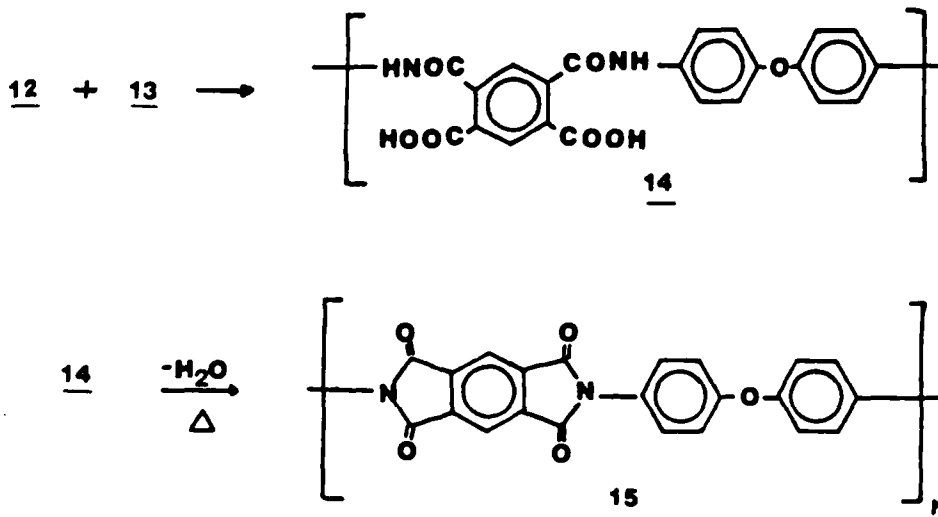
Aromatic polypyromellitimides 11 are prepared by cyclization of soluble polyamic acid precursors.



A commercially available representative example is polymer H 15 (Kapton) which is derived from pyromellitic dianhydride 12 and 4,4'-diaminodiphenylether 13.¹



The polymerization is a two stage process. First the diamine is allowed to react with the dianhydride in a solvent such as N,N-dimethylformamide at room temperature to afford the corresponding polyamic acid 14. Dehydration of 14 produces the polyimide 15.



There are two major disadvantages to this process. The polyamic acid is thermally and hydrolytically unstable, and water is given off during the imidization. The water can cause partial reversal of the amidation reaction.⁶²

Polymer H is completely insoluble in organic solvents and infusible, and must be processed as the unstable polyamic acid. In order to obtain high molecular weight polyimides, two conditions must be met. They are the absence of moisture, and relatively low reaction temperatures.

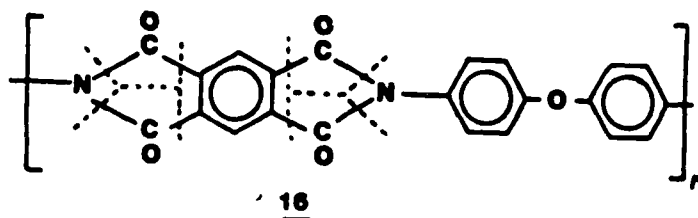
Since polyamic acids are very sensitive to water and hydrolyze easily, the solid dianhydride has often been added to a solution containing the diamine to prevent premature hydrolysis prior to forming the polyamic acid.^{63,64} Reaction temperatures are usually kept below 35°C, since higher temperatures have several destructive effects. Although the presence of water has been shown to catalyze the formation of the polyamic acid, the presence of an o-carboxy group on the polymeric polyamic acid allows water hydrolysis of the intermediate amide at 10^5 times faster than for the unsubstituted analog.⁶⁵

Simultaneously, water can also hydrolyze the dianhydride monomer as well as the anhydride end groups of the growing polymer chain and the rate of hydrolysis increases with temperature.⁶⁶ At higher temperatures imidization begins and additional water is formed. If the imidization proceeds to an appreciable degree, low molecular weight polyimide

precipitates and further chain growth is effectively stopped. For each dianhydride/diamine pair there is an optimum temperature and solvent system for which best results are obtained.^{59,63,64,67-69,71-73}

Improved properties for polypyromellitimides made from aromatic diamines include increased thermal stability, outstanding resistance to irradiation, resistance to mechanical deformation at high temperatures and resistance to solvent attack. Their zero strength temperatures are well above the 550°C value for aluminum. The zero strength temperature is defined as the temperature at which a film supports a load of 20 lb per square inch of film cross section for 5 ± 0.5 sec.

Polymer H has several unique properties. Among them are good mechanical properties to 500-600°C and a zero strength temperature to 800°C. No T_g has been found in the range from -100 to +500°C. It is flameproof and infusible, and hydrolytically stable, with solubility limited to fuming HNO₃. It remains thermally stable in air to 420°C but completely volatilizes in 5 hours at 485°C with an activation energy of 33 kcal/mol. Analysis of the volatile products indicates cleavage along the dotted lines in 16. The remaining carbonized, probably crosslinked residue (45%) displayed semiconducting properties.⁴⁰



The color of aromatic polypyromellitimides is related to the structure of the diamine, as aliphatic derivatives are colorless while aromatic derivatives are tinted yellow.

Crystallinity is related to the symmetry of the diamines with crystallinity occurring upon preparation when p-phenylene diamine is used. However, diamines such as m-phenylene diamine, bis(4-aminophenyl) ether, and bis(4-amino-phenyl) sulfide give polyimides which are not crystalline as prepared but can be crystallized by high temperature annealing.⁵⁷

Solution properties also depend on diamine structure. In general, polypyromellitimides are quite resistant to dissolution and solvents such as concentrated sulfuric acid or cold fuming nitric acid are required. Some examples of polypyromellitimides that are soluble in common solvents are shown in Table 1.

TABLE 1
POLYPYROMELLITIMIDES SOLUBLE IN COMMON SOLVENTS

DIAMINE	SOLVENT	VISCOSITY
$\text{HN}-(\text{CH}_2)_{24}-(\text{CH}_3)_2\text{C}-\text{C}_6\text{H}_4-\text{C}(\text{CH}_3)_2-(\text{CH}_2)_4\text{NH}_2$	m-cresol	1.5-1.8 η_{inh}
$\text{HN}-\text{C}_6\text{H}_3(\text{NH}_2)-\text{CH}(\text{CH}_3)_2$	DMF, DMA	1.17 η_{inh}
$\text{HN}-\text{C}_6\text{H}_4-\text{NH}_2$	DMSO	0.17 η_{sp}
$\text{HN}-\text{C}_6\text{H}_3(\text{NH}_2)_2$	DMSO	0.11 η_{sp}

Many polypyromellitimides exhibit thermal stability in an inert atmosphere up to 500°C without noticeable weight loss (Figure 4). Table 2 demonstrates the effect that diamine structures 17a-17i can have on the properties of polypyromellitimides.⁵⁷

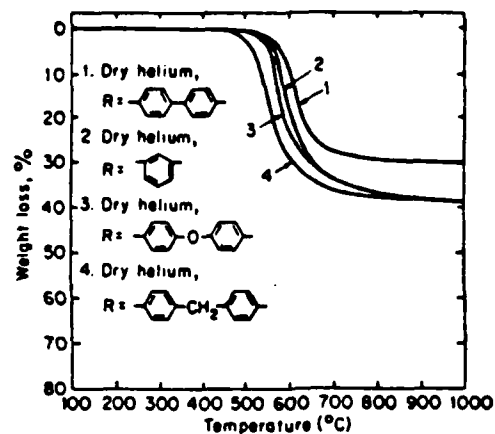
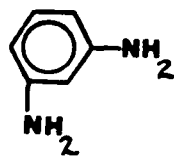
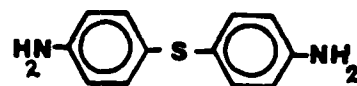


FIGURE 4. THERMOGRAVIMETRIC ANALYSIS OF POLYPYROMELLITIMIDES

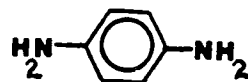
17a



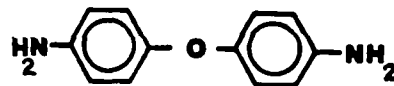
17f



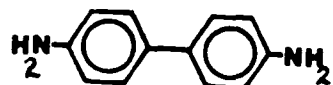
17b



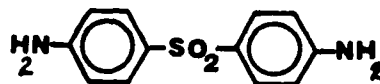
17g



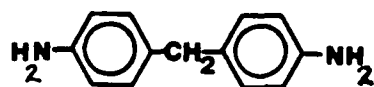
17c



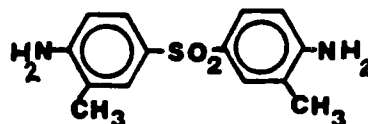
17h



17d



17i



17e

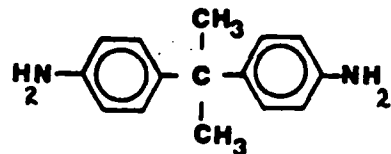


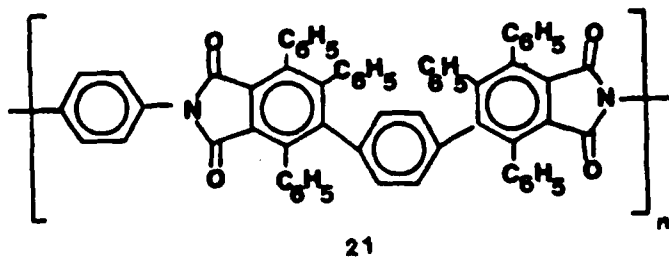
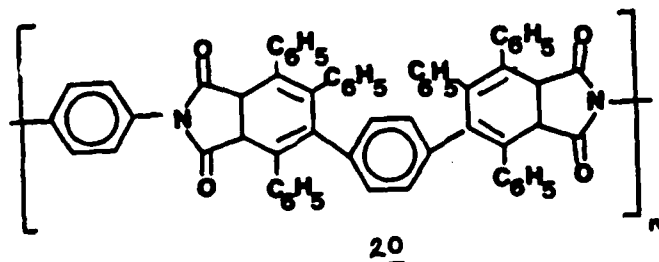
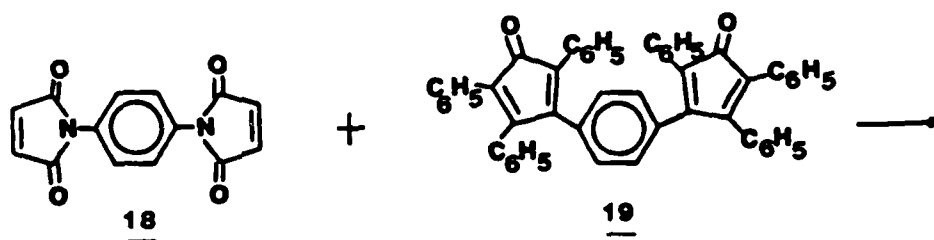
TABLE 2
EFFECT OF AROMATIC DIAMINE STRUCTURE
ON POLYPYROMELLITIMIDE PROPERTIES

DIAMINE	COLOR/ CRYSTALLINITY	SOLUBILITY	THERMAL STABILITY		ZERO STRENGTH TEMP. °C
			275°C	300°C	
<u>17a</u>	Crystallizable	amorphous H_2SO_4 crystalline insol.	>1yr	>1mo	900
<u>17b</u>	"	amorphous H_2SO_4 crystalline insol.	>1yr		900
<u>17c</u>	highly crystalline	fuming HNO_3		1mo	900
<u>17d</u>	slightly crystalline	H_2SO_4		7-10 days	800
<u>17e</u>	crystallizes with difficulty	H_2SO_4		15-20 days	580
<u>17f</u>	deep red/ crystallizable	fuming HNO_3	10-12 mo	6wk	800
<u>17g</u>	yellow/ crystallizable	fuming HNO_3	>1yr	>1mo	850
<u>17h</u>	nearly colorless	H_2SO_4		>1mo	
<u>17i</u>	-----	H_2SO_4		>1mo	

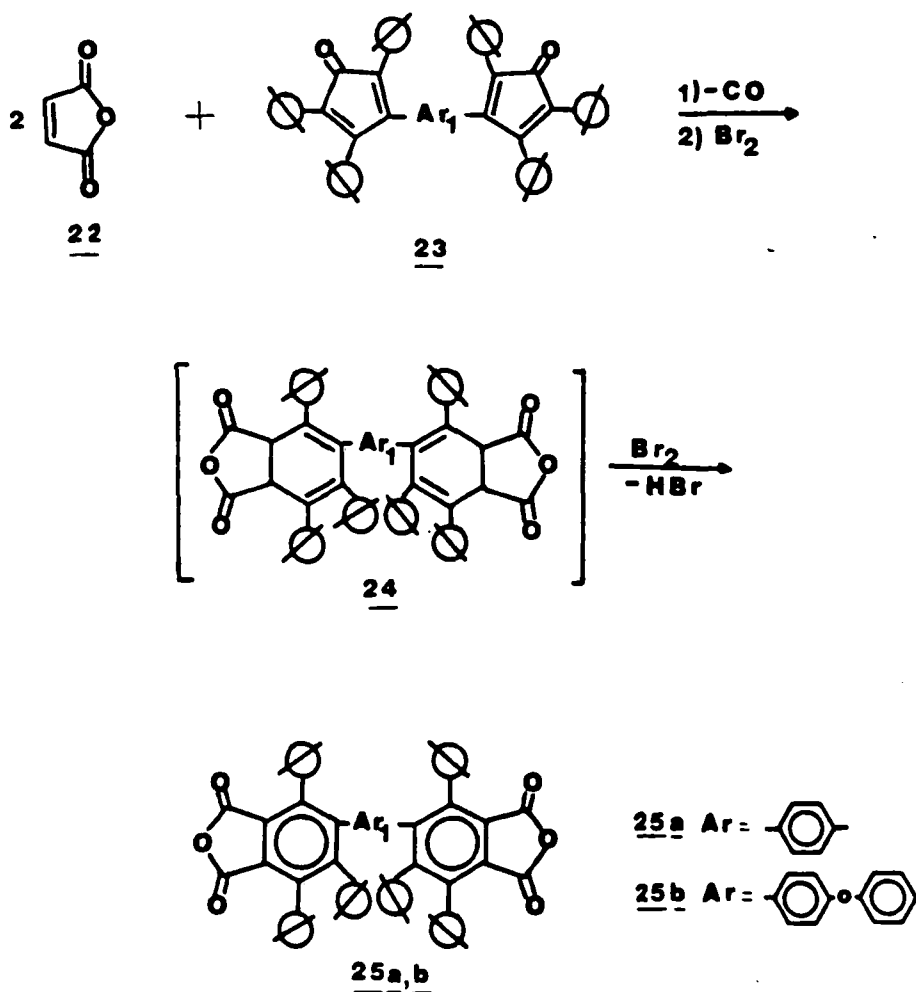
Phenylated Polymers

Pendent phenyl groups on the polyimide backbone have been shown to increase solubility of the polymer in organic solvents.⁸²

The reaction of N,N'-p-phenylene dimaleimide (18) with 3,3'-(p-phenylene)bis(2,4,5-triphenyl-cyclopentadienone) (19) generates a polydihydrophthalimide 20, which can be dehydrogenated to yield the polyimide 21.



Use of phenylated dianhydrides has produced phenylated polyimides with higher intrinsic viscosities. Synthesis of the phenylated dianhydride 25a,b involves the Diels-Alder reaction of maleic anhydride (22) with the phenylated cyclopentadienone (23). The intermediate bis(dihydrophthalic)anhydride (24) can be dehydrogenated with bromine to form the bis(phthalic)anhydride 25.⁸²



A sharp decrease in intrinsic viscosity is observed if the dehydrogenation of polydihydrophthalimides occurs thermally or in refluxing nitrobenzene. This is probably due to decomposition of the dihydrophthalimide linkage.⁸¹

Polyimides 27, formed from dianhydride 25 and various diamines 26 in a refluxing m-cresol, isoquinoline mixture, gave a series of Tg's which are illustrated in Table 3 and show a decrease in Tg as the flexibility of the diamine monomer increases. A flexible ether linkage in the dianhydride monomer results in a more pronounced lowering of Tg than the presence of the same unit in the diamine.^{83,84}

Polyimides made from 4,4'-(oxydi-1,4-phenylene)bis(2,4,5-Triphenylphthalic anhydride) (25b)⁸⁵ and diamine 26-29 were synthesized to study the effects of the diamine flexible linkages on the thermal stability and tractability of polymers 30-33.⁸⁶

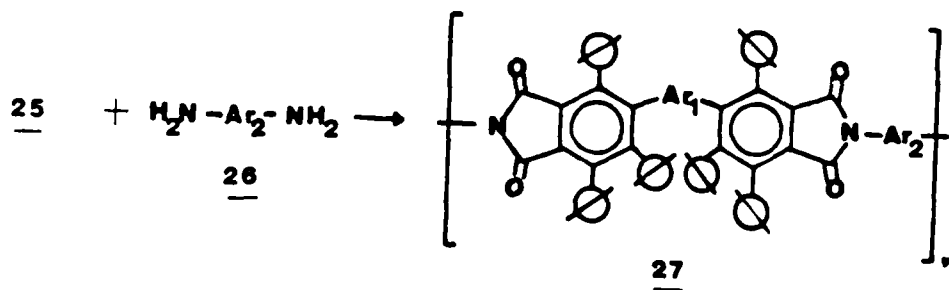



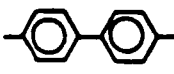
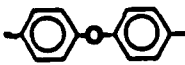
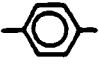
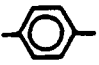
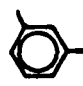
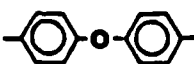
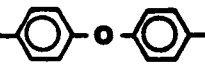
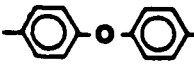
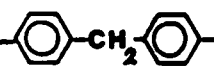
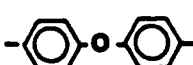
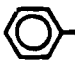

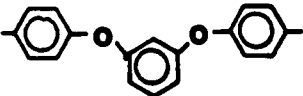
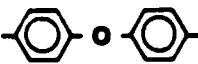

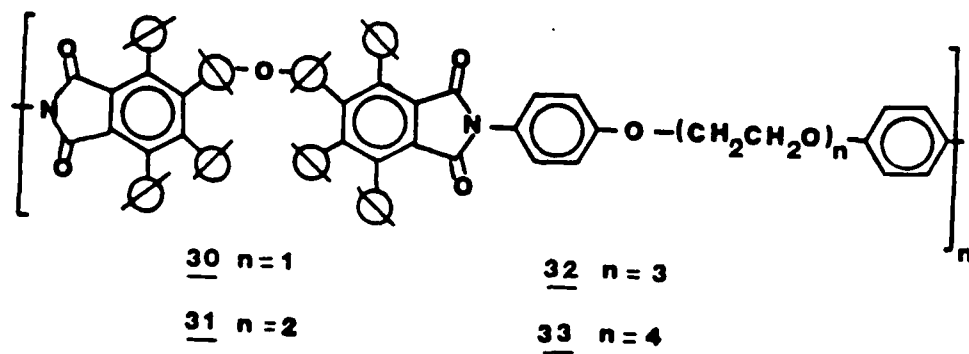
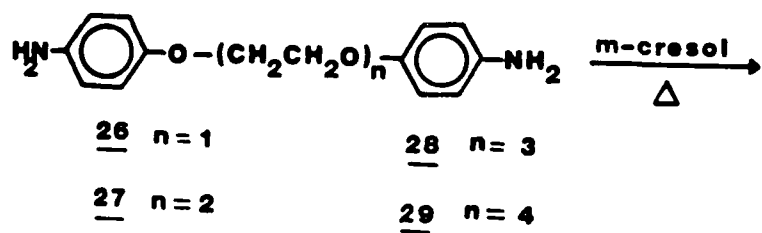
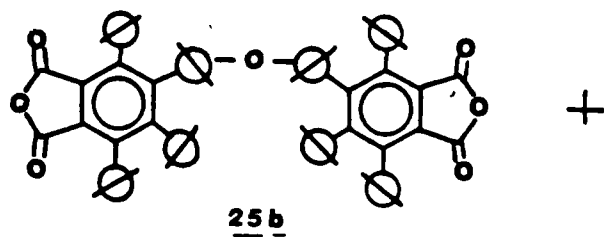


TABLE 3
GLASS TRANSITION TEMPERATURES OF PHENYLATED POLYIMIDES 25

Ar ₁	Ar ₂	T _g
		411
		397
		371
		365
		360
		356
		352
		315
		262



Results indicated increased thermal stability for a phenylated dianhydride as compared to a non-phenylated analog. A decrease in thermal stability is observed as the length of the flexible oxyethylene linkage increased (Table 4). Viscosities also decrease as the length of the linkage increases.

TABLE 4
THERMAL STABILITY OF PHENYLATED POLYMERS

POLYMER	n	η_{inh}	TGA	
			Air	N ₂
<u>30</u>	1	1.06	540	510
<u>31</u>	2	0.89	500	480
<u>32</u>	3	0.65	470	455
<u>33</u>	4	0.46	435	470

Diphenoxypyromellitic Dianhydride and Related Monomers

Pyromellitic dianhydrides with various substituents at the 3 and 6 positions have been synthesized. Twenty examples were found in the literature from 1933 to 1984. Table 5 summarizes the properties and uses of fourteen examples found in the literature.

TABLE 5
SUBSTITUTED PYROMELLITIC DIANHYDRIDES

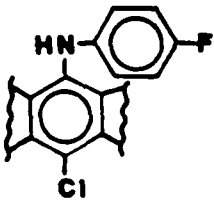
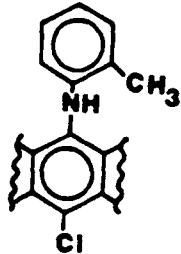
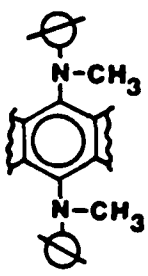
SUBSTITUENT(S)	MP°C	REMARKS	REF.
3-chloro-6-(p-fluoroanilino) 	255-256	brown red yield = 62.5% verify structure by degradation and resynthesis; precursor: (3,6-dichloro) reacted with 6-p-fluoroaniline	87
3-chloro-6-o-toluidino 	233-235	brown red verification of structure by degradation and resynthesis; precursor: (3,6-dichloro) reacted with o-toluidine, yield = 63%	87
3,6-bis(N-methyl-anilino) 	246-250	formation of blue imides, mp = 297-298°C; hydrolysis gave the pyromellitic acid, mp = 314-316°C	88

TABLE 5 continued

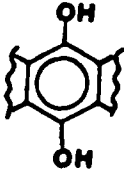
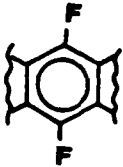
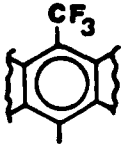
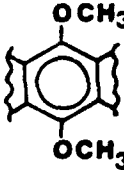
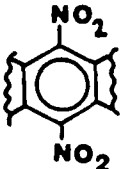
SUBSTITUENT(S)	MP°C	REMARKS	REF.
3,6-dihydroxy 		yellow, red brown fluorescence in uv light, anionic in nature, low solubility in most solvents	89
3,6-difluoro  acid form	270	derivatives useful in polymer synthesis for high boiling fluid; fungicides and bactericides pharmaceutical intermediates	90
3-trifluoromethyl  acid form	280-281	from 1-tri-fluoromethyl durene, precursor iododurene, yield = 89% 1) CF ₃ I, 2) HNO ₃	91
3,6-dimethoxy 	280-283	gold crystals oxidize durene precursor, then sublimed to form dianhydride	92 93 94
3,6-dinitro  acid form	225-230	color due to decreased resonance between carbonyl electrons and N, yield = 75%	94 95 96

TABLE 5 continued

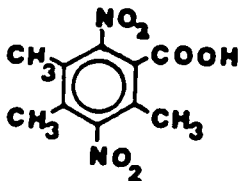
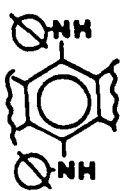
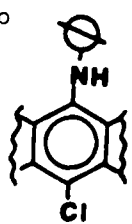
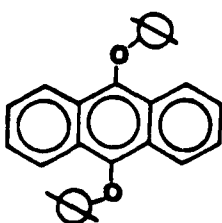
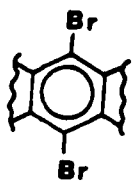

SUBSTITUENT(S)	MP°C	REMARKS	REF.
 durylic acid form	212-213	8 day reflux at 100 °C, filter off MnO ₂ and acidify ² filtrate	97
3,6-dianilino 	268	typical IR bands of anhydride substitute aniline for dichloro; model imide synthesis with aniline blue compounds	98
3-anilino-6-chloro 	285	substitute aniline for chloro, used for forming imide with aniline, gave blue compd.	98
9,10-diphenoxy anthracene (related compd.) 	235-257	pale yellow crystals, yield = 22%	99
3,6-dibromo 	270-275	lemon yellow ozonation of aromatic compds., synthesis from 3,6-dibromodurene	100 101 102

TABLE 5 continued

SUBSTITUENT(S)	MP°C	REMARKS	REF.
3,6-dichloro	265-270	lemon yellow	103
		dissociation constants of polycarbonacids	
		pigments and disperse dyes for resins, fibers, lacquer and printing	104
		vapor-phase oxidation, 70 % yield	105
		poloragraphic determination 1/2 wave potential = 1.1volts.	106
		charge transfer bands and energies determined.	107
		chromatographic study on acceptor crystals, heat of formation calculated	108

Some of the components listed in Table 5 were used in polymer formation reactions. Table 6 summarizes the compounds, the polymers and selected properties.

TABLE 6
SUBSTITUTED PYROMELLITIC DIANHYDRIDES
USED IN POLYMERIZATION

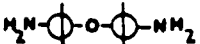
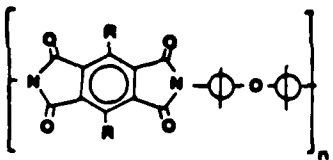
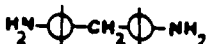
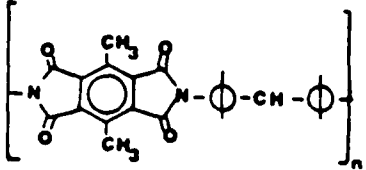
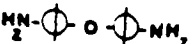
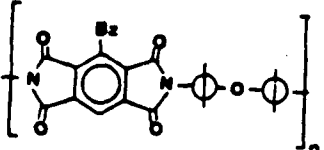
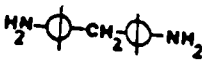
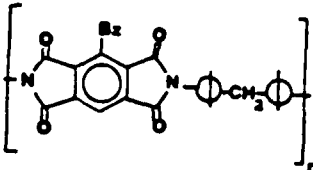
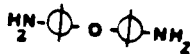
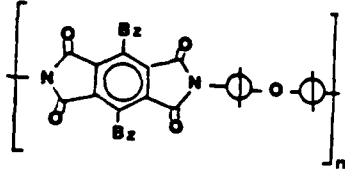

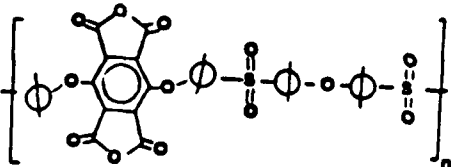
SUBSTITUENT(S)	COMONOMER	POLYMER	REF.
3,6-dibromo			109
		 $R = Br$	
3,6-dichloro	"	$R = Cl$	109
3,6-diiodo	"	$R = I$	109
3,6-dimethyl			110
			
3-benzoyl			111
			

TABLE 6 continued

SUBSTITUENT(S)	COMONOMER	POLYMER	REF.
3-benzoyl			111
			
3,6-dibenzoyl laminates 310°C, good resistance to tensile shearing			112
			
3,6-diphenoxy			113
			

Stabilization of aromatic polyimides was the goal in the dibromo, dichloro and diiodo polyimides. The different substituent effects on stability were studied at 470-500°C and in the presence of oxygen (500 mm Hg) at 360-420°C. The best stability was seen with a 0.1 mole % addition of the dibromo dianhydride. A higher content of additives initiated oxidative thermal degradation. The effectiveness of dibromodianhydride in initiating thermal degradation was inversely proportional to the temperature.

The polyamic acid obtained from 3-benzoylpyromellitic dianhydride (34) and 4,4'-oxydianiline (35) ($\eta_{inh} = 0.96$), or 4,4'-diaminodiphenylmethane (36) was cast into films and heated or chemically treated to convert to the polyimide. A similar polymer was derived from 3,6-dibenzoylpyromellitic dianhydride (37) and 35. Laminates made from this polymer showed good resistance to tensile shearing.

The polymerization of 3,6-diphenoxypyromellitic dianhydride (38) and bisarylsulfonyl halides by a Friedel-Crafts procedure produced a linear poly(arylsulfone) which was useful in the preparation of films and fibers for such applications as ablative re-entry nose cones. Interestingly, no mention of the use of 38 in the preparation of polyimides was made and the details for the synthesis of 38 were lacking.

EXPERIMENTAL

Reagents and Instrumentation

Starting materials included durene, phenol and 3-bromo-o-xylene which were purchased and used without further purification. The diamine 1,3-bis(3-amino-phenoxy)benzene was obtained from the USAF Materials Laboratory, Polymer Branch, WPAFB, Ohio. Solvents for polymerization were purchased in purified grade or purified by distillation before use. Nuclear Magnetic Resonance (NMR) spectra were obtained employing a Varian EM-360-A spectrometer. All samples were run in deuterated chloroform with tetramethylsilane as an internal standard and sample concentrations of approximately 10% (w/v). Infrared spectra (IR) were recorded with a Beckman Model 33 spectrometer and a Nicolet 5DX FTIR using KBr discs and thin films. Mass spectral analysis were performed by AFWAL/MLSA at Wright Patterson AFB, OH. Elemental analysis were performed by Midwest Micro Laboratories, Indianapolis, Indiana and AFWAL/MLSA at Wright Patterson AFB, OH. Viscosities were obtained employing a Cannon Ubbelohde No.75 viscometer at concentrations of .05g/10ml in DMAC at 30°C.

Synthesis of Monomers

Model Compound

3-Phenoxy-o-xylene (40)

In a 250 mL three-necked flask fitted with an air condenser were placed 3-bromo-o-xylene (13.92g, 0.075 mol), potassium carbonate (18.0 g, 0.130 mol), phenol (120.0 g, 1.28 mol), and copper bronze (12.0 g). The mixture was heated to 160°C for twelve hours. The hot maroon solution was poured into a sodium hydroxide (51.0 g, 1.28 mol) solution (780 mL) and stirred to remove excess phenol. The precipitated product was extracted with ether. The ether solution was dried with magnesium sulfate and evaporated. Recrystallization of the residue from methanol yielded pale-yellow, shiny crystals of pure 3-phenoxy-o-xylene¹¹⁷ (9.26 g, 62%): mp 56-57°C; IR (KBr) 3000-2900, 1600, 1500-1450 cm⁻¹; NMR (CDCl₃) δ 2.2 (s, 3H), 2.4 (s, 3H), 7.0 (m, 8H). Anal. Calcd. for C₁₄H₁₄O: C, 84.81; H, 7.12. Found: C, 84.68; H, 7.12.

3-Phenoxyphthalic Acid (41)

A 250 mL three-necked flask equipped with a condenser and magnetic stirrer was charged with 3-phenoxy-o-xylene (4.5 g, 0.0227 mol), pyridine (100 mL), and water (40 mL). After heating to a temperature of 100°C, potassium permanganate (8.96 g, 0.057 mol) was added slowly. The solution was refluxed for 3.5 h at 110-120°C. Vacuum filtration of the

hot reaction mixture through celite yielded a clear, yellow solution, which was evaporated to give a yellow solid. The residue was mixed with a sodium hydroxide (4.0 g, 0.100 mol) solution (73 mL) and heated to 100°C and potassium permanganate (6.45 g, 0.041 mol) was added slowly. After refluxing for 1.5 h, ethanol (10 mL) was added to destroy excess potassium permanganate. A nearly clear filtrate was obtained by vacuum filtration of the hot reaction solution through celite. The filtrate was reduced to a volume of 100 mL and cooled in ice with stirring while cold concentrated hydrochloric acid (12.5 mL) was added dropwise. The pH went from 14 to 2, yielding a white precipitate, which when filtered and dried gave 3-phenoxyphthalic acid (2.67 g, 46%): mp 202-203°C (lit.¹¹⁷ mp 204°C); IR (KBr) 3400-2400, 1700, 1600, 1300 cm^{-1} .

3-Phenoxyphthalic Anhydride (42)

In a 50 mL flask fitted with a condenser was placed 3-phenoxyphthalic acid (0.5 g, 0.0019 mol), and acetic anhydride (25 mL). The mixture was refluxed for one hour at 120-130°C, and then placed in an evaporating dish. Recrystallization of the residue from hexane yielded white crystals of 3-phenoxyphthalic anhydride (0.34 g, 73%): mp 106-107°C (lit.¹¹⁷ mp 106-108°C); IR (KBr) 1850, 1790, 1625-1580, 1475, 1275 cm^{-1} .

9-Oxo-xanthene-1-carboxylic Acid (43)

A mixture of 3-phenoxyphthalic acid (0.5 g, 0.0019 mol), and concentrated sulfuric acid (20 mL) was heated on an oil bath at 90°C for two hours. The yellow solution was poured into water (60 mL), yielding a white precipitate. Vacuum drying yielded a powdery product¹¹⁶ (0.29 g, 31%): IR (KBr) 3000, 1735, 1634, 1625, 1600, 1300, 1075 cm^{-1} .

Monomers

3-Iododurene (45)

In a 500 mL three-necked flask, fitted with an air condenser, were placed durene (50.0 g, 0.373 mol), iodine (38.0 g, 0.150 mol), iodic acid (14.5 g, 0.082 mol), acetic acid (120 mL), sulfuric acid (4 mL), water (20 mL), and carbon tetrachloride (10 mL). The purple-brown mixture was heated on an oil bath with stirring at 75°C for twelve hours. The hot solution was then poured into a stirred aqueous sodium bisulfite solution (150 mL), (10.0 g, 0.096 mol) to destroy excess iodine. The yellow precipitate was collected by vacuum filtration and steam distilled (500 mL) to remove unreacted durene. Crude 3-iododurene was recrystallized from ethanol yielding white, fluffy needles (90.86 g, 94%): mp 80-81°C (lit.¹¹⁴ mp 80°C); IR (KBr) 2980-2825, 1595, 1450, 1375, 1000, 860, 770, 690 cm^{-1} , NMR (CDCl_3) 2.2(s,6H), 2.4(s,6H), 6.7(s,1H).

3-Phenoxydurene (46)

A 500 mL three-necked flask, fitted with an air condenser was charged with 3-iododurene (20.8 g, 0.080 mol), potassium carbonate (12.0 g, 0.080 mol), phenol (80.0 g, 0.850 mol), and copper bronze (8.0 g). The maroon mixture was heated on an oil bath for twelve hours at 160°C. The hot solution was poured into 500 mL of a sodium hydroxide (34.0 g, 0.850 mol) solution to remove excess phenol. The precipitate was filtered and extracted with hot ethanol to produce electrostatic, white crystals (10.8 g, 60%): mp 109-110°C; IR (KBr) 2950-2850, 1590-1575, 1475, 1375 cm^{-1} . NMR (CDCl_3) δ 1.9(s,6H), 2.2(s,6H), 6.5-7.3(m,6H). Analysis calculated for $\text{C}_{16}\text{H}_{18}\text{O}$: C, 84.91; H, 8.02. Found: C, 84.71; H, 8.02.

3-Phenoxypermellitic Acid (47)

In a 1000 mL three-necked flask fitted with a magnetic stirrer and reflux condenser, were placed 3-phenoxydurene (9.21 g, 0.035 mol), pyridine (360 mL), and water (150 mL). This mixture was heated to 100°C and potassium permanganate (32.22 g, 0.204 mol) was added slowly. The solution was refluxed at 110-120°C for 3.5 h. Vacuum filtration of the hot reaction mixture through celite gave a clear, pale yellow filtrate. The filtrate was evaporated and the residue was treated with a sodium hydroxide (12.0 g, 0.300 mol) solution (220 mL). The mixture was heated to 100°C and potassium permanganate (19.3 g, 0.122 mol) was added slowly. After refluxing for 1.5 h, ethanol (15 mL) was added to decompose

excess potassium permanganate. Vacuum filtration of the hot reaction mixture through celite yielded a pale yellow solution. The volume of the solution was reduced to about 75 mL, and the solution was cooled in an ice bath and stirred while cold concentrated hydrochloric acid (24 mL) was added dropwise to produce a white precipitate. Effervescence was observed as the pH went from 14 to 2. The precipitate was filtered to yield 3-phenoxyphthalic acid (9.78 g, 70%): mp 99-101°C IR (KBr) 3600-2400, 1725-1675, 1475, 1375, 1300 cm^{-1} .

Attempted Preparation of 3-Phenoxyphthalic Anhydride (48)

In a 50 mL flask was placed 3-phenoxyphthalic acid (2.0 g, 0.0028 mol). The flask was heated under vacuum (0.1 torr) at 190-210°C, some material sublimed on the flask walls. After 2 h the residue was removed from the flask and recrystallized from toluene yielding yellow needles of 9-oxo-xanthene-1-carboxylic acid phthalic anhydride¹¹⁵ (1.25 g, 63%): mp 215-217 °C IR (KBr) 3000-2500, 1840-1800, 1700, 1300, 900 cm^{-1} ; mass spectrum, m/z (relative intensity) 298(.35, M+), 205(.44, M-O-Ø), 77(.76) (sublimes easily with vacuum). Analysis calculated for $\text{C}_{16}\text{H}_6\text{O}_7$: C, 63.81; H, 1.95. Found: C, 64.16; H, 3.33.

3,6-Dibromodurene (49)

In a 250 mL round bottom flask equipped with a magnetic stirrer and condenser were placed iron (0.2 g, .001 mol) in

chloroform (20 mL) and bromine (10.0 mL). Durene (5.0 g, 0.0373 mol) was dissolved in chloroform (20 mL) and added dropwise to the flask with stirring. Hydrogen bromide gas was evolved as the durene solution was added. The mixture was stirred for 1 h and poured into an evaporating dish to remove excess chloroform and bromine. The residue was washed with 200 mL of aqueous sodium thiosulfate (2 g, .0126 mol), filtered and washed with 100 mL of saturated aqueous sodium carbonate. The mixture was filtered and washed with water (100 mL). Recrystallization from ethanol yielded 3,6-dibromodurene (9.64 g, 89%): mp 200-201°C (lit.¹¹⁸ 200°C), IR (KBr) 2858, 1590, 1072 cm^{-1} . NMR (CDCl_3) δ 2.4(s,12H).

3,6-Diphenoxydurene (50)

A 500 mL three-necked flask fitted with a condenser and magnetic stirrer was charged with dibromodurene (11.67 g, 0.0399 mol), phenol (79.89 g, .8499 mol), potassium carbonate (11.04 g, .0800 mol), and copper bronze (8.0 g). The maroon mixture was heated on an oil bath for 12 h at 160°C. The hot solution was poured into 500 mL of aqueous sodium hydroxide (34.0 g, 0.850 mol) to remove excess phenol. Vacuum filtration produced a tan powdery product mixed with copper. Extraction with ether gave creme colored crystals (5.6 g, 44%): mp 180-181°C; IR (KBr) 3150, 2950, 1600, 1475, 1375, 1200, 730, 710 cm^{-1} . NMR (CDCl_3) δ 2.1(s,12H), 6.6-7.6(m,10H). Analysis calculated for $\text{C}_{22}\text{H}_{22}\text{O}_2$: C, 82.99;

H, 6.97. Found: C, 80.71; H, 6.95.

3,6-Diphenoxypyromellitic Acid (51)

In a 500 mL three-necked flask fitted with a magnetic stirrer and condenser were placed diphenoxydurene (4.33 g, 0.0136 mol), pyridine (120 mL) and water (45 mL). The mixture was heated to 100°C and potassium permanganate (10.74 g, .0679 mol) was added slowly. After refluxing for 3 h at 120°C, the hot solution was vacuum filtered through celite, giving a pale-yellow filtrate. Evaporation produced a residue which was treated with 145 mL of aqueous sodium hydroxide (8 g, 0.2 mol) and heated to 100°C. Potassium permanganate (12.91 g, 0.0817 mol) was added slowly. After refluxing for 1.5 h, ethanol (10 mL) was added to remove excess potassium permanganate. Vacuum filtration of the hot solution through celite produced a pale-yellow filtrate which was evaporated to a volume of 50 mL. The cool stirred solution was treated with cold concentrated hydrochloric acid (15 mL) to produce a white precipitate. Effervescence was observed as the pH went from 14 to 2. The solution was vacuum filtered to yield 3,6-diphenoxypyromellitic acid (4.79 g, 80%): mp 180°C (dec.-H₂O); IR (KBr) 3450-3175, 2975, 1725, 1600, 1475, 1200, 730, 710 cm⁻¹.

3,6-Diphenoxypyromellitic Anhydride (38)

A 50 mL flask was charged with 3,6-diphenoxypyromellitic acid (4.7 g, .0117 mol). The flask was heated under

vacuum at 190–220°C for 2 h. The residue and sublimate were recrystallized from toluene to give yellow needles (3.23 g, 69%): mp 200°C (sub.); IR (KBr) 3175, 1859, 1813, 1590, 1472, 1201, 915; NMR acetone, δ 7.2(m, 10H); mass spectrum, m/z (relative intensity) 402(.72, M^+), 309(.10, $M-O-\emptyset$), 237(.36, 281- CO_2), 209(.15, 2377- CO), 94(.92, $\emptyset-OH$), 77(100, \emptyset). Analysis calculated for $C_{22}H_{10}O_8$: C, 65.67; H, 2.49. Found: C, 64.96; H, 2.51.

Synthesis of Polymers

Model Compound

N,N'-Diphenyl-3,6-diphenoxypyromellitimide (54,55)

In a dry, 25 mL three neck flask, equipped with a nitrogen inlet, magnetic stirrer, stopper and short path distillation head were placed aniline (.11532 g, .00124 mol) in DMAC (2 mL) and isoquinoline (2 drops). The solution was stirred while 3,6-diphenoxypyromellitic dianhydride (.2500 g, 0.00062 mol) was added slowly over 30 min. The solution was heated slowly to 200°C. The DMAC was distilled off and replaced one milliliter at a time for a total of 5 mL. The solution was heated for 1.5 h to close the imide. Precipitation into methanol (300 mL) produced a yellow-gold imide 54 which was recrystallized from dichloromethane (.08 g, 32%): IR (KBr) 3150, 1780, 1720, 1201, 724 cm^{-1} . Analysis calculated for $C_{34}H_{20}N_2O_6$: C, 73.92; H, 3.65; N, 5.07. Found: C, 73.00; H, 3.65; N, 5.37. An additional compound 55 was recovered from the filtrate and

recrystallized from acetone to give orange crystals (.14 g, 56.3%): mp 199–203°C; IR (KBr) 3312, 1768, 1709, 1600, 1475, 1200, 730, 710 cm^{-1} . Analysis calculated for $\text{C}_{34}\text{H}_{20}\text{N}_2\text{O}_6$: C, 73.92; H, 3.65; N, 5.07. Found: C, 74.59; H, 4.41; N, 6.45.

Polymerization Procedures

Procedure 1

In a dry, 25 mL three-neck flask, equipped with a nitrogen inlet, magnetic stirrer, short path distillation head and stopper were placed 1,3-bis(3-aminophenoxy)benzene (.3632 g, .00124 mol) in freshly distilled m-cresol (4 mL) and isoquinoline (2 drops). The diamine solution was stirred while 3,6-diphenoxypyromellitic dianhydride (.5000 g, .00124 mol) was added slowly over 30 min. The last of the dianhydride was washed from the vial with m-cresol (4 mL) and toluene (5 mL). The solution was heated slowly to 80°C to effect solution. The temperature was increased to 140°C to remove toluene and azeotrope water. Additional toluene (5 mL) was added and distilled 1 mL at a time. The solution was heated to 180°C for 1.5 h to close the imide, and then cooled with stirring and diluted with chloroform (10 mL) and pipetted carefully into methanol (1200 mL) with stirring to give a yellow polyimide (58a) (.61 g, 75%): IR (film) from tetrachloroethane 1772, 1730, 721 cm^{-1} . Analysis calculated for $\text{C}_{40}\text{H}_{22}\text{N}_2\text{O}_8$: C, 72.94; H, 3.37; N, 4.25. Found: C, 62.80;

H, 3.42; N, 4.67.

Polyimide (58b)

Procedure 1 was used except that the final solution was diluted with tetrachloroethane (10 mL) and stirred overnight at room temperature. The precipitate (58b) was yellow (.57 g, 70%): IR (film) from tetrachloroethane 1772, 1730, 721 cm^{-1} . Analysis calculated for $\text{C}_{40}\text{H}_{22}\text{N}_2\text{O}_8$: C, 72.94; H, 3.37; N, 4.25. Found: C, 71.34; H, 3.49; N, 4.19.

Polyimide (58c)

Procedure 1 was used except that the final solution was diluted while still hot with tetrachloroethane (10 mL) and precipitated into methanol (1200 mL). The precipitate (58c) was yellow (.59 g, 72%): IR (film) 1774, 1734, 722 cm^{-1} . Analysis calculated for $\text{C}_{40}\text{H}_{22}\text{N}_2\text{O}_8$: C, 72.94; H, 3.37; N, 4.25. Found: C, 70.95; H, 3.40; N, 4.26

Polyimide (58d)

Procedure 1 was changed by decreasing the amount of m-cresol from 8 mL to 5 mL. The temperature was increased from 180°C to 250°C and the water was removed by addition of m-cresol (2 mL) which was distilled and replaced over 4 h. The m-cresol was distilled and replaced with DMAC (10 mL) as a diluting solvent. The polymer was precipitated into methanol (600 mL) yielding a yellow, flaky polyimide (58d) (.65g, 80%): IR (film) (DMAC) vacuum baked 1776, 1730, 1589, 1221, 740 cm^{-1} . Analysis calculated for $\text{C}_{40}\text{H}_{22}\text{N}_2\text{O}_8$:

C, 72.94; H, 3.37; N, 4.25. Found: C, 70.81; H, 3.54; N, 5.50.

Procedure 2

In a dry 25, mL three-neck flask, equipped with a nitrogen inlet, magnetic stirrer, short path distillation head and stopper were placed 1,3-bis(3-aminophenoxy)benzene (.3632 g, .00124 mol) in DMF (4 mL), and isoquinoline (2 drops). The diamine solution was stirred while 3,6-diphenoxypyromellitic dianhydride (.5000 g, .00124 mol) was added slowly over 30 min. The last of the dianhydride was washed from the vial with DMF (4 mL). The solution was heated to 80°C to effect solution. The temperature was increased to 153°C to distill off DMF and water. Additional DMF was added and distilled off 1 mL at a time. The solution was heated to 200°C for 1.5 h to close the imide. The solution was cooled with stirring and precipitated into methanol (1200 mL) to give a powdery Polyimide (58e) (.54 g, 66%): IR (film) (DMF) vacuum baked 3332, 3097, 1776, 1738, 1600, 1219, 724 cm^{-1} .

Polyimide (58f)

Procedure 2 was used except that the room temperature polyamic acid solution was followed by infrared analysis over time to observe conversion to the imide. A sample was vacuum baked at 200°C for 24 h to close the imide (58f). IR (film) (DMF) 0-1.5h 3543, 3437, 2922, 1784, 1701, 1255, 1095, cm^{-1} .

IR (film) vacuum baked 3520, 3117, 1774, 1741, 1593, 1396, 1197, 941, 831, 722 cm^{-1} . Analysis calculated for $\text{C}_{40}\text{H}_{22}\text{N}_2\text{O}_8$: C, 72.94; H, 3.37; N, 4.25. Found: C, 71.21; H, 4.03; N, 5.03.

Procedure 3

In a dry, 25 mL three-neck flask, equipped with a nitrogen inlet, magnetic stirrer, short path distillation head and stopper were placed 1,3-bis(3-aminophenoxy)benzene (.3632g, 0.00124 mol) in vacuum distilled DMAC (4 mL), and isoquino-line (2 drops). The diamine solution was stirred while 3,6-diphenoxypyromellitic dianhydride (.5000g, .00124 mol) was added slowly over 30 min. The last of the dianhydride was washed from the vial with DMAC (4 mL). After stirring at room temperature for 30 min., a sample was transferred to a salt plate and vacuum baked at 200°C for 24 h. Samples of the polyamic acid were taken at 24°C, 45°C, 65°C, and 85°C and compared by infrared analysis. Additional DMAC (5 mL) was added and distilled 1 mL at a time to remove water. The solution was heated to 200°C for 1.5 h to close the imide, cooled with stirring and precipitated into methanol (1200 mL) to give tan powdery flakes of imide (58g) yielding (64 g, 78%): IR (film) (DMAC) amic acid 80°C 3481, 2922, 1720, 1641, 1545, 1180, 1012. IR (film) (DMAC) vacuum baked 1811, 1728, 1591, 1485, 945, 680 cm^{-1} . Analysis calculated for $\text{C}_{40}\text{H}_{22}\text{N}_2\text{O}_8$: C, 72.94; H, 3.37; N, 4.25. Found: C, 69.75; H, 3.57; N, 5.40.

Polyimide (58h)

Procedure 3 was changed in that HPLC grade DMAC was used. precipitate was a gold-tan flaky polyimide (58h) yielding (.37 g, 91%): IR (film) (DMAC) vacuum baked 1811, 1728, 1591, 1485, 945, 680 cm^{-1} . Analysis calculated for $\text{C}_{40}\text{H}_{22}\text{N}_2\text{O}_8$: C, 72.94; H, 3.37; N, 4.25. Found: C, 70.29; H, 4.02; N, 5.45.

Polyimide (58i)

Procedure 3 was altered by halving the molar ratio of the reagents and decreasing the volume of HPLC grade DMAC from 8 mL to 3 mL. Toluene (5 ml) was added and distilled to remove the water. The precipitate (58i) gave burnt orange flakes (.39g, 95.5%) IR (film) (DMAC) vacuum baked 1759, 1725, 1600, 1450, 1200, 742 cm^{-1} . Analysis calculated for $\text{C}_{40}\text{H}_{22}\text{N}_2\text{O}_8$: C, 72.94; H, 3.37; N, 4.25. Found: C, 69.34; H, 3.65; N, 5.77.

Polyimide (58j)

Procedure 3 was altered by reducing the molar ratios of the reagents by half and using 3 mL of HPLC grade DMAC. No samples of the amic acid were taken and the solution was refluxed for 1 h. The DMAC was distilled off and toluene (5 mL) was added and distilled to azeotrope water. This was repeated with a reflux time of 2 h. Repetition of this procedure for an additional two times with reflux times of 3 h each was followed by a final reflux time of 15 h. The

polymer solution was precipitated into methanol (600 mL) to give a dark-orange, flaky product (58j) (.39 g, 95.5%): IR (film) (DMAC) vacuum baked 1759, 1725, 1600, 1450, 1200, 742 cm^{-1} . Analysis calculated for $\text{C}_{40}\text{H}_{22}\text{N}_2\text{O}_8$: C, 72.94; H, 3.37; N, 4.25. Found: C, 71.56; H, 3.97; N, 4.75.

RESULTS AND DISCUSSION

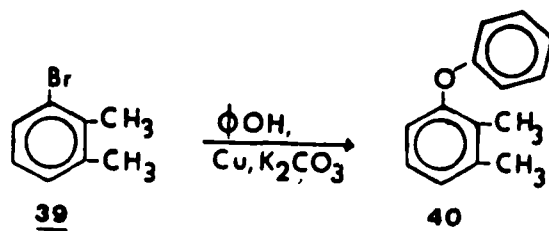
Monomer Synthesis

The major objective of this research was to synthesize a dianhydride with one or more phenoxy substituents which should theoretically lead to an increase in the solubility of a polyimide by decreasing intermolecular interactions. Whereas, the introduction of side-chain or main-chain aliphatic linkages sharply reduced the thermal stability of polypyromellitimides, wholly aromatic polypyromellitimides exhibit excellent resistance to thermal oxidative attack.⁷⁰ Thus, a phenoxy group appeared to be an ideal side-chain pendent because of its thermal stability and relative ease of introduction.

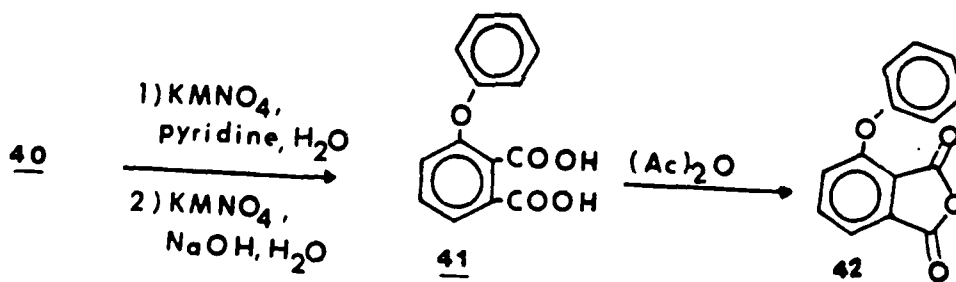
Model Compound

Investigation of a model compound prepared from 3-bromo-o-xylene (39), was investigated to establish synthetic procedures and to determine whether a phenoxy pendent group ortho to an acid function would preferentially cyclize internally to give a xanthone type 43 product.

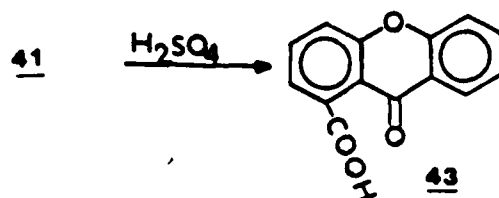
The reaction of 3-bromo-o-xylene (39) with phenol, copper and potassium carbonate yielded 3-phenoxy-o-xylene (40), which was purified by recrystallization from methanol.



Oxidation of (40) was carried out in a two step procedure using potassium permanganate, pyridine and water followed by potassium permanganate, sodium hydroxide and water which produced 3-phenoxyphthalic acid (41). When 41 was reacted with acetic anhydride, 3-phenoxyphthalic anhydride (42) was formed and could be purified by recrystallization from hexane.



The anticipated xanthone product 43 was not found. It could, however, be prepared by the reaction of 3-phenoxyphthalic acid (41) and concentrated sulfuric acid. The infrared spectrum with acid absorption in the 3000 cm^{-1} region and two carbonyl absorptions in the $1700\text{--}1900 \text{ cm}^{-1}$ region is consistent with that expected for 9-oxo-xanthene-1-carboxylic acid (43).



Compounds 40-43 were characterized (Table 7) by known melting points, infrared absorption spectrum (Figures 5-8), an NMR spectrum (Figure 9), and elemental analysis. Conversions in this four step synthesis were reasonable. Interestingly, the conversion of 41 to 42 in acetic anhydride occurred in 73% yield, while the xanthone 43 formation in concentrated sulfuric acid occurred in 31% yield. This may indicate that xanthone formation might be minimized if strong chemical reaction conditions were avoided. Elemental analysis of compound 40 which appears in the literature without reported physical properties is in good agreement with theoretical values.

TABLE 7
PHYSICAL PROPERTIES OF MONOMER MODEL COMPOUNDS

COMPOUND	MP°C (LIT.)	YIELD %	IR (KBr) cm ⁻¹
<u>40</u>	56-57	62	3150-2900 (CH arom., alip.) 1600 (C=C) 1500-1450 (C-O-O)
<u>41</u>	202-203 (204)	46	3400-2400 (OH acid) 1700 (C=O) 1600 (C=C) 1300 (C-O-C)
<u>42</u>	106-107 (106-108)	73	1850 (C=O) 1790 (C=O) 1625, 1475 (C=C) 1275 (C-O-C)
<u>43</u>	175, crude (231-232)	31	3000 (OH acid) 1735 (C=O) acid 1634 (C=O) ketone 1600 (C=C) 1300 (C-O-C)

The infrared spectra of compounds 40-43 (Figures 5-8) are consistent with the functional group conversions carried out. The NMR spectrum of compound 40 (Figure 9) shows nonequivalent methyl groups at δ 2.2 and 2.4 and the aromatic hydrogens at δ 7.0.

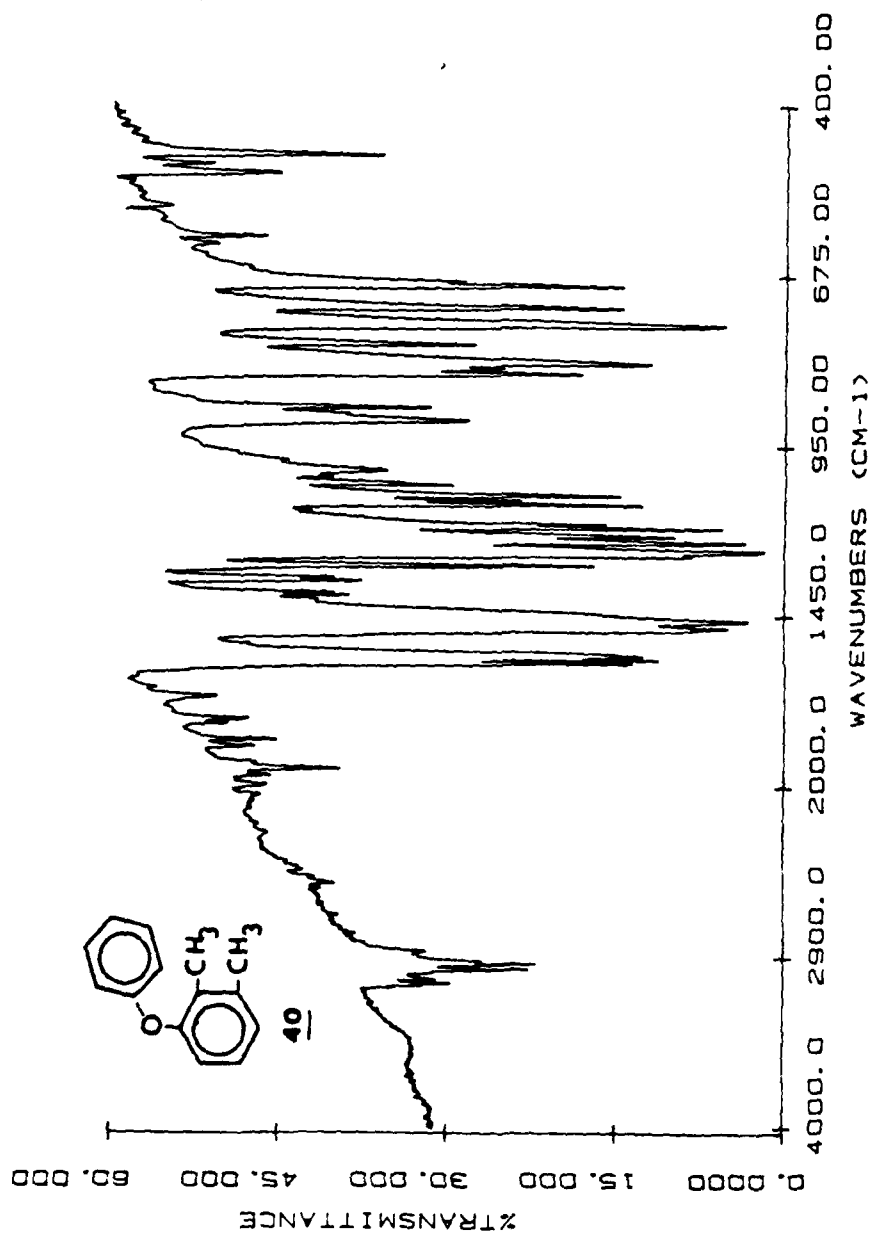


Figure 5. Infrared Spectrum of 3-phenoxy-o-xylene (40).

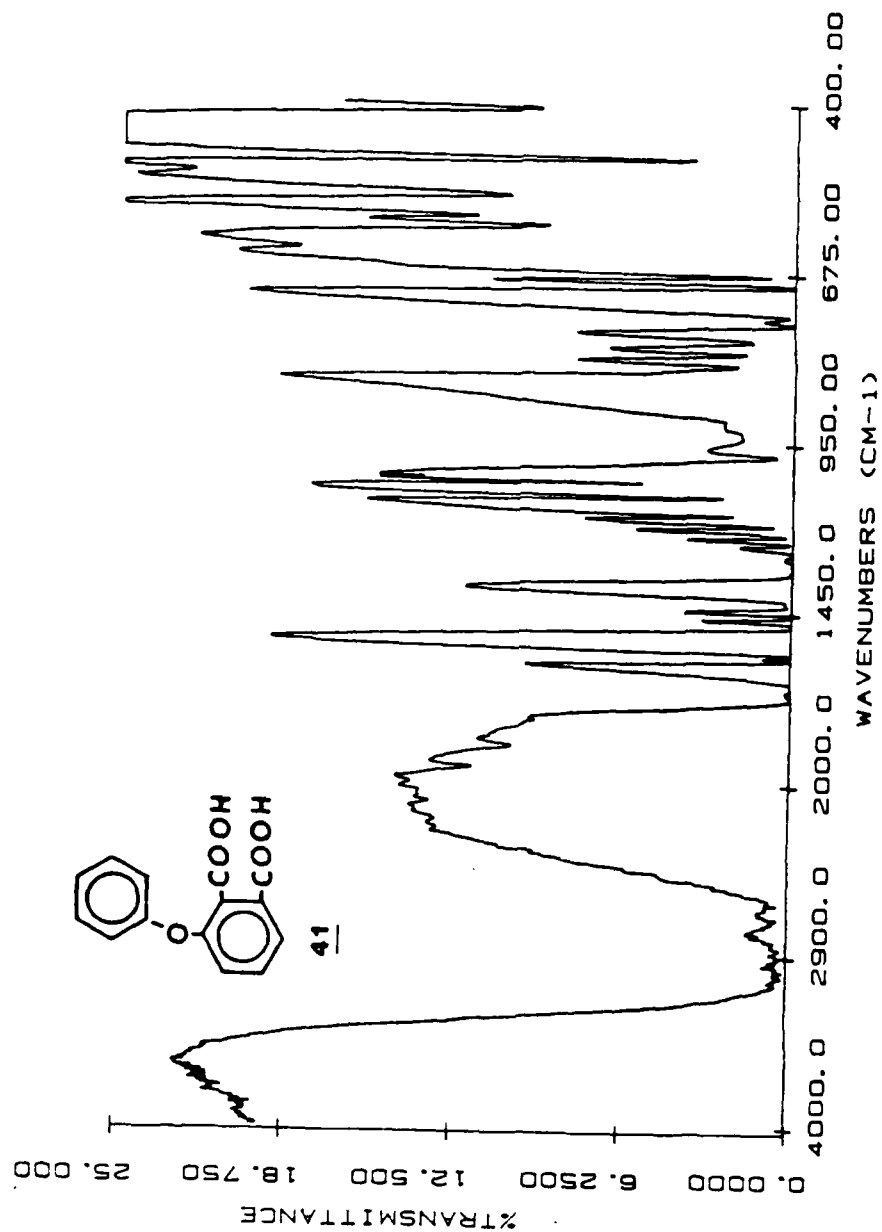


Figure 6. Infrared Spectrum of 3-phenoxyphthalic acid (41).

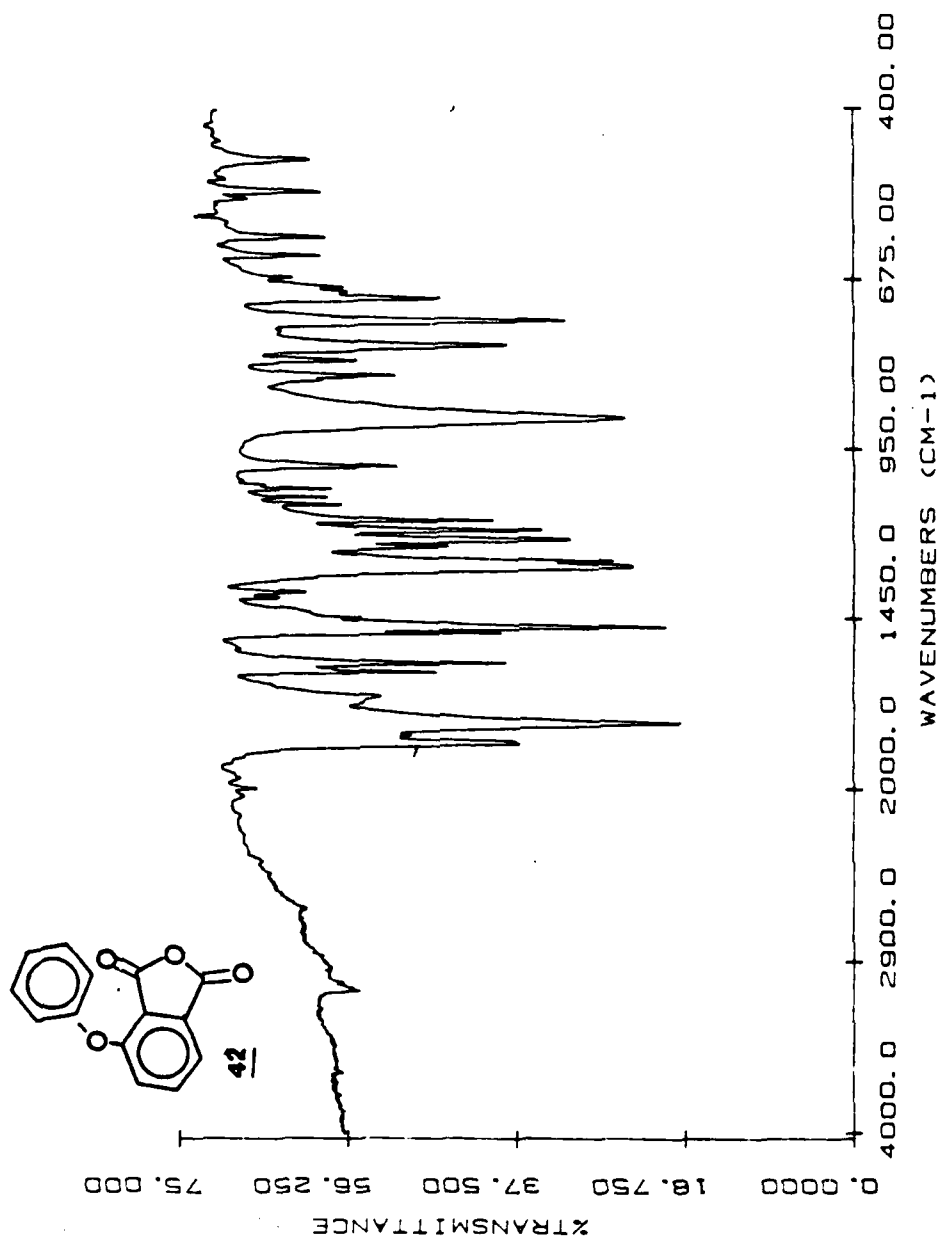


Figure 7. Infrared Spectrum of 3-phenoxyphthalic anhydride (42).

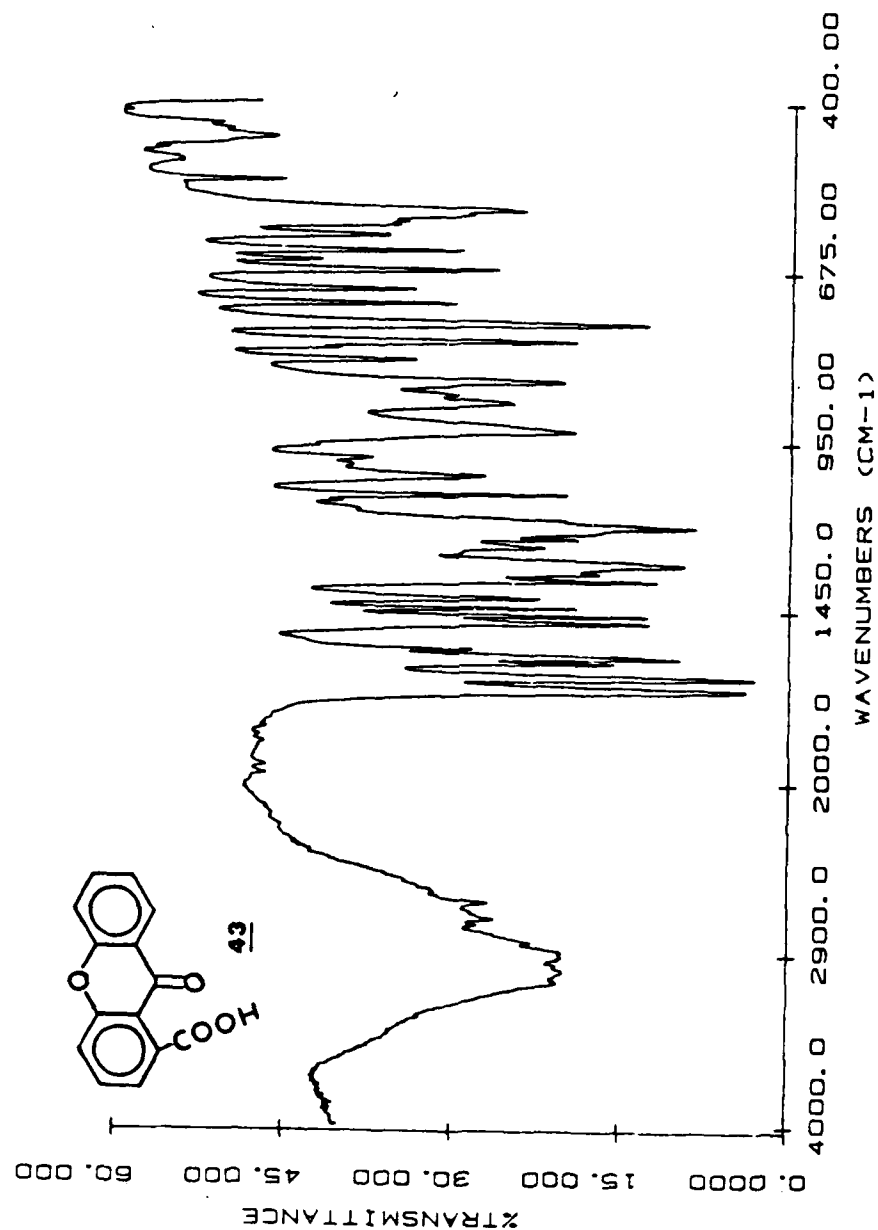


Figure 8. Infrared Spectrum of Compound (43).

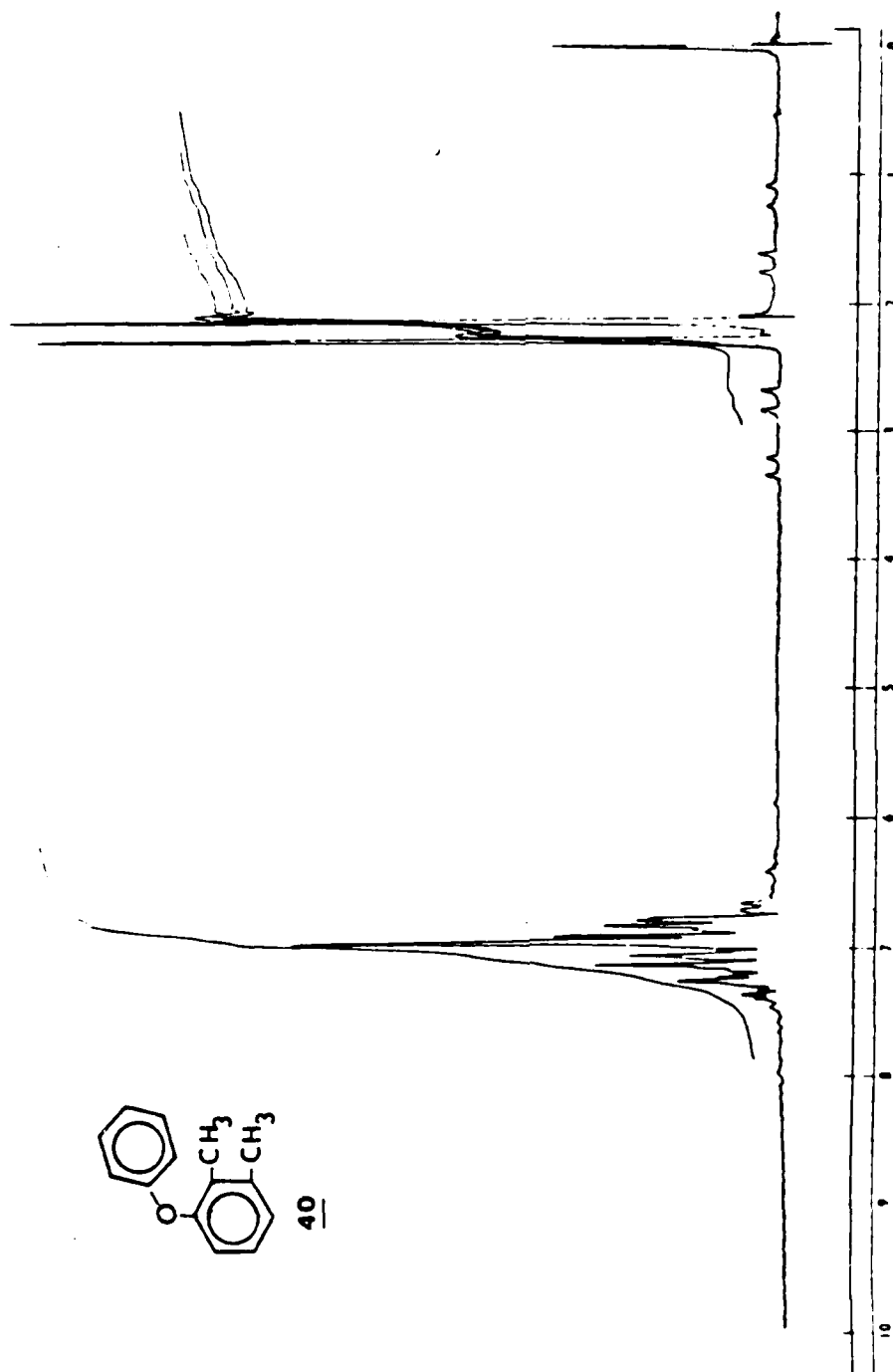
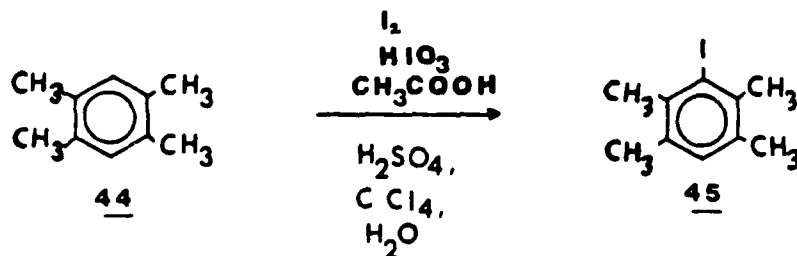


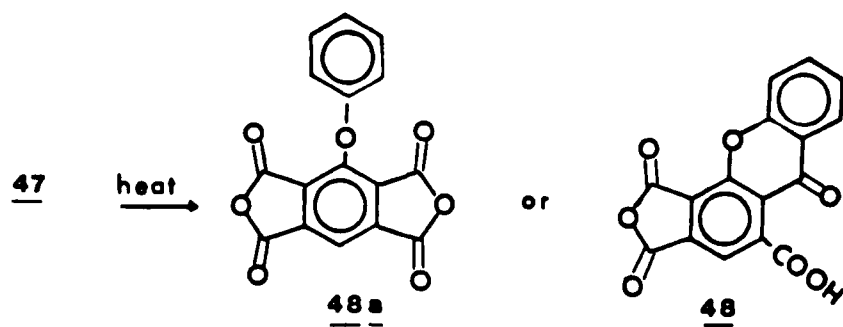
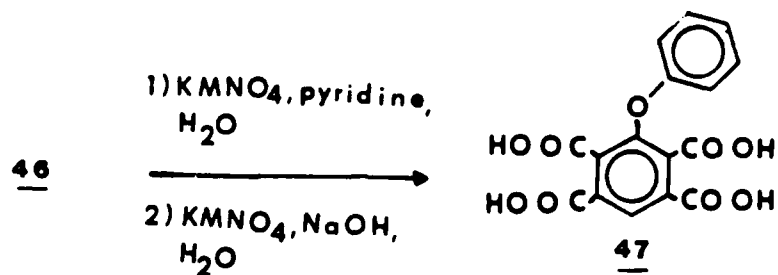
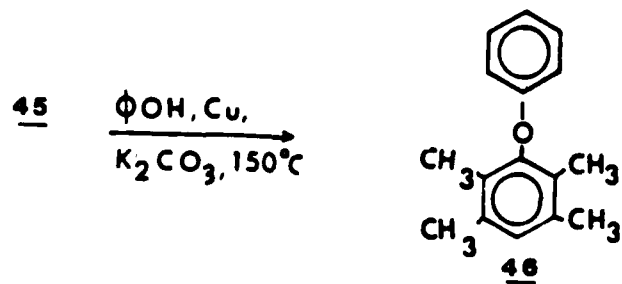
Figure 9. NMR Spectrum of 3-phenoxy-o-xylene (40).

Monophenoxy Dianhydride

The preparation of 3-phenoxydurene dianhydride (48a) was undertaken because the unsymmetrical placement of the pendent group would decrease symmetry and would likely increase the solubility of the dianhydride.

Durene (44) was reacted with iodine, iodic acid, acetic acid, concentrated sulfuric acid, water and carbon tetrachloride to produce known 3-iododurene (45).¹¹⁴ The NMR spectrum of 45 (Figure 15) is consistent with an unsymmetrically substituted benzene indicated by the nonequivalent methyl absorptions at δ 2.2 and 2.4. Compound 45 was used to prepare 3-phenoxydurene (46) using phenol, copper bronze and potassium carbonate as previously discussed. The NMR spectrum of 46 (Figure 16) again shows nonequivalent methyl absorption at δ 1.9 and 2.2 in accord with the electron donating nature of phenoxy as compared to halogen.





Oxidation of 46 in a two step sequence as for the model compound 40 produced the tetraacid 3-phenoxy pyromellitic acid (47). The infrared spectrum of 47 (Figure 13) is consistent with the structure.

Pyrolysis of 47 intended to yield 3-phenoxy pyromellitic dianhydride (48a), gave instead 9-oxo-xanthene-1-carboxylic acid-3,4-dicarboxylic anhydride (48) a lemon yellow compound readily recrystallized from toluene. Mass spectral analysis of 48 (Figure 17) confirmed the molecular weight and infrared analysis (Figure 14) confirmed the presence of acid, anhydride and ketone functions.

A summary of physical properties for the monophenoxy compounds is given in Table 8.

TABLE 8
PHYSICAL PROPERTIES OF MONOPHENOXY COMPOUNDS

COMPOUND	YIELD %	MP°C (lit.)	IR(KBr) cm ⁻¹	NMR δ CDCl ₃	ELEMENTAL ANALYSIS	MASS SPECTRUM
<u>45</u>	94	80-81 (80)	2980-2885 (alip. C-H) 1595 (C=C) 1375 (CH ₃)	2.2 (s, 6H) 2.4 (s, 6H) 6.7 (s, 1H)		
<u>46</u>	60	109-110	2950-2850 (alip. C-H) 1590 (C=C) 1475 (C=C) 1375 (CH ₃)	1.9 (s, 6H) 2.2 (s, 6H) 6.5 (m, 5H)	C=84.91 H=8.02 found: C=84.71 H=8.02	
<u>47</u>	70	99-101	3600-2400 (OH acid) 1725 (C=O) 1675, 1475 (C=C) 1300 (C-O-C)			
<u>48</u>	63	215-217	3000-2500 (OH acid) 1840 (C=O) 1800 (C=O) 1600 (C=C) 1300 (C-O-C) 900 (CO-O-CO)		sent out	(298)M+ 205 (M-O-Ø) 181 152 77 (Ø)

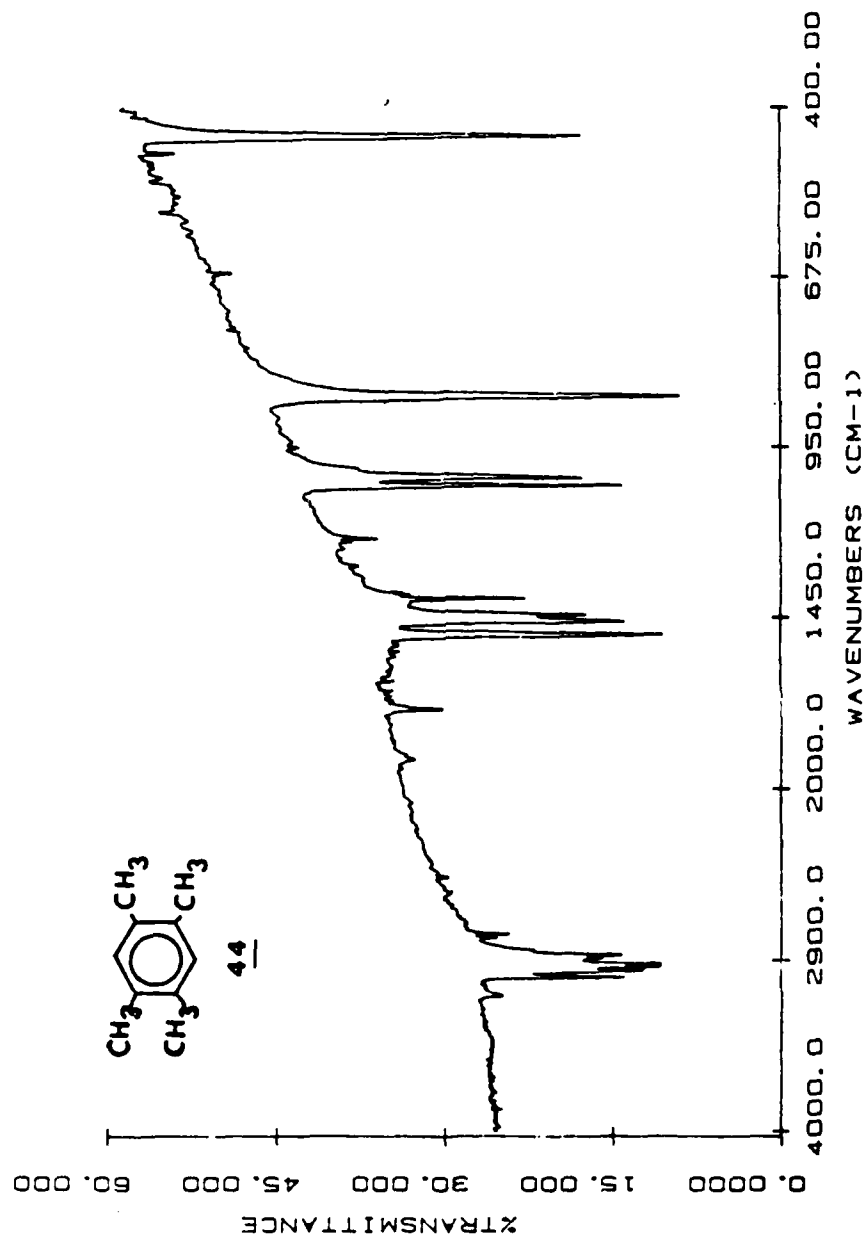


Figure 10. Infrared Spectrum of Durene (44).

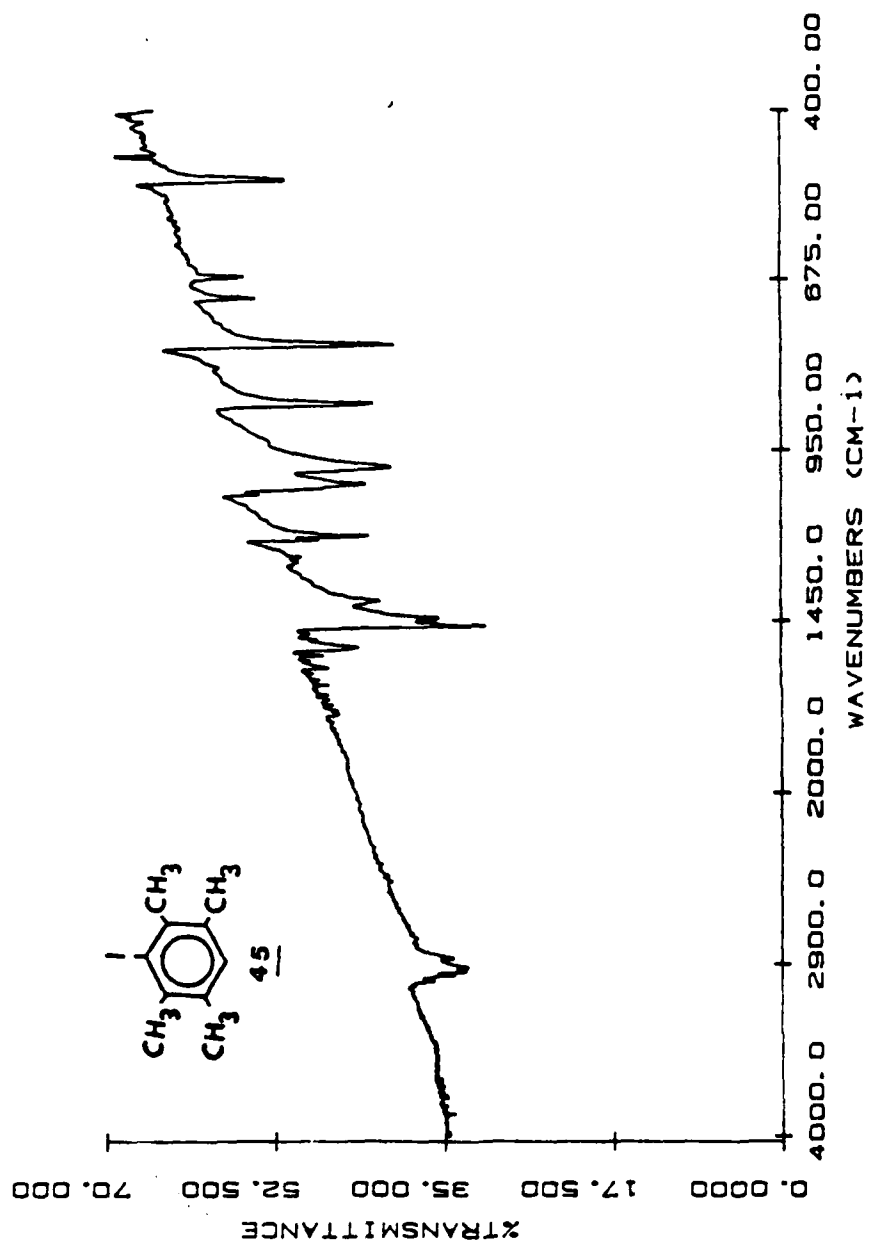


Figure 11. Infrared Spectrum of 3-iododurene (45).

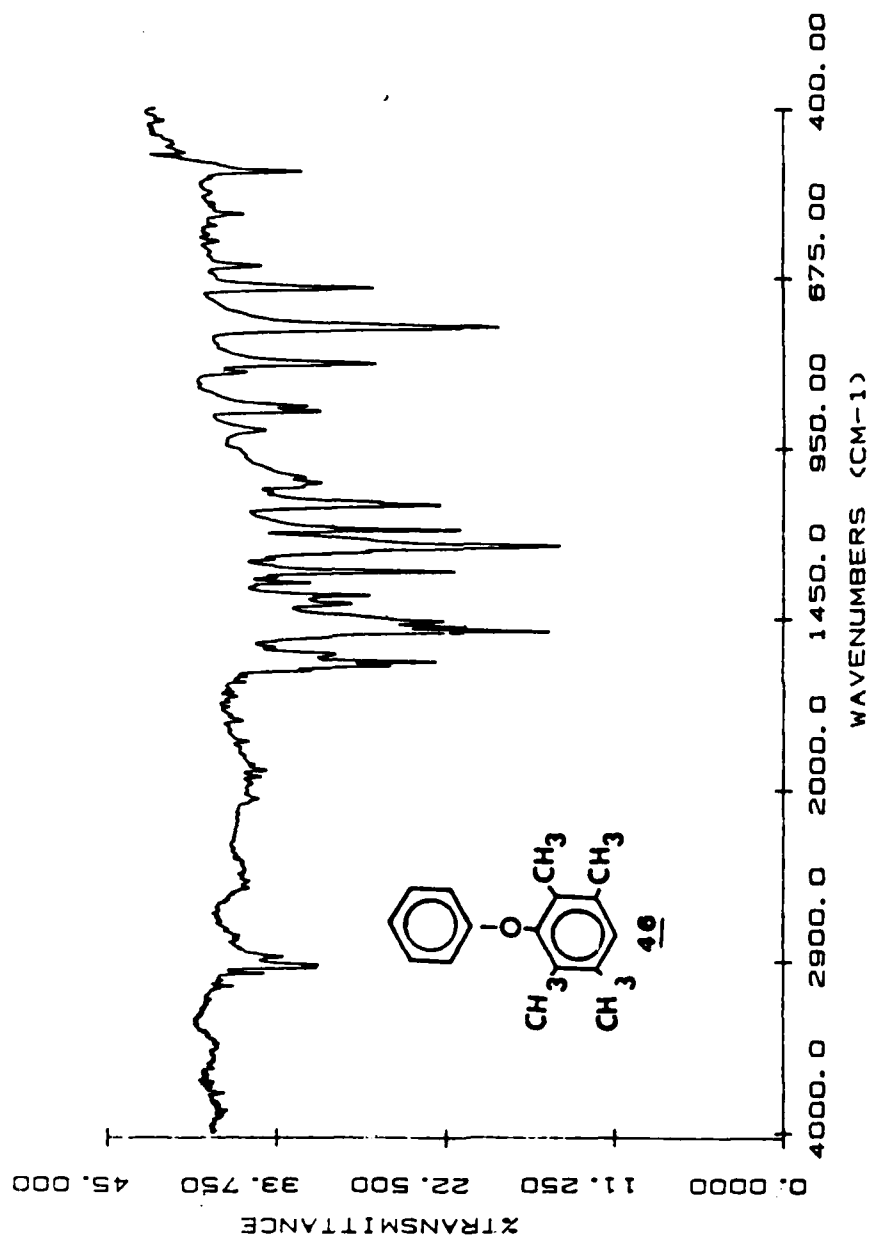


Figure 12. Infrared Spectrum of 3-phenoxydurene (46).

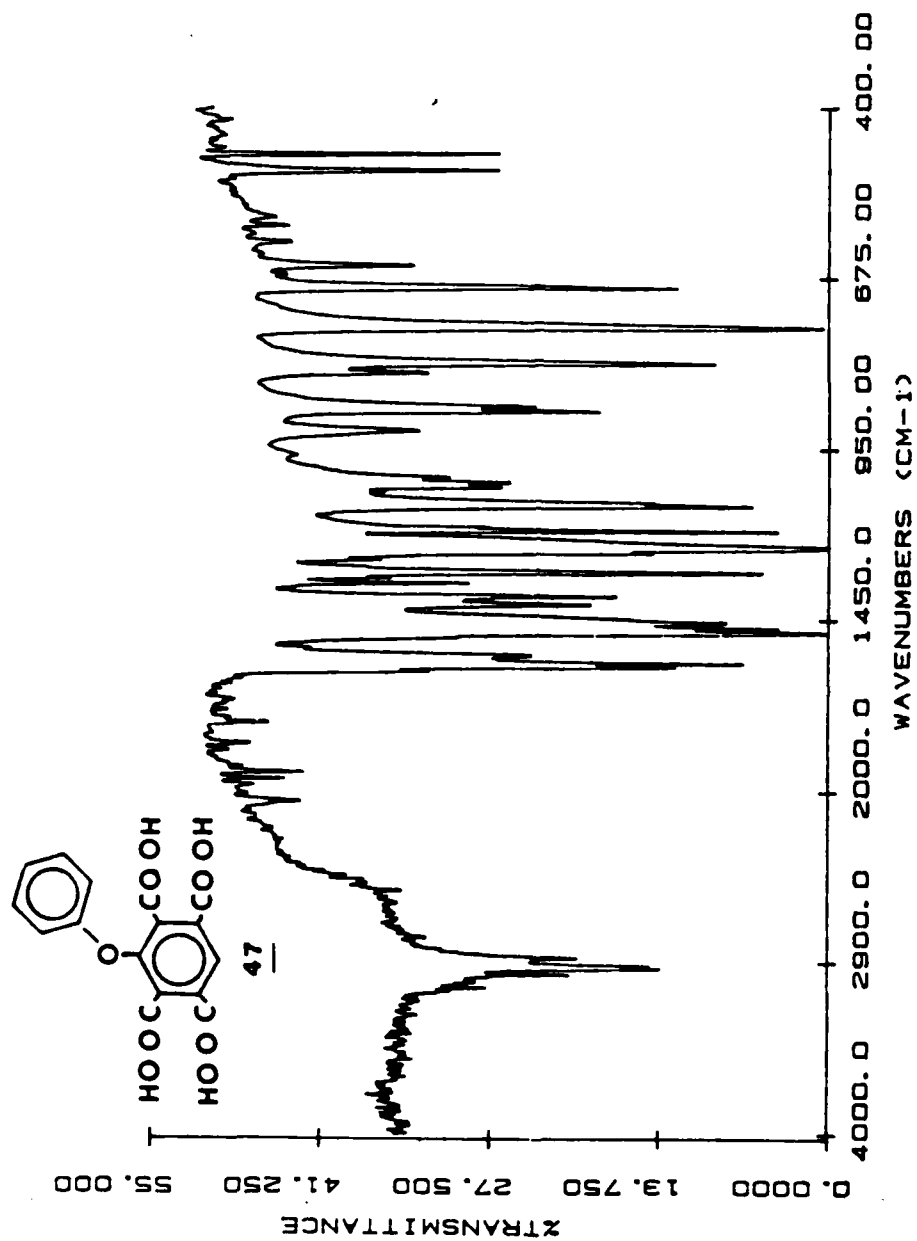


Figure 13. Infrared Spectrum of 3-phenoxyphenylmallic acid (47).

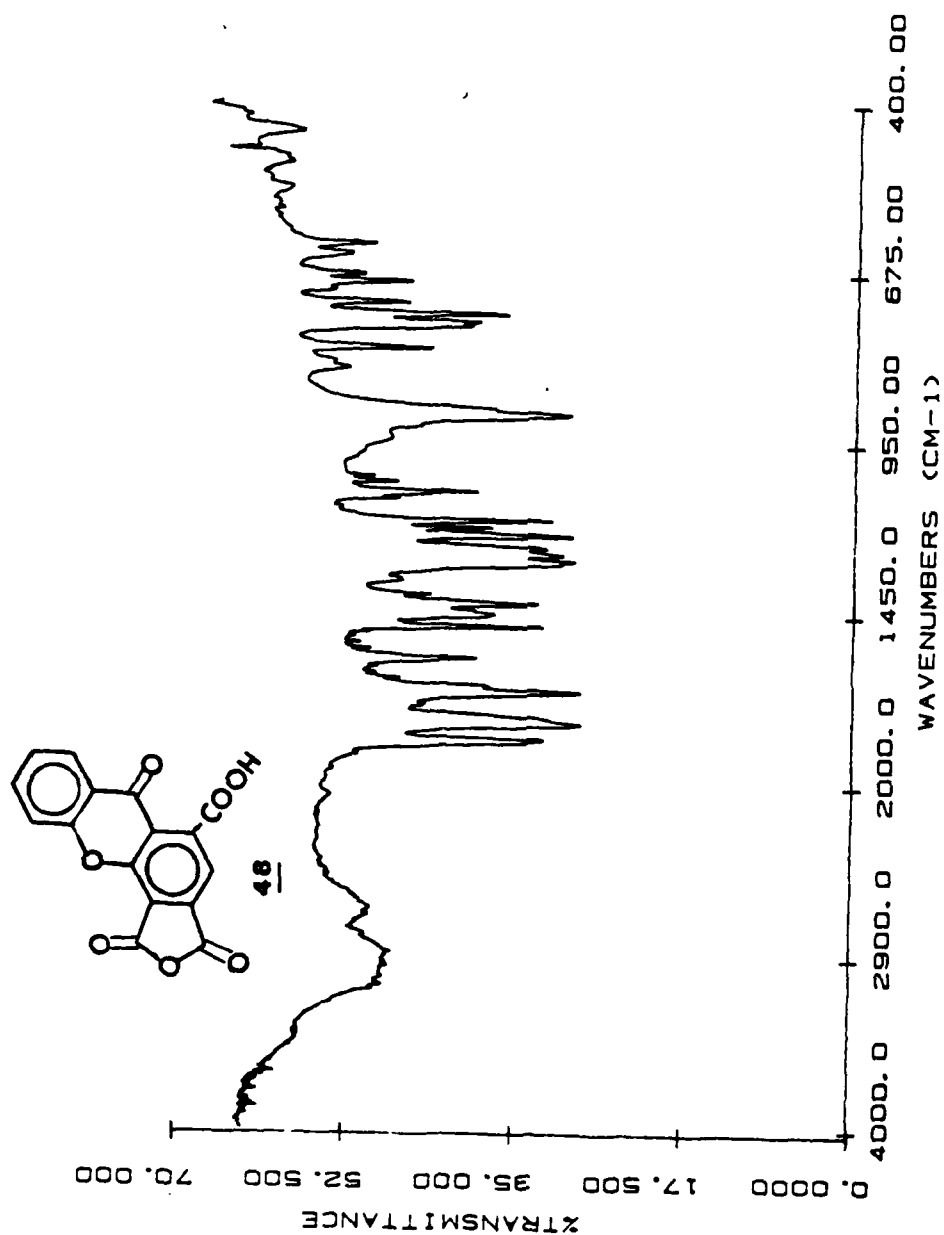


Figure 14. Infrared Spectrum of Compound (4B).

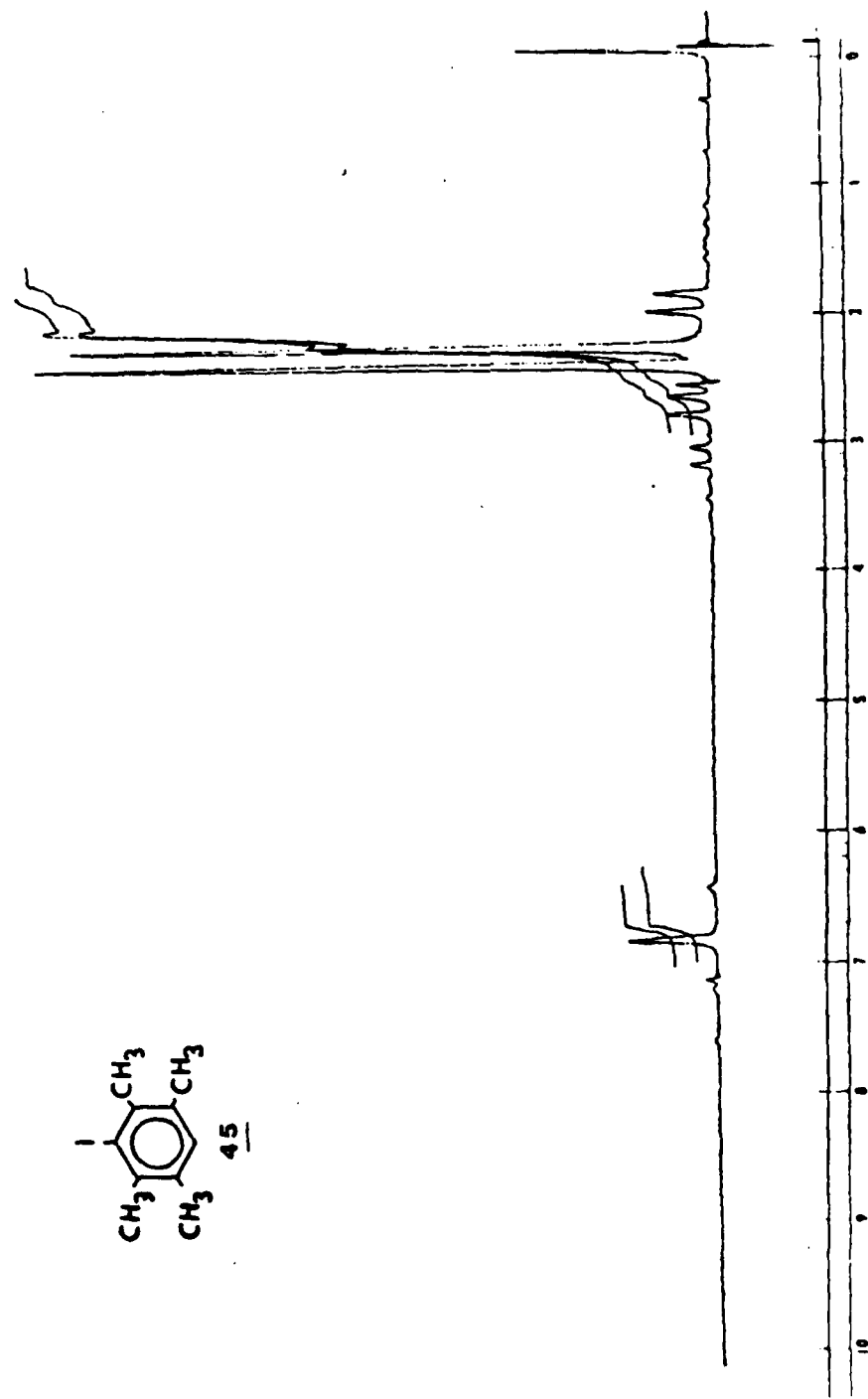
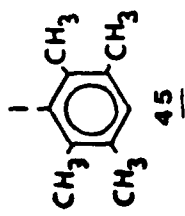


Figure 15. NMR Spectrum of 3-iododurene (45).

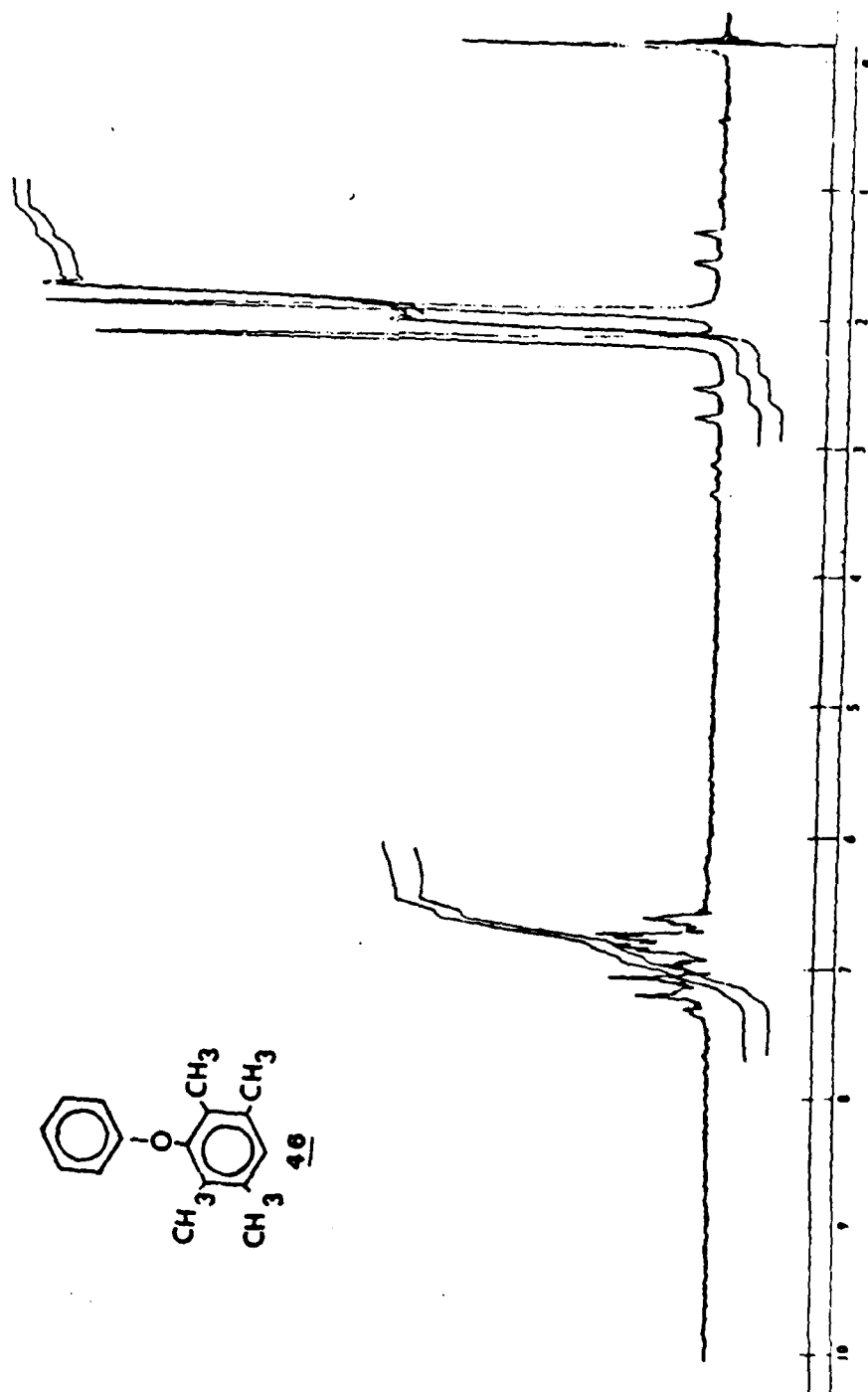
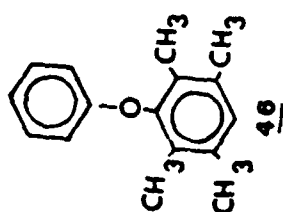


Figure 16. NMR Spectrum of 3-phenoxymethylurene (46).

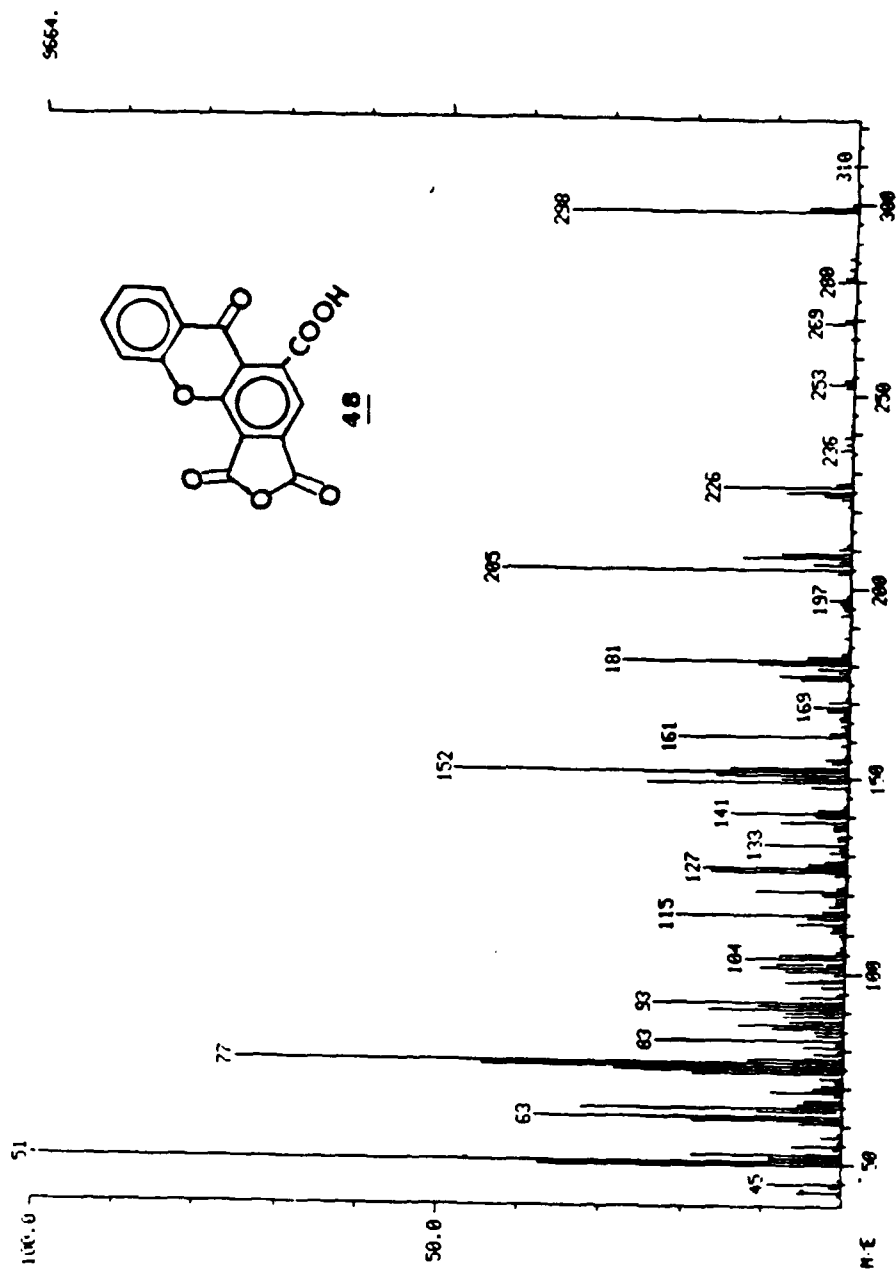
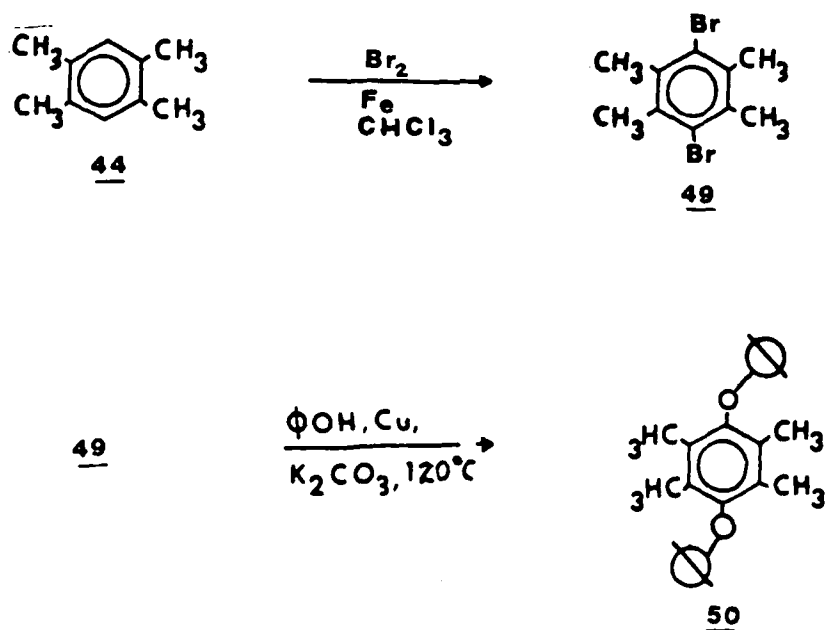


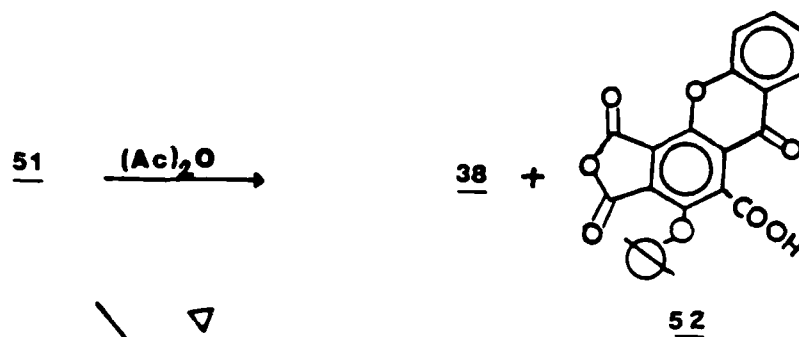
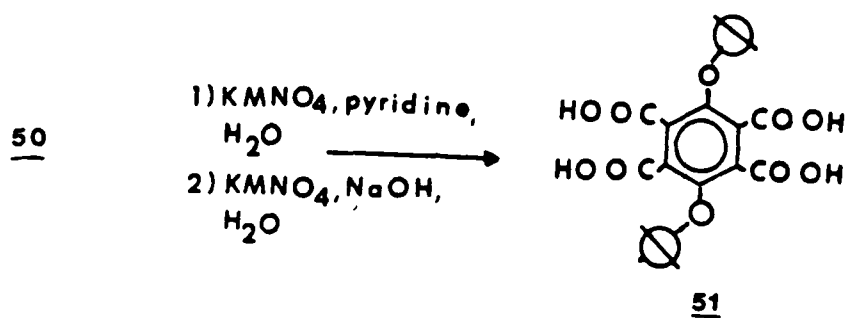
Figure 17. Mass Spectrum of Compound (48).

Diphenoxy Dianhydride

Durene (44) was reacted with bromine and iron in chloroform to produce 3,6-dibromo-durene (49). As expected, 3,6-dibromodurene (49) exhibits a simple NMR spectrum (Figure 21) with a single peak at δ 2.4.

The reaction of 49 with phenol, copper bronze and potassium carbonate gave 3,6-diphenoxydurene (50). The NMR spectrum of 50 is shown in Figure 22. The expected aromatic and aliphatic absorptions are observed.





Steps one through three produced the desired product, but when compound (51) was reacted with acetic anhydride, more than one product was produced as evidenced by a thin layer chromatograph of this material. The desired product was 3,6-diphenoxypyromellitic dianhydride (38), however a possible product was thought to be a xanthene (52). Thermal cyclization of compound (51) gave 3,6-diphenoxypyromellitic dianhydride (38), which was recrystallized from toluene.

The diphenoxy compounds were characterized by melting points, infrared spectrum Figures 18-21, NMR spectrum Figures 22, 23, and 24. Table 9 gives the physical properties and spectral data of the diphenoxy compounds. Infrared analysis of the compounds shows the conversion from 3,6-dibromodurene to 3,6-diphenoxypyromellitic dianhydride through the loss or appearance of functional group bands. The NMR spectrum of 49 shows only one peak for the methyl hydrogens at δ 2.4. Compound 50 has a peak at δ 1.9 for the methyl hydrogens and a broad multiplet at δ 6.5-7.2 for the aromatic hydrogens on the phenoxy pendent groups. The spectrum of 38 shows a multiplet at δ 6.7-7.2 for the phenoxy pendent group hydrogens and a peak at δ 2.2 for the solvent acetone. Elemental analysis and mass spectral analysis confirm the structure of compound 38.

TABLE 9
PHYSICAL PROPERTIES OF DIPHENOXY COMPOUNDS

COMPOUND	YIELD %	MP°C (lit.)	IR(KBr) cm ⁻¹	NMR δ CDCl ₃	ELEMENTAL ANALYSIS	MASS SPECTRUM
<u>49</u>	89	200-201 (200)	2858 (alip. C-H) 1590, 1475 (C=C) 1375 (CH ₃) 1072 (o-p bend CH)	2.4(s, 12H)		
<u>50</u>	44	180-181	3150 (arom. C-H) 2950 (alip. C-H) 1600 (C=C) 1475 (C=C) 1375 (CH ₃) 1200 (C-δ-C) 730, 690 (mono. sub.)	1.9(s, 12H) 6.5-7.2 (m, 10H)		
<u>51</u>	80	180 (dec. -H ₂ O)	3350-3175 (OH) 2875 (C-H alip.) 1725 (C=O) 1600, 1475 (C=C) 1200 (C-O-C) 730, 690 (mono. sub.)			
<u>38</u>	69	200 sub.	3175 (Ar.CH) 1859 (C=O) 1813 (C=O) 1590, 1472 (C=C) 1201 (C-O-C) 900 (CO-O-CO)	6.7-7.2 2.2 (acetone)	CH anal. C=65.67 H=2.49 found C=64.74 H=2.60	(M+) 402 309 281 237 137 94 77

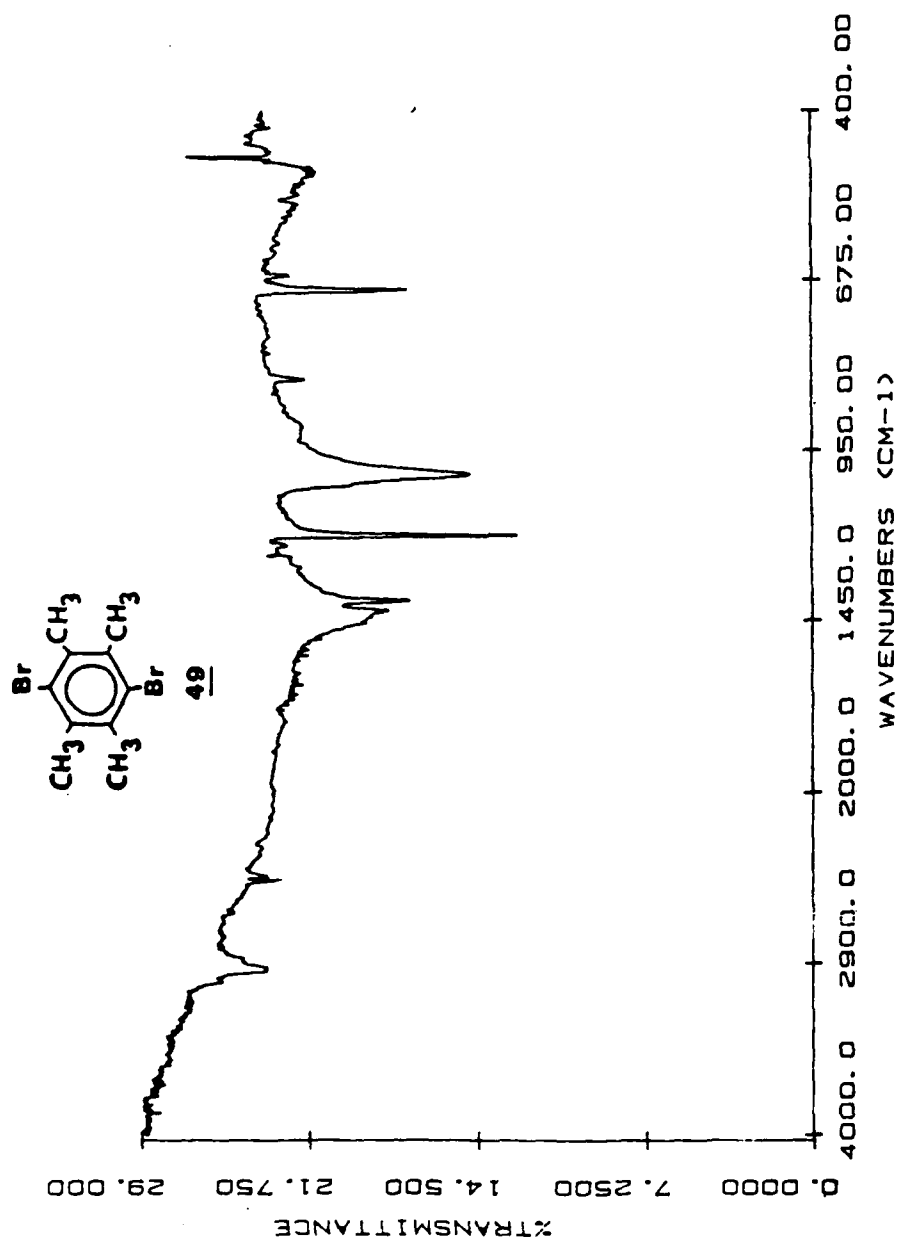


Figure 18. Infrared Spectrum of 3,6-dibromodurene (49).

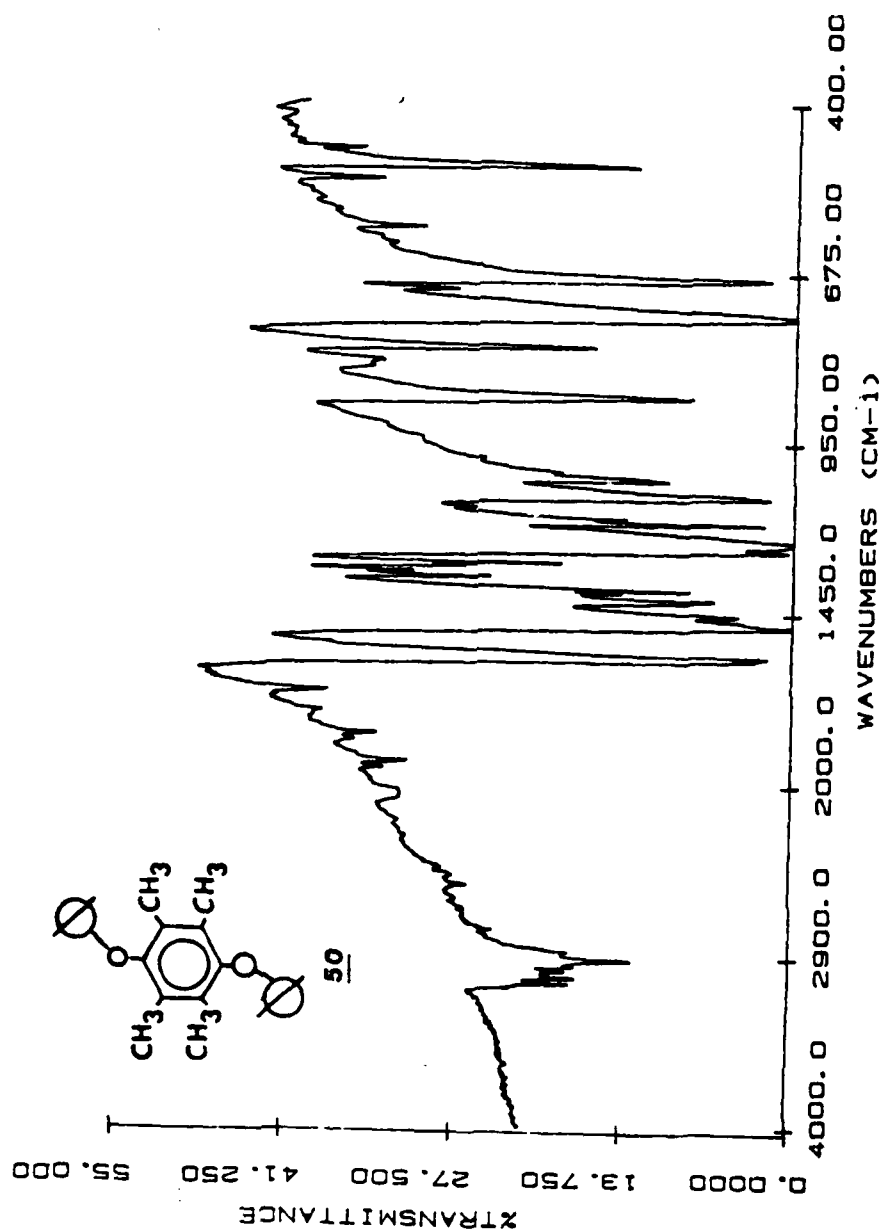


Figure 19. Infrared Spectrum of 3,6-diphenoxydurene (50).

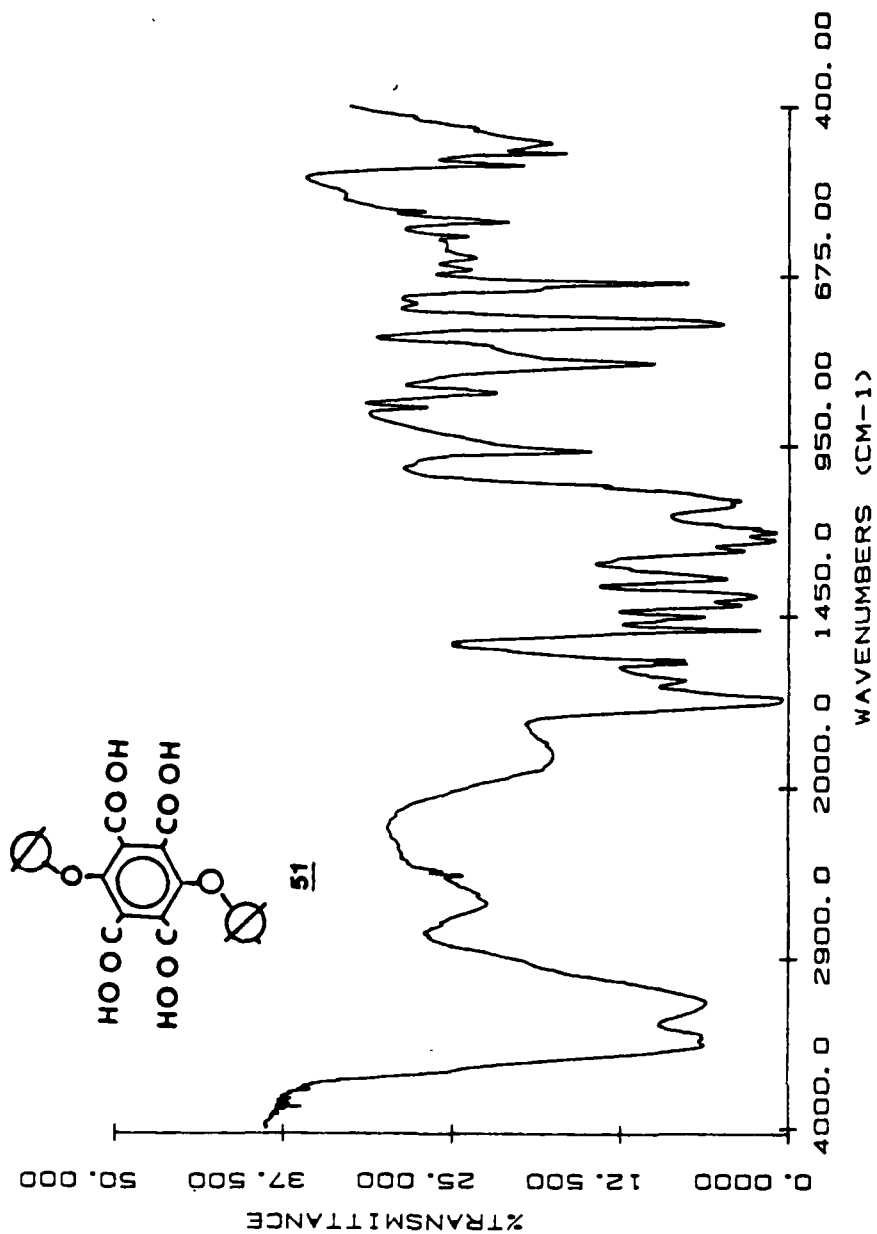


Figure 20. Infrared Spectrum of Compound (51).

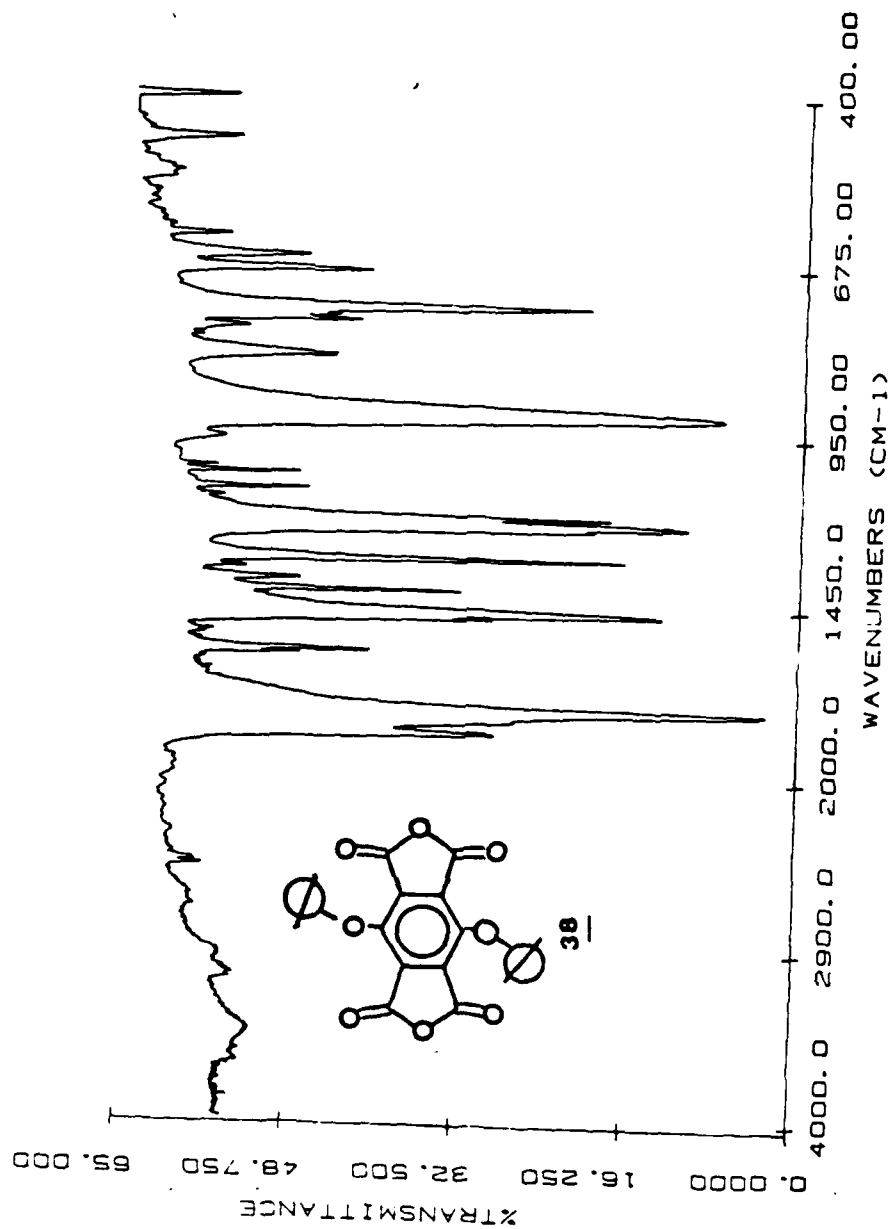


Figure 21. Infrared Spectrum of Compound (38).

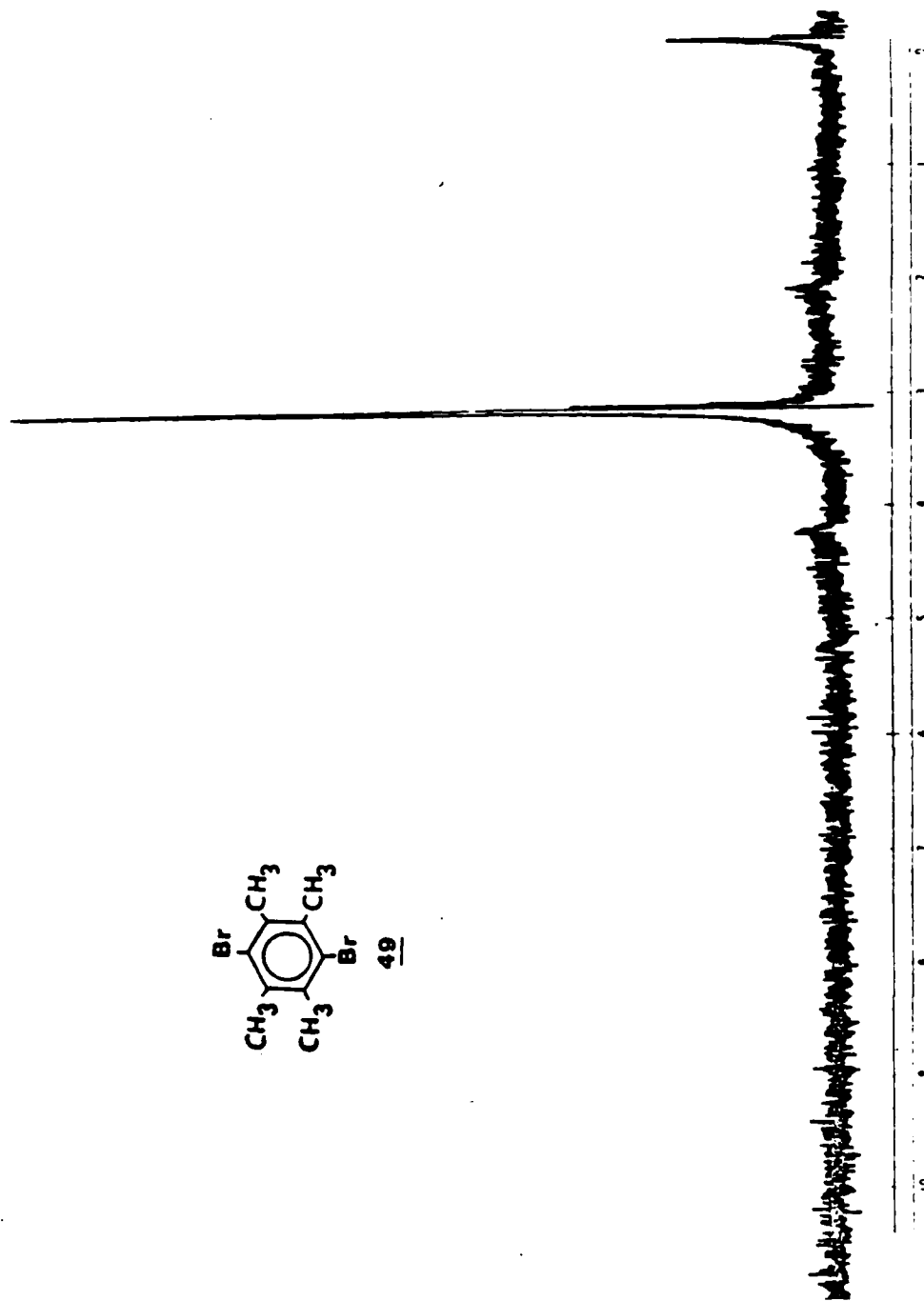
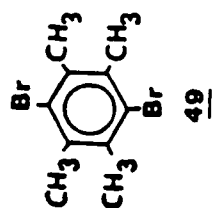


Figure 22. NMR Spectrum of 3,6-dibromodurene (49).

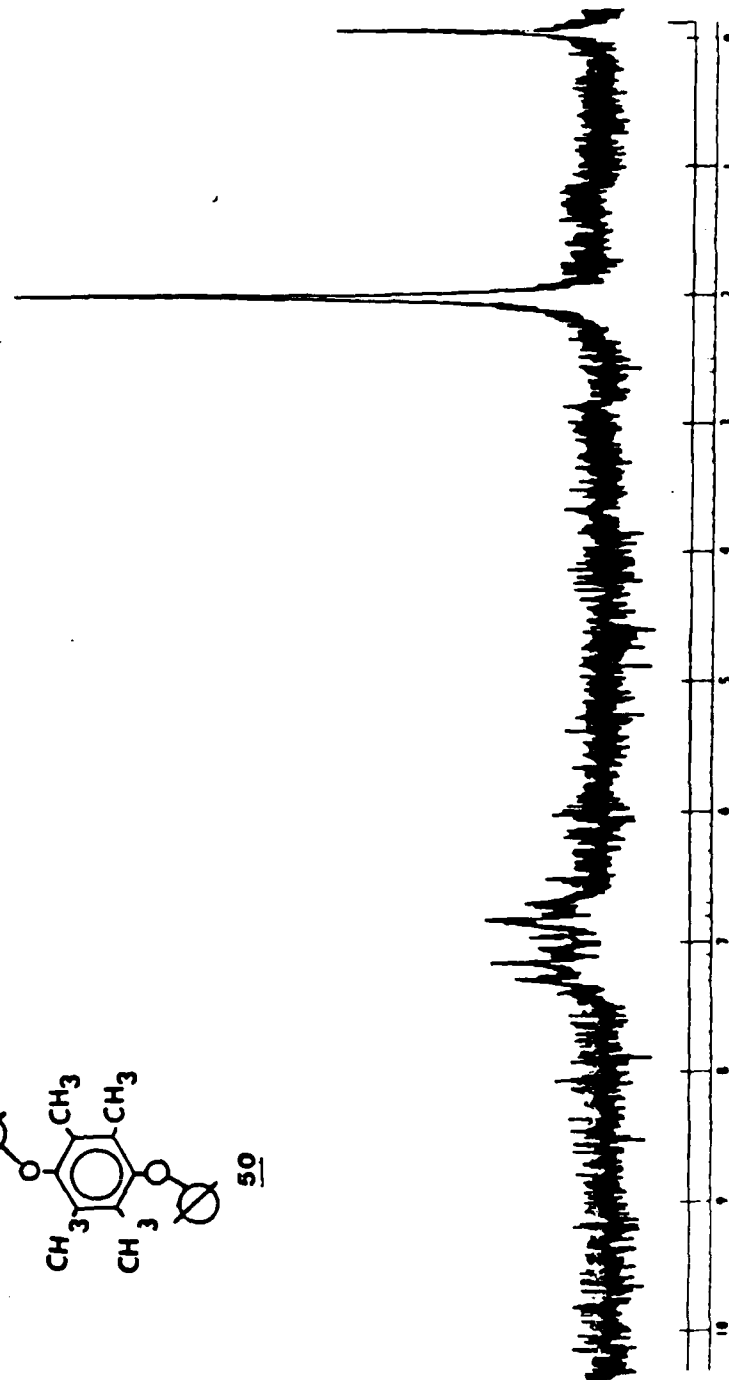
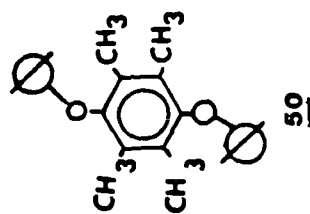


Figure 23. NMR Spectrum of 3,6-diphenoxydurene (50).

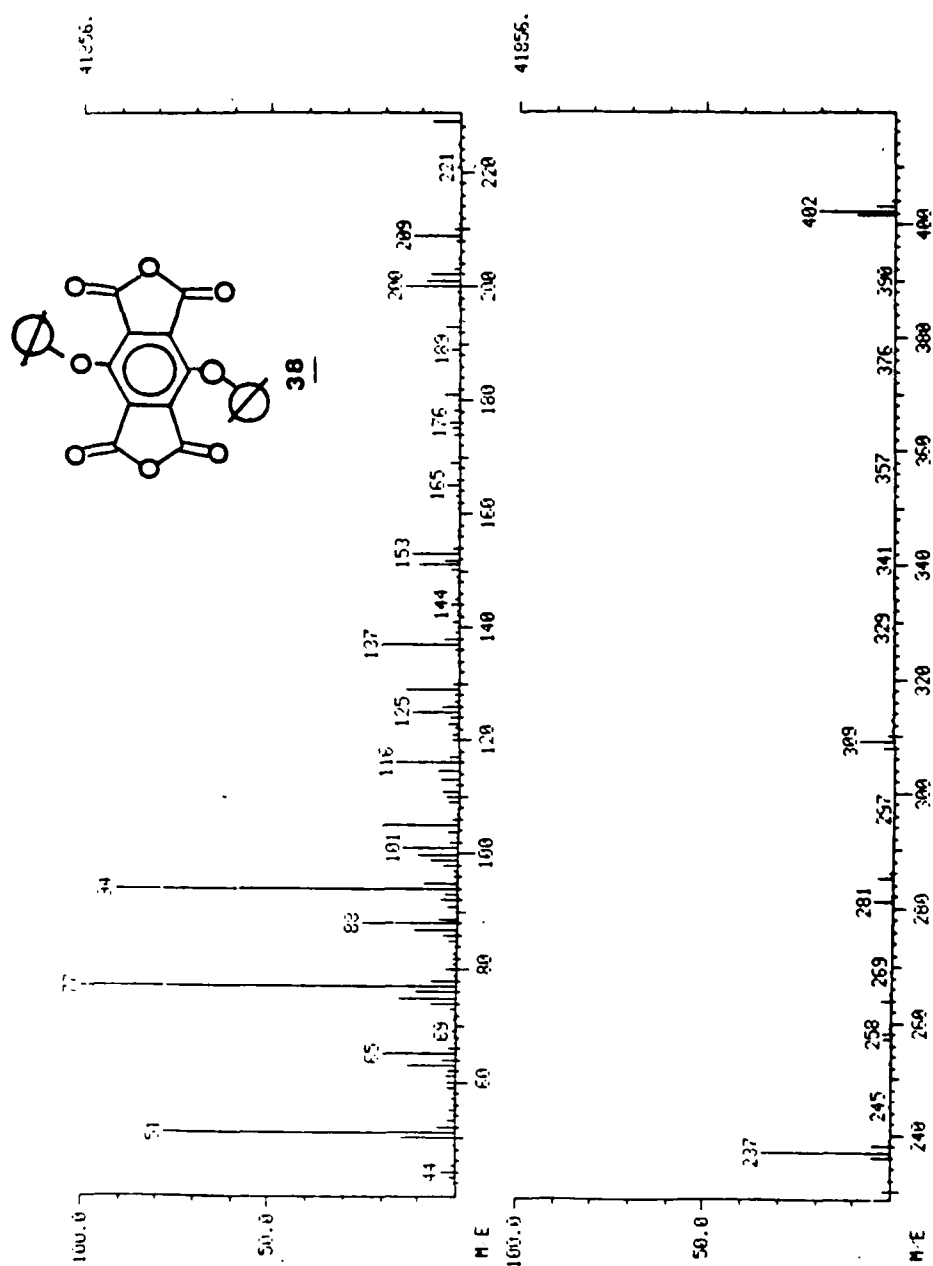


Figure 24. Mass Spectrum of Compound (38).

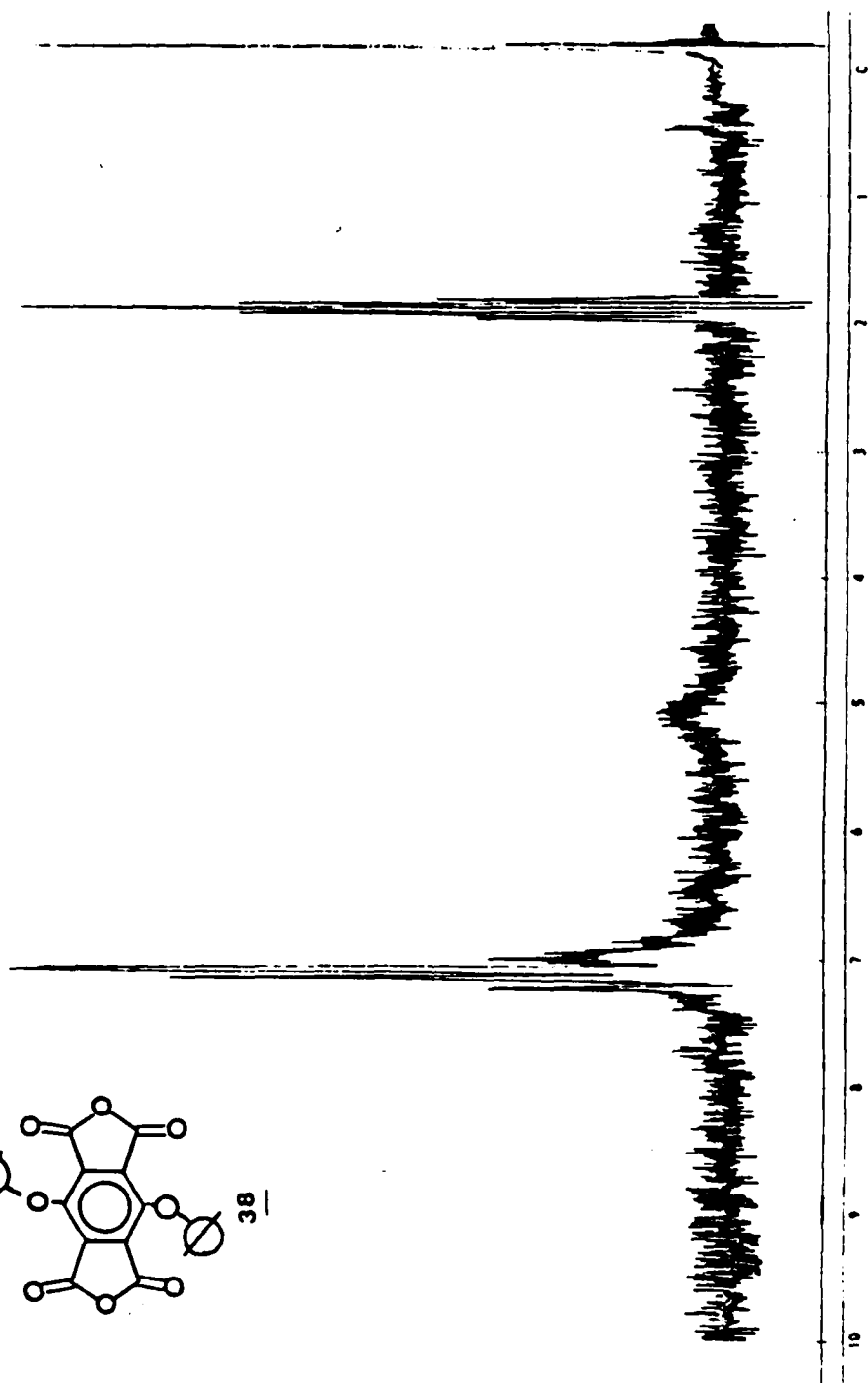
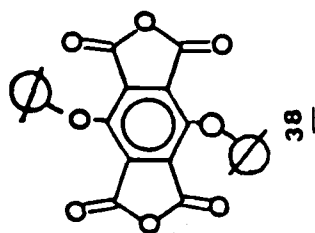


Figure 25. NMR Spectrum of Compound (38).

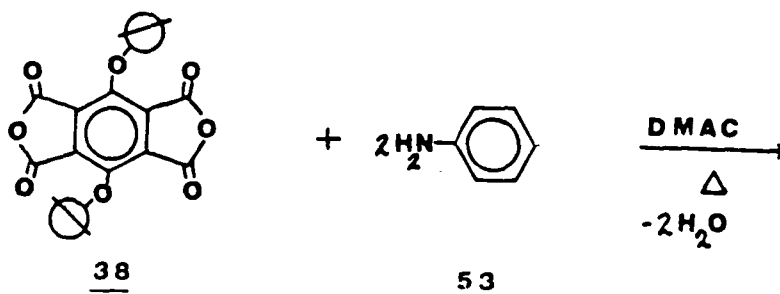
Polymer Synthesis

The second objective of this research was to synthesize a polyimide from the aforementioned dianhydrides 48a and 38. Work with the monosubstituted system 48a/48 was discontinued pending the use of an alternate anhydride formation reaction. The diamine 1,3-bis(3-aminophenoxy)benzene was chosen because it has aromatic units which are associated with thermal stability as well as meta and ether linkages which could add and therefore impart increased solubility to a polyimide.

Model Compound

Reaction of 3,6-diphenoxypyromellitic dianhydride (38) with aniline (53) in DMAC and isoquinoline gave two products.

The physical properties of the two compounds are listed in Table 10 and the infrared spectra are shown in Figure 26 and Figure 27. Compound (54), a bright yellow powder, decomposes at 436 - 438 °C.



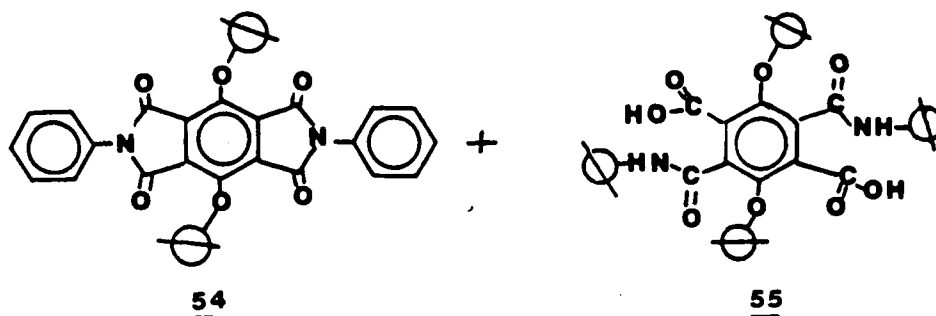


TABLE 10
PHYSICAL PROPERTIES OF MODEL IMIDE AND AMIC ACID

COMPOUND	%YIELD	MP°C	IR (KBr) cm ⁻¹
imide <u>54</u>	32	436-438	3150 (arom. (C-H)) 1780, 1720 (C=O) 1202 (C-O-C) 722
amic acid <u>55</u>	56	199-202	3312 (OH) 1768, 1709 (C=O) 1600 (C=C) 1475 (C=C) 1200 (C-O-C) 730, 710 (mono. sub. arom.)

It was obtained by precipitation of the reaction mixture in methanol and could be recrystallized from methylene chloride. The IR suggests that it is an imide. Compound 55 however was soluble in methanol and did not precipitate. Evaporation of the filtrate gave an orange compound which was recrystallized from acetone and has a melting point of 199-202°C. The infrared spectrum suggests that this compound

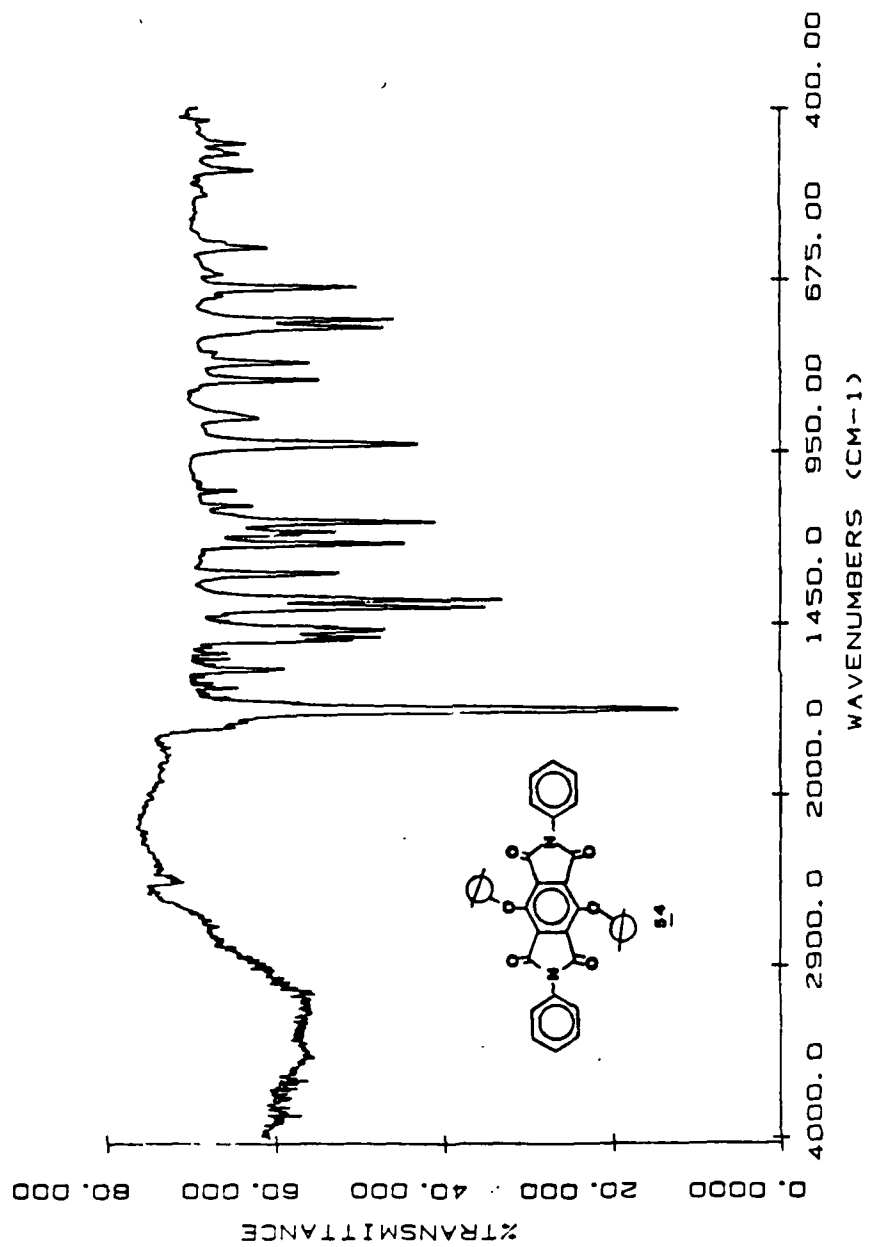


Figure 26. Infrared Spectrum of Compound (54).

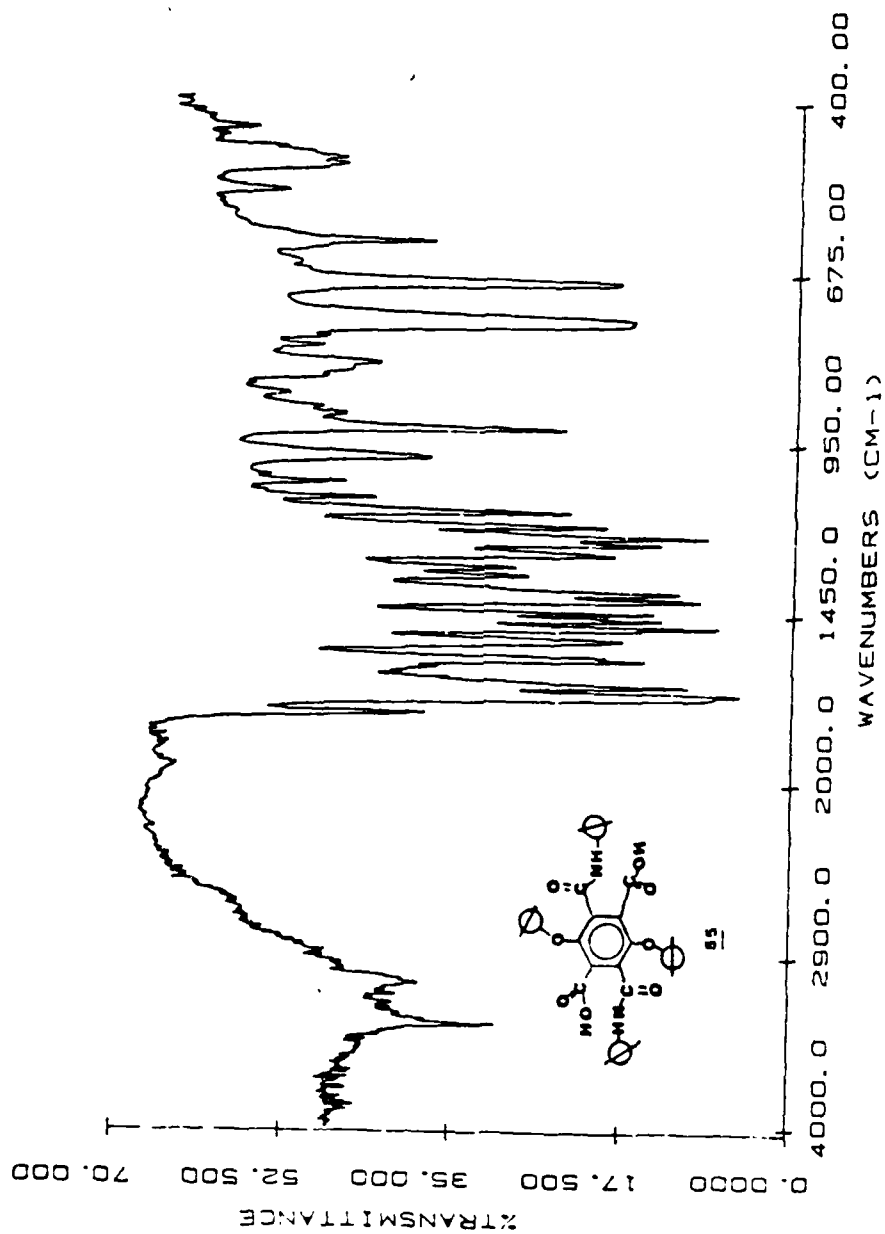


Figure 27. Infrared Spectrum of Compound (55).

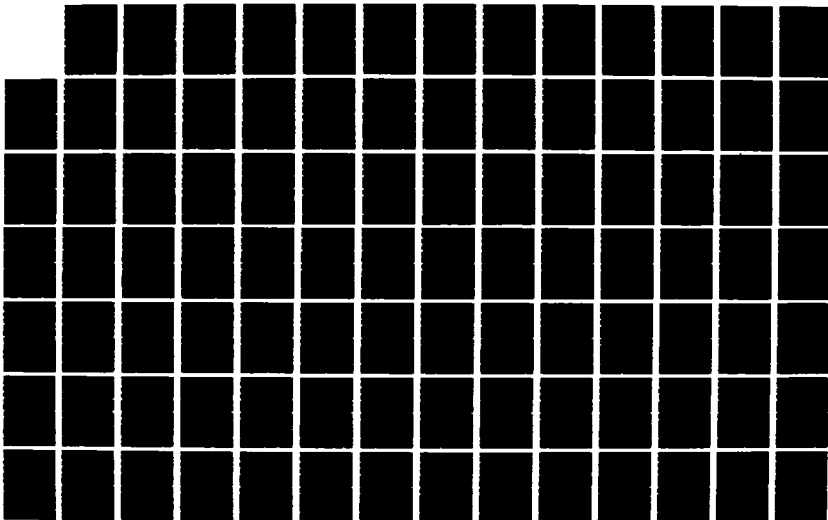
NO-A187 859

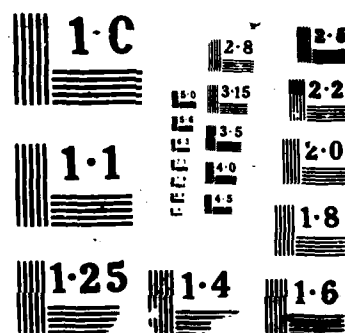
UNITED STATES AIR FORCE RESEARCH INITIATION PROGRAM
1984 RESEARCH REPORTS (U) SOUTHEASTERN CENTER FOR
ELECTRICAL ENGINEERING EDUCATION INC S M D PEELE
MAY 86 AFOSR-TR-87-1722 FF9620-82-C-0035 F/G 7/2

02/10

UNCLASSIFIED

NL

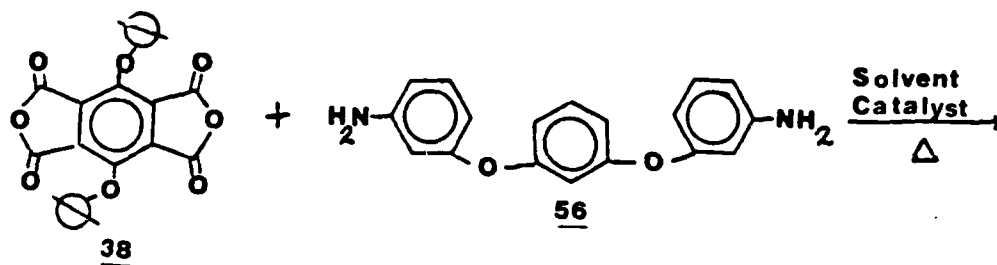


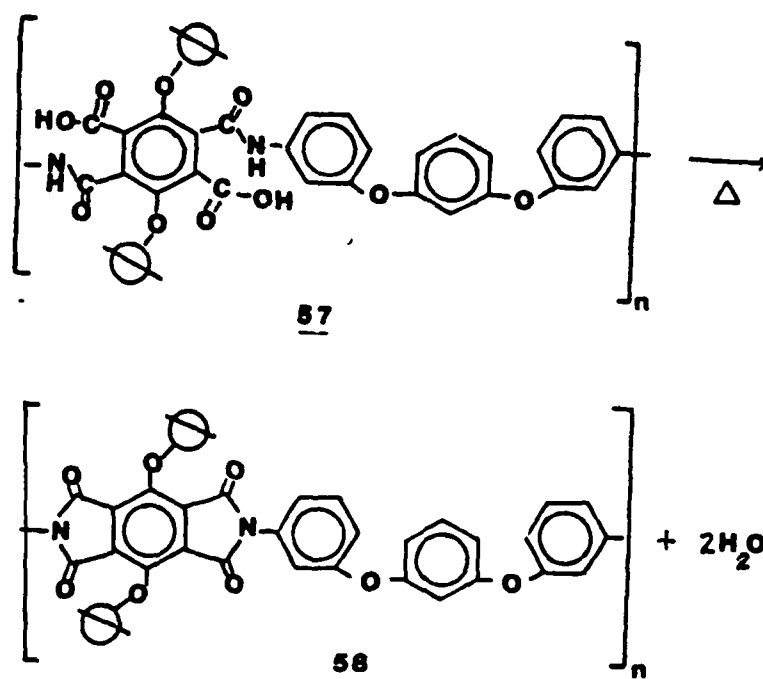


is the amic acid 55. The elemental analysis of compounds 54 and 55 are consistent with either imide, amic acid on a compound with one imide and one amic acid functionality. The results do suggest that ring closure to an imide is a difficult process and should be of importance in polymer formation.

Polymers

The reaction of 3,6-diphenoxypyromellitic dianhydride(38) and 1,3-bis(3-aminophenoxy)benzene (56) was carried out employing three procedures. Each was chosen because it represented an accepted polyimide synthetic procedure. The progress of the reaction was followed by FTIR when possible or desirable.





The first procedure utilized m-cresol as the solvent and toluene or m-cresol as the azeotroping agent. Table 11 summarizes the reactions employing the first procedure.

TABLE 11
PROCEDURE 1 RESULTS

POLYMER	COLOR	%YIELD	η_{inh}	TIME	TEMP. °C
<u>58a</u>	yellow	75	.39	1.5 h	180
<u>58b</u>	yellow	70	.21	2.0 h	180
<u>58c</u>	yellow	72	.25	1.5 h	180
<u>58d</u>	yellow gold	80	.24	4.0 h	250

Polymers 58a, 58b, and 58c were produced using toluene as an azeotroping agent. Polymer 58d was produced using m-cresol as both solvent and azeotroping agent. It is evident from the infrared spectra (Figures 28-31) that imide formation has occurred in each case. The viscosities, however, indicate low molecular weights with 54a being the highest and 58d, in spite of higher yield, the lowest. It is interesting to note that all of these polymers form good films in spite of low viscosities.

The infrared spectra of 58a and 58d exhibit the least absorbance in the NH stretch region (3200 cm^{-1}) and appear to be the most "closed" imides. Absorption in this region can also be due to m-cresol, water, end groups and a variety of other functionalities.

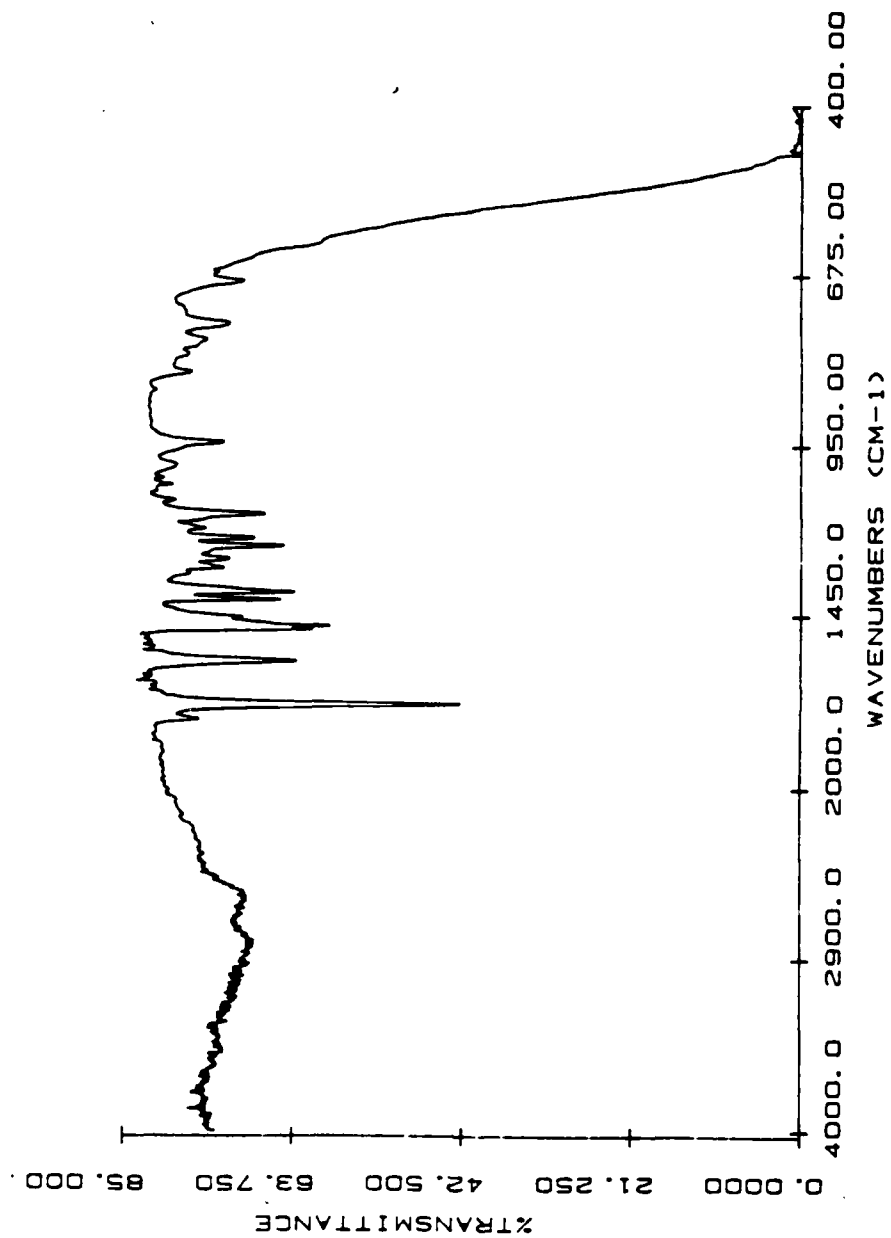


Figure 28. Infrared Spectrum of Polyimide (58b).

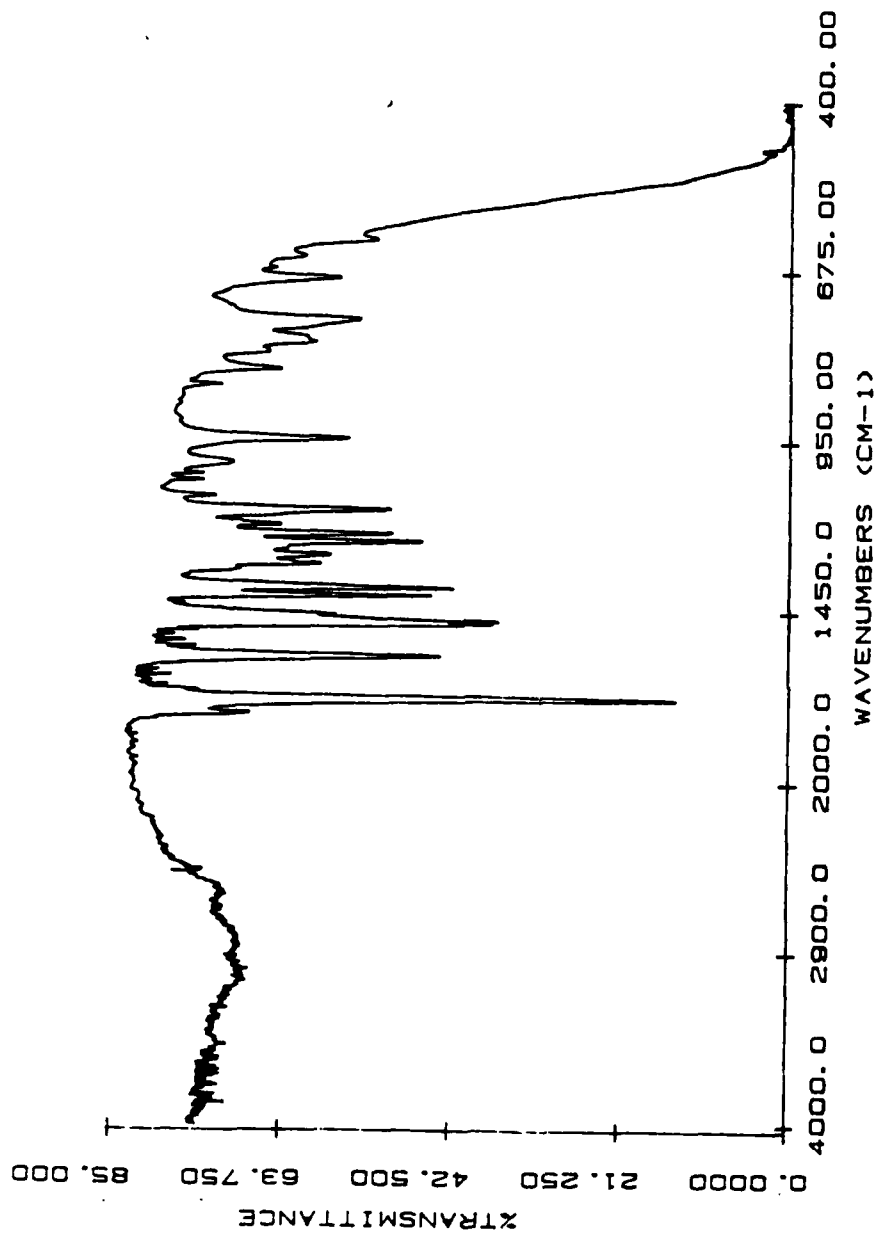


Figure 29. Infrared Spectrum of Polyimide (58g).

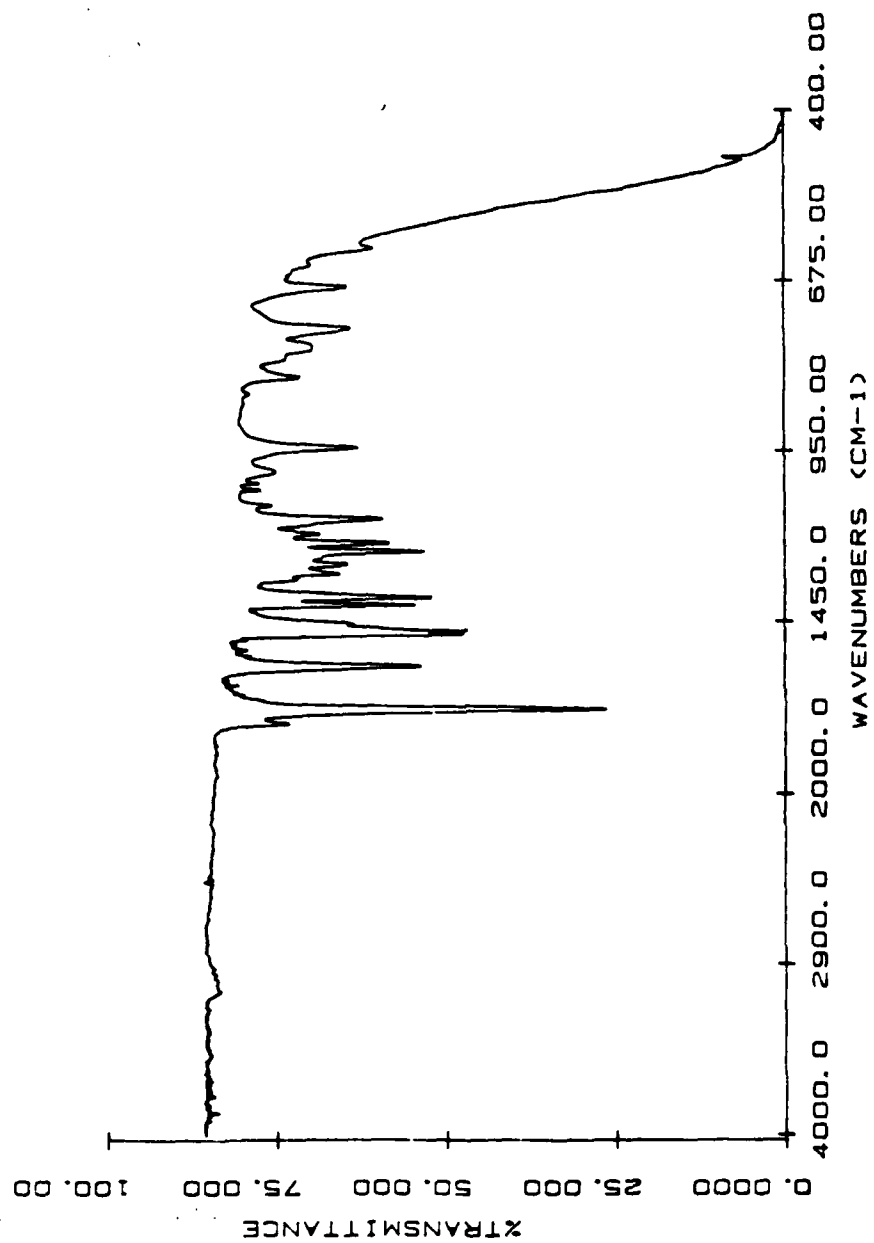


Figure 30. Infrared Spectrum of Polyimide (58a).

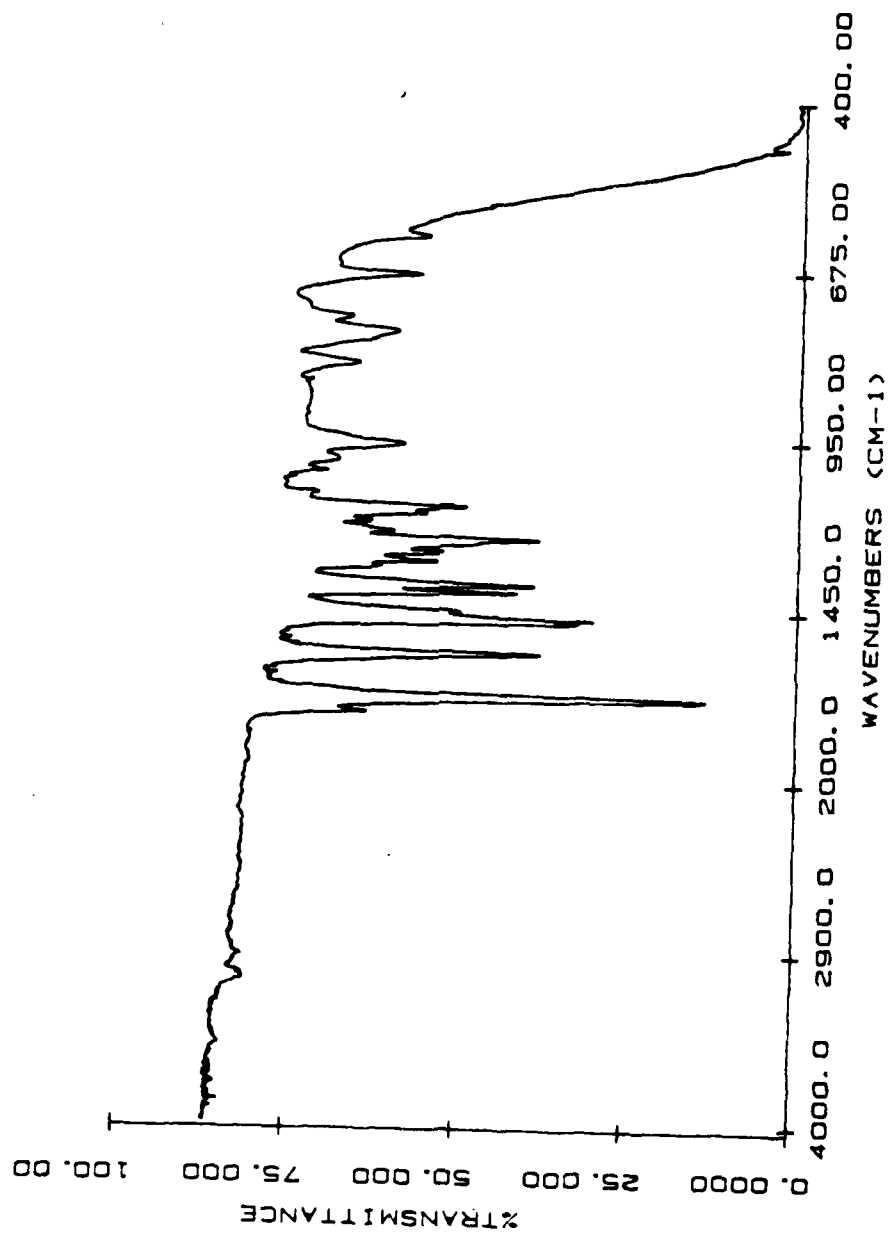


Figure 31. Infrared Spectrum of Polyimide (58d).

The solubility of 58a in common solvents was determined at room temperature at a concentration of 0.02 g/mL solvent and follows the order:

DMF> TCE> DCE> m-cresol> CHCl₃

The second procedure utilized dimethylformamide as the solvent, azeotroping agent, and dilution solvent. Table 12 summarizes the results of this procedure.

TABLE 12
PROCEDURE 2 RESULTS

POLYMER	COLOR	%YIELD	η_{inh}	TIME	TEMP. °C
<u>58e</u>	tan	64	.10	1.5 h	180
<u>58f</u>	orange solution amic acid	NA	NA	24 h vacuum baked	180

Polymer 58e was dissolved in TCE and evaporated to give a film which showed N-H bands at 3250-3150 cm⁻¹ as seen in Figure 32. Vacuum baking the film produced some growth in the length of the imide bands at 1780 and 1740 cm⁻¹ and a small decrease in the N-H band at 3350 cm⁻¹ as seen in Figure 33.

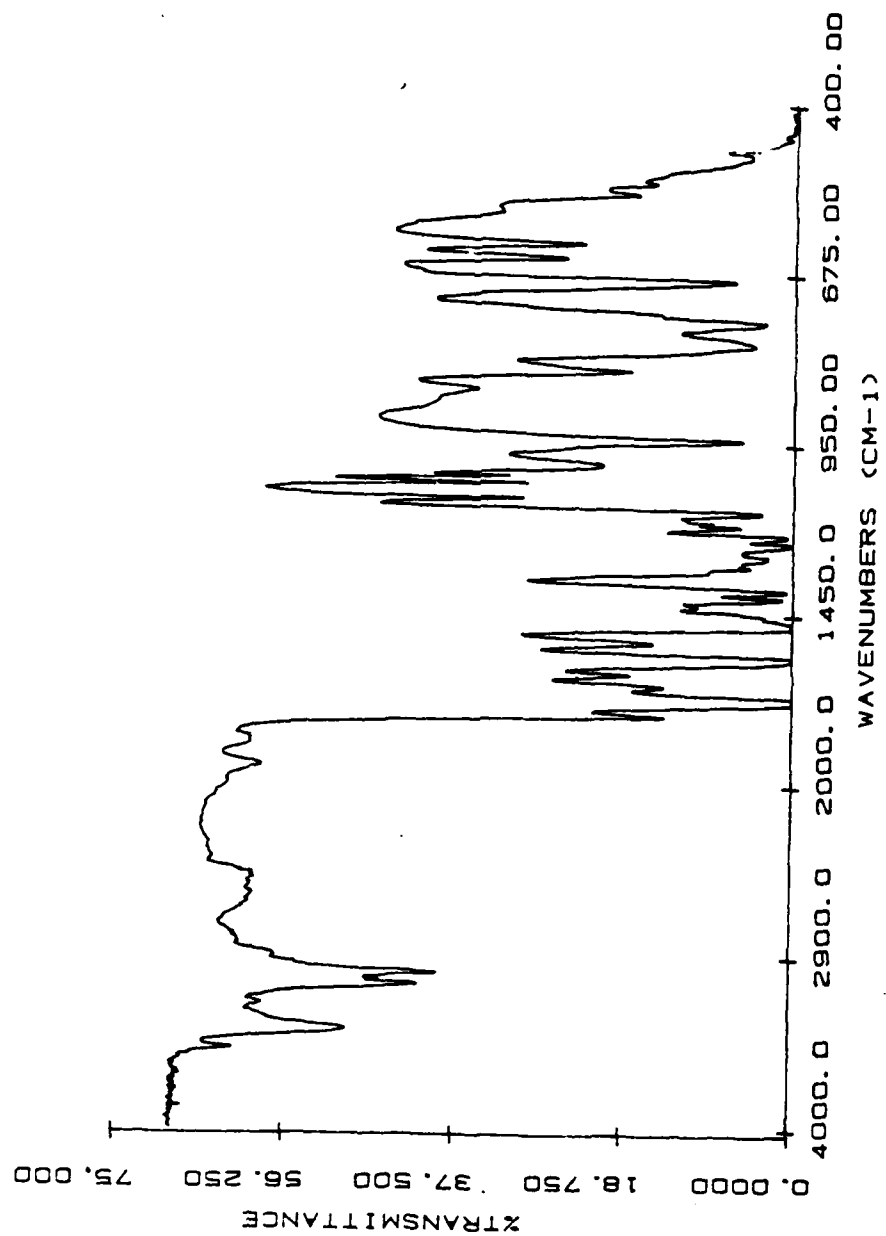


Figure 32. Infrared Spectrum of Polyimide (58g).

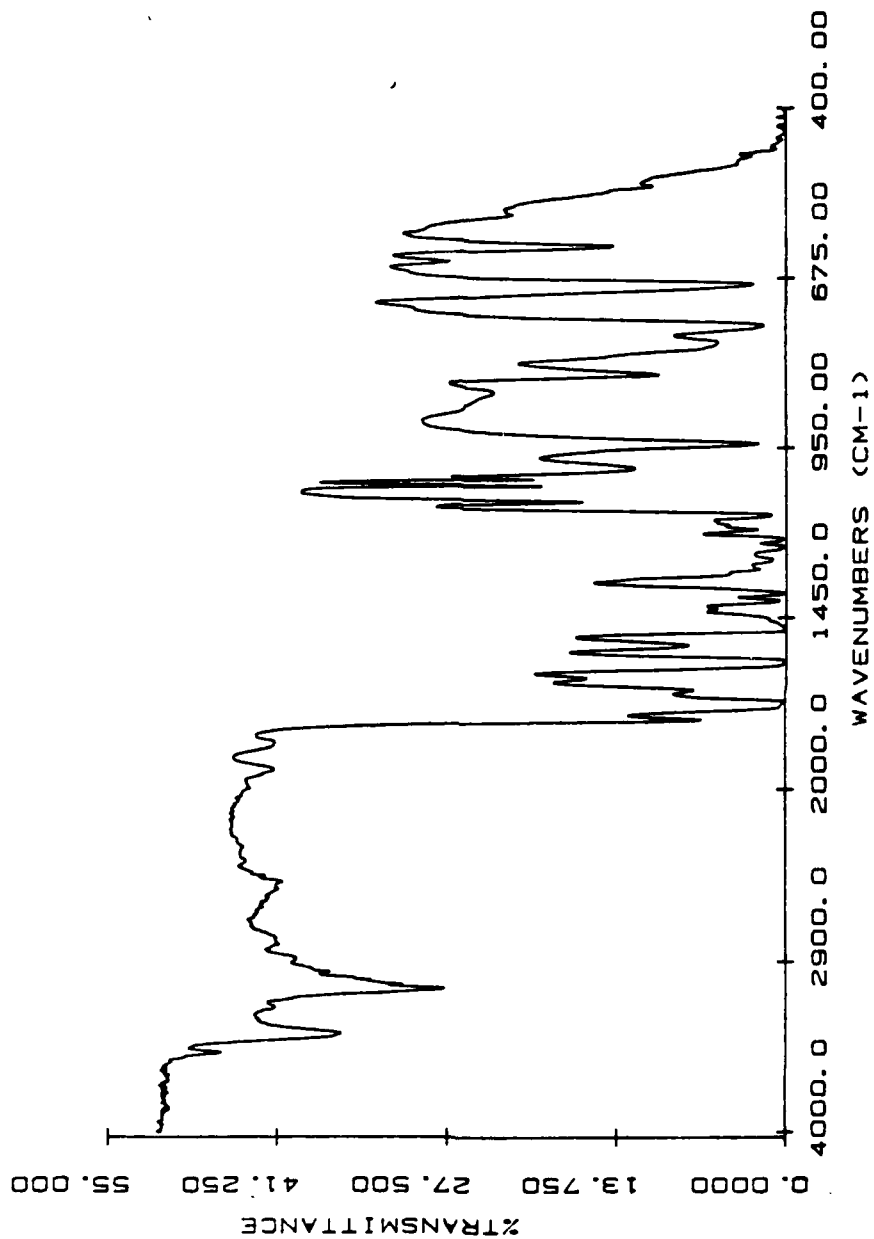


Figure 33. Infrared Spectrum of Vacuum Baked Polyimide (58a).

The generation of polymer 58f was observed by infrared spectroscopy by following the formation of the amic acid at room temperature over time. Figures 34-37 show the change in the IR spectrum at times 0, 0.5, 1.0 and 1.5 h. An N-H band at 3570 cm^{-1} and the C=O bands at about 1750 cm^{-1} show that the amic acid is well formed by .5 h and little change occurs over the last hour of observation. Vacuum baking of the final sample for 24 h at $180\text{ }^{\circ}\text{C}$ produced an IR spectrum (Figure 38) that shows a small absorption at 2950 cm^{-1} and the double carbonyl absorption at 1774 and 1741 cm^{-1} as is usually observed for imides. Absorptions also appear at 1600 , 950 , $750\text{--}850\text{ cm}^{-1}$ region that were not present in the amic acid. Unclosed imide was evident from the band at 3377 cm^{-1} . An IR of the solvent DMF (59) (Figure 39) showed a wide band at 3350 cm^{-1} which could be due to water contamination or dimethylamine produced by dimethylformamide decomposition, either of which could interfere with ring closure to the imide. Figures 33 and 38 show the differences in the infrared spectra of the vacuum baked IR of 58e (vacuum baked for 6 h) and 58f (vacuum baked for 24 h). Prolonged vacuum baking gives a cleaner infrared spectrum region from $4000\text{--}2900\text{ cm}^{-1}$ indicating more complete imide ring closure. It was concluded that solvent may interfere with ring closure and impurities in the solvent can be detrimental to imide formation.

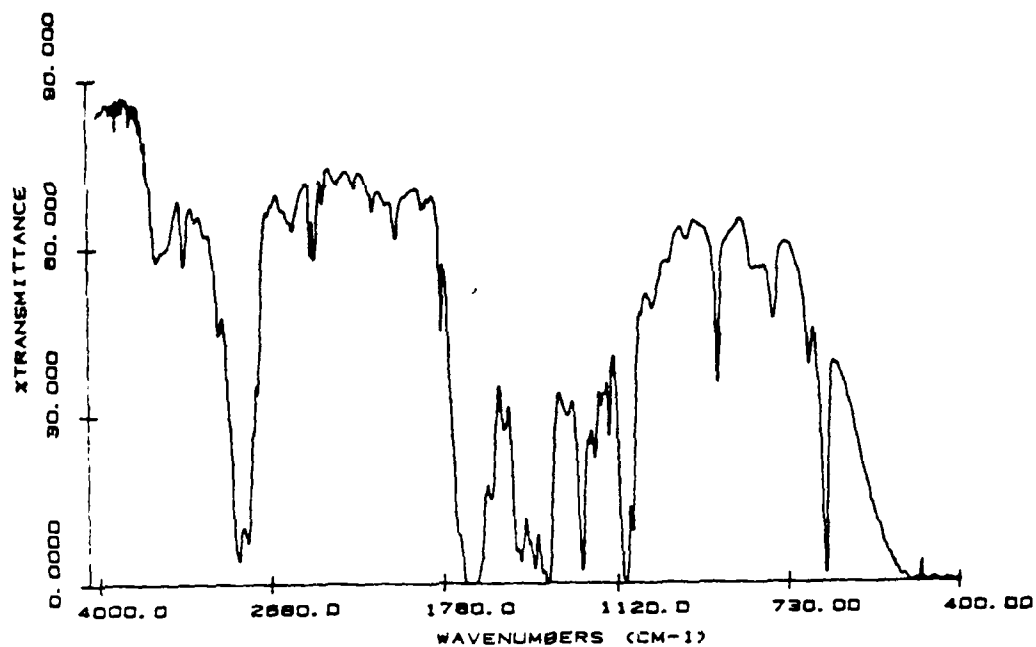


Figure 34. Infrared Spectrum of $t = 0$ Polyamic Acid (58f).

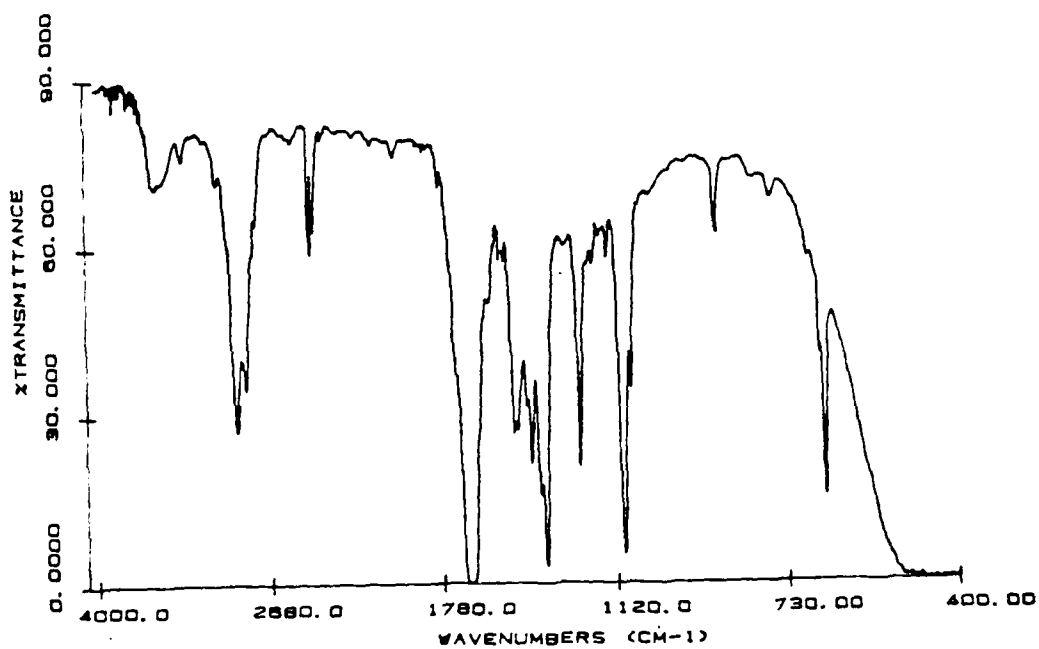


Figure 35. Infrared Spectrum of $t = 0.5$ h Polyamic Acid (58f).

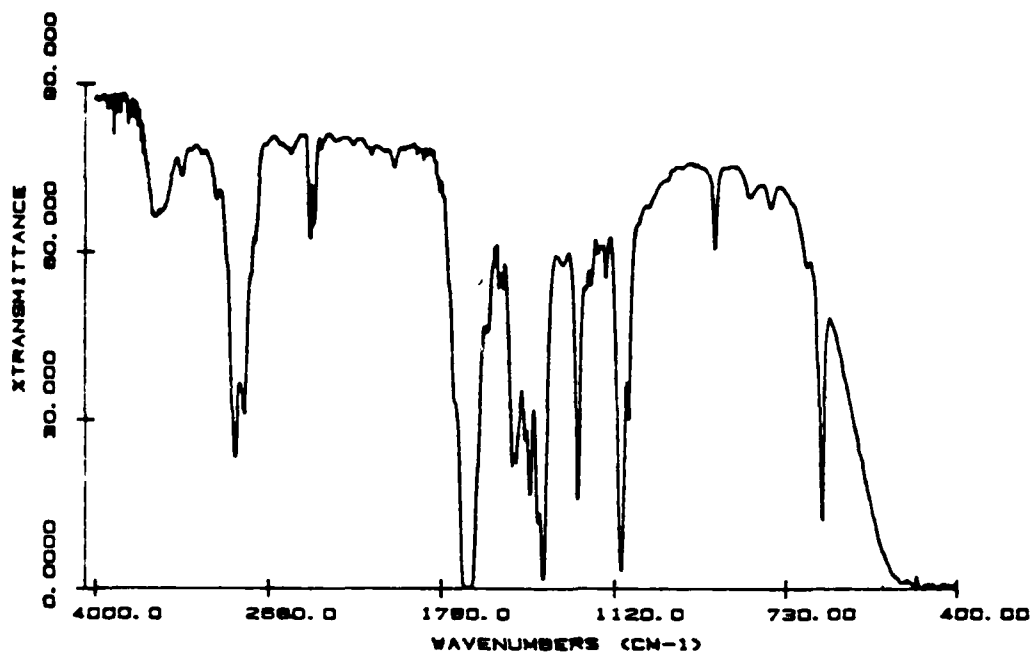


Figure 36. Infrared Spectrum of $t = 1.0$ h Polyamic Acid (58f).

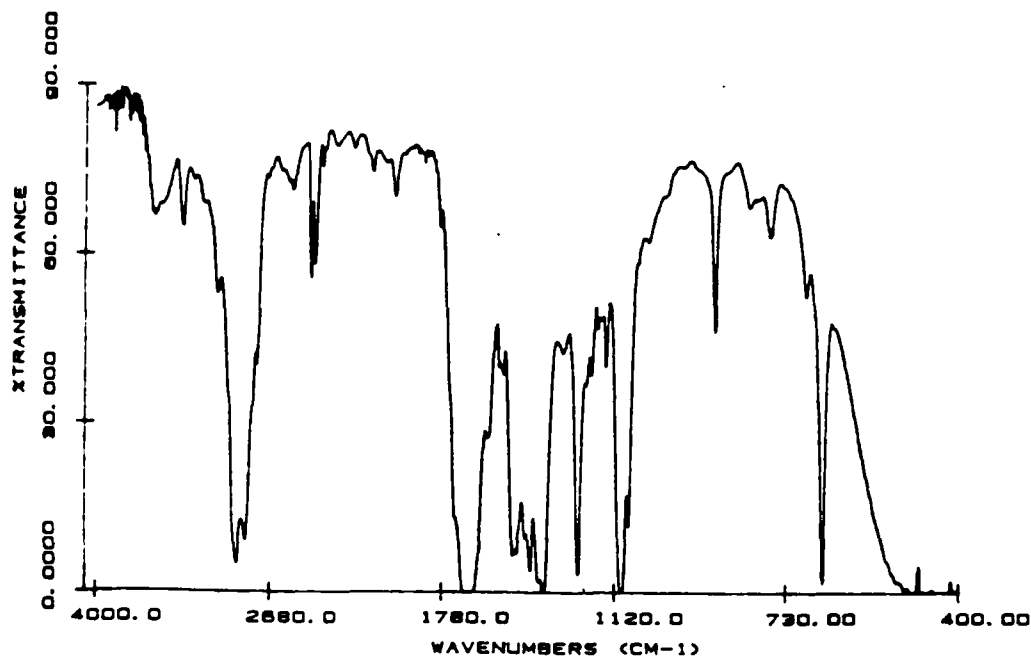


Figure 37. Infrared Spectrum of $t = 1.5$ h Polyamic Acid (58f).

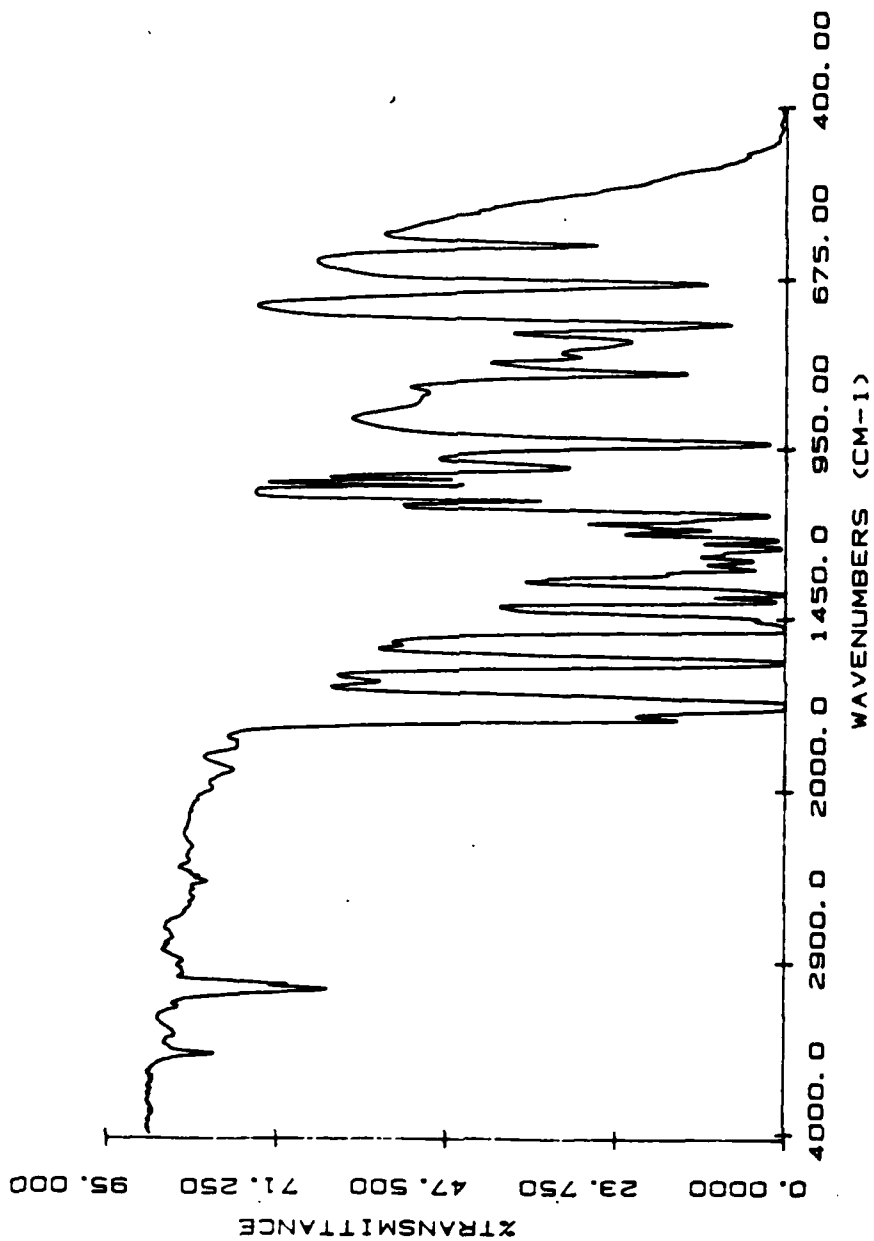


Figure 38. Infrared Spectrum of Vacuum Baked Polyimide (58f).

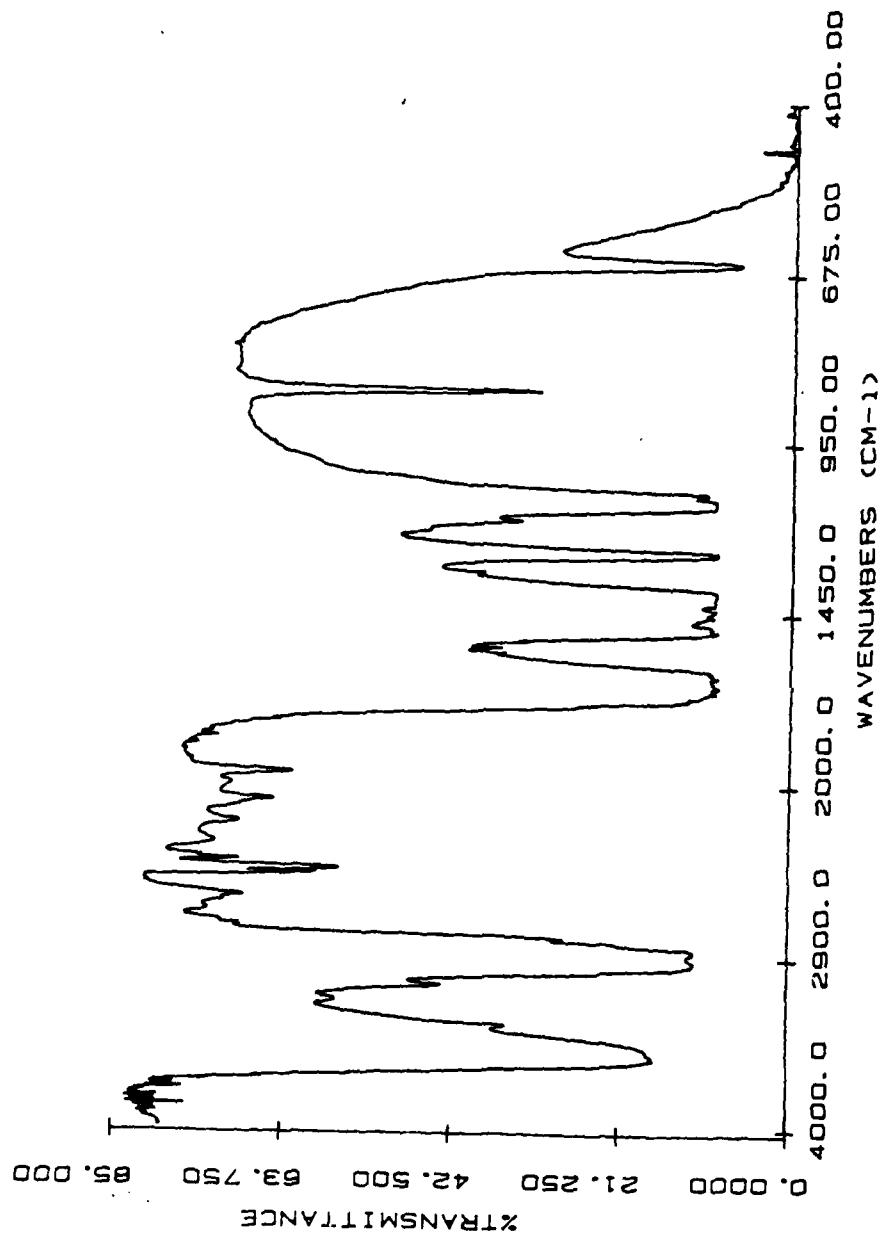


Figure 39. Infrared Spectrum of Solvent DMF (59).

The third procedure employed DMAC as a solvent as it is also considered to be an excellent solvent for the polyimides. Table 13 summarizes the variations and results of this procedure.

TABLE 13

PROCEDURE 3 RESULTS

POLYMER	REFLUX SOLVENT	AZEOTROPE SOLVENT	DILUTION SOLVENT	η_{inh}	TIME hours	YIELD %
<u>58g</u>	DMAC	DMAC	DMAC	.12	1.5	78
<u>58h</u>	HPLC grade DMAC	HPLC grade DMAC	HPLC grade DMAC	.23	1.5	91
<u>58i</u>	"	TOLUENE	"	.25	1.5	95.5
<u>58j</u>	"	" (8 hours)	"	.21	24	95.5

The use of high purity solvents is obviously an important factor. Longer reaction time does not appear to be necessary to increase yield but probably leads to a larger amount of closed imide product.

The formation of the polyamic acid precursor of polymer 58g was followed by infrared spectroscopy with time at increasing temperatures as seen in Figures 40-43.

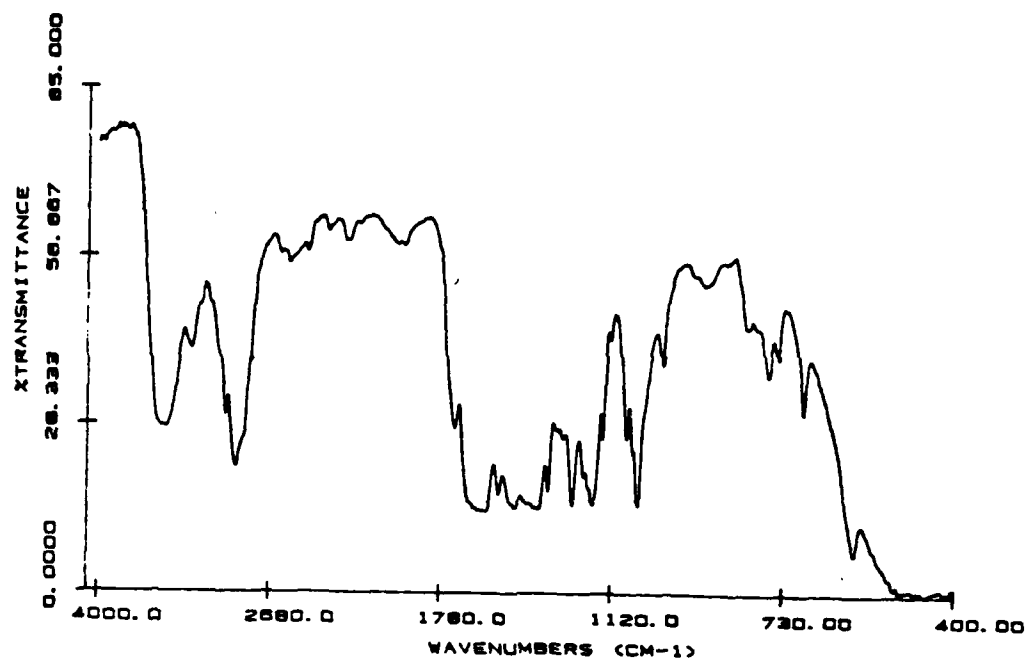


Figure 40. Infrared Spectrum of 24°C Polyamic Acid (58g).

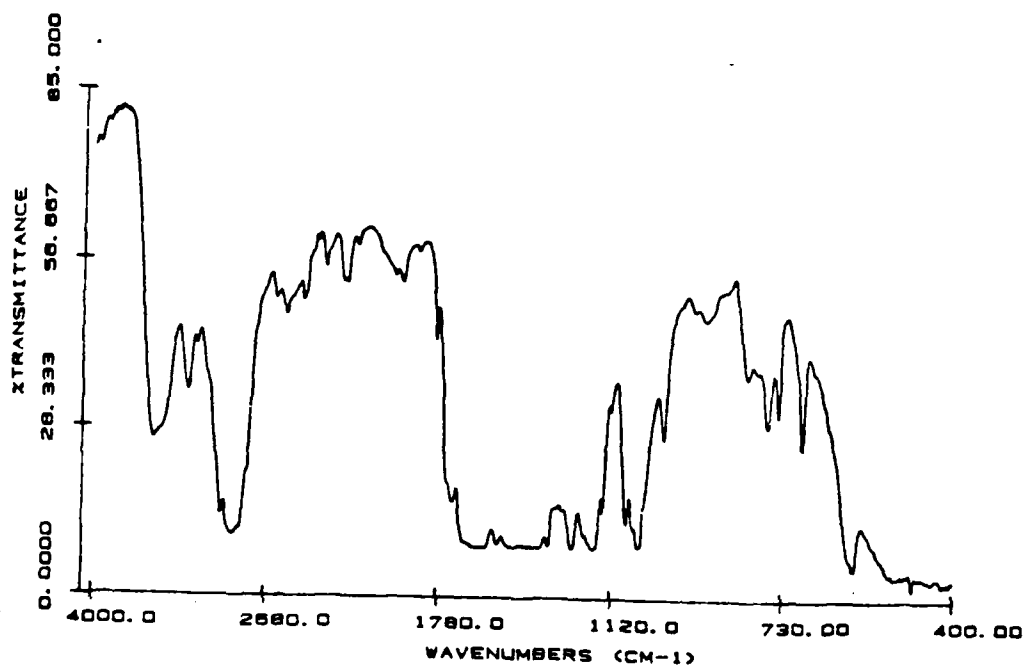


Figure 41. Infrared Spectrum of 45°C Polyamic Acid (58g).

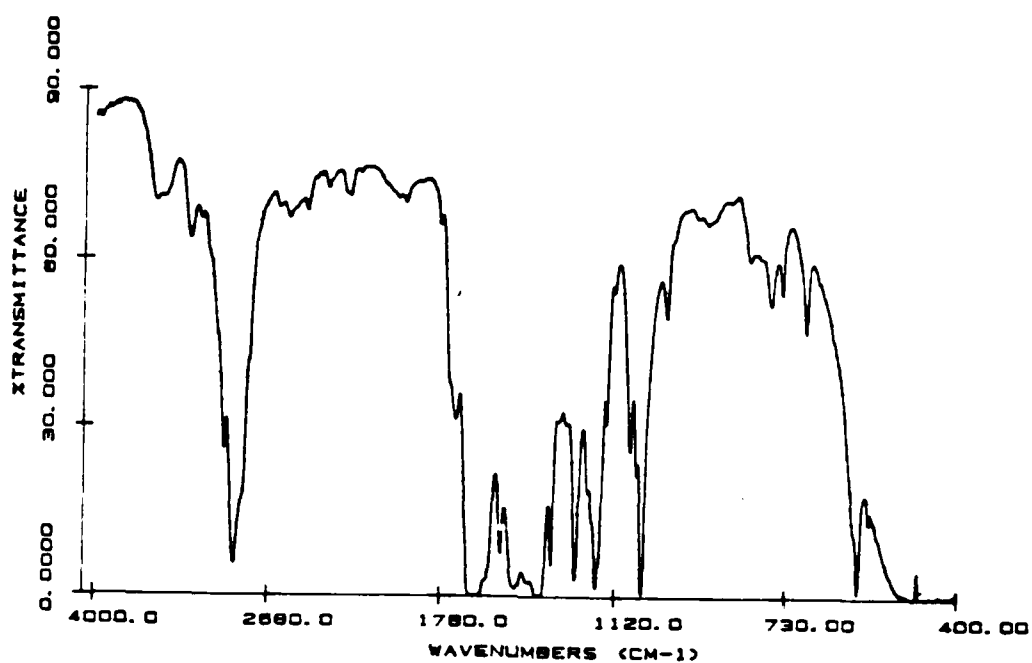


Figure 42. Infrared Spectrum of 65°C Polyamic Acid (58g).

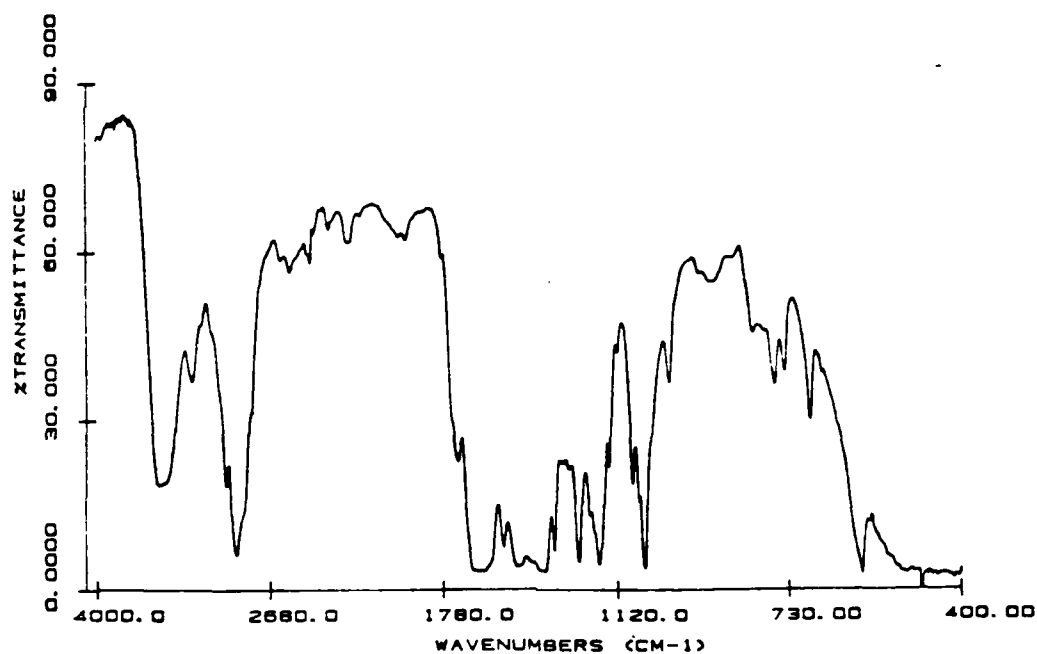


Figure 43. Infrared Spectrum of 80°C Polyamic Acid (58g).

Amic acid is formed early as can be seen in Figure 40. An increase in temperature to 80°C further sharpened the bands but no evidence is seen of imidization (Figures 41-43). A vacuum baked sample of the polyamic acid of 58g in Figure 44 is clearly an imide profile with very little unclosed amic acid.

Comparison of the IR spectra of polymers 58g, 58h, 58i, and 58j in Figures 44-47 illustrates that imide formation is very good for vacuum baked samples regardless of the solvent or time refluxed.

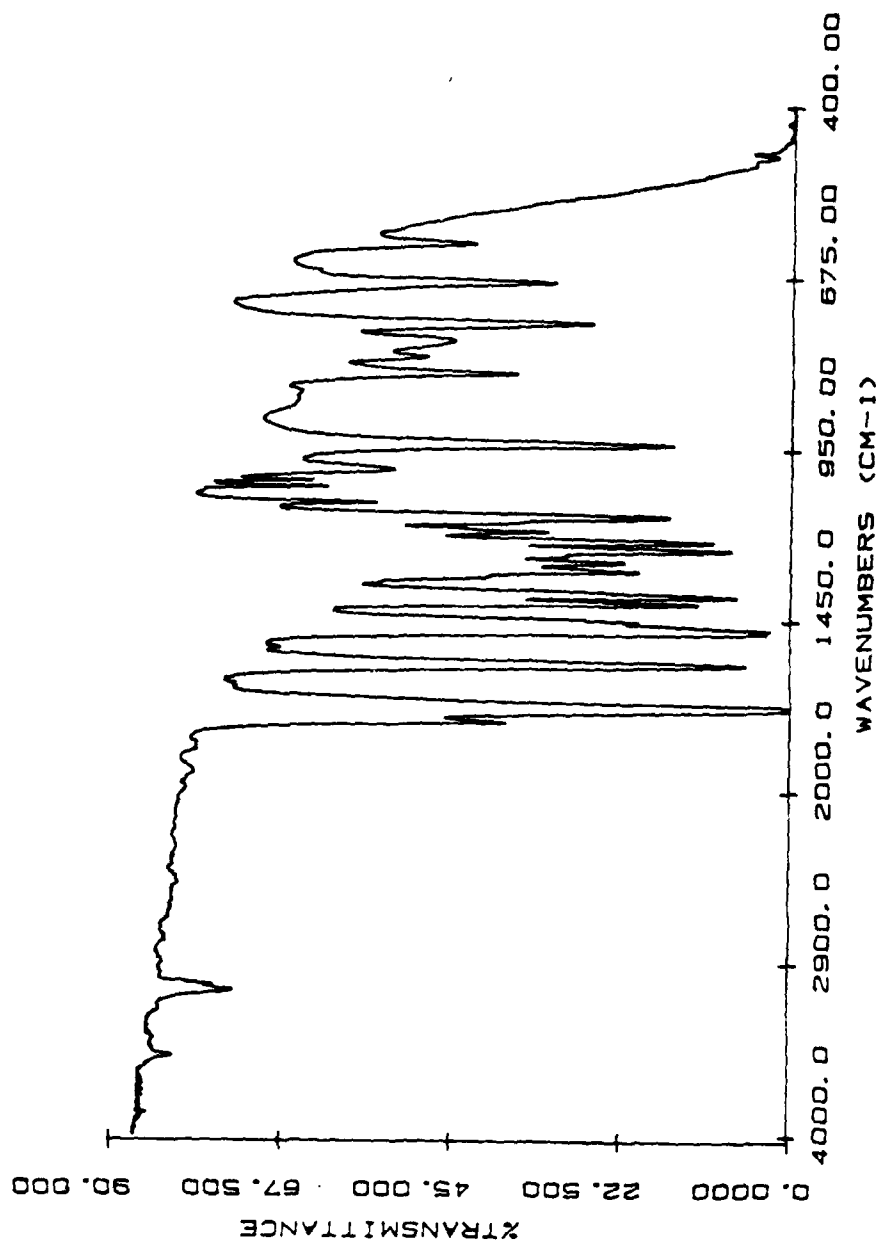


Figure 44. Infrared Spectrum of Vacuum Baked Polyimide (58g).

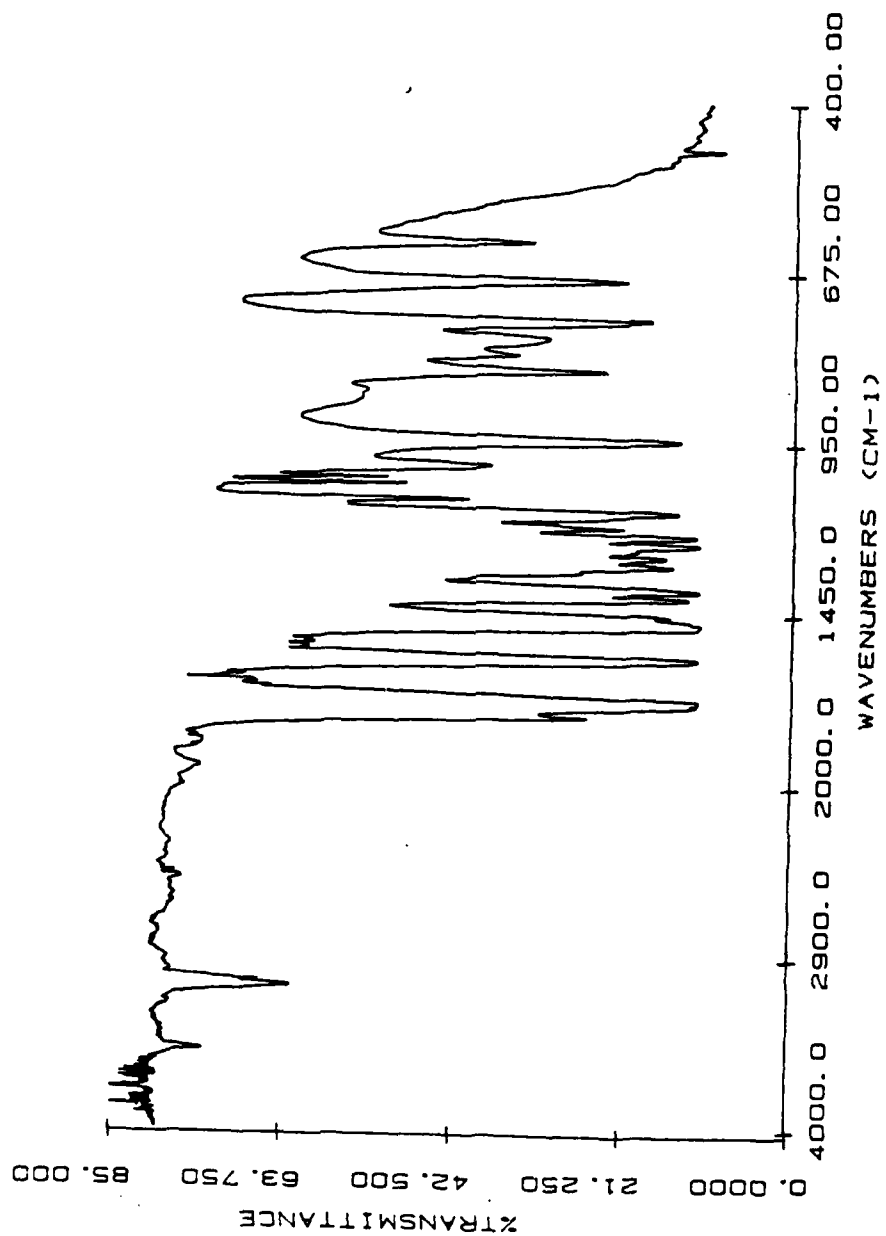


Figure 45. Infrared Spectrum of Vacuum Baked Polyimide (58h).

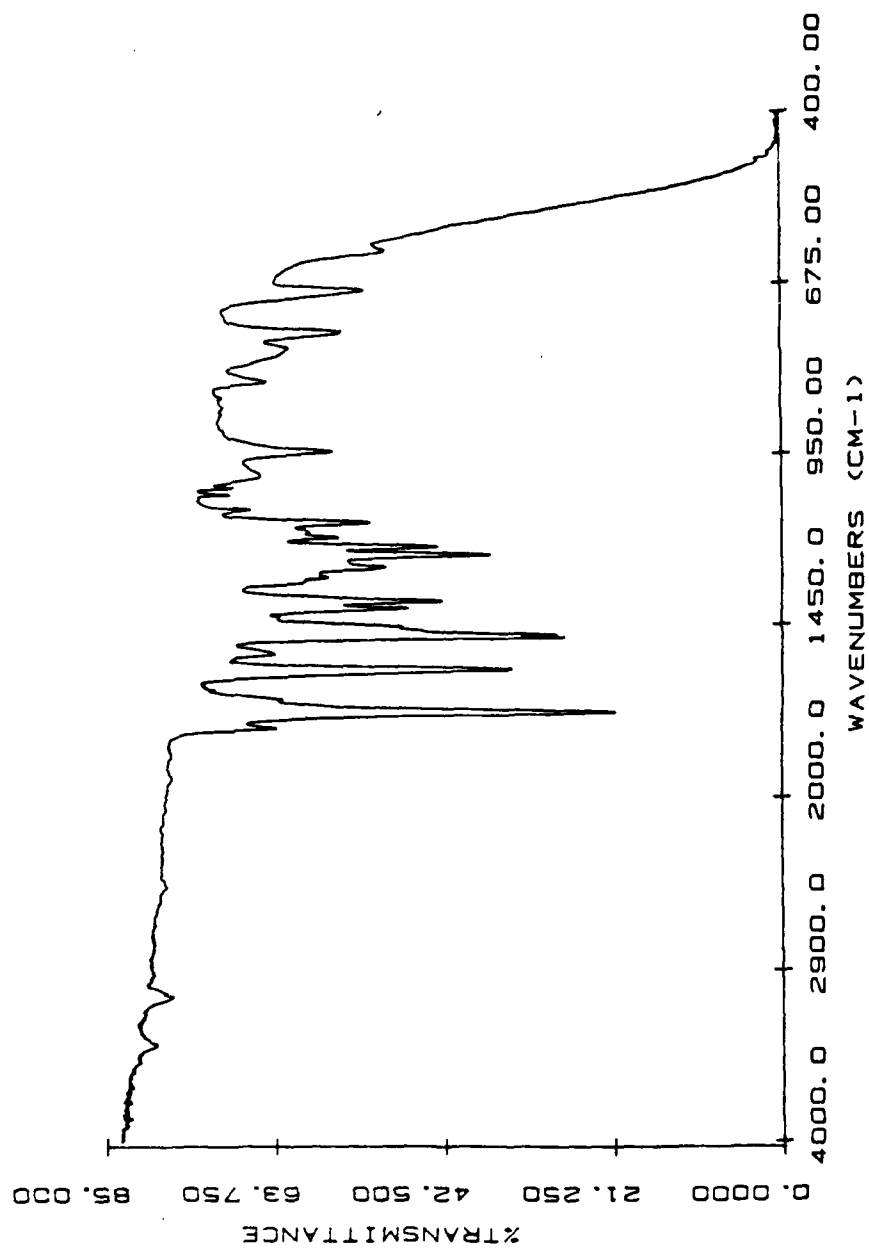


Figure 46. Infrared Spectrum of Vacuum Baked Polyimide (581)

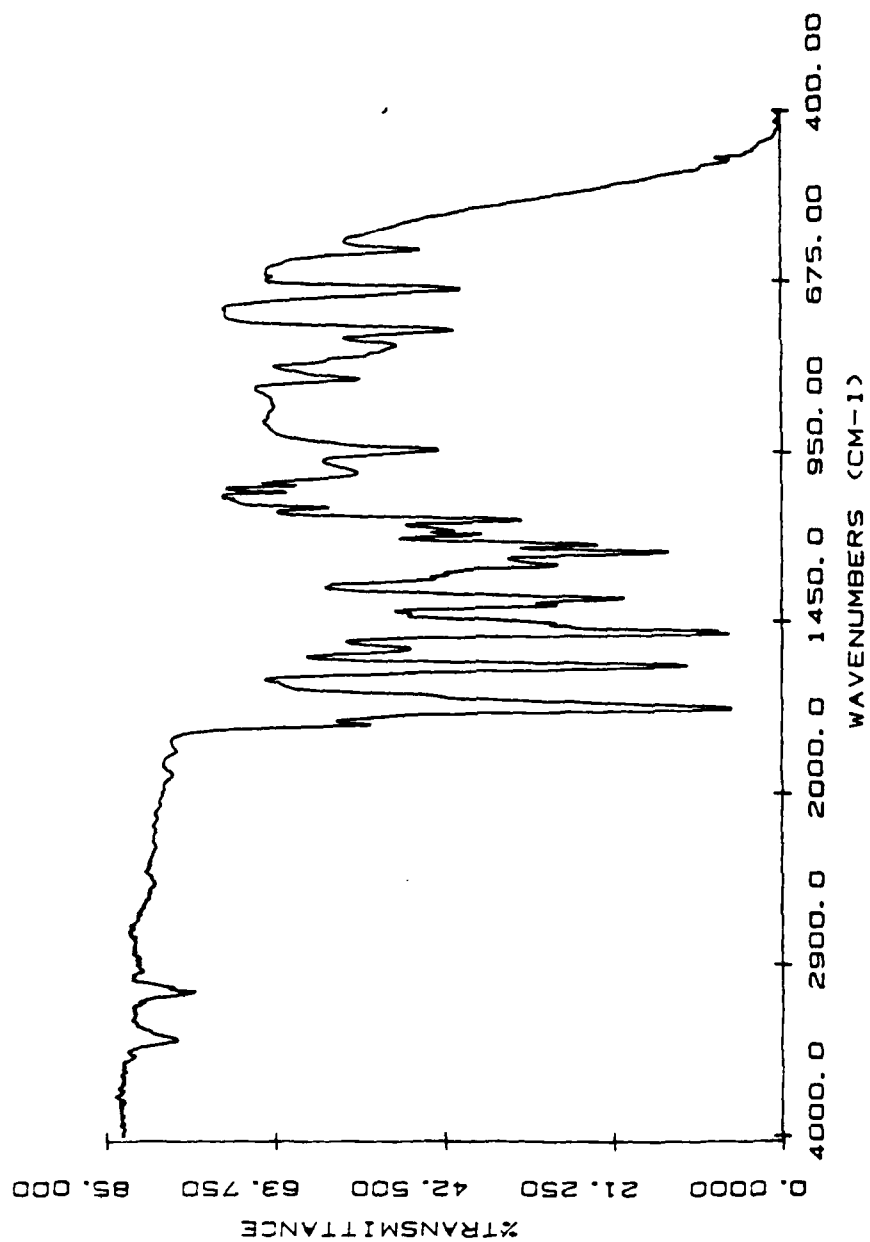


Figure 47. Infrared Spectrum of Vacuum Baked Polyimide (58J).

The factors which influenced the reactions the least were time and concentration. Although concentrated solutions did increase yield, no longer chain length was noticed. The greater stability of the concentrated as compared to dilute solutions of the polyamic acid suggests that the solvent is involved in the degradation of the imide.

Solvent influences on the polymerization are important for two reasons. First the polymer will not gain high molecular weight unless it can stay in solution. Solvents such as m-cresol and tetrachloroethane only allow solubility to be maintained at low concentration. Secondly, the solvent must not interfere with the reaction. Solvents such as DMF and DMAC can release trace amounts of secondary amines into the solution and through transamidation reduce the molecular weight of the polymer.

Since water can hydrolyze the polyamic acid and water is a byproduct of the polymerization procedure, any additional water that is absorbed by solvents like DMF or DMAC can interfere with the imide formation. Therefore, solvent purity is essential. Removal of water from the reaction flask does have a distinct bearing on yield, since the longer the azeotroping time the better the yields.

Reflux temperatures of 180-250°C were used and gave reasonable yields but the vacuum baked samples at 180-200°C gave cleaner IR spectra. This indicates that solvent interferes with ring closure and temperature is not as great

a factor.

Purity of reactants and cleanliness of glassware were small factors since care was taken to insure that no impurities entered the reaction via those sources.

Lastly the structure of the monomer can conceivably interfere with the reaction by sterically hindering the closure of the imide. The phenoxy group lies over the dianhydride part of the time. The phenyl can rotate on its single bond freely over the carbonlys and interfere with ring closure. Also the phenoxy group is an electron donating group and thus helps stabilize the amic acid form.

SUMMARY

Synthesis of 3,6-diphenoxypyromellitic dianhydride was achieved through a four step sequence starting with durene. Polymerization of that monomer with 1,3-bis(3-amino-phenoxy)benzene was carried out using a variety of solvents including: m-cresol/toluene, DMF, DMAC, DMAC/toluene, m-cresol.

From the results, it appears that the factors which most affect the polymerization are solvent, water removal and monomer structure. Although the viscosities of the polyimides were very low the solubility was very good in DMF, and DMAC. It should be noted that vacuum baked films of these polyimides are only slightly soluble and this may be due to crosslinking or increased ring closure.

While achieving a soluble polyimide was a prime objective of this research, low molecular weight will limit its use. The diphenoxy substituent may limit intermolecular interactions but it may also contribute to decreased molecular weight through steric hinderence or a stabilizing effect.

Further research in this area should include 1) changing the substituent on the dianhydride to limit movement. 2) Azeotroping the water continuously to avoid hydrolysis.

CONCLUSIONS

The formation of 3-phenoxy-pyromellitic dianhydride from durene is complicated by internal cyclization which produces a xanthone type product. However, 3,6-diphenoxy-pyromellitic synthesis occurs in good yields to give a well characterized product.

The polymerizations are limited by several factors which influence the overall outcome. The monomer diphenoxy-pyromellitic dianhydride does not appear to undergo polyamic acid formation to high molecular weights in short periods of time. Vacuum baking can lead to imide ring closure, but does not appear to cause increased molecular weight. With respect to imide formation, an electronic effect by the electron-donating phenoxy substituents may prevent efficient attack by nitrogen at carbonyl centers. While a steric effect associated with a hexasubstituted benzene ring may prevent opening of the anhydride ring. In conclusion, the solvent plays an important role in the polymerization with m-cresol/toluene being the most efficient combination.

BIBLIOGRAPHY

1. Fred W. Billmeyer Jr., Textbook of Polymer Science, 2nd Ed., Wiley Interscience, John Wiley and Sons, Inc., New York, p. 124, 458, 506, (1971). Other solvents used include acetone, dimethoxymethane, diglyme, THF, MeCN, nitrobenzene, dioxane and N-methylpyrrolidinone. For further information see references 74 through 80.
2. G. Lubin, Handbook Of Composites, New York, Van Nostrand Reinhold Company, p. 89-114, 772, (1982).
3. L. W. Frost, G. M. Bower, J. H. Freeman, H. A. Bergman, E. J. Traynor, and C. R. Ruffing, J. Polym. Sci., Part A-1, 6, 215 (1968).
4. R. J. Aagelo, U. S. Pat. 3,424,718 (E.I. duPont de Nemours Co.) (1969).
5. H. A. Burgman, J. H. Freeman, L. W. Frost, G. M. Bower, E. J. Traynor, and C. R. Ruffing, J. Appl. Polym. Sci., 12, 805 (1968).
6. J. K. Fincke, AFML-TR-66-188, Monsanto Research Corp. (1966).
7. P. M. Hergenrother, W. J. Wrasedlo, and H. H. Levene, U.S. Govt. Res. Rep. AD 602,679 (1964).

8. Netherlands Patent Application 63/ 00135 (E. I. duPont de Nemours Co.) (1965).
9. H. Lee, D. Stoffey, and K. Neville, New Linear Polymers, p. 205-264, McGraw Hill, New York (1967).
10. R. E. DeBrunner, and J. K. Fincke, U.S. Pat. 3,423, 366 (Monsanto Research Corp.).
11. W. M. Edwards, U.S. Pat. 3,179,634 (E.I. duPont de Nemours Co.) (1965).
12. B. R. Livshits, S. V. Vinogradova, I. L. Knunyants, G. L. Berestneva and T. Kh. Dymshits, Vysokomol. Soedin., A 15: No. 5, 969-968, (1973). Polym. Sci. USSR, A 15, 1078-1087 (1973).
13. F. E. Rogers, U. S. Patent 3,356,648 (1967).
14. Badische Aniline, and Sodal Fabrik, French Patent 2,162,411 (1973).
15. D. R. Heath and J. G. Wirth, U.S. Patent 3,875,116 (1975); Chem. Abstr., 84, 45207y (1976); Chem. Abstr., 83, 59838w (1975).
16. T. Takekoshi and J. E. Kochanowski, U. S. Patent 3,833,546 (1974); Chem. Abstr., 82, 4948f (1975).
17. J. A. Webster, J. M. Butler, and T. J. Morrow, "Advances in Chemistry Series No. 129", Am. Chem. Soc., 61, (1973).
18. G. L. Brode, G. T. Kwiatkowski, and J. H. Kawakami, Am. Chem. Soc., Polymer Preprints, 15 (1), 761 (1974).

19. J. P. Critchley and M. A. White, J. Polym. Sci., 10, 809 (1972).
20. J. P. Critchley, P. A. Grattan, M. A. White, and J. S. Pippett, J. Polym. Sci., A-1, 10, 1789 (1972).
21. O. Ya. Fedotova, V. I. Gorokhov, O. I. Paresishvili, G. S. Karetnikor, and Kolesnikov, Vysokomol. Soedin., A, 14, (6), 1256 (1972).
22. R. J. Angelo, Belgium Patent 655,654 (1965); Chem. Abstr. 65, 2376 (1966).
23. M. L. Wallach, Am. Chem. Soc., Polymer Preprints, 8 (2), 1170 (1967).
24. O. Ya. Fedotova, N. M. Popova, N. Fedotova, Vysokomol. Soedin., B, 15 (10), 760 (1973).
25. W. Dietrich, German Patent 2,115,478 (1972); Chem. Abstr., 78, 17790r (1973).
26. E. Hosokawa, M. Waki, and M. Fukushima, Japanese Patent 74 14,959 (1970); Chem. Abstr., 82, 18202v (1975).
27. V. V. Korshak, A. L. Rusanov, D. S. Tugushi, S. S. Gitis, A. V. Ivanov, and Y. V. Botkina, Vysokomol. Soedin., A, 14 (3), 686 (1972).
28. W. J. Farrissey and P.S. Andrews, U. S. Patent 3,787,367 (1974).
29. H. Mukamal, F. W. Harris, and J. K. Stille, J. Polym. Sci., A-1, 5, 2721 (1967).

30. A. Stoenciu, O. Fedotova, V. V. Korshak, Tr. Mosk. Khim.-Tekhnol. Inst. 74, 130 (1973); Chem. Abstr., 82, 43766q (1975).
31. Y. Imai and H. Koga, J. Polym. Sci., A-1, 11, 2623 (1973).
32. W. J. Farrissey and K. W. Rausch, U.S. Patent 3,870,674 (1975).
33. W. Wrasidlo and J. M. Augl, J. Polym. Sci., A-1, 7, 3393 (1969).
34. F. P. Darmory and M. DiBenedetto, M. S. Patent 3,705,869 (1972); Chem. Abstr., 78, 59024z (1973); Chem. Abstr., 79, 67293x (1973).
35. V. V. Korshak, A. L. Rusanov, R. D. Katsarava, and F. F. Niyazi, Vysokomol. Soedin., A, 15 (12), 2643 (1973); Polym. Sci. USSR, 15, 3000 (1973).
36. V. V. Korshak, A. L. Rusanov, R. D. Katsarava, F. F. Niyazi, and I. Batirov, Vysokomol. Soedin., A, 16 (4), 722 (1974); Chem. Abstr., 81, 121095r (1974).
37. S. V. Vinogradova, N. A. Churochkina, Ya. S. Vygodskii, and V. V. Korshak, Vysokomol. Soedin., 15, 1713 (1973).
38. W. J. Farrissey and P. S. Andrews, U.S. Patent 3,870,677 (1975).

50. W. DeWinter, J. Macromol. Sci.-Revs. Macromol. Chem., 1 (2) 329 (1966).
51. AFWAL-TR-83-4079 Technical report.
52. A. L. Endrey, U. S. Patent 3,179,630; (1965).
53. E. F. Hoegger, U. S., Patent 3,342,774 (E. I. duPont de Nemours Co.) (1967).
54. Netherlands Patent App. 64/08298, Monsanto Co. (1965); Chem. Abstr. 63, 3129 (1965).
55. F. W. Harris and S. O. Norris, J. Polym. Sci., Part A-1, 11, 2143 (1973).
56. C. E. Sroog, A. L. Endrey, S. V. Abramo, C. E. Berr, W. M. Edwards and K. L. Oliver, J. Polymer Science, A, 3, 1374 (1965).
57. C. E. Sroog, Encyclopedia of Polymer Science and Technology, Vol. 11, H. F. Mark, N. G. Gaylord, and N.M. Bikales, Eds., Wiley, New York, 247, (1969).
58. J. I. Jones, F. W. Ochynski, and F. A. Rackley, Chem. Ind., 1686-1688, (1962).
59. G. M. Bower, and L. W. Frost, J. Polymer Sci. A, 1, 3135-3150 (1963).
60. R.J. Angelo, U.S. Patent 3,073,785 (E. I. duPont de Nemours Co.) (1963); Chem. Abstr., 58, 7006 (1963).
61. W. J. Wrasidlo, P. M. Hergenrother, and H. H. Levine, Polym. Prep., Amer. Chem. Soc., Div. Polym. Chem. 5(1), 141 (1964); Chem. Abstr. 64, 3699g (1966).

39. V. V. Korshak, S. V. Vinogradova, Ya. S. Vygodskii, N. V. Gerashchenko, and N. I. Lushkina, Vysokomol. Soedin., A, 14 (9), 1924 (1972); Polym. Sci. USSR, 14, 2153 (1972).
40. V. V. Korshak, A. V. Vinogradov, Al-Khaidar, T. Ziyad, G. M. Tseitlin, and V. V. Rode, Vysokomol. Soedin., B, 14 (8), 592 (1972); Chem. Abstr., 78, 4613k (1973).
41. J. P. Critchley, in Progress In Polymer Science, Vol. 2, A. D. Jenkins, Ed., Pergamon Press, Oxford, p. 51-161, (1970).
42. R. J. Cotter and M. Matzner Ring Forming Polymerizations, Heterocyclic Rings, Part B, 2, Academic Press, New York and London, p. 4-126, (1972).
43. H. Mukamal, F. W. Harris, J. K. Stille, J. Polym. Sci., A-1, 5, 2721 (1967).
44. P.M. Hergenrother, H. H. Levine, J Polym. Sci., A-1, 5, 1453 (1967).
45. H. S. Kaufmann, J. J. Falcetta, Eds., Introduction to Polymer Science and Technology, p. 18-20, John Wiley and Sons, New York, (1977).
46. Kapton Polyimide film H-1, A44627, Product Bulletin.
47. A. Raave, Organic Chemistry of Macromolecules, Chap. 14-19, Marcel Dekker, Inc., N.Y., 1967.
48. H. Mark, Pure and Applied Chemistry, Vol. 12 p. 9 (1966).
49. C. S. Marvel, J. Macromol. Sci., A1 (1), 7 (1967).

62. G. Odian, Principles of Polymerization, McGraw Hill Book Co., New York, p. 139-141, (1970).
63. R. A. Dine-Hart, U. S. Dep. Commun. AD482,530 (1965); Chem. Abstr., 66, 8991, 95736u (1967).
64. R. A. Dine-Hart and W. W. Wright, J. Appl. Polym. Sci., 11, 609 (1967); Chem. Abstr., 67, 3167, 33242s (1967).
65. Belgian Patent 706,049 (Nat. Res. Dev. Corp.)(1968).
66. G. S. Kolesnikov, O. Ya. Fetotova, E. I. Hofbauer, H. H. Al-Sufi, H. H. M. A., ysokmol. Soedin., 8, 1440 (1966).
67. L. W. Frost, and I. Kesse, Polym. Prepr., Amer. Chem. Soc., Div. Polym. Chem., 4(1), 369 (1963).
68. L.W. Frost, and I. Kesse, J. Appl. Polym. Sci., 8, 1039 (1964).
69. C. E. Sroog, J. Polym. Sci., Part C No. 16, Part 2, 1191-1209 (1967); Chem. Abstr., 67, 6113, 64712z (1967).
70. C. E. Sroog, Encyclopedia of Polymer Science and Technology, Vol. 11, H. F. Mark, N.G. Gaylord, and N.M. Bikales, Eds. Wiley, New York, p. 263, (1969).
71. G. M. Bower, and L. W. Frost, Polym. Prepr., Am. Chem. Soc., Div. Polym. Chem., 4 (1), 357 (1963); Chem. Abstr., 62, 641 (1965).
72. J. R. Chalmers, Belg. Pat. 663,771 (E. I. duPont de Nemours Co.) (1965); Chem Abstr. 64, 17816s (1966).
73. J. I. Jones, W. F. Ochynski, F. A. Rackley, Chem. Ind. (London) p. 1686 (1962); Chem Abstr., 57, 15336 (1963).

74. N. A. Adrova, M. M. Koton, I. N. Benma, Vysokomol. Soedin. Ser. B, 10, 137 (1968); Chem. Abstr. 68, 9301, 96238m (1968).
75. A. Ya. Ardashnikov, I. E. Karadash, B. V. Kotov, and A. N. Pravednikov, Dokl. Chm. (English Translation), 164, 1006 (1965).
76. Belgian Patent, 650,774 (Monsanto Co.).
77. Belgian Patent, 654,849 (E. I. duPont de Nemours Co.) (1965).
78. British Patent 1,059,929 (3M Co.) (1967).
79. Netherlands Patent Application 64108298 (Monsanto Co.) (1965); Chem. Abstr., 63 3129 (1965).
80. M. F. Vaughn, J. I. Jones, (National Research Development Corp.) Fr. 1,550,077, 20 Dec. 1968, Brit. Appl. 06 Apr. 1966.
81. T. Takekoshi and J.E. Kochanowski, U. S. Patent 3,833,546 (1974); Chem. Abstr., 82, 4948f (1975).
82. L.H. Lanier, Synthesis and Characterization of Phenylated Polyimides MS thesis WSU, p 27-29, (1976).
83. Badische Anilin and Soda-Fabrik, French Patent 2,162,411 (1973).
84. F. W. Harris, W. A. Feld, L.H. Lanier, Appl. Poly. Symp., 26, 426 John Wiley and Sons, Inc., New York, (1975).
85. F. W. Harris, W. A. Feld, L.H. Lanier, J. Polymer Science, Part A-1, 13, 283 (1975).

86. B. Ramalingam, Polyimides Containing Oxyethylene Units
MS thesis, WSU, (1981).
87. H. Hopff, P. Doswald, and B. K. Manukian, Helv. Chim.
Acta, 46, 757-66, (1963); German, Chem. Abs., 57,
9734e; 58, 5568h.
88. B. K. Manukian, Helv. Chim. Acta 44, 1922-6, (1961),
Chem. Abs., 55, 21043e; 56, 399d.
89. P. R. Hammond, J. Chem. Soc. C, 8, 1521-3 (Eng.),
(1971).
90. Neth. Patent 6,515,806, (1966), Imperial Smelting Corp.
Ltd.
91. V. G. Lukmanov, L.A. Alekseeva, L. M. Yagupolskii,
Zhurnal Organicheskoi Khimii, 10, 9, 2000-2001, (1974).
92. H. Schmid, A. Ebnother and Th. M. Meijer, Helvetica
Chimica Acta, 33, 1751, (1950).
93. Lee Irvin Smith and Henry C. Miller, JACS, 64, 440,
(1942).
94. Lee Irvin Smith and Russel O. Denyes, JACS, 56, 475-6,
(1934).
95. Lee Irvin Smith and Roger L. Abler, JACS, 22, 811-15,
(1957).
96. Lee Irvin Smith and David Tenenbaum, JACS, 57, 1293-6,
(1935).
97. Lee Irvin Smith and Gordon D. Byrkit, JACS, 55, 4305-8,
(1933).

98. H. Hopff and B. K. Manukian, Helv. Chim. Acta , XLIII, VI, 1645-53, (1960).
99. Arnold Zweig, Arthur H. Maurer, and Bernard G. Roberts, JOC, 32, 1322-29, (1966).
100. Frank Dobinson and Phillip S. Baily, Tetrahedron Letters, 13, 14-18, (1960).
101. I. M. Heilbron, and J. S. Heaton, Organic Synthesis, Vol I, John Wiley & Sons, NY, 1941, p. 207-9.
102. H. Hopff, P. Doswald and B. K. Manukian, Helv. Chim. Acta, 61, 1231-7, (1961).
103. H. Hopff and B.K. Manukian, Helv. Chim. Acta, XLIII, 4, 941-8, (1960).
104. Swiss Patent 416,668, (1967), Sandoz Ltd., by Badrig K. Manukian.
105. G. P. Naletova, D. F. Varfolomeev, A. Kh. Sharipov, T. D. Kul'Kova, Yu. V. Kirichenko, Neftepererab. Neftekhim, 8, 33-4 (Russ.), (1968).
106. I. Tokarskaya, N. M. Beksheneva, V. P. Borshehenko, L. Kh. Bikchurina, T. M. Khannanov, Neftekhimiya, 9 (3), 425-8, (Russ.), (1969), Chem. Abs., 71. 91013m, (1969).
107. V. K. Kondratov, L. F. Lipatova, G. M. Karpin, Zh. Obshch. Khim., 49, (10), 2342-6, (1979).
108. V. K. Konfratov, G. M. Karpin, Zh. Fiz. Khim., 53, (1), 211-12, (1979) (Russ.).

109. N. I. Buketova, S. R. Rafikov, I. A. Arkhipova, Izu. Akad. Nauk. Kaz. SSR, Ser. Khim. 19, (6), 77-80 (Russ.).
110. Koji Chiba and, Shinya Tomura, Nippon Kagaku Kaishi, 11 2188-90, (1973).
111. Stanley Tocker, (du Pont de Nemours E. I. & Co.) U.S. 3,437,635, (1969).
112. Maurice Balme, Max Gruffaz, British Patent 1,222,630 (1971).
113. Howard A. Vogel, Hans. T. Oien, U.S. Patent 3,431,240, (1969).
114. H. O. Wirth, F. U. Herrmann, and W. Kern, Makromol. Chem., 80, 120, (1964).
115. D. H. R. Barton, J. C. Blazejewski, B. Charkiot and W. B. Motherwell, J. Chem. Soc. Chem. Comm., 503, (1981).
116. A. A. Goldberg, A. H. Wragg, J. Chem. Soc., 4227, (1958).
117. F. J. Williams, H. M. Relles, P. E. Donahue, and J. S. Manello, J. Org. Chem., 42, 3425, (1977).
118. Hennion and Anderson, JACS 68, 424 (1946).

USAF-SCEEE RESEARCH INITIATION PROGRAM

AIR FORCE OFFICE OF SCIENTIFIC RESEARCH

FINAL REPORT

ANGLE RESOLVED ION-SCATTERING STUDY OF GaAs SURFACES
THE EXPERIMENT DESIGN

PRINCIPAL INVESTIGATOR:	Thomas P. Graham, Ph. D. Physics Department University of Dayton
AIR FORCE RESEARCH COLLEAGUE:	William L. Baun MBM, AFML, WPAFB
DATE:	December 4, 1985
SUBCONTRACT NO.:	84 RIP 38
SUBCONTRACT TO GOVT. NO.:	F49620-82-C-0035

ABSTRACT

Computer programs were developed that permit the design of multi-element cylindrical electrostatic lenses. They permit plotting of ion trajectories through the lense. A five-element cylindrical electrostatic lense, allowing independent control of both angular and energy resolution, was designed and constructed and given preliminary testing with satisfactory results. An experimental facility was assembled to perform angle-resolved ion scattering experiments. The system permits sample rotation as well as rotation of the lense/analyzer/detector subassembly.

Acknowledgement

The author would like thank the Air Force Systems Command, the Air Force Office of Scientific Research and the Southeastern Center for Electrical Engineering Education for the opportunity to participate in the Research Initiation Program. Many thanks go also to his Colleague, William Baun for his many helpful suggestions. The help and hospitality of T. W. Haas and the members of the Mechanics and Surface Interactions Branch at Wright Patterson Air Force Base are also gratefully acknowledged.

I. OBJECTIVES:

This work is part of a longer range program to develop a system for performing angle-resolved ion scattering (ARISS) experiments to aid in the characterization of the surface structure of materials. In particular, this project concentrated on two aspects of the overall plan. One was to develop the ability to design multi-element lenses. Such lenses are needed to permit operation of the ion analyzer in a high resolution mode as well as allowing for efficient collection of scattered ions over a large range of scattering angles. The second aspect was to construct and assemble the experimental facility with which to conduct the experiments.

In Section II a brief background for the experiments and the motivation for pursuing them is given. Section III describes in some detail the work performed. Section IV concludes the report with a brief summary of the status of the experiments and additional steps needed to complete the system.

II. BACKGROUND:

The characterization of the surface properties of electronic materials is a very important requirement for the successful design of semiconducting devices for a number of Air Force programs. At present there is a particular interest in GaAs for use in detectors and FET devices. The characterization includes quantitative and qualitative determination of surface species as well as surface structure.

Ion scattering spectroscopy (ISS), the scattering of low energy ions in the range of 0.2 to 10 kev, exhibits excellent surface selectivity. The ion scattering that results is attributed to scattering from the first one or two surface layers of the sample. This selectivity arises from : (a) large scattering cross-sections

which leads to depletion of the ion beam as it enters and leaves the solid, and (b) to a neutralization effect whereby ions penetrating beyond the first layer of atoms at a solid surface are neutralized very efficiently.¹

When a beam of accelerated ions strikes a crystal surface, each encounter between a projectile ion and a surface atom can be described in terms of an elastic binary collision. Under certain circumstances multiple scattering, blocking, shadowing and channeling effects become important. The energy of an ion making an elastic collision, expressed as a ratio of final energy, E_1 to initial energy, E_0 is determined from energy and momentum conservation to be:

$$E_1/E_0 = \left[M_1^2 / (M_1 + M_2)^2 \right] \left[\cos^2 \theta_L + (M_2^2 / M_1^2 - \sin^2 \theta_L)^{1/2} \right]^2 \quad (1)$$

Here M_1 is the mass of the incoming ion, M_2 the mass of the target atom and θ_L the laboratory scattering angle. By measuring the energy distribution of the scattered ions, the elements in the region of impact can be determined.¹

While ISS is used routinely for elemental characterization, interest has grown in recent years in using angle resolved ion scattering (ARISS) as it is called by some groups²⁾ to determine surface structure often in conjunction with LEED measurements. Analysis of multiple scattering effects and of shadowing and blocking effects can be used to construct models of the surface. When multiple collisions occur, shoulders or peaks occur at energies greater than that of the binary peak for a given element. Since different collision sequences lead to different final energies, knowledge of the energies and angular distributions in principle enable structural analysis. When shadowing, blocking, focusing or channeling effects occur, the intensities of the binary peaks will depend on the energies and incident and final angles.

Heiland and Taglauer³ studied shadowing effects of adsorbed

species on metal surfaces to estimate the positions of the adsorbed atom on the surface. Algra et al⁴ determined the structure of a stepped Cu surface using multiple collision analysis. Overbury et al have investigated the structure of Al(110)² and adsorbate ordering on Mo(001)⁵ using ARISS. Bronckers and de Wit have studied the first two layers of Cu(110) using shadowing effects. Marchut et al⁸ have analysed an unreconstructed Fe(001) surface using a shadow cone analysis involving the second and third atomic layers. From these studies and others it appears that similar studies on GaAs would be of interest.

III RESEARCH PERFORMED:

The work performed in this project was divided between designing a five-element electrostatic lense and constructing and assembling an experimental facility.

A1. Lense Design

A large amount of data, such as that found in Harting and Read⁹, exists for two and three element cylindrical lenses. In order to be able to independently control both the focusing properties and acceptance angle of a scattered ion beam, four or more lense elements are required. Kevan¹⁰ discusses the design of a lense composed of a pair of three-element cylindrical lenses based on Harting and Read's data that would have the desired properties. Kisker¹¹ has recently published a Basic program for the design of a four-element lense that can be used on a personal computer. An attractive feature of this program is that it allows calculation of trajectory data. It was decided that Kisker's program suitably modified could be used to design a variety of lenses and in particular a five-element lense with properties equivalent to the lense described by Kevan¹⁰.

In determining the focal properties of a an electrostatic lense the potential must be calculated first and then the trajectories and consequent focal properties can be found. The program uses an approximation by Bertram¹² who calculated the potential along the axis of a pair of concentric cylinders. One can then determine the potential at nearby off-axis points. From this, trajectories can be calculated. This approach is valid for paraxial rays and thus will give first order focal properties. Read et al¹³ compared their extensive exact calculations with those done using this approximation and found very good agreement as long as the gap between cylinders is small compared to the cylinder diameter. These restrictions have been complied with in the design discussed here.

The main program, TRAJECTORIES, is printed below. The lense potentials and relevant lengths starting from the input end are read in line 60. The lengths give the position of the backend of an element relative to the front of the first lense element. The program allows for a radius change at L2 located part way along the second element (separated by a cylinder diameter from adjacent lens gaps) so that L3 is the distance to the back of the second element. No change in radii was used so L2 was set equal to L1. The radii and gaps are also read in this line. The lengths are normalized to the cylinder radius in line 70 and must be converted back to actual lengths for output in lines 500 and 590. These differ from those given in ref. 11 which seem to be in error. The initial position and slope for two trajectories are given in line 110 in terms of a reduced potential. The radial position is returned by the conversion in line 280 ($P(K/2, I)$). A more detailed description of the method is given by Kisker¹¹ and by Fink and Kisker¹⁴.

```

10 REM TRAJECTORIES
20 REM PROGRAM FOR 5-ELEMENT LENSE
30 REM: ELECTRON RAY TRACING --- SEE RSI V. 53, 115 (1982)
40 DIM I,D,A(8),V(8),U(7),T(3),RS(1)
50 Q=.05:S=20:T=.5:C=3/16:ZV=0
60 READ
VA,VB,VC,VD,VE,L1,L2,L3,L5,L6,L7,R1,R2,S1,S2:S1=INT(S1/R1*10)/10
70
Z1=L1/R1:Z2=L2/R1:Z3=Z2+(L3-L2)/R2:Z5=Z2+(L5-L2)/R2:Z6=Z2+(L6-L2)/R2
:Z7=Z2+(L7-L2)/R2
80 S2=INT(S2/R2*10)/10:DIM VPT(Z7*20+4),B(Z7*20),P(Z7*10,1):FOR I=0
TO 30:READ B(I):NEXT I
90 A=-.12:B=.332:FOR I=31 TO 80:B(I)=B*EXP(A*I):NEXT I:REM EXPAND
THE DATA SET
100
BA=(VB-VA)/S1:CB=(VC-VB)/S2:DC=(VD-VC)/S2:ED=(VE-VD)/S2:ZO=0:GOSUB
190:V=VZ*.25
110 RS(0)=.02*V:RS(1)=0:R(0)=0:R(1)=.15*V
120 ZO=-Q:GOSUB 190:U(2)=VZ:ZO=0:GOSUB 190:U(3)=VZ
130 ZO=Q:GOSUB 190:U(4)=VZ:P(1,0)=R(0)/V:P(1,1)=R(0)/V:R=R1:GOSUB
320
140 REM MAIN PROGRAM
150 FOR K=2 TO Z2*20-2 STEP 2:GOSUB 230:NEXT
160 REM NEW RADIUS R2 AT Z2
170 R=R2:GOSUB 320:FOR K=Z2*20 TO Z7*20 STEP 2:GOSUB
230:NEXT:INPUT"DO YOU WISH TO SAVE DATA (Y/N)";YS:IF YS="Y" THEN
GOSUB 400:END
180 REM POTENTIAL CALCULATION
190
A(1)=ZO-Z1:A(2)=A(1)-S1:A(3)=ZO-Z3:A(4)=A(3)-S2:A(5)=ZO-Z5:A(6)=A(5)
-S2:A(7)=ZO-Z6:A(8)=A(7)-S2
200 FOR I=1 TO 8:A=INT(A(I)*S+T):B=ABS(A):V(I)=Q*A*-(AD)+B(B):NEXT
210
VZ=VA+BA*(V(1)-V(2))+CB*(V(3)-V(4))+DC*(V(5)-V(6))+ED*(V(7)-V(8)):VP
T(ZV)=VZ:ZV=ZV+1:RETURN
220 REM PREPARE NORMALIZED POTENTIALS
230 ZO=K*Q:PRINT ZO::Z=K*T+1:U(0)=U(2):U(1)=U(3):U(2)=U(4)
240 GOSUB 190:U(3)=VZ:ZO=ZO+.05:GOSUB 190:U(4)=VZ:V=U(3)*.25
250 FOR I=1 TO 3:T(I)=C*((U(I+1)-U(I-1))*10/(R*U(I)))^2:NEXT
260 I=0:GOSUB 280:I=1:GOSUB 280:PRINT:RETURN
270 REM HANDLE ONE TRAJECTORY STEP
280
B=R(I):P(K/2,I)=B/V:R(I)=B*(1-G*(T(1)+2*T(2)-U*T(2)))+RS(I)*H*(1-G*T
(2))
290 PRINT P(K/2,I);
300
RS(I)=-B*E*(T(1)+4*T(2)-M*T(1)*T(2))+RS(I)*(1-N*T(2))-E*T(3)*R(I):RE
TURN
310 REM CONSTANTS NEEDED FOR TRAJECTORY CALCULATION, DEPENDING ON
TUBE RADII
320 H=R*.1:E=H/6:F=H*H:M=F/2:N=F/3:U=F/4:G=F/6:RETURN

```



```

330 DATA 1500,250,500,27.5,100:REM LENS VOLTAGES VA,VB,VC,VD,VE
340 DATA 37.25,37.25,42.25,62.75,67.75,79.5:REM TUBE LENGTHS
L1,L2,L3,L5,L6,L7
350 DATA 2.5,2.5,.5,.5:REM TUBE RADII AND GAP WIDTHS
360 REM THIS IS THE "UNIFIED" DATA SET FOR CALCULATING THE AXIAL
POTENTIAL
370 DATA
.2674,.2432,.2207,.1998,.1805,.1627,.1465,.1316,.118,.1057,.0946,.08
45
380 DATA
.0754,.0673,.06,.0534,.0475,.0423,.0376,.0334,.0297,.0264,.0234,.020
8
390 DATA .0185,.0164,.0145,.0129,.0114,.0102,.009
400 INPUT "DO YOU WISH TO SAVE TRAJECTORY DATA (Y/N)";YTS
410 IF YTS="Y" THEN GOSUB 450
420 INPUT "DO YOU WISH TO SAVE POTENTIAL DATA (Y/N)";YPS
430 IF YPS="Y" THEN GOSUB 550
440 RETURN
450 INPUT "WHAT IS FILENAME";RYS
460 RYS=RYS+".DAT"
470 KK=K
480 OPEN"O",#1,RYS
490 FOR K=0 TO KK-2 STEP 2
500 IF K/2=10*Z2 THEN KL=(K/2)*R1/10 ELSE KL=L2+(K/2-10*Z2)*R2/10
510 PRINT#1,K/2,KL,P(K/2,0),P(K/2,1)
520 NEXT K
530 CLOSE
540 RETURN
550 INPUT"DATA FOR POTENTIAL PLOT--NAME'LPOT#' ";PS
560 PS=PS+".DAT"
570 OPEN"O",#1,PS
580 FOR K=0 TO ZV-4 STEP 2
590 IF K=20*Z2 THEN KL=K*R1/20 ELSE KL=L2+(K-20*Z2)*R2/20
600 PRINT#1,K/2,KL,VPT(K)
610 NEXT K
620 CLOSE
630 RETURN

```

The program can be easily modified to calculate trajectories for three element lenses for comparison with the compilation of Harting and Read⁹. By starting with a single input ray parallel to the axis the focal point and, by backward extrapolation of the output ray, the position of the rear principal plane can be found. By reversing the lense, the front focal point and principal plane position can be found. This was done for a few entries in ref. 9 with agreement to less than a percent. Code for this procedure will be added to the program for a more through comparison in the future.

Figure 1 shows an example of a potential distribution obtained with the program. The horizontal portions correspond to the positions of the first, third, and fifth elements. The positions of the second and fourth elements, the focusing elements, correspond to the regions of steep slope. This type of figure is useful in determining the regions of zero field. It is desirable to put additional elements such as deflection plates and apertures in force free regions. In the design shown below, apertures were placed in the region between 48 mm and 58 mm. Another point to be made is that since the region between about 45 mm and 60 mm has a constant potential equal to that of the third element, the five element lens can be thought of as two separate three element lenses. Consequently, focusing conditions for each three element lens can be found independently of the other. In order to determine the focusing conditions for a three element lens the main program was modified for three elements and included a simple routine to search for the focus voltage that give the distance at which a parallel input ray would cross the axis - the focal distance. The program, FOCUS, is given below. Figure 2 shows a plot of the voltage on element two for a range of voltages on the first element for the case where the voltage on the third element was held at 500 V.

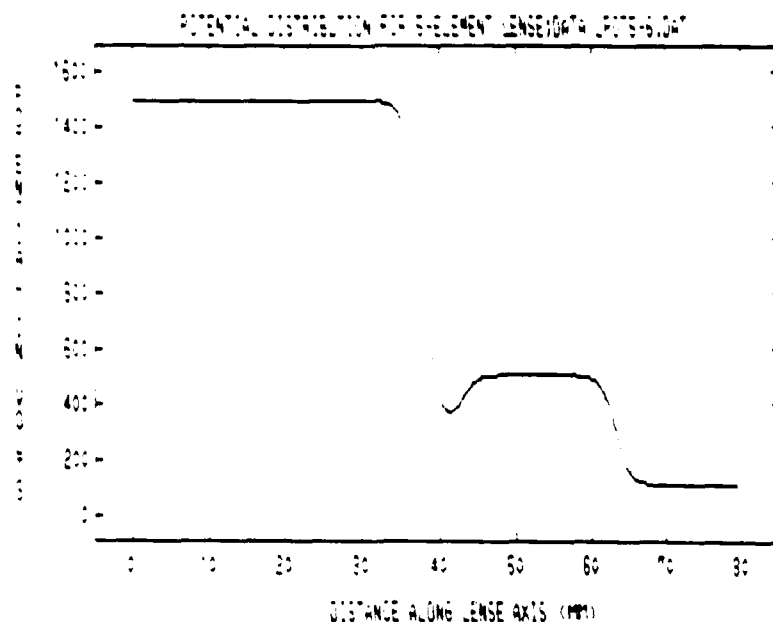


Figure 1. Potential Distribution

```

5  REM FOCUS
10 REM PROGRAM FOR DETERMINING FOCUSING VOLTAGE
20 REM PROGRAM FOR 5-ELEMENT LENSE
30 REM: ELECTRON RAY TRACING --- SEE RSI V. 53, 115 (1982)
40 DIM IM,VAA(20),VCC(20),VDA(20),VCA(20)
50 DIM I,D,A(8),V(8),U(7),T(3),RS(1)
60 Q=.05:S=20:T=.5:C=3/16
70 READ VA,VB,VC,VD,L1,L2,L3,L5,L6,R1,R2,S1,S2:S1=INT(S1/R1*10)/10
80
Z1=L1/R1:Z2=L2/R1:Z3=Z2+(L3-L2)/R2:Z5=Z2+(L5-L2)/R2:Z6=Z2+(L6-L2)/R2
90 KG=L6*10/R1
100 S2=INT(S2/R2*10)/10:DIM VPT(Z6*20+4),B(Z6*20),P(Z6*10,1):FOR I=0
TO 30:READ B(I):NEXT I
110 A=-.12:B=.332:FOR I=31 TO 80:B(I)=B*EXP(A*I):NEXT I:REM EXPAND
THE DATA SET
120 IF MF=0 GOTO 150
130 IF IM=15 GOTO 590
140 VC=VC-7:VA=VA-50:VB=VA
150 VC=VC+10:ZV=0:IF VC=VA/2 GOTO 140
160 PRINT VA,VC
170 BA=0:CB=(VC-VB)/S2:DC=(VD-VC)/S2:ZO=0:GOSUB 260:V=VZ*.25
180 RS(0)=.02*V:R(0)=0
190 ZO=-Q:GOSUB 260:U(2)=VZ:ZO=0:GOSUB 260:U(3)=VZ
200 ZO=Q:GOSUB 260:U(4)=VZ:P(1,0)=R(0)/V:P(1,1)=R(0)/V:R=R1:GOSUB
410
210 REM MAIN PROGRAM
220 FOR K=2 TO Z2*20-2 STEP 2:GOSUB 300:NEXT
230 REM NEW RADIUS R2 AT Z2
240 R=R2:GOSUB 410:FOR K=Z2*20 TO Z6*20 STEP 2:GOSUB 300:NEXT:GOTO
120
250 REM POTENTIAL CALCULATION
260
A(1)=ZO-Z1:A(2)=A(1)-S1:A(3)=ZO-Z3:A(4)=A(3)-S2:A(5)=ZO-Z5:A(6)=A(5)
-S2
270 FOR I=1 TO 6:A=INT(A(I)*S+T):B=ABS(A):V(I)=Q*A*-(AD)+B(B):NEXT
280
VZ=VA+BA*(V(1)-V(2))+CB*(V(3)-V(4))+DC*(V(5)-V(6)):VPT(ZV)=VZ:ZV=ZV+
1:RETURN
290 REM PREPARE NORMALIZED POTENTIALS
300 ZO=K*Q:Z=K*T+1:U(0)=U(2):U(1)=U(3):U(2)=U(4)
310 GOSUB 260:U(3)=VZ:ZO=ZO+.05:GOSUB 260:U(4)=VZ:V=U(3)*.25
320 FOR I=1 TO 3:T(I)=C*((U(I+1)-U(I-1))*10/(R*U(I)))^2:NEXT
330 I=0:GOSUB 350:RETURN
340 REM HANDLE ONE TRAJECTORY STEP
350
B=R(I):P(K/2,I)=B/V:R(I)=B*(1-G*(T(1)+2*T(2)-U*T(2)))+RS(I)*H*(1-G*T
(2))
360 IF K/2=KG AND ABS(P(K/2,0))=.03 THEN 370 ELSE 390
370 MF=1:IM=IM+1:VAA(IM)=VA:VCC(IM)=VC:VDA(IM)=VD/VA:VCA(IM)=VC/VA
380 LPRINT K/2*R1/10,VC,P(K/2,0),VA:PRINT
K/2*R1/10,VC,P(K/2,0),VA:RETURN

```

```

390
MF=0:RS(I)=-B*E*(T(1)+4*T(2)-M*T(1)*T(2))+RS(I)*(1-N*T(2))-E*T(3)*R(
I):RETURN
400 REM CONSTANTS NEEDED FOR TRAJECTORY CALCULATION,DEPENDING ON
TUBE RADII
410 H=R*.1:E=H/6:F=H*H:M=F/2:N=F/3:U=F/4:G=F/6:RETURN
420 DATA 900,900,100,300:REM LENS VOLTAGES VA,VB,VC,VD,VE
430 DATA 25,25,37.25,42.25,55:REM TUBE LENGTHS L1,L2,L3,L5,L6,
440 DATA 2.5,2.5,.1,.5:REM TUBE RADII AND GAP WIDTHS
450 REM THIS IS THE "UNIFIED" DATA SET FOR CALCULATING THE AXIAL
POTENTIAL
460 DATA
.2674,.2432,.2207,.1998,.1805,.1627,.1465,.1316,.118,.1057,.0946,.08
45
470 DATA
.0754,.0673,.06,.0534,.0475,.0423,.0376,.0334,.0297,.0264,.0234,.020
8
480 DATA .0185,.0164,.0145,.0129,.0114,.0102,.009
490 INPUT "DO YOU WISH TO SAVE FOCUS DATA (Y/N)";YFS
500 IF YFS="Y" GOTO 520
510 END
520 INPUT "WHAT IS FILE NAME -- LFOC##";FSS
530 FSS=FSS+".DAT"
540 OPEN"O",#1,FSS
550 FOR I=1 TO IM
560 PRINT#1,VAA(I),VCC(I),VDA(I),VCA(I)
570 NEXT I
580 CLOSE
590 END

```

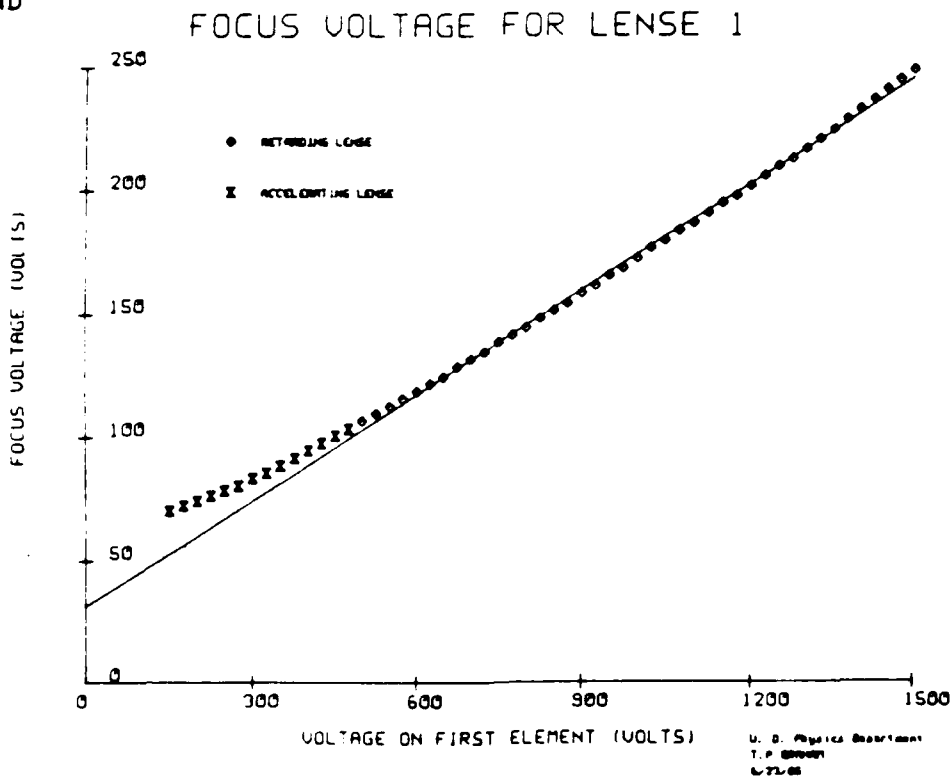


Figure 2. Focus Voltage

Figure 3 gives an example of two trajectories passing through the complete lens with voltages on the elements one through five of 900 V, 150 V, 300 V, 20 V, and 100 V. The position of a pair of apertures is superposed on the figure. In practice the lense as constructed may not exactly duplicate the conditions under which the calculations were made. However it is expected that the theoretical values will provide a good starting point for tuning the lense.

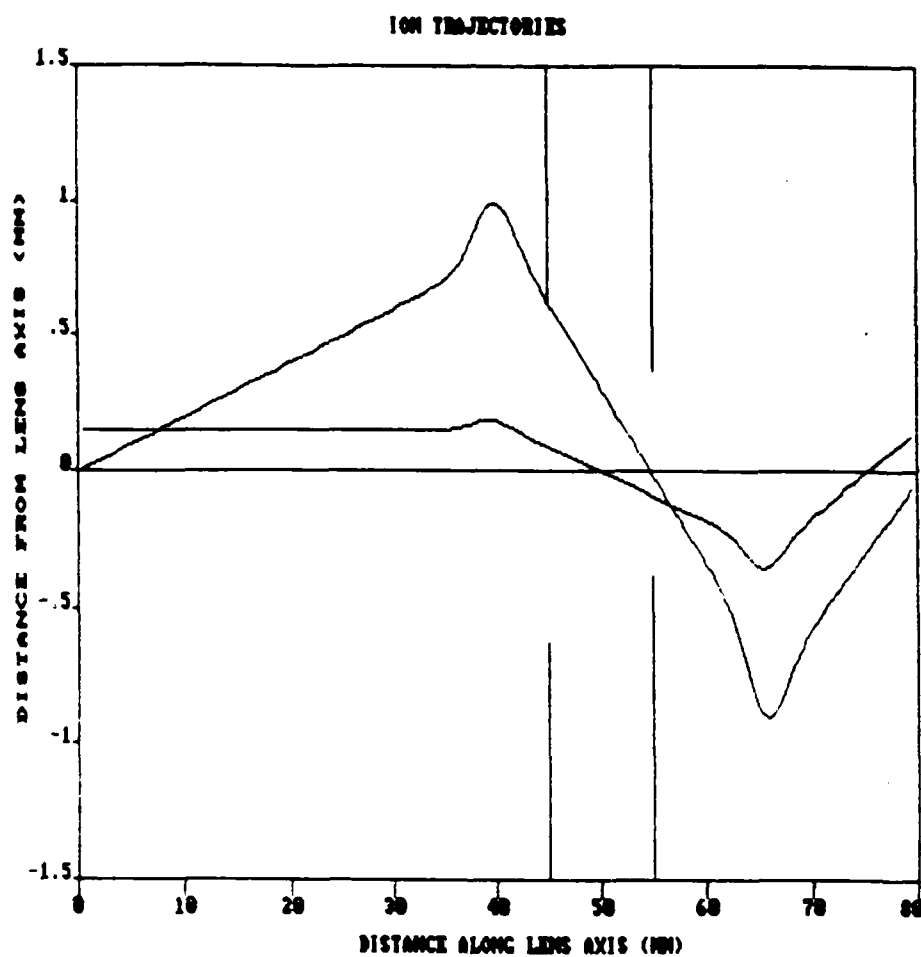
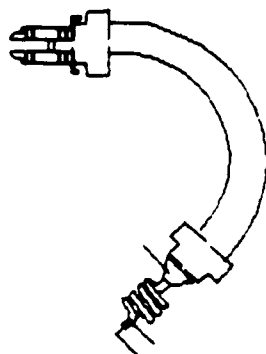


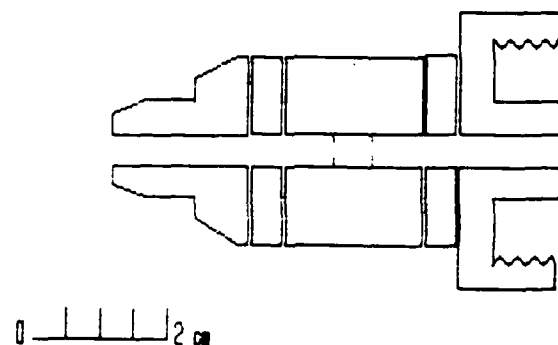
Figure 3. Trajectories through 5-element lense.

sample, an acceptance half-angle varying from $.5$ to 30° , a retarding ratio up to $15/1$ with an energy resolution of 1.5 V.



ANALYZER WITH LENS AND CHANNELTRON

Figure 4. Lense/Analyzer/Channeltron Assembly



FIVE ELEMENT LENSE

Figure 5. Schematic of 5-element lense

B. Experimental Facility

The experiment was assembled in a large UHV chamber that had an inside diameter of 12 inches. Figure 6 shows a schematic diagram of the chamber as viewed from above. Not shown, but indicated, are the instruments and pumps attached to the chamber. The lense/analyzer/channeltron assembly is mounted in a shielding box with the lense protruding. This in turn is mounted on a rotating stage. A sample holder was constructed so that a sample can be placed at the center of the chamber and can be rotated around the holder axis. An ion gun is mounted at 135° to the sample holder. The angle of incidence is fixed. The angle of the beam with respect to crystal axes in the plane of the sample can be varied as the sample holder is rotated. This allows the study of intensity variations with crystallographic direction. The scattering angle can be varied by rotating the analyzer assembly. This rotation is needed to study blocking and shadowing effects.

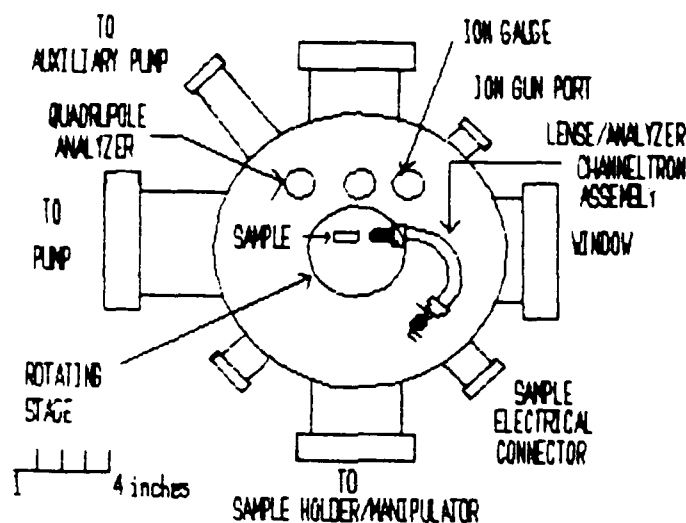


Figure 6. Experimental Chamber

The chamber is mounted on a 400 l/s ion pump through a gate valve. An auxiliary 20 l/s ion pump with a sublimator pump is also attached. A quadrupole analyzer, and various gauges are also mounted on the chamber. Not shown in the figure is the base-plate upon which the chamber is mounted. The rotating stage rests on this plate and is rotated by a manipulator mounted on a feedthrough coaxial with the chamber axis. The base-plate also contains the feedthroughs for the electrical connections. The electrical connections and the operation of the analyzer/channeltron system have been described in the author's final report for the 1984 USAF-SCEEE Summer Faculty Research Program. Additional power supplies and voltage dividers were assembled to provide the required lens voltages. The overall system performs satisfactorily, however the lenses system could not be adequately tested due to a malfunction in the analyzer/channeltron system that occurred as testing of the lense began. The general behavior of the lense could be observed to be satisfactory-- the current through the lense improved by about a factor of five when the lense was used, and changed as expected as the acceptance angle was changed by controlling the front three elements.

IV. SUMMARY AND CONCLUSIONS

Computer programs were developed that permit the design of multi-element cylindrical electrostatic lenses and provide for plotting of ion trajectories through the lense. When the noted limitations are observed, they can provide a convenient replacement for existing tabulations. With the aid of these programs, a five-element cylindrical lens was designed with which both the angular resolution at the sample and the energy resolution can be independently varied. Preliminary testing of the lense indicates satisfactory performance.

An experimental facility was constructed and assembled to perform angle-resolved ion scattering experiments. Two angular degrees of freedom are possible with the system. When

characterization of the lense is completed, studies of surface structure will be initiated.

A number of additional features are contemplated for the future. A more sophisticated sample holder and manipulator is desirable. It would incorporate an additional degree of rotational motion and have provision for both cooling and annealing the sample at high temperatures. A differentially pumped ion gun for use with rare gas ion beams will be necessary when "clean" surfaces are to be studied.

REFERENCES

1. Buck, T. M., "Low-energy Ion Scattering Spectrometry," in Methods of Surface Analysis, Ed. by A. W. Czanderna, (Elsevier, Amsterdam, 1975), Ch. 3.
2. Overbury, S. H., Heiland, W., Zehner, D. M., Datz, S. and Thoe, R. S., "Investigation of the Structure of Au(110) Using Angle Resolved Low Energy K^+ Ion Backscattering," Surface Sci., Vol. 109, pp. 239-262, 1981.
3. Heiland, W. and Taglauer, E., "The Backscattering of Low Energy Ions and Surface Structure," Surface Sci., Vol. 68, pp. 96-107, 1977.
4. Algra A. J., Luitjens, S. B., Suurmeijer, E. P. Th. M. and Boers, A. L., "The Structure of a Stepped Copper(410) Surface Determined by Ion Scattering Spectroscopy," Surface Sci., Vol. 100, pp. 329-341, 1980.
5. DeKoven, B. M. and Overbury, S. H., "Low-Energy K^+ -Ion Scattering as a Probe of Adsorbate Ordering," Phys. Rev. Lett., Vol 53, pp.481-484, 1984.
6. Bronckers, R. P. N. and de Wit, A. G. J., "Shadowing, Focussing and Charge Exchange Effects in the Angular Distributions of keV Ne and H_2O Ions Scattered from Cu(110). I. The Surface Geometry of the First Layer," Surface Sci., Vol. 104, pp. 384-404, 1981.
7. Bronckers, R. P. N. and de Wit, A. G. J., "Shadowing, Focussing and Charge-Exchange Effects in the Angular Distributions of keV Ne $^+$ and H_2O^+ Ions Scattered from Cu(110). II. The Surface Geometry of the First Two Layers," Surface Sci., Vol. 112, pp.111-132, 1981.
8. Marchut, L., Buck, T. M., Wheatley, G. H. and McMahon, C. J. Jr., "Surface Structure Analysis Using Low Energy Ion Scattering. I. Clean Fe(001), " Surface Sci., Vol. 141, pp.549-566, 1984.

9. Harting, E. and Read, F. H., Electrostatic Lenses (Elsevier, Amsterdam, 1976)
10. Kevan, S. D., "Design of a High-Resolution Angle Resolving Electron Energy Analyzer," Rev. Sci. Instrum. Vol. 54, pp 1441-1445, 1983.
11. Kisker, E., "Simple Method for Accurate Ray Tracing in Electrostatic Lenses," Rev. Sci. Instrum. Vol. 53, pp 114-116, 1982.
12. Bertram, S., J. Appl. Phys., Vol. 13, pp 496-502, 1942.
13. Read, F. H., Adams, A. and Soto-Montell, J. R., J. Phys. E: Sci. Instrum. Vol. 4, pp 625-632, 1971.
14. Fink, J. and Kisker, E., "A Method for Rapid Calculations of Electron Trajectories in Multi-Element Electrostatic Cylinder Lenses," Rev. Sci. Instrum., Vol. 51, pp 918-920, 1980.

1984 USAF-SCEEE RESEARCH INITIATION PROGRAM

Sponsored by the

AIR FORCE OFFICE OF SCIENTIFIC RESEARCH

Conducted by the

Southeastern Center for Electrical Engineering Education

FINAL REPORT

THERMAL DECOMPOSITION STUDIES OF SOME SILAHYDROCARBONS

Prepared by: Dr. Vijay K. Gupta, and Lenae V. Tuggle

Academic Rank: Professor of Chemistry

Department and University: Chemistry Department
Central State University, Wilberforce, Ohio 45384

Research Location: Central State University and
Materials Laboratory (AFWAL/MLBT)
Wright Patterson Air Force Base, Ohio

USAF Research: Mr. C.E. Snyder, Jr.

Contract #: F49620-82-C-0035

Date: Nov. 30, 1985

THERMAL DECOMPOSITION STUDIES OF SOME SILAHYDROCARBONS

by

Vijay K. Gupta, and Lenae V. Tuggle

Abstract

Thermal stability characteristics have been investigated for the following advanced synthetic silahydrocarbons, MLO 82-507: the mixture of $\text{CH}_3 \text{Si} (\text{C}_8\text{H}_{17})_3$, $\text{CH}_3 \text{Si} (\text{C}_8\text{H}_{17})_2 \text{C}_{10}\text{H}_{21}$, $\text{CH}_3\text{Si} \text{C}_8\text{H}_{17} (\text{C}_{10}\text{H}_{21})_2$, and $\text{CH}_3 \text{Si} (\text{C}_{10}\text{H}_{21})_3$, MLO 84-350: $\text{CH}_3 \text{Si} (\text{C}_9\text{H}_{17})_3$, MLO 84-193: $\text{CH}_3 \text{Si} (\text{C}_{10}\text{H}_{21})_3$, MLO 85-118: $\text{C}_5\text{H}_9 \text{Si} (\text{C}_8\text{H}_{17})_3$, MLO 85-119: $\text{C}_5\text{H}_{11} \text{Si} (\text{C}_8\text{H}_{17})_3$, and MLO 85-244: $\text{C}_5\text{H}_{11} \text{Si} (\text{C}_8\text{H}_{17})_3$ with branching in the C_5 group. The above studies involved stressing the fluid as a function of time and temperature, analysis of the fluid using GC and viscosity measurements, and characterization of the decomposition products using GC/MS. It has been found that these materials show very little decomposition when stressed at or below 315.6 C for 6 hours, but when stressed at 371.1 C for 6 hours, they undergo significant degradation. Under the stress conditions of 371.1 C and 6 hours, the fluid MLO 84-350 degrades about 10 percent, and the fluids MLO 82-507, and MLO 84-193, degrade about 20 percent. Based on GC/MS data, it appears that these three fluids exhibit similar decomposition pattern. Among the fluids MLO 85-118, MLO 85-119, MLO 85-244, the fluid MLO 85-118 with the double bond in the alpha position of C_5 group is least thermally stable, and the fluid MLO 85-244 with branching at alpha position of C_5 group is slightly more thermally stable as compared to the fluid MLO 85-119 with straight chain substituent groups. The effect of impurity such as disiloxane (MLO 79-182) has also been investigated on the thermal stability of the fluid MLO 84-193, and it is found that addition of disiloxane as impurity to a silahydrocarbon has no catalytic effect on thermal stability characteristics of the fluid MLO 84-193.

Acknowledgements

The authors would like to thank the Air Force Systems Command, the Air Force Office of Scientific Research and the Southeastern Center for Electrical Engineering Education (SCEEE) for providing them with the financial support to conduct this research. We would also like to thank the Nonstructural Materials Branch of the laboratory for the use of their facilities. The authors are thankful to Mr. Lee D. Smithson of the Analytical Services Branch, and Dr. Jeff Workman and Dr. Chin Yu of Technical Services Inc. for providing GC/MS analysis.

We take this opportunity to thank all the members of the Nonstructural Branch of the Materials Laboratory and the UDRI Lubricants Group for their technical assistance in conducting these studies. Finally, we are grateful to Mr. Carl E. Snyder Jr. and Ms. Lois Gschwender for their collaboration and helpful suggestions during the tenure of this project.

I. INTRODUCTION

Recent effort has led to the development of many functional fluids for use in aerospace applications such as jet engine oils, greases, and hydraulic fluids. Since hydraulic fluids are not expected to operate in oxidative environments, therefore thermal and hydrolytic stability are the two main areas of concern(1). In order to meet the need for a high temperature fluid, MIL-H-27601, a -40 C to 288 C hydraulic fluid was developed. A highly refined, deep-dewaxed paraffinic mineral oil was selected as the base stock for the above application, and the fluid provided satisfactory service for over ten years in the temperature range of -40 C to 288 C.

The development of supersonic missiles, like the advanced strategic air launched missiles (ASALM) has created the need for a hydraulic fluid useable over the temperature range of -54 C to 315 C. The mineral oil base stock from which MIL-H-27601 is derived, do not have the needed viscosity-temperature properties to perform satisfactorily in the temperature range of -54 C to 315 C. Synthetic hydrocarbons based on hydrogenated polyalphaolefin oligomers have also been found to be deficient both in viscosity-temperature properties and thermal stability (2). Perfluorinated fluids which have excellent thermal and oxidative stabilities, have several disadvantages such as high density, poor bulk modulus, elastomer incompatibility, and lack of suitable additives (3).

In response to the need for hydrocarbon-type fluids with improved properties, a Materials Laboratory Program has led to the development of a class of compounds called silahydrocarbons. These compounds have excellent viscosity-temperature properties and thermal stability, and are expected to be hydrocarbon like in

their physical and chemical properties. Therefore, silahydrocarbons are good candidates for hydraulic fluids useable over -54 C to 315 C temperature range.

The silahydrocarbons are defined as compounds of silicon substituted by four hydrocarbon groups e.g., SiR_4 . In general, R can be any hydrocarbon group such as CH_3 , C_2H_5 - $\text{C}_{12}\text{H}_{25}$ and be either primary, secondary, tertiary, or a branched alkyl group. The silahydrocarbons may be synthesized as symmetrical SiR_4 , e.g., $\text{Si}(\text{CH}_3)_4$ where all four R groups are identical or unsymmetrical RSiR'_3 , e.g., $\text{CH}_3\text{Si}(\text{C}_{12}\text{H}_{25})_3$ where R and R' groups are different. In the unsymmetrical structures, variations can be made at will by proper selection of the R groups. The properties such as vapor pressure, boiling point, viscosity, and thermal stability can be controlled by the proper selection of the substituent groups (R). For example the length of the R group effects the boiling point, $(\text{CH}_3)_4\text{Si}$ has a boiling point of 26 C while $(n\text{-C}_{12}\text{H}_{25})_4\text{Si}$ has a boiling point of 250 C at 0.06 mm Hg. pressure. One expects some dependence of thermal stability on the structure and size of the substituent groups in the silahydrocarbon. One branched silahydrocarbon $\text{CH}_3\text{Si}(\text{CH}_2\text{CH}(\text{C}_2\text{H}_5)\text{C}_4\text{H}_9)_3$ (1) has been found to be less thermally stable as compared to $\text{CH}_3\text{Si}(\text{C}_{10}\text{H}_{21})_3$. Another branched silahydrocarbon $(\text{CH}_3)_2\text{SiCH}(\text{CH}_3)_2\text{C}_{14}\text{H}_{29}$ (4) has been found to be more thermally stable as compared to $\text{CH}_3\text{Si}(\text{C}_{10}\text{H}_{21})_3$. This raises the question that position of branching in the substituent group of the silahydrocarbon has some impact on the thermal stability characteristics. It was also observed that siloxane which was present as an impurity in $\text{CH}_3\text{Si}(\text{C}_{10}\text{H}_{21})_3$ may also effect the thermal stability characteristics of silahydrocarbons. This report describes the effort to understand the thermal stability characteristics of silahydrocarbons as a function of the variation in the structure of the substituent group. The effect of an impurity such as disiloxane on the thermal stability of a silahydrocarbon has also been reported.

II. OBJECTIVES

The objective of this project were to expand the basic understanding of the thermal stability characteristics of silahydrocarbons with reference to (1) when a straight chain substituent group is replaced by a branched alkyl group, (2) when a disiloxane or a trisiloxane is added as an impurity to the silahydrocarbon. The other objective was to provide the students educational and learning experience with the techniques involved in the analysis and characterization of the decomposition products formed from above compounds.

III. PROPOSED RESEARCH WORK

It was proposed to study the thermal stability characteristics of the following experimental fluids which were assigned MLO numbers as given below:

1. MLO 84-193 $\text{CH}_3 \text{ Si } (\text{C}_{10}\text{H}_{21})_3$
2. MLO 84-350 $\text{CH}_3 \text{ Si } (\text{C}_8\text{H}_{17})_3$
3. MLO 82-507, mixed silahydrocarbon consisting of the following four components: $\text{CH}_3 \text{ Si}(\text{C}_8\text{H}_{17})_3$, $\text{CH}_3 \text{ Si } (\text{C}_8\text{H}_{17})_2 \text{C}_{10}\text{H}_{21}$, $\text{CH}_3 \text{ Si } \text{C}_8\text{H}_{17} (\text{C}_{10}\text{H}_{21})_2$, and $\text{CH}_3 \text{ Si } (\text{C}_{10}\text{H}_{21})_3$.
4. MLO 85-118 $\text{H}_7\text{C}_3\text{HC}=\text{CH Si } (\text{C}_8\text{H}_{17})_3$
5. MLO 85-119 $\text{H}_{11}\text{C}_5 \text{ Si } (\text{C}_8\text{H}_{17})_3$
6. MLO 85-244 $\text{H}_7\text{C}_3 \text{ CH}(\text{CH}_3) \text{ Si } (\text{C}_8\text{H}_{17})_3$

In addition, it was proposed to study the effect of a mixture disiloxane MLO 79-182 on the thermal stability charactersitics of MLO 84- 193. The above disiloxane is a mixture of the following four disiloxanes as determined by GC/MS: $(\text{CH}_3(\text{C}_8\text{H}_{17})_2 \text{ Si})_2 \text{ O}$, $\text{CH}_3\text{C}_8\text{H}_{17}\text{C}_9\text{H}_{19} \text{ Si-O-Si } (\text{C}_8\text{H}_{17})_2\text{CH}_3$, $(\text{CH}_3\text{C}_8\text{H}_{17}\text{C}_9\text{H}_{19} \text{ Si})_2 \text{ O}$, and $\text{CH}_3 \text{ C}_8\text{H}_{17} \text{ C}_9\text{H}_{19} \text{ Si-O- Si } (\text{C}_9\text{H}_{19})_2\text{CH}_3$. The effort involved measuremnts of viscosities before and after decomposition, and characterization of products.

IV. EXPERIMENTAL

This section describes the test procedures.

Thermal Stability Test Procedure: The thermal stability tests were performed in stainless steel bombs. The bombs were made of 9" long stainless steel tubes either 0.25" or 0.375" diameter with swagelok fittings on both ends. The bombs were cleaned with a suitable solvent such as hexane and acetone and dried in an oven at 120 C for at least one hour. Approximately 2 cc. of the test fluid was added to the bomb and the lamp grade nitrogen was bubbled through the fluid for five minutes to remove any air, and the bomb was quickly capped with the swagelok fitting. The bomb was then weighed and placed in the oven at a specified temperature (controlled within 2 C) for a specific time period. After the bomb was heated in the oven for a given length of time, the bomb was removed, allowed to cool, and was weighed again. If the pre-test and the post-test weights differed by more than 0.100g, the test was considered to be a bad test. Generally the weight change was found to be 0.01 g to 0.02 g, but in some cases the bomb developed leak due to some reasons, excessive weight changes were observed and those test were repeated. The thermal degradation products from the bomb were analyzed using viscosity measurements, gas chromatographic analysis for decomposition products both in gaseous and liquid phases, and the GC/MS analysis for identification of decomposition products. In order to analyze the gaseous components, the bomb was placed in a bath maintained at -54 C for at least 30 minutes so that gaseous components liquify or freeze, the bomb was then taken out of the cold bath and one of the cap was replaced by a cap with a small hole containing a septum in order to facilitate the removal of the sample for gas analysis by GC. The method and gas chromatographic conditions for gas analysis are listed in Table 1. After the gas phase sample called headspace was analyzed, the bomb was opened and the liquid sample was

transferred to a glass vial for analysis of liquid components and viscosity measurements. The method and gas chromatographic conditions for the analysis of liquid phase are listed in Table 2. Four mixtures of the disiloxane MLO 79-182 in the fluid MLO 84-193 that were prepared contained 1.42%, 2.42%, 4.73%, and 5.22% of MLO 79-182 and the remaining MLO 84-193. These mixtures were also studied for thermal stability characteristics using the above test procedures and analytical methods.

V. RESULTS AND DISCUSSION

The synthetic fluids as mentioned in section III have been investigated for their thermal decomposition characteristics. For the fluid MLO 84-193, the silahydrocarbon $\text{CH}_3 \text{Si} (\text{C}_{10}\text{H}_{21})_3$, the thermal stability data as a function of time and temperature, and GC/MS analysis of the fluid stressed at 371.1 C for 7 hours characterizing the decomposition products both in the gaseous and liquid phases has been reported elsewhere (4). For the fluid MLO 82-507, the mixture silahydrocarbon consisting of $\text{CH}_3 \text{Si} (\text{C}_8\text{H}_{17})_3$: 29.3%, $\text{CH}_3 \text{Si} (\text{C}_8\text{H}_{17})_2\text{C}_{10}\text{H}_{21}$: 46.4%, $\text{CH}_3 \text{Si} \text{C}_8\text{H}_{17}(\text{C}_{10}\text{H}_{21})_2$: 20.1%, and $\text{CH}_3 \text{Si}(\text{C}_{10}\text{H}_{21})_3$: 3.1%, the thermal stability data as function of time and temperature, and GC/MS data characterizing the decomposition products of the fluid after stress has been included in another report (5). The viscosities of various experimental silahydrocarbon fluids as function of temperature are listed in table 3. It is noted that fluids MLO 84-193 and MLO-79-182 do freeze below - 40 C, whereas the mixture silahydrocarbon MLO 82-507 does not freeze even at -54 C. For the fluids MLO 85-118, MLO 85-119, MLO 85-244, viscosity measurements were made only at 37.8 C before and after the stress due to limited amount of these fluids. The data in table 4 represents the GC and viscosity data for the above experimental fluids both in the unstressed and stressed states. The % concentration represents the amount of silahydrocarbon remaining in the

fluid and is the relative value. It is noted that the fluid MLO 84-350, $\text{CH}_3 \text{Si} (\text{C}_8\text{H}_{17})_3$ is the most stable thermally, and the viscosity and GC data agree with each other. On the other hand the fluid MLO 84-193 $\text{CH}_3 \text{Si} (\text{C}_{10}\text{H}_{21})_3$ has twice as much % change in concentration as compared to MLO 84-350, but the % change in viscosity is about same in both the fluids. The difference in the two fluids may be attributed to the factors such as chain length of the alkyl group, and the presence of impurity di-siloxane in MLO 84-193. In case of the fluids MLO 85-118, MLO 85-119, and MLO 85-244, the differences in thermal stability are significant, whereas the three fluids are with the same number of carbon atoms :29, consisting of three straight chain octyl groups and a 5-carbon group. The 5-carbon group in MLO 85-113 has a double bond in alpha position, in MLO 85-119 is a straight chain alkyl group, and in MLO 85-244 is branched in the alpha position. The fluid MLO 85-244 is relatively more stable than the fluids MLO 85-118 and MLO 85-119, the branching in the alpha position in 5-carbon substituent group may be the factor contributing to the increased thermal stability. The fluid MLO 85-118, which has double bond in 5-carbon substituent group was found to be considerably less thermally stable as compared to the fluid MLO 85-119. In case of fluid MLO 85-118 foaming was also observed in the bomb as the bomb was opened after stress, and the color of the fluid also changed from colorless to yellow. The % changes in viscosity in all three fluids were in the same range. Due to the unusual behavior of MLO 85-118, this fluid was also stressed at lower temperatures, the data in table 5 represents the thermal stability data as function of temperature. The chromatograms in fig. 1 to 5 represent the capillary gas chromatograms of the fluid under different conditions. The chromatogram in fig. 1 indicates that there are four different isomers of the compound $\text{C}_5\text{H}_9 \text{Si} (\text{C}_8\text{H}_{17})_3$. The chromatograms in figures 2,3, and 4 indicate that

there is formation of silahydrocarbons with more than 29 carbon atoms as the fluid is stressed, which is also indicated by the positive change in viscosity (see data in table 5). When the fluid MLO 85-118 is stressed at 371.1 C for 6 hours, the fluid starts breaking into small fragments as indicated by the chromatogram in fig 5.

The data in tables 6 to 9 and figures 6 to 9 represent the GC/MS analysis of the stressed fluids MLO 84-350, MLO 85-118, MLO 85-119, and MLO 85-244 respectively. The above data represents the identification of the decomposition fragments as they are formed. It is noted that in the case of fluid MLO 85-118, significantly larger amounts of hydrocarbons are formed as compared to the fluids MLO 85-119, MLO 85-244, and MLO 84-350. The presence of the silahydrocarbon $\text{Si}(\text{C}_8\text{H}_{17})_4$ in all three fluids after stress indicates that there is recombination of decomposed fragments to form the above compound.

In order to explore the effect of impurities on the thermal stability of a silahydrocarbon fluid, another fluid MLO 79-182, disiloxane, mixture of four different disiloxanes was used. Four mixtures of the above fluid MLO 79-182 in the fluid MLO 84-193 were prepared with the compositions of 1.42%, 2.42%, 4.73%, and 5.22% of MLO 79-182. These mixtures were stressed at 371.1 C for 6 hours in stainless steel bombs. The stressed mixtures contained 71.3%, 70.5%, 73.1%, and 71.4% of the silahydrocarbon $\text{CH}_3\text{Si}(\text{C}_{10}\text{H}_{21})_3$ respectively, whereas the oil MLO 84-193 when stressed under the same conditions contained 77.0% of $\text{CH}_3\text{Si}(\text{C}_{10}\text{H}_{21})_3$ component. These investigations indicate that addition of disiloxane as an impurity does not have any catalytic effect on the thermal stability characteristics of the fluid MLO 84-193. The greater thermal stability of the fluid 84-350 may be due to short chain length of the

alkyl group C_8H_{17} as compared to the longer chain length of the alkyl group $C_{10}H_{21}$ in case of the fluid MLO 84-193. The fluids MLO 85-118, MLO 85-119, and MLO 85-244 contain three straight chain octyl groups and a 5-carbon atom group whereas the fluid MLO 84-350 contains three straight chain octyl groups and a methyl group, but the fluid MLO 84-350 is more thermally stable as compared to the fluids MLO 85-118, MLO 85-119, and MLO 85-244. It appears that substitution of methyl group in MLO 84-350 by 5-carbon atom group has reduced the thermal stability of the silahydrocarbon $CH_3 Si (C_8H_{17})_3$.

On the basis of the results presented in the preceding pages, it is concluded that the candidate silahydrocarbon MLO 84-350 $CH_3 Si (C_8H_{17})_3$ is a fluid possessing highest thermal stability. The presence of double bond in the alpha position of a substituent group in fluid MLO 85-118 has decreased the thermal stability significantly, whereas the presence of branching in the alpha position of a substituent group in the case of the fluid MLO 85-244 has improved the thermal stability slightly. The presence of a disiloxane as an impurity in the fluid silahydrocarbon does not seem to have any catalytic effect on the thermal stability characteristics.

Table 1. Method and Gas Chromatographic Conditions for the analysis of Gases.

METHOD: CAR6
CHANNEL 4

1. DATA INPUT

RUNTM #PKS
40.00, 100

MV/MIN DELAY MIN-AR BUNCH
.300, 0.00, 1000, NO

INTEGRATOR EVENTS
TIME EVENT
1 /E

CONTROL EVENTS
TIME EVENT ECM RLY
1 /E

2. DATA ANALYSIS

PROC RPRT SUP-UNK
ZERO, ME, NO

UNITS TITLE
AREA %

3. USER PROGRAMS

POST-ANAL DIALG-PRG PARAM-FILE
/N

4. REPORTS

RDVC #RPTS
1 T2, 1
2 /E

DONE

GAS CHROMATOGRAPHIC CONDITIONS

Model: Perkin - Elmer 900
Fused Silica Capillary Column
Length: 25 M
Diameter: 0.22 MM
Liquid Phase: Methyl Silicone Carbowax Deactivated
Split Ratio: 100 to 1
Aux: Gas: 40 ml/min Carrier Gas: 1 ml/min
Chart Speed: 1 cm/min
Detector: FID
Attenuation: 10 x 16
Temperatures: Injector: 220°C; Detector: 250°C
Column Temperature: -50°C to 200°C Program Rate: 8 deg/min
Initial Hold: 0 min Final Hold: 20 min
Sample Size: 2 ml
Sample ID: Headspace
Date: 8/24/84

Table 2: Method and Gas Chromatographic conditions for the analysis of liquids.

METHOD: DVK
CHANNEL 2

1. DATA INPUT

RUNTH #PKS
60.00, 200

MV/MIN DELAY MIN-AR BUNCH
.300, 0.00, 10, NO

INTEGRATOR EVENTS
TIME EVENT
1 /E

CONTROL EVENTS
TIME EVENT ECM RLY
1 80.00, CY
2 /E

2. DATA ANALYSIS

PROC RPRT SUP-UNK
ZERO, ME, NO

UNITS TITLE
AREA %

3. USER PROGRAMS

POST-ANAL DIALG-PRG PARAM-FILE
HPGC

4. REPORTS

RDVC #RPTS
1 T2, 1
2 /E

GAS CHROMATOGRAPHIC CONDITIONS

MODEL: HP5710A
FUSED SILICA CAPILLARY COLUMN
LENGTH: 12 M
DIAMETER: 0.23 MM
LIQUID PHASE: METHYL SILICONE CARBOWAX DEACTIVATED
SPLIT RATIO: 100 TO 1
AUX. GAS: 40 ML/MIN CARRIER GAS: 1 ML/MIN
CHART SPEED: 20CM/HR
DETECTOR: FID
ATTENUATION: 10 X 16
TEMPERATURES:
INJECTOR: 300 DEG.C
DETECTOR: 350 DEG.C
COLUMN TEMP: 70-270 DEG.C PROGRAM RATE: 8 DEG/MIN
INITIAL HOLD: 2 MIN FINAL HOLD: 32 MIN
SAMPLE SIZE: STOP1
SAMPLE ID: HYDFL
DATE: 8/24/84
ANALYST: DVK

Table 3: Viscosities of Various Experimental Synthetic Fluids as a Function of Temperature.

Fluid	Viscosity Values at Different Temperature (cSt)				
	98.9	37.3	-40.0	-54.0	37.8*
MLO 82-507	2.75	9.87	-	2216.83	8.60
MLO 84-193	3.53	13.60	solid	solid	12.12
MLO 84-350	2.32	7.99	395.5	-	7.06
MLO 79-182**	3.34	11.99	solid	solid	11.22
MLO 95-118	-	11.02	-	-	8.23
MLO 85-119	-	11.38	-	-	8.37
MLO 85-244	-	13.87	-	-	9.44

* Viscosity value of the fluid stressed at 371.1 C for 6 hours.

** Data for this fluid obtained from 'another report.'

Table 4: Thermal Stability Data of Various Experimental Synthetic Fluids Stressed at 371.1 C for 6 hours

Fluid	% concentration of silahydrocarbon			Viscosity (cSt) of the fluid at 37.8 C		
	Unstressed	Stressed	% change	Unstressed	Stressed	% change
MLO 82-507	99.7	78.9	-20.86	9.90	8.70	-12.10
MLO 84-193	96.4	77.0	-20.12	13.60	12.12	-10.90
MLO 84-350	99.0	89.0	-10.10	7.99	7.06	-10.90
MLO 79-182	-	-	-	11.99	11.22	- 6.40
MLO 85-118*	98.4	35.6	-63.88	11.02	8.23	-25.32
MLO 85-119	99.0	61.8	-37.58	11.38	8.37	-26.45
MLO 85-244	97.6	70.9	-27.36	13.87	9.44	-31.91

* In case of this fluid, foaming was noticed as the bomb was opened after heating.

Table 5: Thermal Stability Data of MLO 85-118 as a Function of Temperature

Temperature (°C)	Time (Hours)	% Concentration	% Change in Concentration	Viscosity(cSt)	% Change in Viscosity
Unstressed	-	98.4	-	11.02	-
315.6	6	88.2	-10.37	11.58	+5.08
315.6	12	87.6	-10.98	12.29	+11.52
343.3	6	72.4	-26.42	12.36	+12.10
371.1	6	35.6	-63.88	8.23	-25.32

Table 6: GC/MS Analysis of MLO 84-350 Stressed at 371.1 C for 6 hours.
(liquid phase)

* These components detected by GC/MS but not detected

Scan No.	Component in GC.	% Concentration	No. C Atoms
46	C ₅ H ₁₀ and C ₅ H ₁₂	0.16	5
49	C ₆ H ₁₂ and C ₆ H ₁₄	0.19	6
52	C ₇ H ₁₄ and C ₇ H ₁₆	0.15	7
75	C ₈ H ₁₆ and C ₈ H ₁₈	1.11	8
206	(CH ₃) ₃ Si C ₈ H ₁₇	*	11
235	H Si CH ₃ C ₂ H ₅ C ₈ H ₁₇	*	11
257	(CH ₃) ₂ Si C ₂ H ₅ C ₈ H ₁₇	*	12
275,291,305	C ₁₃ H ₂₈ , (CH ₃) ₂ Si C ₃ H ₇ C ₈ H ₁₇ , CH ₃ Si (C ₂ H ₅) ₂ C ₈ H ₁₇	*	13
328	(CH ₃) ₂ Si C ₄ H ₉ C ₈ H ₁₇	*	14
365,381,388	(CH ₃) ₂ Si C ₅ H ₁₁ C ₈ H ₁₇ , alkene, H Si CH ₃ C ₆ H ₁₃ C ₈ H ₁₇	*	15
391,401,424	C ₁₆ H ₃₂ , (CH ₃) ₂ Si C ₆ H ₁₃ C ₈ H ₁₇ , H Si CH ₃ C ₇ H ₁₅ C ₈ H ₁₇	*	16
436,439,448,459	(CH ₃) ₂ Si C ₇ H ₁₅ C ₈ H ₁₇ , CH ₃ Si C ₂ H ₅ C ₆ H ₁₃ C ₈ H ₁₇ , HSiCH ₃ (C ₈ H ₁₇) ₂ and its isomer 2.19	2.19	17
470	(CH ₃) ₂ Si (C ₈ H ₁₇) ₂	0.74	18
505	CH ₃ Si C ₂ H ₅ (C ₈ H ₁₇) ₂	0.55	19
525	CH ₃ Si C ₃ H ₇ (C ₈ H ₁₇) ₂	0.37	20
549	CH ₃ Si C ₄ H ₉ (C ₈ H ₁₇) ₂	0.36	21
575	CH ₃ Si C ₅ H ₁₁ (C ₈ H ₁₇) ₂	0.61	22
601	CH ₃ Si C ₆ H ₁₃ (C ₈ H ₁₇) ₂	0.78	23
626	CH ₃ Si C ₇ H ₁₅ (C ₈ H ₁₇) ₂	1.23	24
644,658	CH ₃ Si (C ₈ H ₁₇) ₃	88.22	25
677	C ₂ H ₅ Si (C ₈ H ₁₇) ₃	0.27	26
696	(CH ₃) ₂ C ₈ H ₁₇ Si-O-Si CH ₃ (C ₈ H ₁₇) ₂	0.29	27
704	C ₃ H ₇ Si (C ₈ H ₁₇) ₃	0.13	27

Table 7: GC/MS Analysis of MLO 85-118 Stressed at 371.1 C for 6 hours (liquid phase).

Scan No.	Component	No. of C atoms	% Concentration
53	Mixture of C ₅ to C ₈ Hydrocarbons	5-8	20.91
108	(CH ₃) ₂ Si (C ₈ H ₁₇) ₂	18	0.76
124	CH ₃ Si C ₂ H ₅ (C ₈ H ₁₇) ₂	19	0.63
136	CH ₃ Si C ₃ H ₇ (C ₈ H ₁₇) ₂	20	0.45
150	CH ₃ Si C ₄ H ₉ (C ₈ H ₁₇) ₂	21	0.36
163	H Si C ₅ H ₁₁ (C ₈ H ₁₇) ₂	21	0.83
168	CH ₃ Si C ₅ H ₁₁ (C ₈ H ₁₇) ₂	22	1.81
173	CH ₃ Si C ₅ H ₉ (C ₈ H ₁₇) ₂	22	0.51
183	H Si C ₆ H ₉ (C ₈ H ₁₇) ₂	22	0.66
187,197,201	H Si C ₇ H ₁₁ (C ₈ H ₁₇) ₂ and its isomers	23	2.55
206,216,224	H Si (C ₈ H ₁₇) ₃ and its isomers	24	6.54
229,240	CH ₃ Si (C ₈ H ₁₇) ₃ and its isomer	25	6.08
247	C ₂ H ₅ Si (C ₈ H ₁₇) ₃	26	2.17
256	C ₃ H ₇ Si (C ₈ H ₁₇) ₃	27	4.10
271	C ₄ H ₉ Si (C ₈ H ₁₇) ₃	28	4.32
279,284,290, 294,299, 301, 305, and 309	C ₅ H ₉ Si (C ₈ H ₁₇) ₃	29	40.46
311	C ₆ H ₁₃ Si (C ₈ H ₁₇) ₃	30	0.68
327	C ₇ H ₁₅ Si (C ₈ H ₁₇) ₃	31	0.71
339,352	Si (C ₈ H ₁₇) ₄	32	3.67

Table 8: GC/MS Analysis of MLO 85-119 Stressed at 371.1 C for 6 hours
(liquid phase).

<u>Scan No.</u>	<u>Component</u>	<u>No. of C Atoms</u>	<u>% Concentration</u>
54	Mixture of C ₅ to C ₈ Hydrocarbons	5-8	6.03
117	CH ₃ Si (C ₅ H ₁₁) ₂ C ₈ H ₁₇	19	0.24
126	CH ₃ Si C ₂ H ₅ (C ₈ H ₁₇) ₂	19	0.13
133	C ₂ H ₅ Si (C ₅ H ₁₁) ₂ C ₈ H ₁₇	20	0.26
156	C ₃ H ₇ Si C ₄ H ₉ C ₆ H ₁₃ C ₈ H ₁₇	21	0.24
165	H Si C ₅ H ₁₁ (C ₈ H ₁₇) ₂	21	1.74
170	CH ₃ Si C ₅ H ₁₁ (C ₈ H ₁₇) ₂	22	3.09
189	C ₂ H ₅ Si C ₅ H ₁₁ (C ₈ H ₁₇) ₂	23	2.25
199	C ₃ H ₇ Si C ₅ H ₁₁ (C ₈ H ₁₇) ₂	24	1.44
214	C ₄ H ₉ Si C ₅ H ₁₁ (C ₈ H ₁₇) ₂	25	1.62
226	H Si (C ₈ H ₁₇) ₃	24	1.01
232	(C ₅ H ₁₁) ₂ Si (C ₈ H ₁₇) ₂	26	4.12
249	C ₂ H ₅ Si (C ₈ H ₁₇) ₃	26	1.80
251	C ₅ H ₁₁ Si C ₆ H ₁₃ (C ₈ H ₁₇) ₂	27	0.56
271	C ₅ H ₁₁ Si C ₇ H ₁₅ (C ₈ H ₁₇) ₂	28	1.67
282,296	C ₅ H ₁₁ Si (C ₈ H ₁₇) ₃	29	63.80
310	C ₆ H ₁₃ Si (C ₈ H ₁₇) ₃	30	0.79
330	C ₇ H ₁₅ Si (C ₈ H ₁₇) ₃	31	1.13
355	Si (C ₈ H ₁₇) ₄	32	2.41

Table 9: GC/MS Analysis of MLO 85-244 Stressed at 371.1 C for 6 hours
(liquid phase).

<u>Scan No.</u>	<u>Component</u>	<u>No. of C Atoms</u>	<u>% Concentration</u>
54	Mixture of C ₅ to C ₈ Hydrocarbons	5-8	6.35
105	H Si CH ₃ (C ₈ H ₁₇) ₂	17	0.14
119	H Si C ₂ H ₅ (C ₈ H ₁₇) ₂	18	0.18
126	CH ₃ Si C ₂ H ₅ (C ₈ H ₁₇) ₂	19	0.03
131	H Si C ₃ H ₇ (C ₈ H ₁₇) ₂	19	0.12
137	CH ₃ Si C ₃ H ₇ (C ₈ H ₁₇) ₂	20	0.03
144	(C ₂ H ₅) ₂ Si (C ₈ H ₁₇) ₂	20	0.08
159,164	H Si C ₅ H ₁₁ (C ₈ H ₁₇) ₂	21	2.79
167,169	CH ₃ Si C ₅ H ₁₁ (C ₈ H ₁₇) ₂	22	1.09
186,188	C ₂ H ₅ Si C ₅ H ₁₁ (C ₈ H ₁₇) ₂	23	0.74
194,198	C ₃ H ₇ Si C ₅ H ₁₁ (C ₈ H ₁₇) ₂	24	0.61
209	C ₄ H ₉ Si C ₅ H ₁₁ (C ₈ H ₁₇) ₂	24	0.77
226	H Si (C ₈ H ₁₇) ₃	24	3.17
230	CH ₃ Si (C ₈ H ₁₇) ₃	25	1.45
249	C ₂ H ₅ Si (C ₈ H ₁₇) ₃	26	2.40
260	C ₃ H ₇ Si (C ₈ H ₁₇) ₃	27	1.83
267,278	C ₄ H ₉ Si (C ₈ H ₁₇) ₃	28	4.34
287,300,307	C ₅ H ₁₁ Si (C ₈ H ₁₇) ₃	29	69.89
329	C ₆ H ₁₃ Si (C ₈ H ₁₇) ₃	30	0.44
364	C ₇ H ₁₅ Si (C ₈ H ₁₇) ₃	31	0.60
385,408	Si (C ₈ H ₁₇) ₄	32	4.29

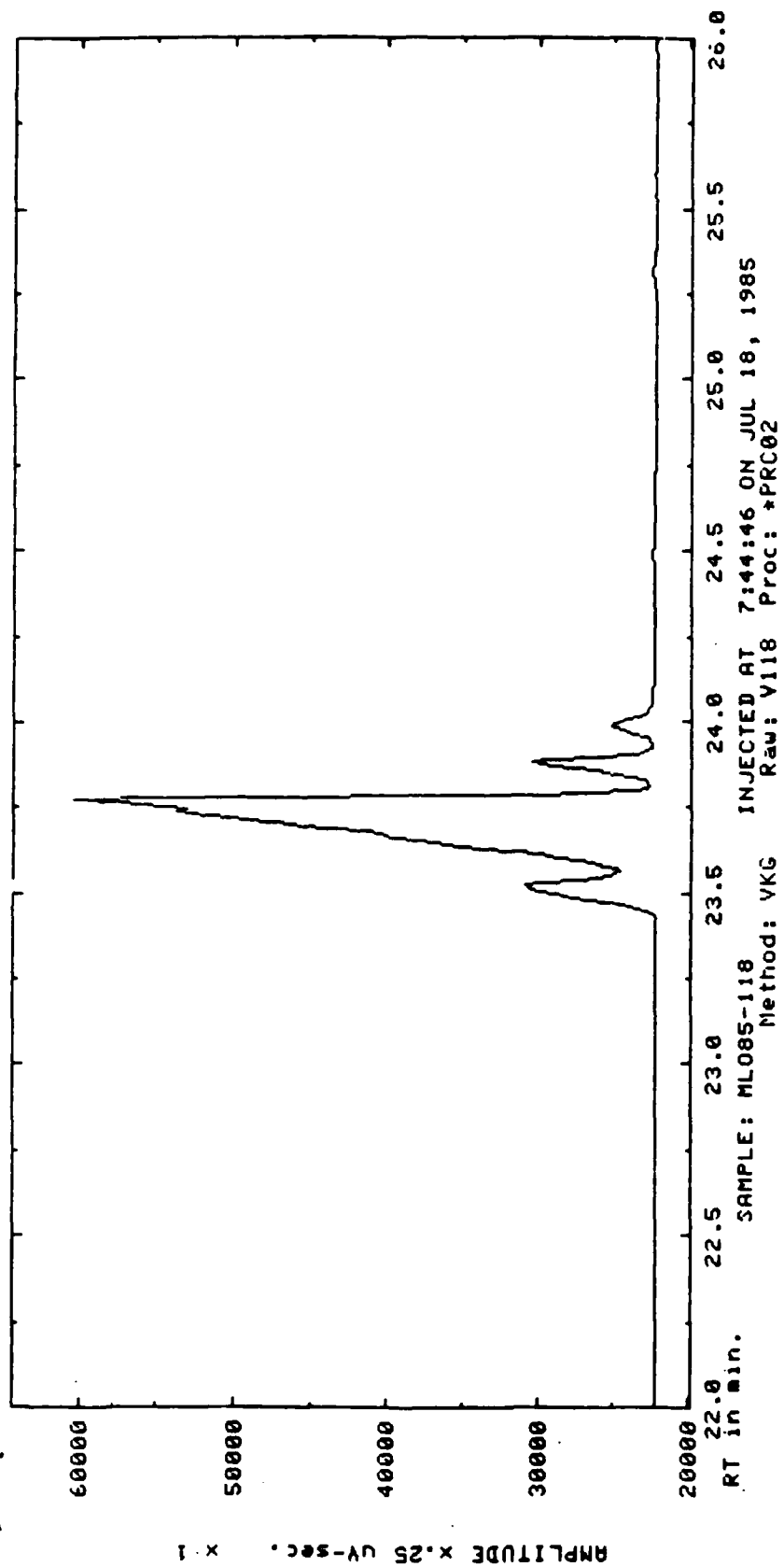


Fig. 1: Capillary GC of MLO 85-118

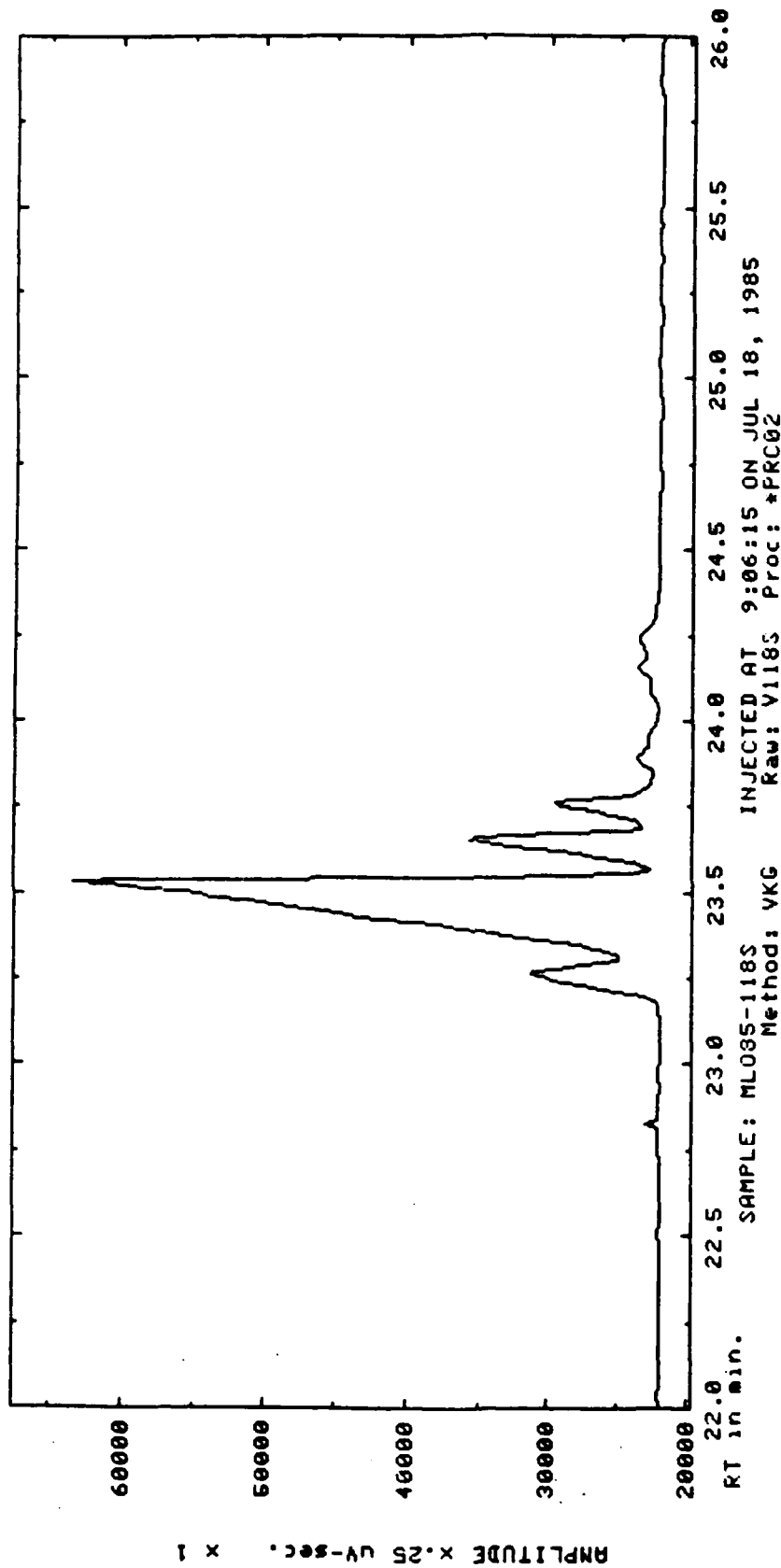


Fig. 2: Capillary GC of MLO 85-118 Stressed at 315.6 C for 6 hours

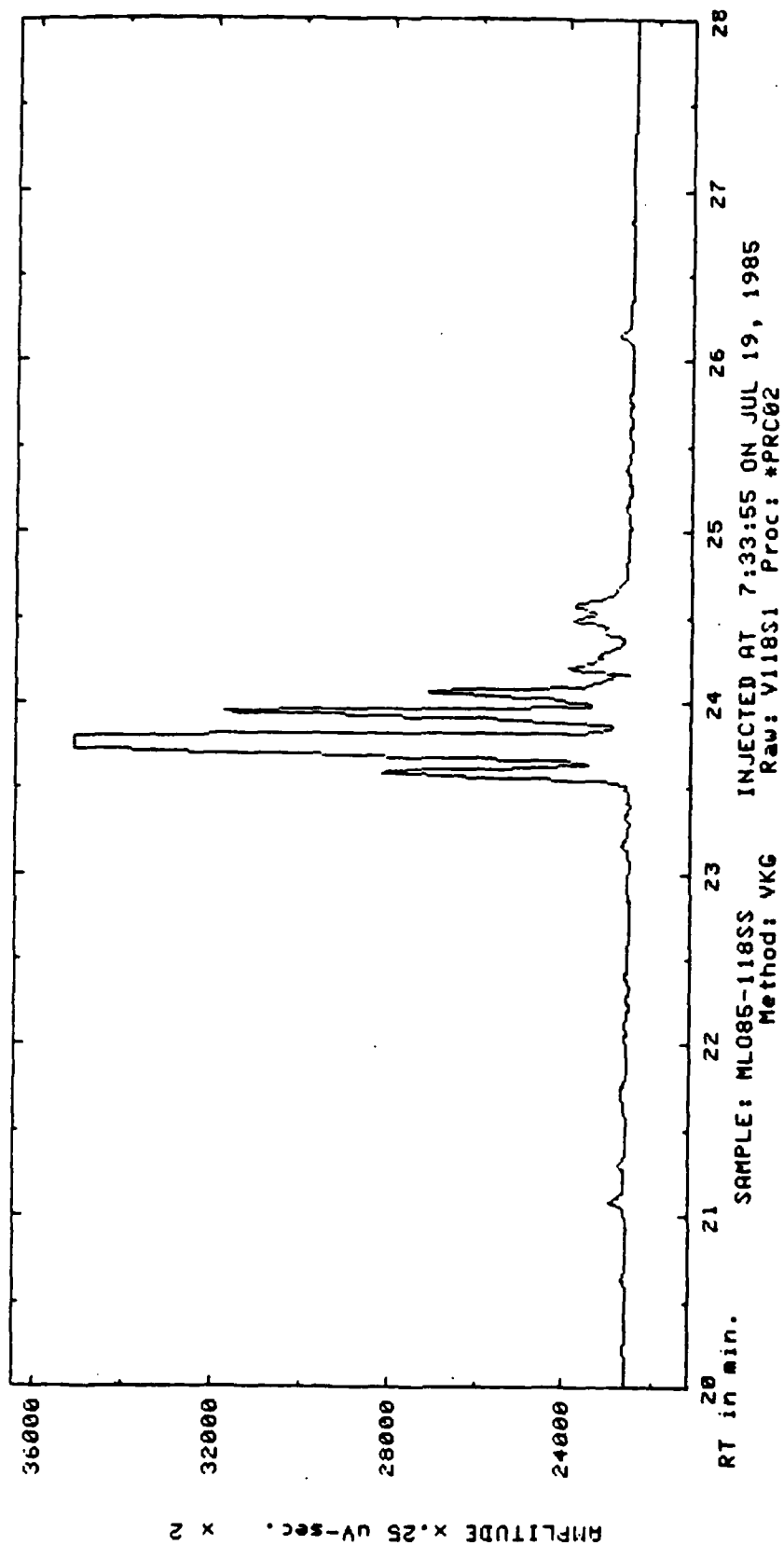


Fig. 2: Capillary GC of MLO 35-118 Stressed at 315.6 C for 12 hours

SAMPLE: MLO85-118SS
Method: VKG
INJECTED AT 7:33:55 ON JUL 19, 1985
Raw: V118S1 Proc: *PRC02

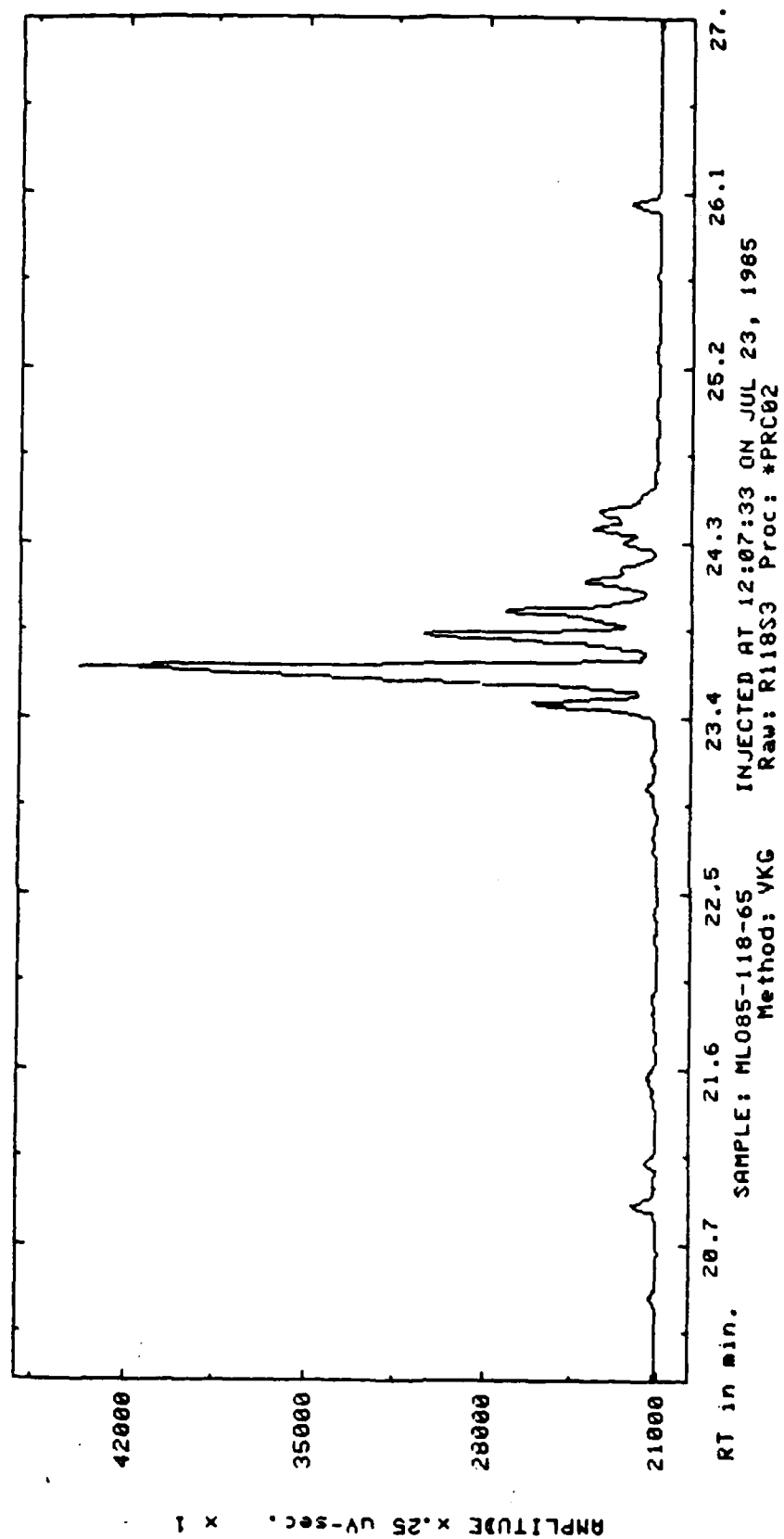


Fig. 4: Capillary GC of MLO 85-118 Stressed at 343.3 C for 6 hours

011

39.25

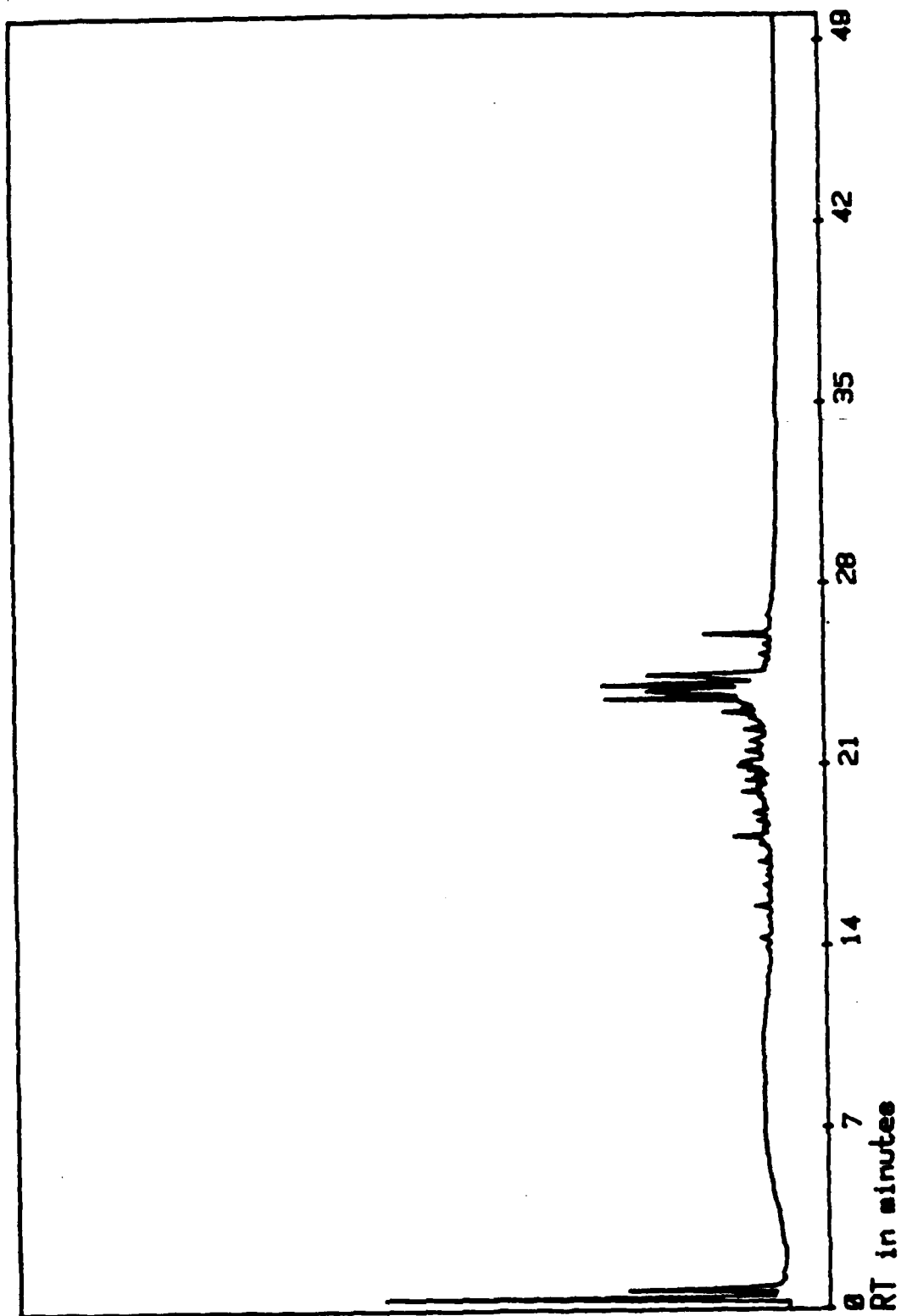
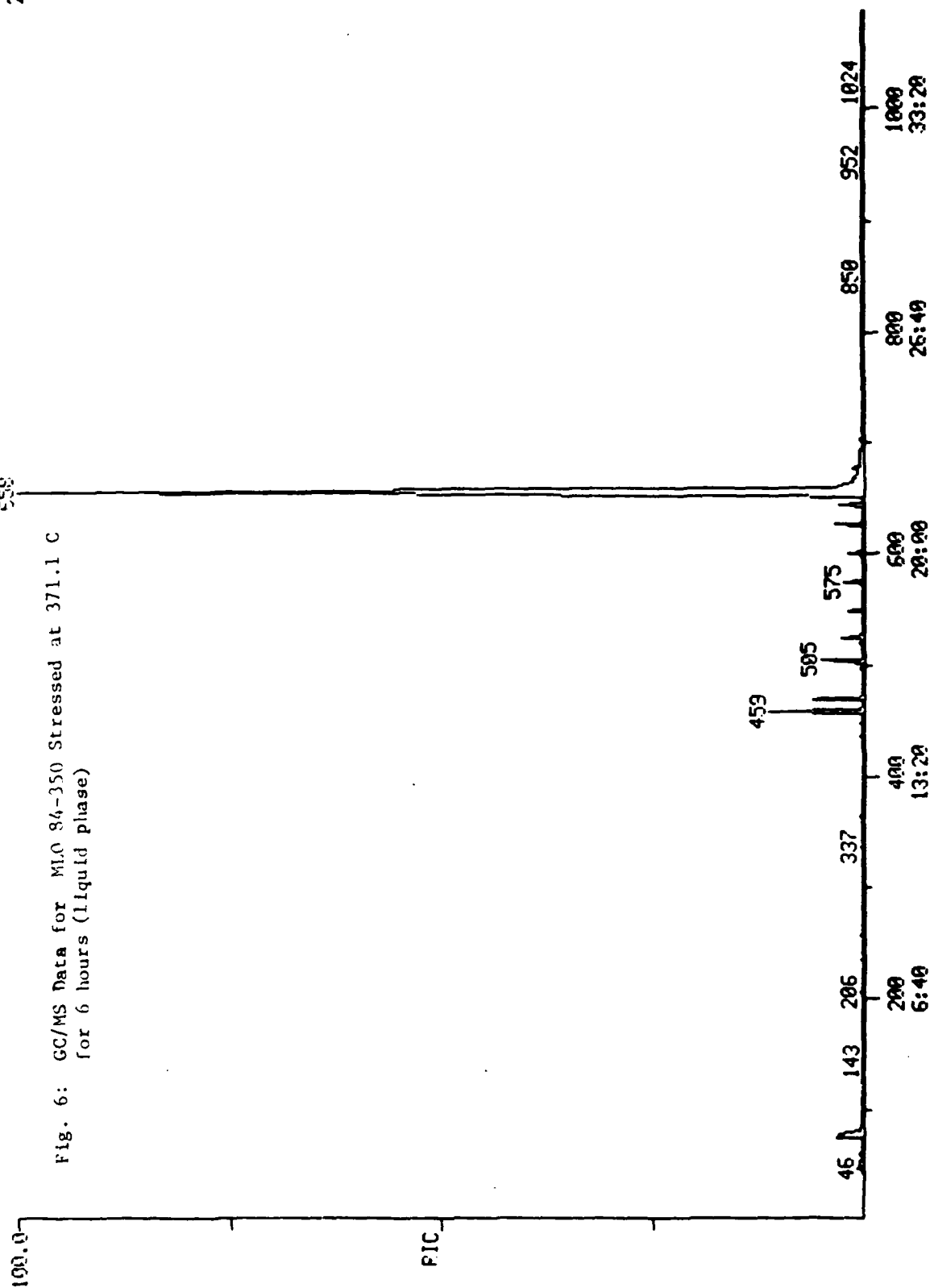


Fig. 5: CAPILLARY GC OF MLD85-118 AFTER 700F MTS 3rd RUN (6 Hours)

PIC
10/26/84 13:53:00
SAMPLE: L-3501
CONDS.: ET
RANGE: G 1.1088 LABEL: H 0. 4.0 RUN#: H 0. 1.0 J 0 BASE: U 20. 3

DATE: 23275 #1
CALL: CAL14 #1
SCANS 1 TO 1089

2174970.



RIC
04/19/85 13:00:00
SAMPLE: ML085-118
CONDS.: EI
RANGE: G 1, 431

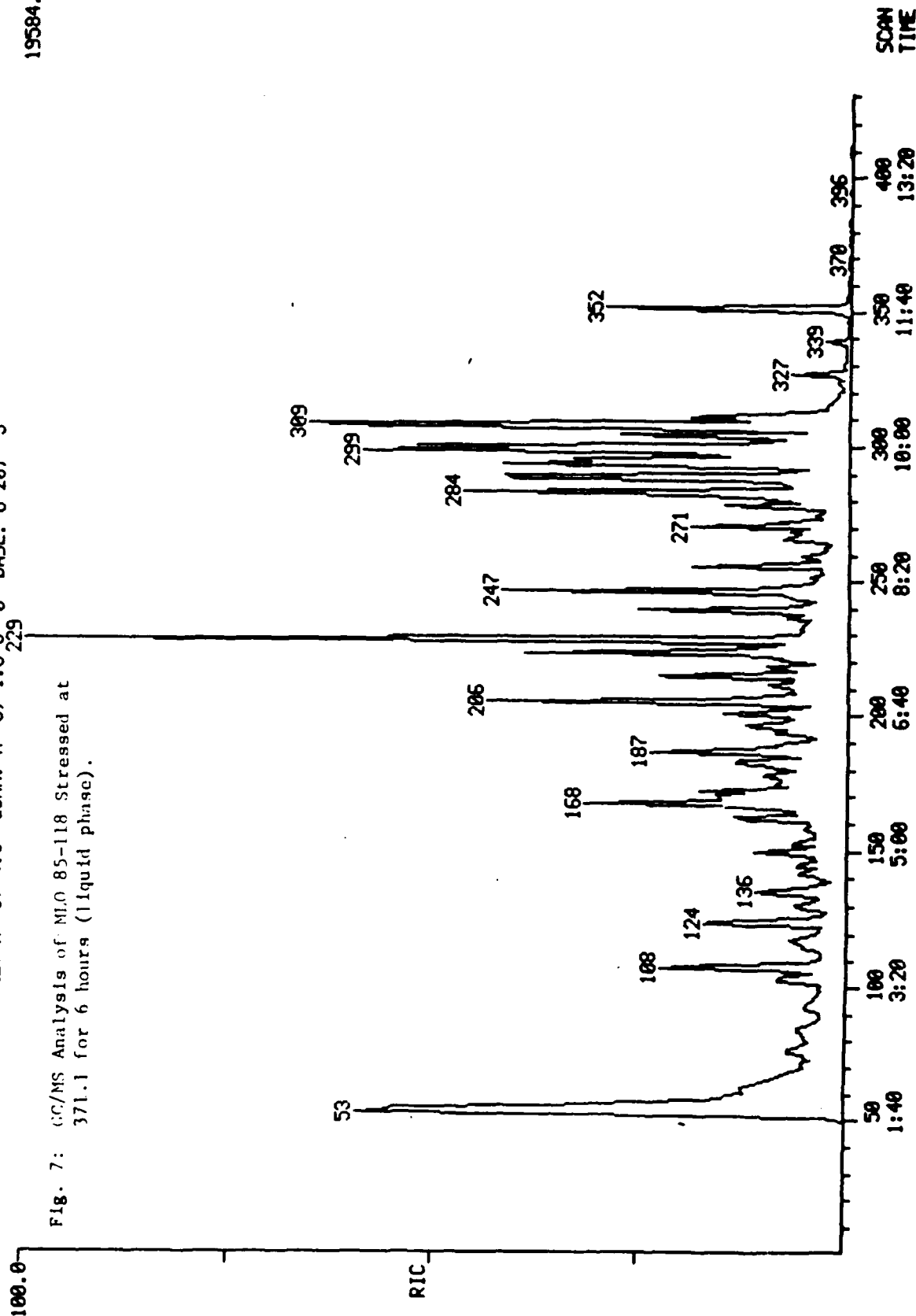
DATA: 30530A #1
CALI: CALI #3

SCANS 1 TO 431

LABEL: N 0, 4.0 QUAN: A 0, 1.0 J 0 BASE: U 20, 3

19584.

Fig. 7: GC/MS Analysis of MLO 85-118 Stressed at
371.1 for 6 hours (liquid phase).



RIC
04/18/85 9:54:00
SAMPLE: MLO-85-119
CONDS.: EI
RANGE: C 1, 549 LABEL: N 0, 4.0 QUAN: A 0, 1.0 J 0 BASE: U 20, 3

DATA: 30529A #1
CALI: CALI1 #3
SCANS 1 TO 549

330240.

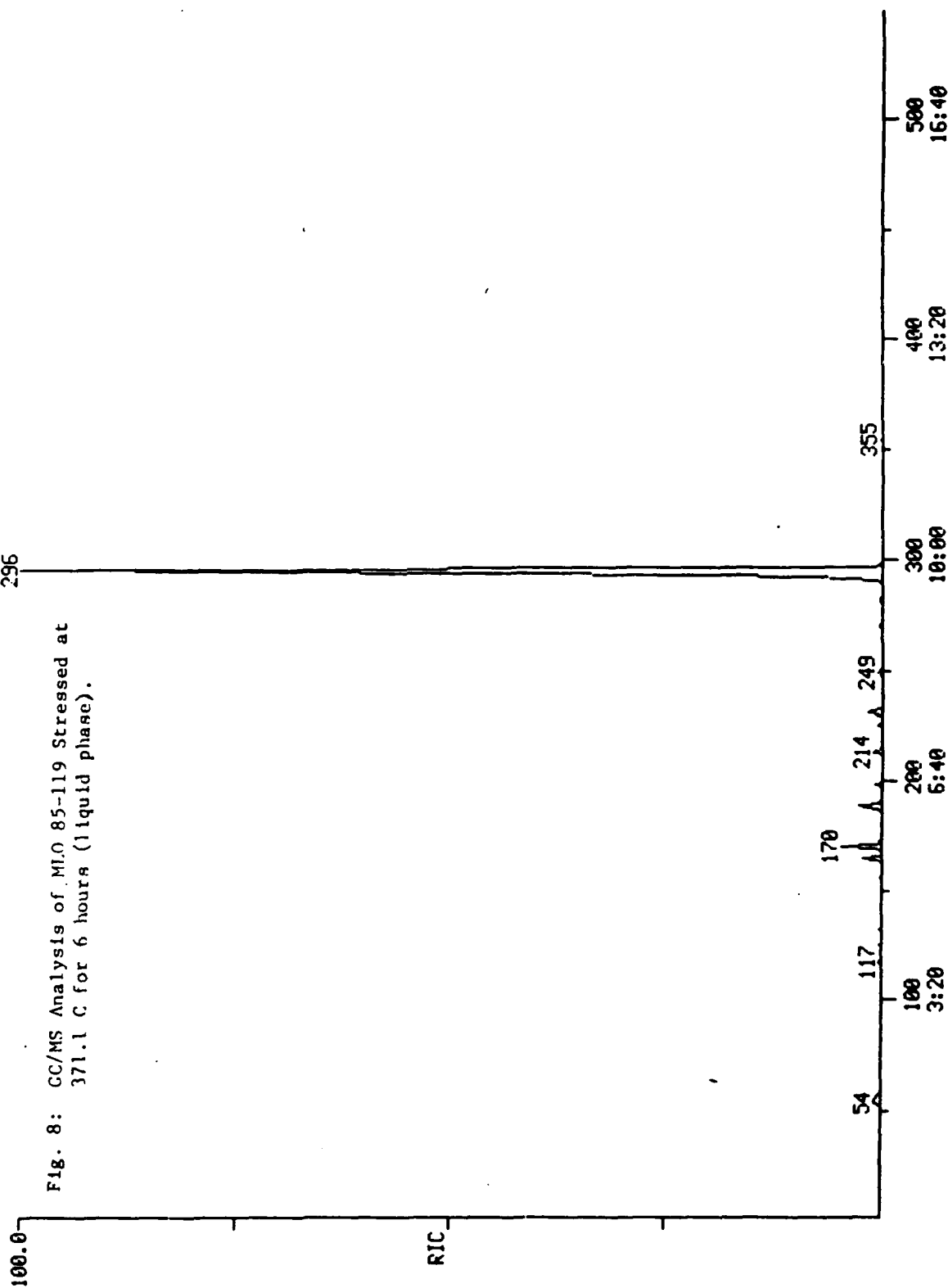
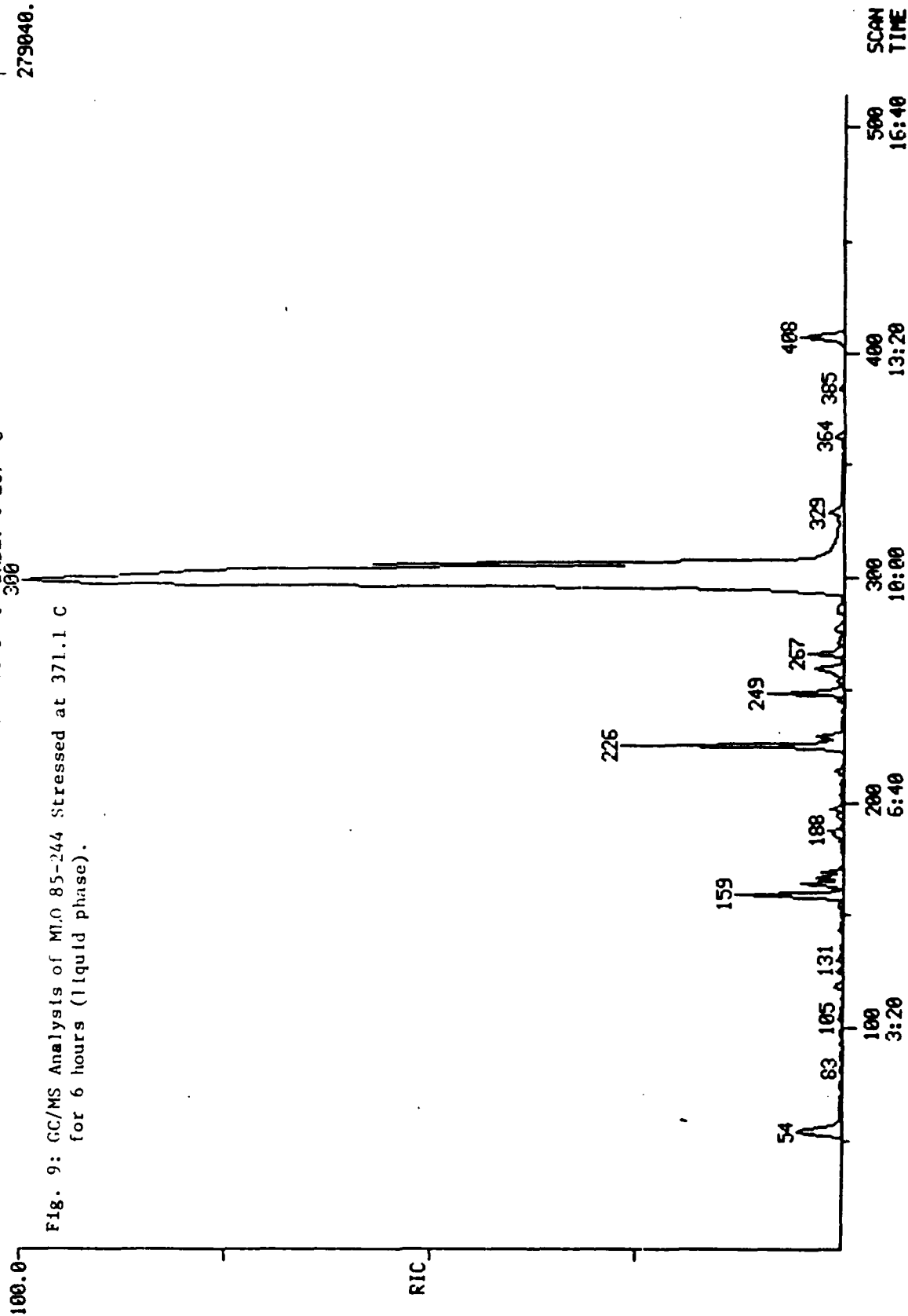


Fig. 8: GC/MS Analysis of MLO 85-119 Stressed at 371.1 C for 6 hours (liquid phase).

RIC
06/03/85 15:13:00
SAMPLE: ML085-244
CONDOS.: EI
RANGE: G 1, 514 LABEL: N 0, 4.0 QUAN: A 0, 1.0 J 0 BASE: U 20, 3

DATA: 30829 #1
CALI: CAL11 #3
SCANS 1 TO 514

279040.



REFERENCES

1. Snyder, C.E. Jr., Gschwender, L.J. and Tamborski, C., "Synthesis and Characterization of Silahydrocarbons - A Class of Thermally Stable Wide-liquid Range Functional Fluids", ASLE Trans. 25, 299-303 (1981).
2. Snyder, C.E. Jr., Tamborski, C. Gschwender, L.J. and Chen, G.J., "Development of High Temperature (-40°C to 288°C) Hydraulic Fluids for Advanced Aerospace Applications", ASLE Preprint No. 80-IC-IC-1.
3. Snyder, C.E. Jr., and Gschwender, L.J., "Development of a Non-flammable Hydraulic Fluid for Aerospace Applications over -54°C to 315°C Temperature Range", Lubr. Engr. 36, 458 (1980).
4. Gupta, V.K., and Weatherby, D.W., "Thermal Stability Characteristics of Silahydrocarbons", Final Report, Contract # F49620-82-C-0035, submitted to South Central Electrical Engineering Education, Miami, Florida, September (1984).
5. Gupta, V.K., Sawyer, William, and Tuggle, Lenae., "Thermal Stability Characteristics of Some Advanced Synthetic Base Fluids", Final Report, Contract No. F49620-85-C-0013, submitted to Universal Energy Systems Inc., September (1985).

1984 USAF-SCEEE RESEARCH INITIATION PROGRAM

Sponsored by the

AIR FORCE OFFICE OF SCIENTIFIC RESEARCH

Conducted by the

SOUTHEASTERN CENTER FOR ELECTRICAL ENGINEERING EDUCATION

FINAL REPORT

SILANE-TREATED SILICA FILLERS FOR
USE IN FULRORSILICONE ELASTOMERS

Prepared by: Larry M. Ludwick

INTRODUCTION

Fumed silica, such as the Cab-O-Sil products produced by the Cabot Corporation, are used extensively as fillers in silicone and fluorosilicone elastomers. Surface treatment of the silica with silanes produces a filler with improved characteristics in the milling process as well as an elastomer with enhanced physical properties. A preliminary study used Cab-O-Sil M-5 for extensive evaluation with various treatment procedures. In addition, during this study a trial using a different filler indicated that an improved elastomer could be produced by increasing the surface area of the filler. The object of this work was to determine the effect of the surface area of the silica fillers, as well as the effect of various surface treatments, on the properties of compounded elastomers. This included the determination of the extent of the silane surface reaction.

EXPERIMENTAL

Materials

Fumed silica (shown on Table 1) were obtained from the Cabot Corporation. These fillers provide a four-fold variation in surface area. The table also lists the physical properties (surface area, particle diameter and average OH groups per gram) as published by the manufacturer.

Hexamethyldisilazane (HMDS) and 1,4-divinyldimethyltetramethyldisilazane (DVMS) were obtained from Petrarch Systems, Inc., and used without further purification. Solvents (toluene and methylene chloride) were used as obtained from Fisher Scientific.

Silastic LS420, a polysiloxane with methyl, trifluoropropyl and vinyl groups attached, was obtained from Dow Corning Corporation.

Treated Fillers

The fumed silica fillers were treated with varying quantities of a solution of hexamethyldisilazane and 0-10 mol% 1,4-divinyldimethyltetramethyldisilazane in toluene. The usual procedure used 20.0 g of the filler dispersed in 600-700 mL toluene with a Ross Micro Mixer-Emulsifier. The amount of solvent varied to assure adequate mixing of the thick mixture. One mL of water was added and blended for about 5 minutes. The disilazane mixture was then added with continued

blending. The mixer was removed and replaced by a magnetic stirrer. The mixture was heated to about 100°C (until it became translucent) and then allowed to cool overnight. The mixture was vacuum filtered and the solid air dried. Final drying was for about 4 hours at 150°C. Additional samples of the Cab-O-Sil M-5 were treated in an analogous manner without the addition of water.

The amounts of disilazane mixture added were based on the published concentration of OH groups per gram for each filler. Thus the amount of the disilazane mixture used for a given treatment level varies from filler to filler when expressed as moles per kilogram filler. The amounts used are expressed as the fraction (X) needed for complete reaction, assuming two OH groups react per disilazane molecule.

Compounding

The fillers (treated and untreated) were compounded with Silastic LS420 according to the following formulation

50.0 g Silastic LS 420
20.0 g filler
1.0 g Luperco CST

Press Cure: 5 minutes at 240°F
Post Cure: 16 hours at 400°F

The silica filler was milled into the elastomer using a 3" x 8" two-roll mill. When the dispersion appeared complete the Luperco SCT was slowly added and followed by additional milling. Approximately thirty minutes were required for the entire process. The mixture was then removed from the mill and immediately press cured in a 6" x 6" x 0.050" mold. With the treated fillers, the tacky mixture had to be scraped from the mill using a putty knife. Although the flow characteristics of the compound were good, the finished sheets had variable thickness and occasionally showed flaws.

Physical Properties

The cured sheets were cut to accommodate the following tests:

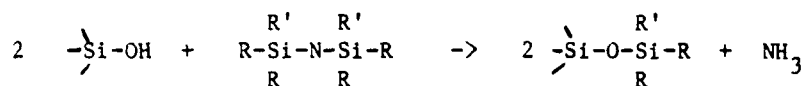
Hardness
Tear Strength, Die B
Tensile Strength, 1/8 inch (constricted width)
dumbbell
Elongation
50 % Modulus
100% Modulus
Compression Set (25% compression, 72 hr at 275°F)

Differential Scanning Calorimetry

Differential scanning calorimetry (DSC) data were obtained using a Perkin-Elmer DSC-4 with control and data storage using a Model 3600 Data Station. Samples (5 to 10 mg) were sealed in aluminum pans and heated in air at either 40 degrees per minute (50°C to 500°C) or 10 degrees per minute (300°C to 500°C). A baseline correction program was used in all cases.

RESULTS

The five fumed silica materials, shown in Table 1, encompassed a four-fold variation in surface area. All were treated with a mixture of disilazanes to provide a surface modified material according to the general reaction



where $\text{R} = \text{R}' = -\text{CH}_3$, HMDS
or $\text{R} = -\text{CH}_3$, $\text{R}' = -\text{CH}=\text{CH}_2$, DVMS

Incorporation of the vinyl functional group, using 1 to 10 mol% DVMS was intended to produce additional reaction sites for crosslinking in the elastomers and thus improve the physical properties.

The treatment level was determined based on the published silanol concentration (OH/nm^2) for each filler. The levels chosen were to provide partial (approximately half), nearly complete (stoichiometric) and complete (two-fold excess) coverage. The treatment procedure followed was that which gave the best results in the preliminary study. A micro-mixer-emulsifier was used to disperse the fillers in the solvent. This was followed by the addition of a small amount of water to ensure the maximum number of free silanols. The desired amount of disilazane solution was then added and the suspension heated to reflux and allowed to cool.

The results of the physical testing of the treated fillers, as compounded with the fluorosilicone elastomer, Silastic LS420, are shown in Tables 2 through 7. With the exception of the Cab-O-Sil M-5, only a limited amount of each was available and duplicate trials were impossible. The conclusions from the testing are complicated by the rather large variations which often occurred in test specimen cut from the same sheet. This is due in part to the stickiness in the compounded materials which made it difficult to remove from the roll mill and properly place in the mold. Nevertheless, some general conclusions seem evident.

In the case of the untreated fillers the surface area correlates with 50% and 100% moduli, hardness, percent compression set and tear strength. The increase in surface area produces a cured elastomer that is harder, with greater resistance to stretching and tearing. The rather large increase in percent compression set (nearly double) is consistent with an increase in available OH groups on the filler which react further under the pressure and temperature conditions of the test. Tensile strengths and percent elongation showed no discernable trend.

In all cases, treatment with the disilazane mixture produced silica fillers with improved properties, although the results do not appear to be entirely consistent for any given filler or treatment regimen. The fillers with the largest surface area produced the elastomers with the largest tensile strength, lowest moduli, the smallest compression set and the greatest tear strength. The change in properties is most particularly apparent in the reduced values for percent compression set. In the case of EH-5, the decrease was greater than fifty percent in all cases. Although the compression set values for the smallest surface area filler (L-90) are nearly the same as those for EH-5, the change with surface treatment is far smaller. In the case of HS-5, with only slightly smaller surface area than EH-5, the compression set remains nearly unaffected by treatment. Factors other than particle size and surface area must distinguish between these two fillers. The results with other physical tests do not show the same behavior.

The presence of the vinyl group does not appear to have a consistent affect on the properties of the formulated elastomers. A 1 mol% DVMS treatment does appear to present the best properties but there is no apparent trend in comparison with 5 and 10 mol% treatments.

Attempts to quantify the presence of the silanes, particularly the vinyl groups, with infra red spectroscopy proved unsuccessful with the techniques and time available. With a KBr disk the absorptions were visible but could not be quantified. Additional investigations will be conducted using infra red spectroscopy.

Using differential scanning calorimetry (DSC) on the treated fillers in oxygen revealed a strong exothermic peak. The exotherm is not reversible and occurs with an onset temperature between 360 and 380°C and a maximum of about 400°C. The peak is completely absent when the sample is heated to 510°C under nitrogen. It is likely that the peak is the result of a radical reaction between the oxygen and the silanoxane surface group. The magnitude of the exotherm correlates reasonably well with the extent of surface treatment as shown by the results on Table 8.

The DSC results do not appear to distinguish between the methyl and the vinyl functional groups. The results on Table 9 show essentially the same results without regard to the percent of the divinyl disilazane in the treating mixture. Preliminary work with a lower treatment level of 0.5 X shows the presence of two exothermic peaks which change with the concentration of vinyl. However the trend is unexpected with two peaks appearing when no vinyl group is present and only one peak appearing when the vinyl concentration approaches 10%. Further

experimentation is needed to verify this result before an explanation can be suggested.

Table 10 shows the effect of surface area using DSC. The amount of reaction observed, reported in cal/gram, varies directly with the surface area of the filler. As expected, with an increase in the surface area there is a larger amount of disilazane incorporated. This correlation does not appear when comparing the physical testing of these samples. As noted before, this may be due in part to the excessive variability frequently encountered when compounding and testing a single sample.

SUMMARY

The results of this work have shown that the surface area of the fumed silica fillers affects the physical performance of the compounded elastomers. Although discrepancies exist with individual test results, the fillers with the largest surface area give the elastomers with the most improved properties. DSC data show that the amount of disilazane incorporated depends of the surface area of the filler and reaches a maximum at approximately the stoichiometric ratio calculated from the published surface area. The presence of the vinyl group does not appear to be a major factor and as yet has not been quantified.

TABLE 1

Cab-O-Sil	Surface Area (m ² /g)	Diameter (μm)	OH/g
L-90	90 (±15)	0.024	4 x 10 ²⁰
LM-130	130 (±15)	0.018	5 x 10 ²⁰
M-5	200 (±25)	0.014	8 x 10 ²⁰
HS-5	325 (±25)	0.008	13 x 10 ²⁰
EH-5	380 (±30)	0.007	15 x 10 ²⁰

All values from Cabot Corporation publication.

TABLE 2

Test Results Using Cab-O-Sil L-90

Treatment ^a	Tensile Strength (lb/in ²)	Modulus		Shore A Hardness	Elong (%)	25% Comp. Set (%)	Tear (lb/in)
		50%	100%				
		(lb/in ²)	(lb/in ²)				
None	890	260	510	62	170	22	66
0.5X 5%	990	180	420	53	180	14	72
1X 5% ^b	860	170	410	53	140	10	68
4X 5%	940	160	380	50	180	9	77
1X 1%	850	160	400	52	170	8	69
1X 5% ^b	860	170	410	53	140	10	68
1X 10%	950	170	370	51	200	16	68

^aCalculated fraction OH groups reacted, % DVMS in treating mixture^bSame Trial

TABLE 3

Test Results Using Cab-O-Sil LM-130

Treatment ^a	Tensile Strength (lb/in ²)	Modulus		Shore A Hardness	Elong (%)	25% Comp. Set (%)	Tear (lb/in)
		50%	100%				
None	910	270	530	70	160	23	74
0.5X 5%	970	200	430	57	190	18	66
1X 5% ^b	730	170	390	53	170	16	61
4X 5%	920	150	360	50	190	15	66
1X 1%	810	160	400	51	180	18	65
1X 5% ^b	730	170	390	53	170	16	61
1X 10%	690	170	360	53	170	16	61

^a Calculated fraction OH groups reacted, 1.00% = 100% reacted.^b Same Trial

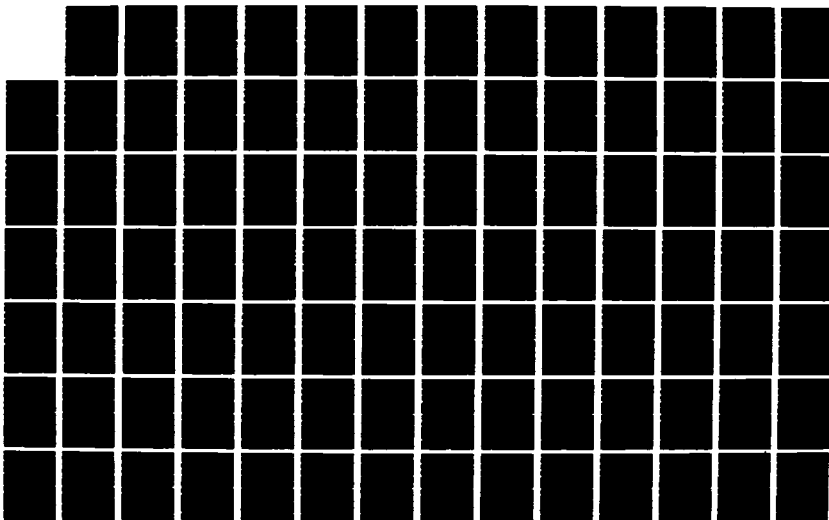
AD-A187 859

UNITED STATES AIR FORCE RESEARCH INITIATION PROGRAM
1984 RESEARCH REPORTS (U) SOUTHEASTERN CENTER FOR
ELECTRICAL ENGINEERING EDUCATION INC S W D PEELE
MAY 86 AFOSR-TR-87-1722 FF9620-82-C-0035 F/G 7/2

01/10

UNCLASSIFIED

NL



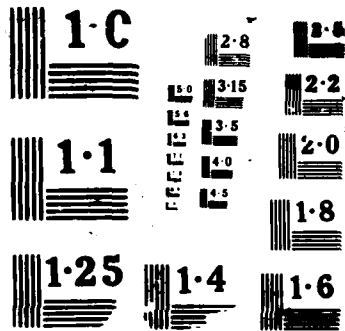


TABLE 4

Test Results Using Cab-O-Sil M-5

Treatment ^a	Tensile Strength (lb/in ²)	Modulus 50% 100% (lb/in ²)		Shore A Hardness	Elong (%)	25% Comp. Set (%)	Tear (lb/in)
None	840	310	520	73	160	32	78
None	750	310	520	72	150	34	76
None	890	380	580	75	160	33	85
0.5X 5%	1000	220	430	61	210	20	77
1X 5% ^b	960	210	400	55	220	22	72
2X 5%	820	170	340	50	210	29	66
1X 1%	1080	190	370	51	230	19	76
1X 5% ^b	960	210	400	55	220	22	72
1X 10%	960	190	350	54	240	26	75

^aCalculated fraction OH groups reacted, % DVMS in treating mixture^bSame Trial

TABLE 5

Test Results Using Cab-O-Sil M-5

Treatment ^a 1% DVMS	Tensile Strength (lb/in ²)	Modulus 50% 100% (lb/in ²)		Shore A Hardness	Elong (%)	25% Comp. Set (%)	Tear (lb/in)
None	820	350	640	76	140	36	71
0.25 X	1120	320	610	71	180	29	85
0.50 X	820	240	520	64	150	25	74
0.75 X	860	210	440	61	190	28	75
1.0 X	1130	200	450	58	190	18	85
1.5 X	760	190	440	56	140	15	82

^a No water added during filler treatment.

TABLE 6

Test Results Using Cab-O-Sil HS-5

Treatment ^a	Tensile Strength (lb/in ²)	Modulus		Shore A Hardness	Elong (%)	25% Comp. Set (%)	Tear (lb/in)
		50%	100%				
		(lb/in ²)	(lb/in ²)				
None	850	380	620	74	150	31	110
1X 5% ^b	900	160	300	53	240	30	80
2X 5%	640	140	270	49	210	33	73
1X 1%	1050	150	310	51	240	26	76
1X 5% ^b	900	160	300	53	240	30	80
1X 10%	730	170	350	55	190	26	86

^aCalculated fraction OH groups reacted, % DVMS in treating mixture

^bSame Trial

TABLE 7

Test Results Using Cab-O-Sil EH-5

Treatment ^a	Tensile Strength (lb/in ²)	Modulus 50% 100% (lb/in ²)		Shore A Hardness	Elong (%)	25% Comp.Set (%)	Tear (lb/in)
None	880	430	660	78	160	42	97
0.5X 5%	1110	170	330	53	270	14	85
1X 5% ^b	780	140	290	48	230	18	72
2X 5%	870	160	320	51	220	9	102
1X 1%	1280	150	320	51	310	15	87
1X 5% ^b	780	140	290	48	230	18	72
1X 10%	940	200	360	56	250	18	85

^aCalculated fraction OH groups reacted, % DVMS in treating mixture^bSame Trial

TABLE 8

Differential Scanning Calorimetry^a of Treated Cab-O-Sil M-5

Treatment Level ^b	Onset (deg C)	Maximum (deg C)	Heat (cal/gram)
0.25 X	389	418	-11 ^c
0.50 X	362	399	-39
0.75 X	369	409	-45
1.0 X	368	401	-58

^aAll values were obtained using heating rate of 40 deg/min.

Later work used 10 deg/min to give more reproducible results.

^b1 mol% DVMS

^cvery broad peak

TABLE 9

Differential Scanning Calorimetry^a of Surface Treated Cab-O-Sil M-5

Treatment Level	Onset (deg C)	Maximum (deg C)	Heat (cal/gram)
2 X 10% DVMS	386	401	-53
2 X 5% DVMS	381	409	-54
2 X 0% DVMS	384	404	-67
1 X 10% DVMS	394	414	-44
1 X 5% DVMS	380	399	-61
1 X 1% DVMS	372	406	-45
1 X 0% DVMS	368	406	-50

^aHeating Rate = 40 deg/min

TABLE 10

Differential Scanning Calorimetry^a of Surface Treated Silica Fillers^b

Cab-O-Sil	Surface Area (m ² /g)	Onset (deg C)	Peak (deg C)	Heat (cal/gram)
L-90	90	381	395	-36
LM-130	130	386	402	-49
M-5	200	374	389	-104
HS-5	325	383	395	-134
EH-5	380	386	397	-148

^aHeating Rate = 10 deg/min^bTreatment Level 1 X 1% DVMS

1984-85 Research Initiation Program (RIP)

SPONSORED BY THE:

AIR FORCE OFFICE OF SCIENTIFIC RESEARCH
Special Faculty Programs AFOSR/XOT
Air Force Systems Command
United States Air Force

Conducted by the

SOUTHEASTERN CENTER FOR ELECTRICAL ENGINEERING EDUCATION
SCEEE Management Office
1101 Massachusetts Ave
St. Cloud, FL 32769

FINAL REPORT

RAMAN SPECTROSCOPIC STUDIES IN EXTRINSIC P-TYPE SILICON

Prepared by:	Dr. James Schneider
Research Location:	Physics Department University of Dayton Dayton, Ohio 45469
Completion Date	December 14, 1985
Contract No.:	F49620-82-C-0035
Subcontract No.:	84 RIP 41

RAMAN SPECTROSCOPIC STUDIES IN EXTRINSIC P-TYPE SILICON

James Schneider

ABSTRACT

The research conducted during this Research Initiation (RIP) Program was a direct follow-on project from work conducted under a 1984 USAF-SCEEE Summer Faculty Research Program (SFRP) at the Materials Laboratory of the Air Force Wright Aeronautical Laboratories. That earlier effort served as a feasibility study that clearly defined the experimental conditions necessary to examine electronic scattering in extrinsic p-type silicon samples by Raman spectroscopy. It was demonstrated in the work of this RIP program that near infrared laser light pulses from a Nd:YAG laser can permit one to effectively probe the bulk of the silicon material when at cryogenic temperatures since the absorption coefficient is low and the samples are sufficiently transparent at several wavelengths available from the Nd:YAG laser. A Raman scattering collection and detection system was assembled that has acceptable efficiency at these near IR wavelengths. New gratings were purchased and installed that were manufactured with the appropriate blaze wavelength of 1250 nm for grating efficiency at wavelengths just beyond 1064 nm and that were ruled with 600 grooves/mm to match the mechanical constraints of an existing double spectrometer. A state-of-the-art extended IR range photomultiplier detector was purchased and used effectively at near -40C in a new "supercooled" thermoelectric cooled housing. This new detector coupled with the gated electronics and digital photon counting system available for use with our pulsed IR laser permitted the collection of data with very small background level signals, even though some fluorescence was obviously coming from the silicon samples when used at temperatures above 4K. A persistent question remains in the literature concerning the existence of Raman active electronic scattering in silicon crystals conventionally doped with group IIIA elements such as boron, aluminum, gallium, indium, and thallium. Data from boron doped silicon material has been interpreted for years by some researchers as resulting from an electronic transition in that material. It is felt that if boron doped silicon has Raman active electronic transitions, then similar Raman active transitions are expected to exist in the other IIIA doped crystals at about the same energy, however these had not been previously reported. It was demonstrated clearly in this work with a series of boron doped silicon samples with doping levels of 2.4×10^{15} , 1.3×10^{16} , and 1.6×10^{17} that there is a Raman active electronic transition shifted by 184 cm^{-1} from the laser energy. Incident laser lines at 1064 nm, 1074 nm, 1116 nm, and 1123 nm were used. The intensities of the Raman active transition observed at 184 cm^{-1} followed the known doping levels of boron in the samples.

I. INTRODUCTION

The research and development of high quality extrinsic silicon material for the fabrication of infrared detectors to be used in operational systems is of continuing importance to the Air Force. The optical and electrical characterization of these materials is necessary for the scientific understanding of the mechanisms and properties that are to be employed in useful devices. Hall effect studies continue to be in the mainstream of techniques that yield interesting and useful details concerning the electrical transport properties of semiconducting materials. Visible and infrared absorption and emission spectroscopies are among the spectral characterization techniques that yield a great deal of information about the electronic excitations in semiconductors. Raman scattering spectroscopy is a useful tool for studying electronic transitions which may be forbidden by selection rules or which occur in experimentally inconvenient spectral regions for IR spectroscopy.

In this study, the application of Raman scattering spectroscopic techniques to silicon samples conventionally doped with one of the group IIIA elements such as boron, aluminum, gallium, indium, or thallium was considered. Silicon is a much studied, technologically important, material. The quality and purity of these crystals has been driven by their frequent use as the base materials for the fabrication of sophisticated devices. Among the open questions in silicon that could yield under the continued improvement in state-of-the-art experimental techniques and the availability of higher quality crystals is a better understanding of shallow p-type acceptor impurities such as the group IIIA elements. Raman spectroscopy has been used extensively to study phonon spectra and phonon interactions in pure and doped silicon,¹⁻⁷ but comparatively few researchers⁸⁻¹¹ have reported studies of electronic transitions in this semiconductor. In their now classic paper, Wright and Mooradian^{8,9} reported on Raman scattering from phosphorus donor and from boron acceptor impurities in silicon. They observed a rather weak, sharp line at 23.4 meV which was attributed to the boron acceptors. Jain, Lai and Klein¹¹ produced an extensive Raman scattering study of phosphorus-doped silicon which included some

observations concerning antimony and arsenic donor impurities in silicon. Their paper also contained a section concerning their observations on p-type acceptors in silicon. They reported a sharp line at 184 cm^{-1} (22.8 meV) in the Raman spectra of boron-doped silicon which was attributed to an electronic transition associated with the boron acceptor state. In addition, they reported unsuccessful attempts to observe similar transitions in aluminum-doped and gallium-doped silicon samples, and commented on not understanding this absence in their spectra.

Due to the extreme similarity of Group IIIA acceptor absorption spectra, it would seem reasonable to expect transitions similar to the reported boron electronic transition to occur in aluminum, gallium, indium, and thallium-doped silicon. To the best of our knowledge, attempts have only been made in aluminum and gallium-doped samples and these previous negative results were reported some years ago when silicon sample quality was less developed. As was pointed out by Klein¹² in a review on electronic scattering in semiconductors, it is generally felt that additional theoretical and experimental work is necessary for better understanding of acceptor states in silicon.

It is, however, not an easy experiment to undertake due to a combination of facts. Firstly, while the ratio of Raman to Rayleigh scattering intensities is generally in the order of 10^{-8} to 10^{-12} , with incident high-power lasers a Raman scattered intensity is, in general, readily detectable. However, Raman interactions in silicon, other than with the LO phonon, are known to be very weak. Signal levels are therefore very low and even small electronic noise such as dark current in the photomultiplier detector is a big problem. Secondly, since silicon is not transparent to visible light, lasers operating at near infrared wavelengths must be employed in order to probe the volume of the silicon samples. Detector sensitivity then becomes a problem at these IR wavelengths because the only photocathode that has any sensitivity in that spectral region is the S-1 cathode and its quantum efficiency for the production of photoelectrons is generally very poor.

II. NEAR IR RAMAN SCATTERING FACILITY

The laser Raman experimental set-up is based on a pulsed Nd:YAG laser, a SPEX model 1401 (0.85 m) double monochromator, photon counting detection, and a gated digital signal processing system. Figure 1 shows a schematic representation of this pulsed laser Raman spectroscopy system¹³. The laser is capable of operating in the burst, Q-switched mode which generates about 10 output pulses of approximately 200 nanosecond duration during each 150 to 200 microsecond long bursts when operated at 1064 nm. When the prism is adjusted for laser output at longer wavelengths, fewer output pulses occur during each burst. Burst rates are normally set at about 50 per second and the average power delivered is in the order of thirty to a hundred milliwatts, with peak power during each of the Q-switched pulses in the kilowatt range.

The basic idea of a pulsed system is to reduce unwanted detection of background signals due to certain fluorescences and from other stray light as well as photomultiplier dark current by gating the digital signal detection electronics "ON" only when there is temporal coincidence with an input laser pulse. A small portion of the incident

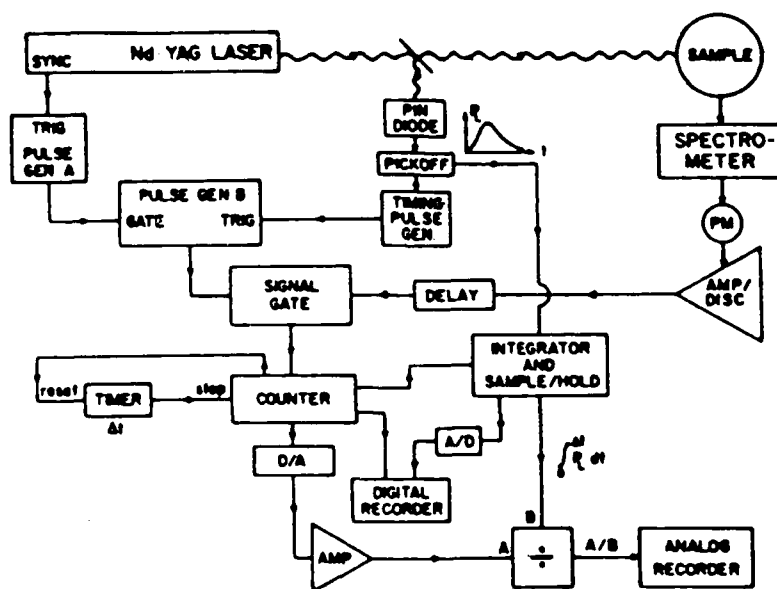


Figure 1. Schematic of Pulsed Laser Raman spectroscopy System

laser light pulse is reflected onto a PIN diode. The output of this diode unit serves both as a timing pulse and as a means to sample, monitor, and record the incident laser power. A Time Pickoff Unit (Ortec 260) feeds this pulse from the diode to an integrator and sample/hold unit that yields an analog signal representative of input laser power. This analog output is both digitized for digital recording and used as the denominator in a divider (PAR 230 Multiplier Unit) to give a normalized output for analog recording used to visually monitor scans. This same output from the PIN diode provides a timing pulse (Ortec 403) to trigger a pulse generator (pulse generator B in figure 1; Systron-Donner 100A Pulse Generator). Additionally, the synchronized output from the Chromatix laser lamp flash circuit is used to trigger another pulse generator (pulse generator A in figure 1; portion of PAR CW-1 Boxcar Integrator) that is used to feed the enable gate of pulse generator B in figure 1. In this configuration, pulse generator B provides an output pulse to open a gate to the digital counter (SSR 1120 Photon Counter) only during the time duration of each pulse of the laser, and spurious firing of pulse generator B is virtually eliminated. Since scattered photons detected by the photomultiplier on the exit slit of the spectrometer are counted by the digital counter only during the short time (100-200 ns) that the laser is active, background signal from photomultiplier dark current, fluorescence, ambient light, etc., are essentially reduced to near zero and weak Raman signals are observable. Typical operation is to hold a spectrometer setting for a fixed number of input laser pulses (e.g. 4000). The signal to noise ratio is improved at larger numbers of input pulses.

Three digital signals are recorded for each setting of the spectrometer, the scattered photon count from the counter, the digitized output from the integrator and sample/hold circuit that is proportional to the incident laser power, and a digitized signal from the spectrometer setting that gives the wavenumber shift measured from the incident laser wavelength. These three signals are processed through a PAR Series 260 multiplexer unit and recorded by an IBM PC/AT microcomputer for display and subsequent processing. The digital output of the photon counter is also converted to an analog signal for analog recording on an x-y plotter as an alternate operator monitor.

This pulsed laser Raman scattering system with gated electronics, photon counting detection and digital recording on magnetic tape was available prior to this work, but Raman studies had been done only in the visible. The NdYAG laser system has an internal doubling crystal for operation at 532 nm output. It was obvious from earlier efforts using this green light to probe near the surface of silicon that the 1064 nm line (or perhaps even longer wavelengths) from the YAG laser should be used to investigate impurities in doped silicon. At low temperatures, this corresponds to a region of low absorption and the volume of the sample can be probed. Several modifications were necessary in the experimental facility before a near infrared Raman system was operational. First, the existing spectrometer with a pair of 1200 g/mm gratings could not mechanically be turned past 1.0 micron position, and we needed to work in the 1064 to 1130 nm range. A pair of new gratings with 600 g/mm were purchased from Spex to meet the specifications of the existing double spectrometer. Thus with these gratings, 1064 nm (9400 cm^{-1}) light shows up at the mechanical position of the spectrometer marked 532 nm (18800 cm^{-1}). These gratings were blazed at 22 degrees (blaze wavelength 1.25 micron) for efficiency ranging from 88% at 1.15 micron to 86% at 1.25 microns.

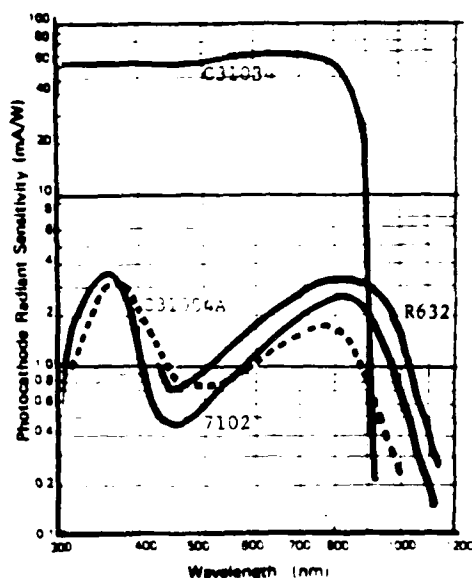


Figure 2. PM Spectral Response

Next, the existing (very efficient in the visible) C31034 end window photomultiplier had to be replaced by one with S1 response so that it possessed some reasonable sensitivity at wavelengths beyond 1064 to perhaps 1250 nm. While tubes with Ag-O-Cs photocathode materials all have the generic S-1 spectral response, side window tubes like the C31004A have reflective type photocathodes and show less sensitivity at the longer wavelengths. End window tubes with a transmissive photocathode on the inside of the glass like the 7102 and the R632 are a little better at the

longer wavelengths. We purchased the smaller diameter (1/2 inch) Hamamatsu R632-01 photomultiplier tube especially selected for high IR response relative to its total white light response. The smaller photocathode surface yields less dark current. Photomultiplier tubes with S1 photocathodes are known to be very noisy and consequently must be cooled to reduce dark current noise. Dark emission is reduced by about an order of magnitude for every 20 degrees cooling (Dark emission from 10^7 electrons per sec per cm^2 at +20C to $10^4 \text{ e s}^{-1} \text{ cm}^{-2}$ at -40C). A model TE210RF super-cooled photomultiplier housing was purchased from Products for Research for use with this tube. It is a water cooled thermoelectric device that maintains the PM tube at 60 degrees below ambient temperature to about -40C.

With the addition of new gratings and a new photomultiplier tube detector in a supercooled housing, an experimental facility was put into operation that was capable of pulsed infrared laser Raman scattering studies. During the time of these modifications and renovations in the system, IBM/XT and IBM/AT computers were also incorporated into the facility as the digital data recorder. Digital data taken earlier in this program was stored on magnetic tapes using the Texas Instruments Silent 700ASR Electronic Data Terminal. Then conversion was made to floppy disk data storage using a Radio Shack TRS80 Model IV microcomputer, to disk storage on an IBM/PC personal computer, to an IBM/XT, and finally an IBM/AT was incorporated into the system. Earlier graphs were presented by way of plots generated on a TRS80 Flatbed Plotter FP-215 using our own software programs. Starting with Figure 13 in this report, a change is noted in the display format. With conversion to the IBM/AT microcomputer we began using Macmillan Software Company's "ASYST" acquisition, analysis, and graphics package of software routines which allowed additional data manipulation and presentation options.

III. RAMAN SPECTRA OF BORON DOPED SILICON

Samples are mounted on a cold finger of an Air Products Heli-Tran using either liquid helium or liquid nitrogen as cryogenic fluids. Figure 3 shows a previous Raman spectra taken from a silicon sample with boron doping using a visible laser. The sample was at 4K and the Raman geometry was 180 degrees, or back scattering of the Raman scattered light from the direction of the incident laser beam. The spectra is plotted in the conventional manner as a wavenumber shift from the energy of the laser which is at zero on the right or high energy side of the plot. With back reflection geometry and opaque samples quite a bit of Raleigh scattered (energy conserved) light makes its way to the detector. The prominent feature is a "line" associated with the LO phonon in silicon shifted at 523 cm⁻¹ (64.9 meV) from the visible 532 nm (2.33 eV or 18797 cm⁻¹) laser line. This phonon energy is characteristic of the silicon crystal at this temperature and serves as a convenient "marker" and as a Raman line with which to peak up the alignment of the system. Between 100 and 500 cm⁻¹ on this spectrum

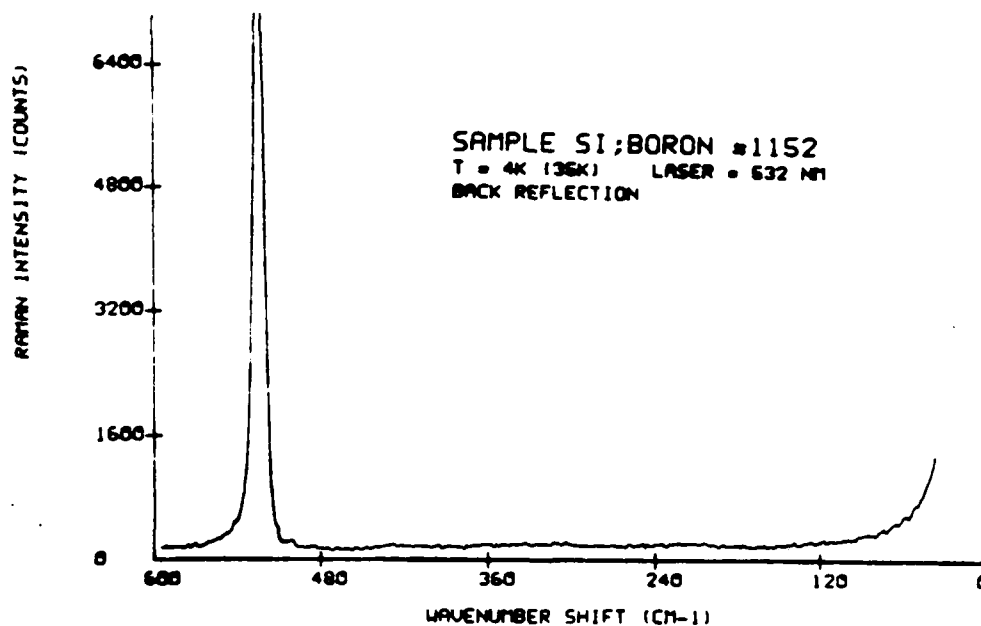


Figure 3. Raman Spectra of Silicon ; Back Refl.; 4K ; 532 nm Laser.

there is only noise background. No features associated with the boron dopant are discernable. In this spectra, each of the 306 data points taken every 1.8 cm⁻¹ represent the scattered photon count per 4000 incident laser pulses.

In the early part of this RIP program liquid helium was not available, so much of the experimental system check out while it was being converted to an infrared system was done taking data from samples at 77K. Figure 4 shows a Raman spectra from a boron doped silicon sample at 77K. In this experiment the Raman scattered light is collected and detected at 90 degrees to the incident IR laser beam which was at 1064 nm (1.165 eV or 9398 cm⁻¹). Again, the main feature is the LO phonon peak at 523 cm⁻¹ shift from the laser energy. Note that the Raman spectra is plotted as energy shift from the laser and is independent of the absolute value of the laser energy used in the experiment. The characteristic energy losses in the interactions with the sample are the parameters sought and observed in Raman scattering experiments. The broad "background" on this figure is fluorescence from just below band gap energy in silicon. Excitation of fluorescence is

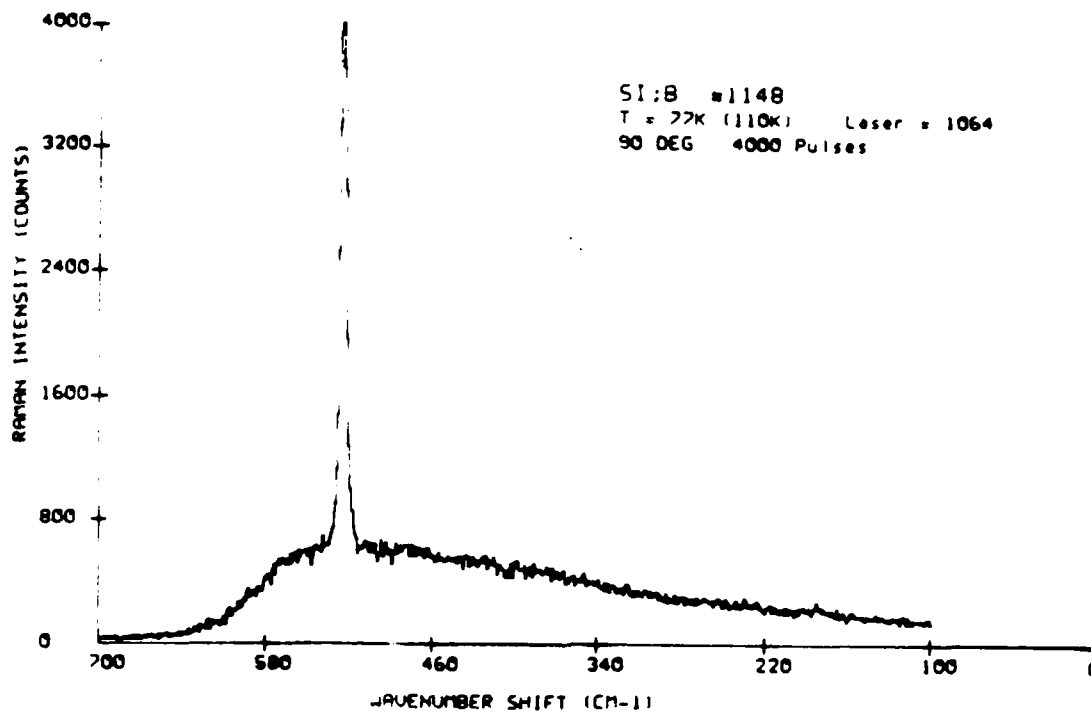


Figure 4. Raman Spectra of Silicon; 77K; 1064 nm Laser.

dependent on the laser energy used. The exciting photon energy must be greater than band gap energy in the material. The fluorescence occurs at absolute energy values just below band gap energy with wavelengths just longer than the wavelength of the band gap radiation. If that energy of this fluorescence happens to be in the same absolute wavenumber region as the energy shift of the Raman scattered light from the incident laser energy, then both are detected by the spectrometer and superimposed on the observed Raman spectrum.

As Figure 5 indicates, the energy of incident 1064 nm laser photons is slightly above the band gap energy of silicon, which changes from about 1.12 eV at room temperature to about 1.16 eV at cryogenic temperatures. Since these 1064 nm excitation photons are above band gap energy of silicon at 77K, recombination emission or fluorescence at energies just below band gap energy would be expected from the silicon.

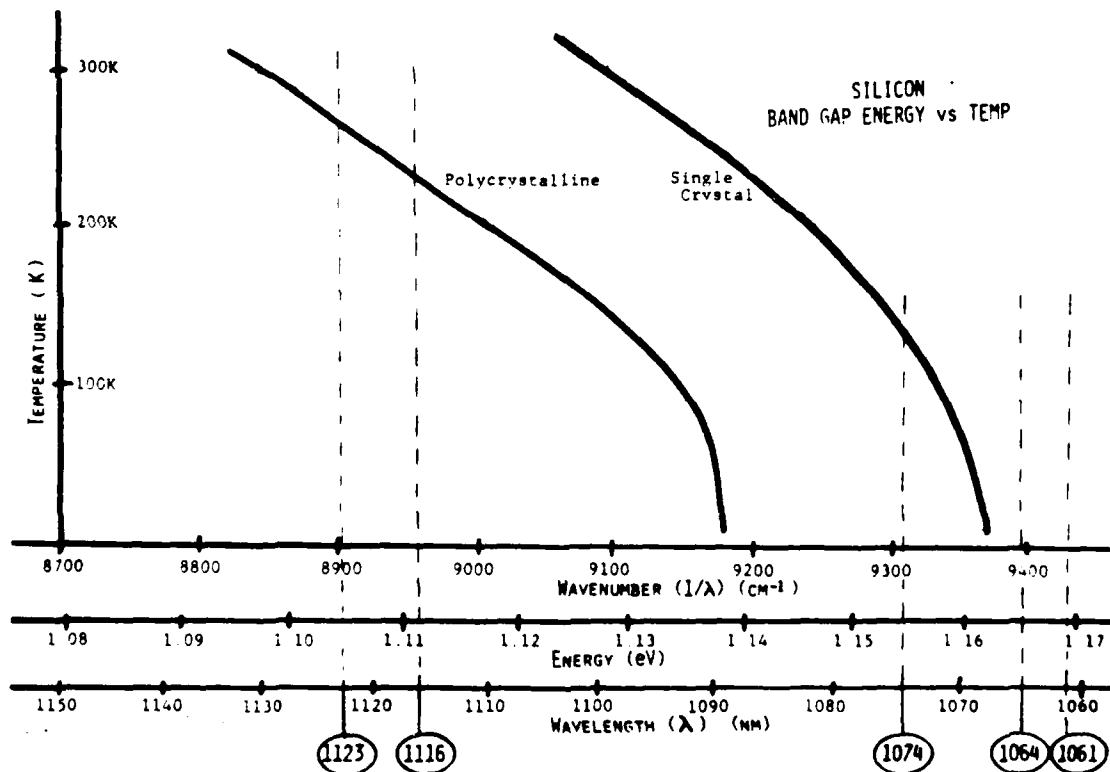


Figure 5. Band Gap Energy in Silicon vs Temperature.

Thus in figure 4, emissions at energies from about 1.09 eV (near 8800 cm^{-1}) to 1.14 eV (near 9200 cm^{-1}) would show up at 600 cm^{-1} to 200 cm^{-1} on the energy shift spectrum where zero represents the 1.165 eV (9398 cm^{-1}) of the incident laser photons. Even though the pulsed laser Raman system used here discriminates against fluorescence that occurs in time after the detection electronics have been turned off, that which occurs during the first 200 nanoseconds after the incident laser photon is detected by the system. In figure 3 on the other hand this fluorescence was not observed superimposed on the Raman energy-shift spectra because the 600 cm^{-1} range over which the spectrometer was swept is in the region 18200 cm^{-1} (2.25 eV and 550 nm) to 18797 cm^{-1} (2.33 eV and 532 nm). The near band gap fluorescence in silicon is still the vicinity of 9000 cm^{-1} (near 1.12 eV and 1110 nm) even though it may be excited by photons with twice that energy.

In order to probe the volume of the silicon crystals, IR laser radiation for which the absorption coefficient is low is necessary. The 1064 nm radiation from NdYAG is acceptable, but an even longer wavelength laser such as the 1074 nm line also available from NdYAG when the laser cavity contains a tuning prism is an even better choice. This 1074 nm line has an energy of 1.154 eV which is below the band gap energy of high quality single crystal silicon at cryogenic temperatures, and should excite little fluorescence noise in the spectra. Other lines such as the laser lines at 1116 nm and 1123 nm would perhaps be even better from the point of view avoiding fluorescence. On the other hand, going to longer wavelengths means that photomultiplier sensitivity is decreasing and overall detection efficiency is reduced. Also, the characteristics of the Q-switched laser cavity are different for these longer wavelengths. Instead of 8 to 10 pulses during each burst which occurs at 1064 and 1074 nm operation, only 1 or 2 pulses are available per burst when the laser is operated at 1116 nm or 1123 nm. This means that the time necessary to collect data from several thousand input pulses at each spectrometer setting is increased significantly. The use of the 1074 nm line seems a good compromise for Raman investigations in low temperature silicon, although some data has been collected at all the above mentioned laser wavelengths.

An important feature of our gated Raman system with a pulsed laser is the effect of an increase in the number of incident laser pulses used at each spectrometer setting. Since the electronics of the detection system are gated "ON" only during the 200 nanoseconds or so that the laser pulse exists and is "OFF" while it waits for the next laser pulse, the signal to noise ratio is increased by using more laser pulses at each setting. Noise is random in time, but signal can only occur only when an incident laser pulse exists. Figure 6 shows the spectrum at 77K of a silicon sample using 1000 pulses of 1074 nm laser light at each spectrometer setting. With the 1074 nm laser, near band gap fluorescence is much reduced by comparison to the case when 1064 nm light was used (figure 4). Again the only feature in the Raman spectrum is the LO phonon peak at 523 cm^{-1} from the laser energy. Figure 7a shows the Raman spectra of this same crystal at the same temperature and same collection geometry, but in this case 10,000 pulses of incident laser light were used at each spectrometer setting. The ratio of Raman

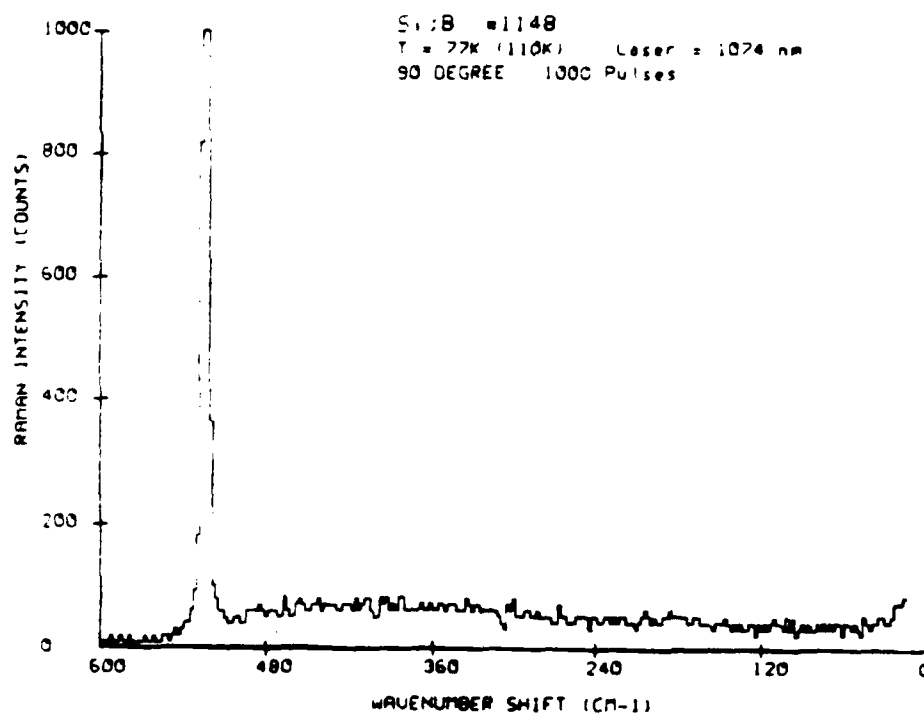


Figure 6. Raman Spectra of Si:B ; 77K ; 1000 Laser Pulses 1074 nm.

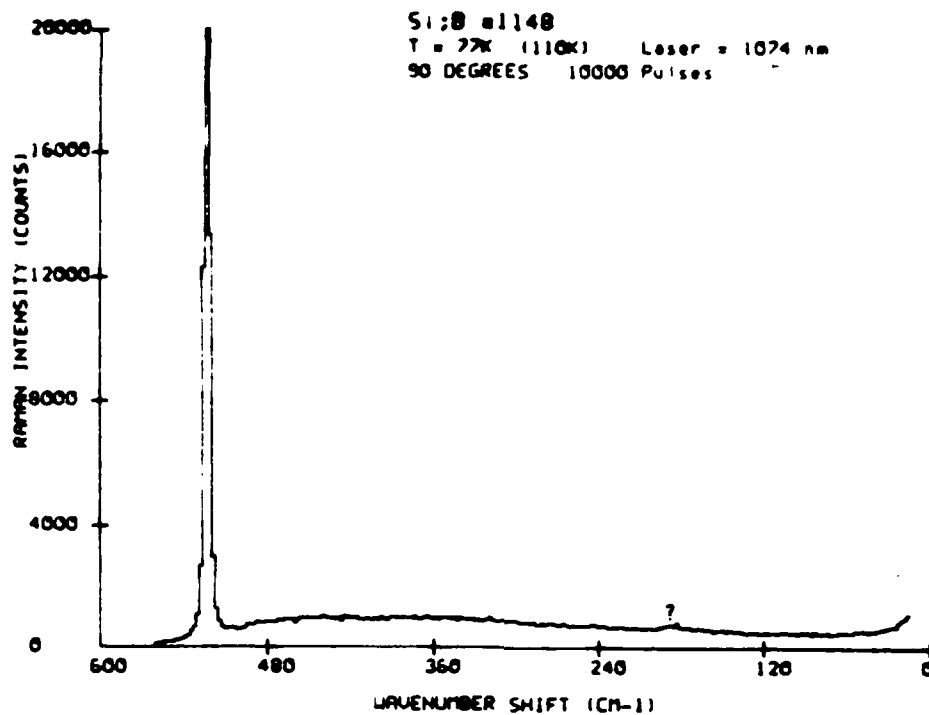


Figure 7a. Raman Spectra of Si:B ; 77K ; 10,000 Pulses 1074 nm.

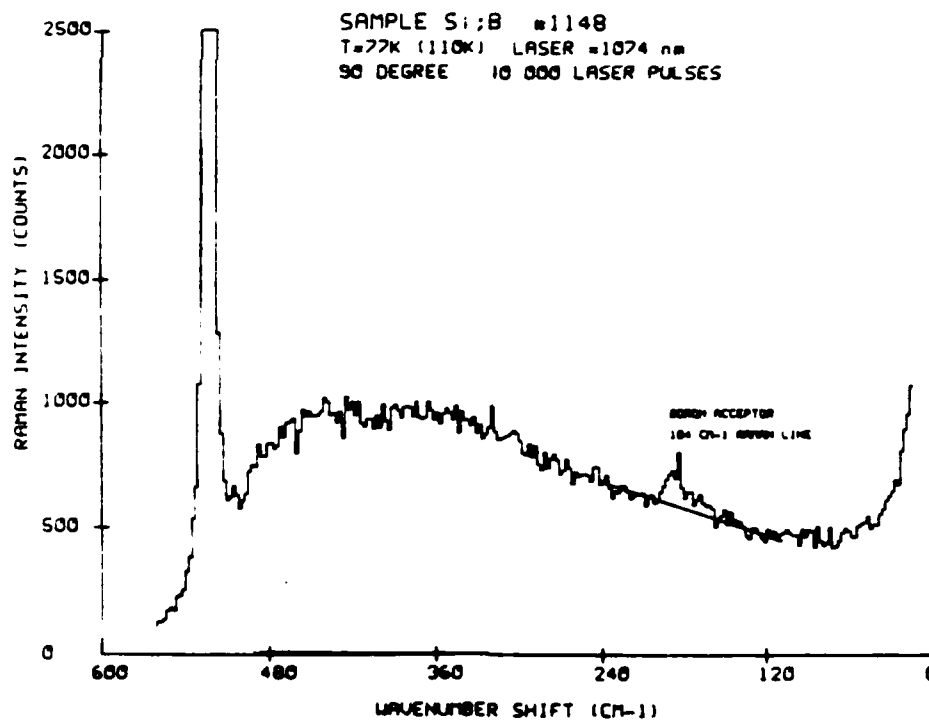


Figure 7b. Raman Spectra of Si:B ; 77K ; 10,000 Pulses 1074 nm.

counts per laser pulse in the region of 300 cm^{-1} to 400 cm^{-1} is observed to be about 0.10 in both cases (about 100/1000 in figure 6 and 1000/10,000 in figure 7). However the curve of figure 7a is much "smoother". If this SAME digital recorded data used to plot figure 7a is replotted as in figure 7b, the reported electronic Raman active interaction with boron acceptor impurities in silicon at 184 cm^{-1} is marginally observed above the fluorescence background noise.

Figure 8 shows two different runs of this same boron doped silicon crystal using 40,000 incident 1074 nm laser pulses. The step size of the wavenumber movement between spectrometer settings is different in the two spectra, but they both clearly indicate the existence of a Raman "line" near 184 cm^{-1} that can be the electronic Raman scattering from boron acceptor impurities.

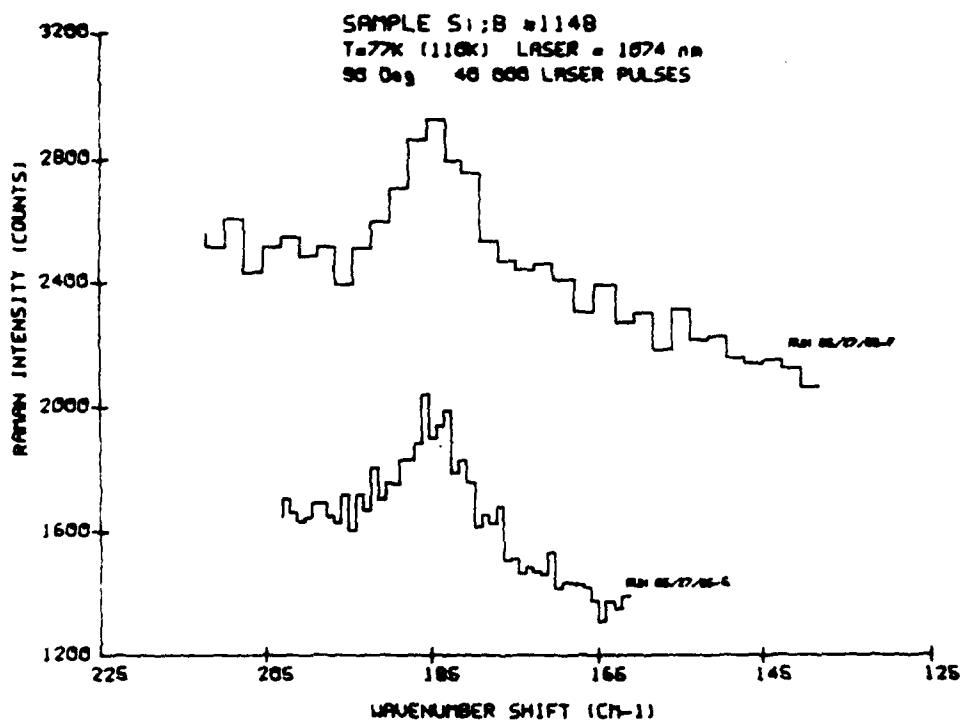


Figure 8. Raman Spectra of Si:B ; 77K ; 40,000 Pulses at 1074 nm.

The spectra in the region of the suspected boron impurity Raman line when 20,000 incident laser pulses were used at each setting and

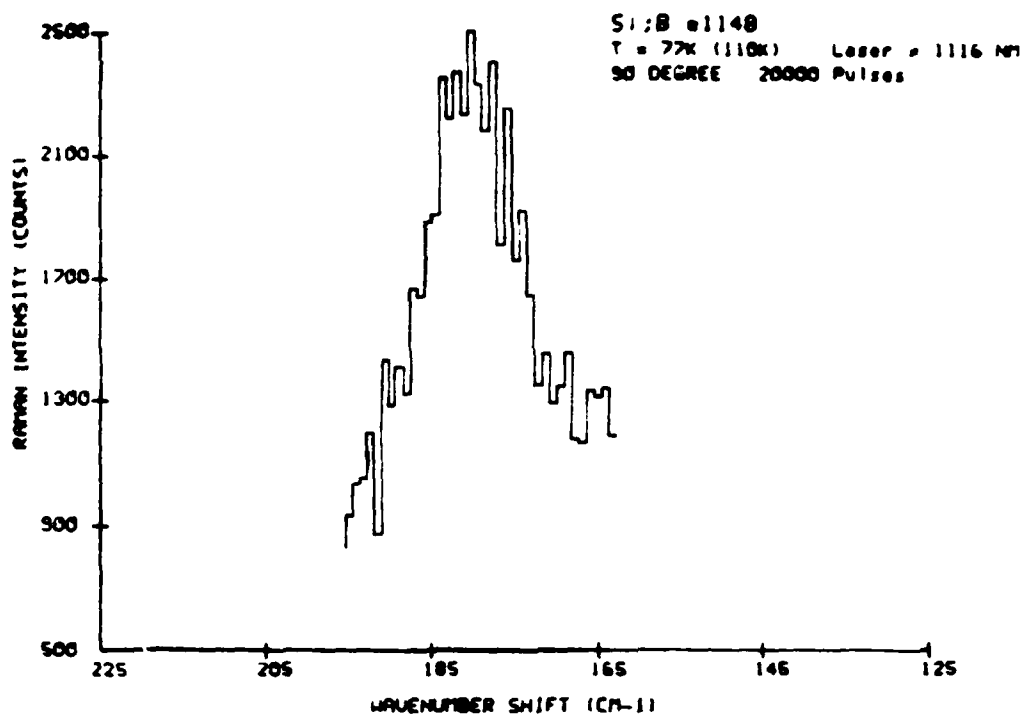


Figure 9. Raman Spectra of Si:B ; 77K ; 20,000 Pulses at 1116 nm.

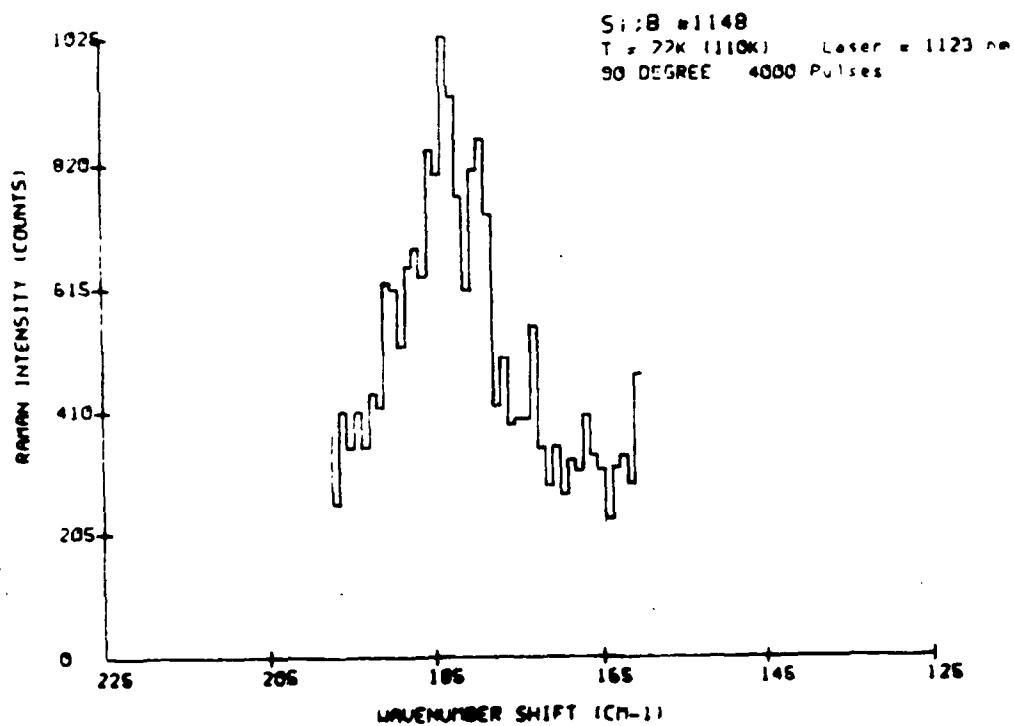


Figure 10. Raman Spectra of Si:B ; 77K ; 4000 Pulses at 1123 nm.

when the wavelength of the laser was changed to 1116 nm is shown in figure 9. At this longer wavelength, the energy of the incident photons is only 1.11 eV and is below band gap energy even though the temperature is only 77K (ref. figure 5). Figure 10 shows similar Raman spectra for a boron doped silicon crystal at 77K, but in this experiment 4000 incident laser pulses at 1123 nm (1.10 eV) were employed at each spectrometer setting. Again the line at 184 cm^{-1} is observed in a region with almost no fluorescence noise background. In all the above Raman scattering experiments of boron doped silicon, the interaction is very weak and the necessity of making concerted efforts to detect small signal levels and to reduce noise is clear.

When it became possible to purchase liquid helium locally, the Raman spectra of this same boron doped sample #1148 was obtained near 4K. Figure 11 shows the spectra obtained using only 4000 incident laser pulses at 1074 nm. Signal to noise could be improved with more incident laser pulses at each data point, but it was not necessary. The "boron line" at 184 cm^{-1} is clearly evident with the sample near helium temperature. Compare this spectra in figure 11 with figures 6 and 7 obtained from this same sample at 77K.

In figure 12 this same sample is used again at near liquid helium temperature but the wavelength of the incident laser pulses was changed by attempting to adjust the inter-cavity prism of the laser for 1064 nm operation. The Raman spectra is plotted as energy shift from the energy of those 1064 nm photons. It is evident both from the "double" LO phonon peaks at 523 cm^{-1} and at about 496 cm^{-1} , as well as from the "double" laser-line peaks obtained by sweeping the spectrometer through the wavenumber region of heavily attenuated Ralleggh scattered laser light, that the laser was operating at two laser wavelengths. It was producing laser pulses both at 1064 nm (9398 cm^{-1}) and at 1061 nm (9425 cm^{-1}) which shows up at -27 cm^{-1} on the scale where 9398 cm^{-1} is set as the "zero" energy shift. The "boron line" likewise shows at the expected 184 cm^{-1} shift from the 1064 nm laser line, but also at 27 cm^{-1} from this location on this scale which is 184 cm^{-1} from the other laser line at 1061 nm. A little bit of fluorescence noise is also observed in this spectra since the photon energies of the 1064 and 1061 nm laser pulses used are above the band gap energy of silicon.

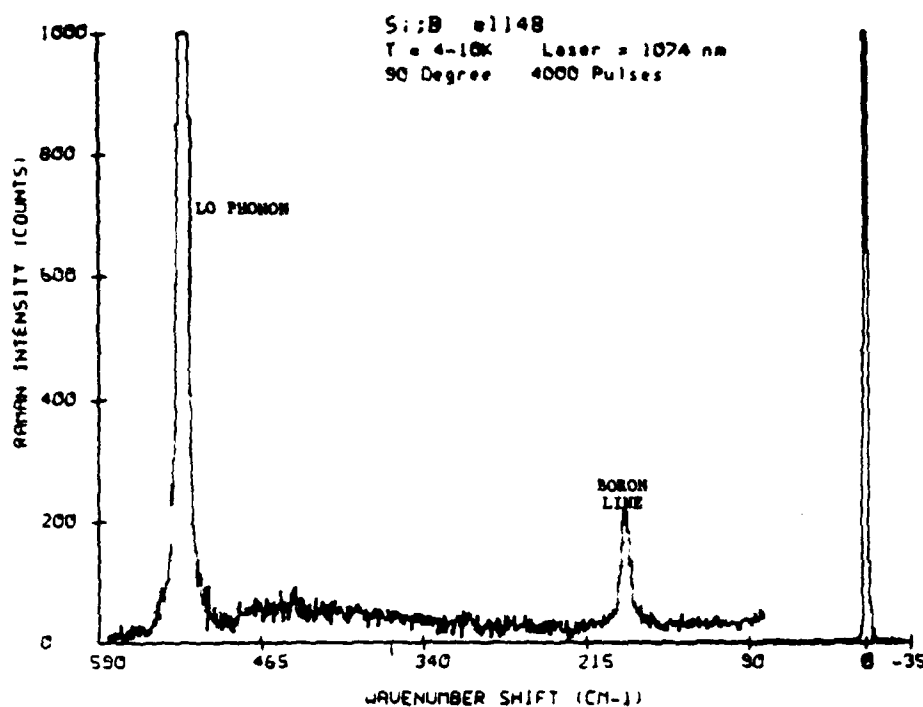


Figure 11. Raman Spectra of Si:B ; 4K ; 4000 Pulses at 1074 nm.

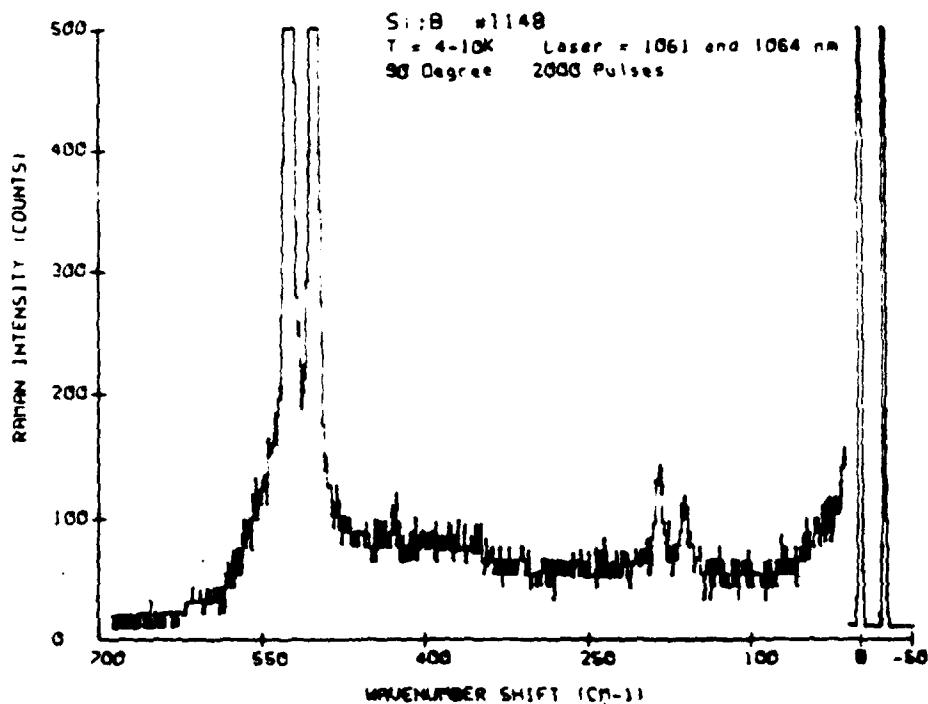


Figure 12. Raman Spectra of Si:B ; 4K ; 2000 Pulses at 1064 + 1061 nm.

IV. RAMAN SPECTRA OF Si;B SAMPLES WITH KNOWN IMPURITIES

A set of three silicon samples was obtained with the number density of the impurity acceptors "known" from previously conducted Hall effect studies on other samples cut from the same silicon crystal boules. These samples were boron doped in the melt and determined to possess 2.4×10^{15} , 1.3×10^{16} , and 1.6×10^{17} acceptor impurities attributed to boron. The ratio of the suspected impurity levels is roughly 0.2 to 1 to 12, so similar ratios of signal levels in the Raman scattering peaks attributed to the boron impurities are expected. However, it must be pointed out that quantitative comparisons require a reasonable amount of data manipulation that was not utilized in this study. The variation in integrated laser power both during a given run, and from one experimental run to the next must be taken into consideration before quantitative comparisons are valid. While the laser was used in a similar mode during this series of experiments, it was not maintained at constant operation from day to day and no attempt was made to correct for the daily variations in output power. The laser wavelength was kept at 1074 nm for this series.

Figure 13 shows the spectra from the Si;B sample with 1.3×10^{16} boron impurities with the sample at 77K; figure 13a used 1000 pulses per data point while figure 13b shows the spectra with 10,000 laser pulses per spectrometer setting. The "boron line" at 184 cm^{-1} is barely above the noise level in 13a but clearly seen in 13b where the signal to noise ratio improvement associated with increased data is observed. Figure 14 shows this same sample, but with the sample temperature lowered to near 4K with liquid helium. Note that the signal due to electronic Raman scattering from the boron acceptor at 184 cm^{-1} may have increased slightly, but the significant improvement in the spectra at 4K is due to a reduction of the background (which was likely fluorescence at 77K). Figure 14a used 2000 pulses per data point while figure 14b utilized 10,000 pulses per spectrometer setting.

The "stray peak" that shows up at 436 cm^{-1} on the scale of figure 14a is actually an LO phonon peak that is shifted by 523 cm^{-1} from incident 1064 nm laser light which was also present.

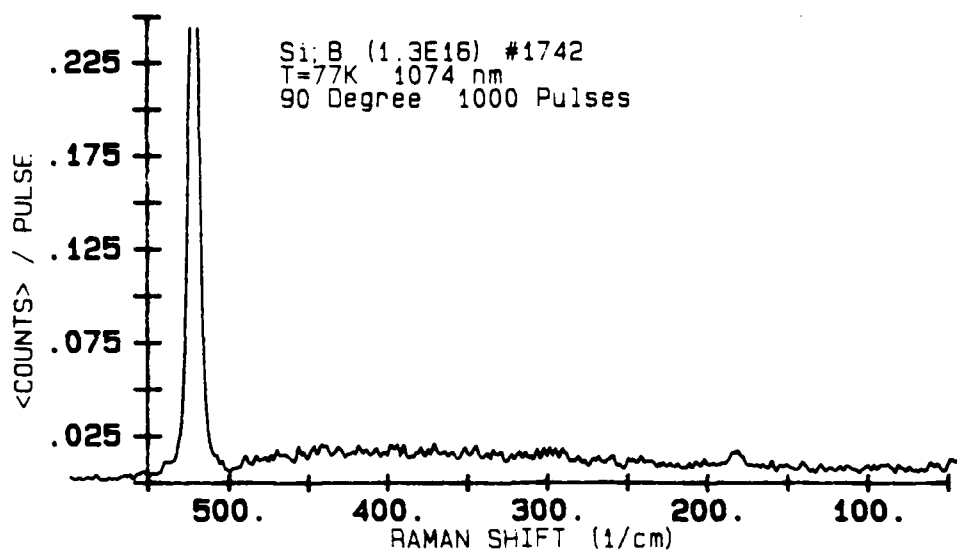


Figure 13a. Raman Spectra of Si:B (1.3E16); 77K ; 1000 Pulses

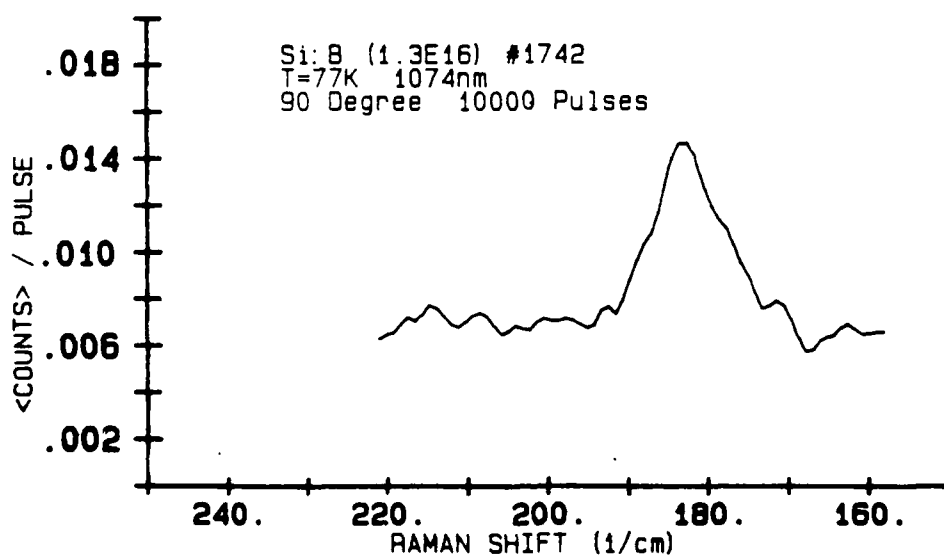


Figure 13b. Raman Spectra of Si:B (1.3E16); 77K ; 10,000 Pulses

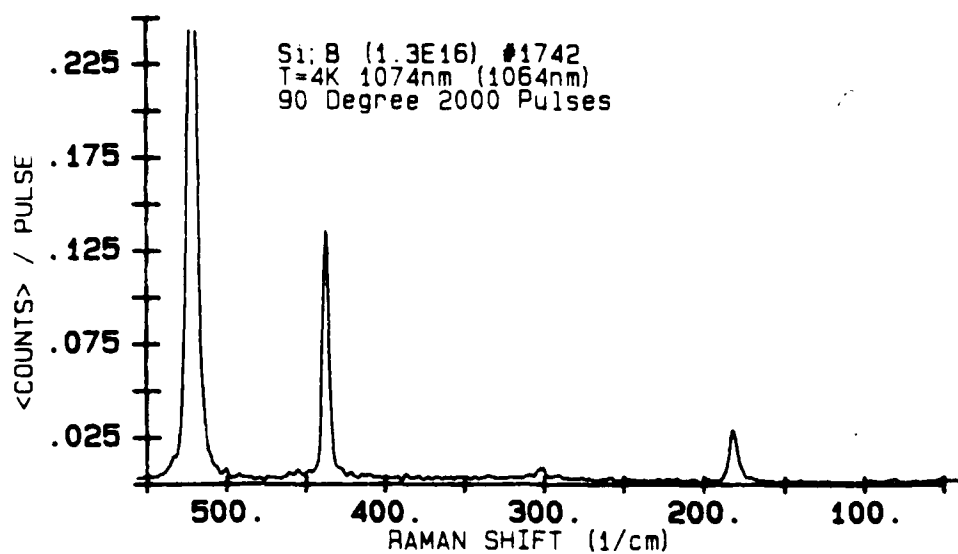


Figure 14a. Raman Spectra of Si:B (1.3E16); 4K ; 2000 Pulses

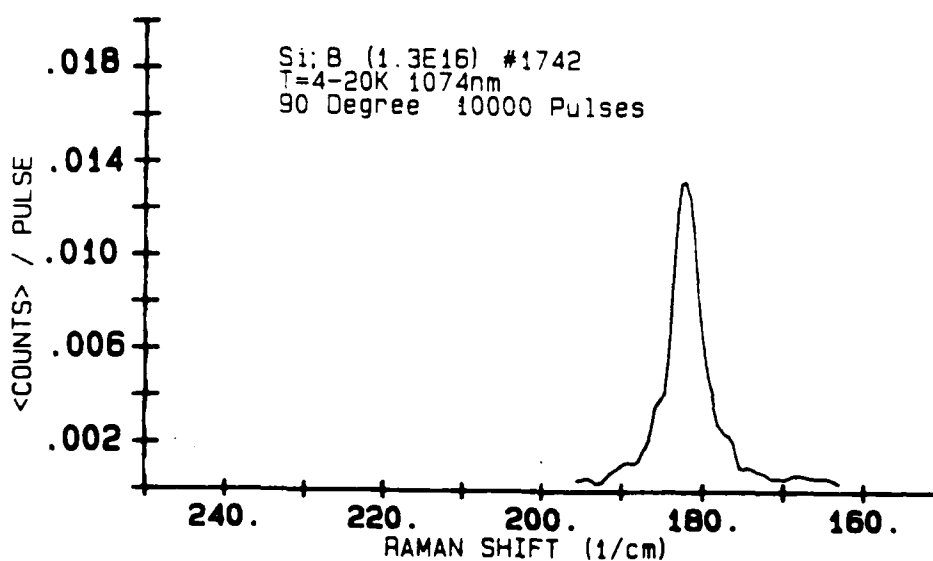


Figure 14b. Raman Spectra of Si:B (1.3E16); 4K ; 10,000 Pulses

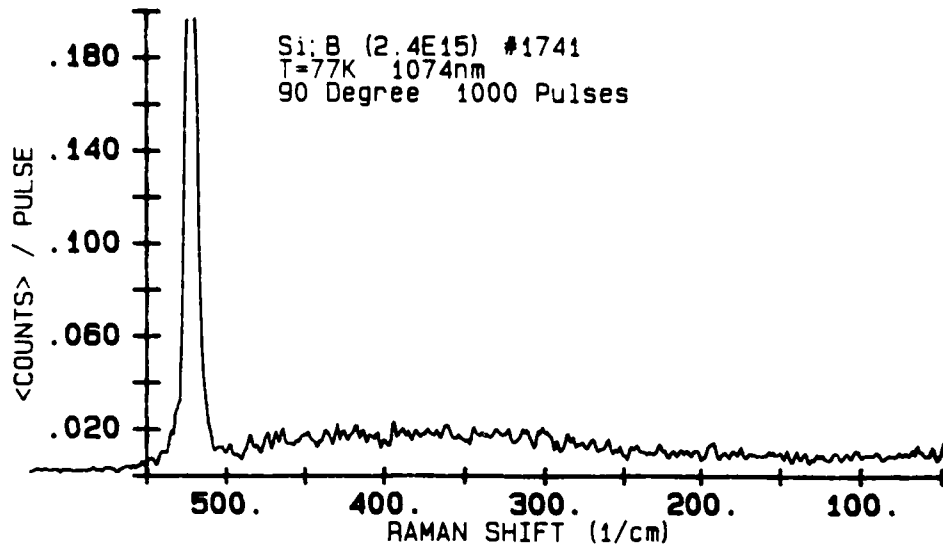


Figure 15. Raman Spectra of Si:B (2.4E15); 77K ; 1000 Pulses

Using the sample with only 2.4E15 impurities, weaker Raman signal was expected. Figure 15 shows the spectrum taken with the sample at 77K. With only 1000 pulses per data point, the signal to noise is such that no signal is apparent. Cooling the sample with liquid helium yielded the spectra of figure 16. In figure 16a the 2000 laser pulses were used, while in figure 16b 10,000 incident laser pulses were utilized for each data point. A comparison of the counts/pulse ratio of peaks on figures 16a with 14a (also of figure 16b with 14b) shows the correct trend in signal sizes but not the factor of 5 that the "known" impurity levels exhibit. The order of magnitude is correct, but quantitative comparison is actually not valid without proper normalization for laser power between runs.

The sample with 1.6E17 boron acceptor impurities shows a very strong Raman peak at 184 cm^{-1} from the 1074 nm laser line in figure 17a. The sample was at 4K and 2000 laser pulses per spectrometer setting were used. The "stray peak" at 436 cm^{-1} on this scale is again an LO phonon peak which is actually 523 cm^{-1} from some 1064 nm laser light that is also present in the beam. Using 4000 laser pulses per data point, figure 17b shows the shape of the 184 cm^{-1} "boron line" in some detail.

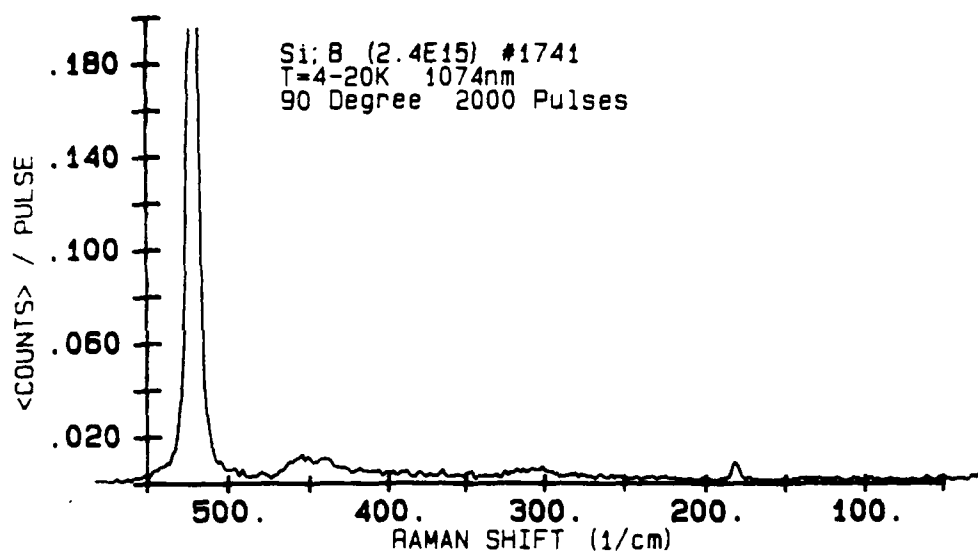


Figure 16a. Raman Spectra of Si:B (2.4E15); 4K ; 2000 Pulses

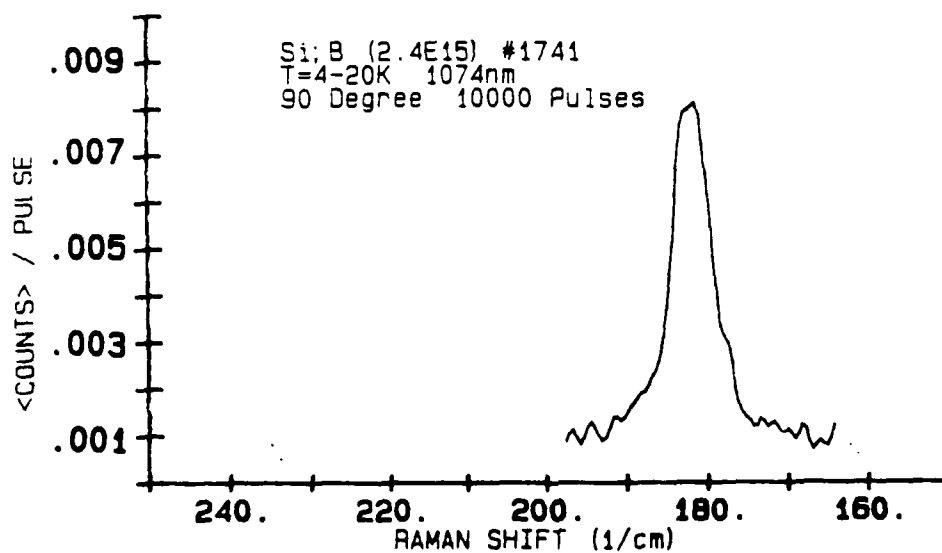


Figure 16b. Raman Spectra of Si:B (2.4E15); 4K ; 10,000 Pulses

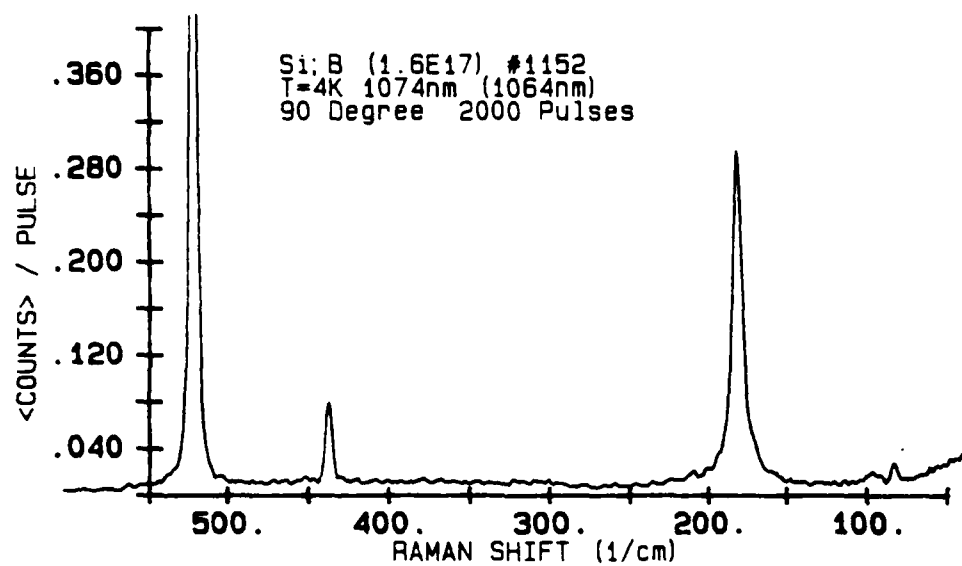


Figure 17a. Raman Spectra of Si:B (1.6E17); 4K ; 2000 Pulses

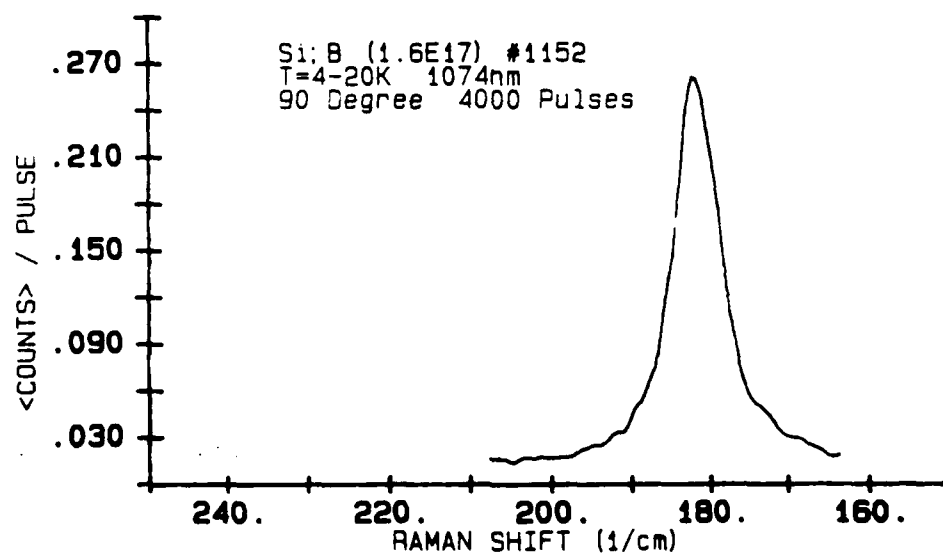


Figure 17b. Raman Spectra of Si:B (1.6E17); 4K ; 4000 Pulses

V. RAMAN SPECTRA OF OTHER GROUP IIIA ELEMENTS IN SILICON

The first goal of this effort was to set up an experimental facility that was capable of reliable Raman scattering studies in silicon. The second goal was to conduct a series of experiments using boron doped silicon samples that would clearly show that the Raman line reported in the literature to exist near 184 cm^{-1} and reported to be an electronic Raman interaction was indeed associated with the boron acceptor impurity. If the first two were successful, then it was reasonable to proceed toward a third and the most scientifically meaningful goal which was to conduct a careful search for similar Raman active electronic transitions in silicon samples doped with the other group IIIA elements, aluminum, gallium, indium, and thallium.

The experience with boron doped samples suggests that the search is essentially doomed unless conducted at helium temperatures and with samples that are known to contain a reasonably high concentration of the impurity dopant. Comparison of 77K and 4K data on the same samples (Figures 13 and 14 for example) suggests that these very weak Raman signals don't get too much stronger at 4K but that the "fluorescence noise" level is significantly reduced, and signal to noise ratios are improved when the samples are held near helium temperature. This series with boron doped samples also demonstrates how hard one needs to work experimentally (use a high number of incident laser pulses at each spectrometer setting, make long experimental runs during which all must remain stable, etc.) when the dopant level is low such as 2.4×10^{15} boron acceptors, and how much easier it was to observe the Raman active interaction with 1.6×10^{17} boron acceptors.

Several attempts were made to observe Raman interactions in silicon samples doped with the other group IIIA impurities, but no careful study was yet made. A sample reported to have aluminum impurity but of unknown level was examined at near 4K. In a "quick" survey run of 2000 pulses per spectrometer setting, only the LO phonon was discernable in the spectra. A similar quick survey run using a silicon sample reported to contain gallium of unknown impurity level did not yield an interpretable spectra because the sample was warming from 50K to 130K during the run; liquid helium was empty and fluorescence

increased as the temperature rose. Another sample reported to be double-doped with boron and thallium gave uncertain results. In experimental runs both at 20K and again in another experimental run at 77K, a peak shows in the Raman spectra at about an 83 cm^{-1} shift from the 1074 nm laser line. A later attempt to repeat this data on the same sample at 77K did not show this peak. These preliminary experiments are inconclusive to say the least.

The question of Raman active interactions with p-type impurities of the group IIIA elements, other than boron, remains open. The next step is obviously to do careful Raman scattering studies near liquid helium temperature with an IR laser on a series of samples that have been previously well characterized by Hall effect data. An attempt is underway to accumulate such a series of samples.

Acknowledgement

The author expresses appreciation to the Materials Laboratory at the Air Force Wright Aeronautical Laboratories, The Air Force Systems Command, the Air Force Office of Scientific Research, as well as the Southeastern Center for Electrical Engineering Education for providing the opportunity to engage in this research project. In particular, I acknowledge the collaboration of Dr. Patrick Hemenger AFWAL/LMPO who suggested this problem and provided the silicon samples. Likewise I recognize the helpful assistance of peers and students at the University of Dayton, especially Dr. Perry Yaney, who originally designed and is responsible for the pulsed laser Raman scattering facility at UD, and Stanley Pruchnic who is involved with the computer software for data acquisition and management on this facility.

REFERENCES

1. J. P. Russel, Appl. Phys. Lett. 6, 223 (1965).
2. J. H. Parker, Jr., D. W. Feldman and M. Ashkin, Phys. Rev., 155 (3) 712 (1967)
3. R. K. Chang, J. M. Ralston and D. E. Keating, Light Scattering Spectra of Solids, Edited by G. B. Wright (Springer-Verlag 1968)
4. Paul A. Temple and C. E. Hathaway, Phys. Rev. B 7 (8), 3685 (1973)
5. B. A. Weinstein and Manuel Cardona, Solid State Com., 10, 961 (1972)
6. K. Uchinokura, T Sekine and E. Matsuura, Solid State Com., 11, 47 (1972)
7. K. Uchinokura, T Sekine and E. Matsuura, J. Phys. Chem. Solids, 35, 171 (1974)
8. G. B. Wright and A. Mooradian, Phys. Rev. Lett., 18 (15), 608 (1967)
9. G. B. Wright and A. Mooradian, Proc. 9th Intern. Conf. Physics of Semiconductors, Moscow, 1067 (1968)
10. J. M. Cherlow, R. L. Aggarwal and B. Lax, Phys. Rev. B, 7 (10), 4547 (1973)
11. Kanti Jain, Shui Lai and M.V. Klein, Phys. Rev. B, 13 (12), 5448 (1976)
12. M. V. Klein, Light Scattering in Solids, Ed. M. Cardona, (Springer-Verlag, 1975, 1983-2nd)
13. P.P. Yaney, J. Raman Spectry., 5, 219, (1976)

Grain Size Control in Meta Stable Beta Titanium Alloys

By

I. Weiss

Materials Science and Engineering

Wright State University, Dayton, OH, 45435

Final Report, Dec 84 - Dec 85

ABSTRACT

The control of grain size, grain shape and uniformity in order to avoid the formation of mixed grain size structure during primary processing from the ingot can be of great importance for further thermomechanical processing and for optimizing of final mechanical properties.

It has been shown that this control can be achieved by processing through a certain temperature range termed the "processing window". The objective of the present work was to follow the effect of hot deformation, post deformation heat treatment and initial ingot grain shape (equiaxed or columnar) and size on the development of mixed grain structure in the metastable beta Ti-15V-3Al-3Cr-3Sn alloy. This is, to determine whether a "processing window" exists, that will allow the determination of the hot working parameters for this alloy, to produce a fine, uniform equiaxed grain material. Forging blanks taken from different locations along the cast ingot (fully equiaxed, fully columnar, and mixed grain structure) were forged to different total reduction of 48% and 65% at temperatures ranging between 790°C (1450°F) to 1365°C (2500°F). Following deformation, the test specimens were annealed under vacuum at temperatures ranging from 870°C (1600°F) to 1255°C (2300°F) for 1 hour. Specimens were then oil quenched so that progress of static recrystallization could be followed. It was found that the appearance of the mixed grain size structure is associated with recrystallization/grain growth behavior at high temperatures. The "processing window" for

material with original elongated (columnar) grains forged to a 48% reduction was observed to extend to a higher processing temperature with minimum processing temperature of 1145°C (2100°F) and higher annealing temperature of 1090°C (2000°F) in comparison to the "processing window" for material contains the same original grains shape forged 65% reduction. Less pronounced "processing window" was observed in material with original equiaxed grains.

I. INTRODUCTION

Because of the interplay between recrystallization and grain growth, processing of beta titanium alloys can lead to the formation of a mixed grain size structure containing large and small grains [1]. The mixed grain size structure is undesirable and contributes to poor high temperature flow, and inferior room temperature properties. Once introduced, it is impossible to remove the mixed grain size structure by heat treatment alone, so that further processing is needed to uniformly refine the microstructure [1].

Mixed grain structures were found after either cold or warm working (below 885°C [1575°F]) the metastable beta titanium alloys, Ti-10Mo-6Cr-2.5Al and Ti-10Mo-8V-2.5Al and annealing at 980°C (1800°F). This microstructure is a result of selective recrystallization in the finer grains, with the driving force for grain growth rapidly decreasing because of the competition from recovery, resulting in a mixed grain size [1]. Similar results were observed in Ti-10V-2Al-3Fe alloy processed below 950°C and subsequent annealed below 1150°C [2].

Studies of the austenite microstructure during hot rolling of steels reveals that under the conditions where partial recrystallization occurs in the transition temperature range from recrystallization to non-recrystallization, the mixed grain structure is produced by preferential recrystallization at austenite grain boundaries, the grain interior being left

unrecrystallized [3]. In addition, when coarse austenite grains are growing rapidly after recrystallization, as a result of light deformation passes, a mixed grain structure also develops [4,5].

The purpose of this study was to examine the effect of hot deformation, post deformation heat treatment, solute concentration level, and initial ingot grain shape (columnar or equiaxed) and size on the development of mixed grain structure in Ti-15V-3Al-3Cr-3Sn alloy. This is, to determine whether a "processing window" exists, that will allow the determination of the processing parameters for this alloy to produce a fine, uniform equiaxed grain material. This in turn will allow achievement of good cold formability conditions.

MATERIALS AND EXPERIMENTAL PROCEDURE

Forging specimens (37.5mm diameter x 50mm) were taken from 750mm cast ingot with a nominal composition of Ti-15V-3Al-3Cr-3Sn. These were hot die forged to total reduction of 48% and 65% at temperatures between 790°C (1450°F) and 1365°C (2500°F). A 50 ton hydraulic press was used at a ram speed of 1.25 cm/min. Deformed specimens were polished and macro etched in Kroll's solution to groove the deformed grain boundaries. The etched specimens were then vacuum annealed for 1 hour at temperatures between 870°C (1600°F) and 1255°C (2300°F). Following oil quenching the polished surface of the annealed specimens simultaneously shows the prior deformed boundaries ("ghost boundaries") and the position of the newly recrystallized grains (thermally etched) [6].

RESULTS AND DISCUSSION

Effect of Processing and Annealing Temperatures

Figures 1 and 2 show the effect of processing and annealing temperatures on the microstructure of specimens containing original elongated (columnar) grains and forged 48% and 65% reduction. Samples with elongated grains forged to a total reduction of 48% at 1145°C (2100°F) were found to require the lowest annealing temperature of 1090°C (2000°F) to produce a fully recrystallized microstructure. These samples have higher driving force for recrystallization and grain growth in comparison with specimens forged above or below 1145°C (2100°F). Specimens with an initial elongated grain structure forged to 65% reduction at 1090°C (2000°F) were found to require a lower annealing temperature of 1035°C (1900°F) to produce a fully recrystallized structure than samples processed at 1365°C (2500°F) and 790°C (1450°F). The processing and annealing temperatures of 1145°C (2100°F) and 1090°C (2000°F) define a "processing window" for which a uniform recrystallized structure results. These observations can be explained in terms of the way elongated grains deform and the driving force for recrystallization and growth during annealing. Similar results are obtained for specimens forged to 65% reduction. The "processing window" was found to shift to lower forging temperatures, with the minimum occurring at an annealing temperature of 1035°C (1900°F) and a

processing temperature of 1090°C (2000°F) as shown in Fig. 2. The shift of the "processing window" is attributed to an increase in driving force for recrystallization and growth when forged to a total reduction of 65% Fig. 3.

Figures 4 and 5 show the effect of processing and annealing temperatures on microstructure of specimens with original equiaxed grain structure forged 48% and 65% reduction. Samples forged at temperatures ranging between 790°C (1450°F) and 1090°C (2000°F) require the same annealing temperature of 1035°C (1900°F) to produce a fully recrystallized microstructure. However, a slightly higher annealing temperature of 1090°C (2000°F) is required for material forged above 1090°C (2000°F) in order to produce similar structure. Processing temperatures between 790°C (1450°F) and 1090°C (2000°F) and annealing temperature of 1035°C (1900°F) define a less pronounce "processing window" for which a uniform recrystallized microstructure results. These observations can be rationalized in terms of the way equiaxed grains deform and the response of the deform material to the annealing process. Similar results are observed for material with equiaxed grain structure forged to 65% reduction. the "processing window" was found to shift to lower annealing temperatures with the minimum occurring at 980°C (1800°F) as shown in Fig. 6. The displacement of the "processing window" to lower annealing temperature is a result of higher driving force for recrystallization and growth in specimens forged to 65% reduction.

Effect of Initial Grain Shape

In earlier study it was found that the "processing window" is affected by the original shape of the ingot grains in addition to the processing and annealing temperatures [2]. Figures 7 and 8 show the combined effect of original grains shape, annealing and processing temperatures on the microstructure of samples forged 48% reduction. Samples with original equiaxed grains require lower annealing temperatures than specimens with original elongated grains to produce fully recrystallized structure. This result can be attributed to more uniform deformation in equiaxed grains as well as an increase in driving force for recrystallization and grain growth during annealing. Similar results are observed in material forged 65% reduction. Relatively lower annealing temperatures are observed when compared to specimens forged 48% reduction, the result of higher driving force for recrystallization during annealing.

Effect of Solute Level

Figure 9 displays the combined effect of solute level, annealing and processing temperatures on the microstructure of specimens with original elongated grains forged 65% reduction. Lower annealing and processing temperatures are detected for Ti-15-3-3-3 (15-3) alloy than for Ti-10-2-3 alloy in order to produce fully recrystallized structure. The higher solute content

in Ti-15-3-3-3 alloy (24 wt% compared to 15%) affects the way elongated grains deform resulting in a different dislocation substructure and higher driving force for recrystallization during annealing.

REFERENCES

1. F.H. Froes, C.F. Volton, J.P. Hirth, R. Ondercin and D. Moracz, "Proceedings of the Beta and Near-Beta Alloys Symposium," TMS-AIME, Atlanta, GA, March (1983).
2. I. Weiss and F.H. Froes, Proceedings of the 5th International Conference on Titanium, Munich West Germany (1985).
3. J.D. Jones and A.B. Rothwell, "Deformation Under Hot Working Conditions," Iron and Steel Inst. Publication 108, Iron and Steel Inst., London (1968).
4. A. Le Bon and L.N. De Saint-Martin, "Microalloying 75," International Symposium on High-Strength, Low Alloy Steel, Union Carbide Corp., New York, NY, (1977).
5. L.J. Cuddy, Met. Trans., 12A, (1981), p. 1313.
6. I. Weiss, F.H. Froes and D. Eylon, Met Trans., A, 1493, (1984).

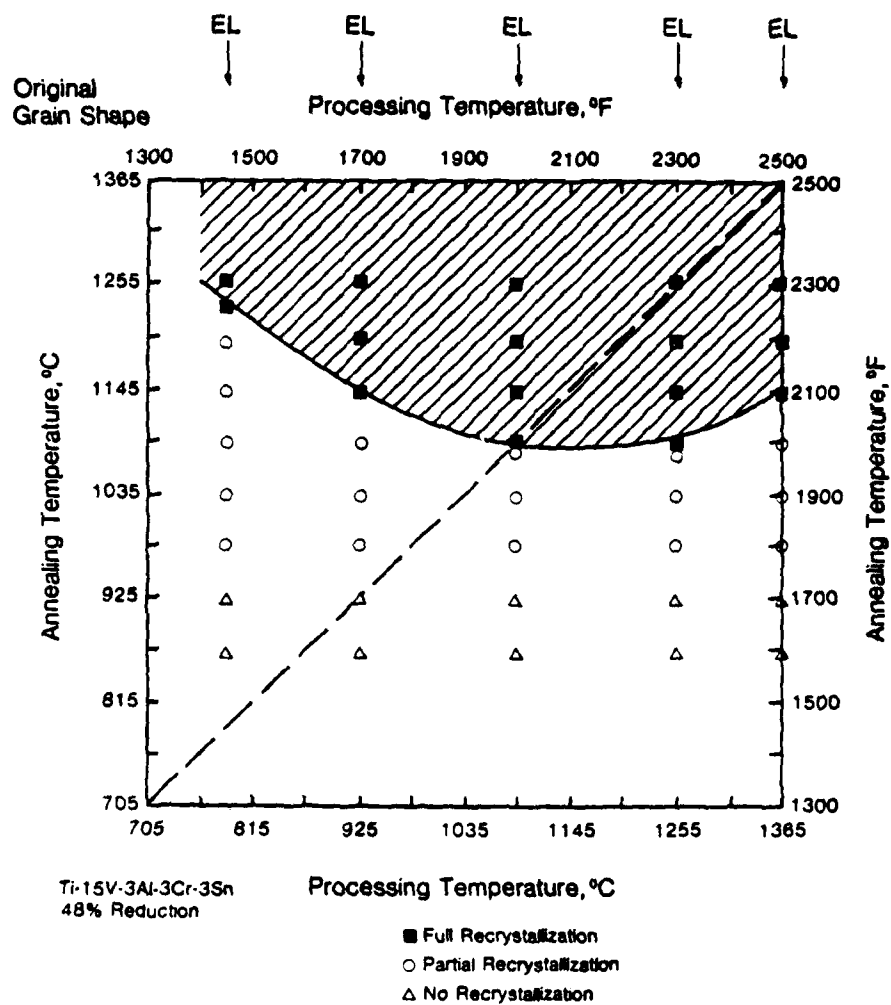


Figure 1

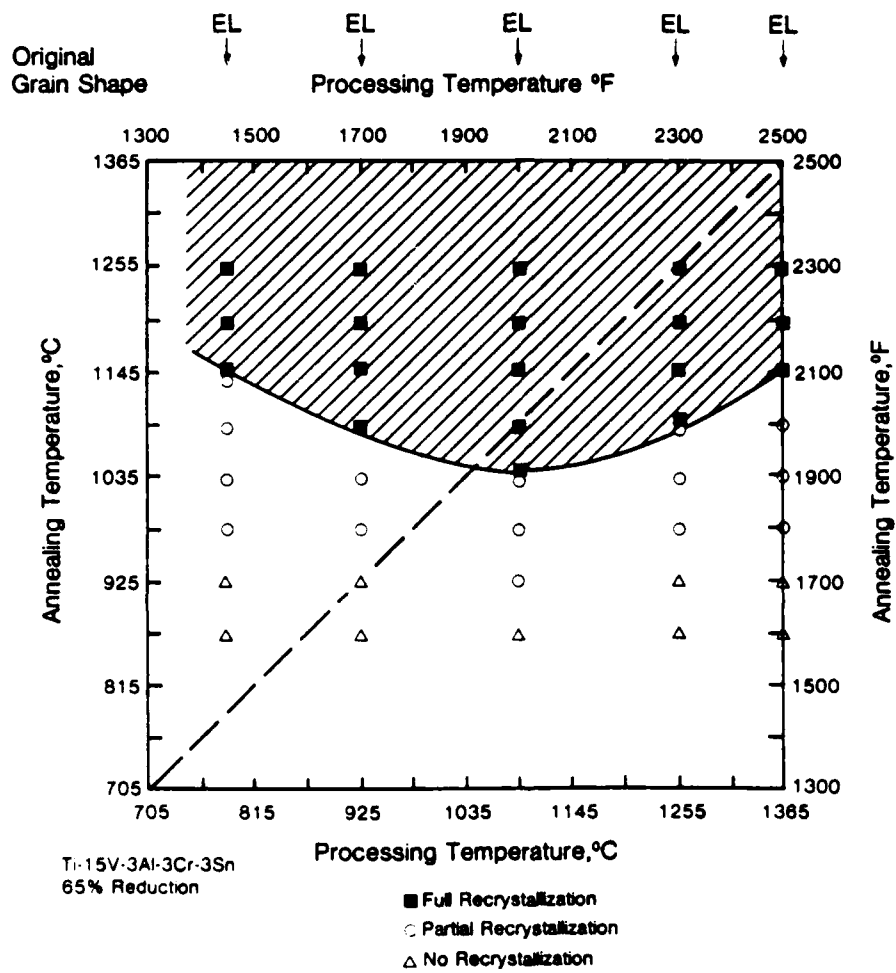


Figure 2

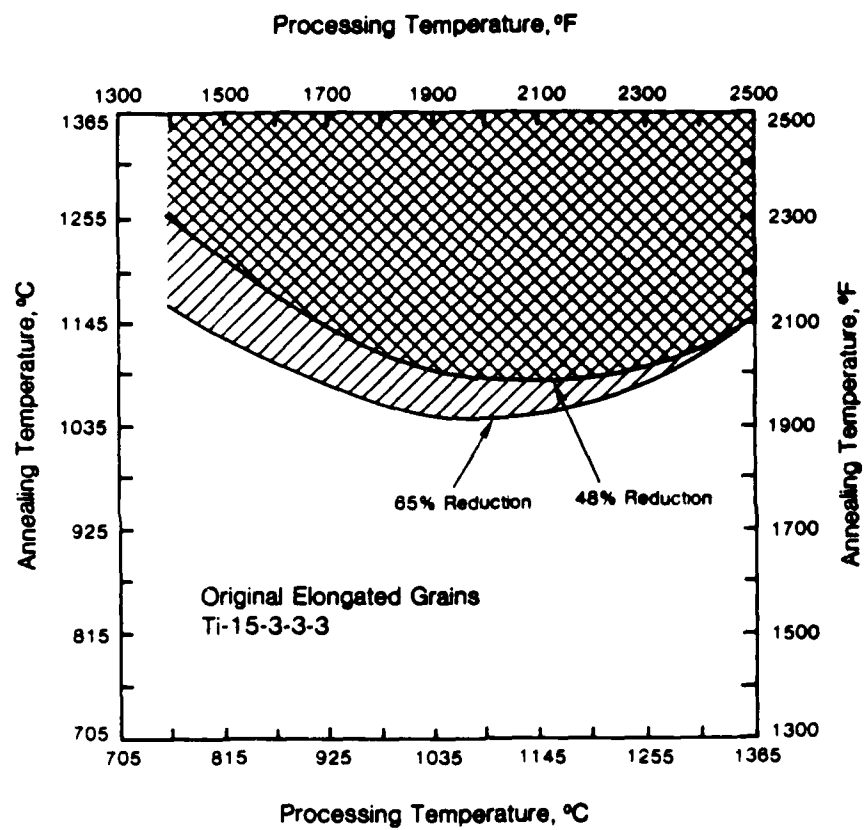


Figure 3

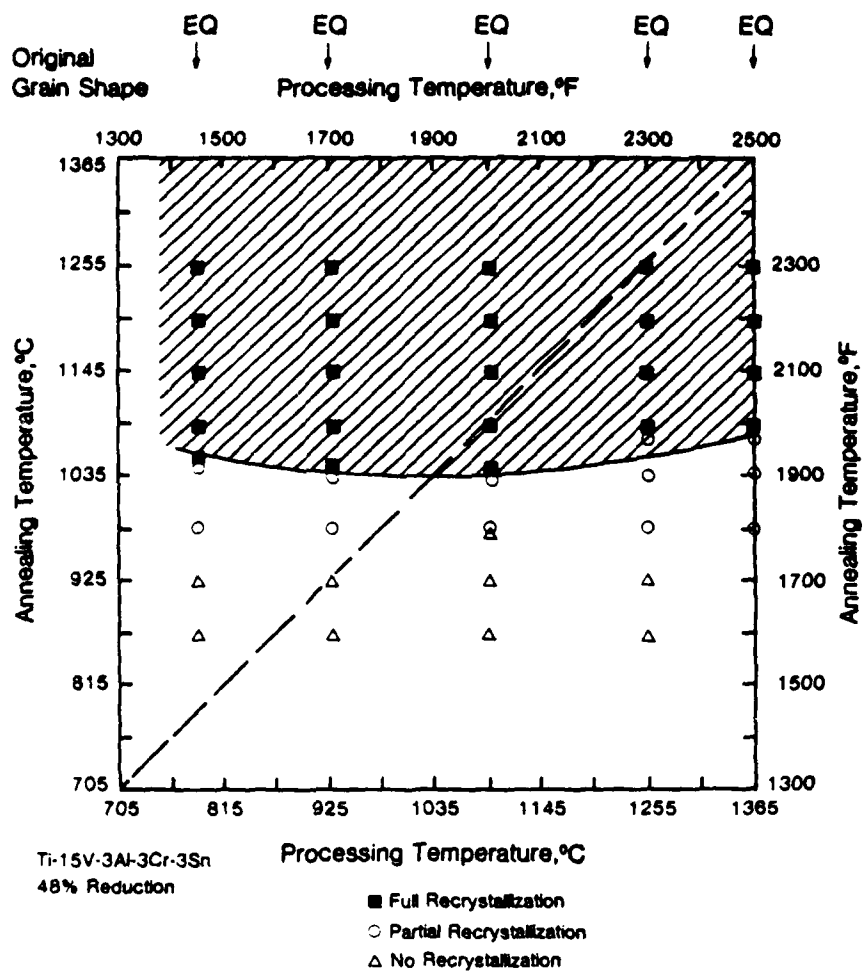


Figure 4

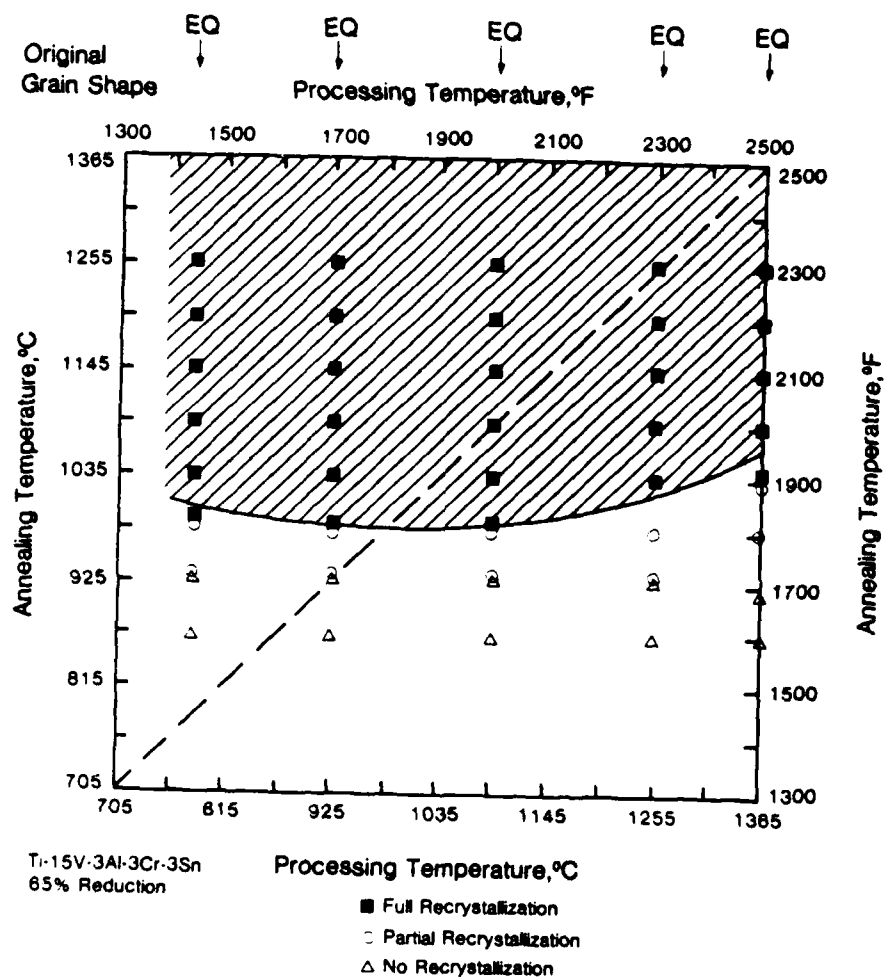


Figure 5

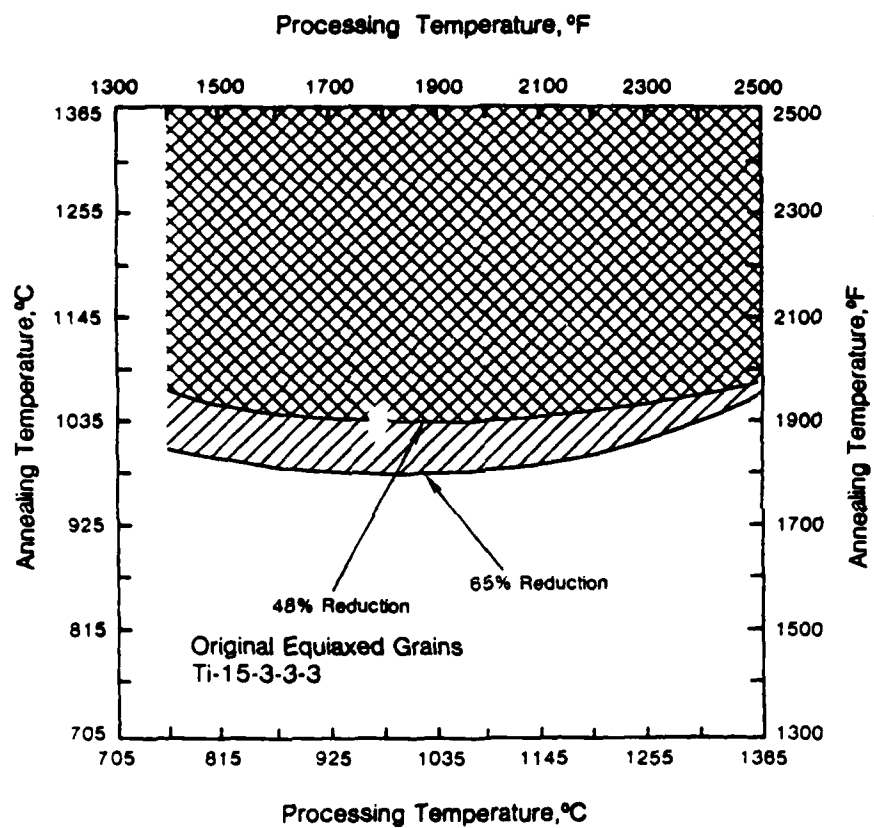


Figure 6

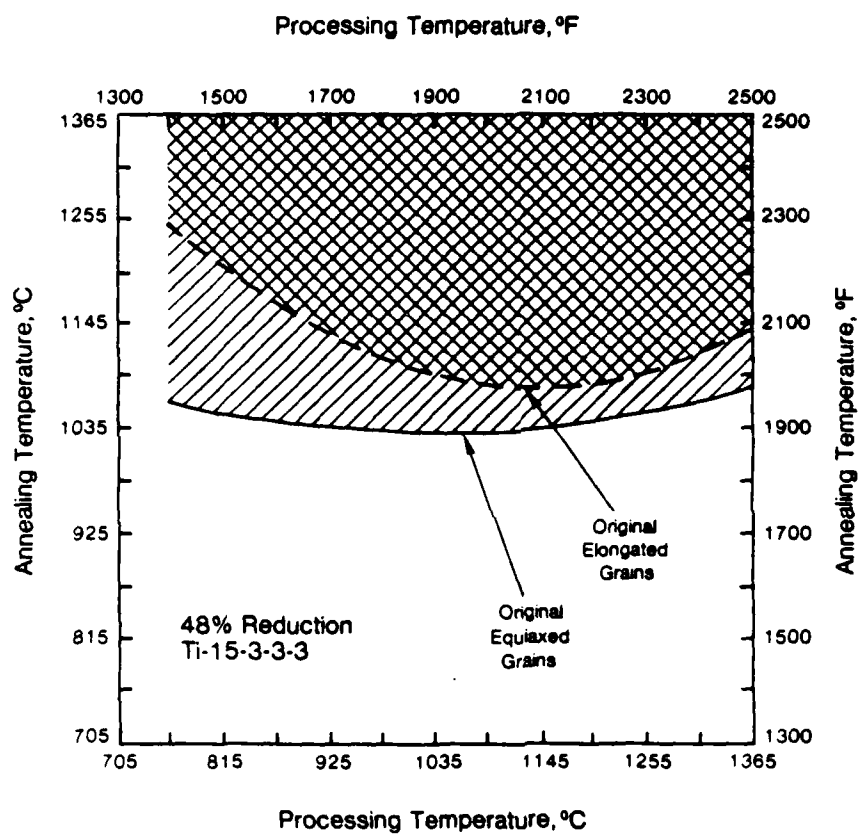


Figure 7

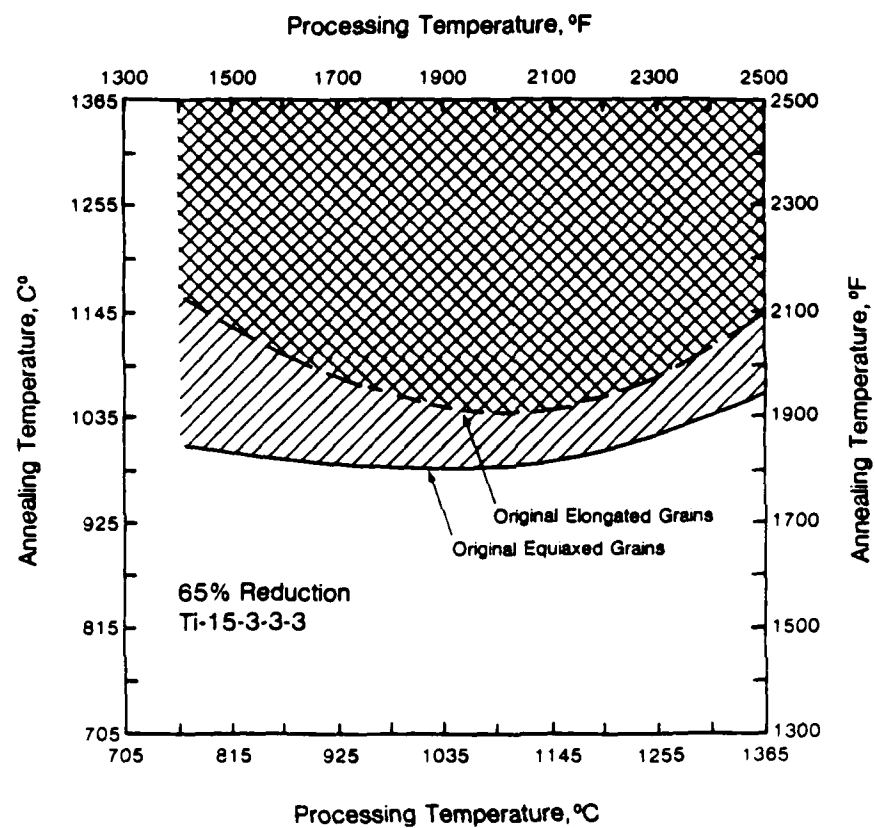


Figure 8

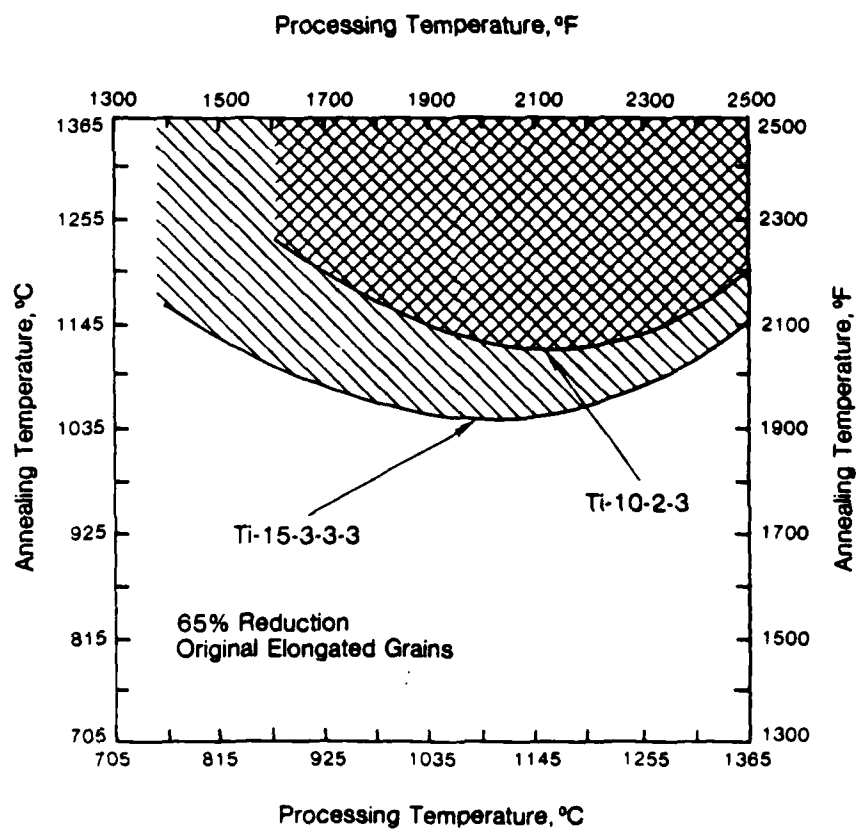


Figure 9

2014

THE IMPACT OF EXPERT SYSTEMS ON PERFORMANCE AND
COGNITIVE STRATEGIES IN DIAGNOSTIC INFERENCE

CONTRACT FINAL REPORT

Sallie E. Gordon
Department of Psychology
University of Idaho

January 1986

Sponsored by:
Air Force Office of Scientific Research
Contract Number: F49620-82-C-0035
Air Force Contact: Rosemarie J. Preidis
Human Resources Laboratory

Conducted by:
Southeastern Center for Electrical
Engineering Education

1. SUMMARY

1.1 Objectives

This report covers a one-year preliminary program of research directed toward assessing the impact of expert computer-aiding systems on the human operator, in particular, when the task is that of "sequential diagnostic inference". The objectives of the program included (1) development of a laboratory task that had the characteristics of real-world sequential diagnostic inference tasks (such as medical diagnosis, radar identification, etc.), (2) assessment of methods to describe and/or quantify the process or "strategy" being used by the operator in the absence of an expert-aid system, (3) empirically specify situational characteristics affecting the performance of the operator (without an expert-aid), and (4) define and assess some of the variables which determine the operator's acceptance and use of a computer-aiding system.

1.2 Technical Approach

These objectives were met by development of a laboratory task involving sequential diagnostic inference, and then using that task to experimentally assess variables affecting human performance on the task, and human use and acceptance of an expert-aiding system.

The laboratory task developed was that of inferring the nature of an animal, given some set of attributes describing the animal. The task was presented on a micro-computer, with attributes given on the display and subjects requesting more information (attributes) as they desired. The subjects requested information until they felt comfortable making a guess, they then entered a guess and confidence rating. The task was entirely automated to allow recording of all subject "moves".

Twenty-four subjects were individually run on the computer, with no help from an expert-aid. Each performed the task during three different sessions, over the course of three days. Performance of these subjects was measured as a function of various task characteristics (difficulty, amount of information available, etc.). Twelve of the subjects were asked to return and performed the task for two more sessions with the help of a computerized expert-aid (built into the computer on which they were performing the task). An additional 12 subjects with no previous experience were run for two sessions with the expert-aid.

1.3 Findings

Several dependent variables were assessed for subjects run under both Manual and Expert-aided conditions. These included accuracy (percent correct), time to perform the task, certainty of response, and number of attributes requested in a given trial.

First, the development of a sequential diagnostic inference task to be used for laboratory research was highly successful; the task was intrinsically interesting for subjects and adequately allows task and expert system characteristics to be manipulated for complex experimental designs.

Task characteristics which were varied did, for the most part, affect subjects' performance in the expected direction. Difficulty of the trial was best manipulated by the Diagnosticity of the cue set; this variable greatly decreased accuracy and certainty, and increased time to perform the trial and number of attributes requested.

Performance under Expert-aid conditions was generally worse than when subjects performed the task on their own. However, this is interpreted to be a function of the particular Expert system utilized in the study. Although the Expert was programmed to know all of the possible causes (animals) and their associated characteristics, it was not given information concerning the relative probability of the animals (some were common and some were rare). This gave the subject a great advantage over the Expert System on those trials where the attribute information given did not allow a reduction of alternatives down to one. The impact of more accurate Expert Systems is currently being assessed.

Finally, an analysis of subjects' strategies in performing the task compared data obtained from Subjects with predictions based on five alternative strategies; Half-Split, Set Reduction, Hypothesis Testing, Favorite Attribute, and Random Request. The data consistently provided support for the Set Reduction strategy, with indications that subjects occasionally leaned towards the more cognitively demanding Half-Split strategy when the characteristics of the task became easy enough.

Overall, the research project was considered highly successful; a sequential diagnostic inference task was developed along with a basic Expert System which can easily be modified for future research, and data was collected on the impact of one particular type of Expert System on both performance and cognitive strategies of the system user.

2. INTRODUCTION

Computerized automation is becoming increasingly prevalent in a wide variety of positions in the armed services. This is especially true in the world of command, control, and communication (C³) where much of the work involves complex "diagnostic inference". Diagnostic inference refers to a task where a person has informational cues, and on the basis of those cues, must infer the nature of the underlying cause or phenomenon. As technological complexities increase, the human operator will have a more difficult time trying to understand, integrate, and utilize the information made available to him. In contrast to man's limited cognitive capacities and well-documented biases [1,2], a computer can utilize and aggregate large volumes of information using pre-determined optimal strategies. It is no longer a question of whether computer aiding will be used, but how it will be used.

Just as there are problems inherent in using a completely "manual" system to perform these functions, there are also problems in using a completely "automated" system. These problems have been discussed in length elsewhere [2,3], but let it suffice to say that at the current time expert systems are not sufficiently advanced to make automated systems infallible or able to deal with the multitude of unforeseen occurrences that are likely in the C³ environment.

Since neither human nor machine are solely capable of performing situational assessment functions, the solution lies in using both together and relying on the strengths of each. To integrate a person and machine successfully for a given task, one must understand how the human perceives and performs the task and analyze the best way to combine man and machine.

In order to optimally integrate human and machine, we need more information concerning two vital questions: (1) What factors influence the optimal performance of the task by the human and by the automation device? and (2) What factors determine operator acceptance and use of the automated system? For example, if the automation is extremely different from or incompatible with a person's way of perceiving and accomplishing the task, then they may be less likely to accept and use the automation.

A review of the literature reveals that there is a large variety of computerized aiding systems being developed. Several of these aiding systems are specifically designed to aid in diagnostic inference types of tasks. For example, the PROSPECTOR [4,5] system helps geologists locate mineral deposits, MYCIN [6,7] and CADUCEUS [8] are systems which aid in medical diagnosis, and DENDRAL and META-DENDRAL [9] analyze chemical data to make inferences about the structure of unknown chemical compounds. Although these systems are often referred to as "decision aids", the tasks fit into our definition of inference. In this type of system, the computer has a large data base of known facts or expert knowledge which is utilized when a new situation arises

for analysis. The characteristics of the new situation are compared with the data base and an "inference" is generated.

Much of the work being done in this area is conducted by computer scientists and "knowledge engineering" experts [10,11]; this work involves two problems in expert systems, the knowledge base and the inference mechanism. Development of the knowledge base is known as knowledge engineering, and the problem is how to best transfer the knowledge that experts have into the most usable form within the computer data base [11,12]. A second problem involves development of the best inference mechanism or "inference engine". A variety of very sophisticated algorithms is currently under development [13].

Researchers are also finally becoming aware of the need to study the human-computer interface with a focus on the operator who will be using the expert system [12,14,15,16]. A volume recently edited by Salvendy [34] contains numerous papers concerned with user interface and acceptance of the automated system. Unfortunately, much of this work is concerned with the literal human-computer interface, that is, the language used, query system, and so forth. There has been very little systematic research on the question of how the human and machine are interfacing at the deeper task level [for exceptions see 17,18,19]. Some researchers have considered the importance of doctor acceptance of the new diagnostic aiding systems [14,15]. Shortliffe [16] provides a list of factors that may influence a physician's decision to use the system; he has also suggested that even a highly reliable system may face difficulty in user acceptance [20].

Finally, Fitter and Cruikshank [21] obtained video-tape data for 3 physicians, 59 consultations WITHOUT a computer system and 93 consultations WITH the system. Although the researchers assessed many interesting facets of the human-computer system, they did not make any attempt to systematically describe or measure the inference process used by the doctors before and after implementation of the system. Their only comment in this regard was that "the doctors appear to be influenced only to a minor extent by the feedback of disease probabilities, they make very little use of feedback during the consultation but tend to check it against their own judgment at the end" (page 252).

It was felt that empirically derived data could be obtained to address the question of how the implementation of an expert system affects the performance of the human operator. A preliminary model was developed of the characteristics of the interaction between the human and the expert system. This model is applicable only to a situation where the human is completely in control of the task and uses the expert system as an aid, and is therefore completely free to consult (or not consult) the system and disregard the answer given by the expert system.

The system model is visually presented in Figure 1, with input to the system presented on the left. It can be seen that some situational variables will affect only the human operator's inference process, some will affect both human and expert system, and some will affect the operators decision to accept the machine answer. Certainly there are other variables which would influence the process in specific task domains, however, it is felt that

the variables listed represent those which are probably characteristic of most diagnostic inference tasks. Not represented here are factors that will be unique to an individual at the time of each inference. Primarily, these are "cognitive set" variables, where the specific information or attributes received will trigger a specific case in the history of the operator (maybe a recent or very common one). This is a process internal to the operator that is an interaction between the attribute set and the

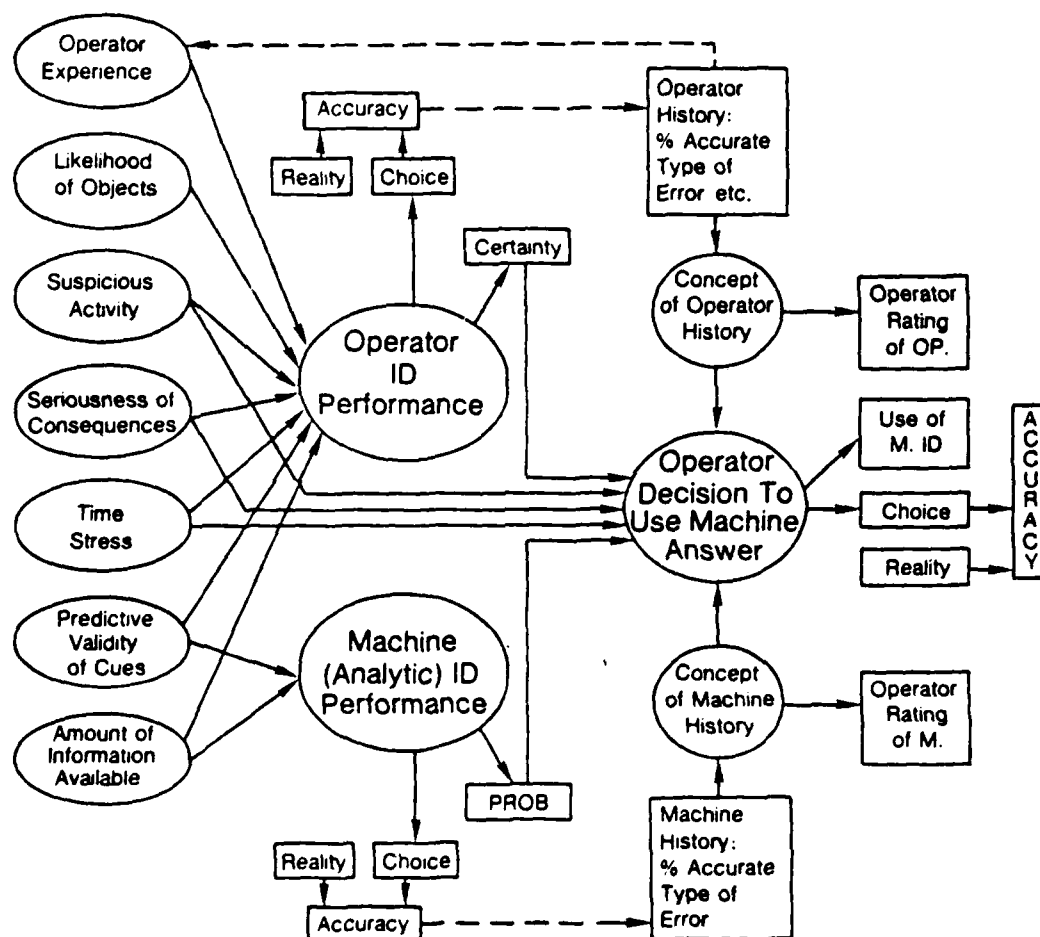


Figure 5. Implementation of Computer-Aiding System

history of the particular operator. An example of this process would be a doctor seeing a patient who is having numbness on one side of the body. The doctor might hypothesize the cause as a stroke because (a) he just had a case similar to this yesterday, or (b) that is the most common cause of the symptom.

Aside from this analogical mechanism, we might expect that to some degree, the operator acts in a rational manner, that is, he considers attributes and searches memory for causes which have matching attributes. To the extent that the subject is experienced and can rely on that memory, he will have confidence in his ability to draw the inference. It is felt that the operator will know when he is definitely certain of the answer or when the inference is tenuous. Especially in the latter case, the operator will consult the expert system for advice. Thus, characteristics causing the human to rely on the expert include (1) small amounts or incomplete information available, (2) low informativeness or predictive validity of the attributes, (3) time stress, (4) perceptions of the person's ability, (5) perceptions of the expert system's ability, and (6) seriousness of the consequences - the more serious the consequence, the less likely the person is to blindly accept the answer of the expert system.

This model guided the experimental design of the research project. A laboratory diagnostic inference task was developed so that most of the input variables outlined on the left could be manipulated while subjects performed the task unaided, and also while they were given the option of consulting an expert system.

3. EXPERIMENTAL METHODOLOGY

3.1 Task Characteristics

The task developed was that of inferring an animal on the basis of a set of characteristics about the animal. An interactive program was written in Turbo Pascal for subjects to perform the task on an IBM personal computer. At the start of a trial, subjects were given an attribute describing an animal. They were then allowed to ask for information regarding other attributes. When subjects felt comfortable with giving a guess, they did so and the trial ended. Under some conditions, the subjects performed the task by themselves, under other conditions subjects were given the opportunity to use an "expert" built into the computer on which they were working. Before describing the task, it should be noted that much thought was given to the decision of using "existing" knowledge sets involving the real world, versus developing a new and artificial set of knowledge that the subjects learn before performing the task. After preliminary development of both kinds of task, it was decided that giving subjects a completely random and arbitrary knowledge base, while being free from previous subject biases, would also be unrealistic and could easily cause cognitive processing different

from that found in most real life tasks.

In order to dampen the effects of subjects' knowledge of animals and/or subject biases, they were "taught" the characteristics of eight animals at the beginning of the first session. Each animal was described in terms of six attributes;

- 1) Size (Large or Small)
- 2) Location (whether found in a Tree or on the Ground)
- 3) Speed (Fast or Slow)
- 4) Color (Brown or Gray)
- 5) Noise (whether the animal makes noise when traveling;
Noise or No Noise)
- 6) Alarm (a chipmunk sounds Alarm for approaching predators;
Alarm or No Alarm).

The attributes taught to subjects for each of the eight animals are listed below:

RABBIT	GROUNDHOG	SQUIRREL
Small	Small	Small
Ground	Ground	Tree
Fast	Slow	Fast
Gray	Brown	Brown
No Noise	No Noise	Noise
No Alarm	No Alarm	No Alarm
DEER	OWL	HAWK
Large	Small	Small
Ground	Tree	Tree
Fast	Fast	Fast
Brown	Gray	Brown
No Noise	No Noise	No Noise
No Alarm	Alarm	Alarm
BEAR	WOLF	
Large	Large	
Ground	Ground	
Slow	Fast	
Brown	Gray	
Noise	No Noise	
Alarm	Alarm	

In the following sections, the inference task will be described in detail. The research was conducted in two phases, one where subjects performed the task under manual conditions (no expert system), and a second phase where subjects performed the same task and had the option of consulting an expert. Subjects in the second phase were partly subjects from phase I and partly new subjects. Task scenarios for each of the two phases will be described separately.

3.1.1 Manual Task Scenario

In the "manual" condition, subjects performed the inference task without the aid of an expert system. This was the first phase of experimentation, and was primarily designed to assess the cognitive processes and strategies being used by subjects. In this condition, subjects were initially given one attribute (i.e., the animal is "small"). Then subjects were asked to provide a preliminary guess of the type of animal. This was simply a way of measuring the subjects' hypothesis at this point.

Figure 2a gives an example of the display screen as it was first presented to subjects. It can be seen that the eight possible answers were always listed at the top of the screen. The "trial" was simply a consecutive running number that informed subjects of the trial number for that session. The "condition" variable always reads either "DAY" or "NIGHT". Subjects were told that if it was daytime, they would receive more information than if the trial occurred during the night. That is, for some attribute categories, subjects were told that the information was "unknown" (this will be demonstrated in Table 2). This was the principle way that task characteristics were varied - by varying the number and informativeness of the attributes. Finally, it can be seen that the attribute first given to this subject was "Small". After entering the subject's first guess, they were asked to give a certainty rating on a scale of 1 to 9, with 1 = not at all certain and 9 = extremely certain. Next, subjects were given a choice as to whether they wished to acquire more information or go on to the next trial. If they chose to continue, subjects were then allowed to ask for information regarding any of the remaining five attributes. As they asked for the information, their choices and the time to perform the choice was recorded. They were always required to give a guess and certainty rating after each new piece of information. The format of the question/ answer interface is shown in Figure 2b. In the example given, the subject has just decided to ask about the animal location. Figure 2c shows the screen after the subject has acquired enough information to make a final guess. When the subject has made their final guess, they press "B" rather than "A" to signal that they are ready to go on to the next trial. At that point, they are informed as to the correct answer for that trial (see Figure 2d).

```

POSSIBLE CHOICES

RABBIT          DEER
SQUIRREL        WOLF
GROUNDHOG       BEAR
HAWK            OWL

TRIAL   :    1
CONDITION :  NIGHT

CODE--ATTRIBUTES :

1--SIZE      :    Small
2--LOCATION    :
3--SPEED     :
4--COLOR     :
5--NOISE     :
6--ALARM     :

GUESS: type the FIRST LETTER of the animal.

```

2a. Initial Display Screen

```

GROUNDHOG       BEAR
HAWK            OWL

TRIAL   :    1
CONDITION :  NIGHT

CODE--ATTRIBUTES :

1--SIZE      :    Small
2--LOCATION    :
3--SPEED     :
4--COLOR     :
5--NOISE     :
6--ALARM     :

GUESS: type the FIRST LETTER of the animal.
R
CONFIDENCE RATING:  1 to 9,
2
CONTINUE :  enter " A " NEXT TRIAL: enter " B "
A
REQUEST ANOTHER ATTRIBUTE:
ENTER the NUMBER to the LEFT of the ATTRIBUTE.
2

```

2b. Display after first Attribute Request

Figure 2. Displays for Manual Diagnostic Inference

POSSIBLE CHOICES

RABBIT
SQUIRREL
GROUNDHOG
HAWK

DEER
WOLF
BEAR
OWL

TRIAL : 1
CONDITION : NIGHT

CODE--ATTRIBUTES :

1--SIZE : Small
2--LOCATION : Unknown
3--SPEED :
4--COLOR : Grey
5--NOISE :
6--ALARM : Alarm

GUESS: type the FIRST LETTER of the animal.

2c. Display after Three Attributes Requested

Your final answer was Owl

The correct answer is Owl

PRESS ANY KEY TO CONTINUE TRIALS

2d. Final Display Screen

3.1.2 Expert-Aid Task Scenario

In the "Expert-aid" condition, subjects performed basically the same task as in the manual condition, however, they were allowed to ask an "expert" for help. This expert was built into the computer system (an integral part of the task program), and required only slight modifications to the task. Subjects were allowed to consult the expert at any time during the trial, and were only allowed to ask twice per trial. The task scenario will be described in this section, and the nature of the expert system will be described in the following section. In addition, Appendix A provides the Pascal program which was used to run subjects in the Expert-aid condition.

It was felt that asking subjects to overtly hypothesize an animal after every attribute was not necessary in the expert-aid phase of the study. After acquiring each attribute, the subject was given three choices, ask for more information, make a guess, or ask the expert. An initial screen state for this task is given in Figure 3a. It can be seen that in general, the display characteristics are similar. (The subjects did not have any problems going from manual task performance to expert-aid conditions.) Figure 3b shows a display after the subject has asked for several attributes and has also asked the expert (expert answer displayed to the right of "EXPERT"). In the example, the subject has just entered a guess (after deciding to use the advice of the expert).

3.2 The Expert System

Because the information base for the task was small and well-defined, it was a simple task to build an "expert" for this particular domain. First, a data bank was built to include all of the animal names and associated characteristics. Thus, the computer expert had perfect knowledge of the attributes and associated animals. Next, a subroutine was written which "read" the screen displayed at the time the subject asked for help. The attributes presented were matched to the attribute sets in the expert memory system and when a match was found, that animal was presented as the answer (see Appendix A). Because the attribute sets were often incomplete, the computer could come up with more than one animal that matched the particular set of attributes being displayed. The subroutine was written such that the order of matching took place randomly, and therefore the "choice" between more than one possible answer was a random one. Notice that in this case, only one answer was provided to the subject, not all possible answers.

```

POSSIBLE CHOICES

RABBIT          DEER
SQUIRREL        WOLF
GROUNDHOG       BEAR
HAWK            OWL

TRIAL   :    1
CONDITION :  NIGHT
EXPERT  :

CODE--ATTRIBUTES :

1--SIZE      :    Small
2--LOCATION    :
3--SPEED     :
4--COLOR     :
5--NOISE     :
6--ALARM     :

(A)--ATTRIBUTE (E)--EXPERT (G)--GUESS

```

3a. Initial Display Screen

```

RABBIT          DEER
SQUIRREL        WOLF
GROUNDHOG       BEAR
HAWK            OWL

TRIAL   :    1
CONDITION :  NIGHT
EXPERT  :          Owl

CODE--ATTRIBUTES :

1--SIZE      :    Small
2--LOCATION    :    Unknown
3--SPEED     :
4--COLOR     :    Grey
5--NOISE     :
6--ALARM     :

(A)--ATTRIBUTE (E)--EXPERT (G)--GUESS
G
GUESS : type the FIRST LETTER of the animal.
O
CONFIDENCE RATING : 1 to 9,
8

```

3b. Display after Guess and Confidence Rating

Figure 3. Displays for Expert-Aided Diagnostic Inference

3.3 Experimental Design

Phase I

In the manual phase of the research, the following independent variables were manipulated:

- (1) Session (1, 2, or 3)
- (2) Likelihood of the animal (Common vs. Rare)
- (3) Number of Attributes available (two vs. four)
- (4) Diagnosticity of attribute set (low vs. high)
- (5) Monetary Payoff (low vs. high)

The first variable was manipulated by telling subjects before performing the task that five of the animals (squirrel, owl, hawk, deer, and rabbit) would be relatively common, and more likely to be the answer than the other three (bear, wolf, and groundhog), which would be relatively rare. In setting up the trials, the common animals were, on the average three times as likely to occur as the rare animals.

The second variable, Attributes available, was manipulated by making either two or four of the six attributes have values (as opposed to being "unknown") on any given trial. To keep this from becoming obvious to the subject, a small number of filler trials were given with either three or five attributes available.

The third variable, Diagnosticity, was one of the most critical of the independent variables. For any given set of attributes that could be potentially available (for example, if the subject asked for all six and received either two or four), that set of information could be highly diagnostic where there was only one possible answer, or it could be low in diagnosticity where there was more than one possible answer. For every trial, attribute sets were developed such that if the subject obtained all available information, there was either only ONE possible answer (high diagnosticity) or there were TWO possible answers (low diagnosticity). This was the primary way in which the difficulty of the trial was manipulated.

Finally, in an effort to manipulate the "seriousness of the consequence" input variable (see Figure 1), the amount of money to be earned by the subject for good performance was varied. One group of subjects was promised \$.50 per day for getting at least 70% of the trials correct. The other group of subjects was promised \$3.00 per day for getting at least 70% of the trials correct. All subjects were also told that they would receive a bonus for simply coming to all three sessions.

The last variable, subject payment, was a between-subjects variable, all others were within-subjects. The general design of each of the three sessions was as follows:

<u>Low Diagnosticity</u>		<u>High Diagnosticity</u>	
Two	3 Common animals	3 Common animals	
Attr.	1 Rare animal	1 Rare animal	
Four	3 Common animals	3 Common animals	
Attr.	1 Rare animal	1 Rare animal	

For each of the three sessions, 16 trials were critical in the assessment of the effects of the independent variables. These 16 trials are those formed by combining the independent variables given above.

The trials were developed so that animals were counter-balanced across the four conditions listed above (i.e. deer was represented equally in all four cells). Two separate sets of trials were developed for replication purposes. The two sets were equivalent in all ways except for the exact animal/attribute combinations.

In the first session, subjects spent some amount of time learning the animal/attribute information, and time only allowed three additional "filler" trials. In the second and third sessions, subjects performed 24 trials resulting from the 16 critical trials plus eight "filler" trials. To maintain consistency across trials and sessions, only the 16 critical trials were used in most of the data analysis.

Information was recorded for attributes requested, guesses, certainty ratings, and asking of the expert. All of these behaviors were recorded as they occurred, preserving the order, and in addition, the time in seconds (down to the hundredth) was recorded for each behavior. Finally, subjects were asked to fill out a questionnaire at the end of the third session (see Appendix B1). Part of this questionnaire involved asking the subject to estimate their performance for each of the three sessions. This allowed, at a minimum, the measurement of the following dependent variables:

- (1) accuracy (Percent Correct)
- (2) Time to perform the task
- (3) subjective Certainty
- (4) Attributes Requested
- (5) Subjective Perception of performance

Phase II

In the second phase of the project, the task differed in two respects; subjects only gave one guess and certainty rating at the end of the trial, and they were allowed to consult the expert. Several of the independent variables were retained in Phase II; Likelihood of the animal, number of Attributes Available, and Diagnosticity of the attribute set.

Twelve of the subjects from Phase I were asked to come back in for two more sessions, six were from the high pay condition, and six were from the low pay condition. They were deliberately chosen to represent a variety of ability in terms of their perfo-

rmance in Phase I. These subjects will be referred to as the "Experienced" subjects. In addition, twelve "Novice" subjects were run in Phase II, thus creating the between-subjects variable of Experience.

The within-subjects variables were combined in the same way as in Phase I, resulting in 16 critical trials during each of the two sessions. All new trials were created so that the experienced subjects would not see any that they had previously performed. Because of the small amount of time required to perform the trials (with only one guess at the end), subjects performed 30 trials total for each session. To ensure equivalency across sessions, most of the data analysis only involved the 16 critical trials. As in Phase I, animals were counterbalanced across the experimental conditions, and two sets of replications were used.

After finishing the second session, subjects were asked to fill out a questionnaire (see Appendix B2). The first two questions asked the subject to rate their own performance on a scale of 1 to 20 (with 1 being "extremely inaccurate" and 20 being "perfect"), and to rate the expert's performance on the same scale of 1 to 20. Additional items asked the subject to estimate their accuracy on each of the two days, describe their strategy, and comment on the expert system.

The design allowed for the following dependent variables to be assessed:

- (1) Accuracy (Percent Correct)
- (2) Time to perform the task
- (3) Subjective Certainty
- (4) Attributes Requested
- (5) number of times the Expert was Asked for an answer
- (6) number of times (or under what conditions) the Expert answer was Used
- (7) at what point in the task the expert was consulted
- (8) Subjective Perception of the subject's performance
- (9) Subjective Perception of the expert's performance.

3.4 Subjects

Subjects were 36 upper level students enrolled at the University of Idaho with a mean age of approximately 21. The subjects were obtained by having several instructors announce the experiment in their classes. Most of the students came from either psychology or engineering classes. Because of the possible difference in the two subject populations, every attempt was made to spread them evenly across the between-subjects variable (high or low payoff).

Four of the subjects who started in Phase I did not complete their three sessions and were replaced with other subjects (their data was thrown out). Three subjects did not complete Phase II and were replaced as well. Finally, one subject in Phase II never asked for the expert advice during any of the 60 trials. It was decided that this was not similar to what would be expected in a real world situation, and the subject was replaced

with a new one.

Subjects were instructed as to the nature of the experiment and treated in accordance with American Psychological Association ethical guidelines. Informed consent was obtained and names were stricken from all records as soon as data collection was complete for the subject.

3.5 Procedure

Subjects were run individually in a small room equipped with several tables, chairs, and one IBM personal computer. The experimenter was with the subject the entire time the subject performed the task, however, the experimenter was usually reading or working at a table behind the subject.

When the subject arrived the first day, they were told that we were studying how people solve problems. They were told that they were going to be playing a simple guessing game, like "I'm thinking of an animal that's small, brown, and noisy, what is it?". The nature of the task was briefly outlined to the subjects and they were shown a list of the eight animals (with the rare animals marked with an *). The subjects were then given a list of the eight animals, each with a list of the associated attributes (similar to the list given previously in this report). Subjects were allowed to study the list as long as they wished up to ten minutes. Most subjects studied the list between six and eight minutes. Subjects were then placed in front of the computer and a practice trial was called to the screen. Subjects in the "Expert-aid" phase were introduced to the use of the expert at this time. The display was explained to the subjects as well as keys to press for each desired action. The subject was allowed to perform the practice trial, and ask the experimenter questions about the task. They were told that they should perform the trials accurately, but also as quickly as possible since they were being timed. Subjects in the low pay condition were told that they would receive \$.50 per session for getting at least 70% right, subjects in the high pay condition were told that they would receive \$3.00 per session for getting at least 70% right.

All subjects completed the trial sets within one hour. In Phase I, most subjects took at least 30 minutes to perform all the trials in a session. In Phase II, experienced subjects usually completed the trials within 30 minutes, while the novice subjects generally took 30-40 minutes.

After subjects were finished with the last session in the phase, they were asked to fill out the questionnaire described earlier. The experimenter was available during that time to answer questions the subjects had on any of the items.

In phase I, all subjects were paid \$20 regardless of performance on the trials. In phase II, all subjects were paid \$14 each regardless of performance on the trials. After the final session and questionnaire, subjects were debriefed and asked not to discuss the experiment with other potential subjects.

4. EXPERIMENTAL FINDINGS

4.1 Phase I: Manual Diagnostic Inference

Results from the first phase which was solely manual performance of the task will be reported first. The results will be presented in three sections, the first deals with overall subject performance on the task, the second summarizes results for subjects' performance estimates, and the third will detail the analysis of subjects' strategies in performing the task.

4.1.1 Performance Measures

A Multivariate Analysis of Variance was performed on the data from the 24 Phase I subjects. The between-subjects variable of "pay condition" did not significantly affect subject's performance. Because of this, it was decided that analysis efforts would concentrate on only those 12 subjects who eventually went on to participate in Phase II (six from High Pay and six from Low Pay). Consequently, the analyses to be described are based on 12 subjects with no payment manipulation.

A Multivariate Analysis of Variance was performed on data for the 12 subjects who later performed under Phase II. The independent variables (all within-subjects) were Session (1 vs. 2 vs. 3), Attributes Available (two vs. four), and Diagnosticity of the cue set (low vs. high). The dependent variables included Percent Correct, Time, Certainty, and number of Attributes Requested (see section 3.3 for the explanation of these variables). The statistical summaries for this analysis are presented in Appendix C. The findings will be described here along with cell means. Only those effects which were significant in the Multivariate test as well as the Univariate test will be reported.

Means for the first dependent variable, Percent Correct (out of four) are presented in the first section of Table 1. A main effect was found for Session, where subjects improved on performance from Session 1 ($\bar{x}=0.68$), to Session 2 ($\bar{x}=0.78$) to Session 3 ($\bar{x}=0.83$). In addition, a main effect was found for Diagnosticity, where trials having a high diagnosticity (ONE animal possible) resulted in better performance ($\bar{x}=0.87$) than trials having a low diagnosticity ($\bar{x}=0.65$). This is reasonable in light of the fact that by nature, the later type of trial is much more difficult. It might be expected that the low diagnosticity trials (resulting in a guess between two animals) should result in Percent Correct scores of approximately 50%, however, it should be kept in mind that subjects knew that the "rare" animals were less likely, and this could help them correctly choose between Common and Rare alternatives.

The second dependent variable, Time to perform the trial (from time of initial presentation to time of final guess) was also affected by Session and Diagnosticity of the Cue Set. The time to perform the task fell from a mean of 85 sec. for the first session, to 65 sec. for the second session, to 58 sec. for the third session. The main effect of diagnosticity resulted in

Table 1. Cell Means for Phase I (all dependent variables)

PERCENT CORRECT				
	Session 1	Session 2	Session 3	
Low Diagnosticity				
Two Attributes Avail.	.50	.67	.79	
Four Attributes Avail.	.71	.69	.56	
High Diagnosticity				
Two Attributes Avail.	.79	.87	.98	
Four Attributes Avail.	.71	.89	.98	
TIME				
Low Diagnosticity				
Two Attributes Avail.	85.7	77.4	63.2	
Four Attributes Avail.	90.3	74.7	72.6	
High Diagnosticity				
Two Attributes Avail.	89.2	50.5	49.1	
Four Attributes Avail.	76.5	57.2	49.6	
CERTAINTY				
Low Diagnosticity				
Two Attributes Avail.	5.48	5.36	5.40	
Four Attributes Avail.	6.47	6.08	5.86	
High Diagnosticity				
Two Attributes Avail.	7.09	7.70	7.80	
Four Attributes Avail.	7.44	8.20	7.87	
ATTRIBUTES REQUESTED				
Low Diagnosticity				
Two Attributes Avail.	3.4	3.6	3.5	
Four Attributes Avail.	3.1	3.3	3.7	
High Diagnosticity				
Two Attributes Avail.	2.7	2.4	2.6	
Four Attributes Avail.	2.6	2.6	2.5	

longer trial times for the low diagnosticity conditions ($\bar{X}=77$) than for the high diagnosticity conditions ($\bar{X}=62$). Finally, an interaction between Session and Diagnosticity (as seen in Figure 4) reveals that, over sessions, subjects improved their trial times much more significantly for the easy trials than for the more difficult trials.

Subjects were asked to rate how certain they were of their guess at the end of each trial (on a scale of 1 to 9). The Certainty ratings for the subjects varied for the two Attributes Available conditions. When there were two possible attributes for subjects to acquire, they gave a mean certainty rating of 6.47. When there were four attributes possible, subjects gave a mean certainty rating of 6.99. Although this difference is statistically significant, it can be seen that the difference between the means is not a particularly great one. Since the number of attributes provided to subjects was manipulated orthogonally to the difficulty of the trials (Diagnosticity), the greater confidence in the trials with four attributes available indicates that subjects were "lulled" into believing that they are more accurate when they have more information.

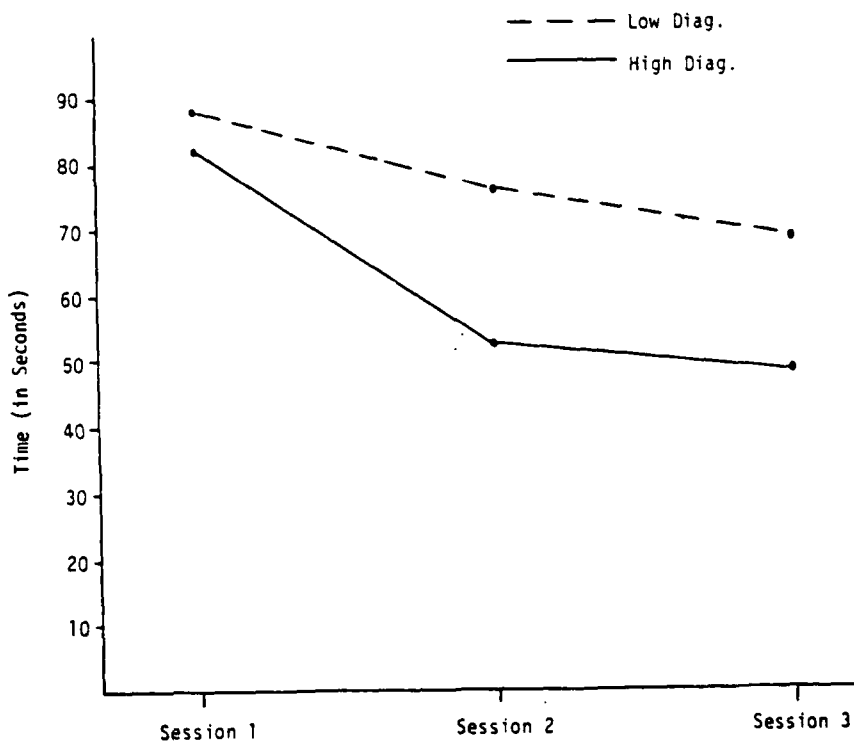


Figure 4. Mean TIME to perform the task as a function of Session and Diagnosticity.

A greater difference in certainty ratings was caused by the Diagnosticity of the trials. The easier high diagnosticity trials resulted in a mean rating of 7.58, while the more difficult low diagnosticity trials resulted in a mean rating of 5.77. Notice that this second rating seems fairly high considering that for all of these trials, subjects, by definition, HAD to be guessing between at least two animals. Finally, an interaction between Session and Diagnosticity reveals that subjects' confidence in their guess went up over sessions for the easy trials, and dropped slightly over time for the more difficult trials.

For the final dependent variable, subjects were assessed on the number of attributes they requested after the first attribute was presented. Means for this variable are thus number of attributes requested out of a total of five possible. A main effect of Diagnosticity was found, where high diagnosticity trials resulted in a mean of 2.6 attributes requested whereas the low diagnosticity trials resulted in a mean of 3.4 attributes requested. In addition, a Session by Diagnosticity interaction (shown in Figure 5) depicts a learning effect, where subjects learned to ask for more attributes for those trials where it was necessary (low diagnosticity trials).

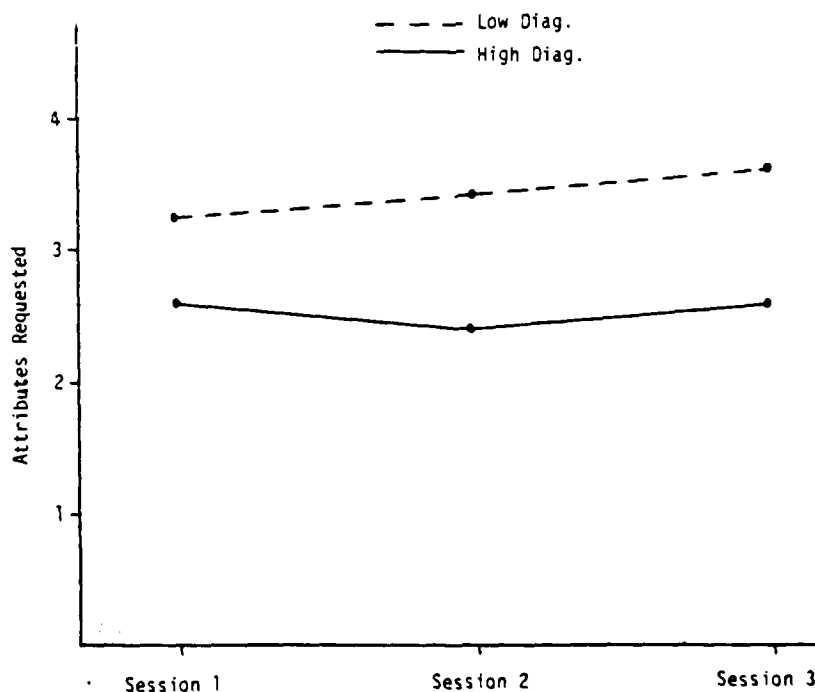


Figure 5. Mean number of Attributes Requested as a function of Session and Diagnosticity.

4.1.2 Performance Estimates

After the completion of Phase I, subjects were asked on a questionnaire to estimate their performance for all three sessions. They were asked to estimate the percent of trials they answered correctly for each of the three sessions. These estimates were then compared to the actual Percent Correct scores. An analysis of variance showed that subjects underestimated their performance for all three sessions, $F(1,11)=4.67, p=.05$. The means are given below for actual vs. estimated performance for all three sessions.

	ACTUAL	ESTIMATED
SESSION 1	.68	.60
SESSION 2	.78	.72
SESSION 3	.83	.79

4.1.3 Strategy Analysis

Strategy Classification

To perform the strategy analysis, subjects' questionnaires were first reviewed to determine what subjects thought they were doing. This resulted in several categories of strategies, and the experimenter also tried to determine a reasonable classification of strategies, partly on the basis of previous research in this area. At this point, the raw data for subjects in sessions 2 and 3 were reviewed to determine whether evidence could be found for any of the strategies defined. On the basis of this data review work, the strategy classifications were slightly revised. The resultant classification system contains five cognitive strategies which subjects might use during the course of the task. These strategies are given below (an example will follow depicting each strategy):

(1) Half-Split. This is a well-known classical strategy that is the most "rational" procedure possible for the task[22]. After the initial attribute acquisition, the subject brings into "working memory" all of the animals which have that attribute. Then a new attribute is requested which comes closest to "splitting" the set of possible animals in half. This procedure is followed until the set is narrowed down to one, or the subject runs out of attribute information. (This strategy is not the only means to the desired end, however, it ensures getting there with the fewest attribute requests.)

EXAMPLE:

First Attribute Given: NO NOISE

Subject:

- (1) Determine possible animals:

RABBIT
HAWK
OWL
DEER
GROUNDHOG
WOLF

- (2) Determine splits:

SIZE	Small(4)	Lge(2)
LOC	Grnd(4)	Tree(2)
SPEED	Fast(5)	Slow(1)
COLOR	Gray(3)	Brwn(3)
ALARM	No(3)	Yes(3)

- (3) Choose attribute resulting in closest to "equal" split:

ASK FOR COLOR OR ALARM

Second Attribute Given: GRAY

Subject:

- (1) Determine possible animals:

RABBIT
OWL
WOLF

- (2) Determine splits:

SIZE	Small(2)	Lge(1)
LOC	Grnd(2)	Tree(1)
SPEED	Fast(3)	Slow(0)
ALARM	No(1)	Yes(2)

- (3) Choose attribute resulting in closest to "equal" split:

REQUEST SIZE, LOC, or ALARM

etc.

(2) Set Reduction. This strategy is an easier way to reduce the alternatives than the first strategy. Again, after the first attribute, the subject must think of a set of animals with that attribute. However, the subject must only think of a set that can be differentiated on SOME other attribute. The subject does not have to think of ALL animals with that attribute, nor then consider ALL possible attribute requests and whether one is best. The subject will simply determine an attribute that is diagnostic

to any degree at all, and request that attribute. The subject then determines a set of animals that fit the two attributes known, and determines whether there is another attribute that can differentiate between them. This continues until the subject narrows down the set enough to ensure consideration of all possible animals with the known attributes (which may not happen at first). A reduction of the set down to two alternatives will place the subject in the same position as for the Half-Split strategy.

EXAMPLE:

First Attribute Given: NO NOISE

Subject:

- (1) Determine some set of animals with known attribute: RABBIT
WOLF
OWL
- (2) Choose any attribute which will differentiate among these: ASK FOR LOCATION

Second Attribute Given: GROUND

Subject:

- (1) Determine some set of animals with known attributes: RABBIT
DEER
GROUNDHOG
- (2) Choose any attribute which will differentiate among these: ASK FOR SIZE

Third Attribute Given: LARGE

Subject:

- (1) Determine some set of animals with known attributes: DEER
WOLF
- (2) Choose an attribute which will differentiate among animals: ASK FOR ALARM

(3) Hypothesis Testing. In this strategy, the subject again considers some subset of animals that have the initial attribute. However, the subject will clearly have a favorite (hypothesis) and will request an attribute to confirm that choice. That is, they will ask for an attribute that characterizes that animal and (optimally) no other.

EXAMPLE:

First Attribute Given: NO NOISE

Subject:

- (1) Determine some of possible animals with one favorite:
GROUNDHOG (favorite)
RABBIT
WOLF
- (2) Choose attribute to request that is most uniquely characteristic of favorite animal:
ASK FOR SPEED (looking for SLOW)

Second Attribute Given: FAST

Subject:

- (1) Determine new set with favorite:
RABBIT (favorite)
HAWK
DEER
- (2) Choose attribute to request that is most uniquely characteristic of favorite animal:
ASK FOR GRAY

etc.

(4) Favorite Attributes. In this strategy, subjects did not attempt to reduce a set of possible alternatives, but rather their attention was focused more on acquiring certain kinds of information. This strategy would lead to having favorite attributes which are always requested first (and second, third, etc.). The subject might still keep track of possible animals to some degree, otherwise they would always ask for the same number of attributes, in the same order, no matter what the trial, and this never seemed to occur.

EXAMPLE:

TRIAL 1

First Attribute Given: NO NOISE

Subject:
ASK FOR SPEED

Second Attribute Given: FAST

Subject:
ASK FOR LOCATION

etc.

TRIAL 2

First Attribute Given: ALARM

Subject:
ASK FOR SPEED

Second Attribute Given: FAST

Subject:
ASK FOR LOCATION

etc.

(5) Random Request This is an unlikely but possible strategy, where after the initial attribute, the subject simply randomly chooses one of the remaining five attributes to request. (Notice that this is compatible with a general hypothesis testing strategy that does not make any effort to assess the best attributes to request; an animal is hypothesized and any attribute might be requested to confirm that hypothesis).

Data Analysis

To determine which of the five strategies subjects were using, it was necessary to derive predictions based on each strategy and compare the data with those predictions. The prediction and relevant data for each strategy will be described in this section. In obtaining data for the strategy analysis, only data from sessions 2 and 3 were included.

To begin, three of the strategies will be covered together because the same set of data is relevant to them.

(1) Half-Split:

The Half-Split strategy predicts that the attribute requested will be that which most evenly splits the possible animals into groups. Thus, for each beginning attribute it was possible to determine the "best" split(s). A second category of splits was determined which were diagnostic but not optimally so, and finally, a third category of attribute requests was identified which was not at all diagnostic. For example, if "Small" is the first attribute given, the best attribute requests are Location, Color, and Alarm. The acceptable attribute requests would be Speed or Noise. The Half-Split strategy predicts that subjects will always request the optimum attribute or the "best" split. Table 2 shows these three categories of attribute request; they are listed as three columns and specify the predicted attribute requests for each possible first attribute. The numbers refer to subject data and will be explained below.

(2) Set Reduction:

The Set Reduction strategy predicts that subjects will request any attribute that is at all diagnostic. In terms of the three types of attribute request listed in Table 2, this strategy predicts that subjects will request the first or second type of attribute, but never the non-diagnostic attribute in the far right column. To summarize, the Half-Split predicts attribute requests only of "best" split variety, while the Set Reduction strategy predicts use of both "best" and "acceptable" split attribute requests.

(3) Random Request:

This strategy predicts that the subjects will not discriminate between the three types of category discussed above and the second attribute requests will be spread equally across the alternative attributes. This means that the expected values for each of the categories can be obtained by determining the proportion of attributes occurring in each category.

The data for subjects' first attribute requests are given in Table 2. The numbers represent the percent of requests that fell in a particular category. For example, when Small was the

Table 2. Percentage of First Attribute Requests Categorized According to Type of Split.

FIRST ATTR.	"BEST" SPLIT REQUESTS	"ACCEPTABLE" SPLIT REQUESTS	NON-DIAG REQUESTS
Small	Loc .40	Speed .00	
	Color .18	Noise .16	
	Alarm .26		
	TOTAL .84	TOTAL .16	--
Large	Speed .09		Loc .07
	Color .27		
	Noise .18		
	Alarm .39		
	TOTAL .93	--	TOTAL .07
Ground	Size .31	Noise .21	
	Speed .17		
	Color .21		
	Alarm .10		
	TOTAL .79	TOTAL .21	--
Tree	Color .40		Speed .00
	Noise .23		Size .01
	Alarm .36		
	TOTAL .99	--	TOTAL .01
Fast	Loc .27	Size .23	
	Color .21	Noise .06	
	Alarm .23		
	TOTAL .71	TOTAL .29	--
Slow	Size .34		Color .07
	Noise .28		Loc .07
	Alarm .24		
	TOTAL .86	--	TOTAL .14
Brown	Size .36		
	Loc .19		
	Speed .14		
	Noise .17		
	Alarm .14		
	TOTAL 1.00	--	--

Table 2 (cont.)

Gray	Size	.32		Noise	.03
	Loc	.37		Speed	.00
	Alarm	.28			
	TOTAL	.97	--	TOTAL	.03
No Noise	Color	.16	Loc	.32	
	Alarm	.10	Size	.38	
			Speed	.04	
	TOTAL	.26	TOTAL	.74	--
Noise	Size	.64		Color	.04
	Loc	.23			
	Speed	.00			
	Alarm	.09			
	TOTAL	.96	--	TOTAL	.04
No Alarm	Size	.28			
	Loc	.37			
	Speed	.05			
	Color	.18			
	Noise	.12			
	TOTAL	1.00	--		--
Alarm	Size	.34	Speed	.04	
	Loc	.24	Noise	.17	
	Color	.21			
	TOTAL	.79	TOTAL	.21	--
Mean Percentage					
OBTAINED for all					
Combined (N=576):					
	(n=479)	.83	(n=85)	.15	(n=12) .02

Mean Percentage					
EXPECTED based on					
Half-Split Strategy:					
	1.00		.00		.00
Mean Percentage					
EXPECTED based on					
Set Reduction Strategy:					
	.83		.17		.00
Mean Percentage					
EXPECTED based on					
Equal Choice:					
	.67		.16		.16

first attribute provided, subjects asked for Location in 40% of the trials. The total for each subset is given below the set of attributes in a given section (eg., when Small was the first attribute, the "best" split attributes were requested 84% of the trials). The percentages for all trials combined are given below the final TOTAL row.

It can be seen by comparing the obtained data with the predictions given at the bottom of Table 2 that the data are much consistent with the Set Reduction strategy than the Half-Split strategy. However, they are not entirely consistent with the Set Reduction strategy because there were a few trials where subjects asked for a NON-DIAGNOSTIC attribute (category #3). Because the expected value for this category is zero, and the obtained value was greater than zero, a Chi-Square analysis for goodness-of-fit could not be conducted for either of the first two strategies. A goodness-of-fit test was conducted using the expected values based on an equal (proportional) use of the three categories (the last set of expected values in Table 2). A χ^2 analysis showed that subjects' requests did differ significantly from these three expected values, $\chi^2(2) = 95.2$, $p < .001$.

To try to determine whether the data fit either strategy (1) or (2) more closely, analysis was conducted using the data for only those trials where subjects had a choice between "best" split attributes and "acceptable" split attributes (Small, Gray, etc.). In this analysis, the Set Reduction strategy produced the expected values, based on the assumption that since subjects did not discriminate between "best" and "acceptable" attribute requests, they would be chosen an equal amount of the time (or more accurately, proportionately to the number of attributes in each category). Thus, a test of the difference between the obtained values and the expected values was a test of the Set Reduction strategy. To the extent that the obtained values differed in the direction of the "best" split, this would provide indirect support for the Half-Split Strategy.

The obtained and expected values for each of the two categories were:

	Best Split	Acceptable Split
OBTAINED	140	85
EXPECTED (Set Reduction)	127	98

A χ^2 test for goodness-of-fit showed that the obtained values did NOT significantly differ from the expected values based on the Set Reduction strategy, $\chi^2(1) = 3.05$. This can be taken as evidence in support of the Set Reduction strategy relative to the Half-Split strategy.

An analysis of second attribute requests was carried out in a manner similar to that just described. The data obtained for this analysis are more complicated because at this point, subjects have obtained information for two attributes (although in some

cases the second piece of information was "unknown"). Frequencies were calculated for all possible combinations of known attributes and the resultant second attribute requests (for example, one combination would be ALARM given first, NO NOISE given after first request, then COLOR as the second request). These combinations were then categorized as to whether they were the "best split" possible, an "acceptable split", or a non-diagnostic request.

It turned out that for all combinations, there were no instances where a decision for the second request had to be made between all three types of category. A decision had to be made between either

- (1) all second requests were category #1
- (2) all second requests were category #2
- (3) all second requests were category #1 or #2
- (4) all second requests were category #1 or #3.

An example of (4) would be SMALL and GRAY given, with the alternative second requests being

Location	Category #1 (Best Split)
Alarm	Category #1
Speed	Category #3 (Non-diagnostic)
Noise	Category #3.

The frequency of choices made between categories 1 and 3 were used to compare the Half-Split and Set Reduction strategies with a simple Random Request strategy. The data for these frequency tabulations are given in the top half of Table 3. The frequencies are listed according to the choices possible. The example given above would fall under the "2 Best, 2 Non-diagnostic" section. Totals were obtained for all choices involving #1 vs. #3 categories. These totals are listed at the bottom of the first section, along with the expected frequencies based on a random choice among the alternative second requests. A χ^2 analysis was performed on these data and showed that the obtained frequencies are nowhere near what would be expected on the basis of random choice, $\chi^2(2)=182.2, p<.001$. This provides support for both the Half-Split and Set Reduction strategies (it is not possible to distinguish between the two in this analysis).

A similar analysis was performed for the data comparing the frequency of choices between category #1 (Best Split) and category #2 (Acceptable Split). These frequencies are given in the lower half of Table 3 and are also arranged according to the division of alternatives (3 out of the four alternatives were the Best-Split, etc.). Totals were obtained for all choices between category #1 and #2, and are listed at the bottom of the table. The Half-Split strategy predicts that category #1 would always be chosen over category #2, whereas the Set Reduction strategy predicts that no preference would be shown for either category type, and therefore the frequencies should be the same as those expected by chance. The expected frequencies based on the Set Reduction strategy were calculated and are given below

Table 3. Frequency of Second Attribute Requests Categorized
According to Type of Split.

CATEGORY 1 VS 3, CHOICE BETWEEN:	"BEST SPLIT" REQUESTS	"NON-DIAGNOSTIC" REQUESTS
3 Best, 1 Non-Diag.		
OBTAINED	75	3
EXPECTED	58.5	19.5
2 Best, 2 Non-Diag.		
OBTAINED	158	9
EXPECTED	83.5	83.5
1 Best, 3 Non-Diag.		
OBTAINED	28	2
EXPECTED	7.5	22.5
TOTAL OBTAINED	261	14
TOTAL EXPECTED (Random)	149.5	125.5
CATEGORY 1 VS 2, CHOICE BETWEEN:	"BEST" SPLIT REQUESTS	"ACCEPTABLE" SPLIT REQUESTS
3 Best, 1 Acceptable		
OBTAINED	28	4
EXPECTED	24	8
2 Best, 2 Acceptable		
OBTAINED	40	21
EXPECTED	30.5	30.5
1 Best, 3 Acceptable		
OBTAINED	9	18
EXPECTED	6.75	20.25
TOTAL OBTAINED	77	43
TOTAL EXPECTED (Set Reduction)	61.25	58.75

the TOTAL OBTAINED values. First, it can be seen that the obtained values do not lend support to the Half-Split strategy predictions (which would predict only category #1 choices). However, a χ^2 analysis showed that the obtained values did significantly differ from the expected values based on the Set Reduction strategy, $\chi^2(1)=8.27, p<.01$. The difference is in the direction of a greater frequency of category #1 choices than would be expected. This is in contrast to the results described previously for the FIRST attribute request analyses (which completely supported the Set Reduction strategy). This difference will be discussed in greater detail in the Summary and Discussion section.

(4) Favorite Attributes:

To determine whether some (or all) subjects had favorite attributes that they requested regardless of the specifics of the trial, their first and second attribute requests were classified for Sessions 2 and 3. This data is provided in Table 4. For a given subject, the most frequent first attribute requested was determined. The percentages given in the first two columns of the table represent how often the subject asked for the most requested attribute in sessions 2 and 3. The columns on the right represent the same type of data for the second attribute requested. For example, subject #11 had a favorite attribute that he/she chose for the first request 50% of the time in Session 2 and 83% of the time in Session 3. However, this subject did not have one consistent second request in both sessions 2 and 3.

The expected value for first requests, given NO favorites would be $1/5$ or 20%, and the expected value for second requests would be $1/4$ or 25%. It can be seen that most subjects seemed to have a favorite first and second attribute request, and some subjects used this strategy more than others.

The data reviewed thus far indicate support for BOTH a Set Reduction strategy AND a tendency to request certain attributes more than others. These two strategies are not at all incompatible given that the Set Reduction strategy often allows flexibility in which attribute should be requested (that is, many will often be diagnostic for a subset of alternatives).

Table 4. Percentage of Favorite Attribute Requests for First and Second Requests (Sessions 2 and 3)

<u>Subject</u>	<u>FIRST REQUEST</u>		<u>SECOND REQUEST</u>	
	<u>Session 2</u>	<u>Session 3</u>	<u>Session 2</u>	<u>Session 3</u>
1	Color .33	Color .29	Color .32	Alarm .38
2	Color .46	Size .33	Alarm .39	Alarm .33
3	Size .37	Size .29	Noise .36	Alarm .25
4	Noise .42	Alarm .37	Noise .27	Noise .35
5	Size .29	Size .29	Noise .26	Size .24
6	Loc .58	Loc .37	Alarm .43	Color .48
7	Size .46	Alarm .58	Loc .33	Noise .40
8	Alarm .37	Size .50	Color .32	Color .33
9	Alarm .29	Speed .25	Alarm .30	Alarm .25
10	Alarm .37	Noise .42	Alarm .40	Alarm .38
11	Color .50	Color .83	Noise .40	Loc .43
12	Size .46	Size .29	Color .28	Color .26
<hr/>				
Mean OBTAINED FREQUENCIES	.41	.40	.34	.34
Mean EXPECTED FREQUENCIES (Random Choice)	.20	.20	.25	.25

(5) Hypothesis Testing Strategy

As explained earlier, this strategy predicts that the subject will request an attribute that is the most unique characteristic of the animal hypothesized by the subject. It was possible to assess the existence of this strategy because subjects were asked to give a hypothesized animal after each attribute acquisition. Thus, for each initial attribute given, it was determined which attribute would be most "unique" for each possible hypothesis. The attributes which were NOT most unique were categorized as to whether they were equally descriptive of all possible alternatives, or "non-unique", that is, they are characteristic of the favorite plus many other animals as well. A frequency count was determined for subjects according to whether their first attribute requested was "unique", "equal", or "non-unique". The percentages of attribute requests falling into each of these three types of category are given in Table 5. A similar analysis was conducted for the second attribute requested. These are shown in the right half of the table.

If this strategy were descriptive of subjects' attribute requests, it would be expected that the attributes in the "unique" column would be chosen over the other two types (equal or non-unique). It can be seen that this is clearly not the case, subjects did not tend to request the attribute that would be most unique to the hypothesized animal. Thus, we can be reasonably confident in ruling out this strategy as a likely description of subjects' cognitive processes.

4.2 Phase II: Expert-Aided Diagnostic Inference

Data analysis from the second phase of the project was performed in three groups of analysis:

- (A) comparison of subjects' performance in Phase I (Sessions 2 and 3) with performance in Phase II (Sessions 1 and 2)
- (B) comparison of Experienced subjects in Phase II with Novice subjects in Phase II
- (C) comparison of Experienced subjects in Phase I (Sessions 1 and 2) with Novice subjects in Phase II (Sessions 1 and 2)

4.2.1 Analysis A: Manual vs. Expert-Aided, Experienced Subjects

(The results reported in this section will be divided into two sections, Performance Measures and Strategy Analysis.)

4.2.1.1 Performance Measures

A Multivariate Analysis of Variance was performed on the data from the 12 subjects who performed in three sessions in

Table 5. Percentage of First and Second Requests Falling into Unique, Equal, and Non-Unique Categories

<u>Subject</u>	<u>FIRST ATTRIBUTE REQUEST</u>			<u>SECOND ATTRIBUTE REQUEST</u>		
	<u>Unique</u>	<u>Equal</u>	<u>Non-Unique</u>	<u>Unique</u>	<u>Equal</u>	<u>Non-Unique</u>
1	.36	.50	.69	.46	.26	.89
2	.27	.61	.46	.31	.56	.70
3	.46	.48	.31	.42	.42	.64
4	.33	.57	.46	.23	.45	.69
5	.39	.57	.36	.38	.50	.56
6	.29	.53	.64	.42	.54	.57
7	.42	.56	.33	.48	.30	.91
8	.50	.42	.31	.45	.37	.78
9	.51	.35	.61	.27	.64	.50
10	.50	.46	.40	.65	.25	.73
11	.42	.42	.75	.40	.48	.62
12	.65	.22	.64	.35	.48	.64

For Subjects
Combined:

Frequency	184	226	72	109	145	82
Total Possible	431	475	145	275	332	119
Total Percent	.43	.48	.50	.40	.44	.69

Phase I and for two sessions in Phase II. The independent variables were Phase (I vs II), Session (2 vs 3 for Phase I and 1 vs 2 for Phase II), Attributes Available (two vs. four), and Diagnosticity (low vs. high). The dependent variables were Percent Correct, Certainty, and Attributes Requested. Each score for these variables was based on three Common and one Rare animal (see p. 16). Statistical summaries from the Multivariate and Univariate Analyses are provided in Appendix D. All effects reported as significant were significant in both the Multivariate and Univariate tests. The means for all three dependent variables are given in Table 6. For the variable, Percent Correct, a main effect was found for Phase, where subjects performed significantly better in Phase I, the Manual condition, ($\bar{x} = .80$) than they did in with the Expert-Aid ($\bar{x} = .74$). At first this finding seemed surprising, however, upon consideration of the expert-aiding system, the probable reason for the findings became clear. Subjects knew that five animals were common and the other three were rare. This information had not been made available to the expert system. Thus, the expert system had the advantage of perfect memory for the animal attributes, but the disadvantage of not knowing the relative odds of occurrence. If subjects relied upon the expert even some of the time, this drawback could lower their performance.

The above possibility is supported by an interaction effect between Phase and Diagnosticity. Figure 6 indicates that subjects' performance remains relatively constant for the easy High Diagnosticity trials, but performance drops considerably for the more difficult Low Diagnosticity trials. These are the trials where subjects would be expected to use the expert most often (it will be shown below that this is exactly what happened). As can also be seen in Figure 6, a main effect was found for Diagnosticity, where the Low Diagnosticity trials resulted in a mean percent correct of .61, and the High Diagnosticity trials resulted in a mean percent correct of .93.

The second dependent variable, Certainty, was affected by several independent variables. The main effect of Phase resulted in a higher mean Certainty for Phase II (7.3) than for Phase I (6.8). There was also a main effect of Session; as expected, the certainty ratings increased over time. As in the Phase I analysis, the number of Attributes Available affected the subjects' certainty ratings, where two Attributes Available resulted in a mean rating of 6.9 and four Attributes Available resulted in a mean rating of 7.2 (see previous discussion of this effect). Finally, Diagnosticity strongly affected subject certainty with a mean rating for Low Diagnosticity trials of 6.0 and a mean rating for High Diagnosticity trials of 8.2. There were no significant interactions for this dependent variable.

The final dependent variable, Attributes Requested, was also affected by Phase. Subjects requested significantly more attributes in Phase II (3.4) than they had in Phase I (3.0). In addition, they requested more attributes for trials with Low Diagnosticity (3.7) than for trials with High Diagnosticity (2.8). There were no interactions for number of Attributes Requested.

Table 6. Cell Means for Experienced Subjects:
Phase I vs. Phase II

PERCENT CORRECT

	(Session) 2	Phase I 3	Phase II 1	Phase II 2
Low Diag.				
Two Att. Avail.	.67	.79	.58	.60
Four Att. Avail.	.69	.56	.50	.48
High Diag.				
Two Att. Avail.	.87	.98	.98	.96
Four Att. Avail.	.89	.98	.85	.94

CERTAINTY

Low Diag.				
Two Att. Avail.	5.4	5.4	6.1	6.3
Four Attr. Avail.	6.1	5.9	6.5	6.1
High Diag.				
Two Attr. Avail.	7.7	7.8	8.4	8.4
Four Att. Avail.	8.2	7.9	8.4	8.6

ATTRIBUTES REQUESTED

Low Diag.				
Two Att. Avail.	3.6	3.5	3.9	3.8
Four Att. Avail.	3.3	3.7	3.7	3.9
High Diag.				
Two Att. Avail.	2.4	2.6	2.9	2.8
Four Att. Avail.	2.6	2.5	2.9	3.4

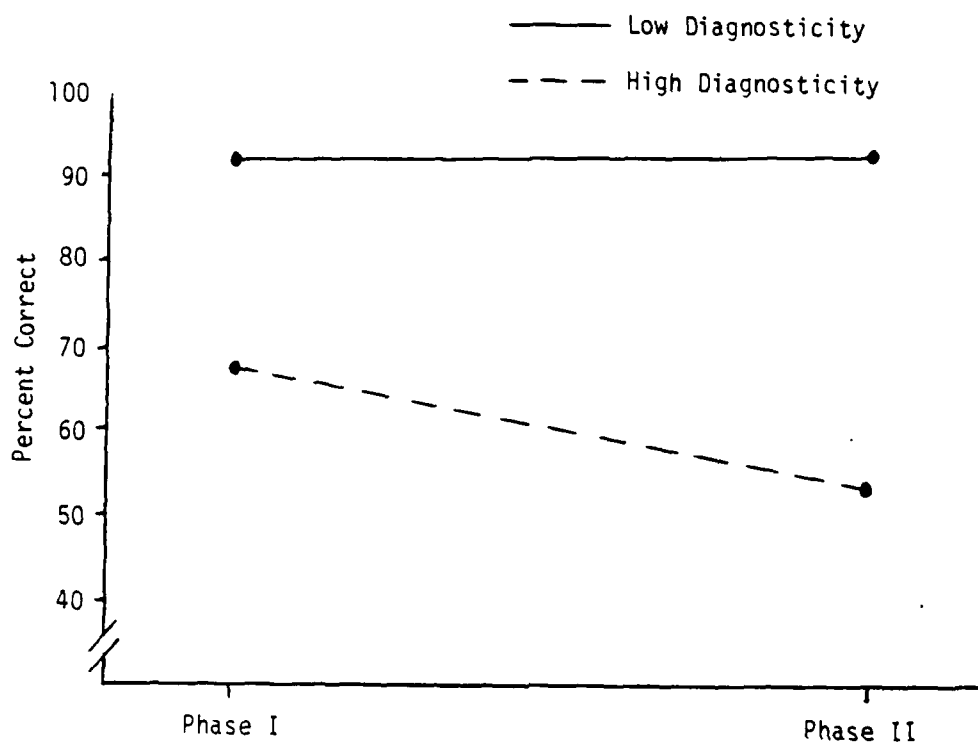


Figure 6. Mean Percent Correct as a Function of Phase and Diagnosticity.

In summary, the major findings in this section include decreased performance on the Low Diagnosticity (difficult) trials in Phase II, an increased overall subjective certainty in Phase II, and an increase in the amount of information requested in Phase II.

4.2.1.2 Strategy Analysis

Strategy analyses were conducted in a manner similar to that described for Phase I. Only four of the five strategies were assessed in this analysis; it was felt that the Hypothesis Testing strategy had been sufficiently ruled out and the analysis should concentrate on the remaining four: Half-Split, Set Reduction, Favorite Attribute, and Random Request.

(1) Comparison of Half-Split, Set Reduction, and Random Request

To assess the likelihood of these three strategies, the frequencies were obtained for "best split, acceptable split, and non-diagnostic" first attribute requests. These data are listed in Table 7. As in the analysis for Phase I (see Table 2), these frequencies are totalled at the end of the table and can be compared with the expected frequencies based on the Half-Split, Set Reduction, and Random Request strategies. As in the Phase I analysis, the obtained values are closest to those predicted by the Set Reduction strategy. A χ^2 analysis showed the frequencies to be significantly different from those predicted on the basis of random attribute request, $\chi^2(2) = 72.8, p < .001$.

To determine whether the request frequencies support the Set Reduction or the Half-Split strategies, the frequencies were tallied for all conditions where a choice was made between the "best split" and "acceptable split" requests. The Half-Split strategy predicts that the "best" split request will always be chosen, whereas the Set Reduction strategy predicts that there will be no preference between the two categories, and therefore the obtained frequencies should follow directly from the proportion of attributes in each of the two categories. The obtained values and the expected values based on the Set Reduction strategy were:

	BEST SPLIT	ACCEPTABLE SPLIT
OBTAINED	219	84
EXPECTED (Set Reduction)	177	126

While the frequencies do not show support for the Half-Split strategy (this would be all frequencies in the "best split" column), a χ^2 test for goodness-of-fit showed that the data did not fit a Set Reduction strategy assuming EQUAL request of all diagnostic attributes, $\chi^2(1) = 23.9, p < .001$. The frequencies were biased in the direction of a Half-Split strategy. The most reasonable explanation of this finding is that the subjects are using a Set Reduction strategy, but are still somewhat more inclined to use attributes that evenly divide the alternative animals than attributes that provide a very uneven split.

An analysis was also conducted for the second attribute requests. As in the analysis for Phase I, these requests were divided into those where a choice was made between category #1 (best split) and category #3 (non-diagnostic), and those where a choice was made between category #1 (best split) and #2 (acceptable split). These data are presented in Table 8.

The expected frequencies are different from Table 2 because they are based on total frequencies for each attribute (on the left), and these were not distributed the same for Phases I and II.

Table 7. Percentage of First Attribute Requests Categorized
According to Type of Split (Phase II)

FIRST ATTR.	"BEST" SPLIT REQUESTS	"ACCEPTABLE" SPLIT REQUESTS	NON-DIAG REQUESTS
Small	Loc .32 Color .41 Alarm .19 TOTAL .92	Speed .02 Noise .06 TOTAL .08	--
Large	Speed .14 Color .31 Noise .14 Alarm .33 TOTAL .92	--	Loc .08 TOTAL .08
Ground	Size .27 Speed .13 Color .33 Alarm .27 TOTAL 1.00	Noise .00 TOTAL .00	--
Tree	Color .50 Noise .14 Alarm .30 TOTAL .94	--	Speed .03 Size .03 TOTAL .06
Fast	Loc .15 Color .33 Alarm .16 TOTAL .64	Size .27 Noise .09 TOTAL .36	--
Slow	Size .50 Noise .33 Alarm .17 TOTAL 1.00	--	Color .00 Loc .00 TOTAL .00
Brown	Size .32 Loc .36 Speed .02 Noise .10 Alarm .20 TOTAL 1.00	--	--

Table 7 (cont.)

Gray	Size	.36			Noise	.07
	Loc	.38			Speed	.03
	Alarm	.16				
	TOTAL	.90		--	TOTAL	.10
No Noise	Color	.20	Loc	.24		
	Alarm	.20	Size	.32		
			Speed	.04		
	TOTAL	.40	TOTAL	.60		--
Noise	Size	.36			Color	.14
	Loc	.21				
	Speed	.00				
	Alarm	.29				
	TOTAL	.86		--	TOTAL	.14
No Alarm	Size	.31				
	Loc	.17				
	Speed	.14				
	Color	.24				
	Noise	.14				
	TOTAL	1.00		--		--
Alarm	Size	.44	Speed	.03		
	Loc	.25	Noise	.11		
	Color	.17				
	TOTAL	.86	TOTAL	.14		--
Mean Percentage						
OBTAINED for all						
Combined (N=576): (n=477) .83 (n=84) .14 (n=15) .03						
Mean Percentage						
EXPECTED based on						
Half-Split Strategy: 1.00 .00 .00						
Mean Percentage						
EXPECTED based on						
Set Reduction Strategy: .78 .22 .00						
Mean Percentage						
EXPECTED based on						
Equal Choice: .67 .22 .11						

Table 8. Frequency of Second Attribute Requests Categorized According to Type of Split (Phase II)

CATEGORY 1 VS 3, CHOICE BETWEEN:	"BEST SPLIT" REQUESTS	"NON-DIAGNOSTIC" REQUESTS
3 Best, 1 Non-Diag.		
OBTAINED	90	8
EXPECTED	73.5	24.5
2 Best, 2 Non-Diag.		
OBTAINED	137	10
EXPECTED	73.5	73.5
1 Best, 3 Non-Diag.		
OBTAINED	22	4
EXPECTED	6.5	19.5
TOTAL OBTAINED	249	22
TOTAL EXPECTED Random	153.5	117.5
CATEGORY 1 VS 2, CHOICE BETWEEN:	"BEST SPLIT" REQUESTS	"NON-DIAGNOSTIC" SPLIT REQUESTS
3 Best, 1 Acceptable		
OBTAINED	4	
EXPECTED	4	
2 Best, 1 Acceptable		
OBTAINED		
EXPECTED		
1 Best, 1 Acceptable		
OBTAINED		
EXPECTED		
TOTAL OBTAINED	4	
TOTAL EXPECTED	4	

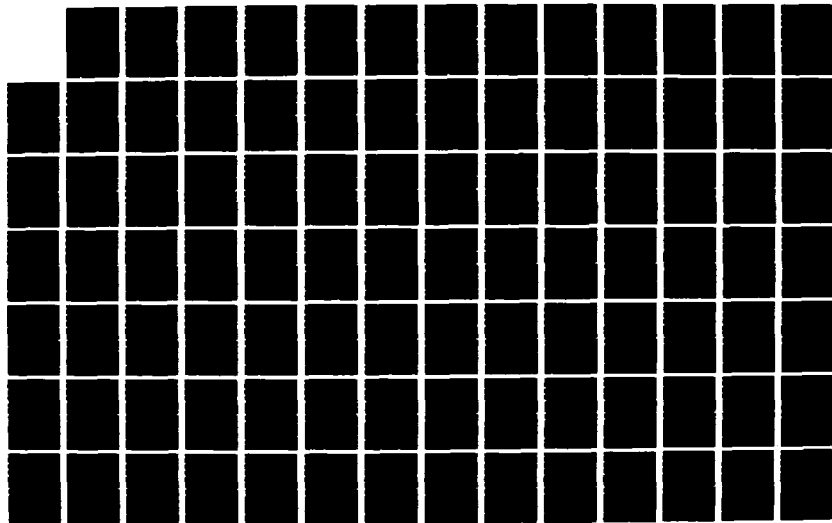
AD-A187 859

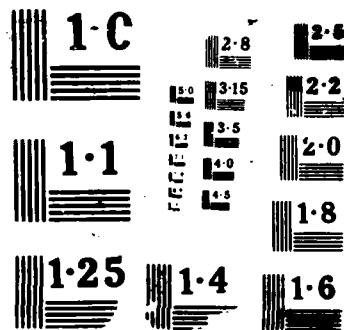
UNITED STATES AIR FORCE RESEARCH INITIATION PROGRAM
1984 RESEARCH REPORTS (U) SOUTHEASTERN CENTER FOR
ELECTRICAL ENGINEERING EDUCATION INC S M D PEELE
MAY 86 AFOSR-TR-87-1722 FF9628-82-C-8035 F/G 7/2

84/10

UNCLASSIFIED

NL





A χ^2 test was conducted for the Best Split vs. Non-Diagnostic requests where the obtained scores were compared with the frequencies expected on the basis of the Random Request strategy. The results showed that the data were significantly different from those expected on the basis of Random Request, $\chi^2(2) = 137$, $p < .001$. It can be seen that relatively few choices were made for a non-diagnostic attribute.

A second χ^2 test was conducted for the Best Split vs. Acceptable Split requests. In this case, the expected frequencies were provided by the Set Reduction strategy. The analysis showed that there was no significant difference between the values obtained and those expected on the basis of this model ($\chi^2 < 3.0$). These results provided direct support for the Set Reduction strategy.

(2) Favorite Attributes

First and second attribute requests were sorted for Phase II to assess whether subjects had favorite attributes (which they did in Phase I), and also to determine whether this tendency changed from Phase I to Phase II.

Table 9 provides information similar to that given in Table 4, that is, the percent of trials each subject asked for a favorite attribute, listed according to session. The mean percentages of favorite attributes are given at the bottom of the table along with what would be expected if there was NO difference in subjects' request for the different attributes. One of the first things which can be noticed is that in general, the tendency to rely on a favorite attribute increased from that found in Phase I, particularly for some of the subjects. Figure 7 shows the mean percentages for first and second attribute requests in Phases I and II.

A 2(Phase) x 2(Session) Analysis of Variance was performed on the percentage scores for the first attribute requests and results showed that subjects did use one favorite attribute more often in their first request during phase II ($\bar{X} = .54$) than in phase I ($\bar{X} = .40$), $F(1,11) = 10.8$, $p < .01$.

A similar analysis was performed for the second attribute requests (this was performed separately because the percentages were based on fewer items than the first requests - subjects sometimes based their final decision on only two attributes). The results of the analysis for second requests showed that although there was a slight trend towards using a favorite more often in Phase II, this trend was not significant.

In summary, there was good support for the Set Reduction strategy, and there was also evidence that subjects were not only relying on favorite attributes within the confines of a Set Reduction strategy, but that this tendency increased in Phase II when they had the availability of the expert system.

Table 9. Percentage of Favorite Attribute Requests for First and Second Requests (Phase II)

Subject	FIRST REQUEST		SECOND REQUEST	
	Session 2	Session 3	Session 2	Session 3
1	Color .58	Color .42	Loc .43	Color .30
2	Loc .37	Loc .42	Color .41	Color .30
3	Size .33	Size .37	Size .27	Size .30
4	Noise .75	Alarm .83	Alarm .62	Noise .67
5	Size .42	Size .71	Noise .27	Color .29
6	Loc .79	Loc .62	Color .62	Color .39
7	Alarm .54	Alarm .54	Noise .32	Size .38
8	Size .42	Size .33	Alarm .32	Alarm .33
9	Speed .21	Speed .33	Speed .32	Color .25
10	Color .42	Color .87	Alarm .30	Alarm .42
11	Color .75	Color .87	Loc .43	Loc .48
12	Size .46	Alarm .54	Alarm .29	Size .27
<hr/>				
Mean OBTAINED FREQUENCIES	.50	.57	.38	.36
Mean EXPECTED FREQUENCES (Random Choice)	.20	.20	.25	.25

4.2.2 Analysis B: Experienced vs Novice Subjects; Phase II

Extensive analyses were performed comparing subjects who had previously learned the inference task on their own before using the expert system, with those (novice) subjects who used the expert system as they were learning the task. The variables were first subjected to a Multivariate Analysis of Variance with the following independent variables: Experience (Experienced vs. Novice), Session (1 vs 2), Attributes Available (two vs. four) and Diagnosticity of the cue set (low vs. high). The dependent variables included:

- (1) Percent Correct
- (2) Time to Perform the Task
- (3) Certainty
- (4) Number of Attributes Requested
- (5) Percent (out of four) the Expert was asked
- (6) Percent of times (out of #5) the Expert was used.

The results from the Multivariate and all Univariate analyses are presented in Appendix E. All results reported in this section were significant for both analyses. The means for the first four dependent variables are given in Table 10. These four "performance" variables will be discussed first.

Results from the analysis for Percent Correct revealed several main effects and one interaction. First, there was a significant difference between Experienced and Novice subjects, where the Experienced subjects overall had higher scores ($\bar{x} = .74$) than the Novice subjects ($\bar{x} = .67$). To give a clearer picture of the overall performance levels, Figure 7 shows the Percent Correct means for Experienced subjects in Phase I and II, and for the Novice subjects in Phase II. The results reported here indicate that there is a difference in performance between the subject groups in Phase II. Since the Novice subjects are just learning to perform the task, it is not surprising that their performance is lower. A more fair analysis will be described shortly comparing the Experienced subjects' first two sessions with the Novice subjects' first two sessions. One point should be noted, however. The novice subjects performed 30 trials on their first day and this should have been sufficient practice for them to reach their normal performance level. Even with this many trials before their second session, their performance doesn't improve.

Other variables affecting the performance of both groups of subjects included Attributes Available, where subjects performed better in trials where only two attributes were available ($\bar{x} = .75$) than where four attributes were available ($\bar{x} = .65$). This is presumably because when only two are available, it is more likely that subjects obtain all attributes necessary to optimally narrow down the alternative answers. Finally, as in previous analyses, Diagnosticity had a strong effect on subject performance, where the High (easy) trials resulted in .89 correct while the Low (difficult) trials resulted in only .51 correct.

Table 10. Cell Means for Analysis B: Experienced vs. Novice
Subjects, Phase II Only

PERCENT CORRECT

(Session)	Experienced		Novice	
	1	2	1	2
Low Diag.				
Two Att. Avail.	.58	.60	.48	.52
Four Att. Avail.	.50	.48	.56	.37
High Diag.				
Two Att. Avail.	.98	.96	.94	.94
Four Att. Avail.	.85	.94	.69	.83

TIME

Low Diag.				
Two Att. Avail.	52.2	40.7	56.3	41.2
Four Attr. Avail.	50.2	44.6	56.0	40.7
High Diag.				
Two Attr. Avail.	37.9	31.3	48.6	34.1
Four Att. Avail.	43.7	37.8	53.1	37.1

CERTAINTY

Low Diag.				
Two Att. Avail.	6.1	6.3	5.8	5.1
Four Attr. Avail.	6.5	6.1	5.8	5.7
High Diag.				
Two Attr. Avail.	8.4	8.4	7.0	7.7
Four Att. Avail.	8.4	8.6	7.3	8.0

ATTRIBUTES REQUESTED

Low Diag.				
Two Att. Avail.	3.9	3.8	3.7	3.6
Four Att. Avail.	3.7	3.9	3.6	3.7
High Diag.				
Two Att. Avail.	2.9	2.8	3.0	2.9
Four Att. Avail.	2.9	3.4	3.2	3.7

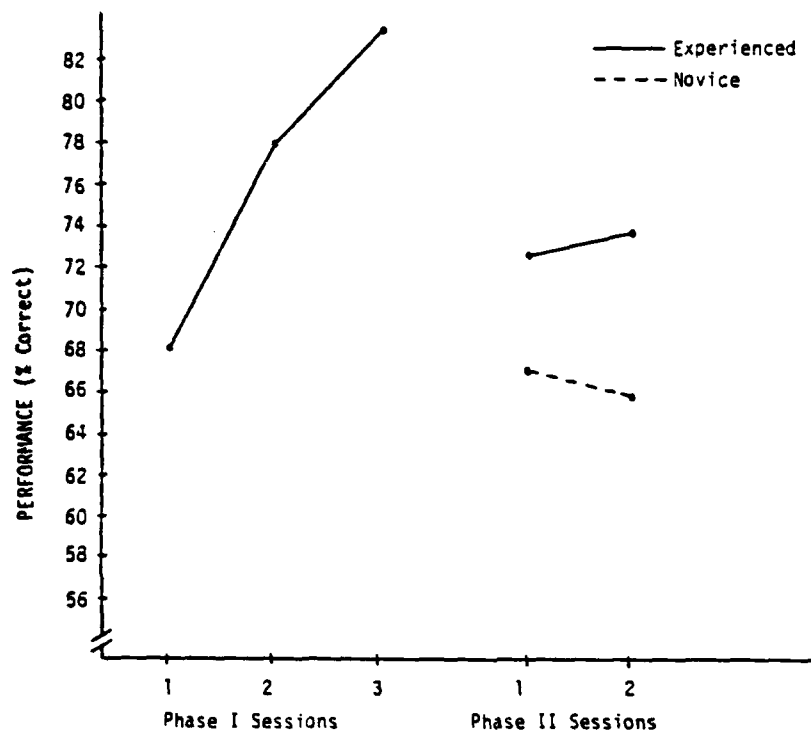


Figure 7. Mean Percent Correct as a Function of Experience and Session.

The interaction between Session and Diagnosticity resulted in borderline significance ($p=.06$). There was a slight tendency for all subjects to improve over sessions for the High diagnosticity trials (from .86 to .92), whereas there was a slight decrease in scores over sessions for the Low diagnosticity trials (from .53 to .49).

The total time that subjects took to complete a trial was measured in seconds (to two decimal places). Recall that for each subjects' score in a given cell, the time was calculated by averaging the times from four trials (three Common animals and one Rare animal). There was no overall difference in time to perform the task for experienced vs. novice subjects. There was a significant effect of Session, where time decreased from 49.7 seconds for session 1 to 38.4 seconds for session 2. In addition, subjects spent less time on trials where two attributes were available ($\bar{x} = 42.8$) than on trials where four attributes were available ($\bar{x} = 45.4$). This is consistent with the results just reported where subjects generally do better on trials where

fewer attributes are available. Subjects spent more time on the more difficult Low diagnosticity trials (47.7 sec) than the easier High diagnosticity trials (40.4). Finally, an interaction between Attributes Available and Diagnosticity revealed that when the trial was Low in diagnosticity, it did not matter whether there were two or four attributes available, subjects took a relatively long time to perform the trial. However, on the easier trials, subjects were quick to perform the inference with only two attributes, but took longer to process the information when there were four attributes available (see Figure 8).

The third dependent variable, Subjective Certainty, was also averaged over four trials for each score (three Common and one Rare animal). Overall, the Experienced subjects were more confident in their guesses ($\bar{x} = 7.4$) than the Novice subjects ($\bar{x} = 6.6$). Again, this is the expected finding since the Novice subjects are learning the task. The scores of the Novice

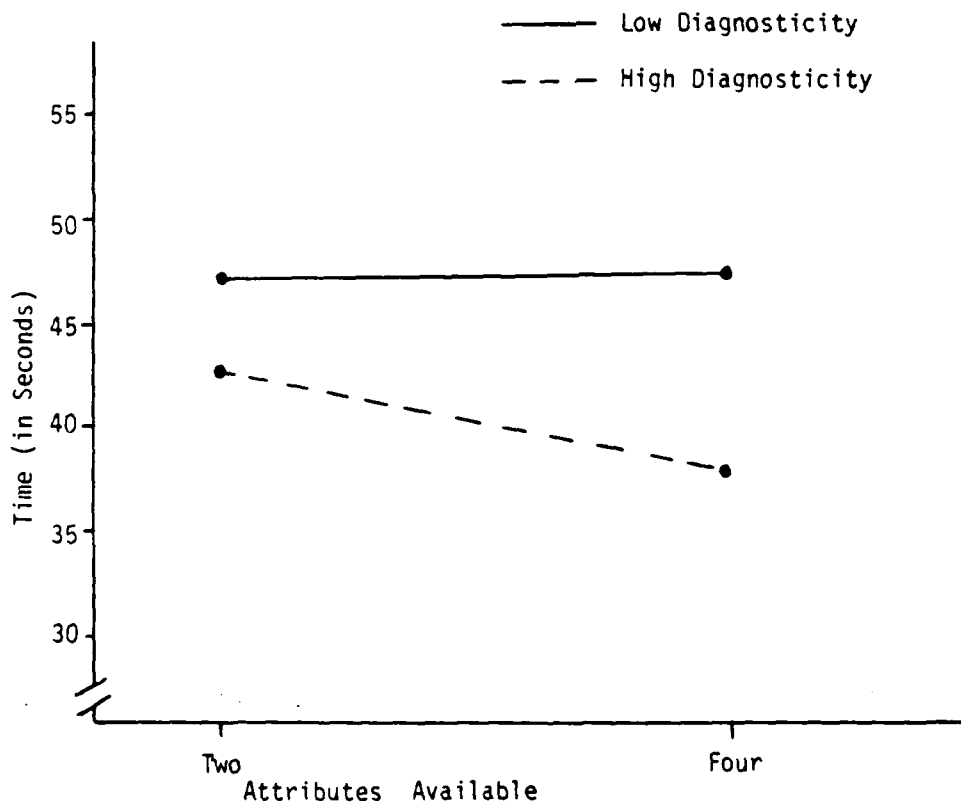


Figure 8. Mean Time to perform the task as a function of Attributes Available and Diagnosticity.

subjects will be compared with the first two sessions of the Experienced subjects in a later analysis. As in previous analyses, the easy High diagnosticity trials resulted in more confidence, with a mean rating of 8.0, while the harder trials resulted in a mean confidence rating of 5.9. Finally, there was a significant interaction between Session and Diagnosticity. For the easier High diagnosticity trials, confidence ratings went up from 7.8 in the first session, to 8.2 in the second session. For the difficult Low diagnosticity trials, the ratings went from 6.0 down to 5.8.

The final "performance" dependent variable found in Table 10 is the number of Attributes Requested by subjects. The only main effect was produced by Diagnosticity of the attribute set. When the attributes had Low diagnosticity, the subjects asked for a mean of 3.7, whereas when the attributes had High diagnosticity, the subjects asked for fewer (3.1) attributes. In addition, there was a two-way interaction between the Attributes Available and Diagnosticity, where the difficult trials resulted in a large attribute request for both two and four attributes available (3.8 and 3.7, respectively), while the easier trials resulted in more requests when there were more attributes available (3.3) than when there were only two available (2.9).

The remaining dependent variables included in the Multivariate analysis have to do with the use of the expert system, and they are therefore discussed together. The means for these variables are presented in Table 11. The first

Table 11. Cell Means for Use of Expert System

PERCENT EXPERT ASKED

	(Session)	Experienced		Novice	
		1	2	1	2
Low Diag.					
Two Att. Avail.		.87	.77	.60	.54
Four Att. Avail.		.77	.57	.52	.48
High Diag.					
Two Att. Avail.		.14	.04	.46	.21
Four Att. Avail.		.29	.12	.33	.12

PERCENT EXPERT USED

Low Diag.					
Two Att. Avail.		.69	.56	.70	.54
Four Attr. Avail.		.61	.56	.65	.60
High Diag.					
Two Attr. Avail.		.33	.17	.57	.42
Four Att. Avail.		.42	.42	.54	.25

dependent variable is the percent of times that the expert was asked for "advice". This percent was obtained by calculating the number of times out of four trials that the subject asked the expert (these four trials are the ones presented on p. 16, with three Common and one Rare animal). Analyses showed that subjects asked the expert more often in the first session ($\bar{x} = .50$) than in the second session ($\bar{x} = .36$). In addition, subjects asked the expert more often for the difficult Low diagnosticity trials ($\bar{x} = .64$) than for the easier High diagnosticity trials ($\bar{x} = .21$). Finally, an interaction showed that Experienced subjects asked the expert LESS often for the easy High diagnosticity trials but MORE often for the harder Low diagnosticity trials (see Figure 9).

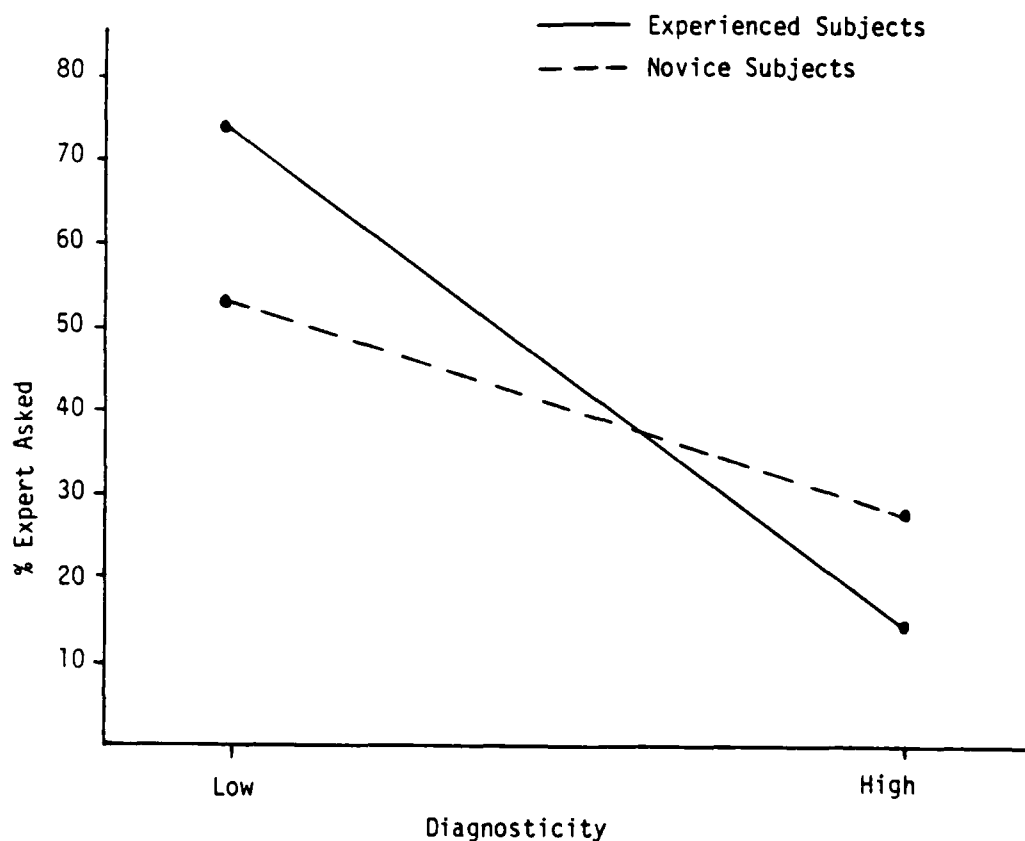


Figure 9. Mean % of Trials the Expert was Asked as a function of Subject Experience and Diagnosticity.

The second variable reflecting subjects' use of the expert was, given that the subject HAD asked the expert for advice, what was the percentage of trials that the subject gave an answer that was the same as the one given by the expert. That is, how often did the subject actually use the expert's advice. First, use of the expert's advice was slightly over half of the time (.56) for session 1, but slightly under half of the time for session 2 (.44), this difference was significant at the .05 level. In addition, the subjects tended to rely on the expert answer more often for the difficult Low diagnosticity trials ($\bar{x} = .61$) than for the easier High diagnosticity trials ($\bar{x} = .39$). There were no other variables which affected this measure, including the experience of the subjects.

One last variable will be discussed; this variable was not an objective measure, but rather the subjective perception of the subjects. On the final questionnaire, subjects were asked to rate both themselves and the expert on a scale ranging from 1 = extremely inaccurate to 20 = perfect. These ratings were subjected to a 2 (Experienced vs. Novice) x 2 (Self vs. Expert) Analysis of Variance. Results showed that overall, subjects rated themselves as better on the task than the expert (mean ratings were 13.7 and 11.3, respectively), $F(1,22) = 6.3, p < .05$. However, the main effect cannot be interpreted independently because an interaction shows that this effect is due entirely to the perceptions of the Experienced subjects. The Experienced subjects strongly considered themselves to be better than the expert (mean Self rating was 14.3 and mean Expert rating was 9.7), while the Novice subjects saw no difference between themselves and the Expert (means were 13 and 13.1, respectively), $F(1,22) = 6.8, p = .01$. To demonstrate this effect in another way, ten out of the twelve Experienced subjects rated themselves as being better than the Expert, while only four of the Novice subjects rated themselves as being better than the Expert.

4.2.3 Analysis C: Experienced vs. Novice; First Two Sessions

A final analysis compared the Experienced subjects with the Novice subjects, using the first two sessions for each group. That is, the data for Experienced subjects was obtained from Sessions 1 and 2 of Phase I, and the data for Novice subjects was obtained from Phase II. Since the total number of trials was not equal for the sessions in Phases I and II, caution must be used in interpreting these data. However, the comparisons are still being made ONLY for the critical trials in both cases, thus the difference becomes one of practice effects caused by having more "filler" trials in Phase II.

A Multivariate Analysis of Variance was conducted for data relevant to Percent Correct, Time to Perform the Task, Subjective Certainty, and number of Attributes Requested. The independent variables were Experience (Experienced vs. Novice), Session (1 vs. 2), Attributes Available (two vs. four), and Diagnosticity (Low vs. High). The results of this analysis are presented in appendix F, and cell means are listed in Table 12. The dependent

Table 12. Cell Means for Analysis C: Experienced vs. Novice
Subjects, First Two Sessions

PERCENT CORRECT

(Session)	EXP. Phase I		NOV. Phase II	
	1	2	1	2
Low Diag.				
Two Att. Avail.	.50	.67	.48	.52
Four Att. Avail.	.71	.69	.56	.37
High Diag.				
Two Att. Avail.	.79	.87	.94	.94
Four Att. Avail.	.71	.89	.69	.83

CERTAINTY

Low Diag.				
Two Att. Avail.	5.5	5.4	5.8	5.1
Four Attr. Avail.	6.5	6.1	5.8	5.7
High Diag.				
Two Attr. Avail.	7.1	7.7	7.0	7.7
Four Att. Avail.	7.4	8.2	7.3	8.0

ATTRIBUTES REQUESTED

Low Diag.				
Two Att. Avail.	3.4	3.6	3.7	3.6
Four Att. Avail.	3.1	3.3	3.6	3.7
High Diag.				
Two Att. Avail.	2.7	2.4	3.0	2.9
Four Att. Avail.	2.6	2.6	3.2	3.7

variable of Time to perform the task is not listed in the table, and will not be covered, because the differences in the task (asking subjects in Phase I to provide intermediate hypotheses) caused large differences in time for the two different phases.

The first dependent variable, Percent Correct, was marginally different for the Experienced subjects ($\bar{x} = .73$) than for the Novice subjects ($\bar{x} = .67$), $p = .06$. Notice that the Novice subjects had the advantage of 60 trials for the two sessions while the Experienced subjects performed only 43. Thus, the Novice subjects would be expected, if anything, to have higher accuracy scores than the Experienced. While inconclusive, this analysis along with the analysis performed on Experienced subjects from the two Phases suggests that in this experiment, use of the expert caused subjects performance to drop. This finding will be discussed in more detail in the following section.

As in previous analyses, the diagnosticity of the trials affected subject performance. Low diagnosticity trials resulted in an average of 56% correct, while the easier High diagnosticity trials resulted in an average of 83% correct. There were several significant two-way interactions:

- (1) Experience x Diagnosticity, where subjects did equally well on the easy trials but the Experienced subjects performed better on the difficult trials (presumably because the Novice subjects asked the expert more often on these trials and this hurt their performance)
- (2) Session x Diagnosticity, where all subjects improved on the easy trials (78% for session 1 and 88% for session 2), but did not improve on the difficult trials (56% both sessions)
- (3) Attributes Available x Diagnosticity, where performance was better on Two Attribute trials (88%) than Four Attribute trials (78%) for the easy High diagnosticity trials, but showed the opposite effect for the difficult Low diagnosticity trials, with a mean of 54% for Two Attribute trials and 58% for Four Attribute trials.

Finally, a three-way interaction occurred for Session, Attributes Available, and Diagnosticity. This interaction is diagrammed in Figure 10. It can be seen that subject's performance went up from Session 1 to Session 2 for all types of trials except for difficult (Low diagnosticity) trials with Four attributes available. This effect may be due to the problem that subjects simply did not learn to ask for enough of the attributes to narrow down the alternatives to the correct two choices.

In making Certainty ratings for each trial guess, there was no significant difference between Experienced and Novice subjects. As before, an effect was found for Attributes Available, where subjects were more confident with more attributes on which to base their judgments ($\bar{x} = 6.9$) than when there were only two attributes available ($\bar{x} = 6.4$). Also, for the easy High diagnosticity trials, subjects' mean rating was 7.6, while the Low diagnosticity trials resulted in a mean certainty rating of 5.7.

Finally, an interaction between Session and Diagnosticity revealed that certainty increased from Session 1 (7.2) to Session 2 (7.9) for the easy trials, but decreased from Session 1 (5.9) to Session 2 (5.6) for the difficult Low diagnosticity trials.

The final dependent variable, number of Attributes Requested, was affected by the type of trial; subjects in the Low diagnosticity trials requested an average of 3.5 attributes, while subjects in the High diagnosticity trials requested only an average of 2.9 attributes. Overall, the Novice subjects asked for significantly more attributes ($\bar{x}=3.4$) than the Experienced subjects ($\bar{x}=3.0$). Finally, an interaction between Attributes Available and Diagnosticity showed that for the easy High diagnosticity trials, subjects asked for more attributes in the Four conditions than in the Two Attributes Available conditions (3.2 and 2.6, respectively), however, in the difficult Low diagnosticity trials, subjects asked for FEWER attributes in the Four attributes conditions than in the Two attributes conditions (3.4 and 3.6, respectively).

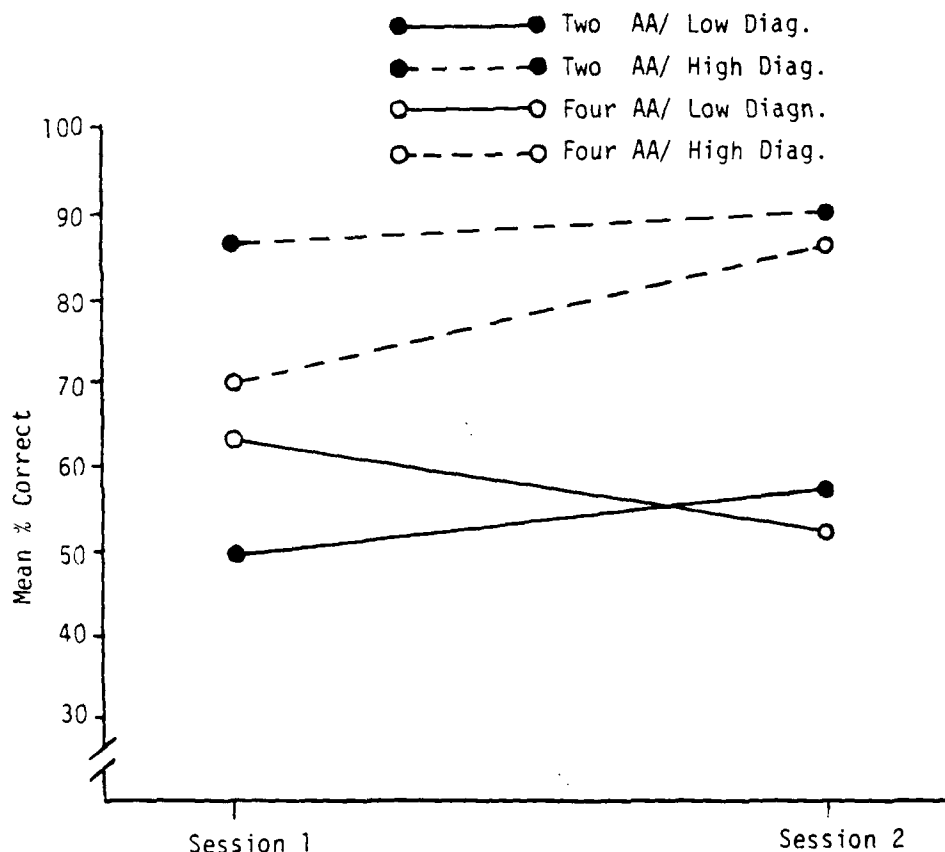


Figure 10. Mean % Correct as a function of Session, Attribute Availability, and Diagnosticity.

5. SUMMARY AND DISCUSSION

The major goal of this section is to first describe subject behavior in the inference task without the support of an expert-aiding system, and then to describe how that behavior changes as a function of introducing an expert-aiding system. To accomplish this, the results will be summarized in two sections; the first dealing with overall performance of the task without and then with expert-aid, and the second dealing with an analysis of cognitive strategies without and with expert-aid.

5.1 Performance

5.1.1 Manual Conditions

Subjects performing the task manually had no trouble learning the material or performing the inference task. Overall, subjects correctly solved an average of 73% of the trials. Subjects also found the task intrinsically interesting and motivation was high. Thus, the development of the task as a research tool was considered quite successful, and will be utilized for extensions of the current research.

Several variables were manipulated to provide information bearing on the model given at the beginning of this report (p. 7). It was felt that several factors would affect the operator's performance, WITHOUT consideration of whether there was a computer-aid available. The input variables which were assessed are given below on the right, with the corresponding manipulation provided on the left:

<u>Manipulation</u>	<u>Model Variable</u>
(1) Session	Operator experience
(2) Monetary Payoff	Seriousness of Consequences
(3) Diagnosticity	Predictive Validity of Cues
(4) Attributes Available	Amount of Information Available

(1) As expected, as subject's experience increased from session to session, their accuracy improved significantly. Also, time to perform the task decreased. When subjects were asked to give a certainty rating for each guess, overall their certainty did not change. However, for the easy High Diagnosticity tasks subjects became more certain of their answers, while for the difficult Low Diagnosticity tasks the certainty levels dropped. Also, with experience, subjects learned to ask for more information on the difficult trials.

(2) The second manipulation, monetary payoff, did not significantly affect any of the performance measures. This is interpreted as indicating that the operational definition of "seriousness of the consequences" was not sufficiently strong to have an effect on subjects. It is felt that the variable does have an impact in real-world inference tasks, but it is difficult to manipulate this variable in a laboratory setting.

(3 and 4) The last two variables are actually two factors which affect information transmitted to the operator. The amount of information can be determined by the "informativeness" of each cue or attribute, and also by how MANY attributes are given to the operator. The Diagnosticity of the attribute set reflected the total number of possible answers, given that the subject had obtained ALL of the attributes available (either ONE possible = high diagnosticity, or TWO possible = low diagnosticity). The number of Attributes Available to the subject was either two or four. These variables can be manipulated independently of one another, and this was accomplished in the current experiment.

As would be expected, the overall diagnosticity of the attribute set had a much greater effect on subjects than the number of attributes available (because if the subject acquired all relevant cues, the number of attributes available did not really affect the difficulty of the trial). In fact, the diagnosticity strongly impacted subject accuracy while the number of attributes available did not affect performance. This indicates that subjects did request information until the relevant information had been obtained.

In addition, low diagnosticity caused subjects to take longer in performing the task, and subjects requested more information in these trials. Interestingly, not only did low diagnosticity cause subjects to lower their certainty ratings, but they also lowered their ratings when there was less information available (which actually did not affect their performance on the trials).

To summarize, subjects became faster, more accurate, and more confident with experience, and the major factor affecting performance was the predictive validity (diagnosticity) of the attribute set. Finally, when subjects were asked to estimate the accuracy of their performance, they consistently underestimated their performance, even with increasing experience over sessions.

5.1.2 Manual vs. Expert-aid Conditions

To assess the impact of introducing an expert-aid, subjects from the manual conditions performed the task in two expert-aided sessions. In addition, new inexperienced (Novice) subjects were asked to perform the task under expert-aid conditions for two sessions. Thus, the Experienced subject's performance could be compared with their own previous unaided performance as well as that of Novice subjects who had not previously learned the task.

The following variables were manipulated for this phase of the project:

Manipulation

- (1) Manual vs. Expert-Aided
- (2) Experienced vs. Novice
- (3) Session
- (4) Diagnosticity
- (5) Attributes Available

(1, 2 and 3) The most important finding was that Experienced subjects' accuracy declined from manual to expert-aided conditions. In addition, the Novice subjects who performed only in Expert-Aided conditions performed worse than the Experienced subjects when they performed the task under manual conditions (see Figure 7, p. 49). This detrimental effect of the Expert System can be explained by the fact that the Expert did not have information concerning the likelihood of each animal (some were common and others were rare). Since subjects did have access to this information, it is reasonable that their performance would be lower if they relied on the expert (which evidence shows that they did). (An interesting side-note is that there was no difference in TIME to perform the task between the Experienced subjects and the Novice subjects, another indication that they were performing the task in much the same way as one another.)

The important implication here is not that subjects did worse with the expert aid, but that Experienced subjects DID rely on it even when they had been performing better on their own. The Experienced subject's final ratings showed that they considered themselves to be much better than the expert (assessment based on their performance under manual conditions) yet they still allowed themselves to be swayed by the expert. Interestingly, the Novice subjects DID NOT realize that they were more capable than the Expert; they relied on it more and also rated it as being equally capable with themselves. The obvious implication here is that system operators should be trained to perform a task on their own in order to become familiar with the task and their own capabilities.

Another difference between the Manual and Expert-aided conditions was that subjects certainty ratings after each guess were generally higher under the expert-aid conditions. However, the Experienced subjects also had higher ratings than the Novice subjects. The overall pattern of data indicates that it was experience and not the Expert System that caused the subjects ratings to increase. There was no evidence that subjects were more certain of their guesses simply because they could consult the advice of the Expert System.

Subjects asked for more attribute information in the Expert-aid conditions than in the Manual conditions. In addition, there was no difference between Experienced and Novice subjects. This suggests that something about the Expert System caused subjects to obtain more attributes before making a guess. However, there is a plausible alternative reason for this effect. In the Manual conditions, subjects were asked to make hypotheses (and associated ratings) after each attribute was provided. This may have caused impatience or frustration in performing the task, thereby reducing the amount of "cognitive effort" a subject wanted to put into any one trial. Thus the overall effect might have resulted in a tendency to rely on fewer pieces of information in the Manual conditions. A study to investigate these alternatives is currently being implemented.

The Experienced and Novice subjects were also compared for overall use of the Expert System. First, use of the system by all subjects in general dropped from the first session (50%) to

the second session (36%). This is not unexpected since the subjects realized that, in general, the expert system was not particularly good. There was no overall difference between use of the Expert by Experienced vs. Novice subjects. However, an interaction suggests that this finding is misleading. The Experienced subjects asked the Expert more often for the difficult Low Diagnosticity items, whereas the Novice subjects asked the expert more often for the Easy High Diagnosticity items.

The percent of trials where the expert answer was used by subjects dropped from 56% for the first session to 44% for the second session. Given the overall negativity of subject's attitudes towards the Expert System, it is surprising that the use rate did not drop more than it did. There were no differences between Experienced and Novice subjects in acceptance of the Expert's answer.

(4 and 5) The characteristics of the trials were varied as before by manipulating Diagnosticity of the total cue set, and number of Attributes Available. The results followed the same pattern as in the Manual conditions. For all subjects, the difficult Low Diagnosticity trials resulted in lower accuracy (percent correct), lower certainty ratings and more Attributes Requested. A Phase (manual vs. expert-aided) x Diagnosticity interaction showed that performance on the easy High Diagnosticity trials remained relatively high when subjects went from Manual to Expert-aid conditions, while performance on the difficult Low Diagnosticity trials dropped when subjects used the Expert System. Finally, as before, number of Attributes Available affected certainty ratings but not actual performance.

In summary, use of the Expert System had a negative impact on subjects' accuracy, did not affect their certainty in making their guesses, and caused subjects to ask for more information than under Manual conditions. Of particular importance, the Experienced subjects showed better discrimination in using the Expert System only for the most difficult trials and revealed in their ratings that they found it to be a less reliable system than their own abilities. On the other hand, Novice subjects had never developed a good perception of the task and their own abilities, and so they used the Expert System less discriminantly, and rated it equally as good as themselves.

5.2 Strategy Analysis

5.2.1 Manual Conditions

To assess the strategies used by subjects in performing the task, five different possible strategies were first identified. In brief these were: (1) Half-Split, the most rational and economical strategy, where subjects determine the set of possible animals based on the currently known set of attributes and another attribute is then requested which most optimally splits this set in half, this strategy is followed until one answer is

determined or no attributes remain, (2) Set Reduction, a strategy where subjects think of SOME subset of possible answers based on the currently available set of attributes, and then requests any attribute which will narrow this subset down (following this procedure means that the set of hypotheses may change substantially from one attribute acquisition to the next), (3) Hypothesis Testing, where the subject determines some subset of possible animals with one obvious favorite, and the subject then requests an attribute that will confirm that favorite choice, (4) Favorite Attributes, where subjects do not attempt to reduce a set of alternatives, but rather they have favorite attributes which they tend to request at first regardless of the initially given attribute, and (5) Random Request, an unlikely but possible strategy, where the subject simply randomly chooses an attribute to request regardless of the initial attribute.

The strategies were compared by inspecting the patterns of attribute requests and also the hypothesized animals following each attribute acquisition. Several comparisons were made since there was no single analysis which could discriminate between all five strategies. In general, predictions were made for each strategy and then data was sorted and analyzed using a Chi-square goodness-of-fit test. To summarize the results, all analyses effectively ruled out the Hypothesis Testing and Random Request strategies.

Two analyses of attribute requests were productive in discriminating between the Half-Split and Set Reduction strategies. The first attributes requested by subjects were analyzed in terms of predictions based on each of the two models and the data clearly supported the Set Reduction strategy. That is, the subjects did not seem to mentally entertain all possible animals based on the initial attribute and then ask for an attribute which most evenly split the alternatives. Instead, they did think of some subset of alternatives and then ask for an attribute which would narrow the subset. This makes intuitive sense, because the Set Reduction strategy requires much less cognitive energy and doesn't really cost the subject anything.

Analysis of the second attribute request was interesting in that subjects seemed to follow the same Set Reduction strategy, but the data was "skewed" towards the Half-Split strategy. This means that, in general, the subjects followed a tendency to reduce the set, but there was a definite indication that subjects were sometimes choosing an attribute which would best split the entire subset of possible animals. This is again intuitively plausible, because once subjects have two attributes, the entire subset of possible alternatives is small, and not difficult for the subject to mentally identify all alternatives at once.

A separate analysis of the attributes requested revealed that within the confines of the general strategy that subjects were using (Set Reduction) they did have some preference for particular attributes. That is, given that two attributes were equally diagnostic they would not randomly choose one, but would always go with a preferred attribute. Also, some subjects showed this tendency more than others. This is presumable an effect of "availability", where some attributes are simply more available in memory than others. This would cause the subject to consider

that attribute first, and if it was diagnostic, the subject would go ahead and request it.

In summary, the data show the general strategy to be that of Set Reduction, but as the task becomes less demanding, the subjects start requesting attributes that are more optimally diagnostic. The implications are that the greater the information load (number of possible attributes and number of possible causes), the greater the tendency to rely on the Set Reduction strategy (rather than the Half-Split). This would be especially important in a real-world task such as medical diagnosis, because the information load is great, and a tendency to mentally consider one small subset of causes (diseases) at first might induce a cognitive set that is never completely overcome. This is probably one area where computer systems may be most helpful (in making sure possible causes are not overlooked by the user). Finally, there seems to be an "availability" effect, where not all equally diagnostic attributes are requested equally often; rather the subjects have favorites that are most accessible in memory, and if those attributes are diagnostic, they will be requested before any others.

5.2.2 Strategy Analysis for Expert-Aid Conditions

The same five strategies were assessed for subjects in the Expert-aid conditions. The analyses were similar to those performed under Manual conditions; attributes requested were compared with predictions based on the models, and Chi-square goodness-of-fit tests were performed. As before, the data were consistent with the Set Reduction strategy, with each subject showing some favoritism as far as requesting some attributes more than others. In fact, this tendency to request favorite attributes was more pronounced in the Expert-aid conditions than under Manual conditions. This is most likely because subjects were more inclined to "get information now" and "solve the problem later" with the Expert System.

Only in one analysis did the data show a slight tendency away from a Set reduction strategy in the direction of the Half-Split strategy (meaning that subjects did not randomly determine a diagnostic attribute to request, but instead sometimes chose one that more evenly split the possible alternatives).

To summarize, subjects used what seems to be a sensible and relatively easy strategy, that of Set Reduction, both in the Manual and Expert-aided conditions. Within the confines of that strategy, when there were several equally diagnostic attributes, they showed a tendency towards favoritism in requesting certain attributes more than others (different subjects favored different attributes). In addition, data indicate that as the set of possible alternatives and relevant attributes becomes small, subjects are more able to utilize a Half-Split strategy. However, in the case of the current study, this is only when this number is 2-4 alternatives, and in the real world environment, this would be towards the very end of the inference process.

5.3 Conclusions

Several useful pieces of information resulted from the present research project. First, it has been shown that the laboratory diagnostic inference task developed for the study is a successful tool to use in studying both manual performance of an inference task, and also the effects of introducing various configurations in an Expert-aiding System.

Second, preliminary studies comparing Manual with Expert-aid performance of the diagnostic inference tasks have given many insights into the impact of introducing an expert system. The most important of these is the benefits of training the system operators to perform the task on their own; both to learn the task characteristics and also become familiar with their own capabilities. This allows them to more effectively use and assess the Expert System.

Finally, an analysis of the strategies used by subjects in both Manual and Expert-Aid conditions, has revealed that subjects use an effective and cognitively undemanding strategy in performing the inference task on their own, and that this strategy does not essentially change as a function of introducing an Expert System.

There are obviously several details concerning the study which make these conclusions tentative until further research is conducted. Primarily, two issues need to be resolved. The first is whether the change in task requirements caused some of the differences seen in the Expert-aid conditions (such as the number of attributes requested). Second, the nature of the Expert System needs to be modified such that it begins with at least as much information (probabilities, etc.) as the subject. This will make the system more accurate and also more closely mirror real world expert systems. Research is currently being implemented to study these and other important questions.

REFERENCES

- [1] Slovic, P., Fischhoff, B., and Lichtenstein, S. "Behavioral decision theory", Annual Review of Psychology, Vol. 28, pp. 1-39, 1977.
- [2] Price, H.E., Maisana, R.E., and Van Cott, H.P. "The allocation of functions in man-machine systems: A perspective and literature review", (NUREG CR-2623). Oak Ridge, Te: Oak Ridge National Laboratory, June 1982.
- [3] Yntema, D.B. and Torgerson, W.S. "Man-computer cooperation in decisions requiring common sense", IRE Transactions on Human Factors in Electronics, Vol. 2, pp.20-26,1961.
- [4] Duda, R., Gaschnig, J., and Hart, O.E., Model design in the PROSPECTOR consultant system for mineral exploration. In B.L. Webber and N.J. Nilsson (Eds.). Readings in artificial intelligence, Palo Alto, CA: Tioga Publishing Co., 1981.
- [5] Duda, R.O. and Gaschnig, J. "Knowledge-based expert systems coming of age", Byte, Vol. 6, pp. 238-281, 1981.
- [6] Shortliffe, E.H., Axline, S.G., Buchanan, B.G., Merigan, T.C., and Cohen, S.N. "An artificial intelligence program to advise physicians regarding antimicrobial therapy", Computers in Biomedical Research, Vol. 6, pp. 544-560, 1973.
- [7] Shortliffe, E.H. Computer-Based medical consultation: MYCIN. Elsevier/North Holland, New York, 1976.
- [8] Pople, H.E. Heuristic methods for imposing structure on ill-structured problems: The structuring of medical

- diagnostics. In P. Szolovitz (Ed.), Artificial intelligence in medicine. Boulder, Co.: Westview Press, 1981.
- [9] Buchanan, B.G., and Feigenbaum, E.A. DENDRAL and Meta-DENDRAL: Their applications dimension. Artificial Intelligence, 11, pp. 5-24.
- [10] Hillman, D.J. "Artificial intelligence". Human Factors, Vol. 27, pp. 21-31, 1985.
- [11] Brachman, R.J., and Smith, B.C. SIGART 70 (special issue on knowledge representation), 1980.
- [12] Salvendy, G. (Ed.) Human-computer interaction. Elsevier/North Holland, New York, 1984.
- [13] Michie, D. Introductory readings in expert systems. New York: Gordon and Breach, 1982.
- [14] Startzman, T.S. and Robinson, R.E. "The attitudes of medical and paramedical personnel towards computers". Computers in Biomedical Research, Vol. 5, pp. 218-227, 1972.
- [15] Teach, R.L. and Shortliffe, E.H. "An analysis of physician attitudes regarding computer-based clinical consultation systems". Computers in Biomedical Research, Vol. 14, pp. 542-558, 1981.
- [16] Shortliffe, E.H. "Medical consultation systems: designing for doctors". In Designing for human-computer communication, London: Academic Press, 1981.
- [17] Price, H.E. "The allocation of functions in systems", Human Factors, Vol. 27, pp. 33-45, 1985.
- [18] Rouse, W.B. "Models of human problem solving: Detection, diagnosis and compensation for system failures", Automatica,

in press.

- [19] Rasmussen, J. On the structure of knowledge - A morphology of mental models in a man-machine system context (Report No. M-1983). Riso, Denmark: Riso National Laboratories, 1979.
- [20] Shortliffe, E.H., Buchanan, B.G. and Feigenbaum, E.A.
"Knowledge engineering for medical decision making: A review of computer-based clinical decision aids. Proceedings of the IEEE, Vol. 67, pp. 1207-1224, 1979.
- [21] Fitter, M.J. and Cruikshank, P.J. "Doctors using computers: A case study". In M.E. Sime and M.J. Coombs (Eds.), Designing for human-computer communication. London: Academic Press, 1983.
- [22] Hunt, R.M. and Rouse, W.B. "Problem-solving skills of maintenance trainees in diagnosing faults in simulated powerplants", Human Factors, Vol. 23, pp. 317-328, 1981.

APPENDICES

APPENDIX A: PASCAL PROGRAM FOR INFERENCE TASK WITH EXPERT-AID

PROGRAM GORDON;

(.....
.....)

This is a program used in the research grant conducted by Dr. Sallie Gordon,
from the University of Idaho. It begins by reading data from the b disk drive.

(.....
.....)

CONST

NUMCODE = 6 ; (* The number of attribute types *)
NUMTRIALS = 30; (* The number of trial per disk *)

TYPE

INFO = RECORD
TRIAL : INTEGER; (* The trial of the session *)
CONDITION : STRING[5]; (* The condition of the day *)
UNANSWER : STRING [10]; (* The answer to the trial *)
UNCH1 : STRING[10]; (* The following six strings *)
UNCH2 : STRING[10]; (* are the strings of attributes *)
UNCH3 : STRING[10]; (* read into the computer that *)
UNCH4 : STRING[10]; (* are unknown to the user until *)
UNCH5 : STRING[10]; (* requested by the user *)
UNCH6 : STRING[10];
end; (* End of the record *)

regpack = record
ax,bx,cx,dx,bp,di,si,ds,es,flags:integer;
end;

VAR

recpack:regpack;
done : integer;

I : INTEGER; (* Integer counter used in prog *)
CODE : CHAR; (* Code of the attribute *)
TEMPCO : CHAR;
KNANSWER : STRING[25]; (* Answer known to the user *)
KNCH1 : STRING[10]; (* The following are the six *)
KNCH2 : STRING[10]; (* attributes shown on the screen*)
KNCH3 : STRING[10]; (* by the computer. These are *)
KNCH4 : STRING[10]; (* only shown when requested by *)
KNCH5 : STRING[10]; (* the user *)
KNCH6 : STRING[10];
EXPERT : STRING[10];

ATTRIBUT : STRING[10]; (* String used in output *)

GUESS : STRING[10]; (* The guess used by the user *)
RATING : CHAR; (* The rating given by the user *)
CONTINUE : CHAR; (* The integer used for continue *)
NUMBER : STRING[2]; (* The subject number of user *)
ANS : CHAR;

GUESSCOD: CHAR;
CORRECT: INTEGER;
PER : REAL;
X: INTEGER;

```

initime,
endtime,
time : integer;
xtime : real;

INFOARRAY : INFO;          (* Record of values          *)
DATAFILE : TEXT;           (* Text file for input  *)
OUTFILE : TEXT;            (* Text file for output  *)

(*****
This procedure is used to give directions to the user as to what he is
to do for the program.
*****)

PROCEDURE DIRECTIONS;
BEGIN                      (* Begin of procedure dirctions      *)

WRITELN(' Welcome to the scientific study conducted by Dr. Sallie Gordon.',
' The object of this study is to guess what animal is being described by ',
' the computer. You will be given the condition of the day and one of ',
' six attributes. ');
writeLn(' You are to guess the animal, ask the expert, or ask for an ',
' attribute. ');

writeLn(' You may only ask the expert twice, and when you have made ',
' your guess. ');
writeLn(' the trial will automatically end. ');

writeLn;
writeLn(' The research assistant will help you go through a practice trial. ');
end;                      (* End of procedure directions      *)

(*****
This procedure asks for the subject number of the user.
*****)

PROCEDURE QSUBNUM;
BEGIN                      (* Begin of procedure qsubnum      *)
WRITELN;
WRITELN;
WRITELN;
WRITELN(' PLEASE ENTER YOUR SUBJECT NUMBER ');
READLN( NUMBER );         (* Reads the subject number      *)
END;                      (* End of procedure qsubnum      *)

(*****
This procedure reads the data. It will read the data one trial at a
time. The procedure first reads a code which then does a case statment
as to what attribute will be read next.
*****)

```

```

PROCEDURE READDATA;
var
  I: INTEGER;
  CODE : CHAR;

BEGIN
  WITH INFOARRAY do
    BEGIN
      READLN(DATAFILE, TRIAL);      (* Begin of procedure readdata *)
      READLN(DATAFILE, CONDITION);  (* Begin of with statement *)
      READLN(DATAFILE, unANSWER);   (* Reads the trial number *)
      READ (DATAFILE, CODE);        (* Reads the condition *)
      TEMPCO := CODE;              (* Reads the answer *)
      CASE CODE OF                 (* Reads the code of the first *)
        '1' : BEGIN                (* attribute. Which is first *)
          READLN(DATAFILE, KNCH1);  (* to be put on the screen *)
          UNCH1:=KNCH1;             (* Reads the attribute with *)
          ATTRIBUT := KNCH1;        (* the code of one *)
        END;
        '2' : BEGIN
          READLN(DATAFILE, KNCH2);  (* Reads the attribute with *)
          UNCH2:=KNCH2;             (* the code of two *)
          ATTRIBUT := KNCH2
        END;
        '3' : BEGIN
          READLN(DATAFILE, KNCH3);  (* Reads the attribute with *)
          UNCH3:=KNCH3;             (* the code of three *)
          ATTRIBUT := KNCH3
        END;
        '4' : BEGIN
          READLN(DATAFILE, KNCH4);  (* Reads the attribute with *)
          UNCH4:=KNCH4;             (* the code of four *)
          ATTRIBUT := KNCH4
        END;
        '5' : BEGIN
          READLN(DATAFILE, KNCH5);  (* Reads the attribute with *)
          UNCH5:=KNCH5;             (* the code of five *)
          ATTRIBUT := KNCH5
        END;
        '6' : BEGIN
          READLN(DATAFILE, KNCH6);  (* Reads the attribute with *)
          UNCH6:=KNCH6;             (* the code of six *)
          ATTRIBUT := KNCH6
        END;
      END;
      FOR I := 1 TO NUMCODE-1
        DO BEGIN
          READ(DATAFILE, CODE);      (* For loop to read the rest of *)
          WRITE( CODE);              (* the attributes which are not *)
          CASE CODE OF               (* shown on the screen *)
            '1': READLN(DATAFILE, UNCH1);  (* Reads the code for the *)
            '2': READLN(DATAFILE, UNCH2);  (* attribute *)
            '3': READLN(DATAFILE, UNCH3);  (* reads attribute one *)
            '4': READLN(DATAFILE, UNCH4);  (* reads attribute two *)
            '5': READLN(DATAFILE, UNCH5);  (* reads attribute three *)
            '6': READLN(DATAFILE, UNCH6);  (* reads attribute four *)
          END;
        END;
      END;
    END;
  END;
END;

```

```

(.....)
This procedure prints out the screen as the attributes are requested.
(.....)

```


PROCEDURE SCREEN;

BEGIN

(* Begin of procedure screen *)

WRITELN;

WRITELN(' POSSIBLE CHOICES ');

WRITELN;

WRITELN(' RABBIT

DEER

');

WRITELN(' SQUIRREL

WOLF

');

WRITELN(' GROUNDHOG

BEAR

');

WRITELN(' HAWK

OWL

');

WRITELN;

WITH INFOARRAY DO

BEGIN

WRITELN(' TRIAL : ', TRIAL); (* Prints out the trial # *)

WRITELN(' CONDITION : ', CONDITION); (* Prints out the condition *)

WRITELN(' EXPERT : ', EXPERT); (* Prints out the answer *)

WRITELN;

WRITELN;

WRITELN(' CODE--ATTRIBUTES : ');

WRITELN;

WRITELN(' 1--SIZE : ', KNCH1); (* The following prints out *)

WRITELN(' 2--LOCATION : ', KNCH2); (* attributes as they are *)

WRITELN(' 3--SPEED : ', KNCH3); (* requested by the user *)

WRITELN(' 4--COLOR : ', KNCH4);

WRITELN(' 5--NOISE : ', KNCH5);

WRITELN(' 6--ALARM : ', KNCH6);

WRITELN;

END;

(* END OF DO BEGIN

*)

END;

(* END OF PROCEDURE

*)

(*****
 This procedure prints out the heading of the output to the output file
 It lists the subject number, trial number, condition, attribute pick
 at that time, guess of the animal, rating on the guess of 1-9, and
 the answer of the trial.
 *****)

PROCEDURE HEADING;

BEGIN

(* Begin of procedure heading *)

WRITELN(OUTFILE);

WRITELN(OUTFILE, ' SUB THI ');

WRITELN(OUTFILE, ' NUM NUM CONDI CODE-ATTRIBUTE GUESS RATING ',

' ANSWER TIME EXPERT');

(* End of the procedure

*)

END;

(*****
 This procedure prints out the data to a file. It prints it as soon as
 the user inputs the data after a rating has been given from the key
 board.
 *****)

PROCEDURE ATTPRINT;

```

BEGIN                                (* Begin of procedure dataprint *)
WITH INFOARRAY DO
BEGIN                                (* Begin of with statement *)
WRITELN(OUTFILE, NUMBER:4, TRIAL:5, CONDITION:8, CODE:6, ATTRIBUT:10, '-':20,
UNANSWER:12, XTIME:9:2);
END;                                (* End of with statement *)
END;                                (* End of procedure dataprint *)

PROCEDURE EXPRT;
BEGIN
WITH INFOARRAY DO
BEGIN
WRITELN(OUTFILE, NUMBER:4, TRIAL:5, CONDITION:8, '-':48, XTIME:9:2, EXPERT:10);
END;
END;

PROCEDURE GUEPRINT;
BEGIN
WITH INFOARRAY DO
BEGIN
WRITELN(OUTFILE, NUMBER:4, TRIAL:5, CONDITION:8, '-':16, GUESS:12, RATING:8, UNANSWER:
XTIME:9:2);
END;
END;

(*****
*****
This procedure is used to exchange the unknown attribute with the known
attribute when an attribute is requested. This is done with a case
statement which cases a code and exchanges the correct attribute.
*****
*****);

PROCEDURE ATTRICODE;
BEGIN                                (* Begin of procedure attricode *)
WITH INFOARRAY DO
BEGIN                                (* Begin of with statement *)
CASE CODE OF                        (* Case statement of the codes *)
'1': BEGIN
KNCH1 := UNCH1;
ATTRIBUT := UNCH1
END;                                (* Exchanges the first attribute*)
'2': BEGIN
KNCH2 := UNCH2 ;
ATTRIBUT := UNCH2
END;                                (* Exchanges the second attribut*)
'3': BEGIN
KNCH3 := UNCH3 ;
ATTRIBUT := UNCH3
END;                                (* Exchanges the third attribute*)
'4': BEGIN
KNCH4 := UNCH4 ;
ATTRIBUT := UNCH4
END;                                (* Exchanges the forth attribute*)
'5': BEGIN
KNCH5 := UNCH5 ;
ATTRIBUT := UNCH5
END;                                (* Exchanges the fifth attribute*)
'6': BEGIN
KNCH6 := UNCH6 ;
ATTRIBUT := UNCH6
END;                                (* Exchanges the sixth attribut*)
END                                (* End of the Case statement *)
END                                (* End of the With statement *)
END;                                (* End of the Procedure *)

```

```

(*****
*****
This procedure asks questions that the study is using.
1.) Guess
2.) Rating
3.) Continue on this trial or go onto next
4.) If continue on this trial, it will ask for an attribute choice.
*****
*****
)

PROCEDURE QUESTION;
BEGIN
REPEAT
WRITELN(' MAKE A GUESS by typing the FIRST LETTER of the animal. ');
READLN(GUESSCOD); (* Reads the guess *)
UNTIL UpCase(guesscod) in ['R','S','G','H','D','W','B','O'];

with reckpt
do begin
ax:=0;
intr($1a,reckpack);
endtime := dx + 32767
END;

xtime:= (endtime - initime)/18.2;
(*TIME:= xTIME div 1*)

REPEAT
WRITELN(' You must enter a CONFIDENCE RATING from 1 to 9, ');
READLN(RATING); (* Reads the rating *)
UNTIL UpCase(RATING) in ['1','2','3','4','5','6','7','8','9'];

guesscod := UpCase(guesscod);
case guesscod of
'R' : GUESS := ' Rabbit';
'S' : GUESS := ' Squirrel';
'G' : GUESS := ' Groundhog';
'H' : GUESS := ' Hawk';
'D' : GUESS := ' Deer';
'W' : GUESS := ' Wolf';
'B' : GUESS := ' Bear';
'O' : GUESS := ' Owl';
END;

GUEPRINT;
done := 1; (* Call to print current data *)

END; (* END OF PROCEDURE GUESSTION *)

PROCEDURE ATTR;
BEGIN (* Begin of ATTR PROCEDURE *)
REPEAT
WRITELN(' ENTER the NUMBER to the LEFT of the ATTRIBUTE. ');
READLN(CODE);
UNTIL UpCase(CODE) IN ['1','2','3','4','5','6'];

ATTRICODE;
done:= 0; (* Reads code of attribute *)

WITH RECKPACK
DO BEGIN
AX:=0;
INTR($1A,RECKPACK);
ENDTIME := DX + 32767
END;

```

XTIME:= (ENDTIME-INITIME)/18.2;

ATTPRINT;

END;

(* End of the ATTR PROCEDURE *)

PROCEDURE EXPERTOP;

VAR

raw: integer;

found : integer;

BEGIN

REPEAT

RAW:= RANDOM(9);

WRITE(RAW);

CASE RAW OF

1 : BEGIN

```
    IF (KNCH1=' Small') or (knch1=' Unknown') or (knch1=' ')
    then if (knch2=' Ground') or (knch2=' Unknown') or (knch2=' ')
    then if (knch3=' Fast') or (knch3=' Unknown') or (knch3=' ')
    then if (knch4=' Grey') or (knch4=' Unknown') or (knch4=' ')
    then if (knch5=' No Noise') or (knch5=' Unknown') or (knch5=' ')
    then if (knch6=' No Alarm') or (knch6=' Unknown') or (knch6=' ')
    then
        begin
            expert := '    Rabbit';
            found := 1
        end
    end;
```

2 : begin

```
    if (knch1=' Small') or (knch1=' Unknown') or (knch1=' ')
    then if (knch2=' Ground') or (knch2=' Unknown') or (knch2=' ')
    then if (knch3=' Slow') or (knch3=' Unknown') or (knch3=' ')
    then if (knch4=' Brown') or (knch4=' Unknown') or (knch4=' ')
    then if (knch5=' No Noise') or (knch5=' Unknown') or (knch5=' ')
    then if (knch6=' No Alarm') or (knch6=' Unknown') or (knch6=' ')
    then
        begin
            expert := ' Groundhog';
            found := 1;
        end
    end;
```

3 : begin

```
    if (knch1=' Large') or (knch1=' Unknown') or (knch1=' ')
    then if (knch2=' Ground') or (knch2=' Unknown') or (knch2=' ')
    then if (knch3=' Fast') or (knch3=' Unknown') or (knch3=' ')
    then if (knch4=' Brown') or (knch4=' Unknown') or (knch4=' ')
    then if (knch5=' No Noise') or (knch5=' Unknown') or (knch5=' ')
    then if (knch6=' No Alarm') or (knch6=' Unknown') or (knch6=' ')
    then
        begin
            expert := '    Deer';
            found := 1;
        end
    end;
```

4 : begin

```
    if (knch1=' Large') or (knch1=' Unknown') or (knch1=' ')
    then if (knch2=' Ground') or (knch2=' Unknown') or (knch2=' ')
    then if (knch3=' Slow') or (knch3=' Unknown') or (knch3=' ')
    then if (knch4=' Brown') or (knch4=' Unknown') or (knch4=' ')
    then if (knch5=' Noise') or (knch5=' Unknown') or (knch5=' ')
    then if (knch6=' Alarm') or (knch6=' Unknown') or (knch6=' ')
    then
```

```

then
  begin
    expert := '      Bear';
    found := 1;
  end
end;

5 : begin
  if (knch1=' Small') or (knch1=' Unknown') or (knch1='
then if (knch2=' Tree') or (knch2=' Unknown') or (knch2='
then if (knch3=' Fast') or (knch3=' Unknown') or (knch3='
then if (knch4=' Brown') or (knch4=' Unknown') or (knch4='
then if (knch5=' Noise') or (knch5=' Unknown') or (knch5='
then if (knch6=' No Alarm') or (knch6=' Unknown') or (knch6='
then
  begin
    expert := '      Squirrel';
    found := 1;
  end
end;

6 : begin
  if (knch1=' Small') or (knch1=' Unknown') or (knch1='
then if (knch2=' Tree') or (knch2=' Unknown') or (knch2='
then if (knch3=' Fast') or (knch3=' Unknown') or (knch3='
then if (knch4=' Grey') or (knch4=' Unknown') or (knch4='
then if (knch5=' No Noise') or (knch5=' Unknown') or (knch5='
then if (knch6=' Alarm') or (knch6=' Unknown') or (knch6='
then
  begin
    expert := '      Owl';
    found := 1;
  end
end;

7 : begin
  if (knch1=' Small') or (knch1=' Unknown') or (knch1='
then if (knch2=' Tree') or (knch2=' Unknown') or (knch2='
then if (knch3=' Fast') or (knch3=' Unknown') or (knch3='
then if (knch4=' Brown') or (knch4=' Unknown') or (knch4='
then if (knch5=' No Noise') or (knch5=' Unknown') or (knch5='
then if (knch6=' Alarm') or (knch6=' Unknown') or (knch6='
then
  begin
    expert := '      Hawk';
    found := 1;
  end
end;

8 : begin
  if (knch1=' Large') or (knch1=' Unknown') or (knch1='
then if (knch2=' Ground') or (knch2=' Unknown') or (knch2='
then if (knch3=' Fast') or (knch3=' Unknown') or (knch3='
then if (knch4=' Grey') or (knch4=' Unknown') or (knch4='
then if (knch5=' No Noise') or (knch5=' Unknown') or (knch5='
then if (knch6=' Alarm') or (knch6=' Unknown') or (knch6='
then
  begin
    expert := '      Wolf';
    found := 1;
  end
end;

(*otherwise : expert:= '      Unknown'*)

```

```

end;                                     (* end of case *)

until found = 1;
done := 0;

WITH RECPACK
DO BEGIN
  AX:=0;
  INTR($1a,recpack);
  endtime:= dx + 32767;
end;

xtime:= (endtime-initime)/18.2;

EXPRINT;
(*
writeln
writeln(' EXPERT GUESS is ', expert)
writeln

REPEAT
UNTIL KEYPRESSED *)

end;                                     (* end of procedure expert *)

PROCEDURE PROMPT;

VAR
  CUE : CHAR;

BEGIN

  done :=0;
  REPEAT
    WRITELN(' (A)--ATTRIBUTE    (E)--EXPERT    (G)--GUESS    ');
    READLN(CUE);
    UNTIL UpCase(cue) in ['A','E','G'];

    CUE := UpCase(cue);
    case cue of
      'A' : ATTR;
      'E' : EXPERTOP;
      'G' : QUESTION;
    end;

  end;

end;

```

```

(*****
*****
*****
*****

```

This is the main part of the program. It calls all of the subroutines as they are called in this portion of the program.
 It will first define all of the files for the input and the output.
 It then proceduces to call the subroutines as instructed by the program.

```

*****
*****
*****
*****
BEGIN      (*      MAIN      *)
  ASSIGN(DATAFILE, 'B:ANIMAL.DAT');      (* Assigns the input file      *)
  RESET(DATAFILE);
  ASSIGN(OUTFILE, 'A:ANIMAL.OUT');      (* Assigns the output file      *)
  REWRITE(OUTFILE);

  DIRECTIONS;      (* Call to procedure directions*)
  QSUBNUM;      (* Call to procedure qsubnum      *)
  CLASCR;      (* Clears the screen      *)

  CORRECT:=0;

  FOR I := 1 TO NUMTRIALS      (* Begin of loop to process      *)
    DO BEGIN      (* program      *)

      HEADING;      (* Calls the heading procedure *)

      KNCH1:=';'      (* Initializes the string      *)
      KNCH2:=';'      (* knch1-knch6 to empty      *)
      KNCH3:=';'
      KNCH4:=';'
      KNCH5:=';'
      KNCH6:=';'
      KNANSWER:=';'
      EXPERT:=';'

      WITH INFOARRAY DO
      BEGIN
        UNCH1:=';'      (* Initializes the string      *)
        UNCH2:=';'      (* unch1-unch6 to empty      *)
        UNCH3:=';'
        UNCH4:=';'
        UNCH5:=';'
        UNCH6:=';'
        UNANSWER:=';'

        END;      (* End of with statement *)

      READDATA;      (* Call to readdata procedure *)

      CODE:= TEMPCO;

      with repack
      do begin
        ax:= 0;

```

```

        intr($la,recpack);
        initime:= dx + 32767
    end;

xtime:= 0.0;

ATTPRINT;

REPEAT                                     (* Repeat the following calls *)
SCREEN;                                  (* Call the screen procedure *)
PRCMT;
CLRSCR;                                  (* Clears the screen *)

UNTIL DONE = 1;                          (* Repeats until continue=B *)

WITH INFOARRAY DO                        (* Being of the with statement*)
BEGIN

    WRITELN(' Your final answer was ', guess);
    WRITELN;

    WRITELN(' The correct answer is ', UNANSWER); (* Writes the answer *)
                                                (* when completed *)
    WRITELN;
    WRITELN;
    WRITELN('PRESS ANY KEY TO CONTINUE TRIALS ');
    WRITELN;

    REPEAT
    UNTIL KEYPRESSED;
    CLRSCR;

    END;                                (* End of the with statement *)

    END;                                (* End of for statement loop *)

    (*WRITELN(' STATEMENT JUST BEFORE PERCENT CALL ')*
    (*PERCENT*)

CLOSE(OUTFILE);

END.                                    (* End of the main program *)

```


APPENDIX B: POST-EXPERIMENTAL QUESTIONNAIRES

Questionnaire for Manual Conditions:

1) What percentage of the trials do you think you answered correctly for each of the three sessions?

% for first day _____

% for second day _____

% for third day _____

2) For each of the eight animals, give the percentage of trials where the animal was the correct answer. That is, out of 100%, what percent accounted for each particular animal?

Rabbit	_____
Groundhog	_____
Deer	_____
Bear	_____
Squirrel	_____
Owl	_____
Hawk	_____
Wolf	_____

3) Try to describe the strategy you used during the trials.

Questionnaire for Expert-Aided Conditions:

1) On a scale from 1 to 20, rate yourself on how accurate you think YOUR OWN unaided guesses were (as you did each trial, how good were your ideas without considering the help you received). In rating yourself, 1 = extremely inaccurate and 20 = perfect.

2) On a scale from 1 to 20, rate the EXPERT on how accurate you think it's answers were, 1 = extremely inaccurate and 20 = perfect.

3) Was the expert better in some situations than others?

4) For each of the eight animals, give the percentage of trials where the animal was the correct answer. That is, out of 100%, what percent accounted for each particular animal?

Rabbit	_____
Groundhog	_____
Deer	_____
Bear	_____
Squirrel	_____
Owl	_____
Hawl	_____
Wolf	_____

5) Try to describe the strategy you used during the trials.

6) What percentage of the trials do you think you answered correctly for each of the two sessions?

% for first day _____

% for second day _____

APPENDIX C: ANALYSIS OF VARIANCE TABLES FOR PHASE I

Multivariate Analysis for All Dependent Variables Combined:

<u>Source</u>	<u>Source df</u>	<u>Error df</u>	<u>Mult F</u>	<u>Prob.</u>
Session	8	40	3.89	.01
Attr. Available	4	8	6.81	.01
Diag.	4	8	43.74	.000
Session x AA	8	40	1.48	ns
Session x Diag.	8	40	2.48	.03
AA x Diag.	4	8	4.01	.04
Session x AA x Diag.	8	40	1.97	ns

Analysis of Variance for PERCENT CORRECT:

<u>Source</u>	<u>Source df</u>	<u>Error df</u>	<u>F</u>	<u>Prob.</u>
Session	2	22	7.58	.01
Attr. Available	1	11	.07	ns
Diag.	1	11	54.92	.000
Session x AA	2	22	1.82	ns
Session x Diag.	2	22	2.42	ns
AA x Diag.	1	11	.12	ns
Session x AA x Diag.	2	22	4.00	.03 *

* Considered not significant because the Multivariate analysis was not significant for the three-way interaction.

Analysis of Variance for TIME to perform the task:

<u>Source</u>	<u>Source df</u>	<u>Error df</u>	<u>F</u>	<u>Prob.</u>
Session	2	22	19.02	.000
Attr. Available	1	11	.18	ns
Diag.	1	11	56.12	.000
Session x AA	2	22	1.75	ns
Session x Diag.	2	22	7.70	.01
AA x Diag.	1	11	2.87	ns
Session x AA x Di.	2	22	2.20	ns

Analysis of Variance for Subjective CERTAINTY:

<u>Source</u>	<u>Source df</u>	<u>Error df</u>	<u>F</u>	<u>Prob.</u>
Session	2	22	.19	ns
Attr. Available	1	11	23.60	.001
Diag.	1	11	52.38	.000
Session x AA	2	22	1.20	ns
Session x Diag.	2	22	4.06	.03
AA x Diag.	1	11	2.07	ns
Session x AA x Di	2	22	.38	ns

Analysis of Variance for Number of ATTRIBUTES REQUESTED:

<u>Source</u>	<u>Source df</u>	<u>Error df</u>	<u>F</u>	<u>Prob.</u>
Session	2	22	.48	ns
Attr. Available	1	11	.73	ns
Diag.	1	11	120.39	.000
Session x AA	2	22	.51	ns
Session x Diag.	2	22	4.30	.03
AA x Diag.	1	11	.59	ns
Session x AA x Di	2	22	1.59	ns

Analysis of Variance for PERFORMANCE ESTIMATES:

<u>Source</u>	<u>Source df</u>	<u>Error df</u>	<u>F</u>	<u>Prob.</u>
Session	2	22	9.22	.001
Est. Vs. Actual	1	11	4.67	.05
Session x E/A	1	11	.55	ns

APPENDIX D: ANALYSIS OF VARIANCE TABLES FOR EXPERIENCED
SUBJECTS, MANUAL VS. EXPERT-AID CONDITIONS; ANALYSIS A

Multivariate Analysis for All Dependent Variables Combined:

<u>Source</u>	<u>Source df</u>	<u>Error df</u>	<u>Mult. F</u>	<u>Prob.</u>
Phase	4	8	28.92	.000
Session	4	8	4.11	.04
Attr. Available	4	8	7.33	.01
Diag.	4	8	55.99	.000
Phase x Session	4	8	.30	ns
Phase x AA	4	8	1.53	ns
Phase x Diag.	4	8	6.59	.01
Session x AA	4	8	1.62	ns
Session x Diag.	4	8	1.33	ns
AA x Diag.	4	8	.95	ns
Phase x Session x AA	4	8	2.56	ns
Phase x Session x Di	4	8	.45	ns
Phase x AA x Diag.	4	8	.95	ns
Session x AA x Diag.	4	8	1.87	ns
Ph x Ses x AA x Diag	4	8	1.11	ns

Analysis of Variance for PERCENT CORRECT:

<u>Source</u>	<u>Source df</u>	<u>Error df</u>	<u>F</u>	<u>Prob.</u>
Phase	1	11	7.41	.02
Session	1	11	2.06	ns
Attr. Available	1	11	2.39	ns
Diag.	1	11	155.46	.000
Phase x Session	1	11	.48	ns
Phase x AA	1	11	.48	ns
Phase x Diag.	1	11	5.98	.03
Session x AA	1	11	1.15	ns
Session x Diag.	1	11	1.74	ns
AA x Diag.	1	11	1.89	ns
Phase x Session x AA	1	11	1.64	ns
Phase x Ses x Diag.	1	11	.34	ns
Phase x AA x Diag.	1	11	.46	ns
Session x AP x Diag.	1	11	4.07	ns
Ph x Ses x AA x Diag	1	11	.15	ns

Analysis of Variance for TIME to perform the task:

<u>Source</u>	<u>Source df</u>	<u>Error df</u>	<u>F</u>	<u>Prob.</u>
Phase	1	11	46.91	.000 *
Session	1	11	12.18	.01
Attr. Available	1	11	7.92	.02
Diag.	1	11	93.45	.000
Phase x Session	1	11	.09	ns
Phase x AA	1	11	.00	ns
Phase x Diag.	1	11	15.31	.01
Session x AA	1	11	2.22	ns
Session x Diag.	1	11	1.29	ns
AA x Diag.	1	11	1.56	ns
Phase x Ses x AA	1	11	.01	ns
Phase x Ses x Diag.	1	11	.09	ns
Phase x AA x Diag.	1	11	.59	ns
Ses x AA x Diag.	1	11	6.01	.03 **
Ph x Ses x AA x Diag	1	11	.72	ns

* This variable is not considered because the subtasks required changed from phase I to phase II, affecting the time variable.

** Considered not significant because the Multivariate analysis was not significant for this three-way interaction.

Analysis of Variance for Subjective CERTAINTY:

<u>Source</u>	<u>Source df</u>	<u>Error df</u>	<u>F</u>	<u>Prob.</u>
Phase	1	11	6.08	.03
Session	1	11	.10	ns
Attr. Available	1	11	18.02	.001
Diag.	1	11	56.60	.000
Phase x Session	1	11	.92	ns
Phase x AA	1	11	3.30	ns
Phase x Diag.	1	11	.00	ns
Session x AA	1	11	1.53	ns
Session x Diag.	1	11	.69	ns
AA x Diag.	1	11	.54	ns
Phase x Ses x AA	1	11	.83	ns
Phase x Ses x Diag.	1	11	.79	ns
Phase x AA x Diag.	1	11	2.05	ns
Day x AA x Diag.	1	11	1.97	ns
Ph x Ses x AA x Diag	1	11	1.07	ns

Analysis of Variance for Number of ATTRIBUTES REQUESTED:

<u>Source</u>	<u>Source df</u>	<u>Error df</u>	<u>F</u>	<u>Prob.</u>
Phase	1	11	11.26	.01
Session	1	11	3.63	ns
Attr. Available	1	11	.43	ns
Diag.	1	11	60.05	.000
Phase x Session	1	11	.01	ns
Phase x AA	1	11	.46	ns
Phase x Diag.	1	11	1.49	ns
Session x AA	1	11	4.05	ns
Session x Diag.	1	11	.05	ns
AA x Diag.	1	11	2.62	ns
Phase x Ses x AA	1	11	1.27	ns
Phase x Ses x Diag.	1	11	.45	ns
Phase x AA x Diag.	1	11	1.48	ns
Session x AA x Diag.	1	11	.19	ns
Ph x Ses x AA x Diag	1	11	3.52	ns

APPENDIX E: ANALYSIS OF VARIANCE TABLES FOR EXPERIENCED
VS. NOVICE SUBJECTS, PHASE II; ANALYSIS B

Multivariate Analysis for All Dependent Variables Combined:

<u>Source</u>	<u>Source df</u>	<u>Error df</u>	<u>Mult. F</u>	<u>Prob.</u>
Exp. vs. Novice	6	17	2.60	.05
Session	6	17	5.72	.002
Attr. Available	6	17	3.60	.02
Diag.	6	17	77.99	.000
E/N x Session	6	17	.85	ns
E/N x AA	6	17	.41	ns
E/N x Diag.	6	17	5.10	.01
Session x AA	6	17	2.57	ns
Session x Diag.	6	17	4.24	.01
AA x Diag.	6	17	3.68	.02
E/N x Session x AA	6	17	1.01	ns
E/N x Session x Di.	6	17	1.37	ns
E/N x AA x Diag.	6	17	1.16	ns
Session x AA x Diag	6	17	1.99	ns
E/N x Ses x AA x Di.	6	17	.97	ns

Analysis of Variance for PERCENT CORRECT:

<u>Source</u>	<u>Source df</u>	<u>Error df</u>	<u>F</u>	<u>Prob.</u>
Exp. vs. Novice	1	22	4.19	.05
Session	1	22	.10	ns
Attr. Available	1	22	9.68	.01
Diag.	1	22	125.22	.000
E/N x Session	1	22	.10	ns
E/N x AA	1	22	.06	ns
E/N x Diag.	1	22	.15	ns
Session x AA	1	22	.01	ns
Session x Diag.	1	22	4.02	.05
AA x Diag.	1	22	.91	ns
E/N x Session x AA	1	22	.36	ns
E/N x Session x Di.	1	22	1.68	ns
E/N x AA x Diag.	1	22	2.17	ns
Session x AA x Diag.	1	22	8.96	.01 *
E/N x Ses x AA x Di.	1	22	1.73	ns

* Not considered significant because the Multivariate analysis was not significant for this interaction.

Analysis of Variance for TIME to perform the task:

<u>Source</u>	<u>Source df</u>	<u>Error df</u>	<u>F</u>	<u>Prob.</u>
Exp. vs. Novice	1	22	.61	ns
Session	1	22	29.43	.000
Attr. Available	1	22	4.43	.05
Diag.	1	22	34.95	.000
E/N x Session	1	22	3.48	.07
E/N x AA	1	22	.60	ns
E/N x Diag.	1	22	2.47	ns
Session x AA	1	22	.26	ns
Session x Diag.	1	22	.26	ns
AA x Diag.	1	22	5.15	.03
E/N x Session x AA	1	22	.79	ns
E/N x Session x Di	1	22	.28	ns
E/N x AA x Diag.	1	22	.06	ns
Session x AA x Diag.	1	22	.38	ns
E/N x Ses x AA x Di	1	22	.14	ns

Analysis of Variance for Subjective CERTAINTY:

<u>Source</u>	<u>Source df</u>	<u>Error df</u>	<u>F</u>	<u>Prob.</u>
Exp. vs. Novice	1	22	10.23	.01
Session	1	22	.67	ns
Attr. Available	1	22	2.36	ns
Diagnosticity	1	22	108.28	.000
E/N x Session	1	22	.24	ns
E/N x AA	1	22	.34	ns
E/N x Diag.	1	22	.54	ns
Session x AA	1	22	.05	ns
Session x Diag.	1	22	11.71	.002
AA x Diag.	1	22	.06	ns
E/N x Session x AA	1	22	1.20	ns
E/N x Session x Diag	1	22	3.97	.06
E/N x AA x Diag.	1	22	.01	ns
Session x AA x Diag.	1	22	.08	ns
E/N x Ses x AA x Di	1	22	4.71	.04 *

* Considered not significant because the Multivariate analysis was not significant for this interaction.

Analysis of Variance for Number of ATTRIBUTES REQUESTED:

<u>Source</u>	<u>Source df</u>	<u>Error df</u>	<u>F</u>	<u>Prob.</u>
Exp. vs. Novice	1	22	.06	ns
Session	1	22	1.50	ns
Attr. Available	1	22	2.91	ns
Diagnosticity	1	22	30.47	.000
E/N x Session	1	22	.14	ns
E/N x AA	1	22	.38	ns
E/N x Diag.	1	22	2.81	ns
Session x AA	1	22	8.85	.01
Session x Diag.	1	22	.86	ns
AA x Diag.	1	22	10.60	.004
E/N x Session x AA	1	22	.01	ns
E/N x Session x Diag	1	22	.07	ns
E/N x AA x Diag.	1	22	.18	ns
Session x AA x Diag	1	22	1.56	ns
E/N x Ses x AA x Di	1	22	.01	ns

Analysis of Variance for Number of times EXPERT was ASKED:

<u>Source</u>	<u>Source df</u>	<u>Error df</u>	<u>F</u>	<u>Prob.</u>
Exp. vs. Novice	1	22	.24	ns
Session	1	22	9.47	.01
Attr. Available	1	22	3.83	.06
Diagnosticity	1	22	119.43	.000
E/N x Session	1	22	.00	ns
E/N x AA	1	22	1.47	ns
E/N x Diag.	1	22	18.99	.000
Session x AA	1	22	.30	ns
Session x Diag.	1	22	.99	ns
AA x Diag.	1	22	3.42	ns
E/N x Session x AA	1	22	1.44	ns
E/N x Session x Diag	1	22	1.60	ns
E/N x AA x Diag.	1	22	5.43	.03 *
Session x AA x Diag.	1	22	.18	ns
E/N x Ses x AA x Di	1	22	.02	ns

* Considered not significant because the Multivariate analysis was not significant for this interaction.

Analysis of Variance for Number of times EXPERT was USED:

<u>Source</u>	<u>Source df</u>	<u>Error df</u>	<u>F</u>	<u>Prob.</u>
Exp. vs. Novice	1	22	.43	ns
Session	1	22	5.24	.03
Attr. Available	1	22	.02	ns
Diagnosticity	1	22	14.69	.001
E/N x Session	1	22	.49	ns
E/N x AA	1	22	.66	ns
E/N x Diag.	1	22	.63	ns
Session x AA	1	22	.47	ns
Session x Diag.	1	22	.26	ns
AA x Diag.	1	22	.25	ns
E/N x Session x AA	1	22	.67	ns
E/N x Session x Diag	1	22	.30	ns
E/N x AA x Diag.	1	22	2.08	ns
Session x AA x Diag.	1	22	.17	ns
E/N x Ses x AA x Di	1	22	.73	ns

APPENDIX F: ANALYSIS OF VARIANCE TABLES FOR EXPERIENCED
VS. NOVICE, FIRST TWO SESSIONS; ANALYSIS C

Multivariate Analysis for All Dependent Variables Combined:

<u>Source</u>	<u>Source df</u>	<u>Error df</u>	<u>Mult. F</u>	<u>Prob.</u>
Exp. vs. Novice	4	19	11.60	.000
Session	4	19	14.80	.000
Attr. Available	4	19	2.80	.05
Diagnosticity	4	19	60.56	.000
E/N x Session	4	19	1.18	ns
E/N x AA	4	19	2.62	ns
E/N x Diag.	4	19	4.06	.01
Session x AA	4	19	1.45	ns
Session x Diag.	4	19	7.44	.001
AA x Diag.	4	19	7.21	.001
E/N x Session x AA	4	19	1.11	ns
E/N x Session x Diag	4	19	2.17	ns
E/N x AA x Diag.	4	19	.73	ns
Session x AA x Diag.	4	19	3.15	.04
E/N x Ses x AA x Di	4	19	1.59	ns

Analysis of Variance for PERCENT CORRECT:

<u>Source</u>	<u>Source df</u>	<u>Error df</u>	<u>F</u>	<u>Prob.</u>
Exp. vs. Novice	1	22	4.02	.05
Session	1	22	3.25	ns
Attr. Available	1	22	1.19	ns
Diagnosticity	1	22	66.39	.000
E/N x Session	1	22	3.25	ns
E/N x AA	1	22	6.45	.02 *
E/N x Diag.	1	22	7.95	.01
Session x AA	1	22	.41	ns
Session x Diag.	1	22	5.85	.02
AA x Diag.	1	22	6.12	.02
E/N x Session x AA	1	22	.00	ns
E/N x Session x Diag	1	22	.93	ns
E/N x AA x Diag.	1	22	.00	ns
Session x AA x Diag.	1	22	7.91	.01
E/N x Ses x AA x Di	1	22	.12	ns

* Not considered significant because the Multivariate analysis was not significant for this interaction

Analysis of Variance for TIME to perform the task:

<u>Source</u>	<u>Source df</u>	<u>Error df</u>	<u>F</u>	<u>Prob.</u>
Exp. vs. Novice	1	22	23.51	.000 *
Session	1	22	33.53	.000
Attr. Available	1	22	.05	ns
Diagnosticity	1	22	45.45	.000
E/N x Session	1	22	.72	ns
E/N x AA	1	22	.82	ns
E/N x Diag.	1	22	8.68	.01
Session x AA	1	22	.60	ns
Session x Diag.	1	22	7.14	.01
AA x Diag.	1	22	.00	ns
E/N x Session x AA	1	22	1.08	ns
E/N x session x Diag	1	22	7.08	.01 **
E/N x AA x Diag.	1	22	1.81	ns
Session x AA x Diag.	1	22	2.21	ns
E/N x Ses x AA x Di	1	22	2.67	ns

* The main effect of Phase cannot be considered because of changes in the subtasks between Phase I and Phase II

** Considered not significant because the Multivariate analysis was not significant for this three-way interaction

Analysis of Variance for Subjective CERTAINTY:

<u>Source</u>	<u>Source df</u>	<u>Error df</u>	<u>F</u>	<u>Prob.</u>
Exp. vs. Novice	1	22	.24	ns
Session	1	22	.63	ns
Attr. Available	1	22	10.66	.01
Diagnosticity	1	22	117.87	.000
E/N x Session	1	22	.01	ns
E/N x AA	1	22	1.92	ns
E/N x Diag.	1	22	.20	ns
Session x AA	1	22	.20	ns
Session x Diag.	1	22	14.85	.001
AA x Diag.	1	22	1.58	ns
E/N x Session x AA	1	22	.49	ns
E/N x Session x Diag	1	22	.04	ns
E/N x AA x Diag.	1	22	.92	ns
Session x AA x Diag.	1	22	.05	ns
E/N x Ses x AA x Di	1	22	2.39	ns

Analysis of Variance for Number of ATTRIBUTES REQUESTED:

<u>Source</u>	<u>Source df</u>	<u>Error df</u>	<u>F</u>	<u>Prob.</u>
Exp. vs. Novice	1	22	9.50	.005
Session	1	22	.13	ns
Attr. Available	1	22	.20	ns
Diagnosticity	1	22	50.84	.000
E/N x Session	1	22	.10	ns
E/N x AA	1	22	3.48	ns
E/N x Diag.	1	22	4.05	.05
Session x AA	1	22	3.13	ns
Session x Diag.	1	22	.35	ns
AA x Diag.	1	22	9.38	.01
E/N x Session x AA	1	22	.85	ns
E/N x Session x Diag	1	22	3.22	ns
E/N x AA x Diag.	1	22	.86	ns
Session x AA x Diag.	1	22	1.42	ns
E/N x Ses x AA x Di	1	22	.01	ns

Effects of Enriching a Computer-Instructed
Proceduralized Task with Explanatory Information

Technical Report

by

Krystine Batcho Yaworsky

Le Moyne College

Contract No: F49620-82-C-0035

Abstract

In this research, 240 undergraduates constructed an electrical circuit by following instructions displayed on a microcomputer. Type of explanatory material, sequential order (before or after instructions), and mode of presentation of explanations (integrated or non-integrated) were manipulated to explore the influence of explanatory text added to instructions on execution of the circuit assembly task as well as on the knowledge learned about the circuit and the ability to apply that knowledge to new problem solving tasks such as fault diagnosis and circuit design. Overall, the pattern of facilitation effects due to the explanatory material suggested an advantage for concrete, structural information, especially when it followed experience with concrete procedures and objects. The pattern of data suggested that facilitation effects obtained in this study were more likely to have been at a higher level of organization (e.g., mental model formation) than at a lower level of priming or repetition processes. A number of significant gender differences raised questions concerning information processing styles of men and women and indicated the importance of caution in generalizing from results obtained with one gender to the other. Further research is needed to explore the mechanisms underlying gender differences and to ascertain how such differences might necessitate modification of guidelines for the design of human-computer interactive systems.

Effects of Enriching a Computer-Instructed Proceduralized Task with Explanatory Information

As aircraft systems become increasingly more complex, the need for automated aids for maintenance on those systems also increases. Assuming that computerized fault isolation will become the rule (and manual fault isolation the exception), the technician's primary task will evolve into one of executing procedures according to instructions from the computer aid. Optimization of the technician's performance in the new situation requires efforts to design aids with attention to the abilities and limitations of the user. If computer-aiding is to be successful, answers must be sought to questions concerning what types of information should be displayed, how information should be presented, and how difficult the system will be for the user to operate. In brief, the success of computer-aided maintenance ultimately depends upon the user's ability to interact with the computer effectively.

At present there exists little research which is directly related to performance in the anticipated computer-aided context. Furthermore, it is not yet clear how extensive--and how reliable--automated maintenance can become. It is probable that, given the current state of technology, there will remain faults that are not located automatically (Gunning, 1984; Smillie, 1984). As the degree of automation of problem solving and decision making increases and the task of the technician becomes

increasingly proceduralized, concern for generating and maintaining competence at levels appropriate to the demands of infrequently occurring circumstances should also increase.

Current research does not point to a clear method of design to maximize competence in such situations. The project reported here represents a first step in beginning a line of research to address this question. Specifically, this study was designed to explore the utility of explanatory material embedded in the computerized system, and to provide a better understanding of the underlying cognitive processes of human-computer interaction.

An important issue is whether the computerized aiding system can be designed so that interaction with it facilitates the development of useful mental representations of the equipment, which would enhance troubleshooting ability. One possibility is the development of enriched procedural modes to facilitate the acquisition of knowledge about the equipment while executing computer-specified instructions.

Existing data do not make clear, however, whether adding educative material (such as explanatory statements) to a set of instructions would always be necessary or desirable. It might be argued that in the proceduralized task supplementary material would be superfluous and possibly costly, distracting the user.

Kieras and Bovair (1983) argued that an understanding of how a system works does not seem to be necessary if either the device is very simple or the procedures for its use are well known (e.g. our use of the telephone). On the other hand, some evidence exists to suggest that enriched understanding may benefit a proceduralized task. For example, using a device designed specifically for their research, Kieras and Bovair found that a mental model facilitated learning to operate the device.

Consistent with the Kieras and Bovair (1983) finding, Smith and Goodman (in press) found that supplementing procedural instructions with explanatory material benefitted performance in a task requiring assembly of an electrical circuit. In particular, explanatory material facilitated understanding of instructions as evidenced by faster reading times. The explanatory statements were of two types, both of which provided higher-level information in an hierarchical arrangement in which instructions often functioned as instantiations (i.e., concrete examples) of higher level concepts. One type of explanation incorporated structural information concerning the components of the circuit and their interconnections. The other type of explanation provided functional information by emphasizing the dynamics of current flow.

One aspect of Smith and Goodman's (in press) results is particularly relevant to the question of facilitating active fault diagnosis. Their findings suggested that functional explanations might enhance the ability to reason about the circuit and to troubleshoot faulty versions of the circuit. Unfortunately, the evidence on this issue was not conclusive, because the obtained differences did not reach statistical significance.

Although these results are suggestive, the presence of some marginal effects and inconsistencies in results across experiments leaves unresolved the issue of the type of effects produced by explanatory enrichment. Also, the formulation of general guidelines for the nature and format of explanatory statements for application to other tasks presupposes some level of understanding of the mechanisms underlying the effects. Although Smith and Goodman offered suggestions as to possible mechanisms such as preactivation, instantiation, context, mental model formation, justification, goal direction, and hierarchical representation, their studies were not designed to distinguish among such different causative factors.

The purpose of the present study was twofold: (1) to obtain more convincing evidence of the utility and effectiveness of explanatory material embedded in computer-aid prompts, and (2) to explore the nature of the mechanisms underlying facilitation effects.

In pursuit of the first objective, pilot testing was used to produce a different version of the task modified to avoid the ceiling effects on performance encountered by Smith and Goodman and to reduce certain inconsistencies in information and presentation. For example, in the explanatory material used by Smith and Goodman, some statements presented a higher level concept which was instantiated in the following instruction. In others, a concept was introduced in the statement and then repeated in the instruction. Also inconsistent was the order of presentation of the explanatory material with explanation sometimes preceding the instruction and sometimes following it.

Such inconsistencies make it difficult to evaluate whether enhancement effects are related to processes such as preactivation in the form of repetition or instantiation, to context effects, or to mental model formation. Toward the second goal, the explanatory statements will be modified to minimize inconsistencies and to promote a better understanding of the cognitive processes responsible for facilitation effects.

The manipulation of two new variables in the current design was intended to contribute both to an understanding of the mechanisms underlying the effects of explanatory material and to an identification of stylistic features of the presentation mode which are important in producing the facilitating effect. The design included two sequential

orders of explanation in each of two conditions of integration. The statements were presented either before or after the instructions to help determine whether the enhancement depends upon preactivation or context effects. Preactivation and context explanations require that the information precede the instructions (Bransford and Johnson, 1972, 1973; Bransford and McCarrell, 1977). Furthermore, lower level preactivation processes would require that each priming concept be displayed immediately preceding its corresponding instruction, whereas a higher-level assimilation-into-context process could function also in a condition in which the explanatory material was given in a block of information prior to the set of instructions in a non-integrated fashion.

The manipulation of the integrated/non-integrated dimension and the type of information were designed to help clarify issues concerning the development of mental models. The quality of the mental model about the circuit acquired during the task was assessed in tests administered following task completion. If concretization is critical to model development, that quality should be superior in the integrated condition.

Method

Subjects

One hundred sixty undergraduates were tested individually, 20 in each of the 8 experimental conditions. An additional 80 subjects participated in the control condition, in which no explanatory material accompanied the assembly instructions. Only students who reported no prior formal or informal training in physics or electronics (other than high school science) were allowed to participate in the study. The total testing session required approximately an hour and 15 minutes, with a few subjects taking up to 2 hours to complete all tests.

Design

The experiment was comprised of two stages. In stage 1, subjects assembled a simple electrical circuit by following instructions displayed on an IBM PC. In stage 2, subjects completed five tests designed to assess their knowledge about the circuit they had constructed and their ability to apply the newly acquired knowledge to new, related tasks.

Three independent variables were manipulated in stage 1 in a 2 X 2 X 2 between-subjects factorial design. The first factor, sequential order, consisted of two levels with explanatory statements presented either before or after the instructions. The second factor, integration, involved the arrangement of the explanatory statements as either incorporated into the set of instructions as did Smith and Goodman (in press) or as a non-integrated block separate

from the instructions. The third factor, type of explanation, refers to the two kinds of information--structural or functional. The study also included a condition in which the instructions were presented without supplementary information. This condition served as a baseline control group.

Procedure

Twenty subjects were tested individually in each of the eight conditions as outlined in Figure 1. The procedures and circuit assembly task were modelled after those used by Smith and Goodman. To avoid ceiling effects encountered by Smith and Goodman, a slightly more complex circuit was used. Each subject assembled a circuit involving a battery, two double-throw switches, and two small light bulbs. Instructions and explanatory statements were displayed by an IBM PC.

Upon reading each statement, the subject pressed one of two keys to signal either readiness to continue or a request to return to a previous statement. The key press enabled times for the first reading to be recorded for each statement and resulted in a prompt which remained on the screen while the subject executed the instructed step. A second key press was required to request display of the next statement so that execution times for each step would be recorded. Reading and execution times are the main dependent variables by which performance on the

proceduralized task can be evaluated.

In the integrated conditions, explanatory statements were interspersed throughout the set of instructions (See Appendix A for instructions and explanatory statements.) In the before condition, explanations always preceded the relevant task instruction, and in the after condition, explanations always followed the relevant instruction. In the non-integrated conditions, all of the explanatory material was presented either before or after the entire set of instructions. The explanatory statements were written to enhance knowledge about the circuit in either of two ways. The structural material emphasized structural, organizational aspects of the circuit (e.g., labelling components and structural units), whereas the functional explanations stressed the way in which the circuit would operate. The structural statements, therefore, contained simpler content, while the functional statements provided information which was probably less familiar to the subjects.

Upon completion of the circuit assembly task, each subject tested the three major portions of the circuit to ensure that the circuit had been constructed correctly. Following the successful construction, the experimenter removed the assembled circuit and gave the subject an identical set of unassembled components for the subject to reconstruct the circuit from memory. Subjects were allowed a maximum of 30 minutes for this reconstruction.

After the reconstructed circuit was removed, each subject was asked to draw a diagram of the interconnections among the battery, the switches, and the lamps using different colors to represent different functional portions of the circuit (See Appendix B for all testing materials.) The diagram task was followed by a fault diagnosis test in which subjects were presented with eight diagrams of circuits intended to achieve the functions of the circuit they had constructed. Their task was to determine whether or not a fault existed, describe any faults, answer questions concerning the function of the faulty circuit, and correct any faults present. Next they were asked to design a new, slightly more complex circuit which would function in a prescribed fashion. Finally, they were to determine the effects of failure of each of two components in two circuits--one identical to the circuit they had assembled and one a modified version of that circuit.

Results

Cell Assembly Task

A 2 X 2 X 2 between-subjects analysis of variance was used to analyze each of 6 dependent measures, four of which were reading times and two of which were execution times. Analysis of total initial reading times for the instructions (Table 1) yielded no significant effects for any of the independent variables (Integration, Order, Type of Explanation). The analysis of total reading times including additional time spent rereading instructions (Table 2) also

demonstrated no significant differences among conditions.

Total times to read the explanatory statements were also analyzed with and without including rereading time. Total initial times to read explanations were significantly longer (Table 3) when the explanations preceded the instructions ($M = 249.60$ sec) than when they followed instructions ($M = 213.03$ sec), $F(1,152) = 5.52$, $p < .02$. As expected, the functional statements took significantly longer to read ($M = 258.06$ sec) than did the structural ($M = 204.57$ sec), $F(1,152) = 11.82$, $p < .001$. Analysis of total times to read explanations including rereading time (Table 4) showed the same significant main effects of order, $F(1,152) = 8.00$, $p < .006$, and of type of explanation, $F(1,152) = 8.81$, $p < .004$.

Although reading time reflects ease or difficulty of comprehension of the instructions, comprehensibility of the instructions should be reflected also in the time needed to execute commands. For example, in certain situations, an instruction might be read quickly with a particular understanding in mind, but the understanding may be in fact erroneous or inadequate and result in interference during execution. From this perspective, therefore, execution times might be considered as another estimate of comprehensibility of instructions. In the analyses of total execution times (Tables 5 and 6), with and without additional time to correct a faulty maneuver, no effects were significant, but the Integration by Order by Type of

Explanation interaction approached significance in both cases, $F(1,152) = 3.57$, $p < .06$ and $F(1,152) = 3.22$, $p < .07$, respectively. The pattern of data, similar for both dependent measures, suggested that explanatory material facilitated execution of commands only when the information was structural and presented in a block prior to the task, i.e., in the structural, non-integrated, before condition.

Variability in the data across subjects was fairly high. Whereas Smith and Goodman had included only women in their experiments, overall the present study included 103 men and 137 women; of most concern, the experimental conditions included 74 men and 86 women. If men and women differ in either aptitude or style of information processing on tasks such as circuit assembly, variability due to gender might mask other effects. In the literature on human cognitive processing, gender differences have been reported in verbal, spatial, and mathematical abilities, perceptual speed, motor skills, and context sensitivity (Hyde, 1985). Therefore, the current data were reanalyzed with gender as a subject variable, despite the presence of unequal numbers of men and women across conditions.

Main effects of gender were significant in the analyses of initial execution times, $F(1,144) = 5.44$, $p < .03$, and total execution times including re-execute time, $F(1,144) = 6.66$, $p < .01$. Men's first execution attempts were faster ($M = 668.41$ sec) than were women's ($M = 743.02$ sec), and men's total times to execute commands were faster ($M = 702.68$ sec)

than were women's ($M = 792.98$ sec).

Analyses of total times to read the explanations, with and without reread times included, again yielded significant main effects of order, $F(1,144) = 4.49$, $p < .04$, and $F(1,144) = 7.04$, $p < .01$, respectively, and of type of explanation, $F(1,144) = 8.65$, $p < .004$, and $F(1,144) = 6.61$, $p < .02$, respectively, but no significant effects due to gender.

While the analysis of initial times to read instructions showed no significant effects, total times to read instructions including rereading time differed significantly as a function of a gender by type of explanation interaction, $F(1,144) = 4.29$, $p < .04$. The pattern of data suggests that men spend more time reading instructions when functional information is present, whereas women spend more time reading instructions when structural information is added. The gender differences obtained in the experimental conditions are particularly interesting, because men and women did not differ significantly on any of the four dependent measures in the control condition (Table 7).

Knowledge About the Circuit

The knowledge and skills acquired during the circuit assembly task were assessed in several tests administered following successful construction of the circuit. Recall for the assembly procedure was tested by having subjects reconstruct the circuit from memory. Since not all subjects

were able to reconstruct the circuit correctly, a scoring system was devised to reflect accuracy of recall. Analysis of these scores (Table 8) indicated no significant effects of the independent variables on recall.

Memory was evaluated also in another format designed to reflect knowledge about the three major functional units of the circuit. In this test, the subject was asked to diagram the interconnections of each of the functional units in a different color. Performance was scored separately for each of the three units, and the three scores were summed to provide an overall measure (Table 9). Of the analyses of these four scores, only one provided a significant result. The Integration by Order interaction was significant in the analysis of scores representing accuracy of the diagram of the first portion of the circuit assembled, $F(1,152) = 5.51$, $p < .02$. The pattern of the data suggested that knowledge was better when explanations followed instructions, but only if they had been integrated into the set of instructions.

Performance on each of the eight fault diagnosis problems was summed to yield a composite fault diagnosis score (Table 10). Analysis of this performance measure demonstrated a significant main effect of type of explanation, $F(1,152) = 5.22$, $p < .03$, with scores for the structural condition higher ($M = 36.70$) than those for the functional condition ($M = 30.46$). One of the eight problems required knowledge that was not presented explicitly during the circuit assembly task. Therefore, the fault diagnosis

data were reanalyzed after removing that problem from the total score. Again, structural information was associated with significantly better performance ($\bar{M} = 32.74$) than was functional ($\bar{M} = 27.43$), $F(1,152) = 4.59$, $p < .04$. Also, scores were higher in conditions in which the explanations followed instructions ($\bar{M} = 32.63$) than in those in which they preceded instructions ($\bar{M} = 27.54$), $F(1,152) = 4.21$, $p < .05$.

A single score was derived to reflect performance on the task requiring subjects to design a new circuit (Table 11). Subjects who had received structural information during the assembly task scored significantly higher ($\bar{M} = 19.26$) than did subjects who had been given functional information ($\bar{M} = 16.94$), $F(1,152) = 4.69$, $p < .04$. Analysis of subjects' ability to predict the effects of failed connections in a circuit like the one they had assembled yielded no significant effects (Table 12).

As with the reading and execution times reported above, the test data were reanalyzed with gender as a subject factor. There were no significant differences between men and women on any of the nine dependent measures in the control condition (Table 13). However, gender differences emerged in almost all of the analyses performed on data from the experimental conditions.

Men reconstructed the circuit from memory significantly better ($\bar{M} = 13.14$) than did women ($\bar{M} = 10.67$), $F(1,144) = 8.50$, $p < .004$. Men also diagrammed the circuit more accurately ($\bar{M} = 21.64$) than did women ($\bar{M} = 18.83$), $F(1,144) = 4.08$, $p < .05$. Men's diagrams were better than women's for 2 of the 3 functional units, $F(1,144) = 4.10$, $p < .05$, and $F(1,144) = 6.44$, $p < .02$. As in the overall analysis reported above, an Integration by Order interaction, $F(1,144) = 4.76$, $p < .03$, suggested that knowledge about the first unit constructed was enhanced only when information was integrated into the instructional set and followed the relevant instruction.

In general, men performed significantly better on the fault diagnosis problems ($\bar{M} = 36.55$) than did women ($\bar{M} = 31.01$), $F(1,144) = 4.39$, $p < .04$. Structural information was somewhat more helpful ($\bar{M} = 36.70$) than was functional information ($\bar{M} = 30.45$), $F(1,144) = 6.16$, $p < .02$. However, these main effects must be considered in light of their interaction with Order and Integration, $F(1,144) = 7.56$, $p < .01$. This pattern of data (Table 14) suggests that women benefitted less from the addition of explanatory material than did the men. Women's performance was enhanced by explanations only when the information was structural and presented in a block prior to the task, i.e., in the structural, non-integrated, before condition. Men's performance was enhanced especially when information was integrated into the instructional set, except if the

information was functional and appeared before the relevant instruction. This pattern of data remained the same after the one problem requiring information not explicitly presented during the assembly task was removed from the overall scores.

A similar pattern of results emerged from the analysis of the scores on the circuit design task (Table 15). The Gender by Integration by Order by Type of Explanation interaction, $F(1,144) = 7.52$, $p < .01$, again suggested that additional information was useful to women in fewer conditions than was the case for men. Women performed best when information was not integrated into the instructional set, but was present as a block--before the instructions when it was structural and after the instructions when it was functional. Men performed best when the information was structural and integrated into the instructions. When the structural information was not integrated, it was better if it followed the task.

A significant four-way interaction was also present in the analysis of the scores (Table 16) on the task requiring an understanding of the effects of failure of different circuit connections, $F(1,144) = 12.29$, $p < .001$. These data suggest little or no positive influence of the explanatory material on this task. However, men's performance was again poor in the integrated, functional, before condition, while women's performance was again best in the non-integrated, structural, before condition.

Discussion

Circuit Assembly Task

Overall, the addition of explanatory material had no effect on the speed of reading the instructions in the circuit assembly task. However, the explanatory statements were read more quickly when they had followed the instructions than when they had preceded them, with functional explanations requiring more time than structural. This finding suggests that concrete experience can serve to provide a useful context within which to assimilate and comprehend more abstract, verbal content. These results imply a facilitation effect which is the reverse, or perhaps the complement of the hierarchical instantiation process described by Smith and Goodman (in press).

While the explanatory material had no significant effect on execution times, the interaction of type of explanation with order and integration approached significance. The pattern of the data suggested that any facilitation of execution due to explanatory material occurred when structural information was presented before the task in a non-integrated block. These data are consistent with the reading times cited above; again, concrete material was useful as a prior context. The presence of the effect in the non-integrated rather than in the integrated condition supports the notion that facilitation takes place at a level of processing which is

higher than that of simple repetition, priming, or lower level preactivation. Rather, it seems more likely that the effect is one of formation of an organizational framework (schema, context, or mental model) within which difficult new material can be understood and retained.

Knowledge About the Circuit

Immediate memory for the assembly task and for the structure of the circuit was not benefitted by the inclusion of explanatory material. The absence of such influence is not surprising, given the fact that the introduction of additional content increased the overall amount of information to be processed during the assembly task. Of greater theoretical as well as practical interest, therefore, are the effects of explanatory content on the tests which required the application of knowledge about the circuit to new types of problems. Performance on fault diagnosis problems was better when subjects had received structural information than when they had been given functional explanations. Also, fault diagnosis scores were higher when the explanations had followed than when they had preceded instructions.

Ability to design a new circuit was also better for subjects who had been exposed to the structural information than for those exposed to the functional. An important question is whether the subjects in the structural conditions solved the fault diagnosis and the new circuit

design problems by using different strategies than did the subjects in the functional conditions. Further research is needed to explore such issues relevant to the influence of explanatory material on mental model formation and problem solving styles.

Gender Differences

Analysis of the current data uncovered an issue important from both theoretical and applied perspectives. The literature on cognitive processing in fault diagnosis and human-computer interaction which is currently available (Yaworsky, 1984) has not addressed the question of possible gender differences in such situations. The finding of gender differences in the present study suggests a need for caution in generalizing results obtained with one gender to the other.

The gender differences obtained in this experiment are especially intriguing, because no gender differences were significant for any of the dependent variables in the control condition. The fact that men and women differed only when explanatory material enriched the instructional set suggests that (1) the task and tests were not biased in themselves in favor of men, at least with respect to the present sample, and (2) overall, men were able to make better use of the added information than were women. In the experimental conditions, men executed commands more quickly, reconstructed the circuit from memory and diagrammed its

functional subunits more accurately, and scored higher on the fault diagnosis problems than did women.

These main effects of gender must be interpreted with caution, however, in light of several significant interactions. One pattern emerging from the data suggested that men had difficulty when functional information preceded instructions in the integrated mode and that women benefitted from the enrichment in fewer conditions than did the men. Women seemed to benefit most when structural information was provided in a block prior to the task. Further research is needed to gain a clear understanding of the mechanisms underlying the gender differences. Also, with regard to practical guidelines for design of computer-aided systems, one cannot assume that conditions which will enhance women's performance will also necessarily enhance that of men.

References

- Bransford, J. D., and Johnson, M. K. (1972). Contextual prerequisites for understanding: Some investigations of comprehension and recall. Journal of Verbal Learning and Verbal Behavior, 11, 717-726.
- Bransford, J. S., and Johnson, M. K. (1973). Considerations of some problems of comprehension. In W. G. Chase (Ed.), Visual Information Processing (pp. 389-392). New York: Academic Press.
- Bransford, J. D., and McCarrell, N. S. (1977). A sketch of a cognitive approach to comprehension: Some thoughts about understanding what it means to comprehend. In P. N. Johnson-Laird and P. C. Wason (Eds.), Thinking: Readings in cognitive science (pp. 377-399). Cambridge: Cambridge University Press.
- Gunning, D. (1984). Integrated maintenance information system. Preliminary Draft, Air Force Human Resources Laboratory, Combat Logistics Branch.
- Hyde, J. S. (1985). Half the human experience. Lexington, MA: D.C. Heath and Company.
- Kieras, D. E., and Bovair, S. (1983). The role of a mental model in learning to operate a device (Technical Report No. 13 UARZ/DP/TR-83/ONR-13). University of Arizona, Department of Psychology.

Smillie, R. J. (1984). Implications of artificial intelligence for a user defined technical information system. In Artificial Intelligence in Maintenance: Proceedings of the Joint Services Workshop, Boulder, Colorado, pp. 353-358.

Smith, E. E., and Goodman, L. (in press). Understanding written instructions: The role of an explanatory schema. Cognition and Instruction.

Yaworsky, K. B. (1984). Cognitive factors in computer-aided fault diagnosis (AFOSR Report, Contract No. F49620-82-C-0035).

Integrated Mode

Type of Explanation

Order	Structural	Functional
Before	n=20	n=20
After	n=20	n=20

Non-Integrated Mode

Type of Explanation

Order	Structural	Functional
Before	n=20	n=20
After	n=20	n=20

Control Condition

n=80

Figure 1. Experimental Design.

Table 1

Mean Total Initial Reading Times for Instructions

Order	Display Mode				Control Mean
	Integrated		Non-Integrated		
	<u>Type of Explanation</u>		<u>Type of Explanation</u>		
	Structural	Functional	Structural	Functional	
Before	384.35	416.74	451.31	432.75	392.32
After	406.50	407.55	426.09	382.11	
Mean	395.43	412.15	438.70	407.43	

Note. Times are reported in seconds.

N = 240.

Table 2

Mean Total Reading Times For Instructions

Order	Display Mode					Control Mean
	Integrated		Non-Integrated			
	<u>Type of Explanation</u>		<u>Type of Explanation</u>			
	Structural	Functional	Structural	Functional		
Before	434.23	456.14	497.33	492.98	432.48	
After	453.55	449.41	460.98	428.73		
Mean	443.89	452.78	479.16	460.86		

Note. Times are reported in seconds.

N = 240.

Table 3

Mean Total Initial Reading Times For Explanations

Order	Display Mode			
	Integrated		Non-Integrated	
	<u>Type of Explanation</u>		<u>Type of Explanation</u>	
	Structural	Functional	Structural	Functional
Before	224.08	259.86	215.36	299.07
After	188.46	257.21	190.35	216.09
Mean	206.27	258.54	202.86	257.58

Note. Times are reported in seconds.

N = 240.

Table 4

Mean Total Reading Times For Explanations

Order	Display Mode			
	Integrated		Non-Integrated	
	<u>Type of Explanation</u>		<u>Type of Explanation</u>	
	Structural	Functional	Structural	Functional
Before	233.67	272.62	246.84	317.22
After	192.73	267.60	196.59	217.73
Mean	213.20	270.11	221.72	267.48

Note. Times are reported in seconds.

N = 240.

Table 5

Mean Total Initial Execution Times

	Display Mode				
	Integrated		Non-Integrated		
Order	<u>Type of Explanation</u>		<u>Type of Explanation</u>		Control
	Structural	Functional	Structural	Functional	Mean
Before	724.24	704.42	648.68	768.73	716.14
After	671.08	723.22	724.98	702.74	
Mean	697.66	713.82	686.83	735.74	

Note. Times are reported in seconds.

N = 240.

Table 6

Mean Total Execution Times

Order	Display Mode				Control Mean
	Integrated		Non-Integrated		
	<u>Type of Explanation</u>		<u>Type of Explanation</u>		
	Structural	Functional	Structural	Functional	
Before	765.94	732.31	687.59	797.90	761.84
After	724.78	787.23	768.44	745.54	
Mean	745.36	759.77	728.02	771.72	

Table 7

Mean Reading and Execution Times For Men and Women in
the Control Group

	Men	Women
Execution Times		
Initial	705.23	717.68
Total	758.80	760.94
Reading Times		
Initial Instruction	401.54	379.48
Total Instruction	442.85	417.91

Note. Times are reported in seconds.

N = 58.

Table 8

Mean Scores on the Reconstruction Task

Order	Display Mode			
	Integrated		Non-Integrated	
	<u>Type of Explanation</u>		<u>Type of Explanation</u>	
	Structural	Functional	Structural	Functional
Before	11.95	10.65	12.20	10.75
After	13.95	10.75	12.25	12.00

Note. Total possible score = 18.

Table 9

Mean Scores on the Circuit Diagram

Order	Display Mode			
	Integrated		Non-Integrated	
	<u>Type of Explanation</u>		<u>Type of Explanation</u>	
	Structural	Functional	Structural	Functional
Total				
Before	20.50	17.35	20.30	18.55
After	22.40	20.85	21.45	19.60
Part A				
Before	6.40	5.00	6.70	6.90
After	7.60	7.10	6.55	6.75
Part B				
Before	6.15	4.65	5.60	5.35
After	6.45	6.00	6.10	5.40
Part C				
Before	7.95	7.70	8.00	6.30
After	8.70	8.10	8.80	7.45

Note. Total possible scores were 9 for Part A, 9 for Part B,
18 for Part C, and 36 for the total.

Table 10

Mean Scores on the Fault Diagnosis Task

Order	Display Mode			
	Integrated		Non-Integrated	
	<u>Type of Explanation</u>		<u>Type of Explanation</u>	
	Structural	Functional	Structural	Functional
Before	38.00	27.15	33.05	27.45
After	38.70	34.80	37.05	32.40

Note. Total possible score = 80.

Table 11

Mean Scores on the Circuit Design Task

Order	Display Mode			
	Integrated		Non-Integrated	
	<u>Type of Explanation</u>		<u>Type of Explanation</u>	
	Structural	Functional	Structural	Functional
Before	19.55	15.30	18.75	15.50
After	20.10	17.65	18.65	19.30

Note. Total possible score = 26.

Table 12

Mean Scores on the Test of Failed Connections

Order	Display Mode			
	Integrated		Non-Integrated	
	<u>Type of Explanation</u>		<u>Type of Explanation</u>	
	Structural	Functional	Structural	Functional
Before	13.65	11.90	13.25	12.80
After	13.40	13.45	13.05	13.55

Note. Total possible score = 16.

Table 13

Mean Test Scores For Men and Women in the Control Group

<u>Test</u>	<u>Men</u>	<u>Women</u>
Reconstruction	11.10	11.55
Diagram, Total	21.31	21.24
Diagram, Part A	6.69	6.62
Diagram, Part B	5.62	5.93
Diagram, Part C	9.00	8.69
Fault Diagnosis	36.03	32.55
Circuit Design	17.93	17.45
Failed Connections	14.45	13.52

Note. N = 58, including 29 men and 29 women.

Table 14

Mean Scores on the Fault Diagnosis Task For Men and Women

Gender	Order	Display Mode			
		Integrated		Non-Integrated	
		<u>Type of Explanation</u>		<u>Type of Explanation</u>	
		Structural	Functional	Structural	Functional
Men	Before	46.13	26.30	30.29	34.50
	After	45.88	44.22	43.78	28.30
Women	Before	32.58	28.00	39.50	24.43
	After	33.92	27.09	31.55	36.50

Note. N = 160, including 74 men and 86 women.

Table 15

Mean Scores on the Circuit Design Task For Men and Women

Gender	Order	Display Mode			
		Integrated		Non-Integrated	
		<u>Type of Explanation</u>		<u>Type of Explanation</u>	
		Structural	Functional	Structural	Functional
Men	Before	21.88	14.70	17.64	19.67
	After	23.38	19.00	22.67	17.10
Women	Before	18.00	15.90	21.33	13.71
	After	17.92	16.55	15.36	21.50

Note. N = 160, including 74 men and 86 women.

Table 16

Mean Scores on the Test of Failed Connections For Men and Women

Gender	Order	Display Mode			
		Integrated		Non-Integrated	
		<u>Type of Explanation</u>		<u>Type of Explanation</u>	
		Structural	Functional	Structural	Functional
Men	Before	15.38	11.30	12.71	14.50
	After	13.63	14.33	14.44	12.70
Women	Before	12.50	12.50	14.50	12.07
	After	13.25	12.73	11.91	14.40

Note. N = 160, including 74 men and 86 women.

APPENDIX A

CONTENTS:

- A1 INSTRUCTIONS
- A2 TEXT FOR THE INTEGRATED BEFORE STRUCTURAL CONDITION
- A3 TEXT FOR THE INTEGRATED AFTER STRUCTURAL CONDITION
- A4 TEXT FOR THE NON-INTEGRATED BEFORE STRUCTURAL CONDITION
- A5 TEXT FOR THE NON-INTEGRATED AFTER STRUCTURAL CONDITION
- A6 TEXT FOR THE INTEGRATED BEFORE FUNCTIONAL CONDITION
- A7 TEXT FOR THE INTEGRATED AFTER FUNCTIONAL CONDITION
- A8 TEXT FOR THE NON-INTEGRATED BEFORE FUNCTIONAL CONDITION
- A9 TEXT FOR THE NON-INTEGRATED AFTER FUNCTIONAL CONDITION

APPENDIX A1

1. Select the single throw switch, that is the switch with contacts on only one side. This will be called switch A.

2. Select a wire with a forked pin on one end and an alligator clip on the other.

3. Keep switch A in the open position, that is with the handle up.

4. Position switch A so that the two metal contacts are on the side of the base farther away from you.

5. With the screwdriver, loosen, but do not remove, the upper left screw.

6. Insert the forked end of the wire under the screw and tighten the screw.

7. Connect the alligator clip on the other end of the wire to the left terminal of lamp A.

8. Select a wire with one forked pin and one circular pin.

9. With the screwdriver, loosen, but do not remove, the lower left screw.

10. Insert the forked pin under the screw and tighten the screw.

11. Select a wire with one alligator clip and one circular pin.

12. Connect the alligator clip to the right terminal of lamp A.

13. Position the second switch below switch A such that the handle may be pulled toward you or pushed away from you. The second switch will be called switch B.

14. Remember to keep the handle in the upright position.

15. Select a wire with one forked pin and one alligator clip.

16. With the screwdriver, loosen, but do not remove, the lowermost left screw.

17. Insert the forked pin under the screw and tighten the screw.

18. Connect the alligator clip to the left terminal of lamp B.

19. Select a wire with one forked pin and one circular pin.

20. With the screwdriver, loosen, but do not remove, the center left screw.

21. Insert the forked pin under the screw and tighten the screw.

22. Select a wire with one alligator clip and one circular pin.

- *****
23. Connect the alligator clip to the right terminal of lamp B.
- *****
24. Select a wire with one alligator clip and one forked pin.
- *****
25. With the screwdriver, loosen, but do not remove, the uppermost left screw on switch B.
- *****
26. Insert the forked pin under the screw, and tighten the screw.
- *****
27. Connect the alligator clip to the left terminal of lamp A.
- *****
28. Select a wire with one forked pin and one alligator clip.
- *****
29. With the screwdriver, loosen, but do not remove, the uppermost right screw.
- *****
30. Insert the forked pin under the screw and tighten the screw.
- *****
31. Connect the alligator pin to the left terminal of lamp B.
- *****
32. With the screwdriver, loosen, but do not remove, the center right screw.
- *****
33. Insert the forked pin of the remaining wire under the screw and tighten the screw.
- *****
34. Thread the wire underneath the switch from the lower right corner to the upper left corner.
- *****
35. Unscrew and remove the two black safety caps from the battery terminals. Keep the caps handy.
- *****
36. Above the circuit, place the battery on its side with the terminals of the battery facing you and the positive (+) terminal on your left.
- *****
37. Locate the three wires which have one of their ends connected to a switch and the other end unattached.
- *****
38. Slip the circular pins of these three wires onto the positive terminal of the battery and screw one of the two black safety caps onto the terminal to anchor the wires.
- *****
39. Connect the two remaining unattached circular pins to the negative (-) terminal of the battery by using the remaining black safety cap.
- *****
40. Push the handle of switch A forward (i.e., in its closed position) to light lamp A.
- *****
41. Place the handle of switch A back in its upright (i.e., open) position.
- *****
42. Pull the handle of switch B toward you to light lamp B.
- *****
43. Push the handle of switch B all the way forward to light both lamps A and B.

44. Return the handle of switch B to its open position.

APPENDIX A2
INTEGRATED (BEFORE)

STRUCTURAL

- * You will construct an electrical circuit that will allow you to light one or two small lamps.
- ** You will build the circuit using the materials you see to the side of the computer.
- A. Assembling a circuit requires that you get the major components ready, then connect them.
- B. This circuit involves three major types of components: (1) a battery, (2) two switches, and (3) two small lamps.
- C. There are 3 main parts to the circuit: (1) a circuit to light lamp A, (2) a circuit to light lamp B, and (3) a circuit to light both lamps with a single switch.
- D. First you will construct the circuit for lamp A.
- E. The lamp A circuit includes the battery, a switch, and lamp A.
- F. First you will make a wire connection from the switch to lamp A.

Instructions 1-7

- G. The switch must be connected to the battery, but all final connections to the battery are made last.
- H. So, now you will attach a wire to the switch, but leave the battery side unattached.

Instructions 8-10

- I. Similarly, the lamp must be connected to the battery, but first you will make only the lamp side of the connection.

Instructions 11-12

- J. Now you will construct the circuit for lamp B.
- K. The lamp B circuit includes the battery, a switch, and lamp B.
- L. First you will make a wire connection from the switch to lamp B.

Instructions 13-18

- M. Now you will attach a wire to the switch to make the switch side of the switch-to-battery connection.

Instructions 19-21

- N. Now you will make the lamp side of the lamp-to-battery connection.

Instructions 22-23

- O. You will wire a circuit so that both lamps A and B can be turned on with a single throw of the switch.
- P. The circuit for both lamps A and B involves the battery, the upper half of switch B, and the two lamps.
- Q. First, you will make a wire connection from the left side of the upper half of switch B to lamp A.

Instructions 24-27

- R. In a similar way, you will make a wire connection from the right side of the upper half of switch B to lamp B.

Instructions 28-31

- S. The right side of the upper half of switch B must be connected to the battery.
- T. At this time, you will make only the switch side of the switch-to-battery connection.

Instructions 32-34

- U. Now you are ready to make the connections to the battery.

Instructions 35-36

- V. First you will connect the wires which are attached to the switches.

Instructions 37-38

- W. Now the wires which are attached to the lamps are connected.

Instruction 39

*** With all connections complete, you will test each portion of the circuit.

- X. First you will test the circuit to light lamp A.

Instructions 40-41

- Y. Now you will test the circuit to light lamp B.

Instruction 42

- Z. Now you will test the circuit to light both lamps A and B.

Instructions 43-44

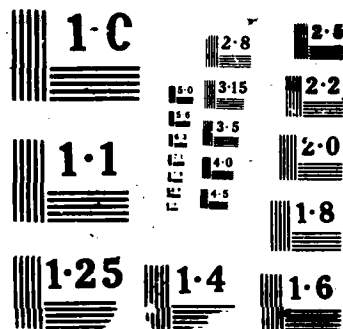
05/10

UNCLASSIFIED

MAY 86 AFOSR-TR-87-1722 FF9620-82-C-0035

F/G 7/2

ML



APPENDIX A3
INTEGRATED (AFTER)

STRUCTURAL

- * You will construct an electrical circuit that will allow you to light one or two small lamps.
- ** You will build the circuit using the materials you see to the side of the computer.

Instructions 1-7

- A. Assembling a circuit requires that you get the major components ready, then connect them.
- B. This circuit involves three major types of components: (1) a battery, (2) two switches, and (3) two small lamps.
- C. There are 3 main parts to the circuit: (1) a circuit to light lamp A, (2) a circuit to light lamp B, and (3) a circuit to light both lamps with a single switch.
- D. You have begun construction of the circuit for lamp A.
- E. The lamp A circuit includes the battery, a switch, and lamp A.
- F. You have made a wire connection from the switch to lamp A.

Instructions 8-10

- G. The switch must be connected to the battery, but all final connections to the battery are made last.
- H. So, you have attached a wire to the switch, but have left the battery side unattached.

Instructions 11-12

- I. Similarly, the lamp must be connected to the battery, but you have made only the lamp side of the connection for now.

Instructions 13-18

- J. You have begun construction of the circuit for lamp B.
- K. The lamp B circuit includes the battery, a switch, and lamp B.
- L. You have made a wire connection from the switch to lamp B.

Instructions 19-21

- M. You have attached a wire to the switch to make the switch side of the switch-to-battery connection.

Instructions 22-23

- N. Now you have made the lamp side of the lamp-to-battery connection.

INTEGRATED (AFTER) CONTINUED

STRUCTURAL

Instructions 24-27

- O. You have begun to wire a circuit so that both lamps A and B can be turned on with a single throw of the switch.
- P. The circuit for both lamps A and B involves the battery, the upper half of switch B, and the two lamps.
- Q. You have made a wire connection from the left side of the upper half of switch B to lamp A.

Instructions 28-31

- R. In a similar way, you have made a wire connection from the right side of the upper half of switch B to lamp B.

Instructions 32-34

- S. The right side of the upper half of switch B must be connected to the battery.
- T. At this time, you have made only the switch side of the switch-to-battery connection.

Instructions 35-36

- U. Now you are ready to make the connections to the battery.

Instructions 37-38

- V. You have connected the wires which are attached to the switches.

Instruction 39

- W. You have connected the wires which are attached to the lamps.

***With all connections complete, you will test each portion of the circuit.

Instructions 40-41

- X. You have tested the circuit to light lamp A.

Instruction 42

- Y. You have tested the circuit to light lamp B.

Instructions 43-44

- Z. You have tested the circuit to light both lamps A and B.

APPENDIX A4
NON-INTEGRATED (BEFORE)

STRUCTURAL

- * You will construct an electrical circuit that will allow you to light one or two small lamps.
- ** You will build the circuit using the materials you see to the side of the computer.
- A. Assembling a circuit requires that you get the major components ready, then connect them.
- B. This circuit involves three major types of components: (1) a battery, (2) two switches, and (3) two small lamps.
- C. There are 3 main parts to the circuit: (1) a circuit to light lamp A, (2) a circuit to light lamp B, and (3) a circuit to light both lamps with a single switch.
- D. First you will construct the circuit for lamp A.
- E. The lamp A circuit includes the battery, a switch, and lamp A.
- F. First you will make a wire connection from the switch to lamp A.
- G. The switch must be connected to the battery, but all final connections to the battery are made last.
- H. So, you will attach a wire to the switch, but leave the battery side unattached until the end.
- I. Similarly, the lamp must be connected to the battery, but first you will make only the lamp side of the connection.
- J. Then you will construct the circuit for lamp B.
- K. The lamp B circuit includes the battery, a switch, and lamp B.
- L. First you will make a wire connection from the switch to lamp B.
- M. Then you will attach a wire to the switch to make the switch side of the switch-to-battery connection.
- N. Next you will make the lamp side of the lamp-to-battery connection.
- O. Then you will wire a circuit so that both lamps A and B can be turned on with a single throw of the switch.
- P. The circuit for both lamps A and B involves the battery, the upper half of switch B, and the two lamps.
- Q. First, you will make a wire connection from the left side of the upper half of switch B to lamp A.

STRUCTURAL

- R. In a similar way, you will make a wire connection from the right side of the upper half of switch B to lamp B.
- S. The right side of the upper half of switch B must be connected to the battery.
- T. First you will make only the switch side of the switch-to-battery connection.
- U. Then you will be ready to make the connections to the battery.
- V. First you will connect the wires which are attached to the switches.
- W. Then the wires which are attached to the lamps will be connected.
- ***With all connections complete, you will test each portion of the circuit.
- X. First you will test the circuit to light lamp A.
- Y. Then you will test the circuit to light lamp B.
- Z. Finally, you will test the circuit to light both lamps A and B.

Instructions 1-44

APPENDIX A5
NON-INTEGRATED (AFTER)

STRUCTURAL

- * You will construct an electrical circuit that will allow you to light one or two small lamps.
- ** You will build the circuit using the materials you see to the side of the computer.

Instructions 1-44

- A. Assembling a circuit requires that you get the major components ready, then connect them.
- B. This circuit involves three major types of components: (1) a battery, (2) two switches, and (3) two small lamps.
- C. There are 3 main parts to the circuit: (1) a circuit to light lamp A, (2) a circuit to light lamp B, and (3) a circuit to light both lamps with a single switch.
- D. First you constructed the circuit for lamp A.
- E. The lamp A circuit includes the battery, a switch, and lamp A.
- F. You began the lamp A circuit by making a wire connection from the switch to lamp A.
- G. The switch had to be connected to the battery, but all final connections to the battery were made last.
- H. So, you attached a wire to the switch, but left the battery side unattached until the end.
- I. Similarly, the lamp had to be connected to the battery, but first you made only the lamp side of the connection.
- J. Then you constructed the circuit for lamp B.
- K. The lamp B circuit includes the battery, a switch, and lamp B.
- L. You began the lamp B circuit by making a wire connection from the switch to lamp B.
- M. You attached a wire to the switch to make the switch side of the switch-to-battery connection.
- N. Next you made the lamp side of the lamp-to-battery connection.
- O. Then you wired a circuit so that both lamps A and B can be turned on with a single throw of the switch.
- P. The circuit for both lamps A and B involves the battery, the upper half of switch B, and the two lamps.

NON-INTEGRATED (AFTER)

STRUCTURAL

- Q. First you made a wire connection from the left side of the upper half of switch B to lamp A.
- R. In a similar way, you made a wire connection from the right side of the upper half of switch B to lamp B.
- S. The right side of the upper half of switch B had to be connected to the battery.
- T. First you made only the switch side of the switch-to-battery connection.
- U. Then you were ready to make the connections to the battery.
- V. First you connected the wires which are attached to the switches.
- W. Then the wires which are attached to the lamps were connected.
- ***With all connections complete, you tested each portion of the circuit.
- X. First you tested the circuit to light lamp A.
- Y. Then you tested the circuit to light lamp B.
- Z. Finally, you tested the circuit to light both lamps A and B.

APPENDIX A6
INTEGRATED (BEFORE)

FUNCTIONAL

- * You will construct an electrical circuit that will allow you to light one or two small lamps.
- ** You will build the circuit using the materials you see to the side of the computer.
- A. In a circuit, electrical current flows from a source to a "consumer" (that is, to something that requires current, like a lamp).
- B. Current can flow only when the circuit's components are interconnected in a complete circle, each connection being made by a wire or other metal object that conducts electricity.
- C. In this circuit, a battery will be the source of the current, lamps will be the consumers, and switches will form connections allowing current to flow when they are closed, that is, in the ON position.
- D. First you will construct a circuit which will allow lamp A to light when a switch is closed.
- E. When the switch is closed, current will flow from the battery to lamp A and then return to the battery.
- F. Current will flow through the switch when it is closed, because closure connects the two metal contacts on the left side of the switch.

Instructions 1-7

- G. For safety, connections to the battery, the source of current, are made last.
- H. But you can now attach a wire to the switch which will bring current to the switch when it is later connected to the battery.

Instructions 8-10

- I. Similarly, to allow current to return to the source, you must connect the lamp to the battery, but leave the battery side unattached for now.

Instructions 11-12

- J. Now you will construct a circuit which will allow lamp B to light when a second switch is closed.
- K. When the switch is closed, current will flow from the battery to lamp B.
- L. Current will flow through the switch when it is closed, because closure will connect the two metal contacts on the left side of the switch.

Instructions 13-18.

INTEGRATED (BEFORE)

FUNCTIONAL p 2.

- M. Now you will attach a wire to the switch which will bring current to the switch when it is later connected to the battery.

Instructions 19-21

- N. To allow current to return to the source you must connect the lamp to the battery, but leave the battery side unattached for now.

Instructions 22-23

- O. You will wire a circuit so that current can flow through both lamps A and B when the upper half of switch B is closed.
- P. When the upper half of switch B is closed, current will flow from the battery, through each lamp, and back to the battery.
- Q. The current for lamp A will flow through the metal contacts on the left side of the upper half of switch B.

Instructions 24-27

- R. The current for lamp B will flow through the two metal contacts on the right side of the upper half of switch B.

Instructions 28-31

- S. The current for lamp B must come from the battery to the right side of the upper half of switch B.
- T. At this time you will attach the wire through which current will flow to switch B, but leave the battery side unattached for now.

Instructions 32-34

- U. Now you are ready to make the connections to the battery.

Instructions 35-36

- V. First you will connect the wires which will carry current to the switches.

Instructions 37-38

- W. Now the wires through which current will return to the battery are connected.

Instruction 39

*** With all connections complete, you will test each portion of the circuit.

- X. First you will determine whether current flows to light lamp A.

Instructions 40-41

- Y. Now you will determine whether current flows to light lamp B.

Instruction 42

INTEGRATED (BEFORE)

FUNCTIONAL p 3.

2. Now you will determine whether current flows to light both lamps A and B.

Instructions 43-44

APPENDIX A7
INTEGRATED (AFTER)

FUNCTIONAL

- * You will construct an electrical circuit that will allow you to light one or two small lamps.
- ** You will build the circuit using the materials you see to the side of the computer.

Instructions 1-7

- A. In a circuit, electrical current flows from a source to a "consumer" (that is, to something that requires current, like a lamp).
- B. Current can flow only when the circuit's components are interconnected in a complete circle, each connection being made by a wire or other metal object that conducts electricity.
- C. In this circuit, a battery will be the source of the current, lamps will be the consumers, and switches will form connections allowing current to flow when they are closed, that is, in the ON position.
- D. You have begun construction of a circuit which will allow lamp A to light when a switch is closed.
- E. When the switch is closed, current will flow from the battery to lamp A and then return to the battery.
- F. Current will flow through the switch when it is closed, because closure connects the two metal contacts on the left side of the switch.

Instructions 8-10

- G. For safety, connections to the battery, the source of current, are made last.
- H. You have attached a wire to the switch which will bring current to the switch when it is later connected to the battery.

Instructions 11-12

- I. Similarly, to allow current to return to the source, the lamp must be connected to the battery, but you have left the battery side unattached for now.

Instructions 13-18

- J. You have begun construction of a circuit which will allow lamp B to light when a second switch is closed.
- K. When the switch is closed, current will flow from the battery to lamp B.
- L. Current will flow through the switch when it is closed, because closure will connect the two metal contacts on the left side of the switch.

Instructions 19-21

FUNCTIONAL

- M. You have attached a wire to the switch which will bring current to the switch when it is later connected to the battery.

Instructions 22-23

- N. To allow current to return to the source you must connect the lamp to the battery, but you have left the battery side unattached for now.

Instructions 24-27

- O. You have begun to wire a circuit so that current can flow through both lamps A and B when the upper half of switch B is closed.
- P. When the upper half of switch B is closed, current will flow from the battery, through each lamp, and back to the battery.
- Q. The current for lamp A will flow through the metal contacts on the left side of the upper half of switch B.

Instructions 28-31

- R. The current for lamp B will flow through the two metal contacts on the right side of the upper half of switch B.

Instructions 32-34

- S. The current for lamp B must come from the battery to the right side of the upper half of switch B.
- T. You have attached the wire through which current will flow to switch B, but you have left the battery side unattached for now.

Instructions 35-36

- U. Now you are ready to make the connections to the battery.

Instructions 37-38

- V. You have connected the wires which will carry current to the switches.

Instruction 39

- W. You have connected the wires through which current will return to the battery.

***With all connections complete, you will test each portion of the circuit.

Instructions 40-41

- X. You have determined whether current flows to light lamp A.

Instruction 42

- Y. You have determined whether current flows to light lamp B.

INTEGRATED (AFTER) CONTINUED

FUNCTIONAL

Instructions 43-44

2. You have determined whether current flows to light both lamps A and B.

APPENDIX A8
NON-INTEGRATED (BEFORE)

FUNCTIONAL

- * You will construct an electrical circuit that will allow you to light one or two small lamps.
- ** You will build the circuit using the materials you see to the side of the computer.
- A. In a circuit, electrical current flows from a source to a "consumer" (that is, to something that requires current, like a lamp).
- B. Current can flow only when the circuit's components are interconnected in a complete circle, each connection being made by a wire or other metal object that conducts electricity.
- C. In this circuit, a battery will be the source of the current, lamps will be the consumers, and switches will form connections allowing current to flow when they are closed, that is, in the ON position.
- D. First you will construct a circuit which will allow lamp A to light when a switch is closed.
- E. When the switch is closed, current will flow from the battery to lamp A and then return to the battery.
- F. Current will flow through the switch when it is closed, because closure connects the two metal contacts on the left side of the switch.
- G. For safety, connections to the battery, the source of current, are made last.
- H. But you will be able to attach a wire to the switch which will bring current to the switch when it is later connected to the battery.
- I. Similarly, to allow current to return to the source, you must connect the lamp to the battery, but you will leave the battery side unattached until the end.
- J. Then you will construct a circuit which will allow lamp B to light when a second switch is closed.
- K. When the switch is closed, current will flow from the battery to lamp B.
- L. Current will flow through the switch when it is closed, because closure will connect the two metal contacts on the left side of the switch.
- M. You will attach a wire to the switch which will bring current to the switch when it is later connected to the battery.
- N. To allow current to return to the source you must connect the lamp to the battery, but you will leave the battery side unattached until the end.
- O. Then you will wire a circuit so that current can flow through both lamps A and B when the upper half of switch B is closed.

NON-INTEGRATED (BEFORE)

FUNCTIONAL

- P. When the upper half of switch B is closed, current will flow from the battery, through each lamp, and back to the battery.
- Q. The current for lamp A will flow through the metal contacts on the left side of the upper half of switch B.
- R. The current for lamp B will flow through the two metal contacts on the right side of the upper half of switch B.
- S. The current for lamp B will come from the battery to the right side of the upper half of switch B.
- T. You will attach the wire through which current will flow to switch B, but leave the battery side unattached until the end.
- U. Then you will be ready to make the connections to the battery.
- V. First you will connect the wires which will carry current to the switches.
- W. Then the wires through which current will return to the battery will be connected.
- ***With all connections complete, you will test each portion of the circuit.
- X. First you will determine whether current flows to light lamp A.
- Y. Then you will determine whether current flows to light lamp B.
- Z. Finally, you will determine whether current flows to light both lamps A and B.

Instructions 1-44

APPENDIX A9
NON-INTEGRATED (AFTER)

FUNCTIONAL

- * You will construct an electrical circuit that will allow you to light one or two small lamps.
- ** You will build the circuit using the materials you see to the side of the computer.

Instructions 1-44

- A. In a circuit, electrical current flows from a source to a "consumer" (that is, to something that requires current, like a lamp).
- B. Current can flow only when the circuit's components are interconnected in a complete circle, each connection being made by a wire or other metal object that conducts electricity.
- C. In this circuit, the battery is the source of the current, the lamps are the consumers, and the switches form connections allowing current to flow when they are closed, that is, in the ON position.
- D. First you constructed a circuit which allows lamp A to light when a switch is closed.
- E. When the switch is closed, current flows from the battery to lamp A and then returns to the battery.
- F. Current flows through the switch when it is closed, because closure connects the two metal contacts on the left side of the switch.
- G. For safety, connections to the battery, the source of current, were made last.
- H. But you were able to attach a wire to the switch which would bring current to the switch when it was later connected to the battery.
- I. Similarly, to allow current to return to the source, you had to connect the lamp to the battery, but you left the battery side unattached until the end.
- J. Then you constructed a circuit which allows lamp B to light when a second switch is closed.
- K. When the switch is closed, current flows from the battery to lamp B.
- L. Current flows through the switch when it is closed, because closure connects the two metal contacts on the left side of the switch.
- M. You attached a wire to the switch which would bring current to the switch when it was later connected to the battery.
- N. To allow current to return to the source you had to connect the lamp to the battery, but you left the battery side unattached until the end.

NON-INTEGRATED (AFTER)

FUNCTIONAL

- O. Then you wired a circuit so that current can flow through both lamps A and B when the upper half of switch B is closed.
 - P. When the upper half of switch B is closed, current flows from the battery, through each lamp, and back to the battery.
 - Q. The current for lamp A flows through the metal contacts on the left side of the upper half of switch B.
 - R. The current for lamp B flows through the two metal contacts on the right side of the upper half of switch B.
 - S. The current for lamp B comes from the battery to the right side of the upper half of switch B.
 - T. You attached the wire through which current will flow to switch B, but you left the battery side unattached until the end.
 - U. Then you were ready to make the connections to the battery.
 - V. First you connected the wires which carry current to the switches.
 - W. Then the wires through which current returns to the battery were connected.
- ***With all connections complete, you tested each portion of the circuit.
- X. First you determined whether current flows to light lamp A.
 - Y. Then you determined whether current flows to light lamp B.
 - Z. Finally, you determined whether current flows to light both lamps A and B.

APPENDIX B

CONTENTS:

- B1 CIRCUIT DIAGRAM TASK
- B2 FAULT DIAGNOSIS PROBLEMS
- B3 CIRCUIT DESIGN TASK
- B4 FAILED CONNECTIONS PROBLEMS

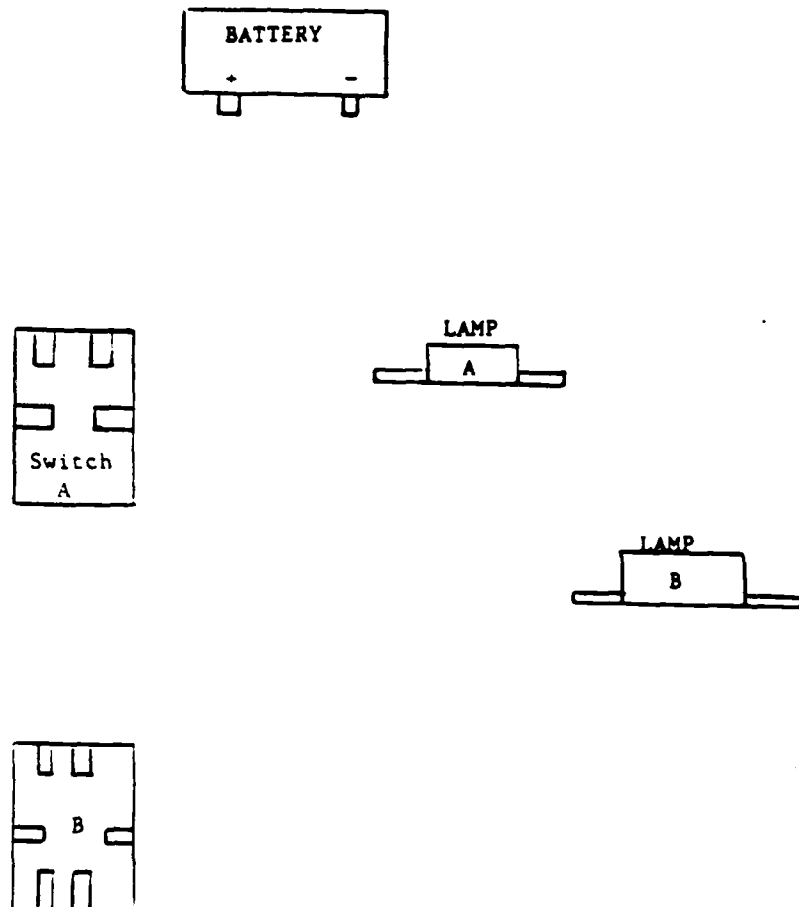
APPENDIX B1

In RED, draw the connections which enable Lamp A to light when switch A is ON.

In BLUE, draw the connections which enable Lamp B to light when switch B is ON in the lower position.

In GREEN, draw the connections which enable both Lamps A & B to light when switch B is ON in the upper position.

If any connection services more than one circuit, indicate service to the second circuit by superimposing dots of the relevant color along the original connection.



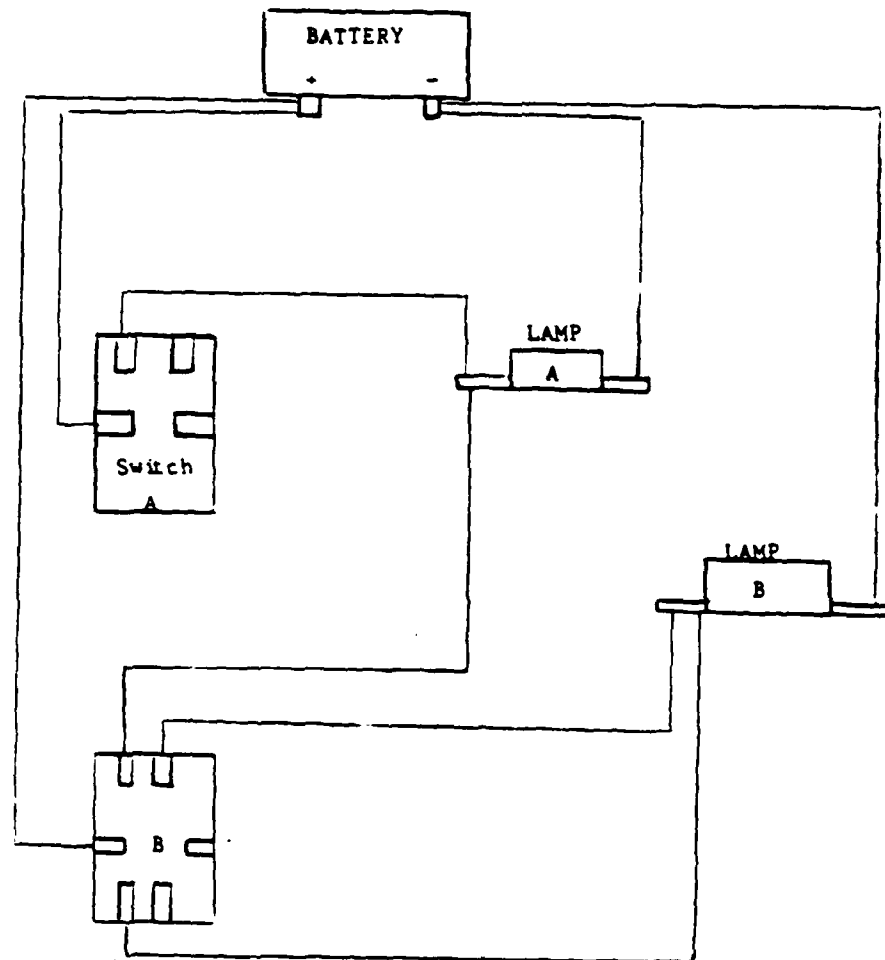
APPENDIX B2

You will be presented with a series of diagrams of circuits intended to achieve the functions of the circuit you have constructed with instructions from the computer. Study each diagram to determine whether or not a fault, that is, an error, exists in the circuit. If a fault is present, (1) describe it briefly in the space provided; (2) answer the questions concerning the function of the circuit by writing in YES or NO. The questions pertain to the circuit as it is diagrammed, that is, with any fault that may be present; (3) correct the diagram by adding any missing connections and/or placing an X over any connection which should not be present.

Describe Fault (if any):

C1

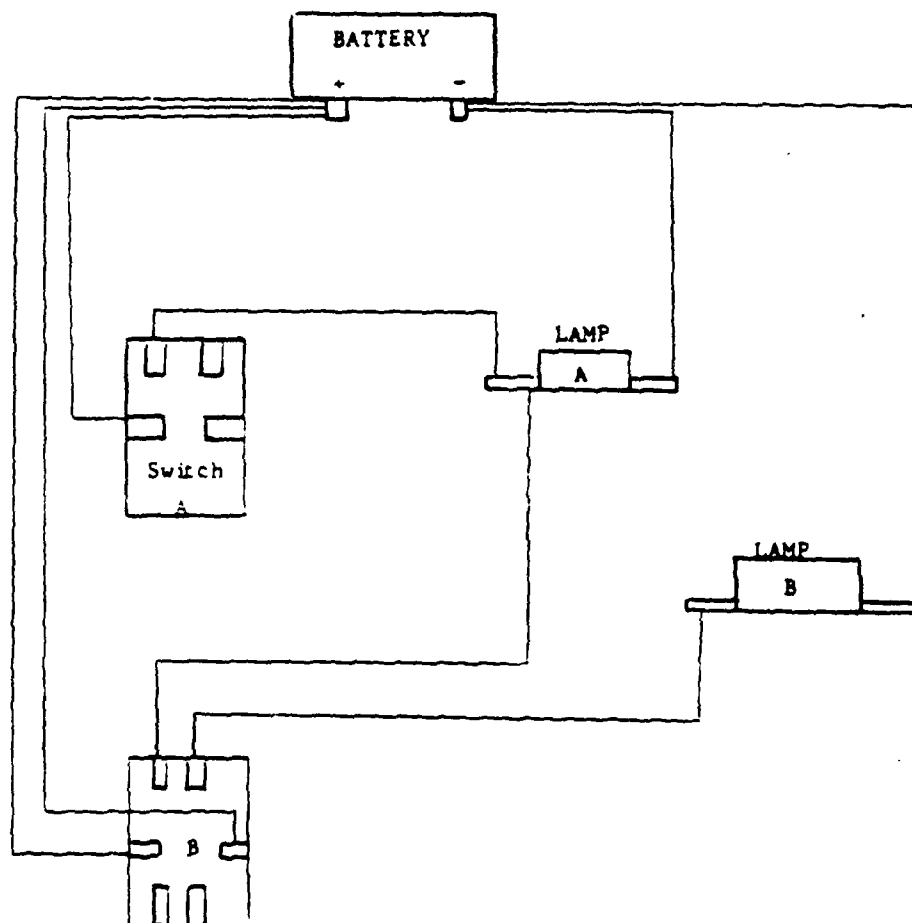
When switch A is ON, will lamp A light? _____
When switch B is ON in the upper position,
will lamp A light? _____
will lamp B light? _____
When switch B is ON in the lower position,
will lamp B light? _____



Describe Fault (if any):

C4

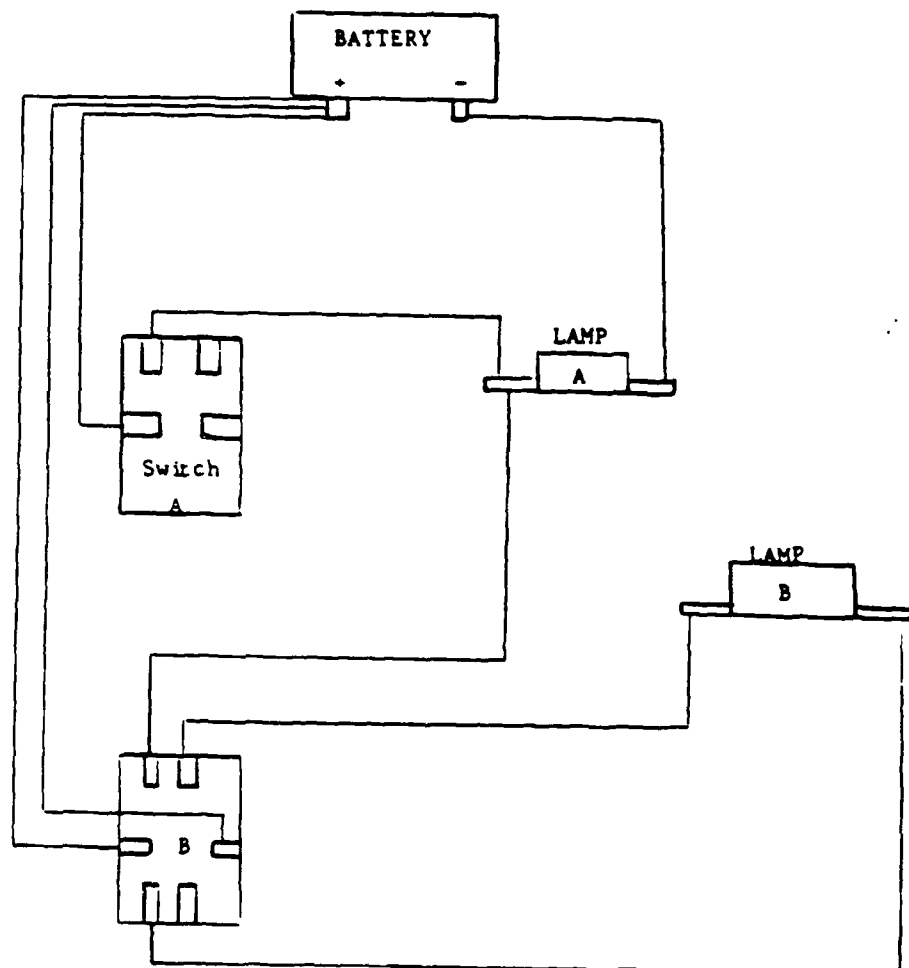
When switch A is ON, will lamp A light? _____
When switch B is ON in the upper position,
will lamp A light? _____
will lamp B light? _____
When switch B is ON in the lower position,
will lamp B light? _____



Describe Fault (if any):

C5

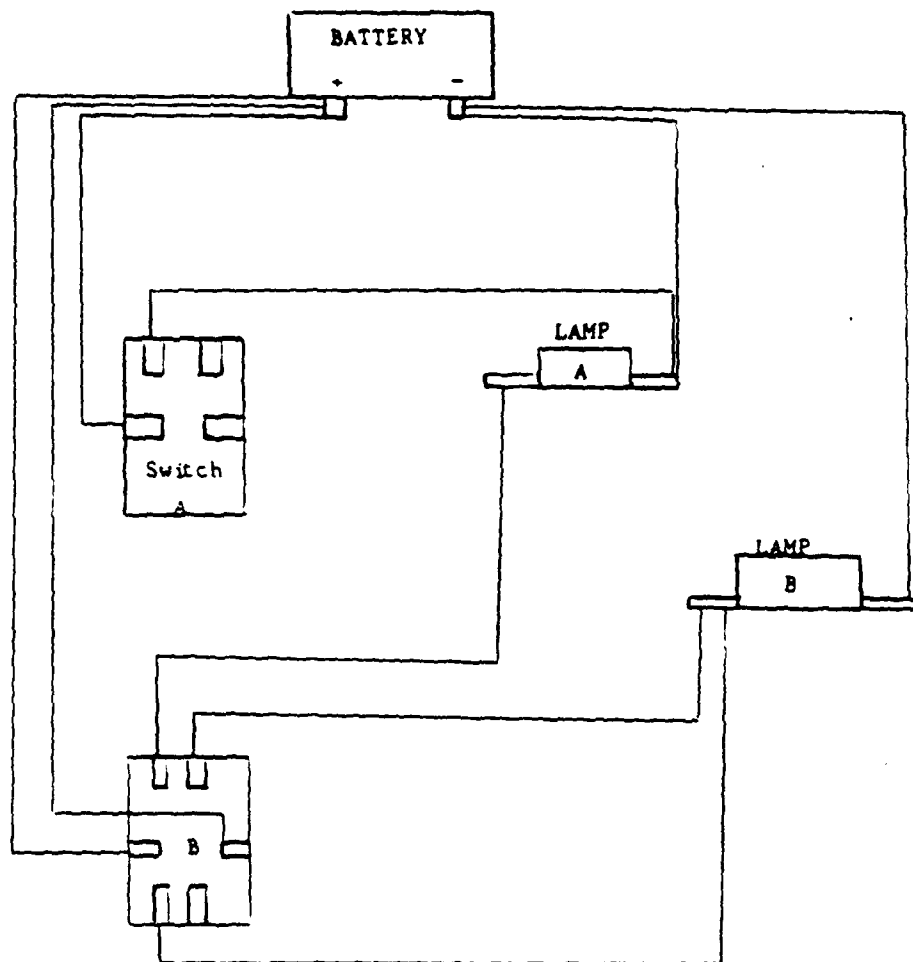
When switch A is ON, will lamp A light? _____
When switch B is ON in the upper position,
will lamp A light? _____
will lamp B light? _____
When switch B is ON in the lower position,
will lamp B light? _____



Describe Fault (if any):

C2

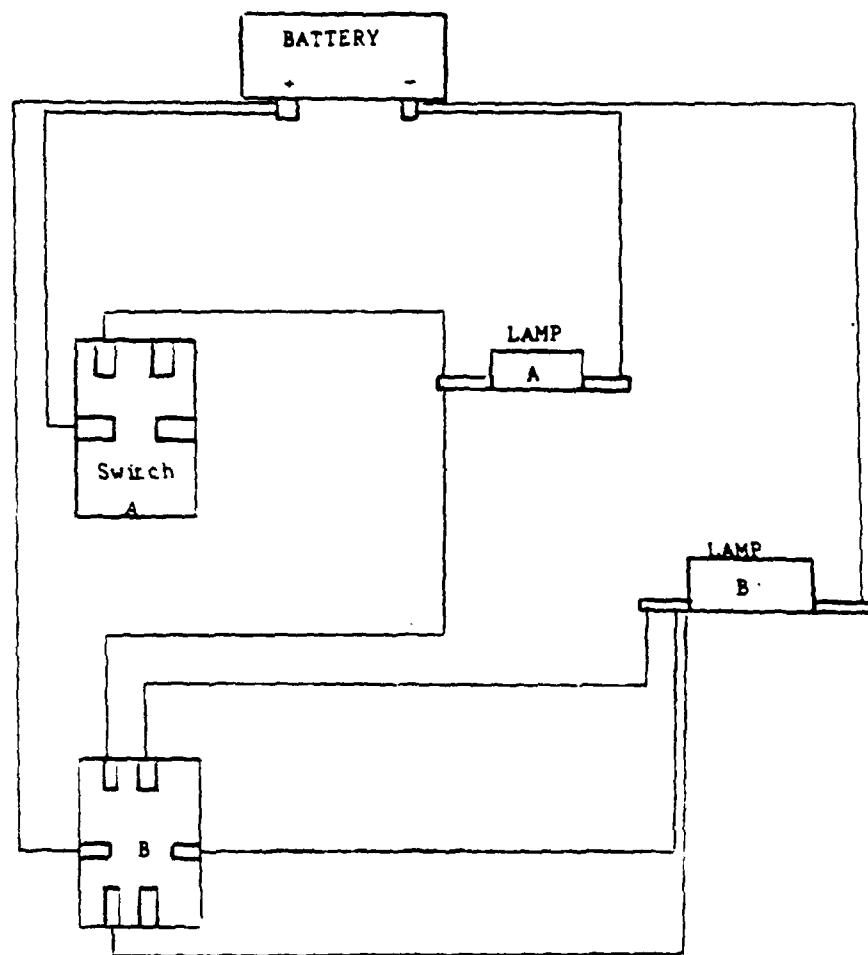
When switch A is ON, will lamp A light? _____
When switch B is ON in the upper position,
will lamp A light? _____
will lamp B light? _____
When switch B is ON in the lower position,
will lamp B light? _____



Describe Fault (if any):

C3

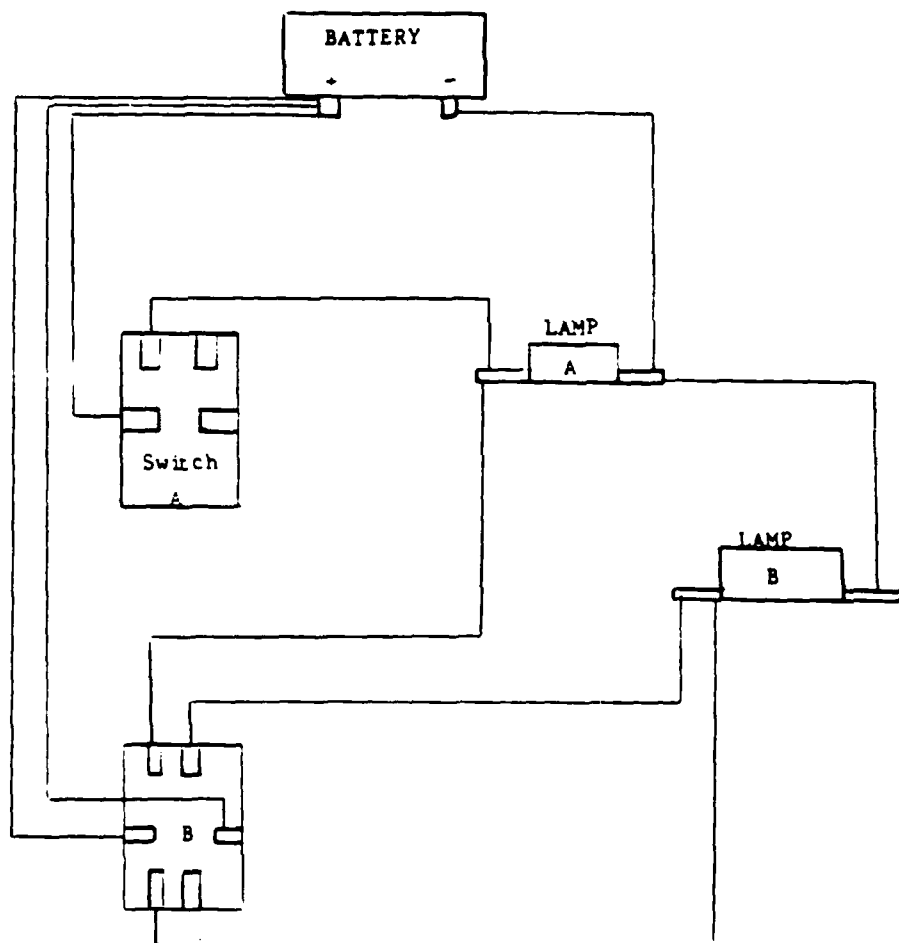
When switch A is ON, will lamp A light? _____
When switch B is ON in the upper position,
will lamp A light? _____
will lamp B light? _____
When switch B is ON in the lower position,
will lamp B light? _____



Describe Fault (if any):

C6

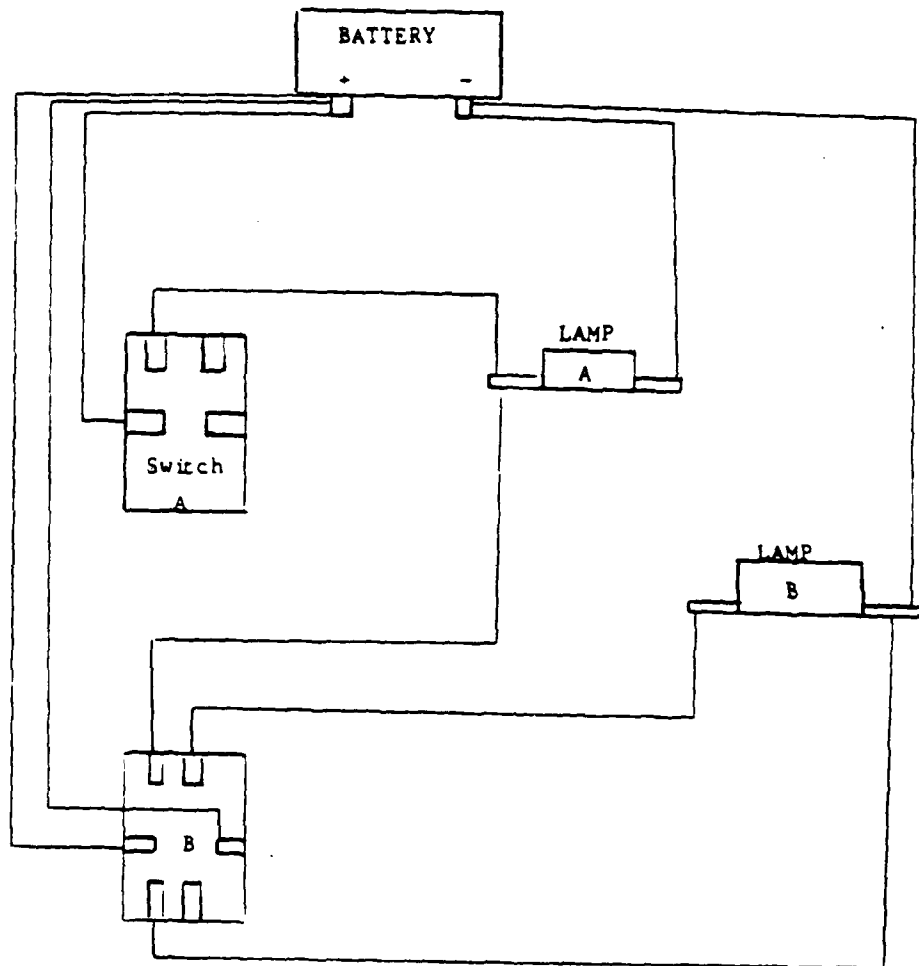
When switch A is ON, will lamp A light? _____
When switch B is ON in the upper position,
will lamp A light? _____
will lamp B light? _____
When switch B is ON in the lower position,
will lamp B light? _____



Describe Fault (if any):

C7

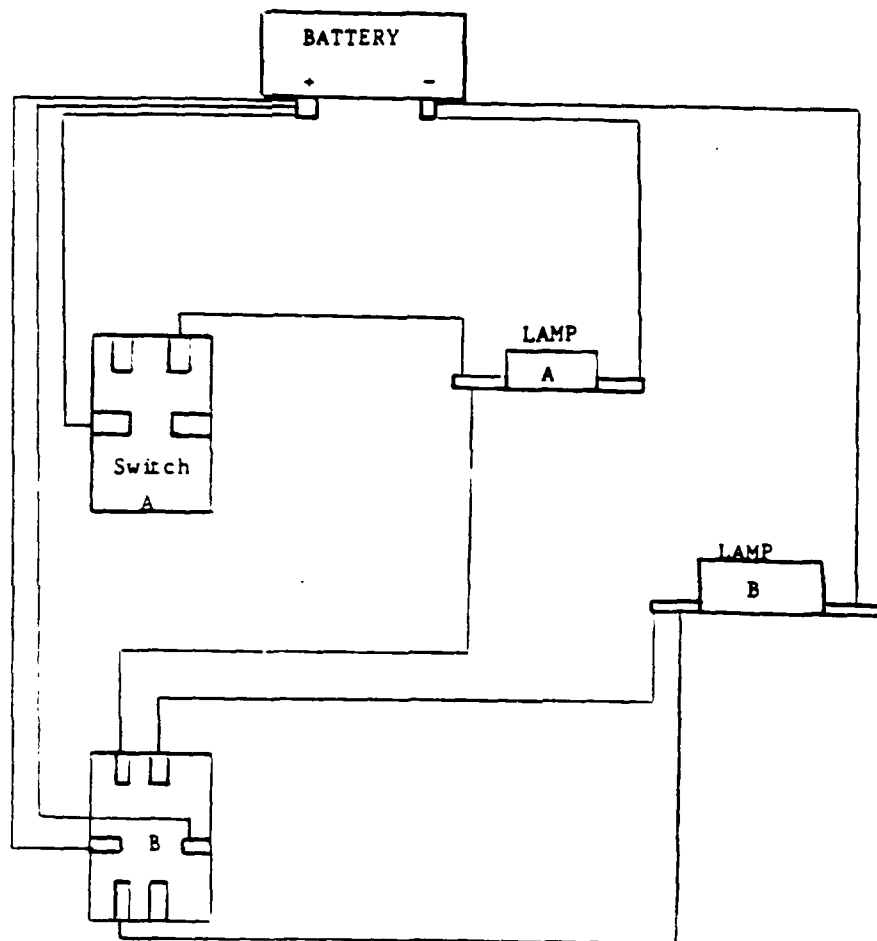
When switch A is ON, will lamp A light? _____
When switch B is ON in the upper position,
will lamp A light? _____
will lamp B light? _____
When switch B is ON in the lower position,
will lamp B light? _____



Describe Fault (if any):

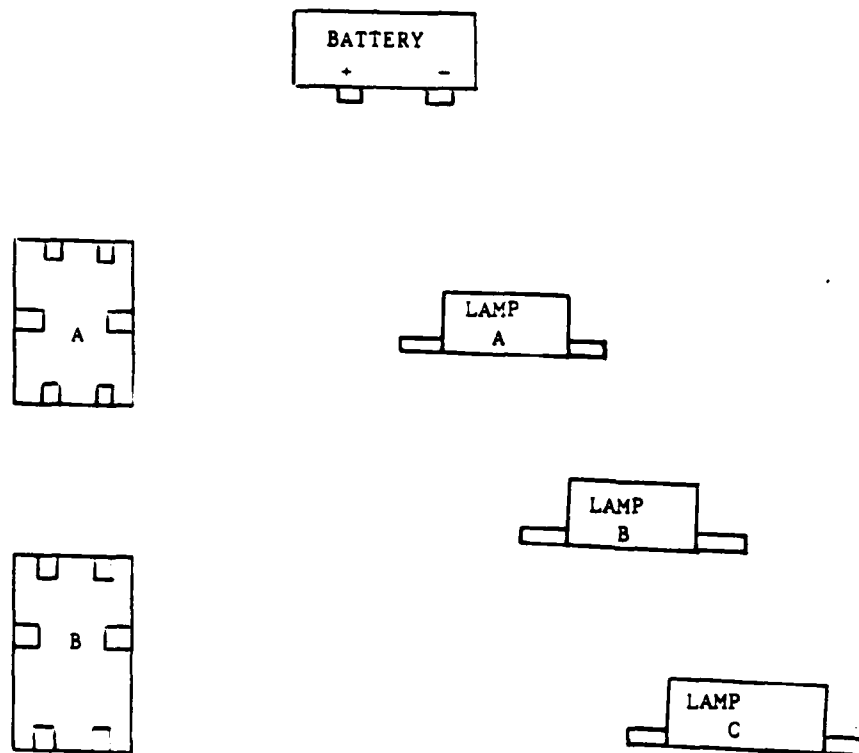
C8

When switch A is ON, will lamp A light? _____
When switch B is ON in the upper position,
will lamp A light? _____
will lamp B light? _____
When switch B is ON in the lower position,
will lamp B light? _____



APPENDIX B3

Design a circuit which will light Lamp A when switch A is ON in the upper position, will light Lamps B & C when switch A is ON in the lower position, will light Lamp C when switch B is ON in the upper position, and will light Lamps A & B when switch B is ON in the lower position. Draw all connections neatly. Work in pencil, and be sure your final design is drawn dark enough to be understood correctly.



PART II IS INDEPENDENT OF PART I.
I. IF THE CONNECTION MARKED * FAILS,

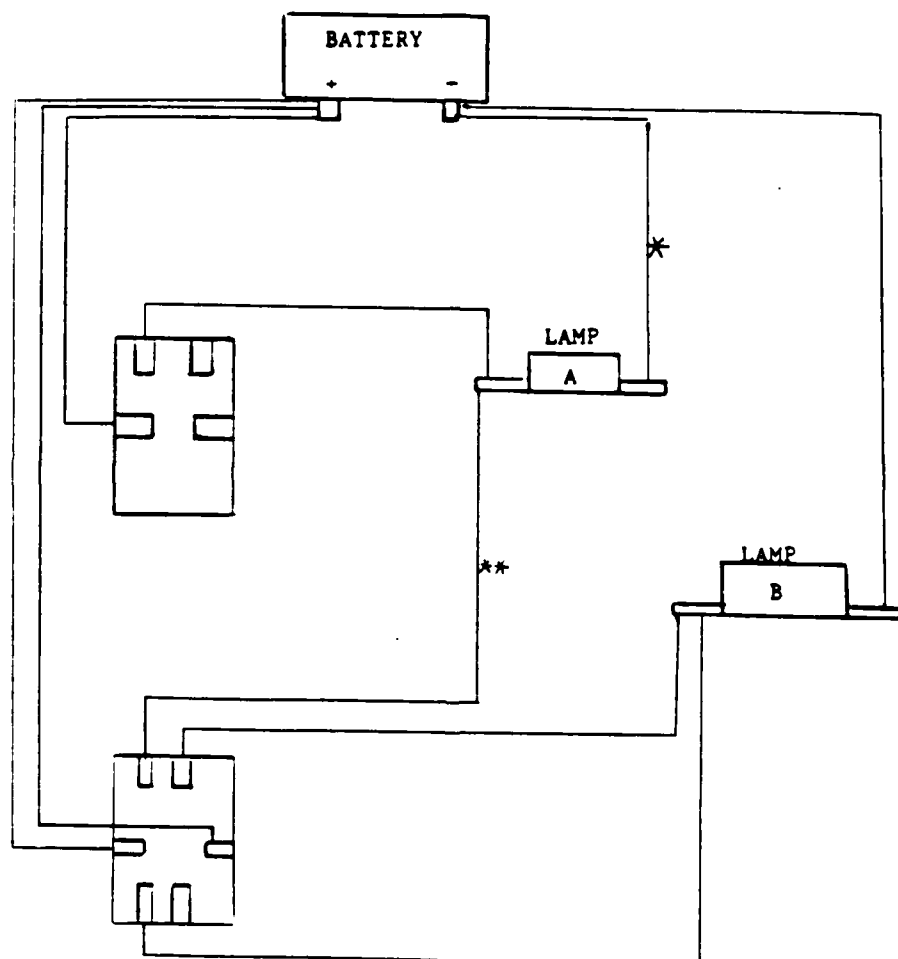
APPENDIX B4

E1

- Will Lamp A light when switch A is ON? _____
Will Lamp A light when switch B is ON in the upper position? _____
Will Lamp B light when switch B is ON in the upper position? _____
Will Lamp B light when switch B is ON in the lower position? _____

II. IF THE CONNECTION MARKED ** FAILS,

- Will Lamp A light when switch A is ON? _____
Will Lamp A light when switch B is ON in the upper position? _____
Will Lamp B light when switch B is ON in the upper position? _____
Will Lamp B light when switch B is ON in the lower position? _____



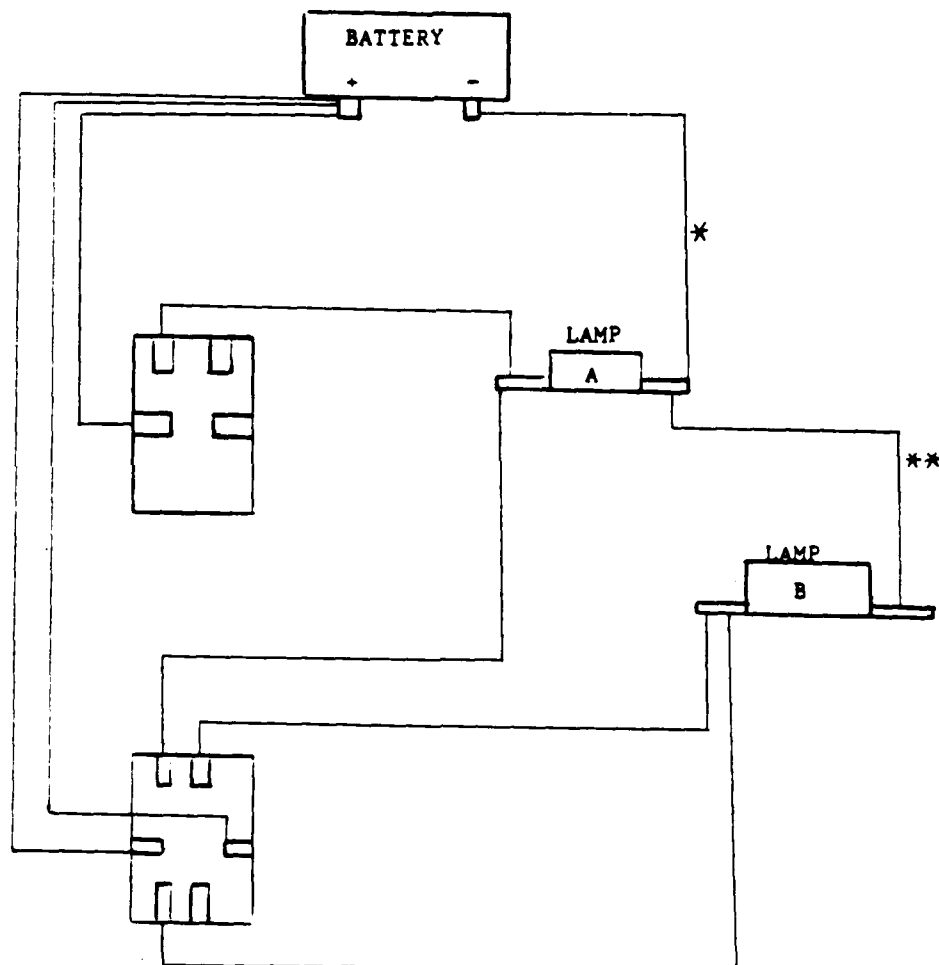
PART II IS INDEPENDENT OF PART I.
I. IF THE CONNECTION MARKED * FAILS,

E2

- Will Lamp A light when switch A is ON? _____
Will Lamp A light when switch B is ON in the upper position? _____
Will Lamp B light when switch B is ON in the upper position? _____
Will Lamp B light when switch B is ON in the lower position? _____

II. IF THE CONNECTION MARKED ** FAILS,

- Will Lamp A light when switch A is ON? _____
Will Lamp A light when switch B is ON in the upper position? _____
Will Lamp B light when switch B is ON in the upper position? _____
Will Lamp B light when switch B is ON in the lower position? _____



Specification Searches in Covariance Structure Modeling

Robert MacCallum

The Ohio State University

Mailing Address: Robert MacCallum
Department of Psychology
404C West 17th Avenue
Ohio State University
Columbus, Ohio 43210

Research sponsored by the Air Force Office of Scientific Research/AFSC,
United States Air Force, under Contract F49620-82-C0035. The United States
Government is authorized to reproduce and distribute reprints for governmental
purposes notwithstanding any copyright notation hereon.

Running Head: SPECIFICATION SEARCHES

Abstract

Many applications of covariance structure modeling include a specification search; i.e., a process of sequentially modifying a model so as to improve its fit and/or parsimony. The present study investigates whether common procedures for conducting specification searches will typically lead to discovery of the correct population model. This is investigated by defining true population models and covariance matrices, then fitting misspecified models to samples from those populations, and carrying out searches. Various phenomena occurring in specification searches are demonstrated and discussed. Results indicate that the likelihood of success in a specification search is optimal when (a) the investigator's initial model corresponds closely to the true model; (b) the search is allowed to continue even when a statistically plausible model is obtained; (c) the investigator is able to place valid restrictions on permissible modifications; and (d) a large sample is used.

Specification Searches in Covariance Structure Modeling

INTRODUCTION

Covariance structure modeling (CSM) (Bentler, 1980; Joreskog, 1974, 1977; Long, 1983) is rapidly becoming an important and widely used research tool in the behavioral sciences. A variety of interesting applications have already been published (e.g., Bentler & Speckart, 1979; Fiske, Kenny, & Taylor, 1982; Fredricks & Dossett, 1983; Maruyama & McGarvey, 1980), and there is wide agreement that use of CSM will continue to grow rapidly and that results provided by this approach will be of significant value in behavioral science research.

Review of Covariance Structure Modeling

Since many readers of this paper will already be familiar with the formal mathematical framework of CSM, only a brief review of that material will be presented here. Readers wishing to review the mathematical model in detail should refer to Joreskog and Sorbom (1984) or Long (1983). Though several variants of the general CSM model have been proposed (e.g., Bentler and Weeks, 1980 ; Joreskog, 1974, 1977; McArdle and McDonald, 1984), the present study will employ that developed by Joreskog (1974, 1977) and represented in the

widely available LISREL computer program (Joreskog and Sorbom, 1984).

A covariance structure model can be defined as an hypothesis of a specific pattern of relationships among a set of measured variables (MV's) and latent variables (LV's). Let ξ be a column vector containing n Independent LV's $\xi_1, \xi_2, \dots, \xi_n$. The Independent LV's are those which, according to the investigator's hypothesis, are not affected by any other variables in the model. Let x be a column vector containing x_1, x_2, \dots, x_q , which are the q indicators of the Independent LV's. These indicators will be referred to as Independent MV's. Let η be a column vector containing m dependent LV's $\eta_1, \eta_2, \dots, \eta_m$. The dependent LV's are those which, according to the investigator's hypothesis, are affected by at least one other variable in the model. Finally, let y be a column vector containing y_1, y_2, \dots, y_p , which are the p indicators of the dependent LV's. These indicators will be referred to as dependent MV's.

CSM can then be defined in terms of a set of three matrix equations. The first two equations, representing what is called the "measurement model," are as follows:

$$x = \Lambda_x \xi + \delta \quad (1)$$

$$y = \Lambda_y \eta + \epsilon \quad (2)$$

Specification Searches

Here Λ_x is a $q \times n$ matrix of coefficients representing the effects of the independent LV's on their indicators, and δ is a $q \times 1$ vector of "errors of measurement" in the indicators. Similarly, Λ_y is a $p \times m$ matrix of coefficients representing the effects of the dependent LV's on their indicators, and ϵ is a $p \times 1$ vector of "errors of measurement" in these indicators. Thus, the measurement model defines each MV as a linear combination of the LV's, plus an error term. The final equation in DSM represents the "structural model," which defines the relationships among the LV's:

$$\eta = B\eta + \Gamma\xi + \zeta \quad (3)$$

In this equation, B is an $m \times m$ matrix of coefficients representing the effect of each dependent LV on each of the other dependent LV's. The matrix Γ is an $m \times n$ matrix of coefficients representing the effect of each independent LV on each dependent LV. Finally, ζ is an $m \times 1$ vector containing residuals, or "errors in equations," for each of the dependent LV's. Thus, the structural model defines each dependent LV as a linear combination of independent LV's and other dependent LV's, plus a residual.

It is also necessary to define the following covariance matrices: (a) $\Phi = E(\xi\xi')$ is an $n \times n$ covariance matrix for the independent LV's; (b) $\Theta_\delta = E(\delta\delta')$ is a $q \times q$

Specification Searches

covariance matrix for the errors of measurement in the independent MV's; (c) $\Theta_{\epsilon} = E(\epsilon\epsilon')$ is a $p \times p$ covariance matrix for the errors of measurement in the dependent MV's; and (d) $\Psi = E(\zeta\zeta')$ is an $m \times m$ covariance matrix for the errors in equations for the dependent LV's.

Given this mathematical representation, it can be shown (Joreskog and Sorbom, 1984) that the population covariance matrix Σ for the $(p+q)$ MV's is a function of eight parameter matrices Λ_x , Λ_y , B , Γ , Θ_{δ} , Θ_{ϵ} , Φ , and Ψ . Thus, given an hypothesized model defined in terms of fixed and free parameters of the eight parameter matrices, and given a sample covariance matrix for the MV's, one can solve for estimates of the free parameters of the model. The most common approach for fitting the model to data is to obtain maximum likelihood estimates of parameters, and an accompanying likelihood ratio χ^2 test of the null hypothesis that the model holds in the population. A variety of other information can be obtained regarding goodness of fit (Bentler and Bonett, 1980; Joreskog and Sorbom, 1984)

Specification Searches

Typical applications of CSM involve (a) the development of a prior model, representing an hypothesized pattern of relationships among a set of MV's and LV's; (b) the fitting of the prior model to sample data; (c) the evaluation of the

Specification Searches

solution in terms of its parameter estimates and goodness of fit; and, very often, (d) the modification of the model so as to improve its parsimony and/or its fit to the data. This last step has been referred to as a specification search (Leamer, 1978; Long, 1983). During such a search the investigator alters the model specification, perhaps numerous times, in search of a parsimonious, substantively meaningful model which fits the data well. Search procedures are designed with the intent to detect and correct specification errors, which represent a lack of correspondence between a proposed model and the true model characterizing the population and variables under study. The ultimate objective of a specification search would be to arrive at the model which correctly represents the network of relationships among the MV's and LV's in the population.

Clearly, a specification search is more critical when an investigator's initial model fits poorly, in which case a successful search can yield a plausible well-fitting model. However, a specification search can be profitable even when an initial model fits well. Such a model may still contain specification errors, and a search may lead to a more correct model which fits as well or better. Leamer (1978), in his discussion of specification searches in linear regression models in economics, distinguishes between searches conducted for the purposes of

Specification Searches

simplification vs. model improvement. However, in CSM a search may include both objectives; e.g., parameters may be added to a model to improve its fit, then other parameters may be deleted from the model to simplify it.

Specification searches are becoming a common part of applications of CSM in the social science literature. For instance, studies by Bentler and Speckart (1979), Bentler and Huba (1979), Fredricks and Dossett (1983), and Smith (1982) include such searches. Indeed, it is unusual to find an application of CSM which does not include any type of specification search. Furthermore, discussions of methodology such as those by Joreskog and Sorbom (1984), Long (1983), and Saris and Stronkhorst (1984) encourage investigators to seek model modifications which would enhance the parsimony of the model and/or its fit to the data.

Though little if any prior research has been done on the success of specification searches per se, the general issues of the consequences and detection of specification errors have received some attention. Gallini (1983) demonstrates some consequences of specification errors in path analysis models, showing that various types of specification errors can cause bias in parameter estimates as well as erroneous decisions about model fit. Billings and Wroten (1978) also discuss consequences of violating the assumptions of path analysis. Such violations

Specification Searches

can be thought of as specification errors. Gerbing and Anderson (1984) discuss alternative interpretations of correlated measurement errors for indicators of a given factor. Their suggestions are relevant in cases where a specification search indicates that allowing such correlations would substantially improve the fit of a model. The interpretation and use of correlated measurement errors is also discussed by Fornell (1983) and Bagozzi (1983), among others. Anderson and Gerbing (1982) discuss the issue of measurement model misspecification, arguing that specification errors in measurement models are common in initial models, and that proper specification of the measurement model is necessary before meaning can be attributed to the results from the structural model. They propose two different procedures aimed at correcting measurement model specification errors so as to obtain unidimensional construct indicators. The problem of detecting specification errors in CSM has also been addressed by Costner and Schoenberg (1973), Joreskog and Sorbom (1984), and Saris, DePijper, and Zegwaart (1979). Thus, the literature on specification errors clearly reveals that they can have serious consequences and that there exists a variety of ways to attempt to identify and correct those errors.

The methodological literature on CSM does not, however, define an optimal

Specification Searches

procedure for conducting a specification search. Rather, the literature recommends that researchers evaluate several types of information and determine changes which seem most meaningful and promising in the context of the research. The information which is most relevant consists of T-values, modification indices (MI's), and residuals. For each free parameter in a model, LISREL provides a T-value, obtained by dividing the parameter estimate by its estimated standard error. Non-significant T-values (usually taken to be those values < 2 in absolute value) represent free parameters whose estimates are not significantly different from zero. If such parameters are not deemed substantively critical to the model, they can be omitted, thereby improving parsimony without severely damaging overall fit. For each fixed zero parameter in a model, LISREL provides a MI, which represents the minimum decrease in the overall χ^2 value that would be achieved if the corresponding parameter were freed. Large MI's represent parameters which, if added to the model, would significantly improve goodness of fit, as measured by the χ^2 test. Thus, if a large MI is deemed to represent a substantively meaningful parameter that was omitted from the original model, that parameter can be added to the model and the resulting modified model will fit the data significantly better. Residuals represent the difference between the observed sample covariances and

Specification Searches

the model estimates of the population covariances. Large residuals reveal those relationships among MV's which are not fit well by the given model. The investigator can attempt to determine meaningful modifications in the model which will reduce the magnitude of the large residuals. Often there will be a convergence between modifications indicated by the MI's and by the residuals. That is, fixed parameters with large MI's would often yield a decrease in large residuals if they were freed. The task for the researcher then is to examine all of this information and to determine whether there are meaningful and productive changes to be made in a model. If so, the model is modified and re-fit to the data. Then results from that model can be evaluated for further modification. The search can continue until no useful modifications are available.

Though there is no single correct strategy for conducting a specification search, there are some guidelines which should be considered. First, it is probably best to attempt to correct specification errors in the measurement model before addressing the structural model, since structural model parameter estimates and related information will be more meaningful if the measurement model is free of specification errors. Second, it is advisable to make only one modification (i.e., the addition or deletion of a parameter) at a time during a search, since a single

Specification Searches

change in a model can affect other parts of the solution. Finally, as discussed by Saris and Stronkhorst (1984), it is preferable to make modifications involving the addition of new parameters prior to deleting parameters. That is, it is recommended that modifications be made so as to improve the fit of the model prior to improving the parsimony.

A critical issue in the conduct of a specification search is the obvious potential for capitalization on chance. That is, model modifications are based on results obtained from fitting an initial model to a particular sample. Therefore, the search process is, to some extent, data-driven, and modified models do not have the status of prior hypotheses (Cliff, 1983). As a result, the external validity of a final model arising from a specification search is open to question. The substantive meaning and goodness of fit of such models must be viewed with caution.

In practice, a specification search is considered successful if it results in an interpretable model which fits the data well. Though these are the most salient criteria available to the applied researcher, there is a more critical criterion which is to be investigated in the present study via simulation techniques. That is, when there exists a model which is correct in the population, and when a model

Specification Searches

different from that correct model is fit to a sample from the population, will a specification search lead the investigator to the correct model? What is the likelihood of a specification search being "successful" in the sense of arriving at the true population model? What factors affect the likelihood of success? What can the researcher do to improve the likelihood of success?

Answers to these questions are of substantial importance in the application of CSM in the social sciences. As noted above, the use of CSM is growing rapidly, and most applications involve a specification search of some degree, followed by an interpretation of the final solution as a plausible representation of the population model. Therefore, it is important to evaluate and, if possible, to improve the likelihood that a specification search will lead an investigator to a correct representation of the population model.

METHOD

Measurement vs. Structural Misspecifications

The general approach used here to investigate the success of specification searches will be to (a) construct artificial data for which there exists a known correct model; (b) fit a misspecified model to the data; and (c) determine whether a specification search would lead to specification of the correct model. Details of

Specification Searches

this procedure are presented below. This study will be restricted to investigating misspecifications and searches involving only the structural model portion of the general model. In terms of population parameters, misspecifications and searches will involve only the B and Γ matrices; i.e., only the directional relationships among the LV's. Thus, the entire measurement model, represented by matrices Λ_x , Λ_y , Θ_δ , and Θ_ϵ , will be correctly specified in all cases. In addition, the Ψ and Φ matrices will be correctly specified.

The primary reason for restricting attention to the structural model in the present study is to keep the problems under study at a more manageable level. Preliminary research shows that when misspecifications exist in both the measurement and structural models, the conduct of a successful specification search can be very problematic. In fact, the author has produced numerous examples in which misspecifications in one part of the model result in the largest MI's occurring in the other part of the model, even when the latter is correctly specified. The reason for such phenomena is that the maximum likelihood estimation technique used in LISREL is a full-information procedure, meaning that all free parameters in both the measurement and structural models are estimated simultaneously by fitting the full model to the full sample covariance matrix. As

Specification Searches

a result, misspecifications in one part of the model can affect results in other parts. Research will continue on the development of strategies for specification searches including both the measurement and structural models. However, given the complexity of the interaction between these, we will focus on the latter in the present investigation.

This restriction does not severely limit the value of this study. In applications of CSM, the structural model is often the focus of attention in specification searches and interpretation. It is unusual for published applications to report serious problems or substantial modifications in measurement models. In addition, there do exist procedures for improving measurement models which can be used fairly independently of the structural model under consideration (Anderson and Gerbing, 1982; Costner and Schoenberg, 1973). Results of the present study will be relevant to applications in which serious measurement problems are not encountered (or, if encountered, have been corrected), and in which the investigator seeks to detect and correct misspecifications in the structural model. In addition, the approach used here can be viewed as representing a "best case" scenario; i.e., the confinement of misspecifications and modifications to the structural model in this simulation should provide the best chance of success for

specification searches.

Starting Points for Specification Searches

From the published applications of CSM, it appears that investigators have employed two different logical starting points for specification searches. The most common is the case in which a substantively meaningful initial model is fit to the data at hand, and the search is based on results from that model. This type of search is illustrated in applications by Bentler and Speckart (1979), Bentler and Huba (1979), and others. An alternative approach is to employ an initial structural model which is not substantively meaningful. Two such non-substantive initial structural models would be (a) an "empty" structural model, in which all elements of B and Γ are fixed at zero, and (b) a "saturated" structural model, in which all potentially meaningful elements of B and Γ are free parameters. Starting from an empty structural model, the search would proceed by successively freeing those fixed parameters which have large MI's and are substantively meaningful. Starting from a saturated structural model, the search would be conducted by fixing those non-critical parameters which display non-significant T-values. Fredricks and Dossett (1983) employed a saturated structural model in their study of attitude-behavior relations, and McAllister,

Specification Searches

Krosnick, and Millburn (1984) used a similar approach in their study of causes of cigarette smoking. The author is not aware of any published applications in which an empty structural model was used to start a specification search. Nevertheless, such an approach represents the logical counterpart to the use of the saturated structural model and may merit consideration. The present study will investigate specification searches based on the common case of substantive initial models. Future research will investigate the use of nonsubstantive initial models.

Generation of Artificial Data

Two different path diagrams were constructed to represent different population covariance structure models. The structural portion of each diagram, using the Joreskog and Sorbom (1984) notation and showing true parameter values, is shown in Figure 1. The models will be referred to henceforth as models A and B. Model A is of the same form as one of the structural models used by Bentler and Speckart (1980) in their study of attitude-behavior relations, and model B was chosen to represent a "chain" of relations among dependent variables. The two models were chosen so as to lend at least a bit of generality to the present results, as well as to provide a basis for demonstrating several different phenomena found to occur in specification searches.

Insert Figure 1 about here

For both models, a measurement model was defined by creating two indicators per LV. Each pair of indicators had true factor loadings of 1.0 and .8 on the corresponding LV, and each indicator had a true unique variance of .6. Given the full set of true parameter values for each model, a population covariance matrix was computed for each model by substituting the true parameter values into the mathematical expression for the covariance form of the model (Equation 1.4; Joreskog and Sorbom, 1994). These two covariance matrices are shown in Table 1, and will be referred to as Σ_A and Σ_B .

Insert Table 1 about here

To illustrate and investigate the issues discussed below, it was necessary to generate sample covariance matrices from each of the populations defined above. This was accomplished via a procedure developed by Kaiser and Dickman (1960). Using this technique, samples of any desired size were generated from a multivariate normal population characterized by either of the population covariance matrices shown in Table 1. From each sample the sample covariance

Specification Searches

matrix was then computed. Details regarding number of samples and sample size are presented below.

Construction of Misspecified Models

For each of the true models, one or more misspecified models were defined. These misspecified models will be presented in the next section of the paper, since they were designed so as to demonstrate the specific issues discussed below. These models were constructed so that the designation of independent and dependent LV's in the true model remained intact in the misspecified models. Though this restriction is not essential, it does serve to avoid unnecessary complications. If a misspecified structural model is constructed which alters the designation of independent and dependent LV's, it is always possible to add parameters to the model so as to obtain a model which can generate the same covariance structure as the true model. The resulting model would be distinguishable from the true model only on substantive grounds. Given this, it was felt that allowing such misspecifications would introduce a very great complication of limited interest. Therefore, the restriction defined above was imposed, which is analogous to granting the validity of an empirical assumption that the initial model contains the correct designation of independent and dependent LV's. The misspecified initial

Specification Searches

models, then, are characterized by two types of specification errors: (a) errors of omission, where a parameter present in the true structural model is omitted in the misspecified model; and (b) errors of inclusion, where a parameter not present in the true structural model is included in the misspecified model. Misspecified initial models will be designated by the letter representing the corresponding true model, followed by an integer (e.g., A1, A2, etc.).

Strategy for Conducting Specification Searches

After misspecified initial models were fit to samples drawn from populations representing models A and B, specification searches were conducted for each sample by following common procedures for using MI's and T values. At each step, the fixed structural parameter with the largest significant ($\alpha=.01$) MI was freed. This was repeated until a model with no significant MI's was obtained. Free parameters with non-significant T's in that model were then identified. This strategy employs the most common information used in specification searches, and follows the guidelines discussed in section 1.2 above. In addition the likelihood ratio χ^2 test was evaluated at each step in each search. It must be emphasized that this statistic does not provide a legitimate hypothesis test for any model beyond the initial model in each search, since modified models are based in part on the

Specification Searches

sample being fit (Cliff, 1983). Nevertheless, the behavior of this statistic is of interest here. Finally, the success of each search was evaluated in terms of whether or not the final step produced a model which matched the correct population model (A or B).

Issues Investigated

Given a substantive initial model, effects of the following factors on the success of specification searches were investigated: (a) the number of specification errors in the structural model; (b) the use of prior restrictions on permissible modifications of the model; and (c) sample size. In one sense, the effects of these factors are somewhat predictable. That is, one would expect specification searches to work better when there are fewer specification errors in the initial model, when correct restrictions on permissible modifications are imposed, and when sample size is large. The purposes of the present study are to investigate and demonstrate the nature and degree of these effects, as well as to shed some light on the likelihood of success of a specification search under various conditions.

The Number of Specification Errors

The general issue to be studied here is whether the likelihood of a successful specification search improves when there are fewer specification errors in the

Specification Searches

structural model. To investigate this phenomenon, the misspecified models shown in Figure 2 were defined so as to represent different degrees of misspecification of model A. Note that model A1 contains one error of omission; A2 contains one omission and one inclusion; and A3 contains two omissions and one inclusion. Based on the population covariance matrix Σ_A , 20 sample covariance matrices were constructed representing samples of $N=300$ cases. Models A1, A2, and A3 were then fit to these samples, and specification searches were conducted to determine whether the true model A could be identified.

Insert Figure 2 about here

Restricted vs. Unrestricted Searches

As mentioned above, an important issue in the conduct of a specification search involves the ability of the investigator to provide substantive support for prospective model modifications. In practice, such an effort should enhance the quality of the search by reducing the likelihood of creating further specification errors via model modifications. In the present study, this issue is investigated by applying two different search strategies. An unrestricted search will be defined as a search wherein model modifications are made without restriction; that is, the

Specification Searches

fixed structural parameter with the largest significant MI is freed, regardless of its nature, and all free structural parameters with non-significant T values are deleted. A restricted search will be defined as a search wherein restrictions are imposed so that no invalid modifications can be made; i.e., no parameter defined as zero in the true model may be freed, and no non-zero parameter in the true model may be fixed during the search. The unrestricted strategy simulates the empirical situation in which the researcher does not attempt to substantively justify modifications, or perhaps worse, finds a way to justify any modification. The restricted strategy simulates the optimal situation in which the researcher has sufficient substantive and theoretical knowledge so as to avoid imposing further specification errors during the search. To investigate the performance of these two strategies, both types of searches were applied to 20 sample covariance matrices generated from population covariance matrices Σ_A and Σ_B , respectively. Sample size was set at 300, which would be considered an adequately large sample size for the models in question. Model A3 was used as the initial model for the samples based on model A, and model B1, shown in Figure 2, was used as the initial model for the samples based on model B.

Sample Size

It seems likely that the success of specification searches should improve as sample size increases. A larger sample yields a covariance matrix which is likely to be a better estimate of the population covariance matrix, and should thus offer a better opportunity of successfully locating the correct model. Furthermore, larger samples should yield more stable ML's and T's, thus reducing the likelihood of invalid modifications of a model.

To investigate these issues, specification searches were conducted for 20 samples of size 100 drawn from populations with covariance matrices Σ_A and Σ_B , using initial misspecified models A3 and B1, respectively. Both unrestricted and restricted searches were conducted. A sample size of 100 would be considered too small, by most criteria, for the models used here. Results from these searches can be compared to results based on similar searches using samples of size 300, as described in the previous section.

Summary

To summarize, unrestricted specification searches were conducted on 20 samples of $N=300$ from population A, using initial models A1 and A2. In addition, 20 samples were analyzed in each of the eight conditions created by

Specification Searches

crossing two initial models (A3 and B1) with two strategies (unrestricted and restricted) with two sample sizes (300 and 100). Given the purposes of the study, it was not deemed necessary to create a complete factorial design or to use a large number of replications per condition. Results will be seen to serve the purposes of revealing and demonstrating some interesting and important phenomena.

All model fitting was carried out using the maximum likelihood option of the LISREL VI computer program, version 6.3 (Joreskog and Sorbom, 1984). Searches were conducted with the aid of the "automatic modification" option, by which the fixed parameter with the largest significant MI is automatically freed to create a new model. Unrestricted searches were conducted by freeing that fixed parameter which exhibited the largest MI significant at the .01 level. In restricted searches, fixed structural parameters which were defined as zero in the true model were not allowed to be freed, regardless of the size of the corresponding MI's.

RESULTS OF SPECIFICATION SEARCHES

This section provides a presentation and summary of results of the 20 specification searches conducted under each of the conditions described above.

Specification Searches

Tables are presented showing the history of steps within each search for all of the large-N conditions. Given the variety of phenomena and the sampling variability which occurred during the searches, the author believes that these individual search histories are quite informative. For the initial model and each modified model created within each search, the tables provide the probability level for the overall χ^2 test; a list of up to three parameters with the largest significant MI's ($\alpha < .01$) ordered from largest to smallest MI; and a list of parameter estimates which yield nonsignificant T-values ($|T| < 2.00$) in the final model. Results for the small-N conditions will be presented in summary form.

Results for Unrestricted Searches Based on N=300

Considering first model A1, recall that the only misspecification in this initial model is the omission of parameter γ_{22} from the true model A. Thus, the ideal result of a specification search beginning with model A1 would be to find a significant χ^2 for the initial model, along with the largest significant MI for γ_{22} . Then, after freeing γ_{22} , we would have the correct model and would hope to find no significant MI's and no non-significant T's. The left side of Table 2 shows the history of the 20 searches using initial model A1. Inspection of these results reveals only one significant difficulty which prevents nearly all the searches from

Specification Searches

following the ideal sequence: the presence of several non-significant χ^2 's for the initial model. Note that these values reflect Type II decision errors; i.e., the failure to reject a model which is, in fact, misspecified. Table 2 shows that six of the 20 searches yielded Type II errors for the initial model. However, if the search were allowed to proceed even in the face of a non-significant χ^2 , it can be seen that 19 of the 20 searches would be successful. The only failure arose in sample # 15, where the MI for γ_{22} is not significant. The occurrence of a substantial number of Type II errors will be seen to be a recurring finding in this study, and is discussed further below. In the remaining presentation of results, it will be assumed that a search may be continued even when the overall χ^2 is non-significant if further significant modifications in the model are available. Finally, it should be noted that all searches based on model A1 stopped after one step, with all solutions showing no significant MI's and no non-significant T's.

Insert Table 2 about here

Results for searches based on initial model A2 are presented in the right side of Table 2. Note that A2 contains one omission (γ_{22}) and one inclusion (γ_{23}). The optimal search beginning with A2 would yield a significant χ^2 for the initial

Specification Searches

model, accompanied by the largest significant MI for γ_{22} . Freeing γ_{22} would yield a model with a non-significant χ^2 , no significant MI's, and one non-significant T for γ_{23} . Considering the search histories, it can be seen that 11 of the 20 samples yielded Type II errors for the initial model. When MI's for all solutions were examined, an interesting, but not unusual phenomenon occurred: MI's for two different structural parameters, γ_{22} and β_{12} , were almost identical in each sample. In fact, it can be shown that freeing either of these parameters would have the same effect on the fit of the model, and that any observed difference in their MI's was due only to rounding error. Thus, for these analyses, automatic modification was not applicable; the user must choose between γ_{22} and β_{12} as the first parameter to be freed. A choice of β_{12} would create a new misspecification in the model, while a choice of γ_{22} would constitute a valid modification. The search histories for model A2 shown in Table 2 represent an assumption that the user could correctly distinguish between these alternatives in practice. Under this assumption, it can be seen that 17 of the 20 searches were successful. The three failures occurred for three different reasons: sample # 6 failed due to the lack of a significant MI in the initial solution; sample # 7 failed due to a Type I error after γ_{22} was added to the model; and sample # 4 showed an

Specification Searches

extra non-significant T in the final model. Though not shown in Table 2, none of the solutions showed any significant MI's after the first modification.

Specification searches beginning with model A3 were much less successful. Note that this model contains two errors of omission (γ_{21} and γ_{22}) and one inclusion (γ_{23}). An ideal search would yield a significant χ^2 for the initial model, accompanied by the largest significant MI for either γ_{21} or γ_{22} . The first modified model would also yield a significant χ^2 , and the largest significant MI for the remaining missing parameter. Freeing that parameter would yield a model with a non-significant χ^2 , no significant MI's, and a non-significant T for γ_{23} . The search histories shown in Table 3 reveal that none of the searches followed this pattern. In addition to the occurrence of five Type II errors for the initial model, a new problem arose. For 19 of the 20 samples, the largest MI in the structural model was for parameter β_{12} , which is not a parameter in the correct model A. Thus, freeing this parameter created an additional specification error in the first step of the search. When this was done, 18 of the 19 samples yielded a non-significant χ^2 , with no large MI's. At first glance, these results suggest that the specification searches produced an alternative model with acceptable fit. However, closer inspection of these solutions revealed symptoms of problems. Most

Specification Searches

Importantly, it was found that 17 of the solutions showed a negative squared multiple correlation for η_1 ; this resulted from the estimate of the residual variance for η_1 being greater than its actual variance. As noted by Joreskog and Sorbom (1984), such events should be interpreted as danger signals. In this case, they arose due to the severe misspecification created in the first step of the specification search. Thus, the failure of the search was revealed for these 17 samples. It is worth noting that these solutions often yielded other strange happenings, such as non-significant T's for β_{12} (after it had been freed due to its large MI), and non-significant T's for other structural parameters. In any case, it is clear that all 20 of these searches failed to locate the correct model.

Insert Table 3 about here

For another illustration, consider model B1, which contains two errors of omission (β_{21} and β_{32}) and two errors of inclusion (β_{31} and γ_{22}). The ideal search in this case would begin with a significant χ^2 for the initial model, accompanied by the largest significant MI for either β_{21} or β_{32} . Freeing one of these would yield a model which would again show a significant χ^2 and the largest

Specification Searches

significant MI for the remaining missing parameter. Freeing that parameter would produce a model which would yield a non-significant χ^2 , no significant MI's, and non-significant T's for β_{31} and γ_{22} . The search histories shown in Table 4 reveal that, while none of the searches followed exactly this pattern, four did arrive at the correct model if searches were continued in spite of non-significant χ^2 's. To summarize the various problems encountered in these searches, there were five Type II errors for the initial solutions, and 19 after one modification. Of the 20 searches, eight failed due to an invalid modification at the first step, three more failed due to an invalid modification at the second step, and five failed due to the lack of any significant MI's after one modification was made. The remaining four searches provided correct identification of the true model.

Insert Table 4 about here

Results for Restricted Searches Based on N=300

As described above, restricted specification searches were conducted using initial models A3 and B1. These initial models were each fit to 20 samples of N=300 drawn from populations represented by covariance matrices Σ_A and Σ_B , respectively, and searches were conducted under the restriction that no parameter

Specification Searches

which did not exist in the true model could be freed during the search, regardless of the magnitude of its MI.

Restricted searches beginning with model A3 required only the restriction that parameter β_{12} not be freed. Table 5 presents results of these searches; note that results for the initial model were the same as those for the unrestricted searches, since the same 20 samples were employed. Type II errors were again found -- five for the initial model, and five after one modification. Of the 20 searches, 11 failed at the initial solution due to the lack of any significant permissible MI's. One more failed for the same reason after one modification. Of the eight searches which made the first two modifications correctly, one failed after that point due to a Type I error. Thus, allowing searches to continue in spite of nonsignificant χ^2 's, seven of the 20 restricted searches based on model A3 resulted in the correct identification of model A.

Insert Table 5 about here

Restricted searches based on model B1 required that the following parameters not be allowed to be freed during the search: β_{12} , β_{13} , β_{23} , β_{14} , β_{24} , β_{34} , β_{41} , β_{42} , γ_{21} , γ_{31} , γ_{32} , γ_{41} , and γ_{42} . Results of these searches are shown in

Specification Searches

Table 6. Type II errors were again common, with five found for the initial model, and 19 after one modification. All 20 searches made a valid modification in the first step, but nine failed after that first step due to the lack of additional significant MI's representing permissible modifications. The remaining 11 made the second valid modification and yielded non-significant χ^2 's and the correct pair of non-significant T's. Thus, 11 of the 20 searches were successful if continued in spite of non-significant χ^2 's.

Insert Table 6 about here

Results for Searches Based on N=100

Both unrestricted and restricted searches were conducted on 20 samples of N=100 observations drawn from populations represented by covariance matrices Σ_A and Σ_C , using initial models A3 and B1, respectively. Results of these searches will be discussed in summary form, without presenting tables of search histories. The searches were uniformly unsuccessful and were characterized by a variety of problems, including improper solutions, lack of significant MI's, and invalid nonsignificant T's. (Note: An improper solution is one in which one or more parameter estimates are out of bounds, such as variance estimates being

Specification Searches

negative. The occurrence of such a solution was considered as sufficient reason to halt the specification search.)

For the 20 unrestricted searches based on model A3, there were four improper solutions for the initial model. Of the 16 proper solutions, 14 yielded Type II errors, and eight showed no significant MI's. Of the eight searches which did carry out a modification, seven freed a parameter which did not exist in the true model. The only search which made a correct first step failed due to the lack of additional significant MI's after that step. Thus, all 20 searches failed, and many solutions exhibited invalid non-significant T's and negative squared multiple correlations for η_1 , as discussed above. The restricted searches for the same samples were also completely unsuccessful. Only two of the 20 searches executed a valid first modification, and both then failed for lack of a significant MI representing the second modification.

Results based on Initial model B1 were equally discouraging. For the 20 samples analyzed, results for unrestricted searches matched those for restricted searches since no invalid modifications were made during the unrestricted searches. For the initial model, 14 solutions were improper. For the six proper solutions, two searches failed immediately due to lack of any significant MI's.

Specification Searches

Four searches did execute a valid first modification, but then failed for the lack of further significant MI's.

The results for the analyses of small samples are easy to summarize: there were numerous improper solutions, and all specification searches conducted on proper solutions failed to locate the correct model.

DISCUSSION

A disturbing aspect of the results presented above was the high frequency of Type II decision errors for all types of searches. The author doubts that this occurred as a function of the particular models used here, since similar results were obtained using a variety of other models. Rather, this phenomenon was probably due to a combination of (a) a relatively low level of power for the models and samples employed, and (b) the phenomenon of capitalization on chance in the search process. The first problem could have been alleviated somewhat via the use of larger samples and/or the use of larger true parameter values for the structural paths. Both of these changes would increase the power of the likelihood ratio test for the misspecified models. However, the large sample size of 300 and the structural path coefficients of .4 do not seem particularly low when compared to published applications. The second problem refers again to the fact

Specification Searches

that, since the search process is in part data-driven, there will be a tendency for this process to capitalize on chance and in turn yield inflated measures of fit for modified models.

The most important implication of the common occurrence of Type II errors in the present study is that investigators should not interpret a non-significant χ^2 as a signal to stop a specification search. Given the high frequency of Type II errors found here, along with the fact that the great majority of successful searches were achieved only by continuing the search beyond a model with a non-significant χ^2 , there is a clear indication that stopping searches as soon as a non-significant χ^2 is obtained may greatly reduce the success rate. Thus, it is recommended that, when a model with a non-significant χ^2 is obtained, the investigator still examine MI's and related information to determine whether there exist further modifications which would significantly improve goodness of fit.

Results presented above also serve to demonstrate the tendency for searches to be less successful when initial models contain more specification errors. Models A1, A2, and A3 contain successively more errors, and the number of successful searches using these initial models becomes successively smaller. (Model B1 actually contains more errors than does A3, but yields more successful searches;

however, given the confounding of number of errors with true model, this comparison probably should not be viewed as contradicting the effect being shown.) The author does not suggest that this effect is exhaustively investigated here. Rather, these results can be considered a demonstration of the importance of close correspondence between initial models and true models. A closer correspondence should enhance the likelihood of a successful specification search. It is quite clear that researchers must not proceed by constructing a haphazard initial model and relying on a specification search to lead them to the true model.

Results also reveal the value of a restricted, as opposed to an unrestricted, search strategy. Successful restricted searches outnumbered successful unrestricted searches 7-0 for model A3, and 11-4 for model B1 (for $N=300$). This emphasizes the point that searches have a greater likelihood of success if investigators can employ substantive and theoretical information to help determine whether particular modifications are permissible. Without such restrictions applied in practice, the likelihood of success will be greatly reduced. A very important condition for this conclusion is that a search be allowed to continue even when a model yielding a non-significant χ^2 is obtained. If the search is required to stop when χ^2 becomes non-significant, then the number of successes falls

dramatically, to two for model A3 and zero for model B1.

The results also demonstrate the drastic effect of sample size on the success of specification searches, with all searches failing when sample size was set at 100. It is well known that large samples are needed in covariance structure modeling in order to provide valid use of the χ^2 test and efficient parameter estimates, and to avoid improper and non-convergent solutions (Boomsma, 1983). Present results show that large samples are needed also in order to enhance the likelihood of a successful specification search. Given these results, it would be very difficult to have any confidence in the validity of the outcome of a specification search based on a small sample.

CONCLUSIONS

These findings suggest that there are several things that empirical investigators can do to enhance the likelihood of success in specification searches. These include (a) careful formulation of the initial model, so as to maximize correspondence between it and the true model; (b) use of as large a sample as possible; (c) use of a restrictive search strategy, wherein no model modifications are made without rigorous substantive justification; and (d) a willingness to continue a search beyond the point of finding a model with a nonsignificant χ^2 .

Specification Searches

However, even under these guidelines, researchers should be quite cautious with respect to their confidence in a good-fitting model which is the product of a specification search. Note that, even with correct restrictions, and allowing searches to continue despite non-significant χ^2 's, only about half of the searches reported in Tables 5 and 6 were successful. This is a discouraging result in that it suggests that the outcomes of many, if not most, specification searches in practice may not correspond to correct population models. Thus, investigators should not interpret their final model as if it corresponds to the correct model, and they should attempt to cross-validate their final model by fitting it to an independent sample (Bentler, 1980; Cliff, 1983). Only with a well-designed initial study, a carefully conducted search, and positive cross-validation results can a researcher begin to argue for the validity of a model which has resulted from a specification search. Despite the fact that results based on only a small number of true and misspecified models are presented here, the author wishes to emphasize that similar analyses were conducted using a variety of other models, and that similar results were obtained.

Finally, the author suggests that results presented here may actually represent a "best case" view of specification searches. Initial model misspecifications and

Specification Searches

modifications were limited to the structural portion of the model, and other simplifying assumptions were made, as discussed earlier. It seems likely that a more realistic simulation of misspecifications and more complex searches would introduce complications which would, if anything, reduce the success rate of the searches. Research continues on a number of these issues.

References

- Anderson, J. C., & Gerbing, D. W. (1982). Some methods for respecifying measurement models to obtain unidimensional construct measurement. Journal of Marketing Research, 19, 453-460.
- Bagozzi, R. P. (1983). Issues in the application of covariance structure analysis: A further comment. Journal of Consumer Research, 9, 449-450.
- Bentler, P. M. (1980). Multivariate analysis with latent variables: Causal modeling. Annual Review of Psychology, 31, 419-456.
- Bentler, P. M., & Bonett, D. G. (1980). Significance tests and goodness of fit in the analysis of covariance structures. Psychological Bulletin, 88, 588-606.
- Bentler, P. M., & Huba, G. J. (1979). Simple minitheories of love. Journal of Personality and Social Psychology, 37, 124-130.
- Bentler, P. M., & Speckart, G. (1980). Models of attitude-behavior relations. Psychological Review, 36, 452-464.
- Bentler, P. M., & Weeks, D. G. (1980). Linear structural equations with latent variables. Psychometrika, 45, 289-307.
- Billings, R. S., & Wroten, S. P. (1978). Use of path analysis in industrial/organizational psychology: Criticisms and suggestions. Journal of

Applied Psychology, 63, 677-688.

Boomsma, A. (1983). On the robustness of LISREL (maximum likelihood estimation) against small sample size and non-normality. Amsterdam: Sociometric Research Foundation.

Cliff, N. (1983). Some cautions concerning the application of causal modeling methods. Multivariate Behavioral Research, 18, 115-126.

Costner, H. L., & Schoenberg, R. (1973). Diagnosing indicator ills in multiple indicator models. In A. S. Goldberger & O. D. Duncan (Eds.), Structural equation models in the social sciences. New York: Seminar Press.

Fiske, S. T., Kenny, D. A., & Taylor, S. E. (1982). Structural models for the mediation of salience effects on attribution. Journal of Experimental Social Psychology, 18, 105-127.

Fornell, C. (1983). Issues in the application of covariance structure analysis: A comment. Journal of Consumer Research, 9, 443-448.

Fredricks, A. J., & Dossett, D. L. (1983) Attitude-behavior relations: A comparison of the Fishbein-Ajzen and Bentler-Speckart models. Journal of Personality and Social Psychology, 45, 501-512.

Gallini, J. (1983). Misspecifications that can result in path analysis structures.

Specification Searches

- Applied Psychological Measurement, 7, 125-137.
- Gerbing, D. W., & Anderson, J. C. (1984). On the meaning of within-factor correlated measurement errors. Journal of Consumer Research, 11, 572-580.
- Joreskog, K. G. (1974). Analyzing psychological data by structural analysis of covariance matrices. In R. C. Atkinson, D. H. Krantz, R. D. Luce, & P. Suppes (Eds.) Contemporary developments in mathematical psychology -- Volume II. San Francisco: W. H. Freeman.
- Joreskog, K. G. (1977). Structural equation models in the social sciences: Specification, estimation, and testing. In P. R. Krishnaiah (Ed.), Applications of statistics. Amsterdam: North-Holland Publishing Co.
- Joreskog, K. G., & Sorbom, D. (1984). LISREL VI user's guide. Mooresville, Indiana: Scientific Software, Inc.
- Kaiser, H. F., & Dickman, K. (1962). Sample and population score matrices and sample correlation matrices from an arbitrary population correlation matrix. Psychometrika, 27, 179-182.
- Leamer, E. E. (1978). Specification searches: Ad hoc inference with non-experimental data. New York: Wiley.
- Long, J. S. (1983). Covariance structure models: An introduction to LISREL.

Beverly Hills, California: Sage Publications, Inc.

Maruyama, G., & McGarvey, B. (1980). Evaluating causal models: An application of maximum likelihood analysis of structural equations. Psychological Bulletin, 87, 502-512.

McAlister, A. L., Krosnick, J. A., & Milburn, M. A. (1984). Causes of adolescent cigarette smoking: Tests of a structural equation model. Social Psychology Quarterly, 47, 24-36.

McArdle, J., & McDonald, R. P. (1984). Some algebraic properties of the reticular action model for moment structures. British Journal of Mathematical and Statistical Psychology, 37, 234-254.

Saris, W. E., dePijper, W. M., & Zegwaard, P. (1979). Detection of specification errors in linear structural equation models. In K. F. Schuessler (Ed.), Sociological Methodology 1979: San Francisco: Josey Bass.

Saris, W. E., & Stronkhorst, L. H. (1984). Causal modeling in nonexperimental research: An introduction to the LISREL approach. Amsterdam: Sociometric Research Foundation.

Smith, E. R. (1982). Beliefs, attributions, and evaluations: Nonhierarchical models of mediation in social cognition. Journal of Personality and Social

Specification Searches

Psychology, 43, 248-259.

Specification Searches

Table 1
Population Covariance Matrices for Models A and B

Model A											
Y1	Y2	Y3	Y4	X1	X2	X3	X4	X5	X6		
Y1	1.868										
Y2	1.014	1.412									
Y3	1.019	.815	2.128								
Y4	.815	.652	1.223	1.578							
X1	.640	.512	.776	.621	1.600						
X2	.512	.410	.621	.497	.800	1.240					
X3	.640	.512	.776	.621	.300	.240	1.600				
X4	.512	.410	.621	.497	.240	.192	.900	1.240			
X5	.640	.512	.496	.397	.300	.240	.300	.240	1.600		
X6	.512	.410	.397	.317	.240	.192	.240	.192	.800	1.240	

Model B													
Y1	Y2	Y3	Y4	Y5	Y6	Y7	Y8	X1	X2	X3	X4		
Y1	1.590												
Y2	.784	1.227											
Y3	.392	.314	1.257										
Y4	.314	.251	.525	1.020									
Y5	.157	.125	.263	.210	1.205								
Y6	.125	.100	.210	.168	.484	.987							
Y7	.063	.050	.105	.084	.242	.194	1.197						
Y8	.050	.040	.084	.067	.194	.155	.477	.982					
X1	.600	.480	.240	.192	.096	.077	.038	.031	1.600				
X2	.480	.384	.192	.154	.077	.061	.031	.025	.800	1.240			
X3	.600	.480	.240	.192	.096	.077	.038	.031	.500	.400	1.600		
X4	.480	.384	.192	.154	.077	.061	.031	.025	.400	.320	.800	1.24	

Specification Searches

Table 2
Unrestricted Specification Search Histories for Initial Models A1 and A2

Sample	Initial Model A1			Initial Model A2			
	χ^2 prob	Sig MI's	Step 1 χ^2 prob	χ^2 prob	Sig MI's	Step 1 χ^2 prob	Nonsig T's
1	.050	γ_{22}	.494	.000	γ_{22}	.195	γ_{23}
2	.099	γ_{22}	.318	.069	γ_{22}	.411	γ_{23}
3	.001	γ_{22}, β_{12}	.496	.054	γ_{22}	.573	γ_{23}
4	.009	γ_{22}, β_{12}	.189	.008	γ_{22}	.592	β_{21}, γ_{23}
5	.005	γ_{22}	.648	.002	γ_{22}	.088	γ_{23}
6	.050	γ_{22}	.311	.040	----		γ_{23}
7	.001	γ_{22}, γ_{23}	.375	.000	γ_{22}	.018	γ_{23}
8	.008	$\gamma_{22}, \beta_{12}, \gamma_{23}$.985	.024	γ_{22}	.303	γ_{23}
9	.000	$\gamma_{22}, \gamma_{23}, \beta_{12}$.244	.604	γ_{22}	.907	γ_{23}
10	.000	γ_{22}, β_{12}	.725	.581	γ_{22}	.979	γ_{23}
11	.107	γ_{22}	.566	.283	γ_{22}	.859	γ_{23}
12	.084	γ_{22}	.924	.011	γ_{22}	.088	γ_{23}
13	.100	γ_{22}, β_{12}	.761	.291	γ_{22}	.853	γ_{23}
14	.027	γ_{22}, β_{12}	.645	.421	γ_{22}	.968	γ_{23}
15	.119	β_{12}	.678	.289	γ_{22}	.730	γ_{23}
16	.012	γ_{22}, β_{12}	.342	.007	γ_{22}	.194	γ_{23}
17	.021	γ_{22}, β_{12}	.393	.449	γ_{22}	.793	γ_{23}
18	.192	γ_{22}	.622	.179	γ_{22}	.711	γ_{23}
19	.018	γ_{22}, β_{12}	.236	.215	γ_{22}	.523	γ_{23}
20	.031	γ_{22}, β_{12}	.493	.048	γ_{22}	.244	γ_{23}

Specification Searches

Table 3
Unrestricted Specification Search Histories for Initial Model A3

Sample	Initial		Step 1		Nonsig T's
	χ^2 prob	Sig MI's	χ^2 prob	Sig MI's	
1	.008	β_{12}	.453	-----	γ_{23}
2	.050	β_{12}	.931	-----	γ_{23}
3	.000	β_{12}, γ_{22}	.328	-----	β_{12}
4	.001	$\beta_{12}, \gamma_{21}, \gamma_{22}$.361	-----	β_{12}
5	.007	β_{12}, γ_{21}	.653	-----	γ_{23}
6	.429	-----			-----
7	.012	β_{12}	.123	-----	β_{12}
8	.000	β_{12}, γ_{21}	.339	-----	-----
9	.003	β_{12}, γ_{22}	.224	-----	-----
10	.000	β_{12}, γ_{22}	.012	-----	$\beta_{12}, \gamma_{11}, \gamma_{12}, \gamma_{13}$
11	.027	β_{12}	.789	-----	$\beta_{12}, \gamma_{11}, \gamma_{12}, \gamma_{13}$
12	.031	β_{12}, γ_{21}	.743	-----	β_{12}, γ_{23}
13	.018	β_{12}, γ_{22}	.250	-----	β_{12}
14	.011	β_{12}, γ_{21}	.526	-----	$\beta_{12}, \gamma_{11}, \gamma_{12}, \gamma_{13}, \gamma_{23}$
15	.002	β_{12}	.104	-----	β_{12}
16	.051	β_{12}	.983	-----	$\beta_{12}, \gamma_{11}, \gamma_{12}, \gamma_{13}$
17	.284	β_{12}	.772	-----	β_{12}
18	.066	β_{12}	.479	-----	β_{12}
19	.080	β_{12}	.586	-----	$\beta_{12}, \gamma_{11}, \gamma_{12}$
20	.027	β_{12}	.428	-----	β_{12}

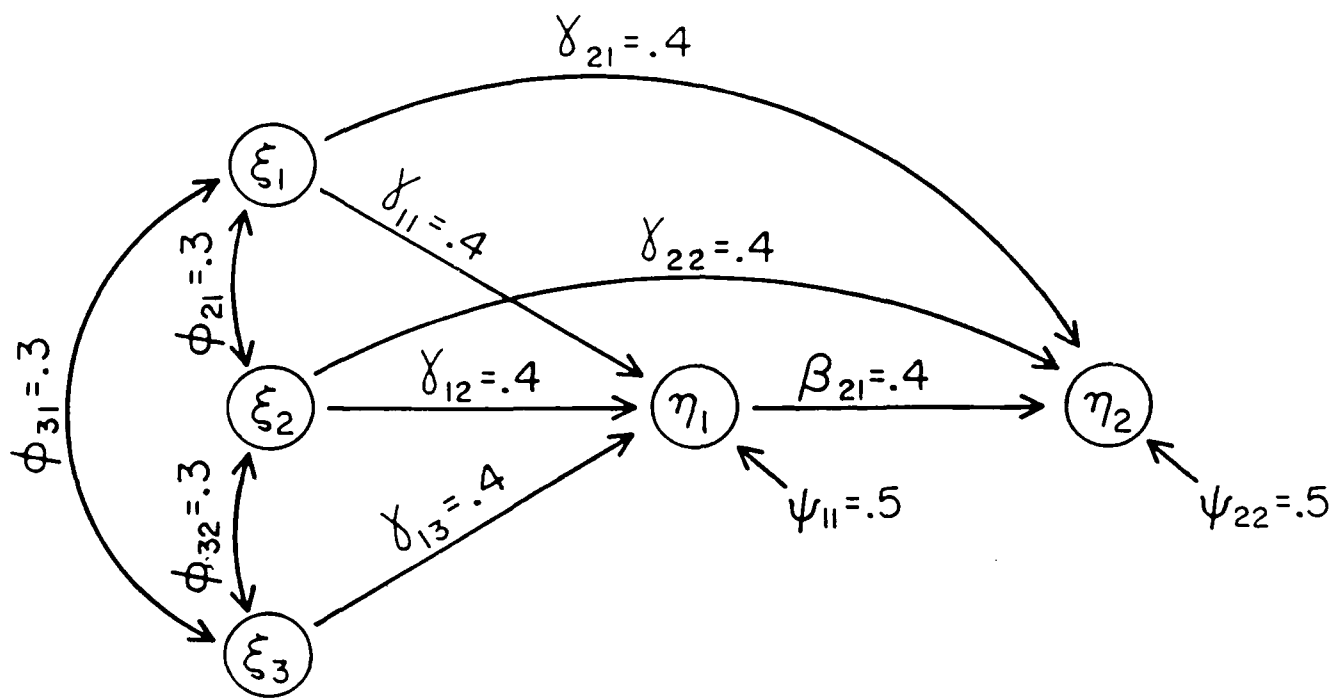
Specification Searches

Table 4
Unrestricted Specification Search Histories for Initial Model B1

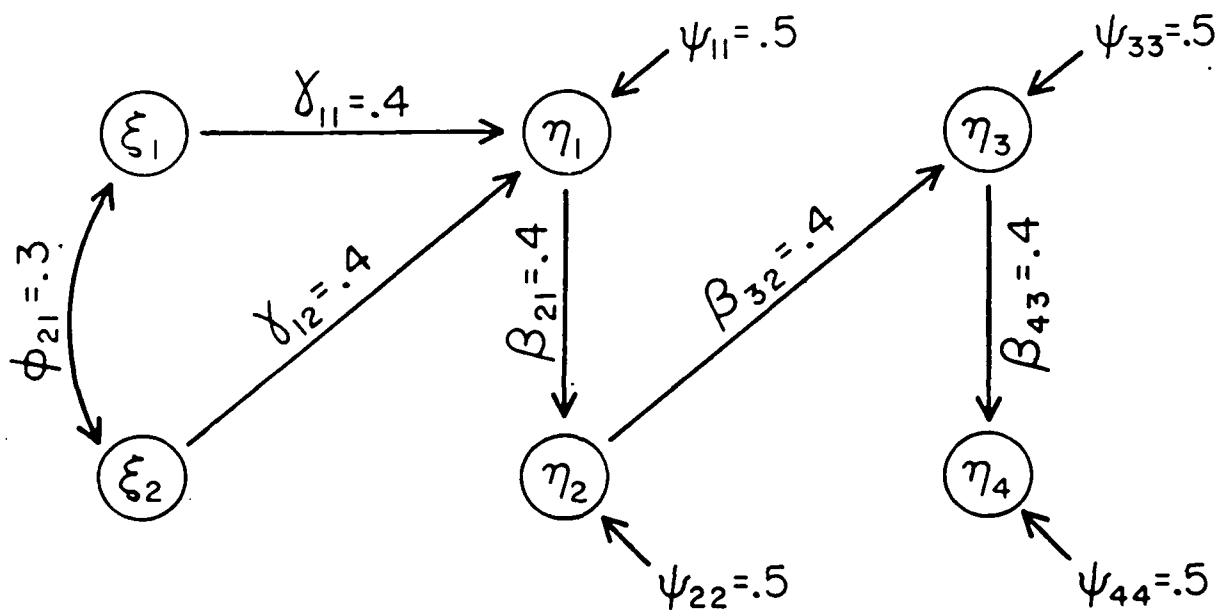
Sample	Initial		Step 1		Step 2	
	χ^2 prob	Sig MI's	χ^2 prob	Sig MI's	χ^2 prob	Nonsig T's
1	.006	$\beta_{23}, \beta_{21}, \beta_{32}$.270	β_{21}, β_{12}	.688	γ_{22}
2	.051	$\beta_{23}, \beta_{32}, \beta_{21}$.286	β_{21}	.505	β_{31}, γ_{22}
3	.022	$\beta_{23}, \beta_{32}, \beta_{12}$.402	β_{21}, β_{12}	.771	β_{31}, γ_{22}
4	.018	$\beta_{32}, \beta_{23}, \beta_{21}$.542	β_{21}, β_{12}	.834	β_{31}, γ_{22}
5	.013	$\beta_{21}, \beta_{23}, \gamma_{21}$.143	β_{23}, β_{32}	.366	β_{31}, γ_{22}
6	.000	$\beta_{21}, \beta_{12}, \beta_{23}$.309	$\beta_{32}, \beta_{23}, \gamma_{41}$.775	β_{31}, γ_{22}
7	.045	β_{21}, β_{12}	.650	----		γ_{22}
8	.059	$\beta_{21}, \beta_{12}, \beta_{23}$.697	----		γ_{22}
9	.001	$\beta_{23}, \beta_{32}, \beta_{21}$.414	----		-----
10	.138	$\beta_{23}, \beta_{32}, \beta_{21}$.858	β_{21}	.982	-----
11	.002	$\beta_{21}, \beta_{12}, \beta_{32}$.258	β_{32}, β_{23}	.629	β_{31}, γ_{22}
12	.000	$\beta_{12}, \beta_{21}, \beta_{23}$.001	----		-----
13	.002	$\beta_{21}, \beta_{12}, \beta_{23}$.154	β_{32}, β_{23}	.584	β_{31}, γ_{22}
14	.165	β_{12}, β_{21}	.546	----		-----
15	.000	$\beta_{21}, \beta_{12}, \beta_{23}$.208	β_{23}	.410	γ_{22}
16	.000	$\beta_{21}, \beta_{12}, \gamma_{21}$.222	----		γ_{22}
17	.031	$\beta_{23}, \beta_{32}, \beta_{12}$.691	β_{12}, β_{32}	.950	β_{32}
18	.002	$\beta_{21}, \beta_{12}, \beta_{23}$.245	β_{23}, β_{32}	.487	γ_{22}
19	.574	β_{32}, β_{23}	.993	----		-----
20	.007	$\beta_{21}, \gamma_{21}, \beta_{23}$.338	----		γ_{22}

Table 5
Restricted Specification Search Histories for Initial Model A3

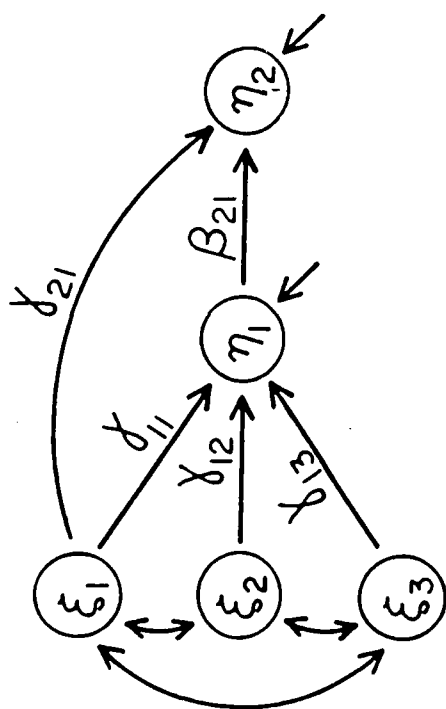
Sample	Initial		Step 1		Step 2	
	χ^2 prob	Sig MI's	χ^2 prob	Sig MI's	χ^2 prob	Nonsig T's
1	.008	----				Y_{23}
2	.050	----				----
3	.000	Y_{22}	.016	Y_{21}	.482	Y_{23}
4	.001	Y_{21}, Y_{22}	.025	Y_{22}	.313	Y_{23}
5	.007	Y_{21}	.238	Y_{22}	.771	----
6	.429	----				----
7	.012	----				----
8	.000	Y_{21}	.075	Y_{22}	.370	Y_{23}
9	.003	Y_{22}	.104	Y_{21}	.364	Y_{12}, Y_{23}
10	.000	Y_{22}	.004	Y_{21}	.018	Y_{23}
11	.027	----				----
12	.031	Y_{21}	.506	Y_{22}	.845	Y_{23}
13	.018	Y_{22}	.249	----		----
14	.011	Y_{21}	.203	Y_{22}	.561	Y_{23}
15	.002	----				----
16	.051	----				----
17	.284	----				----
18	.066	----				----
19	.080	----				----
20	.027	----				----



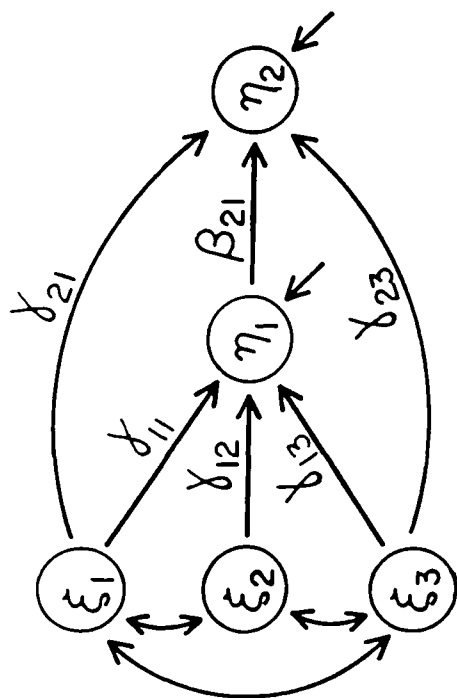
Model A



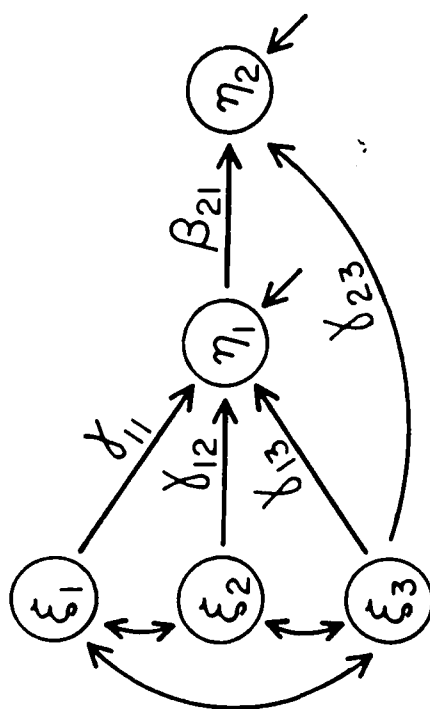
Model B



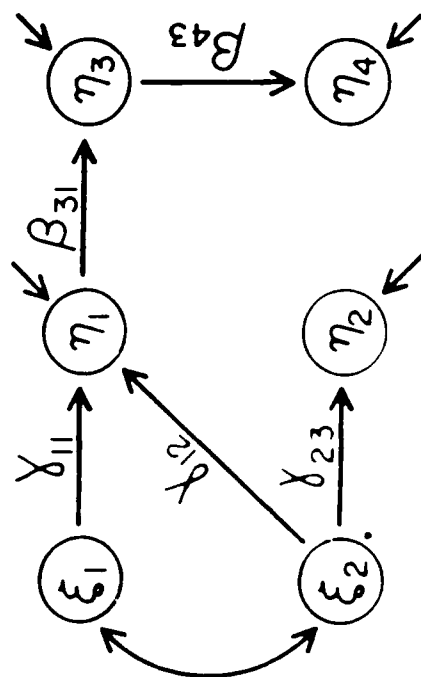
Model A1



Model A2



Model A3



Model B1

Specification Searches

Table 6
Restricted Specification Search Histories for Initial Model B1

Sample	Initial		Step 1		Step 2	
	χ^2 prob	Sig. MI's	χ^2 prob	Sig. MI's	χ^2 prob	Nonsig. T's
1	.006	β_{21}, β_{32}	.101	β_{32}	.694	β_{31}, γ_{22}
2	.051	β_{32}, β_{21}	.314	-----		β_{31}
3	.022	β_{32}, β_{21}	.373	β_{21}	.770	β_{31}, γ_{22}
4	.019	β_{32}, β_{21}	.542	β_{21}	.834	β_{31}, γ_{22}
5	.013	β_{21}	.143	β_{32}	.321	β_{31}, γ_{22}
6	.000	β_{21}, β_{32}	.309	β_{32}	.775	β_{31}, γ_{22}
7	.045	β_{21}	.650	-----		γ_{22}
8	.059	β_{21}	.697	-----		γ_{22}
9	.001	β_{32}, β_{21}	.261	β_{21}	.629	β_{31}, γ_{22}
10	.138	β_{32}, β_{21}	.752	β_{21}	.983	β_{31}, γ_{22}
11	.002	β_{21}, β_{32}	.258	β_{32}	.629	β_{31}, γ_{22}
12	.000	β_{21}	.001	-----		γ_{22}
13	.002	β_{21}, β_{32}	.154	β_{32}	.584	β_{31}, γ_{22}
14	.165	β_{21}	.532	-----		γ_{22}
15	.000	β_{21}, β_{32}	.208	-----		γ_{22}
16	.000	β_{21}	.222	-----		γ_{22}
17	.031	β_{32}, β_{21}	.457	β_{21}	.878	β_{31}, γ_{22}
18	.002	β_{21}, β_{32}	.245	β_{32}	.483	β_{31}, γ_{22}
19	.574	β_{32}	.971	-----		β_{31}
20	.007	β_{21}	.338	-----		γ_{22}

Specification Searches

Figure Captions

Figure 1. True population models A and B

Figure 2. Misspecified initial models

FINAL REPORT

TO

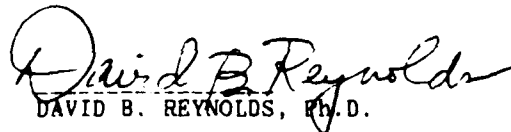
The Southeastern Center for Electrical Engineering Education (SCEEE)

Title: "A Computational Model of the Human Cardiopulmonary System"

Subcontract No.: 84 RIP 46 between SCEEE and Wright State University.

Date: December 12, 1985

By:



DAVID B. REYNOLDS, Ph.D.

Department of Biomedical Engineering

Wright State University

Dayton, OH 45435

ABSTRACT

A non-linear computational model of ventilation distribution in the human lung has been developed. The model is a two alveolar compartment model incorporating compliance, resistance, and inertance elements. Inertance elements are needed to extend the predictions of the model to include ventilation distribution during high frequency mechanical ventilation, which is a recent therapeutic modality. At normal breathing frequency, i.e. less than 1 breath per second, inertance can be neglected and resistance and compliance elements determine ventilation and its distribution to the two compartments. A strong dependence of ventilation distribution on the functional residual capacity of the lung is shown. As frequency is increased above 1 breath per second, the effects of inertance elements become increasingly important. At frequencies representative of high frequency ventilation, ventilation distribution is strongly affected by driving pressure amplitude, resulting in more ventilation to the upper compartment at low driving pressure amplitudes with increasing lower compartment ventilation as driving pressure amplitude is increased. High frequency pendelluft or gas mixing between alveolar compartments is also predicted by the model. These predictions are in qualitative agreement with recent experimental observations.

INTRODUCTION

There has been a growing interest in pulmonary ventilation and its distribution in the lungs under normal and abnormal situations. Of particular current interest are ventilation distribution and gas exchange during mechanical ventilation by high frequency oscillation (4,20). Consequently, in a first attempt to extend previous ventilation modeling (5,6,12,19) to include higher frequencies and flow amplitudes, we present the model which is to follow.

This research began as an effort to improve, update and generally build upon cardiopulmonary models developed by Collins and co-workers (6). This phase of the research has concentrated on improving their pulmonary ventilation model. We believe the following model is conceptually much "cleaner" and much less cumbersome to use and interpret than the one originally presented (6). Our criticism of their model has been presented elsewhere (18). In addition, we have added elements to the model which allow application and prediction of events during high frequency ventilation, a topic of considerable current interest. Of course, this is a first attempt and we anticipate refinements in the model in the future. Our lack of knowledge of regional properties in the tracheobronchial tree and alveolar spaces is one area in which additional research is direly needed. In addition to regional resistances and compliances of bronchial segments, we can now add regional inertances to the list, since these become important in high frequency ventilation. Unfortunately, the bronchial tubes do not behave as straight tubes, for which much engineering information is known. In this respect, the field of biomedical engineering has added much to the knowledge

base of flows in complex branching systems since they are seen so much in physiological systems. The physics of unsteady flow has also seen a contribution from biomedical engineering as well, and will continue to do so in the future when computational methods will be the predominant research and design tool.

MODELS AND METHODS

Because the six alveolar compartment pulmonary ventilation model originally proposed by Collins et al (6) is redeveloped here to include inertance elements as well as resistance and compliance elements, a simpler two alveolar compartment model is presented here. The present model builds on the ventilation model of Shykoff and co-workers (19) and Chang and Shykoff (5) which is applicable to normal (low frequency) ventilation.

Two Alveolar Compartment Model

The two alveolar compartment model is shown in Fig. 1. Upper and lower alveolar compartments (i.e., upper and lower in the normal upright posture) having compliances C_2 and C_1 are connected to two bronchial compartments having flow resistances R_2 and R_1 and inertances L_2 and L_1 , respectively. The latter parallel compartments are in series with a central bronchial compartment having resistance R_c and inertance L_c . The alveolar compliances C_1 and C_2 are computed as the slope of the transpulmonary pressure-volume curve of the lung, which is modeled by the hyperbolic-sigmoid relationship given by Murphy and Engel (11). For each alveolar compartment:

$$P = \frac{\Lambda_1}{V_{\max} - V^*} + \frac{\Lambda_2}{V_{\min} - V^*} + \Lambda_3 \quad (1)$$

Where P is regional transpulmonary pressure, i.e. compartment alveolar pressure minus pleural pressure, (i.e., pressure in the pleural space

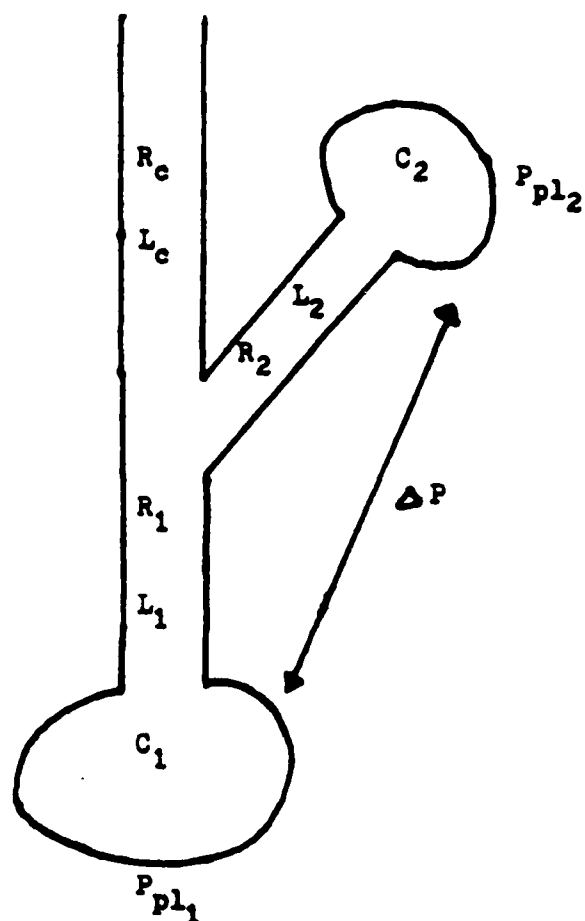


FIGURE 1. TWO COMPARTMENT MODEL GEOMETRY.

surrounding the lungs), $V^* = 100(V - RV)/VC$, V is alveolar compartment volume, RV is compartment residual volume and VC is compartment vital capacity. V_{\max} , V_{\min} , λ_1 , λ_2 , λ_3 are constants used to fit experimental pressure-volume data. We used the values suggested by Shykoff et al (19), i.e. $V_{\max} = 135\%$, $V_{\min} = -2.0\%$, $\lambda_1 = 1500 \text{ cmH}_2\text{O}$, $\lambda_2 = 50 \text{ cmH}_2\text{O}$ and $\lambda_3 = -8.5 \text{ cmH}_2\text{O}$.

The same pressure-volume (P-V) relationship is used for each compartment, which is shown in Fig. 2. However, due to the nonlinear P-V curve and the fact that transpulmonary pressures are different in the two alveolar compartments due to the pleural pressure gradient, the compliance of the alveolar compartments are different. For the two alveolar compartment model, the pleural pressure of the lower compartment is $2 \text{ cmH}_2\text{O}$ greater than that of the upper compartment. However, this gravity-dependent pressure difference is a parameter of the model and may be adjusted. As a result of this pleural pressure difference, the following regional lung volumes result:

$$RV_1 = 0.684 \text{ l}; \quad VC_1 = 2.916 \text{ l}; \quad FRC_1 = 1.52 \text{ l}$$

$$RV_2 = 1.044 \text{ l}; \quad VC_2 = 2.556 \text{ l}; \quad FRC_2 = 2.18 \text{ l}$$

where FRC is functional residual capacity. These volumes were computed as the product of regional percentage volumes experimentally found by Milic-Emili (9,10) and the corresponding lung subdivisions found by Gibson et al (8) in normal young men. Note that the RV , VC , and FRC of the entire lung can be found by summing the contribution from each compartment. Regional total lung capacity (TLC_r) is by definition the sum of regional RV and VC . TLC of the entire lung is the sum of the TLC_r . Note also that the $TLC_r = 3.6 \text{ l}$ for each of the two compartments, thus the TLC of the entire lung is 7.2 l . Thus the

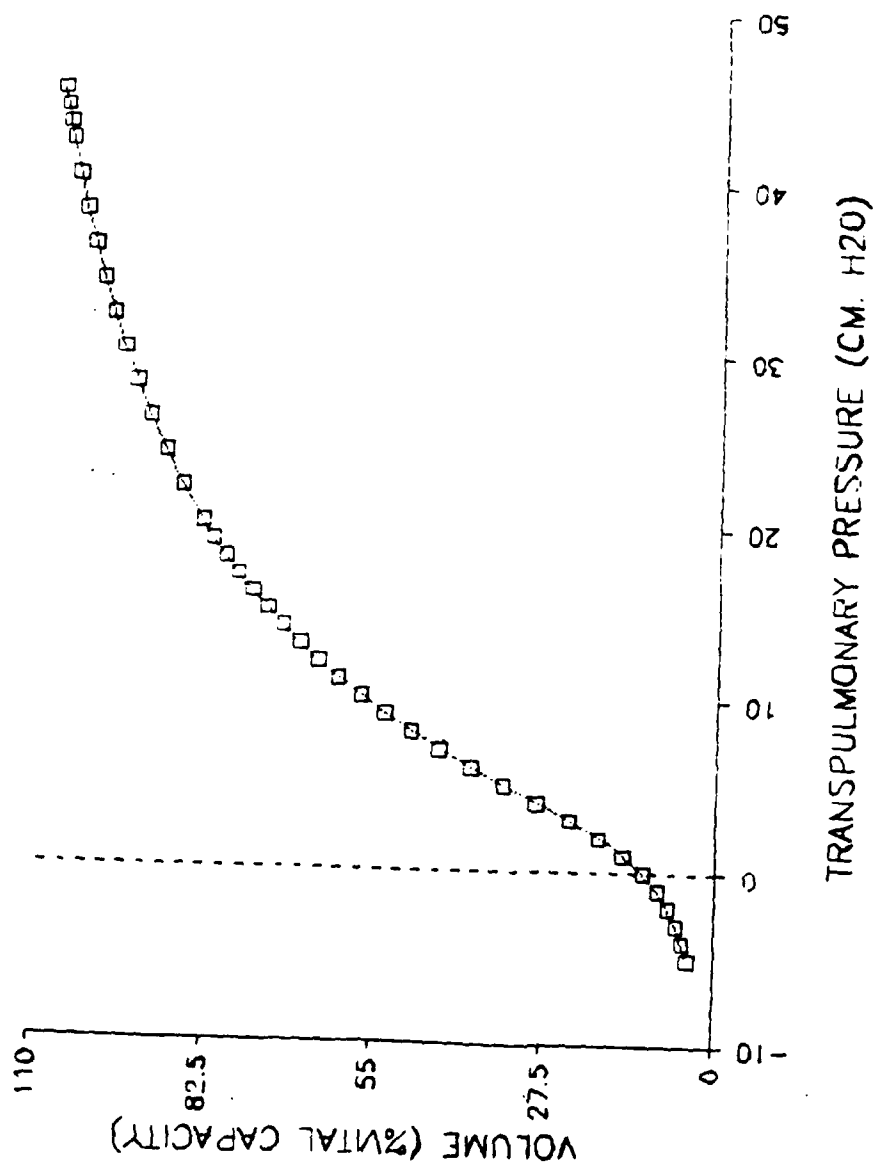


FIGURE 2. STATIC PRESSURE-VOLUME CURVE OF MURPHY AND ENGEL.

only point at which the two alveolar compartments have the same volume is at TLC. This is consistent with the static lung volume studies of Milic-Emili (9,10).

Bronchial flow resistances R_1 and R_2 were modeled by a modified Rohrer's equation. Rohrer's equation is a pressure-flow relationship of the airways in which a flow squared term accounts for turbulent losses and pressure differences due to convective acceleration and linear term in accounts for pressure drop in laminar flow. While we have shown in past studies (15,16,17) that Rohrer's equation is applicable to bronchial pressure flow relationships, the interpretation of the two terms as being due to laminar and turbulent losses is probably not valid. In all likelihood the laminar pressure losses are probably in the linear term and some of the flow squared term. However, Rohrer's equation is generally accepted as a convenient empirical relation. For R_1 and R_2 , the resistance equation is given by

$$R [\text{cm H}_2\text{O} \cdot \text{s} \cdot \text{l}^{-1}] = \frac{0.3 + 0.4 \dot{V} [\text{l/s}]}{0.17 + 0.3 V [\text{l}]} \quad (2)$$

where \dot{V} is the local flow rate and V is the volume of the corresponding alveolar compartment and the quantities in brackets indicate the units for which the equation is valid. The denominator function in volume is attributed to Blide and coworkers (2). The central resistance is given by

$$R_c [\text{cm H}_2\text{O} \cdot \text{s} \cdot \text{l}^{-1}] = 0.3 + 0.4 \dot{V}_c [\text{l/s}] \quad (3)$$

where \dot{V}_c is the flow rate in the central airway. These equations were also used by Chang and Shyoff (5) and Shyoff et al (19) in their two alveolar compartment model of ventilation distribution.

Inertance of bronchial tubes has been little investigated (13). Presumably, the inertance is mostly dependent on the gas inertance in

bronchial tubes (13). In any case, we used the following inertance values suggested by some recent experimental work in the human respiratory tract (14):

$$L_c = 0.0035 \quad ; \quad L_1 = 0.005 \quad ; \quad L_2 = 0.005.$$

The units for inertances above are $\text{cm H}_2\text{O} \cdot \text{s}^2 \cdot \text{l}^{-1}$

The system was driven with a sinusoidal pleural pressure. This was done to simulate actual breathing at low driving frequencies or forced oscillation at higher frequencies.

The following differential equations can be derived for the two alveolar compartment model.

$$\frac{dP_1}{dt} = R_c \frac{d\dot{V}_c}{dt} + L_c \frac{d^2\dot{V}_c}{dt^2} + R_1 \frac{d\dot{V}_1}{dt} + L_1 \frac{d^2\dot{V}_1}{dt^2} + \frac{\dot{V}_1}{C_1} \quad (4a)$$

$$\frac{dP_2}{dt} = R_c \frac{d\dot{V}_c}{dt} + L_c \frac{d^2\dot{V}_c}{dt^2} + R_2 \frac{d\dot{V}_2}{dt} + L_2 \frac{d^2\dot{V}_2}{dt^2} + \frac{\dot{V}_2}{C_2} \quad (4b)$$

$$\frac{d\dot{V}_c}{dt} = \frac{d\dot{V}_1}{dt} + \frac{d\dot{V}_2}{dt} \quad (4c)$$

$$\frac{d^2\dot{V}_c}{dt^2} = \frac{d^2\dot{V}_1}{dt^2} + \frac{d^2\dot{V}_2}{dt^2} \quad (4d)$$

where $P_{1,2} \equiv P_{pe_{1,2}} - P_m$, the overall pressure difference across the system, i.e., the differences between the compartmental pleural and mouth pressures for the two pathways. Equations (4a, b) result from equating the overall pressure difference to the sum of the pressure differences across elements of the model along the two pathways. Equations (4c, d) are based on mass balance for an incompressible fluid. Thus, the model assumes that the gas is incompressible. This assumption is reasonable as long as the amplitude of pressure fluctuations are a small fraction of atmospheric pressure. Assuming

incompressibility of the air passages is probably more important to consider and will be discussed later.

The above equations were combined to produce two second order differential equations in \dot{V}_1 and \dot{V}_2 . Initial conditions for \dot{V}_1 , \dot{V}_2 , $d\dot{V}_1/dt$ and $d\dot{V}_2/dt$ were set at zero. The system of equations was solved numerically using an Adams-Bashford integration scheme (1).

RESULTS AND DISCUSSION

At low frequencies of pleural pressure driving, our results should be similar to those of Chang and Shykoff (5) and Shykoff et al (19). However, the latter investigators did not report values for vital capacity (VC), residual volume (RV), and functional residual capacity (FRC) of each alveolar compartment. Indeed, the two studies referred to above presumably used different values of whole lung FRC (3.7l in (5) vs. 2.8l in (19)) yet similar results were obtained. Our results indicate that very different results should occur, even for a smaller difference in total FRC. It should be reiterated that compartmental RV and VC are needed to set limits for the transpulmonary pressure-volume curve (P-V curve) of a compartment via Eq. (1) and regional FRC defines the equilibrium state of a compartment on the P-V curve.

Normal whole lung FRC in the upright posture range between 30 and 55% of the TLC, with normal values in males of about 42% of TLC (22). To illustrate the effect of whole lung FRC on ventilation distribution at low frequencies, we chose FRC's of 3.06 liters and 3.7 liters, corresponding to 43% and 51% of the TLC. The smaller FRC was partitioned between the two compartments in the same proportion as was for the larger value, which is reported in the Methods section.

To quantify ventilation distribution, the ratio of tidal volume of the upper to lower compartments was computed from the numerical solution. Tidal volume is the amount of gas volume that enters and leaves an alveolar compartment over a cycle.

Fig. 3 shows tidal volume ratio as a function of driving pleural pressure amplitude for the two values of FRC at a breathing frequency of 0.25 Hz or 15 breaths/min. As reported by Shykoff et al (19), the tidal volume ratio for an FRC = 3.7l is nearly invariant with pleural pressure amplitude. However, a striking dependence of tidal volume ratio on FRC is readily seen. Apparently, Shykoff et al (19) did not study the effect of even normal variations in FRC on tidal volume distribution.

The phenomena presented in Fig.3 has been explained qualitatively by West (21). Briefly, because the pleural pressure is greater (i.e., less negative) at the basal region than at the apical region of the lungs, the expanding pressure, i.e., alveolar pressure minus pleural pressure, is smaller. The lower region thus has a smaller resting volume (FRC) but it lies on a steeper portion of the sigmoid-shaped P-V curve (Fig. 1). Thus, the compliance (slope of the P-V curve) is greater for the basal region. In contrast, due to the lower pleural pressure in the apical lung, the expanding pressure is greater but the P-V curve is flatter. This results in a larger regional FRC for the apical region but a lower compliance. Since compliance of the alveolar regions controls ventilation distribution at low pleural pressure driving frequencies and amplitudes, the basal region expands more than the apical region.

This results in tidal volume ratio of upper to lower regions of less than unity, as shown in Fig. 3 for FRC = 3.7l. For the smaller FRC = 3.06l, the

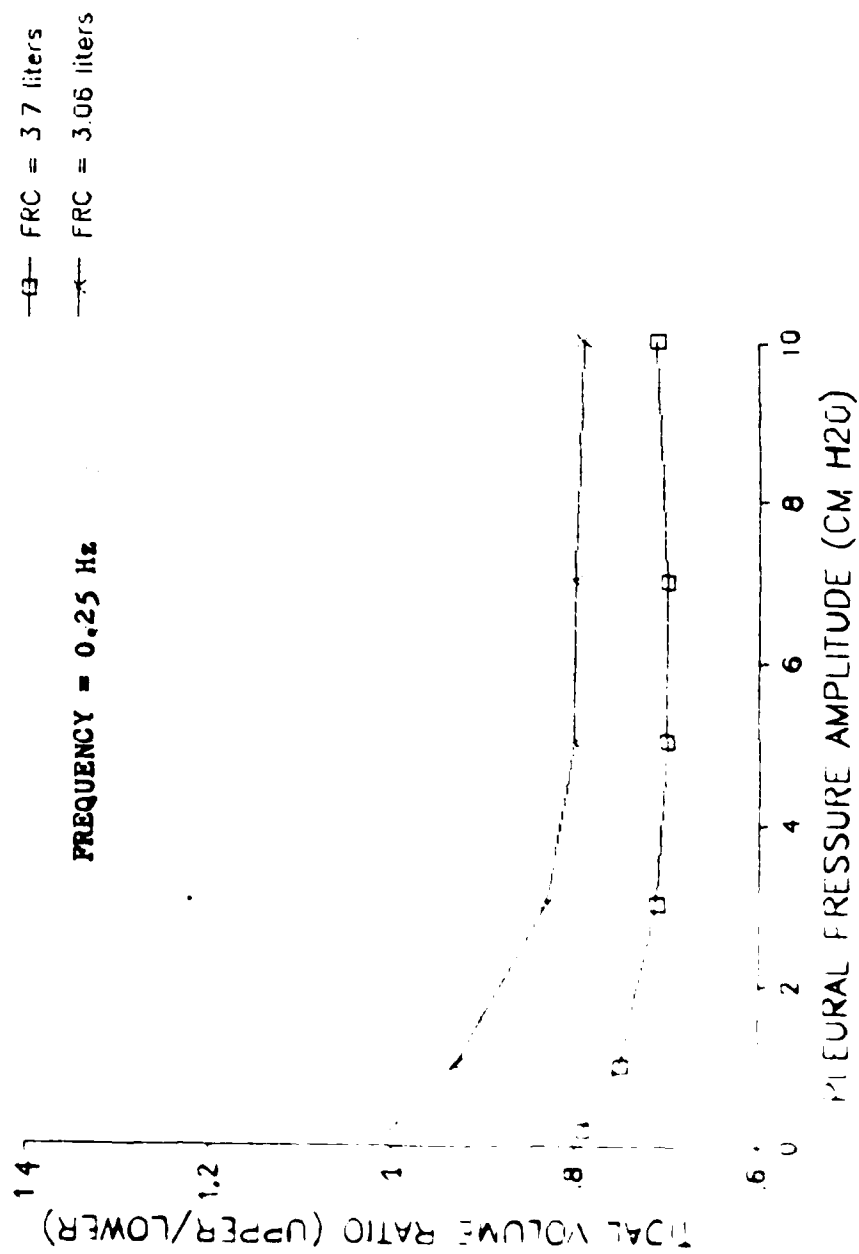


FIGURE 1. TWO COMPARTMENT MODEL RESULTS OF TIDAL VOLUME RATIO VERSUS PLEURAL PRESSURE AMPLITUDE.

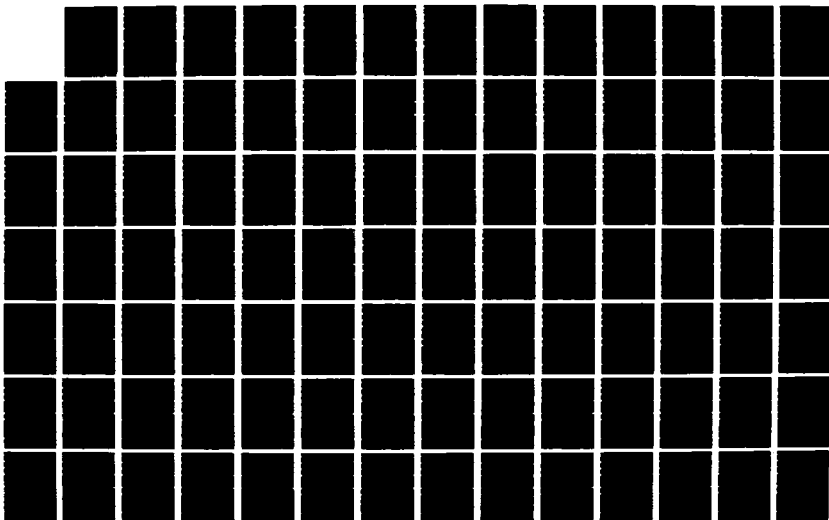
AD-A187 859

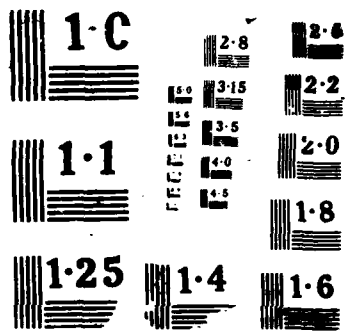
UNITED STATES AIR FORCE RESEARCH INITIATION PROGRAM
1984 RESEARCH REPORTS (U) SOUTHEASTERN CENTER FOR
ELECTRICAL ENGINEERING EDUCATION INC S W D PEELE
MAY 86 AFOSR-TR-87-1722 FF9628-82-C-8835 F/G 7/2

06/10

UNCLASSIFIED

ML





regions have compliances which are closer to being equal. This results from the upper region moving to a point on the P-V curve which is steeper while the lower region moves to a less steep point than for the higher FRC case. The tidal volume ratio thus approaches unity at low driving pressure amplitudes.

For frequencies above 1 breath/sec (1 Hz), inertance must be included. This observation is based on running the model with and without the inertance terms and comparing results. Above 1 Hz, the tidal volume ratios with and without inertance elements began to differ by more than 10%. The values of inertance chosen produced a 4.5 Hz resonant frequency of the system when driven at the smallest pleural pressure amplitudes. Driving the system at small pressure amplitudes produced a nearly linear system, for which a resonant frequency is clearly defined. The resulting resonant frequency is in agreement with reported values (13). High frequency results reported below were obtained after initial transients had died out, i.e., steady state oscillation.

Fig. 4 shows the effects of the driving pleural pressure frequency and amplitude on tidal volume ratio. Frequency appears to have only a small effect on tidal volume ratio at a constant pleural pressure amplitude. Lower driving pressure amplitudes show a tendency for tidal volume ratio to decrease with frequency while higher amplitudes show a trend toward increasing tidal volume ratio with frequency. In all cases, more uniform distribution of ventilation occurs than was seen at lower frequencies. Similar results have been shown by Brusasco and coworkers during high frequency ventilation in dogs (3). However, studies such as the latter usually keep tidal volume entering the lungs nearly constant while frequency is adjusted to find a near optimal gas exchange performance. Consequently, driving pressure amplitude would

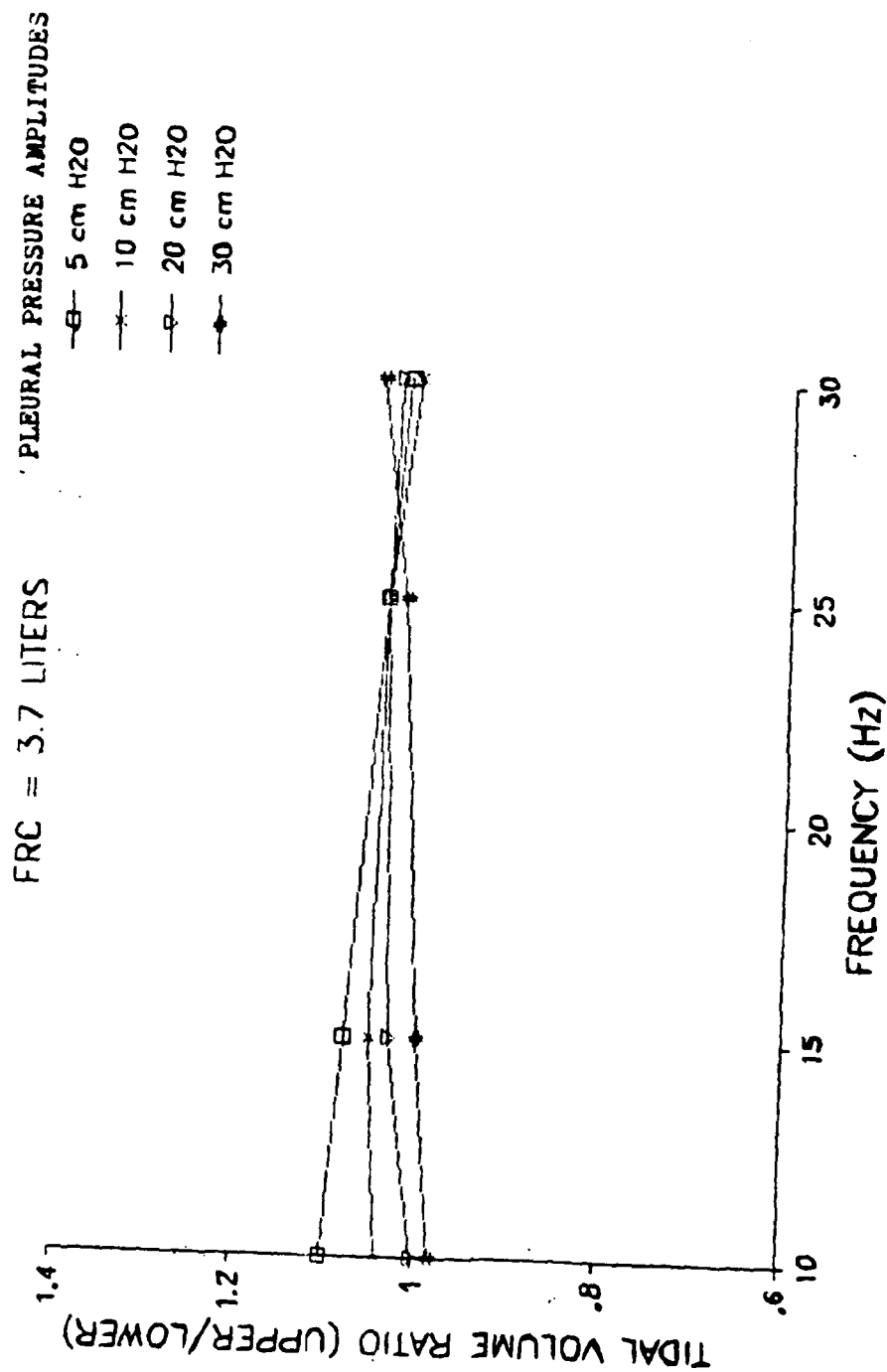


FIGURE 4 • TWO COMPARTMENT MODEL RESULTS OF TIDAL VOLUME RATIO VERSUS FREQUENCY DURING HIGH FREQUENCY ANALYSIS.

increase with frequency to maintain the tidal volume. A logical next study would be to look at tidal volume ratio as a function of frequency at several constant levels of total tidal volume delivered to the central bronchus. This study would better simulate ventilation distribution during mechanical ventilation by high frequency oscillation.

The effect of pleural pressure amplitude on tidal volume ratio for a constant frequency of 10 Hz is shown in Fig. 5. Since increasing pleural pressure amplitude at a given frequency produces an increase in the tidal volume delivered (it does so in a nonlinear way due to the nonlinear system), Fig. 5 can also be viewed as a plot of tidal volume ratio versus tidal volume delivered to the central bronchus. This result demonstrates a fairly strong decrease in the tidal volume ratio with increasing pleural pressure amplitude. This curve is similar in shape to the low frequency results of Fig. 3, but is shifted considerably upwards such that tidal volume ratios of considerably greater than unity result for pleural pressure amplitudes below 10 cm H₂O. This phenomenon has been observed in dogs by Fredberg and coworkers (7). They observed that "at high frequencies, distension of the lung apex is favored when tidal volume is small, whereas distension of the lung base is favored when tidal volume approaches or exceeds dead space".

High frequency pendelluft is also seen in the model. Pendelluft is the "sloshing motion" of air between two neighboring lung units during cyclic ventilation (4,20). It is observed during the time interval between inspiration and expiration. For example, near the end of an inspiration, a lung unit with a smaller RC time constant (the "faster" unit) will be finished inspiring and ready to expire while an adjoining unit with a larger RC time constant (the "slower" unit) is still inspiring. Thus, the faster unit will

FRC = 3.7 liters and FREQUENCY = 10 HZ

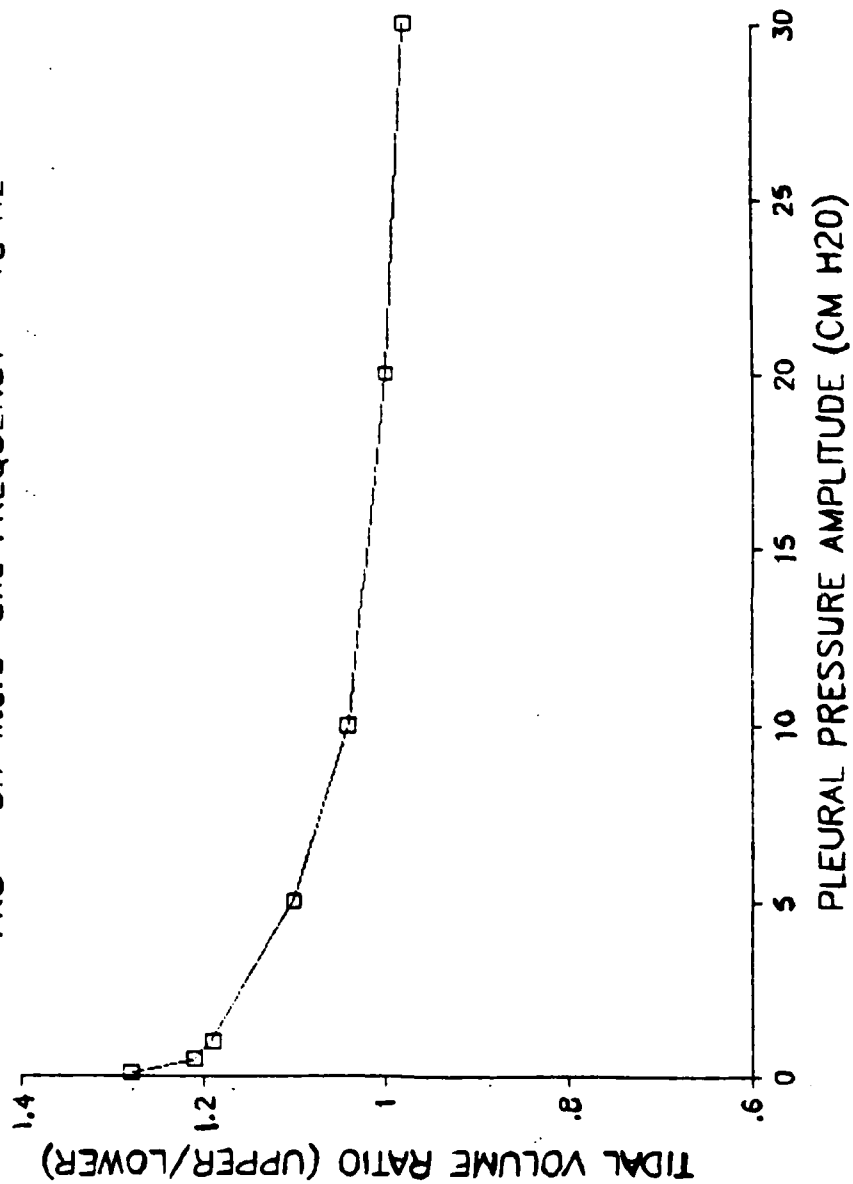


FIGURE 5 • TWO COMPARTMENT MODEL RESULTS OF TIDAL VOLUME RATIO VERSUS PLEURAL PRESSURE AMPLITUDE DURING HIGH FREQUENCY ANALYSIS.

expire into the still inspiring slower unit as well as into the airway common to the two units. Near the end of an expiration, the slower unit will expire into the ready to inspire faster unit. Although little discussed in the literature, L/R would also be a time constant which would be especially important at frequencies above resonance.

The phenomenon of pendelluft is illustrated in Fig. 6. Flow rates in the central airway and in the airways leading to the upper and lower compartments are shown as functions of time for a frequency of 10 Hz. Note that near the end of an inspiration (at ~ 0.98 sec.), the lower compartment is still inspiring while the upper compartment is already expiring. Near the end of an expiration (at ~ 1.03 sec.), the lower compartment is still in expiration while the upper compartment has begun inspiration. Thus, in this case, the upper compartment is the faster compartment and the lower compartment is the slower one.

CONCLUSIONS AND RECOMMENDATIONS

A two alveolar compartment model of the human lung predicting distribution of ventilation has been developed. It appears to be at least qualitatively accurate in its predictions both at low breathing frequencies and high ventilation frequencies. The former are physiological and the latter are intended to simulate mechanical ventilation by high frequency oscillation of the pleural pressure. Experimental data of the type needed to quantitatively verify the model are meager. As more information becomes available, especially on high frequency ventilation, verification and subsequent modification of the model will be done.

In the meanwhile, parameter values need to be less empirically obtained. For example, not enough is known about oscillatory pressure-flow relations in

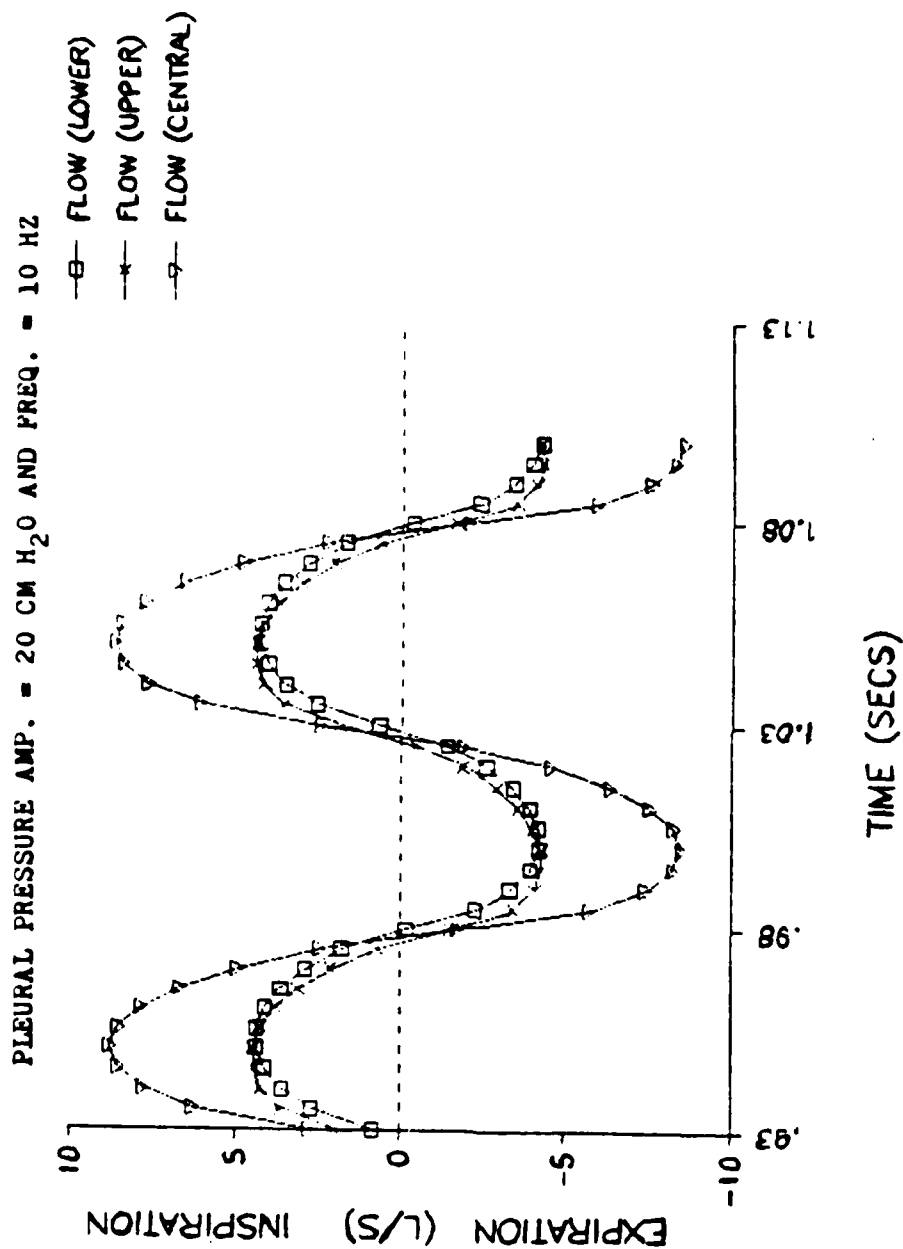


FIGURE 6 . TWO COMPARTMENT MODEL RESULTS OF FLOW VERSUS TIME DURING HIGH FREQUENCY ANALYSIS

the bronchial tree, especially on a regional level. How the nonlinear properties of inertance and resistance are regionally distributed has not been fully answered. For that matter, bronchial compliance (as distinct from alveolar compliance) also has not been considered in this model. The latter is a complication which may have large effects on the ventilation distribution, mixing, and overall gas exchange (4). Relating bronchial geometry, mechanical properties of the bronchial walls, and gas properties to the compliance, resistance and inertance is recommended for future work.

For example, resistance is a function of the flow rate, bronchial lengths, diameters, branching angles, gas density and viscosity, flow direction, and oscillation frequency. The main problem is to be able to handle the distribution of resistance with a reasonable number of resistance elements for which a reliable equation is available. This will probably need to involve experimental work in models of the bronchial tree, since laws for straight tubes are not applicable and secondary flows due to bifurcations and turbulence itself produce unknown dissipative effects. Also, the effects of frequency and driving pressure or tidal volume amplitude on resistance in the bronchial tree has been little investigated. The same as the above can also be said of inertance in branched tubes. The effects of the waveform shape of the driving function should also be investigated. Driving the system with a flow generator rather than a pressure generator also needs to be studied. In spite of the many additional problems which need to be addressed, we believe that the model is new information and an addition to the present state of modeling of the pulmonary ventilation system.

REFERENCES

1. Beckett, R. and J. Hurt. Numerical Calculations and Algorithms, New York, McGraw Hill, 1967.
2. Blide, R.W., H.D. Kerr, and W.S. Spicer. Measurement of upper and lower airway resistance and conductance in man. J. Appl. Physiol. 19(6): 1059-1069, 1964.
3. Brusasco, V., T.J. Knopp, and K. Rehder. Gas transport during high-frequency ventilation. J. Appl. Physiol.: Respirat Environ. Exercise Physiol. 55(2): 472-478, 1983.
4. Chang, H.K. Mechanisms of gas transport during ventilation by high-frequency oscillation. J. Appl. Physiol.: Respirat. Environ. Exercise Physiol. 56(3): 553-563, 1984.
5. Chang, H.K. and B.E. Shykoff. A model simulation of ventilation distribution. Bull.Europ.Physiopath.Resp., 18:329-338, 1982.
6. Collins, R.E., R.E. Calvert and H.H. Hardy. Mathematical simulation of the cardiopulmonary system. Progress Report, AFOSR 79-0123, December 1979.
7. Fredberg, J.J., S.L. Allen, I.D. Frantz. Regional alveolar pressure during periodic flow. Proc. 38th Ann. Conf. Engr. Med. Biol., Chicago, 1985, p.72.
8. Gibson, G.J., N.B. Pride, C. O'Cain and R. Quagliato. Sex and age differences in pulmonary mechanics in normal non-smoking subjects. J. Appl. Physiol., 41: 20-25, 1976.
9. Milic-Emili, J. Ventilation. Ch. 4 in Regional Differences in the Lung, Ed. J.B. West, New York, Academic Press, pp 167-200, 1977.
10. Milic-Emili, J. Inter-regional distribution of ventilation. Bull. Europ Physiopath., 18: 325-327, 1982.
11. Murphy, B.G. and L.A. Engel. Models of the pressure-volume relationship of the human lung. Resp. Physiol. 32: 183-194, 1978.
12. Pedley, T.J., M.F. Sudlow and J. Milic-Emili. A non-linear theory of distribution of pulmonary ventilation. Resp. Physiol., 15: 1-38, 1972.
13. Pedley, T.J., Gas flow and mixing in the airways. In Bioengineering Aspects of the Lung. Ed. J.B. West, Marcel Dekker, New York, p. 163-265.
14. Peslin, R., G. Duvivier, and C. Gallina. Total respiratory input and transfer impedences in humans. J. Appl. Physiol., 59(2): 492-501, 1985.

15. Reynolds, D.B. and J.S. Lee. Steady pressure-flow relationship of a model of the canine bronchial tree. J. Appl. Physiol.: Respirat. Environ. Exercise Physiol., 51: 1072-1079, 1981.
16. Reynolds, D.B. Steady expiratory flow-pressure relationship in a model of the human bronchial tree. J. Biomech. Engr., 104: 153-158, 1982.
17. Reynolds, D.B. and C.A. Phillips. Steady inspiratory pressure-flow relationship in a human bronchial tree model. In Biomedical Engineering II: Recent Developments, Ed. C.W. Hall, Pergamon Press, New York, 1983. p.157-160.
18. Reynolds, D.B. Mathematical modeling of the human cardiopulmonary system. Final Report, AFOSR F49620-82-0035b, August 1984.
19. Shykoff, B.E., A. Van Grondelle and H.K. Chang. Effects of unequal pressure swings and different waveforms on distribution of ventilation: A non-linear model simulation. Resp. Physiol., 48: 157-168-1982.
20. Stutsky, S., J.M. Drazen and R.D. Kamm. High-frequency ventilation. Critical Reviews in Biomedical Engineering, Vol. 9,4: 347-379.
21. West, J.B. Respiratory physiology - the essentials, 2nd Ed. Williams and Wilkins, Baltimore, 1979, p.96-98.
22. West, J.B. Pulmonary pathophysiology - the essentials, Williams and Wilkins, Baltimore, 1977, p.202-203.

FINAL REPORT

**DEVELOPMENT OF AN OPTIMAL TESTING PROTOCOL
FOR THE USAF CRITERION TASK SET (CTS)**

submitted to

**Southeastern Center for Electrical Engineering Education (SCEEE)
11th & Massachusetts Avenue
St. Cloud, Florida 32769**

Contract: SCEEE-84 RIP 47

submitted by

**Dr. Robert E. Schlegel
Assistant Professor
School of Industrial Engineering**

**The University of Oklahoma
1000 Asp, Room 314
Norman, Oklahoma 73019**

ABSTRACT

The USAF Criterion Task Set (CTS) is a human performance test battery composed of nine tasks which measure independent information processing resources. One task measures perceptual input, six tasks measure central processing and two tasks measure motor output.

An evaluation of the CTS was conducted with the following objectives:

- (1) determine the required number of sessions to achieve asymptotic performance on each CTS task when naive subjects are trained on all tasks or some subset of tasks concurrently,
- (2) compare the performance of subjects trained on all nine tasks with the performance of subjects trained on various three-task subsets,
- (3) relate task performance to a subjective workload assessment measure, and
- (4) examine the inter-subject variability and inter-task performance relationships.

Twenty subjects were divided into four groups. One group trained on all nine tasks. The other three groups trained on different three-task subsets. All subjects trained for two hours per day on five consecutive days. Performance measures for the majority of tasks included response time and accuracy. Subjective workload measures were also obtained.

For the majority of tasks and levels, a traditional learning curve effect was observed with little difference in the shape of the curves for the group trained on all nine tasks vs. the other groups. The required number of trials for initial stabilized performance ranged from two to six with a mode of four. Continued improvements were observed on some tasks after eight to ten trials for the groups trained on the three-task subsets. With one exception, there were no statistically significant differences between the groups. The subjective workload ratings showed consistent ordered differences between workload levels for all tasks and provided a comparison of the relative difficulty across tasks.

ACKNOWLEDGEMENTS

This research was sponsored by the Air Force Office of Scientific Research through the Southeastern Center for Electrical Engineering Education under contract F49620-82-C-0035.

The author would like to thank the entire staff of the Workload and Ergonomics Branch, Human Engineering Division of the Armstrong Aerospace Medical Research Laboratory at Wright-Patterson AFB, including the many employees of Systems Research Laboratories, Inc. (SRL). Assistance in supplying human subjects for the research effort was provided by SRL under contract number F33615-82-C-0511.

Specifically, appreciation is expressed to Dr. Clark A. Shingledecker for his support and to David Patterson, Doug Stewart and Betina Schlegel, Graduate Students at the University of Oklahoma, for their assistance in data collection, data analysis and report preparation.

Special thanks are extended to Col. Robert D. O'Donnell and Dr. Kirby Gilliland for their help in making the research opportunity possible.

1.0 INTRODUCTION

Recent trends in workload research have concentrated on two areas. The first area has been the development of workload theory, that is, models which can predict human information processing/performance capability. The second area of concentration has been the development of specific measurement techniques. Unfortunately, there have been very few attempts to coalesce these theory and task developments into a unified workload assessment methodology. The Air Force Criterion Task Set (Shingledecker, 1984) is part of an effort to develop such a methodology to aid in the design and operation of systems.

1.1 Criterion Task Set (CTS)

The Criterion Task Set (CTS) is a battery of tasks developed to provide a practical instrument for human performance assessment. It was designed to provide a set of standardized loading tasks to evaluate the relative sensitivity, reliability and intrusiveness of a variety of available workload measures. Preliminary workload metric evaluation studies (Shingledecker et al., 1983) have initiated the development of appropriate experimental procedures and illustrated the potential variation in diagnosticity that exists among workload measures.

In addition to the original design intention, the CTS forms an independent Performance Assessment Battery which may be used to assess the effects of various stressors and work environments on individual components of the human information processing system.

The CTS is based on a model which represents a synthesis of current information processing theories (primarily Wickens, 1981 and Sternberg, 1969). According to these theories, human mental performance is dependent on a number of information processing resources, stages and specific functions. The CTS model was constructed to outline a minimal set of potential processing resources, and to identify a group of basic information processing activities that are performed by these structural elements.

The model hypothesizes three primary stages of processing and associated resources dedicated to perceptual input, central processing, and motor output or response activities. Within each of these stages, separate resources are associated with the mode of input (visual/auditory), the code in which central processing is performed (spatial imaginal/abstract symbolic), and the mode of response output (manual/vocal). In addi-

tion, the central processing stage is divided to differentiate between working memory and the specific types of processing or decision functions that occur at this stage.

To develop the model, separate elements were defined to specify the basic limits of short-term storage and recall, and to identify qualitatively different levels of central decision activity. The most elementary level is information manipulation or transformation based on implicit or memorized rules. Such activity is common in language comprehension, mathematical computation, and pattern analysis. Reasoning functions represent a higher level of central activity involving the extraction of relational rules from the information presented. This activity occurs during problem solving and in tasks requiring logical analysis.

The above elements were further defined in terms of the characteristics of tasks which would place predominant demands on them. These definitions were then used to select candidate tasks for the CTS. In each case, the ability to manipulate task demand and to minimize loading on resources not tested by the task were used as major selection criteria. Iterative screening of a wide range of tasks from the literature on cognitive and psychomotor performance resulted in the selection of nine tasks for CTS Version 1. These tasks are listed in Table 1 according to their hypothesized relationship to the information processing divisions. A brief description of each task follows.

Empirical evaluation or parametric studies were performed on each task to determine:

**Table 1. CTS Version 1.0 Tasks Listed by
Information Processing System Division.**

STAGE	TASK	CODE
Input/Perceptual	Probability Monitoring	PM
Central Processing	Continuous Recall	CR
	Memory Search	MS
	Linguistic Processing	LP
	Mathematical Processing	MP
	Spatial Processing	SP
	Grammatical Reasoning	GR
Output/Motor	Unstable Tracking	UT
	Interval Production	IP

- (1) ways of manipulating task difficulty to produce three distinct loading levels,
- (2) appropriate task pacing rates to keep the tasks self-paced but within certain limits, and
- (3) adequate training times for stable performance.

Comparisons performed on the post-asymptotic performance indices were used to select three loading levels for each of the individual tasks except Interval Production. These levels were corroborated by subjective ratings of task difficulty and complexity.

1.2 CTS Task Descriptions

The following are brief descriptions of the CTS Version 1 tasks. Detailed descriptions and initial parametric results are provided by Shingledecker (1984).

Visual Probability Monitoring (PM). The subject is required to monitor 1, 3 or 4 simulated meters and determine whether a bias condition is present. This occurs when a pointer stays on one side of the meter center line a higher percentage of time than on the other. The percentages for the 1-, 3- and 4-dial conditions are 95%, 85% and 75% respectively.

Continuous Recall (CR). The subject is presented with pairs of 1-, 2- or 4-digit numbers, one below the other, and must compare the top number with a previous display as well as memorize the bottom number for later comparison.

Memory Search (MS). An initial set of 1, 4 or 6 letters is presented to the subject for memorization. Following this, the subject must identify whether a randomly generated letter is a member of that set.

Linguistic Processing (LP). At the low level, the subject decides whether presented pairs of letters are physically identical. For the medium level, the subject decides whether both letters are vowels or consonants. At the high level, the subject is required to identify antonyms.

Mathematical Processing (MP). The subject is required to decide whether the result of a mathematical expression involving 1, 2 or 3 operators (+ or -) is greater than or less than the value 5.

Spatial Processing (SP). The subject compares an initial histogram of 2, 4 or 6 bars with a second histogram that has been rotated 0, 90, 180 or 270 degrees.

Grammatical Reasoning (GR). Sentences describing the positioning of symbols are presented with the symbols below. The subject must determine whether the sentences correctly describe the positioning of the symbols.

Unstable Tracking (UT). The subject attempts to maintain the position of an object, representative of an airplane, in the middle of the screen using a rotating control knob. The dynamics of the task magnify the control error to prevent stable control of the object.

Interval Production (IP). The subject attempts to create regular timing intervals using a tapping paddle at a rate between 1 and 3 taps per second.

Additional members of the CTS are under development to provide tasks related to planning and scheduling activities characterized by multiattribute decision requirements. These activities are typical in complex system supervision and planning tasks.

2.0 OBJECTIVES

To further the use of the CTS in both basic and applied research programs, it is essential to develop a comprehensive performance data base and to investigate the interrelatedness of the subtests, i.e., to determine the internal structure of the task set. A preliminary requirement for the development of this comprehensive data base is to establish a task administration methodology including an optimal testing protocol.

The development of an optimal training protocol is even more crucial in light of the amount of time required to administer the entire battery. A single subject may require up to two hours for an administration involving the performance of each task once at each workload level. This emphasizes the importance of optimally allocating a limited amount of training time to each of the tasks since some tasks require few training trials while others require extensive training for stabilized performance.

During the development of the CTS, human subjects were trained and tested on each task separately. The data reflect the learning characteristics of each task on an individual task basis often involving subjects with prior experience on the same or related tasks. Little information has previously been available on the crossover learning that may exist or the training characteristics for the three final workload levels of each task. Until the current study, no comprehensive administration of the entire test battery had been made to a group of naive subjects.

The combined replication study reported here was performed to assess the reliability of the findings obtained in the individual task parametric studies. The specific objectives of this study were to:

- (1) determine the required number of sessions to achieve asymptotic performance on each task when naive subjects are trained on all tasks or some subset of tasks concurrently,
- (2) compare the performance of subjects trained on all nine tasks with the performance of subjects trained on various three-task subsets,
- (3) relate task performance to a subjective workload assessment measure, and
- (4) examine the inter-subject variability and inter-task performance relationships.

3.0 EXPERIMENTAL METHODOLOGY

3.1 General Approach

Four different subject groups were established to compare the performance of subjects trained on all nine tasks vs. individual three-task subsets. In assigning tasks to groups, an attempt was made to balance the category of information processing, type of visual stimuli, task difficulty and other characteristics (Table 2).

Each task was assigned to the overall set and one subset. A comparison of learning patterns would determine performance differences between subjects trained on a large set of tasks vs. a smaller subset. Due to training time limitations, five trials of each

Table 2. Basis for Task Assignment.

GROUP	TASK	TYPE I/P/O	CHARACTERISTICS	VISUAL STIMULI
A	-----all nine tasks-----			
B	MS	P	memory	alpha
	PM	I	visual, probability assessment	graphic
	GR	P	logic, spatial, grammar	symbol/alpha
C	MP	P	math, logic	numeric
	UT	I/O	visual/motor	graphic
	SP	P	spatial, visual memory	graphic
D	LP	P	matching, grammar	alpha
	IP	O	timing, motor	-----
	CR	P	memory, spatial	numeric

workload level of each task were performed for Group A tasks and fifteen trials were performed for Group B, C and D tasks.

3.2 Subjects

Twenty male subjects, age 18 to 25 years, were recruited from the Wright State University Campus. All subjects were enrolled in Air Force ROTC and were naive with respect to the CTS battery and other research efforts at AAMRL/HE. The subjects attended an orientation session to become acquainted with the CTS and the goals of the study, and to perform a "SWAT sort" related to the subjective workload measure. The voluntary informed consent of each subject was obtained at this time in accordance with AFR 169-3.

Subjects were randomly assigned to Groups A, B, C and D, five subjects per group. Each subject trained on the appropriate CTS tasks for two hours per day on five consecutive days. Groups B and D trained during the first week of data collection, Groups A and C during the second week.

3.3 Equipment and Software

The CTS is implemented on a Commodore 64 microcomputer system. Two such systems were used, each consisting of the following units: Commodore 64 microcomputer, Commodore 1541 disk drive, Commodore 1526 printer, monochrome Panasonic experimenter's monitor, color Commodore 1702 subject's monitor and three subject response devices.

Modifications were made to the CTS software to provide automatic sequencing through the task levels and automatic filename construction for data storage. A coding scheme was devised which included Group, Subject, Task, Level and Trial identifiers. CTS tasks and data were all stored on floppy disk with separate diskettes for each task group and each subject. On the average, two 5-1/4" data diskettes were required per subject with a total of 2500 trials (data files) for the entire study.

3.4 Subjective Workload Assessment Technique (SWAT)

To relate task performance to a subjective workload measure, the SWAT Scale was used. The SWAT Scale (Reid, 1982; Reid, Eggemeier, and Nygren, 1982) is a psychometric instrument subjectively measuring three major dimensions of workload: Time, Effort, and Stress. Given the demands of any specified workload period, sub-

jects rate each dimension on a 1 to 3 Likert-type scale.

The unique aspect of this scale is that it not only provides a means for obtaining an individual subject's workload ratings, but also a method for establishing across-subject comparability. This is accomplished by having each subject complete a SWAT Sort, i.e., each subject sorts a card deck of all 27 combinations of the three rating levels for all three workload dimensions. The sorting order is then subjected to conjoint scaling yielding a standardized rating metric which can be used for comparisons across subjects (Nygren, 1982).

Subjects performed the initial SWAT card sort during the orientation session. Following each trial, the subject provided his SWAT ratings on a data collection form for later incorporation into the performance data base.

3.5 Procedure

Subjects were trained on their assigned tasks during the same two hour time block on five consecutive days. Subjects in Group A sequenced through the set of tasks in the following order: MS, PM, GR, MP, UT, SP, LP, IP, CR. All tasks have three levels except IP, thus yielding 25 trials per subject during the two-hour period. Within each task, subjects sequenced through the levels from low to high in order.

All other subjects performed three trials at each level of each task. The sequence for Group B was MS, PM, GR with a total of 27 trials per day. Group C followed the sequence MP, UT, SP with 27 trials per day and Group D followed the sequence LP, IP, CR with a total of 21 trials due to the single level of the IP task. One trial at each level of each task was completed before repeating the task sequence. As in Group A, subjects sequenced through the levels from low to high in order.

Two subjects from different groups were tested simultaneously by the experimenter, one subject on each Commodore system. All data was stored on floppy disk for later data reduction and analysis.

4.0 DATA REDUCTION

4.1 Description of the Data Base

Each trial involved the presentation of 20 to 200 individual stimuli. For all central processing tasks, response time and accuracy were the measures recorded for each stimulus. For the input/output tasks, alternative measures were used.

A summary of the performance for a single trial was obtained using the CTS "STATISTICS" software option. The measures provided by this option are summarized for each task in Table 3.

In addition to the measures provided by the CTS "STATISTICS" option, separate analyses for each task can be performed using the individual stimulus data saved on the disks. Examples include the relationship of performance to specific characters presented in the memory search tasks or to the ability to cancel digits in the mathematical processing task. However, these analyses require examination of the raw data

Table 3. Summary Measures for Each Task.

TASK	MEASURES	CODE
All Central Processing Tasks	Mean correct response time (RT) Standard deviation of RT Total number of stimuli Number of correct responses Total number incorrect Total number of errors Total number missed	MN SD
Probability Monitoring	Number of correct detections Number of missed biases Number of false responses Response time	FR RT
Unstable Tracking	Mean absolute error Total edge violations	AE EV
Interval Production	Number of intervals Mean interval duration Standard deviation of interval IPT variability score	MN SD VS

through additional software development on the Commodore 64.

In order to meet the objectives of the study, a SAS (Statistical Analysis System) data base was established incorporating the performance summary measures for all tasks and trials. Including the identification variables for group, subject, task, task level and trial number, the data base contained 124 variables and 750 observations.

4.2 Data Reduction and Transfer

Additional Commodore software was developed to facilitate the data reduction and transfer. As an intermediate step, programs were developed to automatically sequence through the files on each data disk, compute the summary statistics and write them to a disk file in a format appropriate for SAS input. Transfer of this information from the Commodore disks to the IBM 3081 was achieved through the use of a VAX 11/780 and additional transfer software.

5.0 RESULTS

The results from the study are summarized in Tables 4 through 12 which present the means and standard deviations of selected response variables across subjects in Groups A, B, C and D. Part (a) of each table provides summary statistics for each trial for Group A subjects while Part (b) provides statistics for subjects in the corresponding task subset group. Following the tables, Figures 1 through 9 provide a graphical representation of the learning curves and the differences between the groups for the two primary dependent variables for each task.

For the majority of tasks and levels, a traditional learning curve effect was observed with little difference in the shape of the curves for Group A vs. the other groups. The required number of trials for stable performance ranged from two to six with a mode of four. Slight improvements were observed on some tasks after eight to ten trials.

With one exception, there were no statistically significant differences between the performance of Group A and the performance of the other groups. Only at the low level of Continuous Recall was a difference detected with Group A performing significantly worse than Group D. Similar differences, although not statistically significant, were observed at the other levels of CR. These differences may have been due to individual subject or strategy differences between the groups, or to fatigue since Continuous Recall was the last task in the sequence for Group A.

A discussion of the results for each task along with the results of several analyses of variance comparing groups, workload levels and trials is presented following the figures.

THE UNIVERSITY OF OKLAHOMA
CTS 1984 SCHLEGEL SUMMER STUDY

Table 4a. MEMORY SEARCH TASK

----- GROUP = A WORKLOAD LEVEL = LOW -----						
TRIAL	MEAN	(*)	STD_DEV	(*)	PCT COR	(*)
	(msec)		(msec)		(%)	
1	646	(125)	385	(309)	98.8	(1.1)
2	568	(80)	151	(65)	99.3	(0.6)
3	536	(95)	170	(91)	98.2	(1.3)
4	512	(81)	160	(60)	97.6	(1.9)
5	501	(69)	176	(59)	97.2	(3.4)

----- GROUP = A WORKLOAD LEVEL = MEDIUM -----						
TRIAL	MEAN	(*)	STD_DEV	(*)	PCT COR	(*)
	(msec)		(msec)		(%)	
1	752	(108)	278	(96)	98.7	(1.2)
2	750	(151)	345	(154)	98.0	(2.0)
3	697	(168)	255	(153)	97.4	(2.8)
4	670	(132)	318	(166)	96.8	(2.0)
5	657	(120)	273	(120)	96.0	(2.8)

----- GROUP = A WORKLOAD LEVEL = HIGH -----						
TRIAL	MEAN	(*)	STD_DEV	(*)	PCT COR	(*)
	(msec)		(msec)		(%)	
1	907	(99)	564	(251)	84.5	(3.9)
2	758	(144)	398	(191)	88.3	(5.3)
3	769	(191)	380	(208)	86.6	(2.9)
4	760	(163)	396	(192)	86.8	(3.9)
5	742	(144)	391	(144)	83.4	(5.0)

* - STANDARD DEVIATION FOR PRECEEDING VARIABLE

THE UNIVERSITY OF OKLAHOMA
CTS 1984 SCHLEGEL SUMMER STUDY

Table 4b. MEMORY SEARCH TASK

----- GROUP = B WORKLOAD LEVEL = LOW -----						
TRIAL	MEAN	(*)	STD_DEV	(*)	PCT COR	(*)
	(msec)		(msec)		(%)	
1	630	(148)	141	(67)	98.6	(2.0)
2	558	(77)	155	(66)	98.3	(2.0)
3	542	(79)	147	(93)	99.4	(0.6)
4	533	(38)	126	(36)	98.7	(1.2)
5	518	(73)	168	(83)	98.6	(0.6)
6	495	(56)	146	(67)	98.0	(1.5)
7	520	(86)	164	(36)	98.0	(1.3)
8	517	(98)	179	(115)	97.8	(1.3)
9	475	(32)	121	(44)	98.1	(2.2)
10	488	(54)	158	(50)	97.6	(1.1)
11	478	(43)	117	(48)	98.2	(2.1)
12	462	(59)	142	(29)	97.4	(1.8)
13	496	(104)	159	(73)	97.0	(1.7)
14	498	(113)	198	(162)	97.0	(1.2)
15	454	(70)	100	(44)	98.2	(1.5)
----- GROUP = B WORKLOAD LEVEL = MEDIUM -----						
1	752	(144)	260	(102)	98.4	(1.5)
2	764	(61)	296	(149)	97.0	(1.7)
3	737	(93)	290	(87)	98.0	(2.7)
4	654	(76)	211	(59)	97.4	(1.3)
5	665	(105)	227	(114)	98.1	(1.9)
6	667	(45)	254	(89)	96.1	(2.4)
7	631	(82)	201	(114)	97.4	(1.9)
8	652	(99)	312	(201)	94.9	(2.7)
9	613	(89)	236	(151)	92.9	(1.3)
10	598	(61)	198	(89)	96.1	(3.0)
11	592	(26)	178	(37)	95.9	(2.9)
12	597	(41)	232	(43)	96.8	(1.4)
13	555	(61)	163	(69)	96.4	(2.2)
14	620	(136)	253	(159)	96.1	(2.4)
15	576	(46)	163	(46)	95.6	(1.9)
----- GROUP = B WORKLOAD LEVEL = HIGH -----						
1	1050	(225)	556	(179)	85.7	(7.1)
2	956	(157)	494	(215)	84.1	(5.0)
3	891	(135)	534	(252)	87.3	(5.4)
4	819	(139)	369	(115)	85.7	(8.4)
5	758	(73)	367	(209)	89.3	(3.6)
6	749	(57)	351	(128)	79.9	(7.9)
7	755	(46)	474	(147)	84.6	(5.2)
8	840	(167)	629	(451)	81.6	(4.1)
9	782	(151)	540	(406)	86.1	(5.3)
10	735	(84)	433	(167)	79.5	(8.0)
11	670	(82)	289	(103)	84.7	(6.1)
12	779	(175)	436	(298)	84.4	(5.4)
13	648	(78)	315	(146)	86.4	(1.2)
14	740	(110)	447	(218)	77.5	(3.3)
15	678	(61)	304	(114)	83.1	(4.2)

* - STANDARD DEVIATION FOR PRECEEDING VARIABLE

THE UNIVERSITY OF OKLAHOMA
CTS 1984 SCHLEGEL SUMMER STUDY

Table 5a. PROBABILITY MONITORING TASK

----- GROUP = A WORKLOAD LEVEL = LOW -----							
TRIAL #	COR	(*)	FALSE RESP	(*)	MISSED BIAS	(*)	RESP TIME (sec) (*)
1	3.0	(0.0)	2.4	(3.5)	0.0	(0.0)	8.1 (3.4)
2	3.0	(0.0)	0.6	(1.3)	0.0	(0.0)	9.7 (4.2)
3	3.0	(0.0)	0.8	(1.3)	0.0	(0.0)	9.7 (7.4)
4	3.0	(0.0)	0.4	(0.5)	0.0	(0.0)	11.0 (6.3)
5	3.0	(0.0)	0.6	(0.5)	0.0	(0.0)	10.8 (5.0)

----- GROUP = A WORKLOAD LEVEL = MEDIUM -----							
TRIAL #	COR	(*)	FALSE RESP	(*)	MISSED BIAS	(*)	RESP TIME (sec) (*)
1	2.2	(0.8)	2.2	(1.6)	0.8	(0.8)	18.7 (8.1)
2	2.0	(1.0)	0.6	(0.8)	0.4	(0.8)	21.6 (6.9)
3	1.8	(1.3)	0.0	(0.0)	1.4	(0.5)	18.5 (9.8)
4	2.8	(0.4)	0.2	(0.4)	0.2	(0.4)	17.3 (5.4)
5	1.8	(0.8)	0.6	(0.8)	1.0	(1.4)	16.8 (6.0)

----- GROUP = A WORKLOAD LEVEL = HIGH -----							
TRIAL #	COR	(*)	FALSE RESP	(*)	MISSED BIAS	(*)	RESP TIME (sec) (*)
1	1.6	(1.1)	3.0	(1.8)	1.0	(1.0)	16.4 (10.0)
2	1.2	(1.0)	3.2	(1.9)	1.2	(1.0)	22.0 (7.1)
3	1.4	(0.8)	1.2	(0.8)	1.0	(0.7)	16.3 (8.1)
4	1.4	(0.5)	2.0	(1.2)	1.2	(0.8)	9.4 (6.9)
5	1.4	(0.8)	1.6	(0.5)	1.6	(1.1)	19.3 (10.8)

* - STANDARD DEVIATION FOR PRECEEDING VARIABLE

THE UNIVERSITY OF OKLAHOMA
CTS 1984 SCHLEGEL SUMMER STUDY

Table 5b. PROBABILITY MONITORING TASK

----- GROUP = B WORKLOAD LEVEL = LOW -----							
TRIAL #	COR	(*)	FALSE RESP	(*)	MISSED BIAS	(*)	RESP TIME (sec)
1	3.0	(0.0)	1.2	(1.7)	0.0	(0.0)	9.7 (2.0)
2	3.0	(0.0)	0.0	(0.0)	0.0	(0.0)	11.6 (6.9)
3	3.0	(0.0)	0.2	(0.4)	0.0	(0.0)	12.0 (5.6)
4	3.0	(0.0)	0.5	(1.0)	0.0	(0.0)	11.1 (3.6)
5	2.8	(0.4)	0.2	(0.4)	0.0	(0.0)	11.5 (5.8)
6	3.0	(0.0)	0.0	(0.0)	0.0	(0.0)	11.1 (6.0)
7	3.0	(0.0)	0.4	(0.5)	0.0	(0.0)	10.8 (5.8)
8	3.0	(0.0)	0.0	(0.0)	0.0	(0.0)	10.4 (3.9)
9	3.0	(0.0)	0.6	(0.5)	0.0	(0.0)	10.1 (5.7)
10	3.0	(0.0)	0.2	(0.4)	0.0	(0.0)	10.9 (4.8)
11	3.0	(0.0)	0.2	(0.4)	0.0	(0.0)	10.3 (3.7)
12	3.0	(0.0)	0.2	(0.4)	0.0	(0.0)	11.6 (4.5)
13	3.0	(0.0)	0.2	(0.4)	0.0	(0.0)	10.6 (3.9)
14	3.0	(0.0)	0.0	(0.0)	0.0	(0.0)	8.6 (2.4)
15	3.0	(0.0)	0.4	(0.8)	0.0	(0.0)	10.8 (2.4)
----- GROUP = B WORKLOAD LEVEL = MEDIUM -----							
1	2.6	(0.5)	0.8	(0.4)	0.4	(0.5)	14.1 (1.7)
2	2.2	(0.8)	0.6	(0.8)	0.8	(0.8)	22.5 (5.6)
3	1.8	(1.3)	1.0	(1.0)	1.0	(1.0)	20.4 (4.5)
4	2.2	(0.9)	0.4	(0.8)	0.6	(0.5)	17.3 (3.8)
5	2.4	(0.5)	0.2	(0.4)	0.2	(0.4)	14.5 (9.2)
6	2.0	(1.2)	0.4	(0.5)	0.8	(0.8)	16.6 (6.7)
7	2.4	(0.5)	0.4	(0.8)	0.6	(0.5)	15.7 (6.8)
8	2.2	(0.4)	0.8	(0.8)	0.6	(0.5)	19.8 (4.7)
9	2.2	(0.4)	0.4	(0.5)	0.6	(0.5)	20.0 (5.4)
10	1.6	(0.8)	0.8	(0.8)	1.0	(1.0)	21.6 (9.2)
11	1.4	(0.5)	0.6	(0.8)	1.4	(0.5)	17.3 (7.3)
12	2.0	(1.0)	0.6	(0.8)	0.4	(0.5)	26.6 (7.0)
13	1.6	(0.8)	0.6	(0.5)	1.0	(0.7)	21.5 (5.0)
14	2.4	(0.8)	0.2	(0.4)	0.4	(0.5)	25.7 (5.2)
15	2.3	(0.9)	0.0	(0.0)	0.8	(0.9)	21.1 (5.4)
----- GROUP = B WORKLOAD LEVEL = HIGH -----							
1	1.0	(1.0)	1.0	(1.7)	2.0	(1.0)	23.9 (6.8)
2	0.8	(1.0)	1.4	(1.6)	1.4	(1.5)	22.4 .
3	0.8	(0.8)	2.0	(1.5)	1.6	(0.5)	23.1 (4.3)
4	0.8	(0.4)	2.0	(1.8)	1.6	(0.5)	17.0 (9.1)
5	1.2	(0.8)	1.2	(0.8)	1.4	(0.5)	15.6 (0.1)
6	1.0	(0.7)	1.4	(1.1)	1.4	(0.8)	21.9 (5.3)
7	1.0	(0.0)	0.6	(0.8)	1.8	(0.4)	22.6 (4.1)
8	1.6	(0.5)	0.2	(0.4)	1.0	(0.7)	27.1 (6.2)
9	1.2	(0.4)	1.4	(1.1)	1.4	(0.5)	23.4 (10.5)
10	0.6	(0.8)	1.4	(1.1)	1.8	(1.0)	18.4 (1.8)
11	1.4	(0.8)	0.6	(0.5)	0.8	(0.8)	26.9 (8.6)
12	1.2	(0.4)	0.4	(0.5)	0.8	(0.4)	29.0 (2.8)
13	1.8	(0.8)	0.8	(1.3)	1.0	(0.7)	22.7 (5.1)
14	1.0	(1.0)	0.8	(0.8)	1.2	(0.8)	13.1 .
15	0.8	(0.8)	0.8	(0.4)	1.6	(0.5)	16.2 (2.8)

* - STANDARD DEVIATION FOR PRECEEDING VARIABLE

THE UNIVERSITY OF OKLAHOMA
CTS 1984 SCHLEGEL SUMMER STUDY

Table 6a. GRAMMATICAL REASONING TASK

----- GROUP = A WORKLOAD LEVEL = LOW -----						
TRIAL	MEAN	(*)	STD_DEV	(*)	PCT COR	(*)
	(msec)		(msec)		(%)	
1	4453	(1075)	2310	(790)	84.5	(8.4)
2	4065	(1358)	1470	(390)	83.0	(20.0)
3	3381	(1036)	1216	(373)	85.4	(15.9)
4	3396	(1310)	1227	(419)	88.3	(10.6)
5	3561	(1642)	1294	(317)	90.9	(9.5)

----- GROUP = A WORKLOAD LEVEL = MEDIUM -----						
TRIAL	MEAN	(*)	STD_DEV	(*)	PCT COR	(*)
	(msec)		(msec)		(%)	
1	7528	(776)	1997	(750)	84.5	(9.9)
2	6599	(1575)	1590	(256)	93.7	(7.8)
3	5797	(1421)	1419	(521)	87.7	(11.4)
4	5548	(1193)	1439	(378)	90.5	(8.8)
5	5662	(410)	1881	(825)	86.2	(16.0)

----- GROUP = A WORKLOAD LEVEL = HIGH -----						
TRIAL	MEAN	(*)	STD_DEV	(*)	PCT COR	(*)
	(msec)		(msec)		(%)	
1	9562	(1108)	2070	(444)	71.0	(18.3)
2	9111	(1529)	1726	(235)	68.9	(7.2)
3	8291	(1731)	2019	(564)	76.5	(14.7)
4	7810	(1472)	1637	(187)	79.3	(22.7)
5	7849	(1605)	2093	(553)	82.2	(19.2)

* - STANDARD DEVIATION FOR PRECEEDING VARIABLE

THE UNIVERSITY OF OKLAHOMA
CTS 1984 SCHLEGEL SUMMER STUDY

Table 6b. GRAMMATICAL REASONING TASK

----- GROUP = B WORKLOAD LEVEL = LOW -----						
TRIAL	MEAN	(*)	STD_DEV	(*)	PCT COR	(*)
	(msec)		(msec)		(%)	
1	3848	(547)	1390	(368)	95.0	(7.4)
2	3833	(327)	1552	(135)	96.1	(2.2)
3	3663	(637)	1473	(617)	96.3	(2.0)
4	3036	(249)	1070	(262)	96.3	(1.1)
5	3136	(292)	1192	(268)	98.0	(1.4)
6	3132	(250)	1209	(313)	93.7	(3.5)
7	3072	(390)	1311	(583)	96.7	(2.1)
8	3183	(324)	1300	(293)	95.9	(2.9)
9	3145	(252)	1574	(480)	94.1	(4.1)
10	2511	(192)	964	(295)	99.3	(0.8)
11	2570	(136)	1058	(225)	95.1	(4.4)
12	2640	(206)	973	(319)	97.1	(2.9)
13	2481	(396)	948	(334)	96.7	(2.2)
14	2771	(620)	1256	(512)	96.1	(2.0)
15	2627	(300)	1173	(561)	94.7	(5.8)
----- GROUP = B WORKLOAD LEVEL = MEDIUM -----						
1	7095	(1098)	1689	(360)	90.4	(10.7)
2	6467	(618)	1496	(245)	95.6	(2.8)
3	6485	(1482)	1698	(347)	90.2	(10.5)
4	5482	(508)	1296	(326)	95.5	(1.7)
5	6054	(741)	1529	(393)	96.2	(8.2)
6	5702	(811)	1498	(382)	96.3	(3.6)
7	5548	(525)	1386	(355)	93.0	(8.4)
8	5814	(714)	1629	(497)	96.0	(4.1)
9	5796	(971)	1654	(589)	97.4	(4.0)
10	5224	(786)	1576	(623)	94.1	(6.9)
11	5391	(497)	1694	(299)	93.5	(9.4)
12	5076	(599)	1562	(633)	96.3	(2.6)
13	5013	(763)	1604	(346)	97.0	(3.8)
14	5378	(1170)	1628	(687)	95.1	(6.3)
15	4900	(561)	1493	(509)	98.8	(1.5)
----- GROUP = B WORKLOAD LEVEL = HIGH -----						
1	8867	(1596)	1902	(588)	69.3	(18.5)
2	8371	(1253)	1943	(346)	80.4	(10.1)
3	8108	(1849)	1764	(550)	81.9	(18.4)
4	7687	(1449)	1787	(754)	87.6	(11.6)
5	7718	(1238)	2008	(529)	88.7	(10.5)
6	8185	(1246)	2013	(682)	84.1	(14.5)
7	7718	(1452)	1754	(384)	88.6	(15.7)
8	7826	(1200)	2228	(435)	88.2	(14.3)
9	8014	(1355)	1979	(316)	94.9	(6.8)
10	6485	(906)	1555	(837)	90.9	(12.8)
11	7154	(1641)	1769	(363)	94.1	(6.8)
12	6893	(1320)	1881	(485)	84.1	(22.9)
13	6912	(1704)	1959	(625)	91.5	(10.0)
14	7352	(2488)	1872	(841)	90.4	(14.5)
15	6959	(1569)	1803	(370)	92.9	(12.1)

* - STANDARD DEVIATION FOR PRECEEDING VARIABLE

THE UNIVERSITY OF OKLAHOMA
CTS 1984 SCHLEGEL SUMMER STUDY

Table 7a. MATHEMATICAL PROCESSING TASK

----- GROUP = A WORKLOAD LEVEL = LOW -----						
TRIAL	MEAN	(*)	STD_DEV	(*)	PCT COR	(*)
	(msec)		(msec)		(%)	
1	757	(141)	445	(124)	97.3	(2.0)
2	630	(143)	498	(589)	97.3	(3.4)
3	548	(116)	217	(93)	98.6	(1.9)
4	534	(152)	240	(118)	96.6	(3.5)
5	531	(129)	238	(110)	98.4	(2.1)

----- GROUP = A WORKLOAD LEVEL = MEDIUM -----						
TRIAL	MEAN	(*)	STD_DEV	(*)	PCT COR	(*)
	(msec)		(msec)		(%)	
1	1817	(254)	756	(198)	95.9	(1.9)
2	1783	(435)	930	(436)	95.6	(6.0)
3	1511	(256)	723	(301)	94.5	(5.2)
4	1435	(212)	646	(203)	94.7	(7.7)
5	1480	(303)	854	(307)	95.6	(5.6)

----- GROUP = A WORKLOAD LEVEL = HIGH -----						
TRIAL	MEAN	(*)	STD_DEV	(*)	PCT COR	(*)
	(msec)		(msec)		(%)	
1	3011	(724)	1143	(423)	93.8	(7.3)
2	2875	(602)	1224	(524)	91.0	(10.6)
3	2718	(589)	1192	(476)	90.5	(14.5)
4	2467	(748)	1076	(343)	87.5	(18.6)
5	2455	(763)	1055	(392)	88.8	(17.4)

* - STANDARD DEVIATION FOR PRECEEDING VARIABLE

THE UNIVERSITY OF OKLAHOMA
CTS 1984 SCHLEGEL SUMMER STUDY

Table 7b. MATHEMATICAL PROCESSING TASK

----- GROUP = C WORKLOAD LEVEL = LOW -----						
TRIAL	MEAN	(*)	STD_DEV	(*)	PCT COR	(*)
	(msec)		(msec)		(%)	
1	832	(239)	697	(640)	99.0	(2.1)
2	684	(130)	332	(153)	98.0	(1.5)
3	573	(131)	244	(79)	98.6	(1.3)
4	499	(104)	210	(81)	98.4	(1.6)
5	474	(94)	164	(54)	98.4	(1.4)
6	473	(134)	171	(60)	98.9	(1.1)
7	500	(136)	203	(86)	97.8	(1.9)
8	688	(534)	263	(243)	99.2	(0.7)
9	527	(121)	222	(93)	98.3	(1.1)
10	434	(82)	181	(57)	98.1	(1.9)
11	469	(184)	224	(108)	98.7	(1.7)
12	456	(104)	181	(38)	97.6	(1.6)
13	406	(67)	175	(99)	98.1	(1.4)
14	454	(90)	207	(73)	98.1	(1.7)
15	401	(82)	162	(45)	97.2	(4.3)
----- GROUP = C WORKLOAD LEVEL = MEDIUM -----						
1	2078	(813)	784	(284)	96.6	(3.2)
2	1628	(438)	595	(230)	98.7	(1.1)
3	1802	(436)	795	(446)	98.5	(1.3)
4	1483	(294)	533	(142)	99.5	(0.9)
5	1441	(245)	516	(110)	98.7	(1.1)
6	1542	(320)	696	(277)	99.1	(1.1)
7	1420	(217)	601	(201)	98.7	(1.8)
8	1224	(554)	518	(275)	98.9	(1.6)
9	1436	(265)	625	(181)	98.3	(1.7)
10	1288	(345)	539	(213)	97.2	(2.3)
11	1288	(307)	556	(189)	98.3	(1.7)
12	1358	(234)	607	(133)	99.2	(1.0)
13	1093	(203)	407	(107)	98.1	(2.3)
14	1262	(265)	537	(149)	97.7	(2.4)
15	1268	(258)	619	(205)	98.0	(1.4)
----- GROUP = C WORKLOAD LEVEL = HIGH -----						
1	3174	(1171)	1016	(558)	98.6	(1.8)
2	2977	(744)	1338	(736)	97.4	(4.3)
3	2778	(862)	991	(396)	98.2	(1.6)
4	2457	(463)	902	(272)	97.9	(2.0)
5	2388	(627)	832	(432)	100.0	(0.0)
6	2458	(333)	1086	(565)	99.4	(1.2)
7	2190	(427)	875	(371)	97.8	(2.3)
8	2156	(392)	827	(226)	99.4	(1.1)
9	2394	(507)	956	(303)	98.4	(1.4)
10	2149	(510)	873	(284)	98.9	(1.4)
11	2171	(432)	827	(264)	96.3	(3.5)
12	2183	(536)	859	(367)	97.9	(2.0)
13	2085	(599)	836	(396)	98.9	(1.3)
14	1976	(445)	732	(107)	99.5	(0.9)
15	2106	(437)	822	(207)	97.5	(1.7)

* - STANDARD DEVIATION FOR PRECEEDING VARIABLE

THE UNIVERSITY OF OKLAHOMA
CTS 1984 SCHLEGEL SUMMER STUDY

Table 8a. UNSTABLE TRACKING TASK

----- GROUP = A WORKLOAD LEVEL = LOW -----

TRIAL	MEAN ABS ERROR	(*)	MEAN EDGE VIOL	(*)
1	9	(4)	3	(5)
2	9	(4)	2	(3)
3	8	(2)	0	
4	9	(3)	3	(4)
5	9	(3)	1	(2)

----- GROUP = A WORKLOAD LEVEL = MEDIUM -----

TRIAL	MEAN ABS ERROR	(*)	MEAN EDGE VIOL	(*)
1	40	(1)	243	(66)
2	37	(2)	158	(53)
3	36	(4)	130	(69)
4	34	(4)	115	(59)
5	35	(3)	112	(65)

----- GROUP = A WORKLOAD LEVEL = HIGH -----

TRIAL	MEAN ABS ERROR	(*)	MEAN EDGE VIOL	(*)
1	37	(2)	406	(70)
2	38	(3)	386	(102)
3	38	(3)	383	(85)
4	36	(5)	358	(77)
5	37	(4)	373	(63)

* - STANDARD DEVIATION FOR PRECEEDING VARIABLE

THE UNIVERSITY OF OKLAHOMA
CTS 1984 SCHLEGEL SUMMER STUDY

Table 8b. UNSTABLE TRACKING TASK

----- GROUP = C WORKLOAD LEVEL = LOW -----				
TRIAL	MEAN ABS ERROR	(*)	MEAN EDGE VIOL	(*)
1	12	(8)	13	(15)
2	6	(3)	1	(2)
3	6	(3)	1	(1)
4	5	(2)	0	
5	6	(3)	0	
6	5	(2)	0	
7	7	(2)	0	
8	6	(3)	0	
9	8	(2)	0	
10	7	(2)	0	
11	7	(2)	0	
12	9	(2)	1	
13	6	(2)	0	
14	9	(3)	0	
15	9	(5)	1	(1)
----- GROUP = C WORKLOAD LEVEL = MEDIUM -----				
1	37	(5)	222	(106)
2	31	(11)	117	(83)
3	29	(11)	97	(76)
4	29	(9)	86	(81)
5	28	(10)	61	(65)
6	29	(7)	64	(63)
7	31	(3)	74	(48)
8	31	(3)	75	(57)
9	30	(5)	65	(46)
10	33	(4)	90	(58)
11	32	(3)	73	(65)
12	32	(3)	82	(68)
13	29	(8)	67	(73)
14	32	(6)	74	(62)
15	30	(2)	62	(32)
----- GROUP = C WORKLOAD LEVEL = HIGH -----				
1	38	(3)	400	(91)
2	35	(3)	320	(61)
3	35	(2)	321	(73)
4	36	(2)	339	(70)
5	37	(2)	373	(107)
6	38	(4)	429	(244)
7	38		356	(56)
8	36	(2)	337	(51)
9	35	(3)	321	(65)
10	38	(1)	370	(46)
11	36		332	(35)
12	36	(2)	350	(42)
13	38	(1)	369	(83)
14	37	(2)	335	(42)
15	36	(2)	354	(74)

* - STANDARD DEVIATION FOR PRECEEDING VARIABLE

THE UNIVERSITY OF OKLAHOMA
CTS 1984 SCHLEGEL SUMMER STUDY

Table 9a. SPATIAL PROCESSING TASK

----- GROUP = A WORKLOAD LEVEL = LOW -----						
TRIAL	MEAN	(*)	STD_DEV	(*)	PCT CCR	(*)
	(msec)		(msec)		(%)	
1	1061	(330)	432	(192)	95.8	(3.0)
2	932	(293)	379	(160)	93.7	(5.7)
3	862	(198)	355	(156)	96.5	(5.9)
4	770	(287)	343	(232)	94.4	(6.6)
5	803	(158)	361	(162)	93.4	(6.3)

----- GROUP = A WORKLOAD LEVEL = MEDIUM -----						
TRIAL	MEAN	(*)	STD_DEV	(*)	PCT COR	(*)
	(msec)		(msec)		(%)	
1	1680	(486)	795	(480)	91.2	(2.8)
2	1503	(437)	509	(202)	93.3	(9.3)
3	1372	(421)	469	(181)	93.0	(6.5)
4	1368	(412)	596	(106)	92.9	(11.6)
5	1242	(371)	431	(76)	87.0	(15.4)

----- GROUP = A WORKLOAD LEVEL = HIGH -----						
TRIAL	MEAN	(*)	STD_DEV	(*)	PCT COR	(*)
	(msec)		(msec)		(%)	
1	1815	(395)	645	(207)	88.5	(13.8)
2	1566	(226)	616	(85)	91.3	(10.2)
3	1651	(458)	730	(245)	90.0	(14.7)
4	1648	(269)	778	(117)	89.7	(13.2)
5	1682	(648)	677	(271)	84.8	(19.1)

* - STANDARD DEVIATION FOR PRECEEDING VARIABLE

THE UNIVERSITY OF OKLAHOMA
CTS 1984 SCHLEGEL SUMMER STUDY

Table 9b. SPATIAL PROCESSING TASK

----- GROUP = C WORKLOAD LEVEL = LOW -----						
TRIAL	MEAN	(*)	STD_DEV	(*)	PCT COR	(*)
	(msec)		(msec)		(%)	
1	904	(209)	245	(63)	95.9	(5.7)
2	750	(177)	258	(149)	93.8	(7.5)
3	732	(160)	290	(163)	92.2	(6.1)
4	618	(120)	237	(102)	98.5	(3.3)
5	702	(196)	237	(96)	93.9	(5.8)
6	611	(136)	199	(76)	96.8	(5.2)
7	563	(112)	148	(54)	94.7	(6.4)
8	745	(292)	260	(69)	96.9	(3.2)
9	616	(198)	246	(130)	96.2	(2.7)
10	559	(166)	175	(77)	96.2	(2.5)
11	598	(194)	183	(58)	95.6	(6.4)
12	620	(216)	230	(162)	94.6	(3.2)
13	549	(170)	174	(121)	94.9	(5.3)
14	589	(217)	193	(92)	95.4	(3.1)
15	578	(182)	190	(127)	98.4	(2.1)
----- GROUP = C WORKLOAD LEVEL = MEDIUM -----						
1	1362	(308)	438	(197)	90.6	(7.8)
2	1288	(220)	521	(213)	89.9	(9.8)
3	1202	(181)	498	(269)	90.9	(9.3)
4	1286	(295)	499	(175)	90.7	(6.2)
5	1293	(160)	550	(183)	93.2	(6.3)
6	1359	(356)	617	(318)	93.3	(4.6)
7	1040	(240)	423	(215)	95.1	(1.7)
8	967	(355)	442	(308)	93.4	(8.6)
9	1083	(229)	491	(152)	95.1	(4.4)
10	1183	(247)	577	(275)	93.2	(6.3)
11	1198	(267)	534	(317)	95.0	(3.5)
12	1244	(318)	559	(267)	94.0	(5.0)
13	1186	(298)	636	(355)	92.4	(4.4)
14	1045	(168)	473	(304)	91.9	(6.4)
15	1052	(176)	723	(670)	95.9	(5.7)
----- GROUP = C WORKLOAD LEVEL = HIGH -----						
1	1604	(413)	662	(235)	83.4	(15.1)
2	1466	(301)	559	(207)	79.5	(20.7)
3	1661	(580)	817	(604)	88.0	(16.9)
4	1611	(435)	671	(204)	75.9	(22.9)
5	1662	(403)	746	(475)	96.5	(5.6)
6	1698	(593)	677	(269)	96.5	(5.6)
7	1509	(491)	663	(245)	88.6	(9.5)
8	1408	(333)	524	(213)	93.1	(7.7)
9	1399	(400)	541	(202)	92.3	(6.4)
10	1330	(206)	629	(251)	97.4	(2.3)
11	1574	(503)	849	(443)	91.3	(3.1)
12	1463	(491)	738	(194)	92.2	(3.5)
13	1449	(742)	657	(504)	97.5	(3.7)
14	1306	(362)	604	(124)	95.7	(4.3)
15	1429	(621)	615	(277)	93.0	(4.8)

* - STANDARD DEVIATION FOR PRECEEDING VARIABLE

THE UNIVERSITY OF OKLAHOMA
CTS 1984 SCHLEGEL SUMMER STUDY

Table 10a. LINGUISTIC PROCESSING TASK

----- GROUP = A WORKLOAD LEVEL = LOW -----						
TRIAL	MEAN	(*)	STD_DEV	(*)	PCT COR	(*)
	(msec)		(msec)		(%)	
1	680	(103)	285	(144)	98.2	(1.2)
2	611	(102)	255	(171)	97.8	(2.0)
3	611	(115)	204	(96)	98.7	(1.5)
4	547	(79)	199	(94)	94.4	(5.7)
5	545	(78)	163	(76)	96.5	(1.7)

----- GROUP = A WORKLOAD LEVEL = MEDIUM -----						
TRIAL	MEAN	(*)	STD_DEV	(*)	PCT COR	(*)
	(msec)		(msec)		(%)	
1	1439	(393)	895	(577)	95.6	(3.7)
2	1170	(406)	634	(403)	95.9	(3.6)
3	1035	(318)	496	(298)	96.0	(4.1)
4	895	(227)	356	(157)	94.4	(5.1)
5	885	(273)	399	(264)	94.3	(5.7)

----- GROUP = A WORKLOAD LEVEL = HIGH -----						
TRIAL	MEAN	(*)	STD_DEV	(*)	PCT COR	(*)
	(msec)		(msec)		(%)	
1	2398	(810)	1036	(269)	86.7	(4.4)
2	1923	(695)	762	(332)	89.3	(5.3)
3	1929	(539)	931	(555)	89.1	(4.4)
4	1620	(290)	691	(260)	87.4	(3.8)
5	1608	(347)	692	(358)	84.3	(6.7)

* - STANDARD DEVIATION FOR PRECEEDING VARIABLE

THE UNIVERSITY OF OKLAHOMA
CTS 1984 SCHLEGEL SUMMER STUDY

Table 10b. LINGUISTIC PROCESSING TASK

----- GROUP = D WORKLOAD LEVEL = LOW -----						
TRIAL	MEAN	(*)	STD_DEV	(*)	PCT COR	(*)
	(msec)		(msec)		(%)	
1	675	(155)	171	(57)	97.6	(0.9)
2	650	(140)	181	(61)	98.1	(1.5)
3	580	(83)	157	(71)	98.2	(0.9)
4	539	(72)	119	(46)	97.6	(1.7)
5	543	(77)	123	(68)	96.7	(2.7)
6	531	(48)	129	(55)	96.8	(2.8)
7	525	(54)	158	(97)	95.5	(2.4)
8	521	(37)	136	(61)	97.3	(3.2)
9	532	(35)	124	(53)	99.3	(0.7)
10	507	(34)	132	(55)	97.6	(1.0)
11	530	(43)	119	(53)	98.2	(0.6)
12	539	(49)	124	(59)	97.9	(1.3)
13	499	(38)	96	(38)	97.9	(0.6)
14	507	(53)	121	(61)	96.2	(3.7)
15	504	(51)	118	(46)	96.8	(2.2)
----- GROUP = D WORKLOAD LEVEL = MEDIUM -----						
1	1170	(241)	427	(56)	92.4	(4.2)
2	1113	(270)	420	(127)	94.8	(3.4)
3	1036	(275)	406	(204)	89.6	(12.1)
4	951	(262)	290	(179)	93.2	(3.5)
5	874	(222)	246	(111)	93.9	(2.6)
6	834	(174)	265	(113)	94.9	(2.6)
7	818	(175)	237	(79)	94.5	(2.5)
8	819	(155)	281	(139)	95.2	(2.7)
9	868	(181)	333	(177)	95.0	(3.0)
10	779	(97)	212	(64)	96.4	(1.8)
11	764	(108)	296	(169)	96.5	(2.1)
12	747	(191)	261	(168)	95.5	(1.3)
13	698	(135)	191	(95)	96.4	(2.2)
14	717	(149)	221	(105)	94.9	(2.3)
15	702	(146)	233	(127)	94.7	(1.9)
----- GROUP = D WORKLOAD LEVEL = HIGH -----						
1	1875	(512)	724	(295)	89.0	(7.5)
2	1762	(393)	776	(412)	88.2	(2.8)
3	1558	(341)	556	(158)	87.5	(4.2)
4	1478	(299)	489	(136)	88.9	(4.5)
5	1387	(351)	512	(171)	88.1	(3.7)
6	1425	(381)	608	(303)	88.1	(5.5)
7	1390	(348)	495	(216)	87.4	(5.5)
8	1461	(394)	793	(605)	89.1	(6.7)
9	1362	(315)	543	(287)	88.3	(4.0)
10	1286	(345)	448	(177)	91.1	(4.5)
11	1407	(372)	684	(416)	89.2	(2.1)
12	1341	(453)	531	(360)	91.4	(2.3)
13	1282	(292)	487	(189)	87.6	(6.1)
14	1269	(267)	457	(183)	92.4	(3.7)
15	1281	(256)	478	(208)	89.8	(4.3)

* - STANDARD DEVIATION FOR PRECEEDING VARIABLE

THE UNIVERSITY OF OKLAHOMA
CTS 1984 SCHLEGEL SUMMER STUDY

Table 11a. INTERVAL PRODUCTION TASK

----- GROUP = A -----						
TRIAL	INTRVAL MEAN (msec)	(*)	INTRVAL STD_DEV (msec)	(*)	VARIBLTY SCORE	(*)
1	517	(141)	79	(94)	23.7	(5)
2	450	(117)	40	(17)	35.4	(22)
3	449	(83)	48	(20)	38.2	(27)
4	450	(70)	68	(55)	51.9	(56)
5	439	(88)	67	(58)	51.8	(47)

Table 11b. INTERVAL PRODUCTION TASK

----- GROUP = D -----						
TRIAL	INTRVAL MEAN (msec)	(*)	INTRVAL STD_DEV (msec)	(*)	VARIBLTY SCORE	(*)
1	635	(116)	52	(46)	24.1	(27)
2	584	(90)	54	(45)	24.4	(21)
3	545	(97)	39	(17)	20.4	(7)
4	498	(43)	39	(10)	23.0	(6)
5	489	(66)	30	(7)	22.8	(8)
6	510	(86)	36	(16)	21.2	(7)
7	502	(75)	34	(17)	21.4	(12)
8	504	(41)	37	(22)	21.8	(12)
9	508	(42)	47	(36)	21.4	(9)
10	512	(38)	27	(8)	17.9	(5)
11	517	(43)	41	(32)	21.4	(13)
12	515	(45)	27	(11)	18.4	(8)
13	538	(57)	25	(7)	15.2	(1)
14	503	(55)	25	(5)	18.6	(7)
15	524	(44)	29	(14)	18.1	(5)

* - STANDARD DEVIATION FOR PRECEEDING VARIABLE

THE UNIVERSITY OF OKLAHOMA
CTS 1984 SCHLEGEL SUMMER STUDY

Table 12a. CONTINUOUS RECALL TASK

----- GROUP = A WORKLOAD LEVEL = LOW -----						
TRIAL	MEAN	(*)	STD_DEV	(*)	PCT COR	(*)
	(msec)		(msec)		(%)	
1	1794	(702)	1004	(347)	90.7	(14.2)
2	1527	(561)	709	(344)	92.9	(11.2)
3	1575	(411)	725	(217)	92.1	(12.4)
4	1450	(384)	733	(215)	91.6	(14.2)
5	1352	(406)	774	(227)	92.0	(14.2)

----- GROUP = A WORKLOAD LEVEL = MEDIUM -----						
TRIAL	MEAN	(*)	STD_DEV	(*)	PCT COR	(*)
	(msec)		(msec)		(%)	
1	2636	(1168)	1247	(537)	84.1	(15.0)
2	2602	(1226)	1040	(506)	86.5	(20.8)
3	2723	(941)	1044	(261)	89.1	(14.6)
4	2403	(855)	847	(248)	91.7	(13.6)
5	2299	(516)	887	(258)	94.1	(10.3)

----- GROUP = A WORKLOAD LEVEL = HIGH -----						
TRIAL	MEAN	(*)	STD_DEV	(*)	PCT COR	(*)
	(msec)		(msec)		(%)	
1	4002	(1966)	1737	(1007)	75.6	(17.1)
2	464	(2146)	1603	(588)	81.5	(16.5)
3	4134	(1985)	1383	(376)	84.9	(14.5)
4	3489	(1573)	1361	(433)	81.0	(17.0)
5	3823	(1574)	1328	(523)	79.7	(12.3)

* - STANDARD DEVIATION FOR PRECEEDING VARIABLE

THE UNIVERSITY OF OKLAHOMA
CTS 1984 SCHLEGEL SUMMER STUDY

Table 12b. CONTINUOUS RECALL TASK

----- GROUP = D WORKLOAD LEVEL = LOW -----						
TRIAL	MEAN	(*)	STD_DEV	(*)	PCT COR	(*)
	(msec)		(msec)		(%)	
1	1207	(267)	485	(150)	94.6	(3.4)
2	1067	(144)	454	(114)	95.7	(2.6)
3	946	(97)	413	(141)	96.3	(1.9)
4	879	(196)	327	(131)	95.8	(2.8)
5	848	(191)	323	(171)	96.7	(2.9)
6	777	(167)	340	(173)	95.5	(0.6)
7	781	(186)	344	(169)	96.4	(4.9)
8	742	(133)	360	(221)	97.2	(1.7)
9	795	(173)	337	(219)	96.8	(1.4)
10	752	(171)	360	(194)	95.8	(1.9)
11	757	(156)	405	(223)	96.1	(2.6)
12	730	(150)	292	(149)	97.7	(1.1)
13	637	(160)	263	(144)	96.5	(1.4)
14	670	(185)	295	(201)	95.6	(1.6)
15	615	(153)	209	(146)	97.0	(1.7)

----- GROUP = D WORKLOAD LEVEL = MEDIUM -----						
1	2939	(887)	1104	(322)	80.6	(7.4)
2	2113	(401)	801	(137)	79.7	(9.2)
3	2151	(711)	970	(284)	80.7	(9.2)
4	2155	(975)	701	(388)	87.1	(11.5)
5	1933	(830)	849	(728)	82.5	(11.2)
6	1862	(769)	775	(481)	87.7	(9.1)
7	1808	(790)	654	(380)	86.2	(14.1)
8	1807	(808)	722	(434)	84.3	(10.9)
9	1737	(668)	725	(447)	87.0	(14.7)
10	1852	(967)	731	(527)	85.1	(18.0)
11	1805	(983)	718	(478)	87.0	(13.4)
12	1672	(808)	681	(394)	88.3	(10.6)
13	1585	(746)	559	(291)	86.8	(13.9)
14	1565	(756)	653	(453)	87.8	(8.4)
15	1498	(711)	494	(247)	84.8	(10.6)

----- GROUP = D WORKLOAD LEVEL = HIGH -----						
1	2781	(894)	1101	(347)	65.5	(5.2)
2	2345	(587)	1008	(484)	71.7	(12.3)
3	3328	(1552)	1145	(877)	78.7	(6.2)
4	2809	(1339)	1003	(808)	71.1	(14.0)
5	2433	(1046)	830	(497)	74.7	(11.3)
6	2636	(1364)	891	(708)	74.8	(14.9)
7	2513	(1222)	845	(644)	76.7	(13.2)
8	2449	(1198)	772	(575)	75.1	(13.6)
9	2431	(1062)	1079	(722)	76.1	(10.1)
10	2605	(1393)	947	(706)	74.5	(14.3)
11	2596	(1395)	1141	(768)	75.7	(14.3)
12	2533	(1291)	1016	(706)	75.0	(10.2)
13	2318	(1345)	736	(460)	77.9	(13.8)
14	2082	(1034)	717	(397)	76.5	(12.6)
15	2258	(1286)	788	(555)	74.7	(10.6)

* - STANDARD DEVIATION FOR PRECEEDING VARIABLE

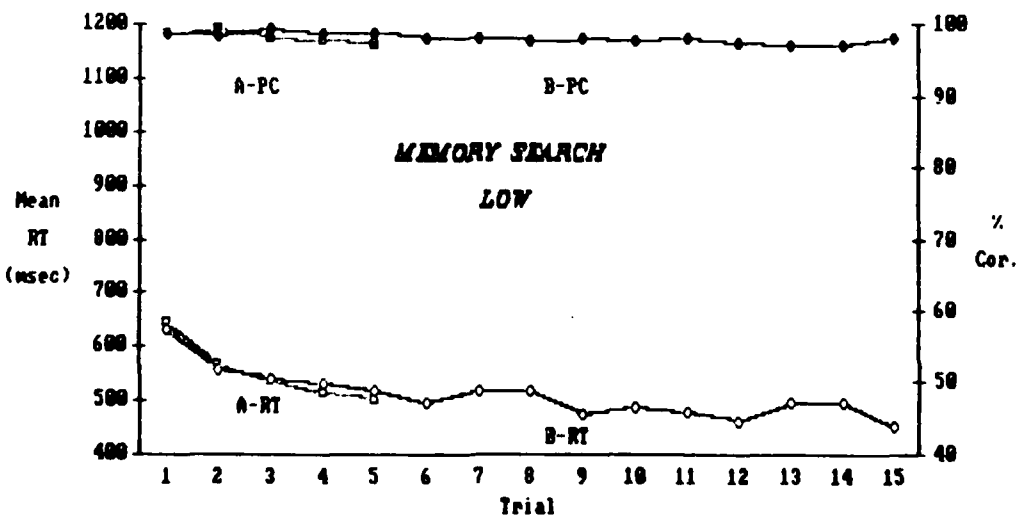
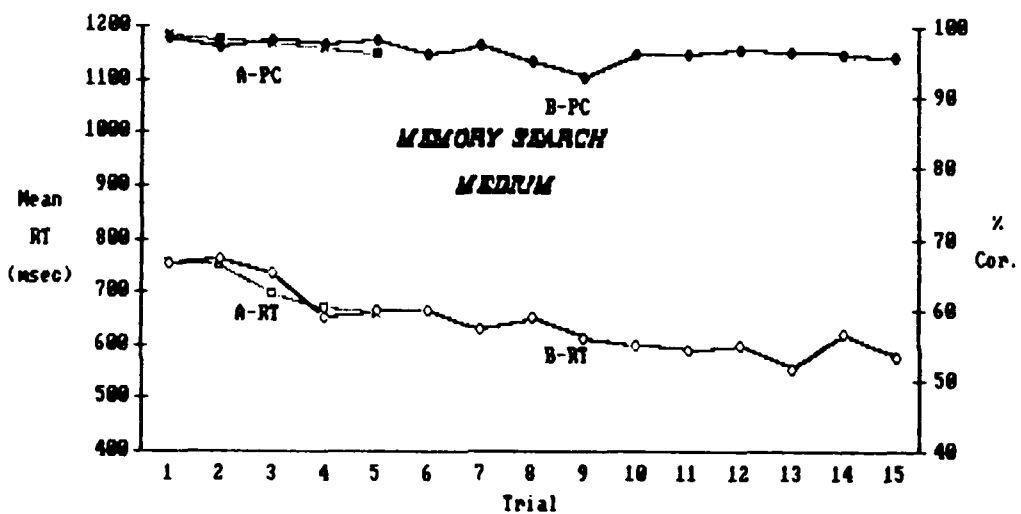
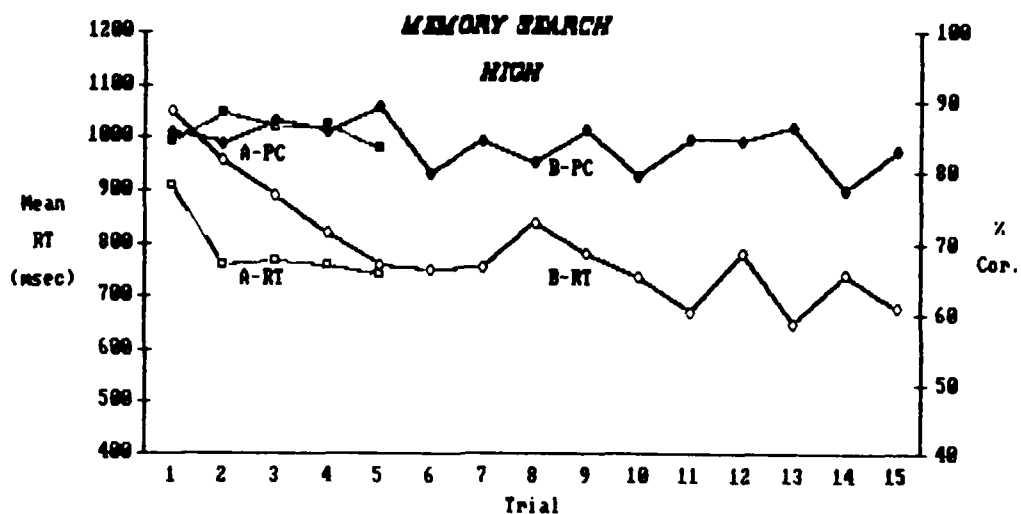


Figure 1. Memory Search.

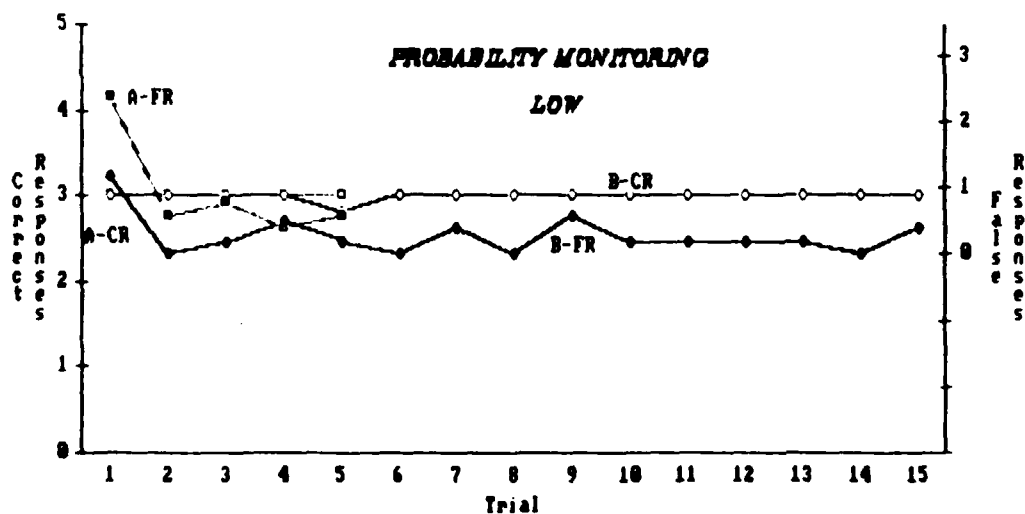
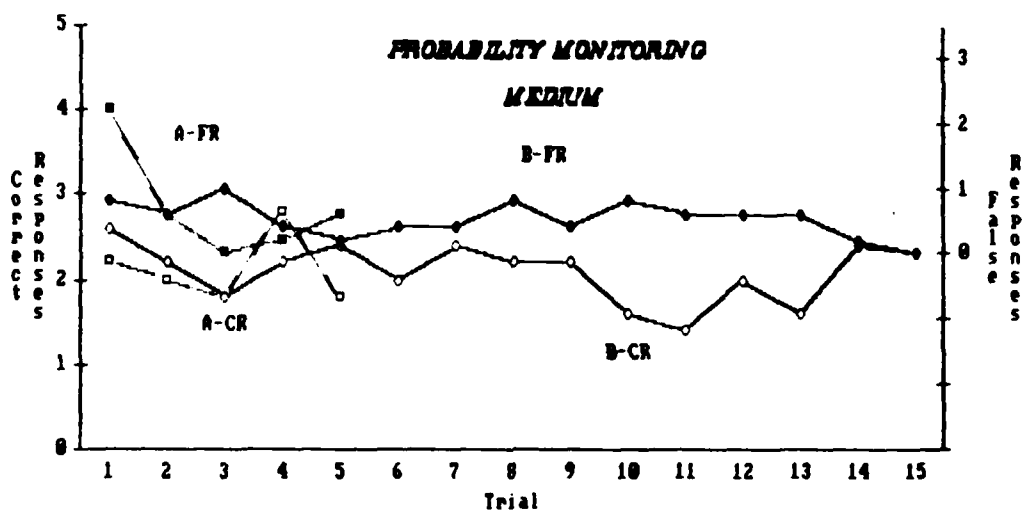
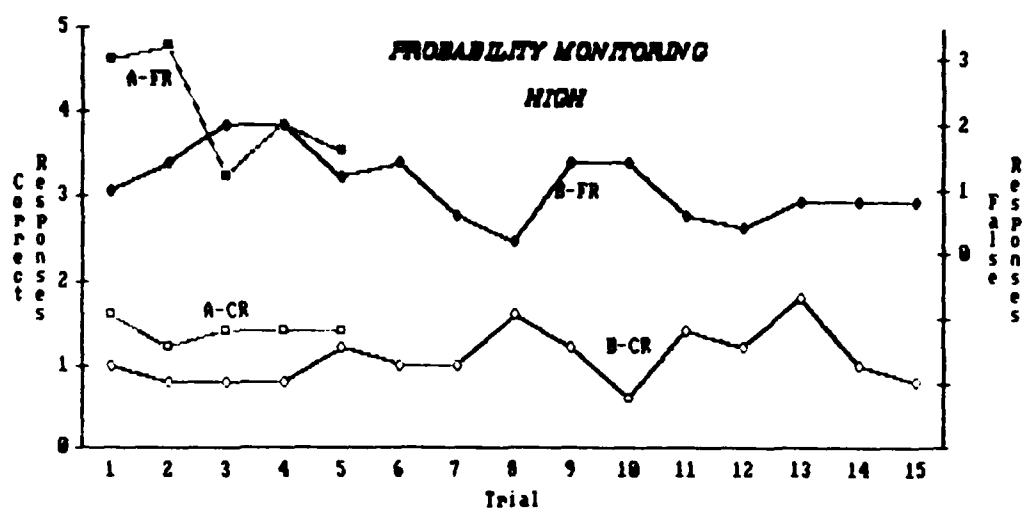


Figure 2. Probability Monitoring.

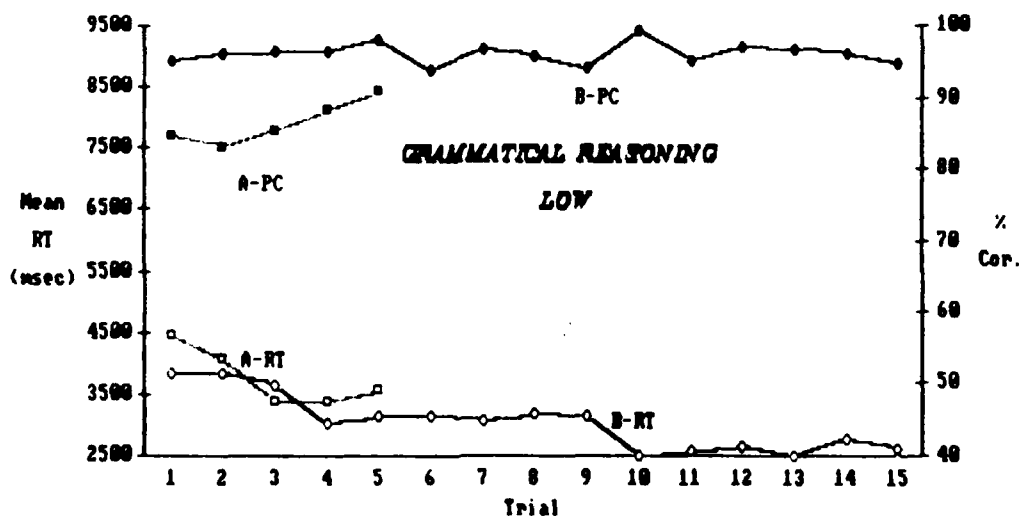
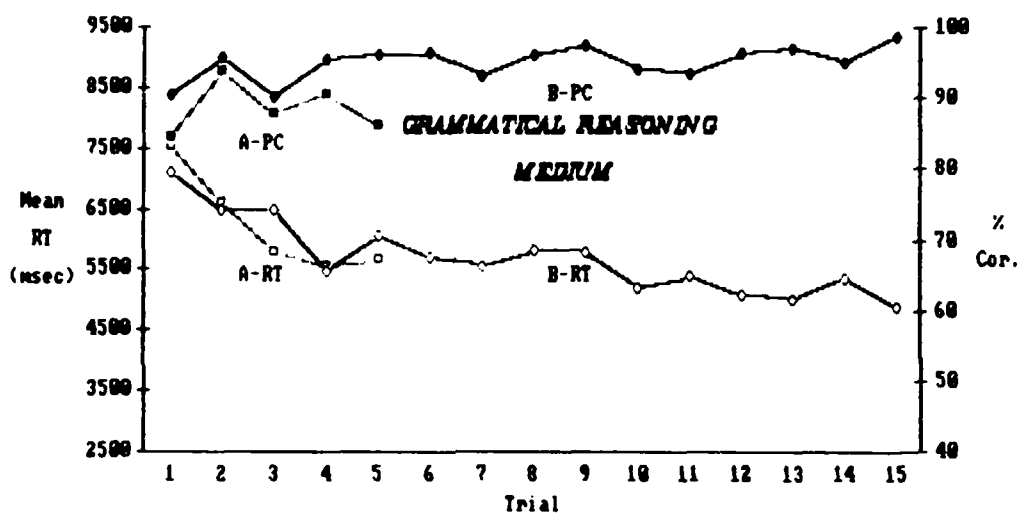
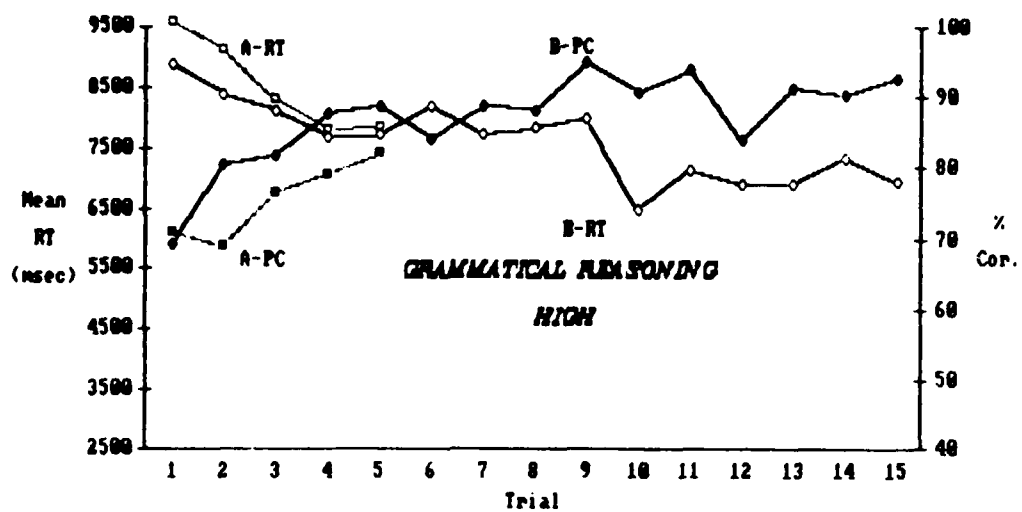


Figure 3. Grammatical Reasoning.

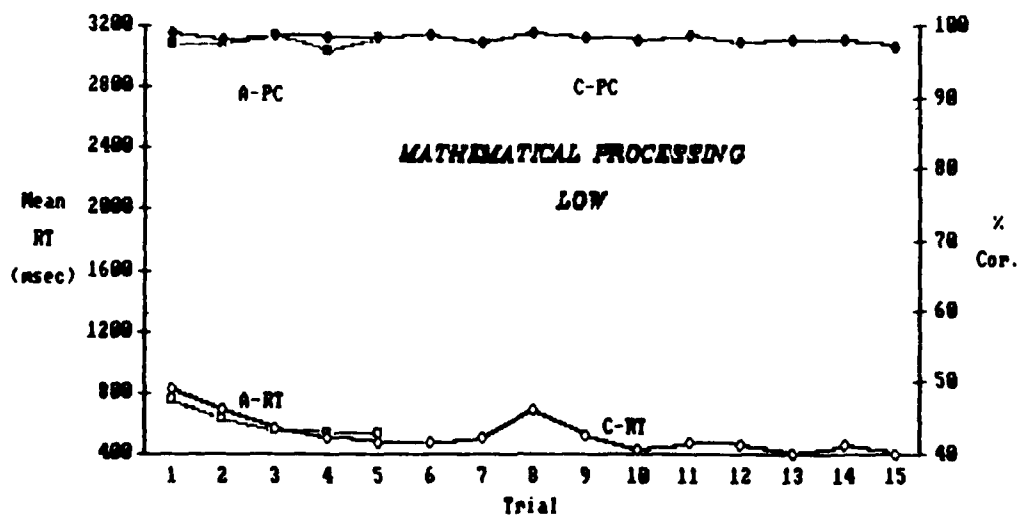
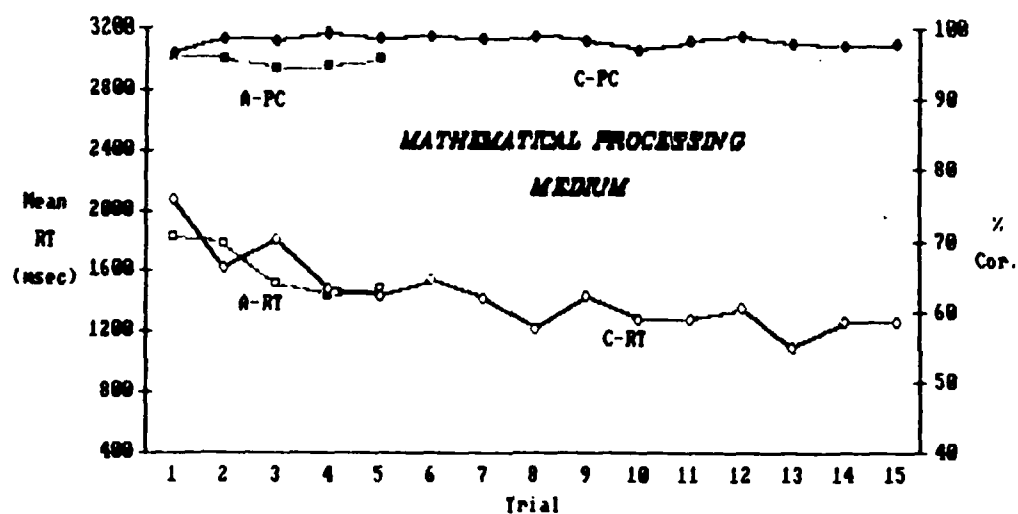
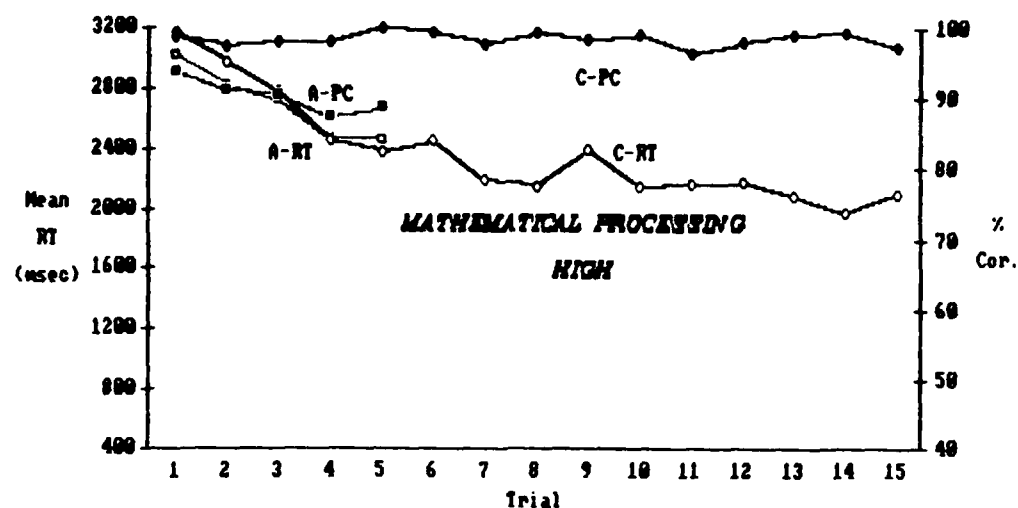


Figure 4. Mathematical Processing.

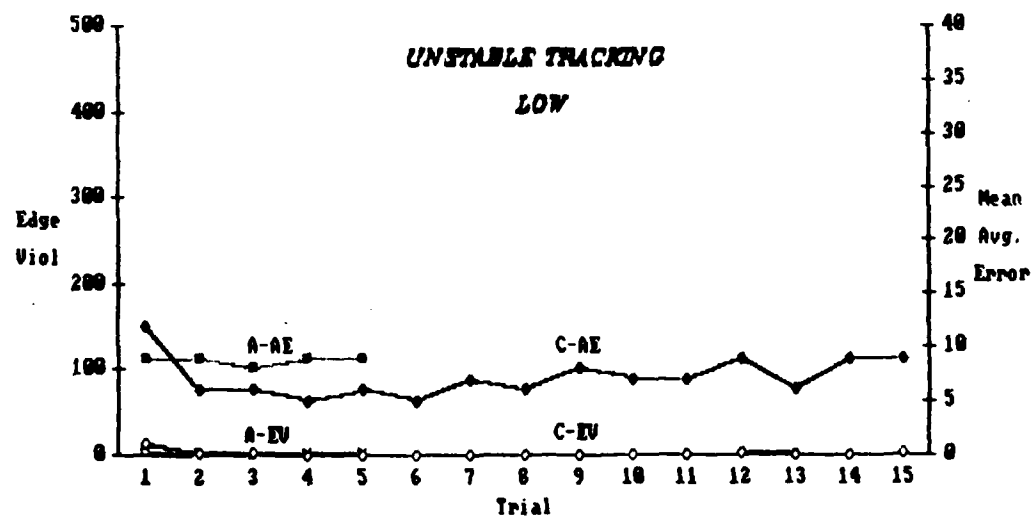
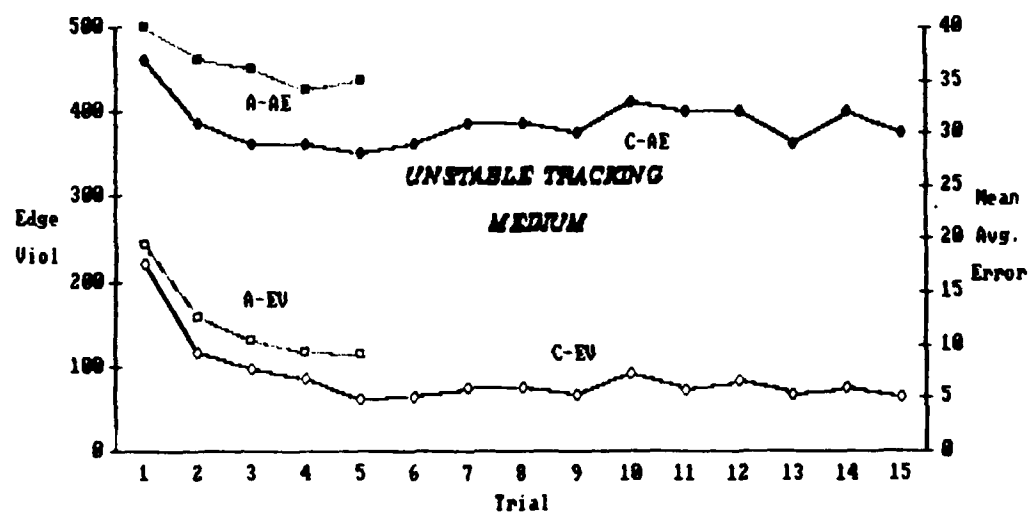
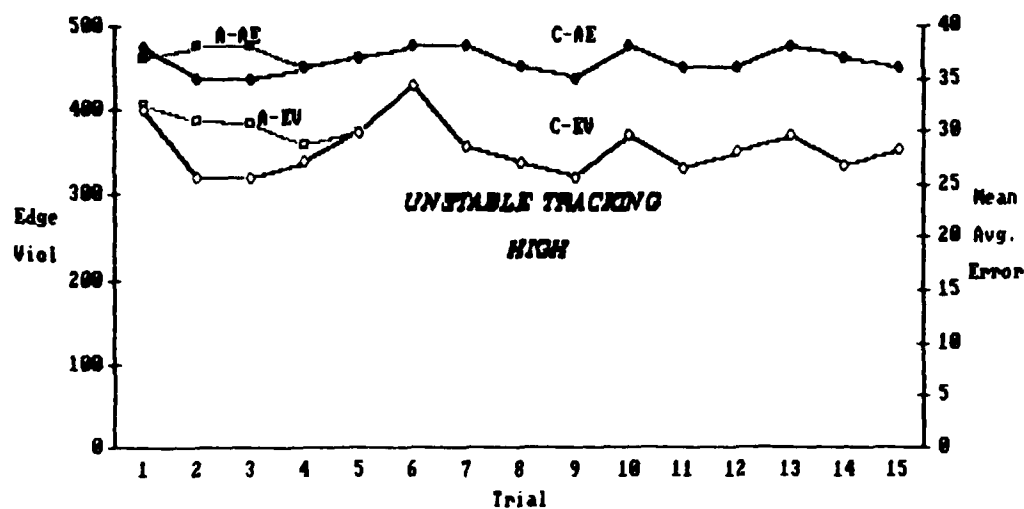


Figure 5. Unstable Tracking.
47.35

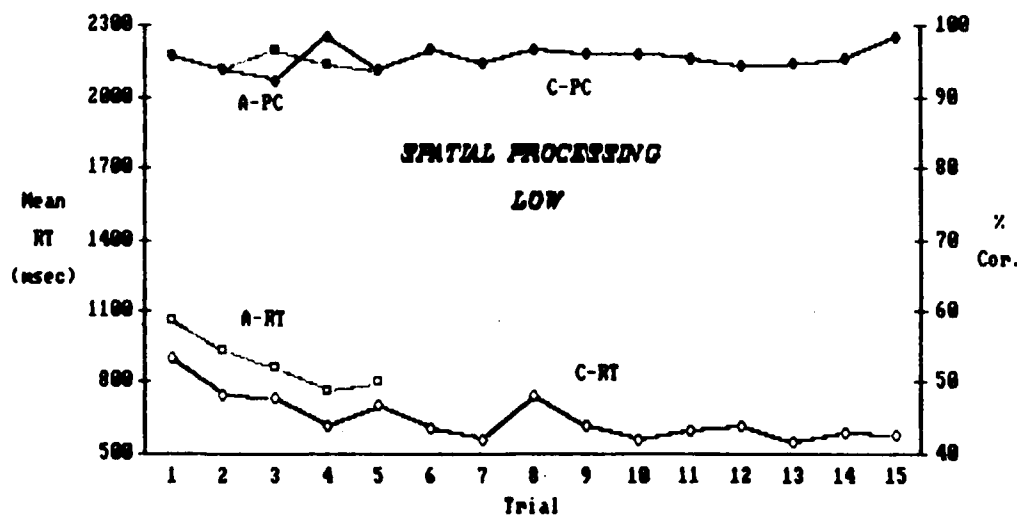
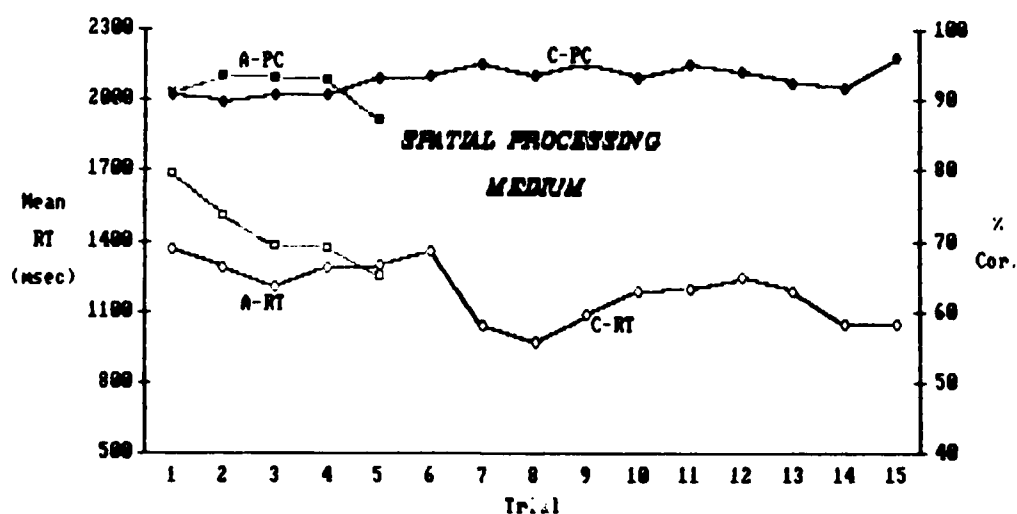
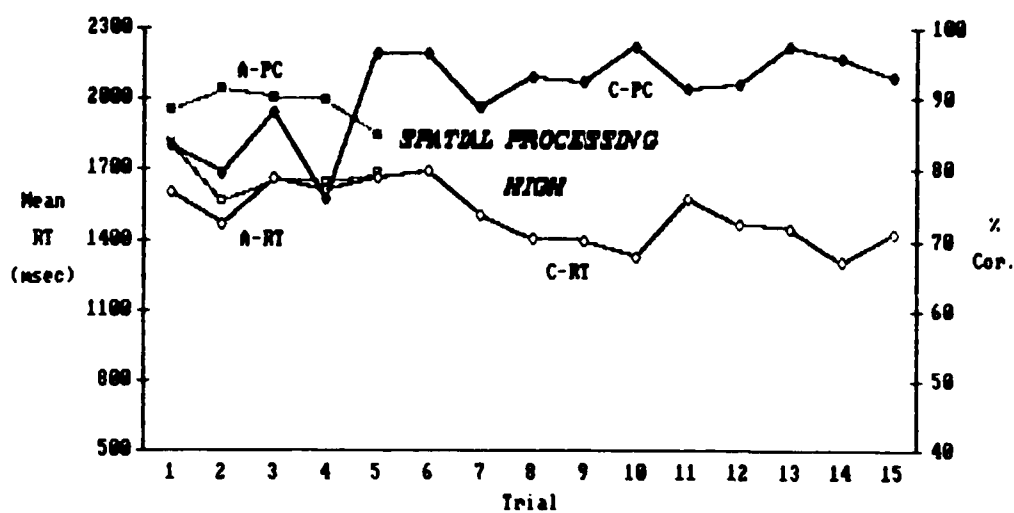


Figure 6. Spatial Processing.
47.36

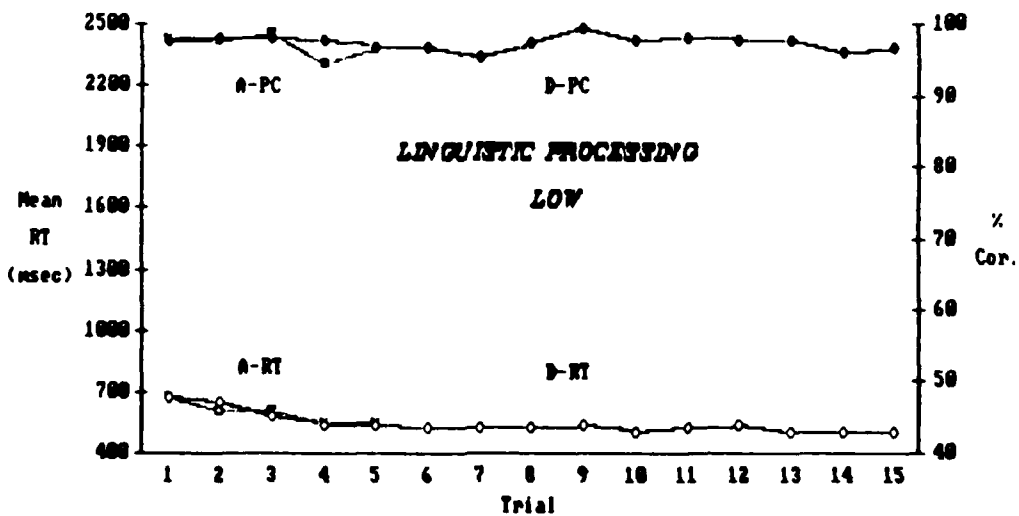
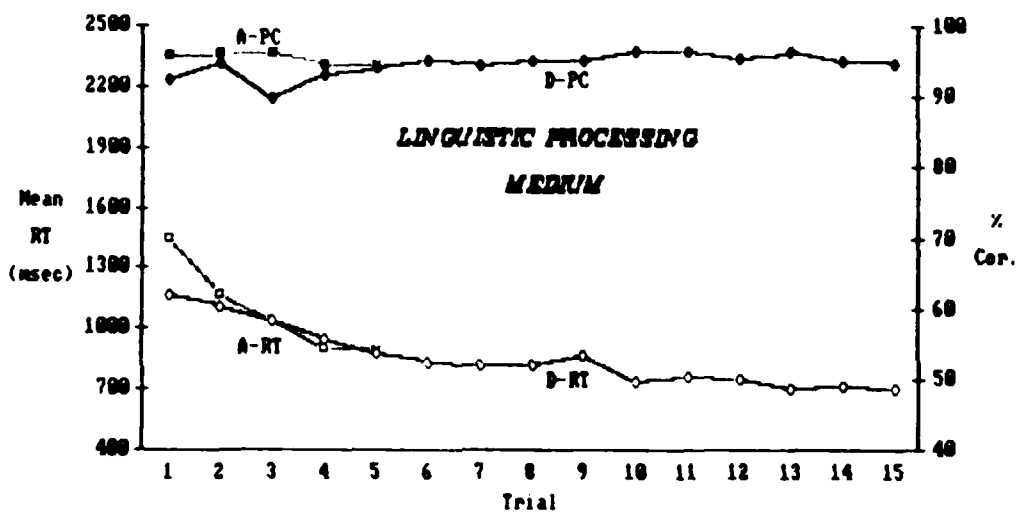
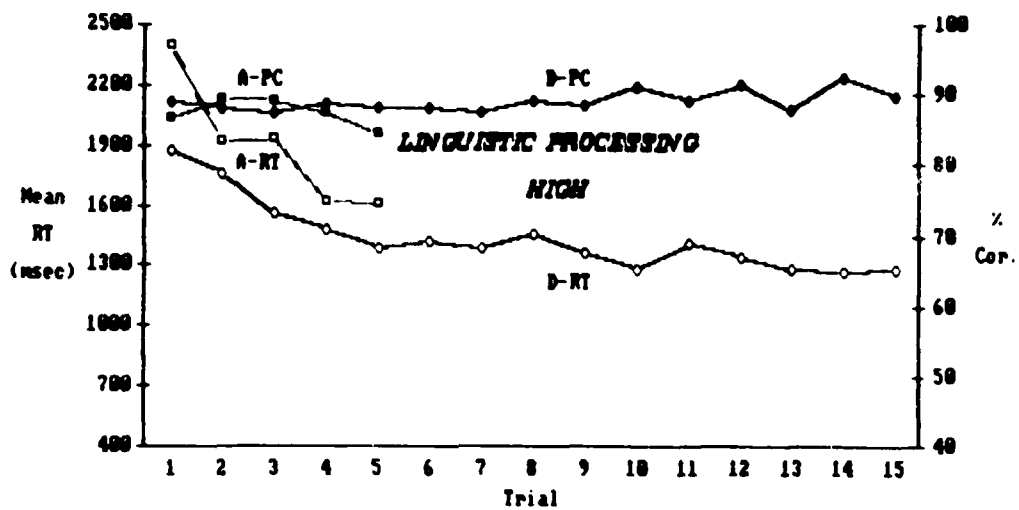


Figure 7. Linguistic Processing.
47.37

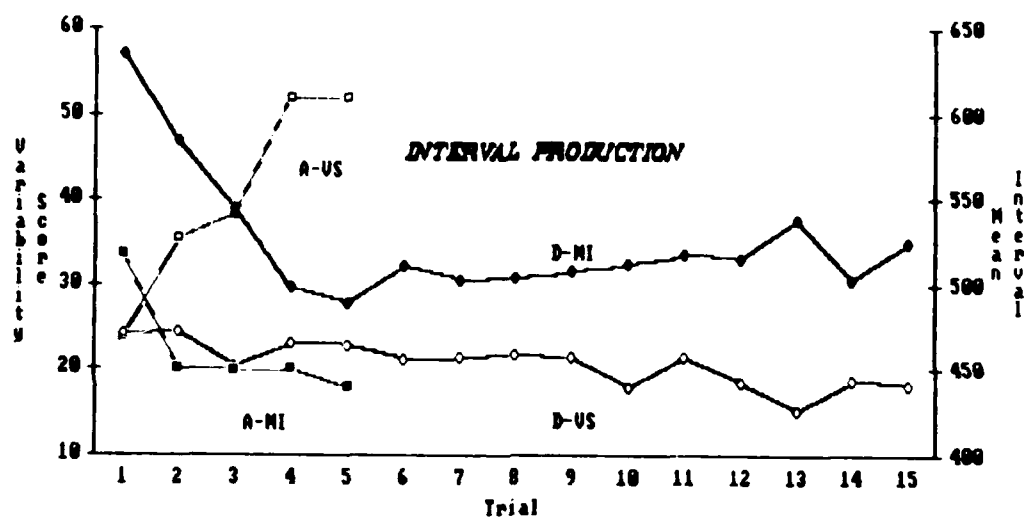


Figure 8. Interval Production.

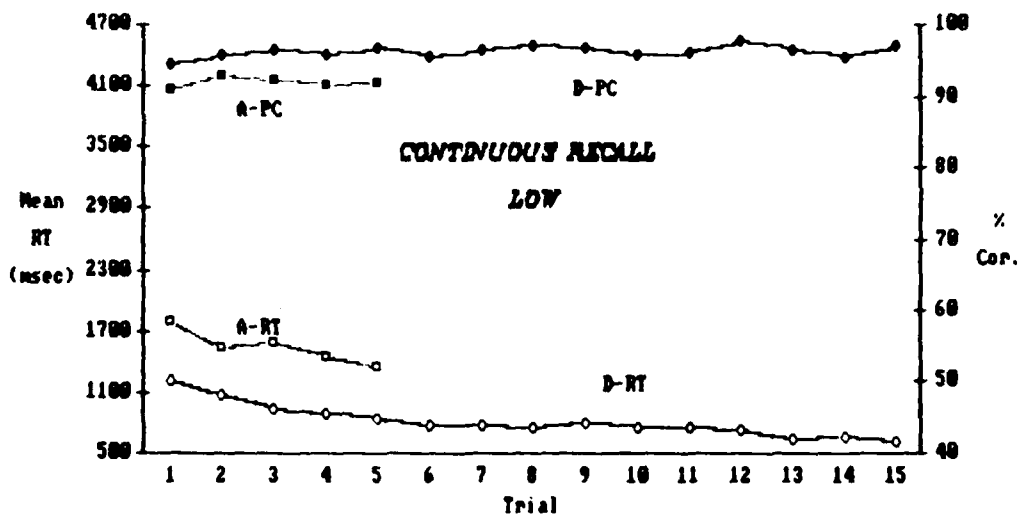
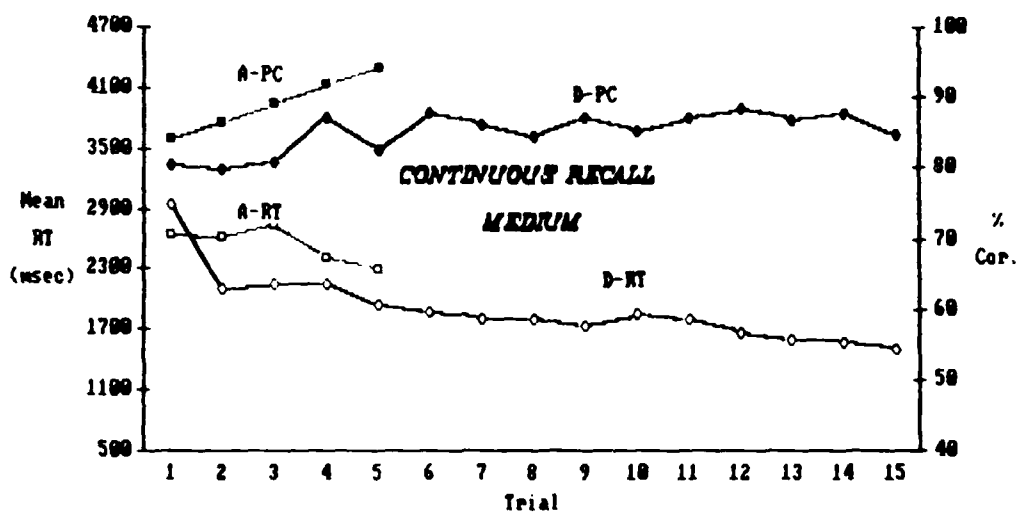
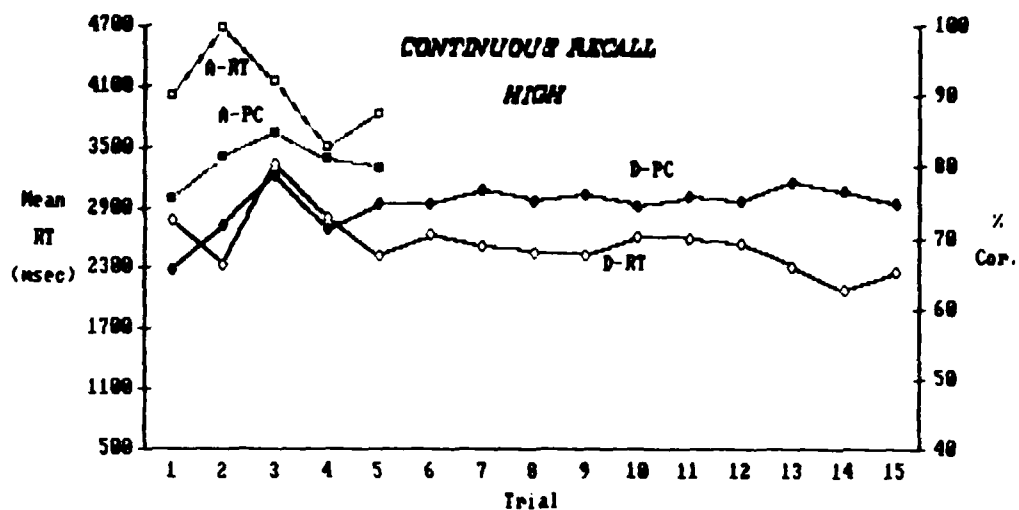


Figure 9. Continuous Recall.

6.0 ANALYSIS AND DISCUSSION

Three separate analysis of variance models were used to isolate the response differences between the groups, trials and workload levels for each task. The first analysis employed a within-subjects factorial design involving the entire data set for a given task, and including Group (G), Trial (T) and Level (L) as the main factors. Only trials 1 through 5 were included in this analysis. The results from this analysis are summarized in Table 13 which gives the value of p for each significant hypothesis test. The variable names for this and subsequent tables consist of a two-letter task code followed by a two-letter code for the dependent variable. The task codes were defined in Table 1 and the variable codes were given in Table 3. In addition, PC represents the percentage correct accuracy score and was obtained by dividing the number of correct responses by the total number of stimuli for each three-minute trial.

As seen in the table, there were no overall differences between the groups and few significant interactions between Group and the other factors. In general, the trial by level interaction was not significant. There were highly significant differences between subjects for virtually every task measure. Differences between trials will be discussed separately for each task.

Because of the highly significant ($p < 0.0001$) differences between workload levels for all task variables, a second set of analyses were performed after isolating the individual data sets for the low, medium and high levels. The major factors in this set of analyses were Group (G) and Trial (T). The results are summarized in Table 14. This approach proved very helpful in isolating the trial differences that were identified in the first set of analyses.

A final set of analyses were performed to determine if the significant trial differences for a given task existed in Group A, Group X (Groups B, C or D) or in both groups. All fifteen trials were included in the analyses for the task subset groups. These results are presented in Table 15.

Summaries of the unique results for each task are given in the sections following the tables and a discussion of the results from the Subjective Workload Assessment Technique concludes the report.

Table 13. Summary of Overall Analyses of Variance.

DEPENDENT VARIABLE	FACTOR				INTERACTION		
	Group	Trial	Level	Subject	GxT	GxL	TxL
MS-MN		*	*	*		.003	
MS-SD		.015	*	*			
MS-PC			*		.071		
PM-RT			*	.085		.059	
PM-PC			*	.064			
PM-FR		.013	*	.001	.025		
GR-MN		*	*	*			
GR-SD		.001	*	*	.070		
GR-PC		.028	*	*			
MP-MN		*	*				
MP-SD		.005	*	*			
MP-PC			.001	*		.001	
UT-AE		.001	*	*		.022	
UT-EV		*	*	*			.001
SP-MN		.012	*	*			
SP-SD			*	*	.044		
SP-PC			*	*			
LP-MN		*	*	*		.007	.070
LP-SD		*	*	*		.053	
LP-PC			*	*			
IP-MN	.089	.008	.	*			
IP-SD			.	.			
IP-VS			.	*			
CR-MN		.086	*	*		.002	
CR-SD		.016	*	*		.050	
CR-PC		.011	*	*		*	

* $p = 0.0001$

Table 14. Summary of Analyses of Variance by Workload Level.

FACTOR	WORKLOAD LEVEL								
	Low			Medium			High		
	G	T	GxT	G	T	GxT	G	T	GxT
DEPENDENT VARIABLE									
MS-MN		*			.001			.002	
MS-SD			.081						
MS-PC									
PM-RT									
PM-PC							.070		
PM-FR					.009	.024			
GR-MN		*	.073		*			.012	
GR-SD		.001	.008						
GR-PC	.087							.076	
MP-MN		*			.001			.003	
MP-SD		.002							
MP-PC									
UT-AE		.059	.073		*				
UT-EV		.006	.047		*				
SP-MN		.001			.014				
SP-SD						.082			
SP-PC									.040
LP-MN		*			*	.030		*	
LP-SD		.022			*	.092		.058	
LP-PC		.037							
IP-MN	.089	.008							
IP-SD									
IP-VS									
CR-MN	.027	.006			.048				.084
CR-SD	.010	.012			.097				
CR-PC					.076			.005	

* p = 0.0001

Table 15. Summary of Individual Analyses of Variance
on Trial Factor by Workload Level and Group.

DEPENDENT VARIABLE	WORKLOAD LEVEL					
	Low		Medium		High	
Groups A and B	A	B	A	B	A	B
MS-MN	.005	*	.028	*		
MS-SD				.035		
MS-PC				*		
PM-RT				.050		
PM-PC						
PM-FR			.006		.096	
GR-MN	.001	*	.001	*	.002	.001
GR-SD	.001	.048				
GR-PC			.041			*
Groups A and C	A	C	A	C	A	C
MP-MN	.001	*	.013	*	.071	*
MP-SD		.002				
MP-PC						
UT-AE		.020	.003	.096		
UT-EV		*	*	*		
SP-MN	.023	*	.009	.020		
SP-SD			.090			
SP-PC						.015
Groups A and D	A	D	A	D	A	D
LP-MN	*	*	*	*	.008	*
LP-SD			.013	*		
LP-PC	.063					
IP-MN		.009
IP-SD		
IP-VS		
CR-MN		*		*		
CR-SD	.079	.012		.017		
CR-PC						

* $p = 0.0001$

6.1 Memory Search Task

Response Time Mean (MS-MN). The mean correct response time for MS, although not significantly different for Groups A and B was faster for Group A especially at the high level. Trials differed significantly at all three levels, especially the low level. As in most tasks, the change in performance was most drastic from trial 1 to trial 2 with trials 2 through 5 not significantly different. For Group B, further improvement was seen for the **middle** trials (8, 9, 10) and the **late** trials (13, 14, 15). Average times for the late trials (L=483, M=584 and H=689 msec) were comparable to the data reported by Shingledecker (1984).

The above results were quite common and may be assumed for the other variables unless stated otherwise. A ranking of subject performance verified a random assignment of subjects to Groups A and B. This result also holds for most variables and tasks and will not be restated.

RT Standard Deviation (MS-SD). The trial standard deviation of response time followed the same pattern as the means except for a lack of difference between trials. Only the medium level for Group B exhibited a significant difference between trials and even in this case there was no clear pattern.

Percentage Correct (MS-PC). Identical statements may be made for response accuracy as measured by percentage correct. In general, accuracy was high across all trials but was significantly lower at the high workload level (L=97%, M=96% and H=82% in latter trials).

6.2 Probability Monitoring Task

Percentage Correct (PM-PC). Aside from the significant differences between workload levels, little can be said with respect to the number or percentage of correct responses for Probability Monitoring. At the low level, 100% accuracy was achieved by all subjects on all trials. At the other levels, this dropped to a range of 50% to 90% over various trials with no clear learning pattern. With only two or three bias signals per trial it is difficult to measure accuracy with adequate precision. An increase in the number of signals during a three-minute trial would reduce this problem.

Response Time (PM-RT). Data for response times is somewhat unreliable due to the small number of signals which means that the **average** response time for a trial may

be based on a single response. The times differed significantly only for the low level (10.5 sec) and could not distinguish between the medium (18.1 sec) and high (18.2 sec) levels. They were comparable to Shingledecker's data except at the high level where the times for the current study were approximately 2 seconds faster. The times showed high variability across trials especially at the medium and high levels with no evidence of improvement with practice at any level.

False Responses (PM-FR). The number of subject responses when no signal was present was significantly higher at the high workload level. There was a constant decrease in the number of false responses over time which was particularly evident for Group A at all levels and for both groups at the medium level.

6.3 Grammatical Reasoning Task

Response Time Mean (GR-MN). The mean correct response time for GR did not differ significantly between Groups A and B. Trials differed significantly for all three levels with a smooth transition from trial 1 through trial 5. For Group B, substantial improvement occurred at trial ten especially at the low and medium levels. This trial represented the beginning of the fourth day of testing and may represent a strategy change on the part of some subjects. Average times even during the latter trials (L=2626, M=5097 and H=7074 msec) were substantially longer (1000-1500 msec) than the data reported by Shingledecker with times for the middle trials an additional 400 to 600 msec higher.

RT Standard Deviation (GR-SD). Overall the trial standard deviation of RT does not distinguish between the low and medium workload levels. Differences between trials existed primarily at the low level for Group A which exhibited a drastic decrease from trial 1 to trial 2.

Percentage Correct (GR-PC). The accuracy score also did not distinguish between the low and medium levels (L=96%, M=97%, H=92% for late trials). In general, accuracy was quite high and may have accounted for some of the differences in the mean RT comparison with Shingledecker. This is one of few variables which exhibited group differences, with Group A having lower accuracy than Group B at the low workload level (86% vs. 96%). Trials differed significantly for the high level only, ranging from 70% for trial 1 to 85% for trial 5 to 92% for the later trials.

6.4 Mathematical Processing Task

Response Time Mean (MP-MN). The response time mean did not differ between Groups A and C. There was definite improvement over time for both groups at all three workload levels. The improvement was smooth yielding average times during the latter trials (L=420, M=1208 and H=2056 msec) that were identical with the data from Shingledecker.

RT Standard Deviation (MP-SD). The standard deviation distinguished between all three workload levels and decreased steadily over time particularly at the low level.

Percentage Correct (MP-PC). Accuracy was uniformly high across all trials and workload levels (L=98%, M=98% and H=99% for late trials). The significant Group by Level interaction was a result of lower accuracy for Group A subjects primarily at the high workload levels.

6.5 Unstable Tracking Task

Mean Absolute Error (UT-AE). This variable differentiated all three workload levels although the difference between medium (34) and high (37) was small compared with the difference between medium (34) and low (8). Data from latter trials (L=8, M=30 and H=37) agreed with that of Shingledecker except at the low level where the current value was higher. The significant Group by Level interaction was due to the poorer performance of Group A subjects which was evident primarily at the medium level.

Performance improved with practice with the greatest gain from trial 1 to trial 2. However, the pattern was different at each workload level. At the low level, Group A's performance did not change while the performance of Group C improved from trial 1 to trial 2 and gradually deteriorated. The task is very easy at this level and substantial improvement is not possible. The medium level has the greatest potential for improvement and both groups improved over the first two or three trials. At the high level, no improvement took place since the task is so difficult that the available level of training did not improve each subject's inherent tracking skill. This contradicts earlier data indicating that six to twelve practice trials are needed to eliminate major training effects (Shingledecker, 1984). With the current data, one or two trials were sufficient at the low and medium levels whereas 15 trials did not provide any improvement at the high level.

Edge Violation (UT-EV). The edge violations or control losses differed widely

between the three workload levels (L=0, M=68 and H=353 for late trials). These data were very close to the values given by Shingledecker. Trial differences were significant especially at the medium level which provided classic learning curve data. As with the absolute error measure, improvement was not possible at the low level beyond the first trial and could not be achieved at the high level.

6.6 Spatial Processing Task

Response Time Mean (SP-MN). Trial differences were evident primarily at the low and medium levels for both Groups A and C with the largest differences within the first two or three trials. Group C demonstrated a decrease in response time during the later trials (L=572, M=1094 and H=1395 msec) yielding data approximately equal to that reported by Shingledecker for all levels.

RT Standard Deviation (SP-SD). Trial standard deviation easily distinguished all three levels. Only Group A at the medium level demonstrated a marginally significant decrease in standard deviation over time.

Percentage Correct (SP-PC). The accuracy score marginally distinguished between the low and medium levels with the accuracy for the high level substantially lower. Data for the latter trials (L=96%, M=93% and H=95%) showed no difference between the levels. Group C at the high level demonstrated a substantial improvement following the first four trials.

6.7 Linguistic Processing Task

Response Time Mean (LP-MN). The results for LP are very similar to those for the Memory Search Task. Trials differed significantly for all three levels following a smooth learning curve. Group D showed little improvement beyond that obtained in the first five trials with times (L=503, M=706 and H=1277 msec) that agreed with Shingledecker's data for the low and the medium levels but were substantially faster (by 50%) for the high level antonym matching task. This may have been due to stimulus memorization by the current study subjects.

RT Standard Deviation (LP-SD). The standard deviation measure decreased smoothly over trials for all three levels. In addition, it easily differentiated all three workload levels (L=186, M=457 and H=717 msec).

Percentage Correct (LP-PC). Percentage correct remained constant across trials but

differed significantly between all three workload levels (L=97%, M=95% and H=76% for latter trials).

6.8 Interval Production Task

Interval Mean (IP-MN). The mean interval duration was the only variable in the CTS which differed between the two groups. The average interval for Group A was approximately 90 msec shorter than that for Group D. Although not the primary performance criterion for this task, the mean interval duration perhaps indicates a stronger desire on the part of Group A subjects to hurry through the remaining part of the battery as this task was near the end of the sequence. For both groups the mean interval became shorter over the course of the first few trials.

Interval Standard Deviation (IP-SD). No significant differences were observed for this measure partly due to the high degree of inherent subject variability.

Variability Score (IP-VS). Although no significant differences were found for this primary performance measure of the IP task, the performance of Group A deteriorated greatly over the first five trials (24 to 52) while that of Group D remained constant or improved. One plausible explanation is that the Group A subjects used the IP task as a rest break since minimal attention is required to actually perform the task. This inattentiveness possibly increased from the first to the last trial.

6.9 Continuous Recall Task

Response Time Mean (CR-MN). Overall, the mean correct response time did not differ between the groups. However, at the low level, Group A was substantially slower than Group D (1540 vs. 989 msec). Trials differed significantly at the low and medium levels only. Group D continued to improve at all levels during the latter trials (L= 641, M= 1549 and H= 2219 msec). However, these times were substantially longer than those reported by Shingledecker.

RT Standard Deviation (CR-SD). Standard deviation easily differentiated all three workload levels (L=595, M=949 and H=1250 msec). The Pattern across trials and groups was similar to the above mentioned pattern for RT mean.

Percentage Correct (CR-PC). Percentage correct differed substantially between levels even following substantial training (L=96%, M=86% and H=76%). Steady improvement over time was achieved particularly at the medium level.

6.10 Subjective Workload Assessment Technique

The SWAT ratings showed consistent ordered differences between workload levels for all tasks (Table 16). Examination of the ratings also provided a comparison of the relative difficulty across tasks (Table 17). Of the tasks with three distinct workload levels, Mathematical Processing had the lowest rating (*easiest*) and Continuous Recall the highest (*most difficult*).

Table 16. Average SWAT Ratings for Each Task.

TASK	WORKLOAD LEVEL		
	Low	Medium	High
MS	4.6	14.2	29.2
PM	4.6	18.0	35.8
GR	15.5	26.0	37.9
MP	0.0	4.9	14.8
UT	5.6	28.4	57.7
SP	0.0	7.4	14.2
LP	5.4	23.0	38.1
IP	1.9	.	.
CR	27.9	36.5	75.0

Table 17. Subjective Task Difficulty Based on SWAT.

WORKLOAD	TASK
Low	Interval Production
	Mathematical Processing
	Spatial Processing
	Memory Search
	Probability Monitoring
	Linguistic Processing
	Grammatical Reasoning
High	Unstable Tracking
	Continuous Recall

REFERENCES

- Nygren, T.E. (1982, April). *Conjoint Measurement and Conjoint Scaling: A Users Guide*. (Tech. Report AFAMRL-TR-82-22), Wright Patterson Air Force Base, Ohio: Air Force Medical Research Laboratory.
- Reid, G.B. (1982). Subjective Workload Assessment: A Conjoint Scaling Approach. In *Aerospace Medical Association Annual Scientific Meeting* (pp.153-154). Bal Harbor, Florida.
- Reid, G.B., Eggemeier, F.T. and Nygren, T.E. (1982). An Individual Differences Approach to SWAT Scale Development. In *Proceedings of the Human Factors Society 26th Annual Meeting*. (pp. 639-642). Rochester, New York: Human Factors Society.
- Shingledecker, C.A. (1984, November). *A Task Battery for Applied Human Performance Assessment Research*, (Tech. Report AFAMRL-TR-84-071). Wright Patterson Air Force Base, Ohio: Medical Research Laboratory.
- Shingledecker, C.A., Acton, W.H. and Crabtree, M.S. (1983, October). *Development and Application of a Criterion Task Set for Workload Metric Evaluation* (SAE Technical Paper 831419). Aerospace Congress & Exposition, Long Beach, California.
- Sternberg, S. (1969). The Discovery of Processing Stages: Extension of Donders' Method, *Acta Psychologica*, 30, 276-315.
- Wickens, C.D. (1981). *Processing Resources in Attention, Dual Task Performance, and Workload Assessment*, (Tech. Report EPL-81-3). University of Illinois, Illinois: Engineering Psychology Research Laboratory.

Research Report to
SCEEE

Construction of Concept-Atoms

Yin-Min Wei

SCEEE 84-RIP-48

A FINAL RESEARCH REPORT TO
SOUTHEASTERN CENTER FOR ELECTRICAL
ENGINEERING EDUCATION

Construction of Concept-Atoms -- the building blocks
for a semantic-net interface for
interactive information retrieval

Prepared by: Yin-min Wei

Academic Rank: Professor

Department and University: Department of Computer Science
Ohio University

Date: November, 1985

Contract No.: F49620-82-C-0035
SCEEE 84-RIP-48

1. Introduction

This research deals with information systems that hold collections of data records. Each record can be the citation of a journal article, a book, or an information module composed for a special purpose. A special characteristic of these systems is that each data record is represented by a set of index terms first. At the indexing time, the problem of the indexer is to select a proper set of subject terms to represent each record. "How to select a proper set of terms for each record," has been discussed in depth by Salton [1]. In general, a term A would be chosen as an index-term for this particular record, if this record contains significantly more information about subject A than most of the other data records in the collection.

However, the term A might have a number of close relatives (e.g. the word "computer" is closely related to "computing", "computers", "calculating", "calculator", etc.). At the time of indexing, the concept of "computer" might be indexed by the term "computer" or any one of its close relatives as mentioned above.

At the time of a search, the problem of the user is: "how to select a proper term for search", in order to reach the desired information. This is a problem because in most retrieval systems, the retrieval mechanism is based on the "perfect" or "fuzzy" match of query-terms with index-terms (see for example, in Salton [2]). In the latter case, the similarity between query-terms and index-terms

ABSTRACT

This report describes the development of a methodology for constructing concept-atoms which are the building blocks for a semantic-net interface between the human users and the information system database. The objective of this interface is to assist users in selecting the proper vocabulary terms for searching through the information database. This interface is particularly helpful for those who are not familiar with the vocabulary used in the information system database. Most of the current online information systems are good illustrations of this situation. Even the subject experts of a given information area may encounter difficulty in online information searches, because they are not familiar with the restricted indexing vocabulary selected for this particular subject area of an online information database.

of data-records are computed and ranked, such that only the most relevant records are retrieved for the user.

In the past, our attention has been centered on information users who depended upon online search specialists to handle their searches of information. As online information systems become more widely available, people from all walks of life begin to hunt for information through the online information system files. An inherent problem in this situation is that most information users are not familiar with the indexing vocabulary used by each of the online information systems; and many of the enthusiastic users are not even familiar with the vocabulary of the subject area, in which they have newly acquired interest. All these users use whatever relevant terms come into their minds for search. However, they usually have the knowledge to recognize the proper terms representing their interest at sight.

Many libraries do have online search specialists to assist these information system users in translating the user's concept of information need into proper subject terms for online searches. But there are not enough of these specialists to handle the service load of the user's needs satisfactorily. Thus, it is desirable to have an interface substituting the human specialist between the database of records and the user, so that the online databases can be more readily accessible to the information users. As can be expected, this new computerized interface would not be as accommodative as the human information specialists, but it is readily accessible by the

users.

As a realization of the interface, Doyle proposed; "Semantic Road Map for Literature Searches", in 1961 [3], but did not provide any details of its implementation. Research for its implementation have been carried out by Wei since 1975 [4], when he proposed the use of concept-atoms to implement the semantic road map for literature searches. Over the next nine years, his research with co-workers continued and results were published [5,6,7].

2. Representation of Real World Knowledge

The online information search specialist mediates between the information system user and the data base system, thus to aid the user in his information searches. In that process, the specialist uses his knowledge about the database. If a computerized interface is to perform the task of a human specialist, it must include a knowledge-base with contents comparable to those possessed by the human specialist.

The information in a knowledge-base can be stored in a network similar to that in Figure 1 [9], which contains the categorical identifiers: WEDGE, BRICK, BLOCK, and the individual identifiers: WEDGE18, BRICK12. Also included in the network are the descriptors: "triangular" and "rectangular". The arrow-headed lines illustrate the relation between the nodes. For example, it says: "BRICK12 is a BRICK", "BRICK is a kind of (AKO) BLOCK", and "BRICK has a shape that is rectangular". A network of this kind carries detailed knowledge about the real world. But it is very costly to store a large knowledge-base of this kind on the computer.

To assist users in information retrieval, the system knowledge as represented by a simplified network similar to that in Figure 2 can be very helpful. A pair of closely related nodes are linked by a line. Two nodes which are linked through one or more nodes, are remotely related. In fact, the network in Figure 2 is similar to the "road map for searches" first proposed by Doyle in 1961. Today,

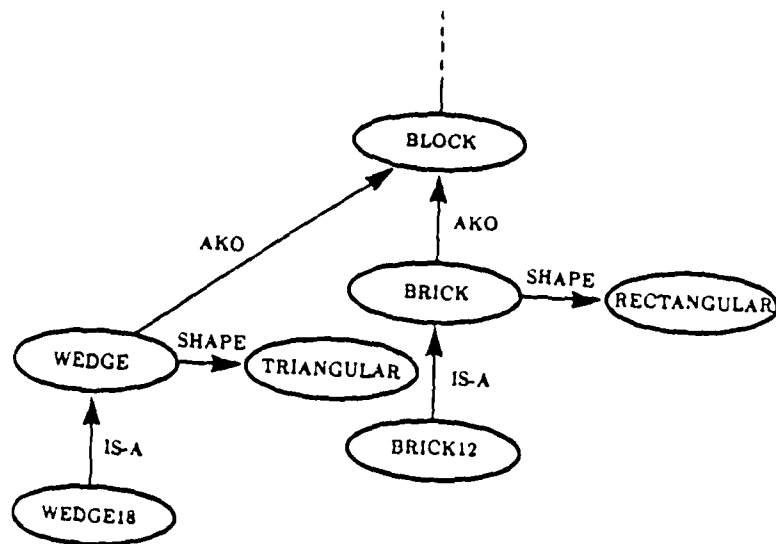


Fig. 1 An example of knowledge representation.

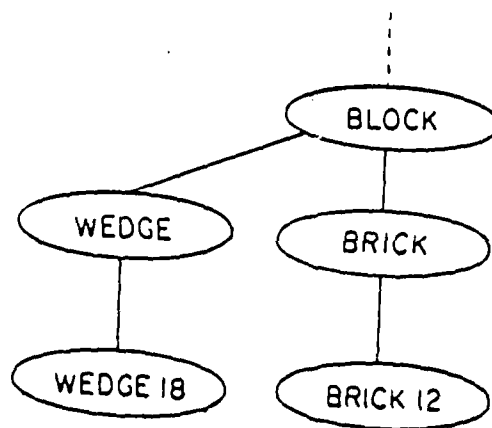


Fig. 2 A Simplified Version of the Network in Fig. 1

that kind of map is better known as semantic-net (network).

As another illustration, a semantic-net fragment appears in Figure 3. Suppose an information searcher begins with a term

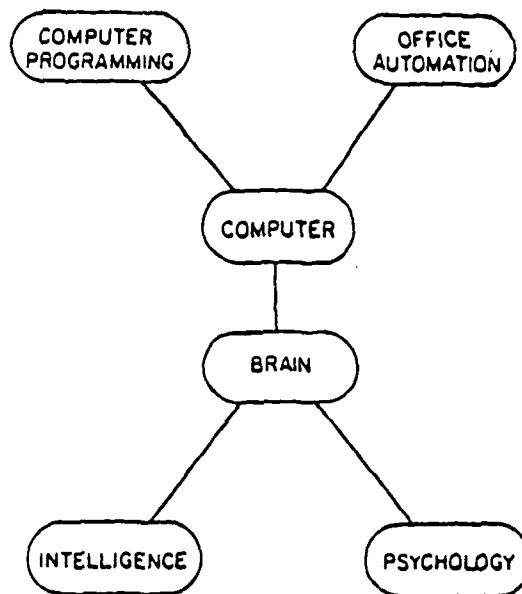


Figure 3. An example of a semantic net fragment.

residing in one of the nodes in the net. If provided a means to navigate through the net, he will be able to find all terms in the net, which are related to the concept as represented by his selected term with which he entered into the semantic-net. The net contains all index-terms used in the database as well as those related terms which might be used by information searchers to enter the system for retrieval. For the convenience of the searchers, all index-terms are marked with a "*". So the users know that data-records are available in the database for those terms.

The index-terms for all records in the database are automatically added to the semantic net. Other terms in the net are added by the system designers with the view that they might be used by information users to begin their searches. Additional terms are to be collected online from entries by users. They are those terms failed to retrieve any record for a user, but relevant records are available in the database.

3. An Information Retrieval System with a Semantic-Net Interface

At Ohio University, Wei conceived, in 1975, the idea using concept-atoms as the building block for a semantic-net. A net was implemented on a HP-3000 computer with IMAGE database management software. Each concept-atom has an appearance similar to the one in Figure 4. The concept-atoms were individually constructed and were entered into the computer separately. However, they are automatically linked into isolated semantic patches. Each patch is similar to the one in Figure 3. Some patches are much larger than others. The entry of one additional concept-atom may link a few patches together into a large patch. Eventually, most of the patches are linked together to have the appearance of the cities and highways on a continent.

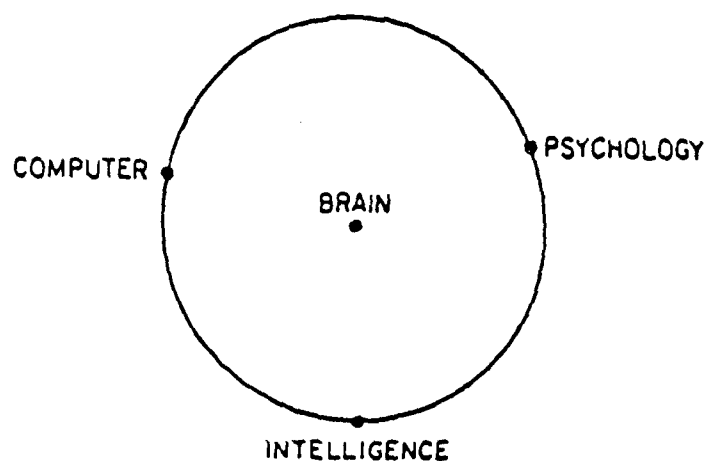


Figure 3. An example of a concept-atom

The configuration of an information retrieval system with index and semantic-net interface is illustrated in Figure 5. The user interacts with the retrieval management program. That program receives request (in the form of a subject term) from user, delivers to user the final result of search or subject-terms for user's selection in order to decide on the direction of further searches. That program also sends request to database management system (DBMS) for a search through the index, the semantic-net or the database records.

The diagram in Figure 6 illustrates the retrieval process which starts when the user enters a search term into the retrieval system. Immediately, the process searches through the index-terms of database records for a match. If a match is found, records indexed under that term are delivered to the user. Otherwise, the process searches through the semantic-net for terms closely related to the entry term. These terms, if found, are delivered to the user for selection. The user selects one of them as an entry term for the next search. Thus, the search process starts on another search cycle. The search cycle repeats until the user is satisfied or the user has given up the hope of finding another valuable data-record after navigating through the semantic-net. However, during a search, the user having retrieved data-records can continue to navigate through the semantic-net for extended searches. A fragment from an actual search session is attached in appendix , as an illustration.

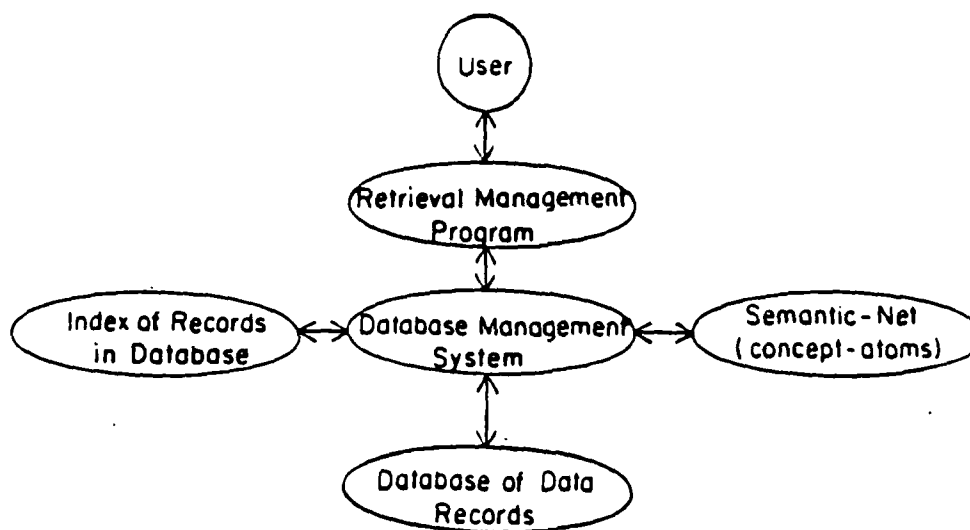


Figure 5 Configuration of an Information Retrieval System with Index and Semantic-Net Interface.

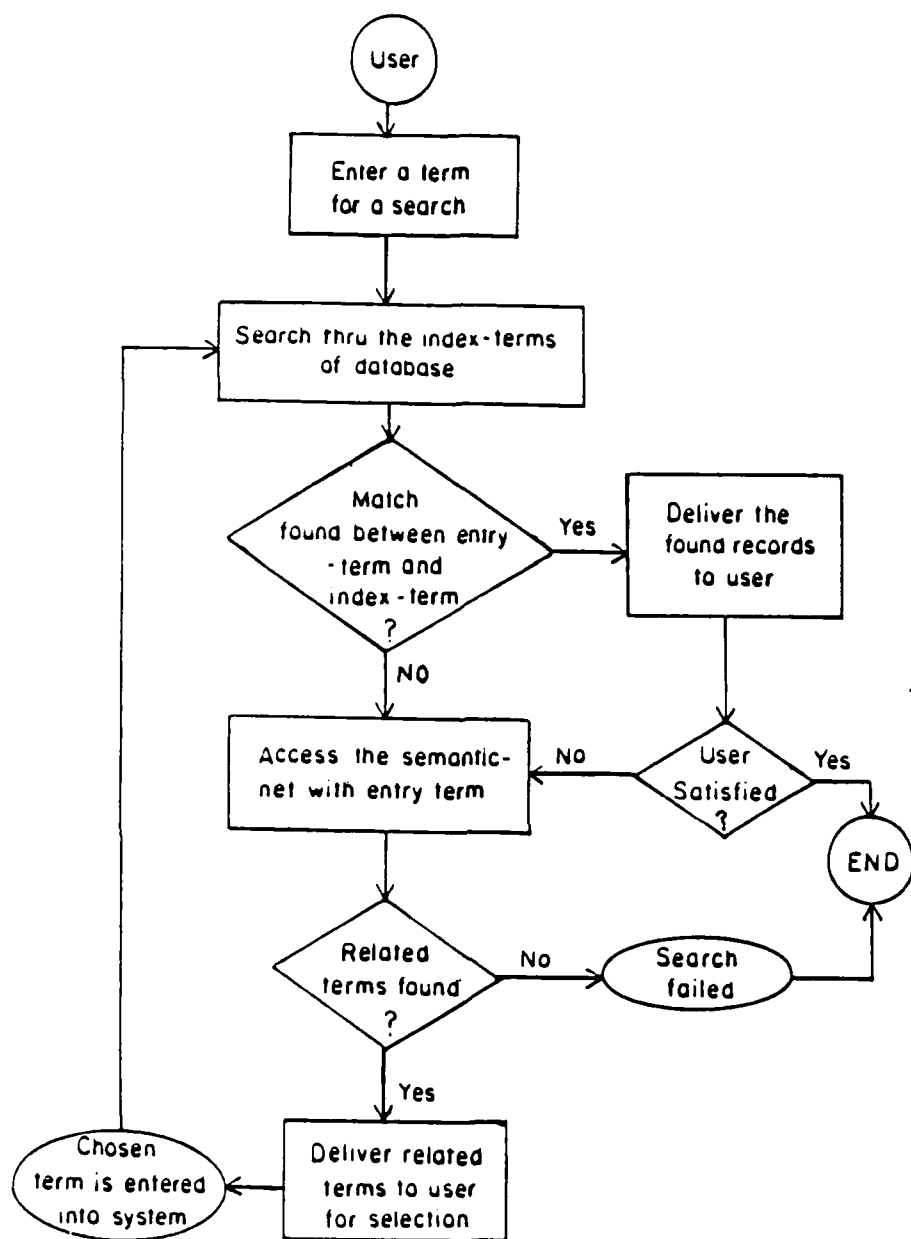


Fig. 6 The Information Retrieval Process

4. Semantic Distance and Concept-atoms

Sowa [10] defined semantic distance between a pair of terms as the minimum number of steps from one term to the other term in a hierarchical graph, in which both terms are present with their super- and sub-types. However, Rosch [12] assigned semantic distance between terms based on the average response time of her test subjects in experiments to questions related to that term-pair. In essence, by her method, the semantic distance (in inverse to strength of association) is dependent to large extent upon the co-occurrence frequency of the term-pair under consideration. The accumulated co-occurrence experience of the term-pair in each test subject's mind determines his response time to the test questions.

We follow, in essence, Rosch's method in determining semantic distances between term-pairs. The values arrived at in this method may subject to variation from person to person. But it is a quicker method to obtain values for semantic distances. Perhaps, for similar reasons, Roger Schank has assigned interest values by hand [11]. In fact, our experience indicates that the strength of association between a pair of terms in our mind does change with time. For example, our library installed a computer system for circulation control and book catalog searches a couple of years ago. Since then the association between the terms: Library and Computer is much stronger, i.e. the semantic distance between those two terms much reduced.

Because of the time-dependent characteristic of semantic

distance, the semantic net constructed to aid information retrieval needs to be revised periodically. The revision is actually simpler, if concept atoms are used as the building blocks. Because each concept-atom can be changed independently.

Since the performance of a semantic-net depends upon the quality of its building blocks (i.e. the concept-atoms) and there are many concept-atoms to construct. Then the question is: "How to construct quality concept-atoms with the aid of computer?"

A concept-atom is a cluster of closely related terms which together represent a concept. Thus, the idea of using statistical cluster analysis method has come up for consideration. Our approach to using statistical method is described in the next section.

5. Cluster Analysis

Understanding our world requires conceptualizing the similarities and differences between the entities that compose it. Clustering analysis is the general logic, formulated as a procedure, by which we objectively group together entities on the basis of their similarities. Therefore, cluster analysis has been used extensively by social science researchers [13, 14, 15]. The cluster analysis method was pioneered by Tryon in the 1930's. He published, in 1939, a monograph, "Cluster Analysis" containing the methodology and theoretical principles of cluster analysis and calculator programs utilizing those methodology and principles. He and his students continued the work into the next 30 years.

The cluster analysis, as originally conceived by Tryon, was a poor man's Factor Analysis. He also wanted methods which relied as much as possible upon logic, and as little as possible upon mathematics. When Tryon worked mathematically, his usual choice was for geometry. He seems to have seen clusters in his space much like astronomers see galaxies in theirs. Some psychologists believe Tryon's cluster approach was a stimulant to the multi-group method of factor analysis, in which axes were put through the centers of clusters.

It came as no surprise that Bailey (Tryon's student) wrote a computer program for cluster analysis of variables from a correlation matrix input [13]. In 1959, Tryon and his associates conceived a general computer program to perform all the main forms

of cluster and factor analysis as mere special cases or options within the system. That project was carried out in the 1960's with funding from the National Institutes of Health. Thus, the pioneering work of Tryon and associates has evolved into the cluster and factor analysis programs in commercially available programming packages such as: SPSS, SAS and BMDP [16, 17, 18].

The cluster analysis programs are to group a set of variables into clusters. The factor analysis programs are to reduce a set of variables into major components, so that the effects of those variables are adequately represented by a fewer number of group-variables called major components. The factor analysis is performed through sophisticated mathematical manipulations as illustrated by Tabachnick and Fidell [19] and Gorsuch [20]. We have used cluster analysis programs in SAS and SPSS, but found the factor analysis program in SPSS provides more options for us to choose from for grouping variables into clusters. An example illustrating the use of factor analysis program in arriving at concept atoms is explained in the next section.

6. Concept-Atoms Construction Using Factor Analysis Method

The factor analysis program in SPSS has been selected for clustering subject terms. This program was designed to cluster variables into groups by taking correlation matrix of the variables as input. In adapting the program for clustering terms, a matrix containing the estimated semantic distance between terms in the range of: from 0 to 1, is used as a substitute for the input correlation matrix. Because of this, the input matrix for our factor analysis (FA) run is not as consistent as a true correlation matrix, whose elements were computed from the values of the input variables.

As a result of the slight inconsistencies in the input matrix, the FA program run can be unstable at times, and refuse to converge onto a result. Fortunately, there are quite a few of parameters to choose from for each of the key commands in the FA program. Those key commands and their parameters are explained as follows:

- a) The EXTRACTION command may use any one of the selected parameters tabulated in Figure 7 to specify a method for computation.

Parameter	Method indicated by parameter
PC	Principal component analysis
PAF	Principal Axis factoring
ALPHA	Alpha factoring
IMAGE	Image factoring
ULS	Unweighted least squares
GLS	Generalized least squares
ML	Maximum likelihood

Figure 7. A list of parameters for the EXTRACTION command.

- b) The CRITERIA command can use one of the selected parameters tabulated in Figure 8 to specify the criteria for stopping the FA program run.

Parameter	Criteria indicated by parameter
Factors(n)	The number of factors (i.e. clusters to be extracted.
Mineigen(val)	Minimum eigen-value used to control the number of factors extracted.
Iterate(n)	Number of iterations for the factors solution.
Econverge(val)	A value is specified as converge criteria for extraction.
Rconverge(val)	A value specified as converge criteria for rotation.
Delta(val)	The value of delta for direct oblimin rotation.

Figure 8. A list of parameters for the CRITERIA command.

- c) The ROTATION command can use one of the selected parameters tabulated in Figure 9 to specify the procedure for rotating the major coordinate axes in arriving at the clusters.

Parameter	Method of rotation indicated by parameter
Varimax	Varimax rotation
Equamax	Equamax rotation
Quartimax	Quartimax rotation
Oblimin	Direct oblimin rotation

Figure 9. A list of parameters for governing the procedure of coordinate axes rotation.

Since there are a large number of combinations of the parameters for the three key commands: EXTRACTION, CRITERIA and ROTATION in a Factor Analysis program, we have conducted extensive program runs to determine the parameter combinations that would produce better clustering results. One of the better FA programs is listed in Figure 10, wherein 14 subject-terms were used as variables: V1 to V14, in the clustering operations. Those variables are:

V1=philosophy	V2=religion
V3=programming	V4=operating system
V5=software	V6=computer
V7=hardware	V8=solid-state chip

```

TITLE CLUSTER ANALYSIS
INPUT PROGRAM
NUMERIC V1 TO V14
INPUT MATRIX FREE
END INPUT PROGRAM
COMMENT      V1=philosophy      V2=religion      V3=programming
COMMENT      V4=oper-sys        V5=software      V6=computer
COMMENT      V7=hardware        V8=solid-chip      V9=cpu
COMMENT      V10=peripheral      V11=network      V12=info-sys
COMMENT      V13=tele-comm      V14=database
FACTOR      READ CORRELATION/
            VARIABLES=V1 TO V14/
            ANALYSIS=V1 TO V14/
            PRINT=CORRELATION ROTATION/
            FORMAT=SORT BLANK (0.1)/
            EXTRACTION=ULS/
            CRITERIA=FACTORS(5)/
            ROTATION=OBLIMIN/
BEGIN DATA
1 .8 0 0 0 0 0 0 0 0 0 0 0 0
.8 1 0 0 0 0 0 0 0 0 0 0 0 0
0 0 1 .7 .9 .9 .7 .5 .9 .5 .5 .7 .5 .8
0 0 .7 1 .8 .9 .6 .5 .7 .5 .5 .8 .5 .8
0 0 .9 .8 1 .9 .9 .1 .7 .5 .5 .8 .5 .8
0 0 .9 .9 .9 1 .9 .8 .9 .9 .8 .8 .5 .8
0 0 .7 .6 .9 .9 1 .9 .9 .9 .5 .5 .5 .7
0 0 .5 .5 .1 .8 .9 1 .7 .5 .4 .4 .4 .4
0 0 .9 .7 .7 .9 .9 .7 1 .8 .5 .4 .3 .6
0 0 .5 .5 .5 .9 .9 .5 .8 1 .3 .6 .3 .6
0 0 .5 .5 .5 .8 .5 .4 .5 .3 1 .3 .8 .4
0 0 .7 .8 .8 .8 .5 .4 .4 .6 .3 1 .4 .8
0 0 .5 .5 .5 .5 .5 .4 .3 .3 .8 .4 1 .5
0 0 .8 .8 .8 .8 .7 .4 .6 .6 .4 .8 .5 1
END DATA

```

Figure 10. An example of a Factor Analysis program for clustering subject-terms.

V9=CPU	V10=peripheral-equipment
V11=network	V12=information system
V13=tele-communication	V14=database

Their estimated semantic distance are tabulated in a matrix between BEGIN DATA statement and END DATA statement in the FA example program listed in Figure 10. This program performed clustering operations for the above listed 14 subject terms using:

EXTRACTION = ULS/

CRITERIA = FACTORS(5)/

ROTATION = OBLIMIN/

to produce 5 clusters (i.e. factors).

The most important output from the program run are displayed in Figures 11. The output in Figure 11(a) is called the pattern matrix which shows the relative contributions of the 5 factors (i.e. clusters) in representing the 14 variables (i.e. subject-terms) with all overlapping parts of the factors removed. This provides a rather simplified clear picture, but is insufficient for all purpose.

The output in Figure 11(b) is called the Structure Matrix which displays the relative contributions of the 5 factors in representing the 14 variables. As Tabachnik [19] has pointed out, in an obliquely rotated solution, which is the case of our example, the factors are correlated; they share overlapping variability, so that assignment of variance to individual factors is somewhat ambiguous.

(a) PATTERN MATRIX:

	FACTOR 1	FACTOR 2	FACTOR 3	FACTOR 4	FACTOR 5
V5	.97113				
V4	.79812			-.15962	
V3	.73265			.10918	
V6	.64127	.21911		-.28363	.46589
V11		1.02084			
V13		.65961			
V1			1.01757		
V2			.71523		
V14	.12683	-.14009		-.98382	.16267
V12		.22627		-.69420	
V9	.23582			.23131	.85229
V10	-.16819			-.34266	.85090
V7	.30745			-.10623	.78783
V8					.50413

(b) STRUCTURE MATRIX:

	FACTOR 1	FACTOR 2	FACTOR 3	FACTOR 4	FACTOR 5
V5	.97400			-.25135	.44935
V6	.94777	.40044		-.58376	.85256
V4	.80248			-.32990	.33093
V3	.74705	.11768			.38773
V11	.14219	1.02767		-.20017	.14189
V13		.66279		-.12321	
V1			1.01757		
V2			.71523		
V14	.41846			-1.03061	.43939
V12	.20803	.33463		-.72409	.14080
V7	.67943			-.35330	.94144
V9	.57355	.13860			.90924
V10	.29155			-.49481	.84751
V8	.20988	.12255			.49354

(c) FACTOR CORRELATION MATRIX:

	FACTOR 1	FACTOR 2	FACTOR 3	FACTOR 4	FACTOR 5
FACTOR 1	1.00000				
FACTOR 2	.12263	1.00000			
FACTOR 3	.00000	.00000	1.00000		
FACTOR 4	-.23866	-.16082	.00000	1.00000	
FACTOR 5	.45493	.12252	.00000	-.24007	1.00000

Figure 11. Output from running the factor analysis program listed in Figure 10.

However, the greater the overlap between a variable and a factor, the more that variable is a pure measure of the factor.

Thus in our program example, the terms (i.e. variables) within a factor will make up a cluster to represent a concept-atom. The subject-term which has the highest weight within the factor (i.e. cluster) will be appropriately chosen as the nucleus, and the other terms within the cluster (i.e. factor) are made the satellites of a concept-atom.

In constructing concept-atoms from the output of our FA example program run, the process is based on the structure matrix in Fig. 11(b), but factor-to-factor correlation matrix in Figure 11(c) and our knowledge about semantic net provide additional guidance for the process. Thus, factor analysis is a computerized aid for our concept-atom construction process, and concept-atoms are the building blocks for a semantic net.

The five concept-atoms sketched in Figure 12 are constructed based on the FA program run output in Figure 11. A few lines with arrow-head were drawn from satellite terms of each concept-atoms to the nucleus of other concept-atoms to show the search paths traveled when a semantic net is referenced during an interactive session for information search.

For the purpose of illustration, the terms: "philosophy" and "religion" were among the terms for clustering. Those two terms belong to concept-atom 3 (i.e. factor 3) in Figure 12, and stand out as an isolated island among the other four concept-atoms: 1, 2,

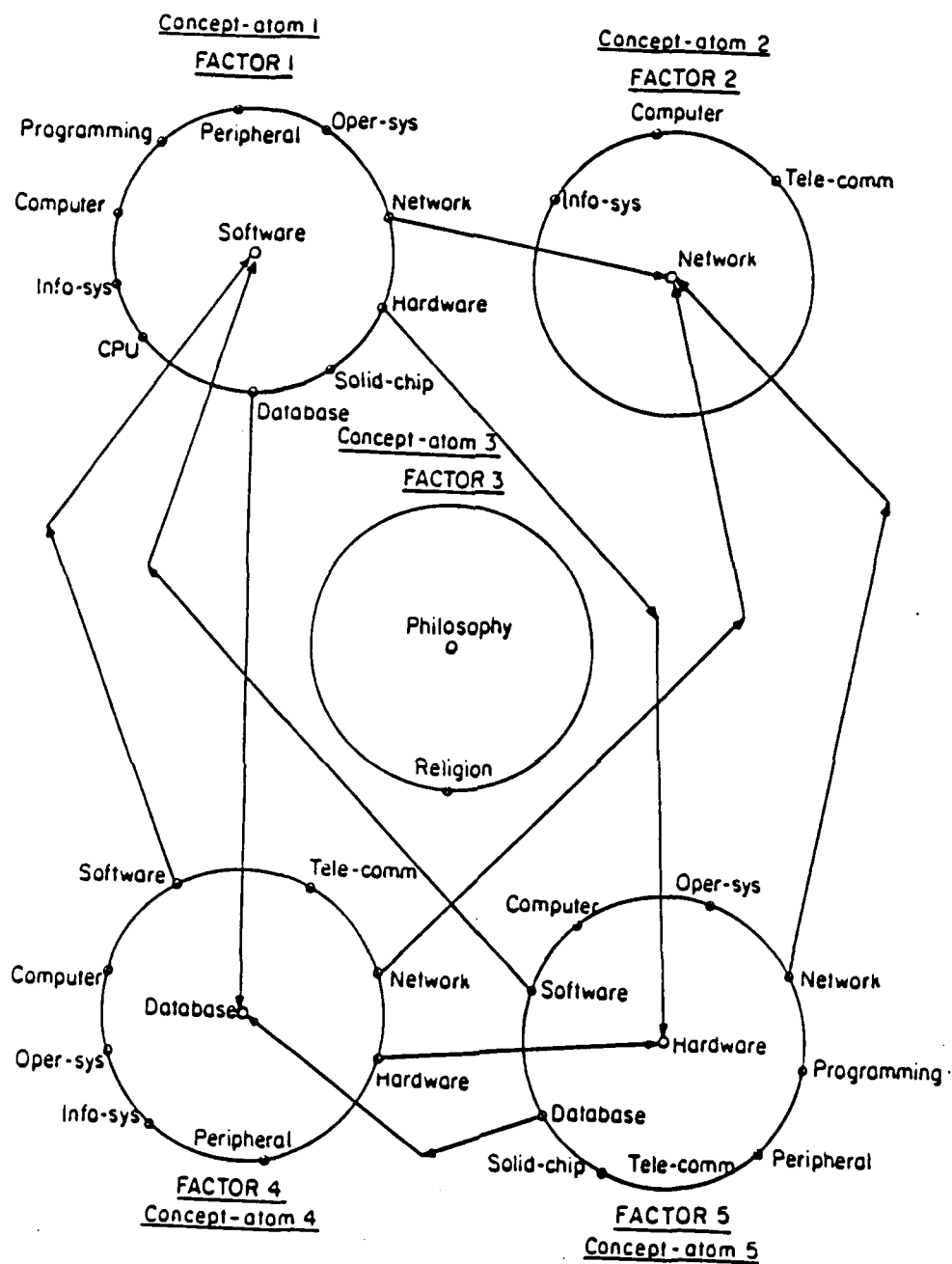


Figure 12. Concept-atoms sketched from factor analysis program output listed in Figure 11.

4, and 5, which are linked together through sharing of common terms.

Those 4 concept-atoms form a semantic patch through the linkage of arrow-headed lines. For example, "software" is the nucleus of concept-atom 1. Starting from "software", we can travel to each one of its satellite terms. Most of those satellite terms would lead us beyond this particular semantic patch. However, "network" would lead us, following an arrow-headed line, to concept-atom 2 at upper right corner, "hardware" leads us to concept-atom 5 at lower right corner, and "database" leads to concept-atom 4 at lower left corner.

Similarly, if starting from "database" at the nucleus of concept-atom 4, we can reach concept-atom 1 through its satellite term "software", to concept-atom 2 through "network", to concept-atom 5 through "hardware". Alternately, if starting from the nucleus of concept-atom 5, we are able to reach concept-atoms: 1, 2, and 4, in the semantic patch.

However, if starting from "network" at the nucleus of concept-atom 2, we can only reach, through its satellite terms, to concept-atoms in other semantic patches.

Since the running time of a Factor Analysis Program increases exponentially with the size of its input matrix (i.e. with the number of subject terms to be clustered), the size of a semantic patch that can be created by a FA program run is restricted by

necessity. Thus, "How to piece together semantic patches created by individual FA program runs?" becomes a topic for our future research.

7. Directions for Future Research

Our research goal is to extend our abilities for building better and better information systems. Naturally, the question: "What is a good information system?", would arise. Since information systems are used to complement the information storage and processing capabilities of human brains, a good information system should possess all the capabilities of a human being if possible.

That means information systems should be made intelligent by some artificial means. Thus, the study of all aspects of artificial intelligence (AI) are within the domain of information system research.

Sowa states in his book [10] that, "artificial intelligence is the study of knowledge representation and their use in language, reasoning, learning, and problem solving." Thus there are five broad areas for our future research. Among those five, knowledge representation is the most fundamental element of them all. Since 1974, this writer has begun research on semantic network which is a sub-area of knowledge representation. He plans to move his research into the area of knowledge representation, because it is not only an entity that aids information search, it also is the foundation for user language to system language translation. On the other hand, this writer is interested in the use of expert system (another AI application area) methodologies in MIS to enhance the system capabilities and its flexibility for modifications.

Acknowledgement

This author would like to thank the Air Force System Command, the Air Force Office of Scientific Research and the Southeastern Center for Electrical Engineering Education for providing a research opportunity at Armstrong Aerospace Medical Research Laboratory in the summer of 1984 and for providing support to continue his research for building a better semantic-net interface between human-user and a database.

Further, he would like to thank Professor Peele and Mr. Slator of SCEE for their assistance and support during this research effort. His appreciation goes to Mr. Robert Bachert, his effort-focal-point at AAMRL/TID, for encouraging this area of research and for his guidance in the research planning; to Dr. Billy Crawford and Mr. Dave Brungart, also of AAMRL/TID, for technical discussions that helped to establish his long range research goals for years to come; and in particular to Dr. George Mohr, Commander of AAMRL, for discussion of his expectations for an information system for a R & D organization.

References

1. G. Salton, A Theory of Indexing, Society for Industrial and Applied Mathematics, Philadelphia, PA., 1975.
2. G. Salton, The SMART Retrieval System, Prentice-Hall, 1971.
3. L. B. Doyle, "Semantic Road Maps for Literature Searches," Journal of ACM, Vol. 8, No. 4, 1961, pp. 553-576.
4. Y. M. Wei, "Concept Atom: A Component in Information Organization and Retrieval," Department of Computer Science, Ohio University, 1975.
5. Y. M. Wei, "Variable Extent of Online Retrieval with Aid of Concept-Atoms," (abstract and presentation), ACM Computer Science Conference, 1979.
6. Y. M. Wei, K. Mulliner, et. al., "An Experimental Interactive Information Retrieval System Utilizing Concept-Atoms," Policy and Information, Vol. 7, No. 1, 1983, pp. 17-24.
7. Y. M. Wei, K. Mulliner, et. al., "Constructing a Semantic Network with Concept-atoms", Proceedings of International Computer Symposium 1984; Taiwan, R.O.C., 1984; pp. 483-488.
8. Scott E. Fahlman; NETL -- A System for Representing and Using Real-World Knowledge, MIT Press, 1979.
9. Patrick H. Winston, Artificial Intelligence, Addison-Wesley, 1984, p. 257.
10. John F. Sowa, Conceptual Structures, Addison-Wesley, 1983.
11. Reference No. 10, p. 203.
12. E. H. Rosch, "On the internal structure of perceptual and semantic categories" in Cognitive Development and the Acquisition of Language, Editor: E. T. Moore, Academic Press, 1973, pp. 111-144.
13. Robert C. Tryon and Daniel E. Bailey, Cluster Analysis, McGraw-Hill, 1970.
14. Barbara G. Tabachnick and Linda S. Fidell, Using Multivariate Statistics, Harper and Row, 1983.
15. Maurice Lorr, Cluster Analysis for Social Scientists, Jossey-Bass Publishers, 1983.
16. SPSS User's Guide, McGraw-Hill, 1983.

17. SAS User's Guide, SAS Institute Inc., Box 8000, Cary, North Carolina.
18. BMDP Statistical Software, Univ. of California Press, Berkeley, CA.
19. B. G. Tabachnick and L. S. Fidell, Using Multivariate Statistics, Harper & Row, 1983.
20. R. L. Gorsuch, Factor Analysis, W. B. Saunders, 1974.

APPENDIX

Sample Search

JOURNAL TITLE RETRIEVAL SYSTEM

M E N U

- [1] HELP : Causes immediate return to this MENU so you may choose another command.
- [2] SEARCH : Asks you to enter a keyword, searches the database for journals relating to the keyword and then produces a terminal and/or printer report of all journals found.
- [3] EXTEND : Extends searches on conceptwords if you cannot find journal titles using the SEARCH command.
- [4] EXIT : Stops execution of this program, prints reports and logs you off so someone else can use the terminal.

Enter your selected COMMAND number.

2

Enter KEYWORD <<maximum of 30 characters>>.
psychology

List of JOURNAL TITLES found using KEYWORD: PSYCHOLOGY

- PSYCHOLOGICAL BULLETIN
- AMERICAN BEHAVIORAL SCIENTIST
- JOURNAL OF ADOLESCENCE
- JOURNAL OF MATHEMATICAL PSYCHOLOGY
- CONTEMPORARY PSYCHOLOGY
- PSYCHOLOGY TODAY

...end of retrieved JOURNAL TITLES

List of CONCEPTWORDS available for EXTEND searching of
KEYWORD: PSYCHOLOGY

- [1] LEARNING
- [2] SOCIAL PSYCHOLOGY
- [3] SOCIOLOGY
- [4] GROUPS

Enter your selected CONCEPTWORD number:

3

List of JOURNAL TITLES relating to the
CONCEPTWORD: SOCIOLOGY

- SOCIOLOGY
- SOCIOLOGICAL QUARTERLY

...end of retrieved JOURNAL TITLES.

DEVELOPMENT OF A HIGH-FREQUENCY LUNG VENTILATION
MODEL FOR TESTING UNDER HYPOBARIC CONDITIONS

Mukul R. Banerjee, Ph.D.
Department of Physiology
Meharry Medical College
Nashville, Tennessee

The project titled "Development of a high-frequency lung ventilation model for testing under hypobaric conditions" described in this report was funded by a RISE grant from SCEE/AFOSR (Subcontract No. 84 RIP 49 and 52, Contract F 49620-82-C-0035).

The project was initiated during my SCEE research fellowship in summer 1984 at the School of Aerospace Medicine, Brooks Air Force Base, Texas. During the tenure of the fellowship, I was able to develop , in collaboration with my effort focal point, Dr. Stephen Haswell a high-frequency ventilation (HFV) system along the lines of Fletcher et al (5). We made satisfactory progress in ventilating a mechanical lung model. The main objective in the RISE grant application was to duplicate our efforts and accomplishments at the Brooks Air Force Base in my laboratory at Meharry Medical College upon my return. With the help of this grant and the support and facilities provided by my home institution we wanted to achieve that goal. Acquiring the capabilities of developing the high-frequency ventilating system locally and having tested the system on an artificial lung model, our next goal was to try the system on live animals. Our purpose is to evaluate the

efficiency of the HFV system on pulmonary gas exchange in animals. The final objective, however, was to examine the performance of the HFV system on animals exposed to sea level condition, particularly under hypobaria.

INTRODUCTION:

High-frequency ventilation is a relatively new technique in providing an adequate gas exchange in the lungs. The journal, Critical Care Medicine devoted its entire volume 12, number 9, 1984 to different aspects of high-frequency ventilation. In this technique, tidal volumes provided to the animals are close to their dead space volumes(4,5,7,8,9). Some of the major disadvantages associated with conventional mechanical ventilators are: injury to the lung tissue from high volume ventilation and depressed cardiovascular function(6,8,9). The HFV technique appears to minimize these disadvantages. However, it is critical that the HFV technique ensures an adequate carbon dioxide removal from the body tissues. HFV falls into three somewhat arbitrary categories: high-frequency positive pressure ventilation, high-frequency jet ventilation and high-frequency flow

440-H-87 859

UNITED STATES AIR FORCE RESEARCH INITIATION PROGRAM

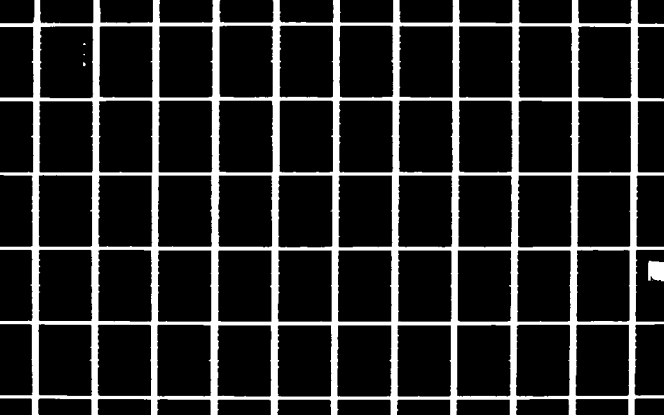
6740

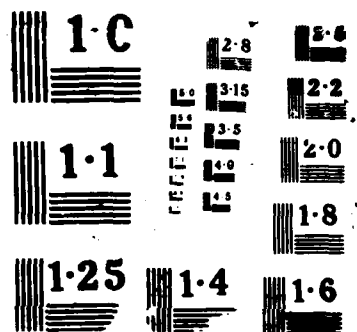
UNCLASSIFIED

MAY 86 AFOSR-TR-87-1722 FF9620-82-C-0035

F/G 7/2

ML





interruption and high-frequency oscillatory ventilation. Of these three techniques, high-frequency oscillatory ventilation has gained widespread attention (3). However, this technique does not appear to be superior to other techniques(1,2). Fletcher et al (5) have described a high-frequency flow interruption technique which prevents an admixture of inspired and expired gases. It allows collection of expired gas for an accurate measurement of volume and gas composition during ventilation at rates upto at least 20 Hz.

METHODOLOGY:

With some modifications of the technique of Fletcher et al (5) a high-frequency flow interruption system was developed. Compressed air was provided to the system from the air outlet in the laboratory. The air was filtered by passing it through tubing packed with fiber glass. The air supply was controlled by a pressure regulator and monitored by a pressure gauge. The different settings of the needle valve connected to the tubing determined the air flow rate chosen. This was indicated by a rotameter which was pre-calibrated with the use of a spirometer. A

bleeder valve regulated the airway pressure developed in the system. A rubber bag connected in series between the rotameter and the rotary valve but in parallel with the bleeder valve prevented the initial rise in inspiratory pressure developed during the expiratory phase of the breathing cycle. The rotary valve, on the other end alternated between inspiratory and expiratory lines. The rotational speed of the rotary valve was controlled by a variable speed DC motor with its speed control unit. The different respiratory frequencies thus obtained were monitored by the digital meter of a Universal Counter Timer Model 5001. On the inspiratory side, the rotary valve was connected to a two-liter glass beaker packed with copper scrubber to prevent adiabatic changes in ventilating volumes. The lateral pressure recorded from the tygon tubing in close proximity to the beaker served as the proximal airway pressure. This pressure was recorded by using a Statham differential pressure transducer, Model PM5E. The pressure recorded by a Validyne differential pressure transducer, Model DP 103-26 and CD 15 Carrier Demodulator in the distal part of the beaker provided the lung pressure or alveolar pressure in the mechanical lung. Inspiratory tidal volume was calculated by multiplying the compliance of the mechanical lung and the changes in

lung pressure during the breathing cycle. The expiratory tidal volume was obtained by the electrical integration of the expiratory flow signal. The expiratory flow rates were determined by the use of a Hans Rudolph Pneumotachograph Model 8311 and a Validyne DP 45 differential pressure transducer system. The integration of the signal was done by using a Narco Biosystems Integrator, Model GPA-10. The pressure and flow tracings were continuously recorded at different frequencies on a Beckman Type RM strip chart recorder.

RESULTS:

Compliance of the lung model. This parameter was determined by using the tygon tubing and the pressure transducer system which were subsequently utilized for determining the ventilator performance characteristics. The calculated average compliance of the mechanical lung model was 2.86 ml/cmH₂O. The individual values are presented in Table 1.

Leakage testing. Initially there was an air leakage between the alumina ceramic cylinder and the surrounding triple-ported stainless steel cylinder

housing. The application of a thin layer of low temperature silicone grease between the ceramic rotary piston and the ceramic cylinder and between the ceramic cylinder and the metal housing stopped the air flow away from the designated pathway. Thus, no airflow was detected through the expiratory port when the air pressure was applied on the inspiratory port under static conditions. Similarly, there was no air exchange directly between the inspiratory and expiratory ports when the air pressure was applied on the expiratory port side.

Leakage under dynamic conditions was tested by comparing expiratory tidal volumes obtained by integrating the expiratory flow with the inspiratory tidal volumes obtained by multiplying the lung compliance with the lung pressure changes. The data in Table 2 show that the inspiratory and expiratory tidal volumes were very close indicating little leakage, if any in the system at different frequencies of ventilation. Also, careful examination of different Figures presented, particularly Figure 1 with expanded time scale shows that there was no expiratory flow tracing as the airway and alveolar pressures rose during inspiration. Similarly, the expiratory flow started to rise as the airway and

alveolar pressures began to fall during expiration.

Pressure waveforms. Typical tracings of airway pressure, lung pressure, expiratory air flow and the integrated signal representing expiratory ventilation are presented in Figures 1-6. It is evident that the rise in pressure during inspiration was essentially smooth. The introduction of the compliant rubber bag in the system along with the use of the bleeder valve minimized the pressure spike developed in the inspiratory line during the expiratory phase of the breathing cycle. The inspiratory phase of the ventilating system is active while the expiratory phase is passive. Thus, the tracings show that the airway pressure fell more slowly during expiration. A major part of the remaining noise in the pressure wave appears to be associated with the inertia of the system.

The time available for passive expiration is inadequate to empty the lung completely particularly at higher frequencies of ventilation. Thus, at the end of expiration the airway pressure did not reach the zero value. Similarly, the lung pressure was above the base line at higher frequencies.

We had problems in obtaining readable complete tracings at higher frequencies in our strip chart recorder. The capillarity of the inking system failed to record the very fast component. In future we plan to store these physiological parameters on an analog tape recorder (Ampex, Model PR 2200).

An analog to digital signal converter for our micro computer has recently been ordered. In future we plan to do microprocessor integration of the digitized signal of the expiratory flow transducer to determine the expiratory ventilation rate.

During the past summer with a UES/AFOSR Research Fellowship I worked with Dr. Neel Ackerman at the Brooks Air Force Base. The other objectives mentioned earlier in this report were accomplished in a preliminary way during that time.

We used the high-frequency flow interruption technique on adult New Zealand White male rabbits. The efficiency of the technique in maintaining an adequate gas exchange in the rabbit was tested first at ground level and then in a hypobaric chamber simulating an altitude of 8000 feet. This was

immediately followed by retesting the same animals under ground level conditions. The anesthetized and intubated rabbits, injected with a muscle relaxant were ventilated at 1, 5 and 7 Hz with a minute ventilation of 1, 2 and 3 liters per minute respectively. Data were collected for approximately one hour at each frequency. Our results suggested that the HFV technique we utilized did not adversely affect the arterial partial pressure of carbon dioxide of rabbits at high altitude. Also, the arterial-alveolar partial pressure of oxygen ratio showed an improvement at high altitude with high-frequency ventilation.

REFERENCES.

1. Ackerman, N.B. and R.A. DeLemos. High frequency ventilation in Current Problems in Pediatrics, ed. L. Barness, Year Book Medical Publishers, 1984, pp 259-293.
2. Ackerman, N.B., R.A. DeLemos and N.M.I. El-Baz. Clinical applications of high frequency oscillation. Ch. 13 in High-Frequency Ventilation in Intensive care and during Surgery High-Frequency

Ventilation in Intensive Care and during Surgery.
Lung Biology in Health and Disease series, Vol. 26,
eds. G.C. Carton and W.S. Holland. Morsel Decor,
Inc. N.Y. 1985 pp 239-260.

3. Chang, H.K. Mechanisms of gas transport
during ventilation by high-frequency oscillation. J.
Appl. Physiol.: Respirat. Environ. Exercise
Physiol., 56:553-563, 1984.

4. Drazen, J.F., R.D. Kamm and A.S. Slutsky.
High-frequency ventilation. Physiol. Rev.,
64:505-543.

5. Fletcher, P.R., M.A. Epstein and R.A.
Epstein. A new ventilator for physiologic studies
during high-frequency ventilation. Resp. Physiol.,
47:21-38, 1982.

6. Gillespie, D.J. High-frequency ventilation.
A new concept in mechanical ventilation. Mayo Clin.
Proc., 58:187-196, 1983.

7. Kamm, R.D., A.S. Slutsky and J.M. Drazen.
High-frequency ventilation. CRC Rev. Biomed. Engg.,
9:347-379, 1983.

8. Quan, S.F., J.C. Calkins, T.J. Conahan and C.K. Waterson. High-frequency ventilation--a promising new method of ventilation. Heart and Lung, 12:152-155, 1983.

9. Slutsky, A.S., R. Brown, J. Lehr, T. Rossing and J. M. Drazen. High-frequency ventilation: a promising new approach to mechanical ventilation. Med. Instr., 15:229-233, 1981.

Table 1. Determination of compliance in the mechanical lung.

<u>Injected air volume (ml)</u>	<u>Change in lung pressure (cmH₂O)</u>
1	0.38
1	0.36
2	0.71
2	0.69
3	1.04
3	1.04
4	1.37
4	1.42
5	1.73
5	1.65
6	2.08
6	2.11
7	2.44
7	2.44
8	2.79
8	3.02
9	3.15
9	3.12
10	3.48
10	3.48

Table 2. Comparison of inspired and expired minute ventilation at different frequencies and at different rates of air flow.

<u>Hz</u>	<u>Inspired minute volume (ml)</u>	<u>Expired minute volume (ml)</u>
1.0	1.218	1.200
1.5	1.283	1.200
2.0	1.111	1.200
3.0	1.796	1.700
4.0	1.539	1.700
5.0	1.283	1.200
5.5	1.881	1.950
6.0	1.026	1.200
8.0	1.026	1.200
10.0	1.710	1.700
15.0	1.924	1.950
20.0	1.928	1.950

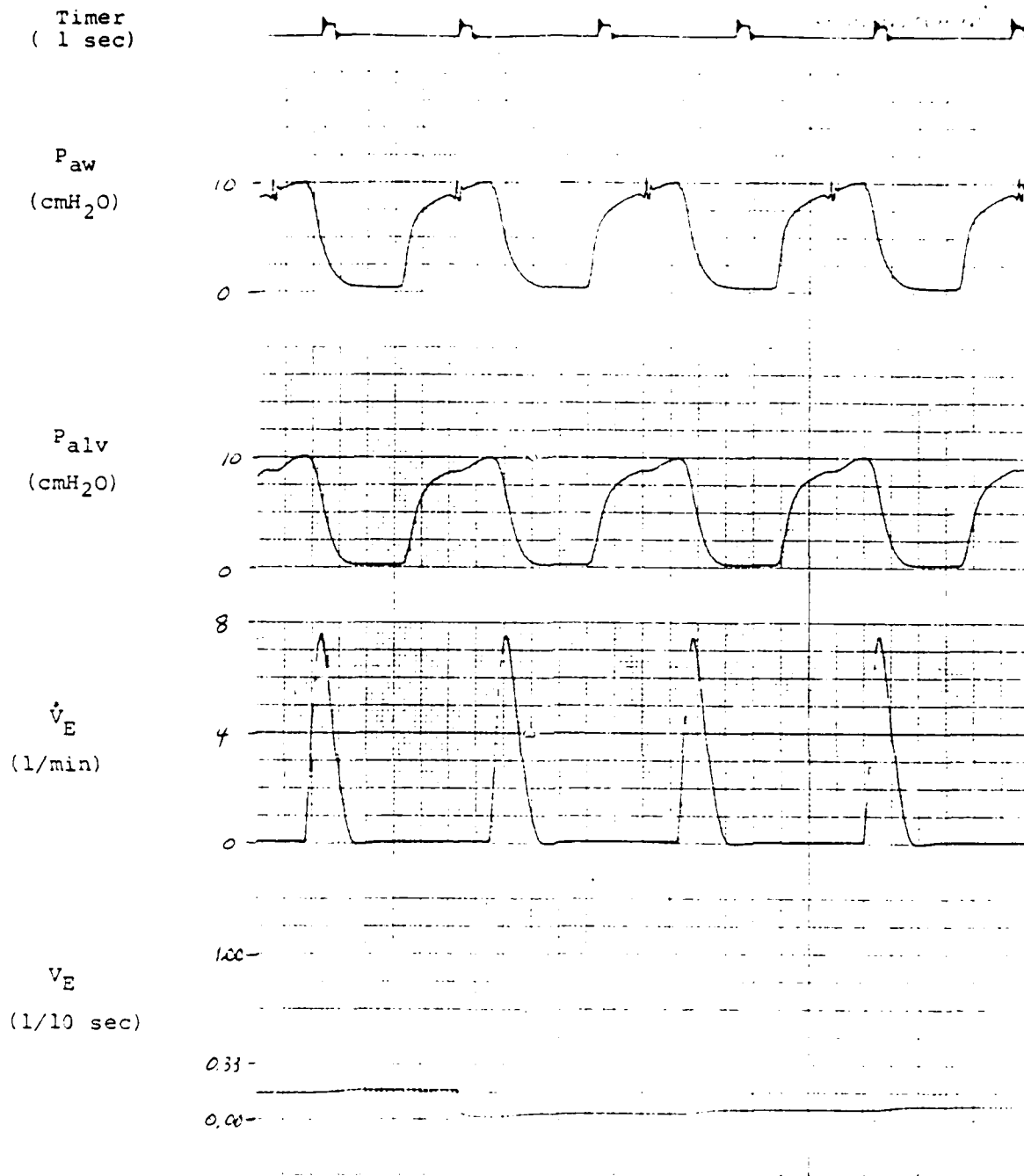


Figure 1. Airway pressure (P_{aw}), alveolar pressure (P_{alv}), expiratory flow (\dot{V}_E) and expiratory volume (V_E) recorded at 1 Hz. Paper speed is 25 mm/sec.

Timer
(1 sec)

P_{aw}
(cmH₂O)

P_{alv}
(cmH₂O)

\dot{V}_E
(l/min)

V_E
(1/10 sec)

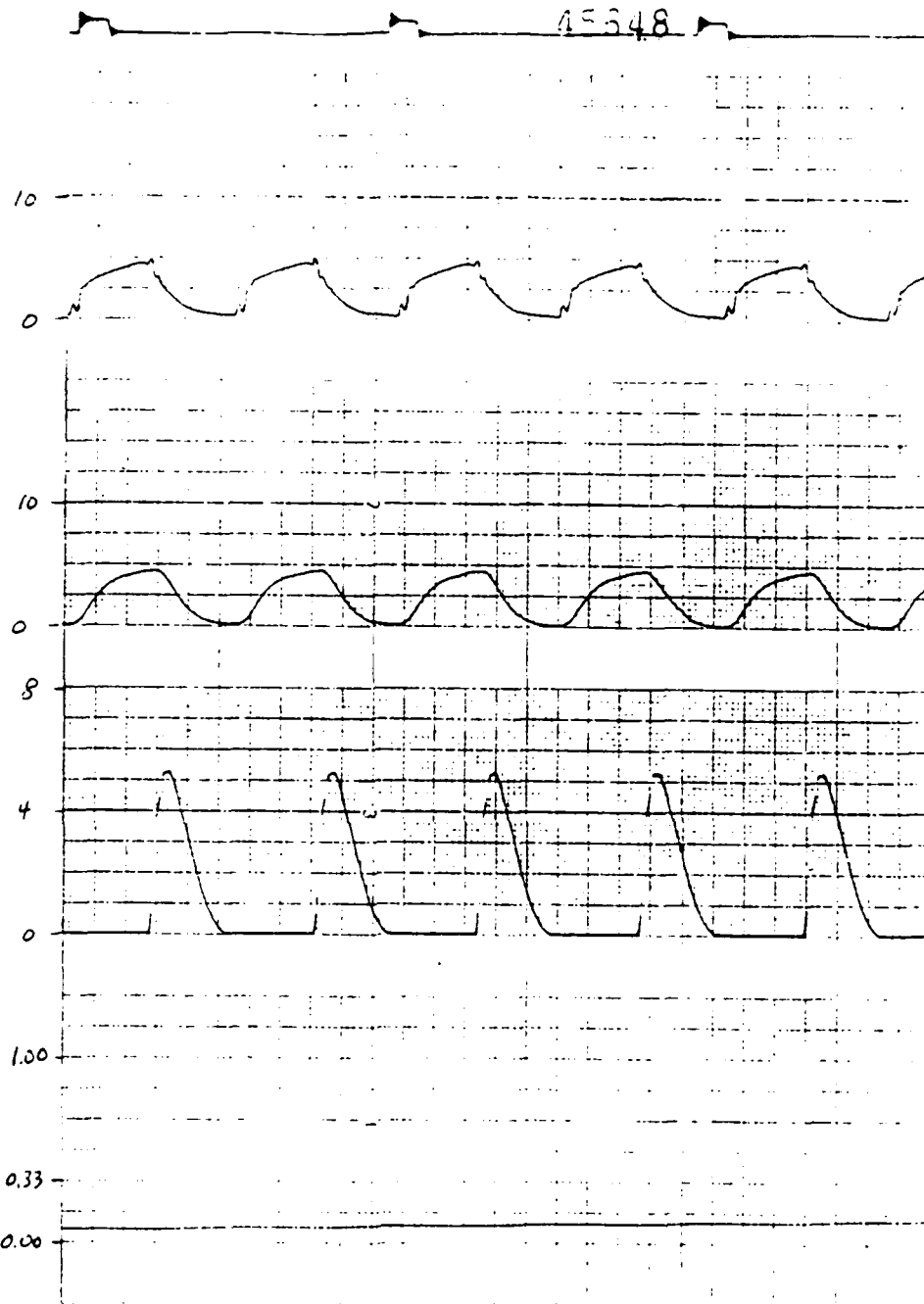


Figure 2. Data recorded at 2 Hz. Paper speed is 50 mm/sec.

Timer
(1 sec)

P_{aw}
(cmH₂O)

P_{alv}
(cmH₂O)

\dot{V}_E
(l/min)

V_E
(1/10 sec)

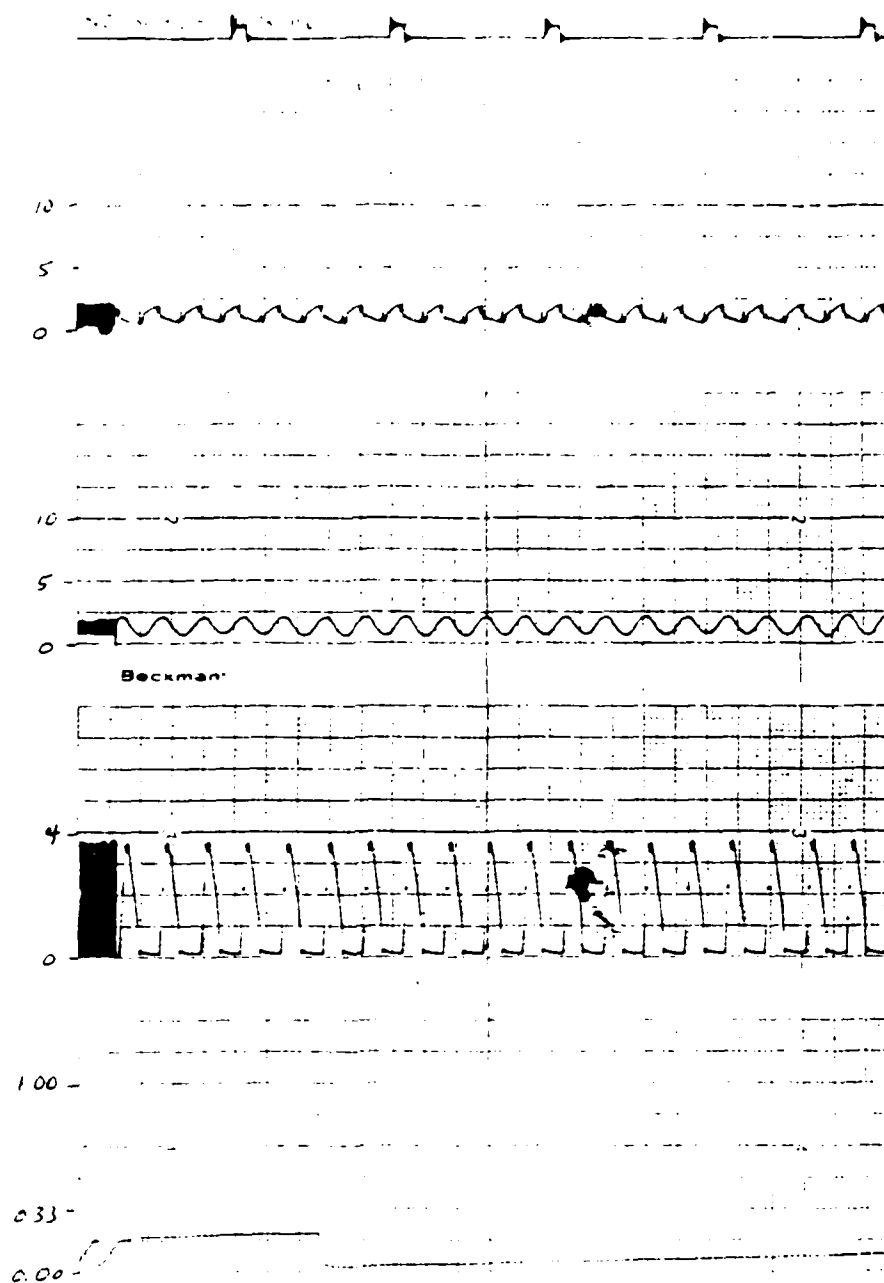


Figure 3. Data recorded at 4 Hz. Paper speed is 25mm/sec

Timer
(1 sec)

P_{aw}
(cmH₂O)

P_{alv}
(cmH₂O)

\dot{V}_E
(l/min)

V_E
(l/10sec)

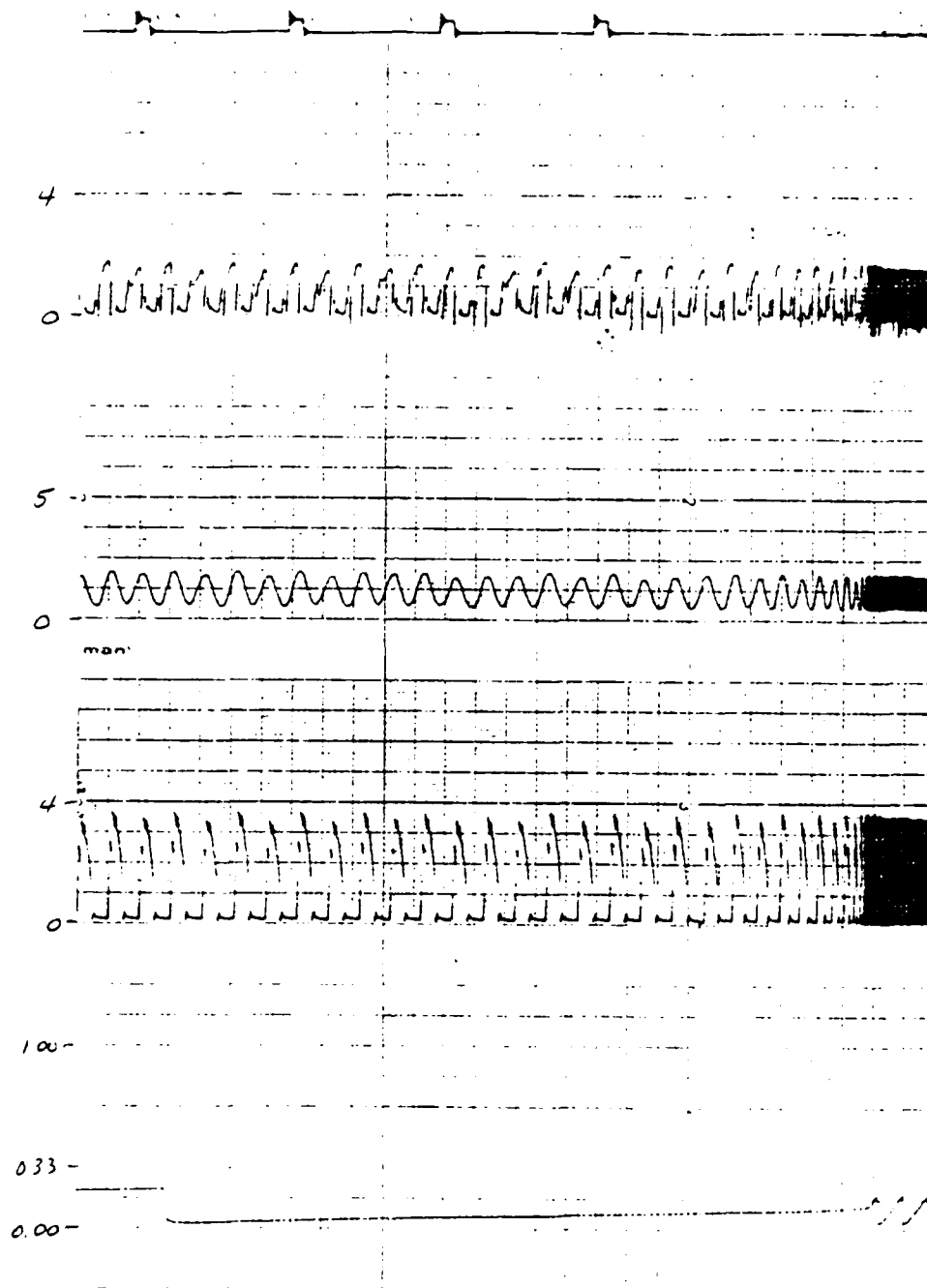


Figure 4. Data recorded at 5 Hz. Paper speed is 25mm/sec.

Timer
(1 sec)

P_{aw}
(cmH_2O)

P_{alv}
(cmH_2O)

\dot{V}_E
(1/min)

V_E
(1/10 sec)

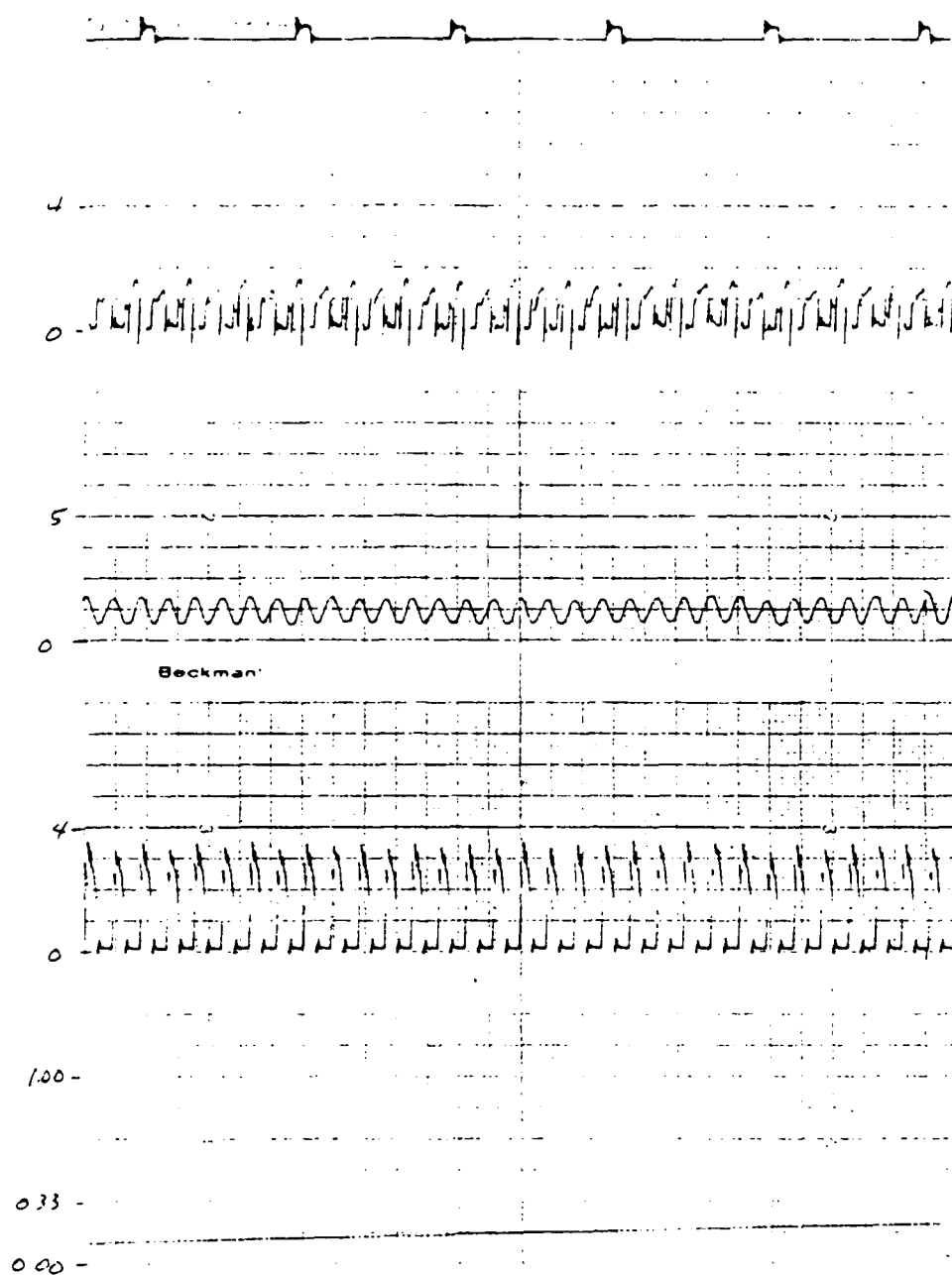


Figure 5. Data recorded at 6 Hz. Paper speed is 25mm/sec.

Timer
(1 sec)

P_{aw}
(cmH₂O)

P_{alv}
(cmH₂O)

\dot{V}_E
(l/min)

V_E
(1/10 sec)

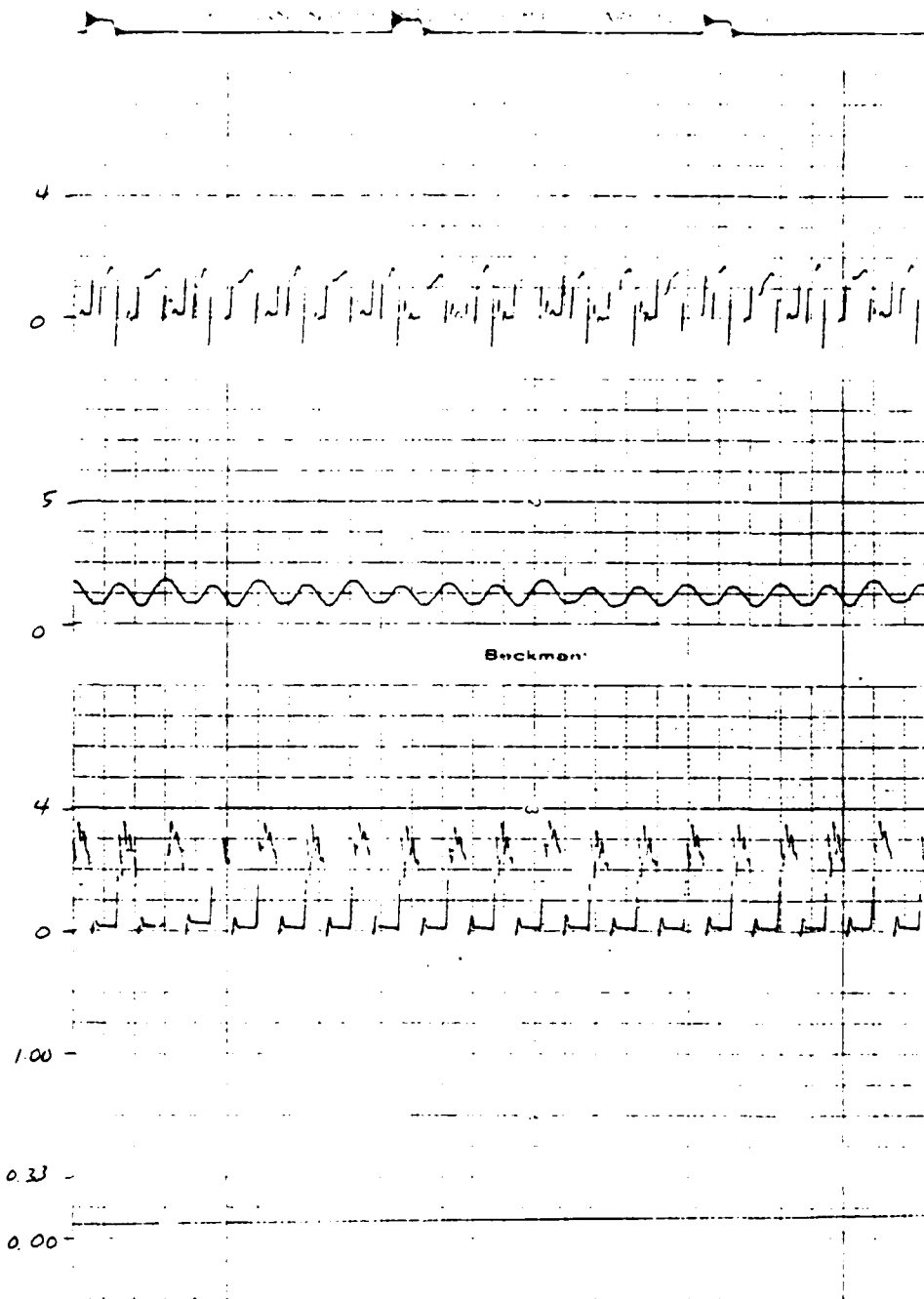


Figure 6. Data recorded at 7 Hz. Paper speed is 50mm/sec.

1984 USAF-SCEEE RESEARCH INITIATION PROGRAM

Sponsored by the

AIR FORCE OFFICE OF SCIENTIFIC RESEARCH

Conducted by the

SOUTHEASTERN CENTER FOR ELECTRICAL ENGINEERING EDUCATION

FINAL REPORT

BRILLOUIN SPECTROSCOPY IN SYSTEMS
OF BIOLOGICAL SIGNIFICANCE

Prepared by: Raj M. Krishnan

REPORT ON THE PROGRESS ON SUBCONTRACT 84RIP50, entitled,
"Brillouin Spectroscopy in Systems of Biological Significance".

The project included the setting up of a Brillouin Scattering Spectrometer for the purpose of studying biological systems. A triple pass piezoelectric scanning interferometer was purchased. We also purchased a photon counting system. An unusual amount of delay was encountered in obtaining the latter. At the present time work is progressing in interfacing the photon counting system with the scanning interferometer. This includes developing a computerized data acquisition system. We hope to get the whole system in operation by the end of summer, 1986.

STABILIZATION OF MODE-LOCKED LASERS

Final Technical Report on
Subcontract 84 RIP 51

Submitted to

1984 USAF-SCEEE Research Initiation Program
Sponsored by the
Air Force Office of Scientific Research
Conducted by the
Southeastern Center for Electrical Engineering Education

Prepared by

Odis P. McDuff
Professor of Electrical Engineering
Department of Electrical Engineering
The University of Alabama
P. O. Box 6169
University, Alabama 35486

and

The Bureau of Engineering Research
College of Engineering
The University of Alabama
P. O. Box 1968
University, Alabama 35486

Submitted by

The University of Alabama
P. O. Box 2846
University, Alabama 35486

BER Report No. 362-70

December, 1985

ABSTRACT

In many applications of mode-locked short pulsed lasers the stability of the system and reproducibility of the pulses are of paramount importance. Such is the case for non-invasive studies of the eye. Although passive mode locking schemes produce short pulses, they tend to have large shot-to-shot variations. Active mode locking produces more stable pulsing when the modulator frequency is carefully controlled. Research is reported which has produced a feedback control system which gives very stable active mode-locked pulsing without the necessity for having precisely controlled laser cavity length and modulator drive frequency. The research included a computer theoretical study and experimental work using an argon laser as a model.

ACKNOWLEDGEMENT

The author would like to thank the Air Force Office of Scientific Research and the Southeastern Center for Electrical Engineering Education for the support of this research. He especially would like to thank Dr. John Taboada, Air Force School of Aerospace Medicine, who was a constant supporter of the effort and who contributed many useful ideas.

The author would like to acknowledge the excellent work of Mr. Adel Atashi and Mr. Derric Scott, graduate students in the Electrical Engineering Department, and Mr. Subhash Jain, an Indo-American Fellow.

Finally the author would like to acknowledge the excellent administrative support of the Electrical Engineering Department and Bureau of Engineering Research and especially the excellent assistance of Ms. Kathy Adams in typing the manuscript.

TABLE OF CONTENTS

ABSTRACT

ACKNOWLEDGEMENT

I. INTRODUCTION

II. OBJECTIVES

III. APPROACH

IV. THEORETICAL STUDY

A. THE COUPLED MODE DIFFERENTIAL EQUATIONS

B. DISCUSSION OF PARAMETERS

1. Inhomogeneous Saturation

2. Homogeneous Saturation

C. DIGITAL COMPUTER SOLUTION

D. SIMULATION RESULTS

1. Homogeneous Laser Simulation

2. Inhomogeneous Laser Simulation

3. General Conclusions Regarding the Simulations

V. EXPERIMENTAL WORK

A. THE DISCRIMINANT

B. THE STABILIZATION CIRCUIT

C. CHECKING SYSTEM PERFORMANCE

D. EFFECTS OF CAVITY LENGTH VARIATION

E. CLOSED LOOP DRIFT

VI. CONCLUSIONS

VII. CONFERENCE PRESENTATIONS

VIII. REFERENCES

APPENDIX A. DEVELOPMENT OF THE COMPUTER SOLUTION

A. PROBLEM DEFINITION

B. SCALING THE EQUATIONS

1. Homogeneous Broadening

2. Inhomogeneous Broadening

C. SELECTION OF SCALED PARAMETERS

D. SOLUTION METHOD

1. Runge-Kutta

2. Parameters

E. COMPUTER VERSION OF EQUATIONS

1. Amplitude Equations
2. Phase Equations
3. Saturation Effects
 - a. Homogeneous Saturation
 - b. Inhomogeneous Saturation

F. CUSTOMIZING THE PROGRAM

1. Modulation
2. Saturation
3. Number of Modes
4. Autostop Feature
5. Multiple Plot Options

G. THE PROGRAM OUTPUT

APPENDIX B. LISTING OF PROGRAM CODE AND SAMPLE OUTPUT DATA
FOR HOMOGENEOUS SATURATION

APPENDIX C. LASER CHARACTERISTICS

APPENDIX D. MODE-LOCKER SPECIFICATIONS

I. INTRODUCTION

The mode-locked laser, first reported in 1964,¹ provides a means for producing short optical pulses. Since 1964, workers in the field have produced shorter and shorter pulses and used various combinations of active and passive elements within the optical cavity for Q-switching and/or mode locking of various types of lasers.

It is understood that the Air Force School of Aerospace Medicine (SAM) is interested in non-invasive studies of the eye by the use of optical pulses short enough that physical mechanisms other than thermal effects come into play.^{2,3} Stability of the system and reproducibility of the pulses is of paramount importance in work of this nature.

Simultaneously Q-switched and mode-locked lasers using a saturable absorber for both the Q-switcher and mode-locker produce short, high peak power pulses but tend to have large shot-to-shot variations in pulse width and energy. The use of the colliding pulse technique⁴ in an antiresonant ring cavity⁵ has been shown to provide shorter and more stable pulsing in a passively Q-switched and mode-locked Nd:YAG laser.⁶ A number of active-passive systems have been described⁷ in which the Q-switching was done passively and the mode locking done actively.

In the case of a cw Nd:YAG laser, the Q-switching must be done actively but the mode locking could be done either actively or passively. The colliding-pulse, antiresonant cavity mode-locking scheme, with its potentially greater stability over other passive mode-locking schemes and its possibility of producing shorter pulses than active mode locking, seemed a good candidate for the production of a stable pulsed source derived from an actively Q-switched Nd:YAG laser and was the subject of an experimental investigation by the author

during the Summer of 1984.⁸ The laser used was a Laser Application Inc. Model 9560T actively Q-switched cw Nd:YAG laser. The conclusion reached was that the laser gain was too low to use saturable absorber mode locking with the mirrors available. Furthermore, there is some doubt whether the active Q-switched, passive mode-locked antiresonant scheme would have been stable enough for the SAM applications, based upon the previous work with non-cw Nd:YAG lasers.⁶

Potentially, the active Q-switched active mode-locked system, followed by harmonic doubling, is the most stable configuration. Previous work has shown the mode-locked pulses not to be as short as with passive mode locking; however, regenerative amplification and pulse compression techniques^{9,10} or synchronous pumping of a mode-locked dye laser^{11,12} could be used to increase the pulse amplitude and reduce pulse width. Workers have used both mode-locked argon and frequency doubled mode-locked Nd:YAG lasers as pump sources for dye lasers. The initial workers used passive mode locking of the pump source but later work¹³ was with active mode-locked pump sources.

Commercial active-active systems are becoming available which use complicated temperature compensation techniques in stabilizing the laser cavity and the mode-locker individually,¹⁴ but they are quite expensive. This is so because, with separate stabilization of the combination line-selecting-prism and mode-locker, it is necessary to control the mode-locker temperature to within a very small fraction of a degree.

It was recommended by the Principal Investigator in the report of his Summer 1984 work⁸ that an active Q-switched, active mode-locked system be considered, to be followed by amplification, harmonic doubling, and pulse compression techniques. This was not to be a

conventional system in which both the laser and mode-locker were separately stabilized;^{15,16} instead, the mode-locker frequency would be actively controlled to be the same as the laser $c/2L$ axial mode spacing frequency. The requirement for an active-active system where the modulation frequency is locked to the $c/2L$ frequency is that the system must be able to sense when the two frequencies are different. Once this difference was sensed, then the modulator drive frequency could be controlled to equal the $c/2L$ frequency and highly stable pulsing obtained. The problem was to determine if such a discriminant existed and whether it could be used for stabilization of a mode-locked laser.

II. OBJECTIVES

An objective of the proposed research was to investigate possible mechanisms for locking the modulator frequency in an active Q-switched, active mode-locked laser to the $c/2L$ mode-spacing frequency. A further objective was to construct, once such a mechanism was identified, a system to lock the two together in an operating laser, thereby producing a very stable mode-locked laser, and to determine the characteristics of such a system. The plan was to do the experimental work with an argon laser at the Principal Investigator's institution but the ultimate goal was to obtain information that could lead to the stabilization of a Nd:YAG laser.

III. APPROACH

At the beginning of this research, some of the performance parameters in an actively mode-locked laser had been known to depend on

the modulator drive frequency. Both the peak amplitude of the pulse and the location of the pulse in the time domain, relative to the phase of the modulator drive, were shown to be dependent upon the frequency of the drive in an early experimental study with loss modulation of an inhomogeneously broadened laser.¹⁷ A nonlinear theoretical analysis of inhomogeneously broadened lasers showed both of these effects to occur in the case of a loss-modulated laser¹⁸ and the variation in pulse amplitude to occur in the case of a phase-modulated laser¹⁹ (the phase of the pulse was not studied in the latter case). Experimental work with an argon loss-modulated laser also showed both effects to occur.²⁰ Experimental work with a phase modulated Nd:YAG laser showed the phase-of-pulse effect to occur.²¹ An early linearized theory²² for the homogeneously broadened laser predicted both effects to occur with phase modulation but only predicted that the amplitude decrease with modulator detuning would occur in the case of loss modulation. In conclusion, both effects had been shown both theoretically and experimentally to occur in the case of loss-modulated inhomogeneously broadened lasers and in the case of phase-modulated homogeneously broadened lasers. Furthermore, the pulse amplitude variation had been shown to occur theoretically in the other two cases--phase-modulated inhomogeneous and loss-modulated homogeneous lasers. However, the linearized theory²² specifically predicted against the phase-of-pulse variation in the loss-modulated homogeneously broadened laser (This would be the desired configuration for a Nd:YAG laser).

It was essential for the phase-of-pulse effect or some similar effect to occur since it would give the direction of departure of the modulating frequency from the $c/2L$ mode spacing frequency. This

information was needed for a feedback control system to lock the two frequencies together.

It was the expectation of the Principal Investigator that both effects would occur in all four cases--phase- and loss-modulated homogeneous and inhomogeneous lasers. This could be explained as follows. When the modulator drive frequency is greater than the mode spacing frequency, the pulsing would be forced to occur at a frequency higher than the natural $c/2L$ frequency. The pulsing mechanism would resist this and the phase of the pulse would lag behind the modulator drive frequency. When the modulator drive frequency is less than the mode spacing frequency, the pulsing would be forced to occur at a frequency lower than the natural $c/2L$ frequency. The pulsing mechanism would resist this also and the phase of the pulse would lead the modulator drive frequency. At the same time, the detuning of the modulator drive frequency would reduce the efficiency of the coupling mechanisms and add effective losses to the pulse path, reducing the pulse output amplitudes. There seemed to be no reason, intuitively, why all four cases would not operate qualitatively the same and it was believed that both effects would be observed in all cases.

Once a discriminant for controlling the modulator frequency was shown to exist then the effects of the various parameters were to be studied. For example in none of the previous work had a study been made of the effects of detuning the modulator when the center mode of the set of oscillating modes was off line center of the gain medium. If the modes were going to be permitted to "float" and the modulator frequency locked to the mode-spacing frequency, then this departure from line center had to be considered. Furthermore, it remained to be determined

whether the phase-of-pulse effect would occur in a Nd:YAG laser (homogeneous broadening) with loss modulation, the combination most desirable for the basic mode-locked source.

The approach had two basic directions of effort. An experimental effort included the loss modulation mode locking of an Argon laser, Spectra Physics Model 170, which was available at The University of Alabama and the characterization of the mode-locked performance. Using the appropriate results of these measurements a feedback control system was developed to lock the modulation frequency to the mode spacing of the laser. The phase-of-pulse effect together with a phase-locked loop were used in this system and performance data were measured.

A theoretical effort included a computer simulation of a mode-locked laser to determine whether the phase-of-pulse effect would exist with a loss-modulated homogeneously broadened laser (such as Nd:YAG). The work confirmed that such an effect would be present and considered the effects of the various operating parameters. The effort used theoretical mode coupling equations developed earlier¹⁸ but modified them to include the effects of homogeneous line broadening and saturation.

IV. THEORETICAL STUDY

A computer simulation study was made of the mode locked laser. The purpose of the study was to determine whether the phase-of-pulse effect existed with a loss-modulated homogeneously broadened laser and to serve as a guide for the experimental modeling using an inhomogeneously broadened laser.

A. THE COUPLED MODE DIFFERENTIAL EQUATIONS

The starting point was the coupled mode differential equations developed earlier.^{18,19,20} As shown in these references one can express the total electromagnetic field in the cavity as a sum of normal mode eigenfunctions,

$$E(z,t) = \sum_n E_n(t) \cos [\nu_n t + \phi_n(t)] U_n(z), \quad (1)$$

where $U_n(z) = \sin(n_0 + n) \pi z/L$. The $E_n(t)$ and $\phi_n(t)$ are the slowly time varying amplitude and phase of the n th mode, ν_n is its frequency,* L is the cavity length, and n_0 is the number of spatial variations of some central mode whose frequency is chosen to be closest to the center of the atomic fluorescence line. Starting with Lamb's self consistency equations²³ and including the effects of atomic polarization and the parametric polarization due to the loss modulator, one obtains coupled first order differential equations as follows^{18,19,20}

$$\begin{aligned} (\dot{\phi}_n - n\Delta\nu + \frac{c}{2L} \psi_n) E_n = \\ \frac{-c\alpha_c}{2L} [E_{n+1} \sin(\phi_{n+1} - \phi_n) - E_{n-1} \sin(\phi_n - \phi_{n-1})] \end{aligned} \quad (2)$$

$$\begin{aligned} (\dot{E}_n + \frac{c}{2L} \alpha_n E_n - \frac{c}{2L} G_n E_n = \frac{-c\alpha_a}{2L} E_n \\ \frac{-c\alpha_c}{2L} [E_{n+1} \cos(\phi_{n+1} - \phi_n) + E_{n-1} \cos(\phi_n - \phi_{n-1})] \end{aligned} \quad (3)$$

B. DISCUSSION OF PARAMETERS

In equations (1) and (2) the frequency ν_n of the n th mode has been expressed in terms of the detuning $\Delta\nu$ of the modulator drive frequency

* In the theoretical discussion all symbols for frequencies will denote circular frequencies unless otherwise noted.

ν_m from the axial mode spacing, $\Delta\nu = \Delta\Omega - \nu_m$, such that

$$\Omega_n - \nu_n = n\Delta\nu. \quad (4)$$

The parameter Ω_n is the frequency of the nth cavity resonance and is given by

$$\Omega_n = \Omega_0 + (n\pi c)/L, \quad (5)$$

where Ω_0 is the frequency of some center mode. Also $\Delta\Omega$ is the frequency interval between axial resonances ($\Delta\Omega = \pi c/L$).

The atomic contribution to the polarization of the nth mode is introduced by means of macroscopic quadrature and in-phase components of susceptibility, denoted by χ_n'' and χ_n' , respectively. Then an optical signal propagating through a length L of the cavity undergoes additional phase retardation $\nu L \chi_n'/2c$ because of the presence of the atomic medium. At the same time, the output optical intensity is increased by an amount equal to $\exp(-\nu L \chi_n''/2c)$. It is useful to define a factor G_n such that

$$G_n = -\frac{\nu L}{c} \chi_n'' . \quad (6)$$

Thus the fractional single pass power gain of the nth mode is given by

$$\left(\begin{array}{c} \text{Single Pass} \\ \text{Power Gain} \end{array} \right)_{\text{nth mode}} = \left(\frac{I_{\text{out}} - I_{\text{in}}}{I_{\text{in}}} \right)_{\text{nth mode}} = e^{G_n - 1}. \quad (7)$$

At small gains, $e^{G_n} \approx 1 + G_n$ and therefore G_n is approximately equal to the fractional single pass power gain. The parameter G_n depends nonlinearly upon frequency and power level. Similarly, it is useful to define a phase retardation ψ_n such that

$$\psi_n = \frac{\nu L}{c} \chi_n' , \quad (8)$$

where ψ_n is the additional round trip phase retardation which is seen by the nth mode as a result of the insertion of the atomic medium. This also depends nonlinearly upon frequency and power level. In the

computer simulation a specific dependence upon frequency and power level must be assumed for G_n and ψ_n . These differ for inhomogeneous and homogeneous broadening and are considered in detail in later subsections of this discussion.

The quantity α_n is defined in terms of Q_n of the nth mode by the expressions

$$\alpha_n = \frac{\nu L}{c} \frac{1}{Q_n} \quad (9)$$

and includes both dissipative and output coupling loss (mirror transmission). Since loss is small, α_n is approximately equal to the fractional single pass power loss of the nth mode (i.e., $e^{\alpha_n} \approx 1 + \alpha_n$). In typical cases α_n is independent of n .

In practice the perturbing element or modulator extends over a short distance in the axial, or z direction and usually will have no significant spatial variation over its length in that direction. The expression for the attenuation through a loss modulator perturbing element, per pass through the element, can be written

$$\alpha(t) = \alpha_M (1 + \cos \nu_m t). \quad (10)$$

As previously, if the loss is small, $e^{\alpha_M} \approx 1 + \alpha_M$ and therefore α_M is approximately the average single pass loss through the perturbing element.

This yields a cross coupling term α_c which is given by the expression¹⁸

$$\alpha_c = \frac{L}{l} \frac{\alpha_M}{\pi} \sin \frac{\pi l}{2L} \cos \frac{z_0 \pi}{L}, \quad (11)$$

where l is the axial length of the modulator centered at z_0 , and for $l \ll L$ is approximately

$$\alpha_c = \frac{\alpha_M}{2} \cos \frac{z_0 \pi}{L}. \quad (12)$$

The cross coupling loss term α_c is maximized by making z_0 small and then becomes

$$\alpha_c = \frac{\alpha_M}{2}. \quad (13)$$

The self-coupling term

$$\alpha_a = \alpha_M \quad (14)$$

and therefore is equal to the average loss per pass through the modulator.

Several loss terms have been defined in this section and are summarized as follows: * α_n , the single pass power loss of the n^{th} mode with is usually independent of n ; α_M , the average loss per pass through the perturbing element; a self-coupling term α_a which is equal to α_M ; and a cross-coupling term α_c which is approximately equal to one half of this average loss, α_M .

1) Inhomogeneous Saturation

It remains to give the form of G_n and ψ_n depending on the particular type of line broadening or saturation. For the inhomogeneous case the principal features of the problem are considered to be treated adequately by assuming the example of a Doppler broadened Gaussian atomic line with homogeneous linewidth much smaller than both the axial mode interval $\Delta\Omega$ and Doppler linewidth. For these cases the gain is expressed as

$$G_n = \frac{g_n}{\sqrt{1 + C E_n^2}}, \quad (15)$$

* These descriptions are applicable to the low loss case, otherwise the terms should more correctly be called attenuation constants.

where g_n is the unsaturated per pass fractional power gain of the n th mode and C is the saturation parameter. For the Doppler broadened Gaussian line then, g_n is given by

$$g_n = g_0 \frac{Z_1 \left(\frac{\nu_n - \nu_0}{Ku} \right)}{Z_1(0)} \quad (16)$$

and corresponding this, ψ_n is taken to be

$$\psi_n = g_0 \frac{Z_r \left(\frac{\nu_n - \nu_0}{Ku} \right)}{Z_1(0)} \quad (17)$$

where power dependent mode pulling and pushing effects have been neglected. In (16) and (17) g_0 is the unsaturated line-center power gain and Z_r and Z_1 are the real and imaginary parts of the plasma dispersion function, as described by Lamb.²³ For vanishingly small homogeneous linewidth, (16) and (17) become g_0 times the normalized Gaussian and Hilbert transform of the Gaussian, respectively. The parameter ν_0 is the center frequency of the atomic line and Ku has units of angular frequency and equals 0.6 times the half power Doppler linewidth. It often is convenient to express the axial mode interval in terms of Ku and thus make use of the tables of Fried and Conte.²⁴

2) Homogeneous Saturation

The prior work had not considered the case of homogeneous line broadening or saturation and in order to do the numerical work it was necessary to derive the appropriate expressions.

The population inversion $(N_1 - N_2)$ in a two-level atomic system which is homogeneously broadened varies with the optical intensity, I , at a frequency ν according to the expression²⁵

$$(N_1 - N_2) = \frac{(N_1 - N_2)_e}{1 + \frac{I}{I_{sat}} \frac{\tau}{2} \Delta \nu_L g_L(\nu)} \quad (18)$$

where $(N_1 - N_2)_e$ is the zero-signal inversion, $\Delta\nu_L$ is the Lorentzian linewidth, I_{sat} is the optical intensity level at which the population inversion is reduced to one-half its unsaturated value, and $g_L(\nu)$ is the Lorentzian line shape function

$$g_L(\nu) = \frac{1}{\pi} \frac{\Delta\nu_L/2}{(\nu_0 - \nu)^2 + (\frac{\Delta\nu_L}{2})^2} \quad (19)$$

where ν_0 is the line-center frequency.

Following the work of Kuizenga and Siegman,²² but writing a summation of discrete modes rather than a continuous integral over the whole linewidth, one can modify (18) to account for the presence of several non-zero modes as follows.

$$(N_1 - N_2) = \frac{(N_1 - N_2)_e}{1 + \frac{1}{I_{sat}} \frac{\pi}{2} \Delta\nu_L \sum_m I_m g_L(\nu_m)}, \quad (20)$$

where I_m is the m th mode intensity and the summation is over all non-zero modes.

Corresponding to the population inversion there are in-phase and quadrature components of susceptibility²⁵

$$\chi'_n = (\text{constant})(N_1 - N_2) \frac{2}{\Delta\nu_L} (\nu_0 - \nu_n) g_L(\nu_n) \quad (21)$$

and

$$\chi''_n = (\text{constant})(N_1 - N_2) g_L(\nu_n) \quad (22)$$

where (constant) depends upon the dipole matrix element of the transition, etc.

Then, from (6), (20), and (22) the gain factor is given by

$$G_n = g_0 \frac{\pi}{2} \Delta\nu_L \frac{g_L(\nu_n)}{1 + C \frac{\pi}{2} \Delta\nu_L \sum_m E_m^2 g_L(\nu_m)}, \quad (23)$$

where g_0 is the unsaturated line-center power gain and $C = (A I_{sat})^{-1}$ (writing $E_m^2 = A I_m$).

Similarly, from (8), (20), (22) and (23), the phase retardation ψ_n is given by

$$\psi_n = \frac{g_o \pi (\nu_n - \nu_o) g_L(\nu_n)}{1 + C \frac{\pi}{2} \Delta \nu_L \sum_m E_m^2 g_L(\nu_m)} \quad (24)$$

The saturation parameter C is of course different from that in the inhomogeneous case shown in (15).

C. DIGITAL COMPUTER SOLUTION

Equations (2) and (3) were solved on a digital computer, IBM 3081D, for various operating conditions. The development of the program is described in detail in Appendix A, and a copy of the program listing for the homogeneous broadening case is included in Appendix B. The differential equations were started on the computer, after selecting initial mode amplitudes and phases and the laser parameters, and permitted to run until a steady state condition was reached (all $\dot{E}_n = 0$ and $\dot{\phi} = 0$ to 3 decimal places). The $n = 0$ mode was generally taken at line center, with a frequency $\nu_o = \Omega_o$, except when specifically the effects of shifting the center mode away from line-center were being studied. The solution gives all the mode amplitudes E_n and mode phases ϕ_n .

The laser output pulse envelope was plotted to observe the time-domain behavior. If the output signal of the laser is written

$$E(t) = \sum_n E_n \cos[(\Omega_o + n\nu_m)t + \phi_n], \quad (25)$$

then the low passed portion (or envelope) of $E^2(t)$, such as would be obtained if the signal were incident on a photodetector, is given by¹⁹

$$W(t) = \frac{1}{2} \sum_s \sum_n E_n E_{n+s} \cos(s\nu_m t + \phi_{n+s} - \phi_n). \quad (26)$$

From this output pulse envelope the pulse width and the phase shift of

the pulse relative to the modulator can be determined. With an assumed modulation phase as in (10), the pulse under ideal zero detuning conditions has its peak at $\nu_m t = \pi$ (lowest modulator loss).

D. SIMULATION RESULTS

The most important element of the study was the determination of the effects of modulator detuning upon the phase of the output pulse. It also was of interest to know the effects of modulation strength upon this phase shift. In the homogeneous case it was not known beforehand whether the phase shift would occur with loss modulation.

In general in the homogeneous case it was more difficult to obtain a steady state solution that gave constant mode amplitudes and phases. In some runs a limit-cycle type of steady state was reached in which the peak in the mode spectrum would oscillate back and forth from line-center to the wings of the lineshape. This behavior tended to occur at low modulation strength (small α_c) and at large detuning of the modulator frequency. The pulse produced also varied in a cyclic manner, alternately contracting and spreading in width. This behavior was attributed to the fact that under these conditions there was insufficient mode coupling to produce a steady state mode locking. A relaxation type of behavior had been observed experimentally by others²¹ and in general the tendency for homogeneous mode locked lasers to be unstable had been noted. Some had attributed the phenomenon to the effects of noise;²⁶ however, the equations presented here do not include the effects of noise, and the effect apparently is due to the dynamics of the coupled mode system. A similar limit cycle behavior was observed experimentally under certain conditions by the author in the case of a Nd:YAG laser.²⁷

Experimentalists have used an intracavity etalon to make a mode-locked homogeneous laser more stable. In the simulation described in the following such a system was modeled.

1. Homogeneous Laser Simulation

A Nd:YAG laser, an example of homogeneous broadening, was modeled. A linewidth of 120 GHz was assumed, together with an axial mode spacing of 150 Mz, to give a ratio of mode spacing to linewidth, $\Delta\Omega/\Delta\nu_L$, of 0.00125. A 10% transmission output mirror and an additional 10% round trip cavity loss were assumed, giving a single pass loss of 10%, or $\alpha_n = 0.1$. These parameters were chosen to match the approximate characteristics of the Nd:YAG laser at the Air Force School of Aerospace Medicine. Furthermore, comparing the excitation currents at oscillation threshold and at operating conditions for that laser, a single pass unsaturated gain of 16% was assumed, or $g_0 = 0.16$. Figures 1, 2, and 3 show the variation of pulse phase shift, pulse width, and pulse amplitude versus modulator detuning at several values of cross coupling, α_c (data points for the limit-cycle behavior were not plotted). These curves show the great sensitivity of pulse phase to both modulator detuning and cross coupling. They show that the desired effect does indeed occur but, as will be seen from Argon laser simulations to follow, the effect is not as great as in the case of inhomogeneous broadening. The difference between the Nd:YAG and Argon lasers appears to be due more to the value of $\Delta\Omega/\Delta\nu_L$ than to the type of broadening, however. It was impossible to tell exactly whether $\Delta\Omega/\Delta\nu_L$ is the reason because an inhomogeneous laser with this value of $\Delta\Omega/\Delta\nu_L = 0.00125$ would have too many free-running modes to be modeled. The statement can be inferred, however, from the observation of what happens when an etalon

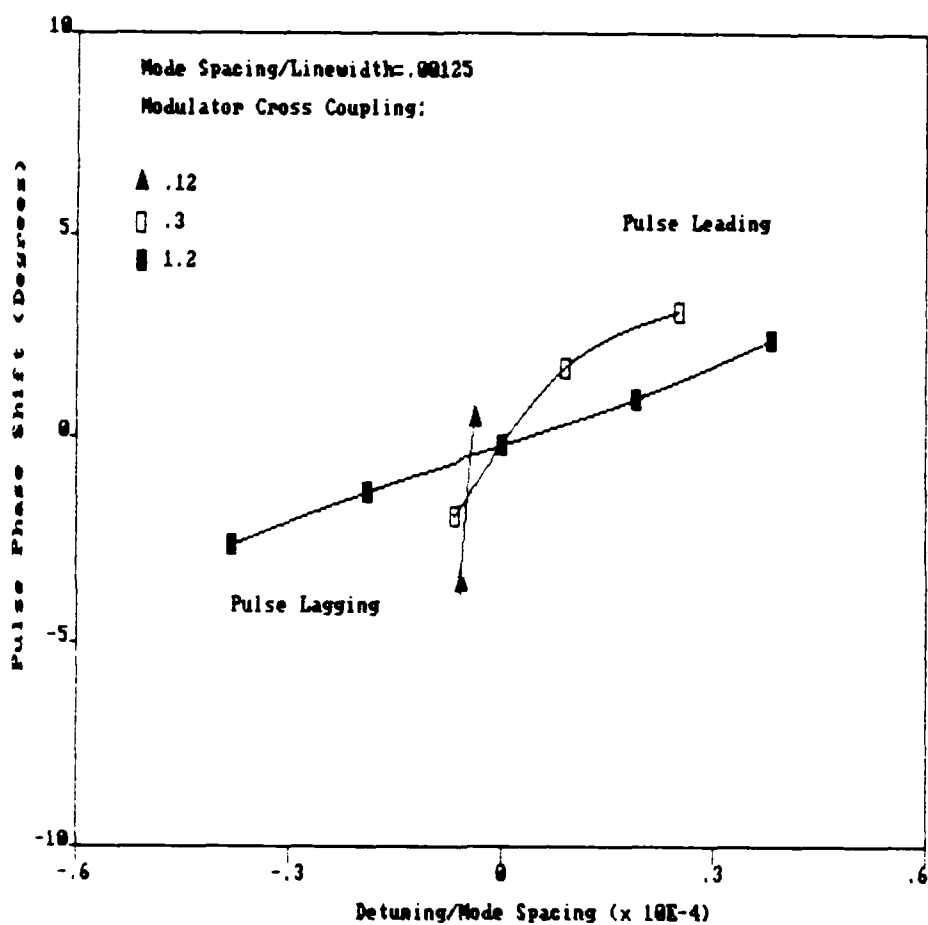


Figure 1. Phase Shift of pulse versus normalized modulator detuning in a simulated mode-locked Nd:YAG laser.

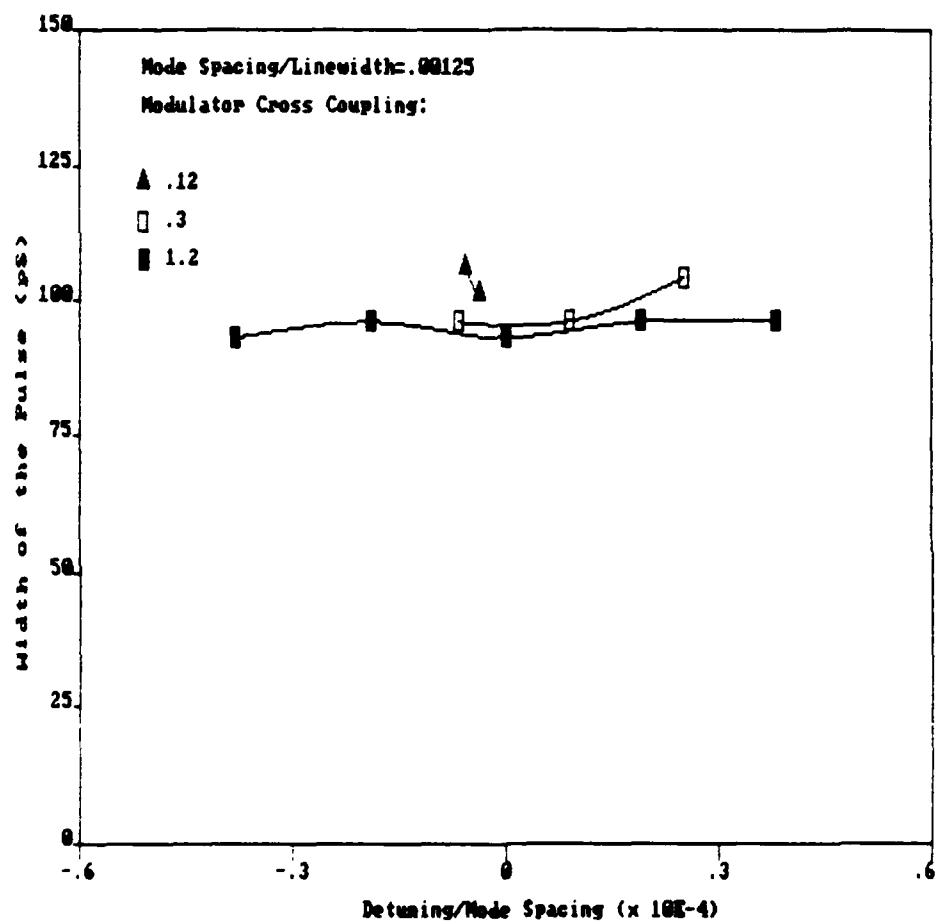


Figure 2. Width of pulse versus normalized modulator detuning in a simulated mode-locked Nd:YAG laser.

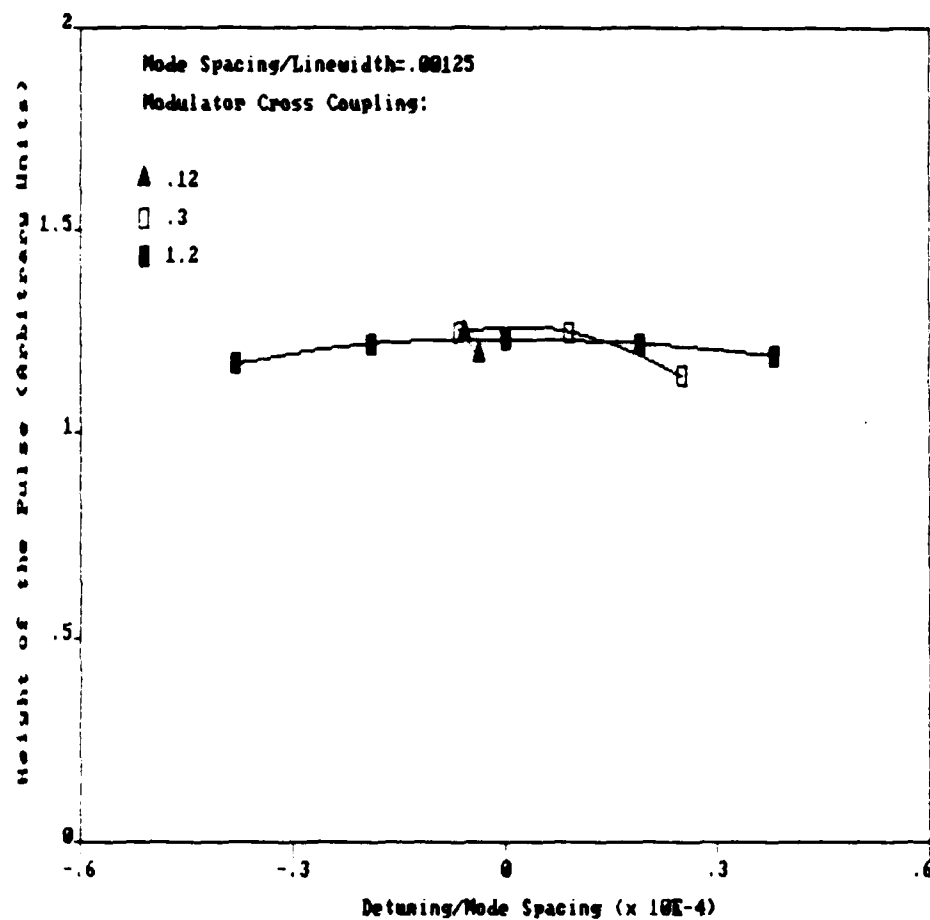


Figure 3. Pulse height versus normalized modulator detuning in a simulated mode-locked Nd:YAG laser.

is placed inside the cavity of the homogeneous laser (the next model). The pulse widths in Figure 2 compare quite favorably to those measured experimentally by the author with the School of Aerospace (SAM) laser.²⁷

Next, the laser was modeled as if an etalon with an effective linewidth of 30 GHz had been placed in the laser cavity. This gave a value of $\Delta\Omega/\Delta\nu_L = 0.005$. The mode spacing, loss per pass, unsaturated gain, etc were assumed to remain the same. Figures 4, 5, and 6 show the variation of the same parameters as with the previous laser. The computer solutions were much more stable with less difficulty arising due to limit-cycle type of behavior. One notes from the figures that a larger detuning is tolerated but that a larger phase shift is experienced, and that the pulses are wider (they also were of smaller peak values although it is not shown by the curves since a different pulse height normalization was used in Figure 6 and in Figure 3). These results are in conformance with the explanation that fewer modes are produced due to the more rapid drop-off in effective mode gain for modes away from line center. In addition, the more rapid drop-off in gain helps the system of modes to center on line center, producing a more stable coupled mode system.

As pointed out in Appendix A, it should be emphasized that this set of computer runs could be interpreted differently by assuming different laser constants for the set of normalized constants (see equations (41)-(48) of Appendix A). Of particular interest would be the interpretation that the run represented an increase in mode spacing to 300 MHz and the insertion of a 60 MHz linewidth etalon. If all the other laser parameters remain the same, then the curves of Figures 4, 5, and 6 still apply except that the pulse widths are halved, and a given

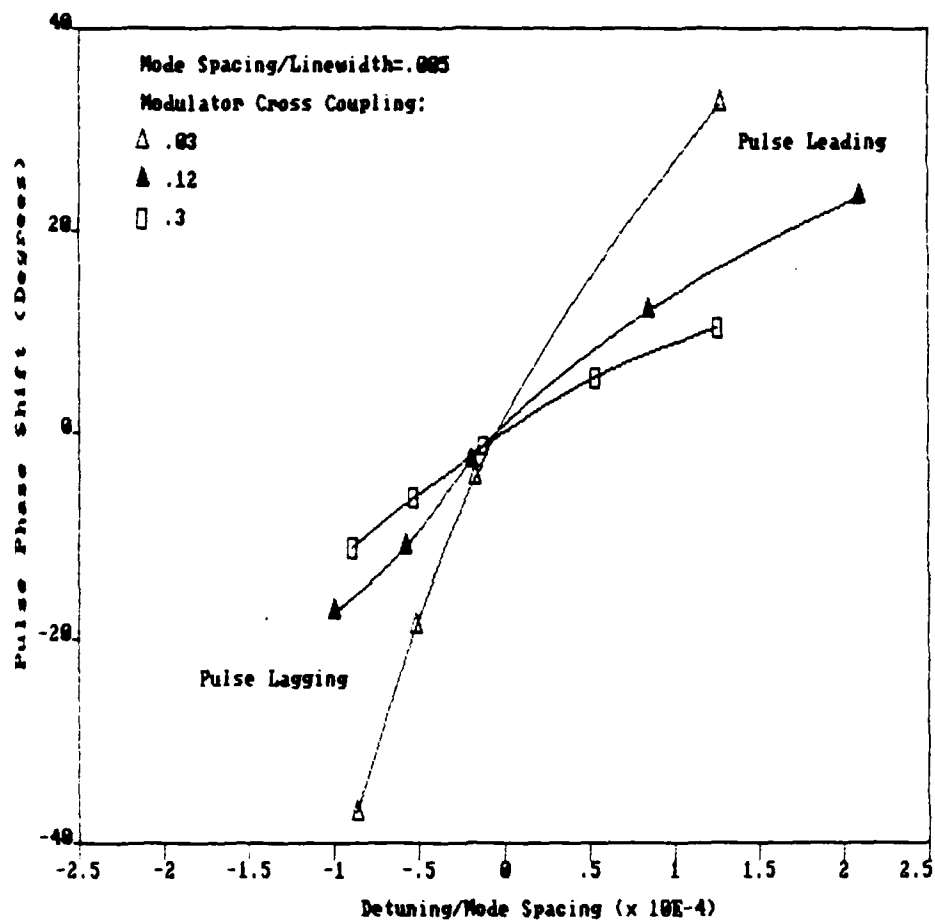


Figure 4. Phase shift of pulse versus normalized modulator detuning in a simulated mode-locked Nd:YAG laser having a 30 GHz linewidth intracavity etalon.

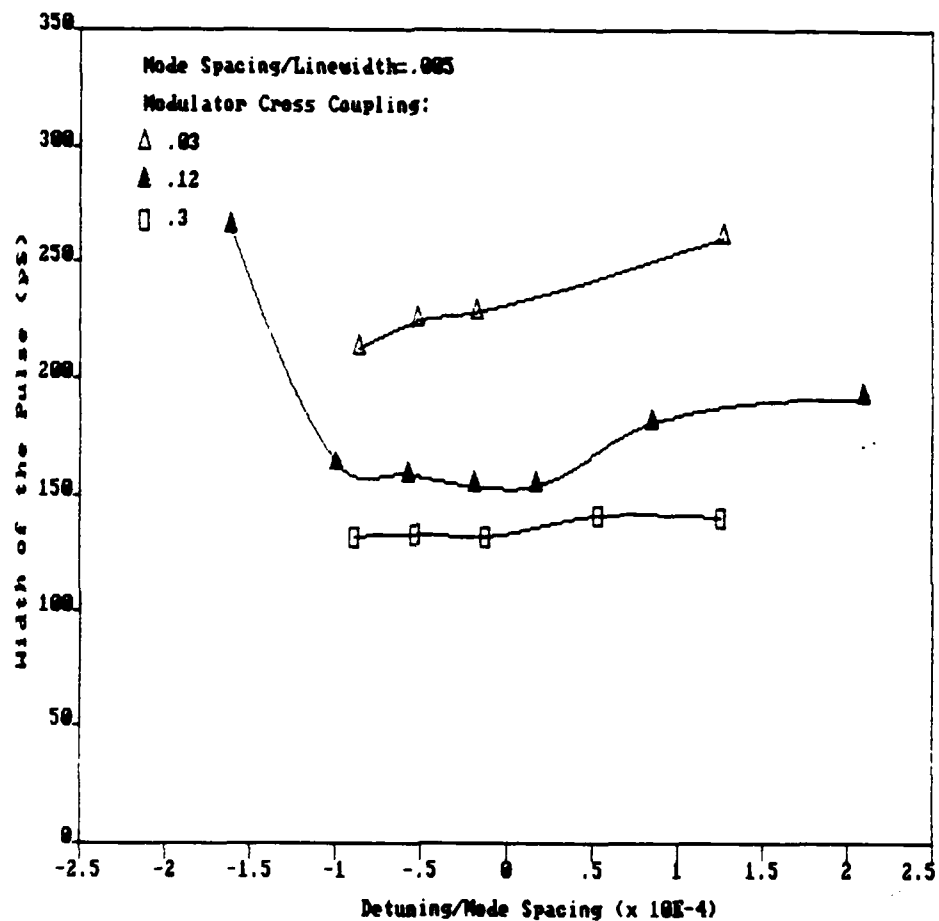


Figure 5. Width of pulse versus normalized modulator detuning in a simulated mode-locked Nd:YAG laser having a 30 GHz linewidth intracavity etalon.

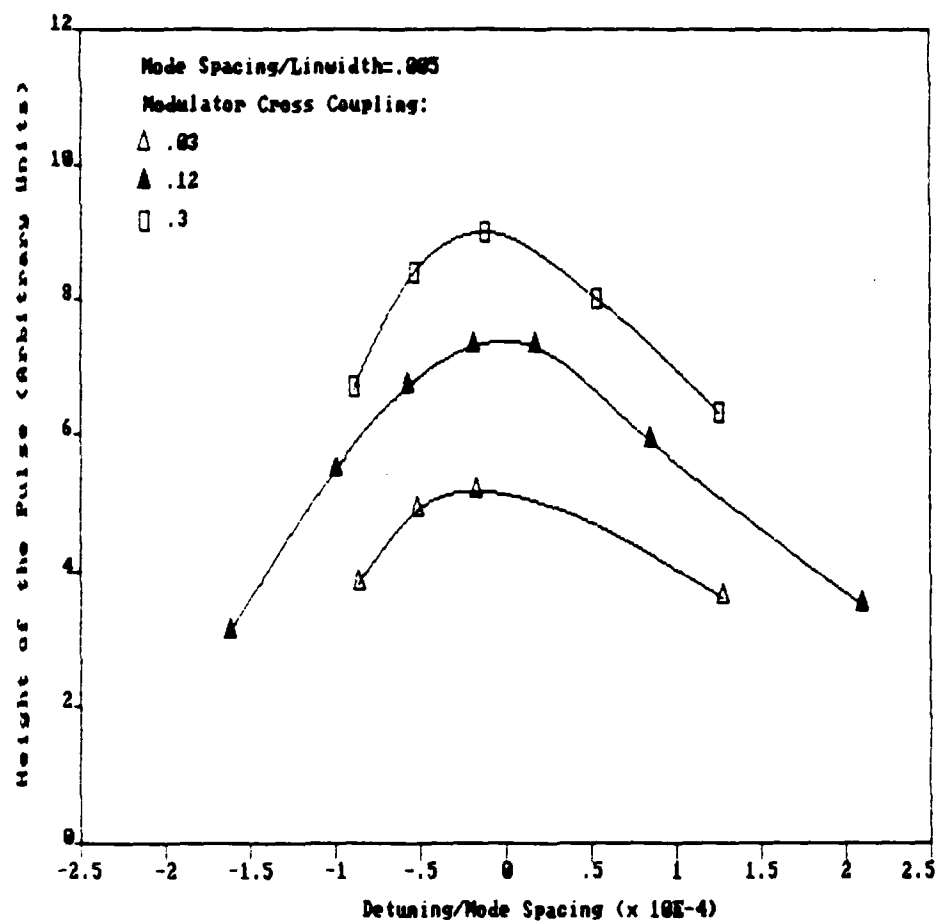


Figure 6. Pulse height versus normalized modulator detuning in a simulated mode-locked Nd:YAG laser having a 30 GHz linewidth intracavity etalon.

value of detuning $\Delta\nu/\Delta\Omega$ means an actual $\Delta\nu$ twice as large. The pulse widths are halved but their repetition rate is doubled, so that the laser average power output remains the same since the pulse peak amplitude does not change.

A third case was modeled in which the first laser had inserted an etalon with a 15 GHz linewidth. The same trends were observed; a more stable set of solutions producing wider pulses having reduced amplitudes, and an increased phase shift with detuning. These results are shown in Figures 7, 8, and 9. An additional characteristic of the computer runs with smaller values of $\Delta\Omega/\Delta\nu_L$ was that they reached steady state more rapidly, requiring less computer time.

In conclusion, the homogeneous case simulation showed that the desired phase-shift effect would occur and indicated the range of values of α_c necessary and the actual sensitivity to detuning. The phase-shift effect was later observed experimentally by the author with the SAM laser.^{27,28}

2. Inhomogeneous Laser Simulation

An Argon laser, used in the experimental work described in Section V following, was modeled. This was done to provide confidence in the computer results, since the phase-of-pulse effect was known to occur with Argon, and to serve as an aid in the experimental work.

An Argon linewidth of 5 GHz was assumed with a mode spacing of 71.6 MHz to match the laser used for the experimental work. Complete inhomogeneous broadening was assumed, although the homogeneous linewidth in Argon may be as large as 100-200 MHz. A single pass loss of 10% was assumed meaning $\alpha_n = 0.10$. The unsaturated line-center gain was assumed to be 12.8%, i.e. $g_0 = 0.128$, giving 41 modes free running, a figure in

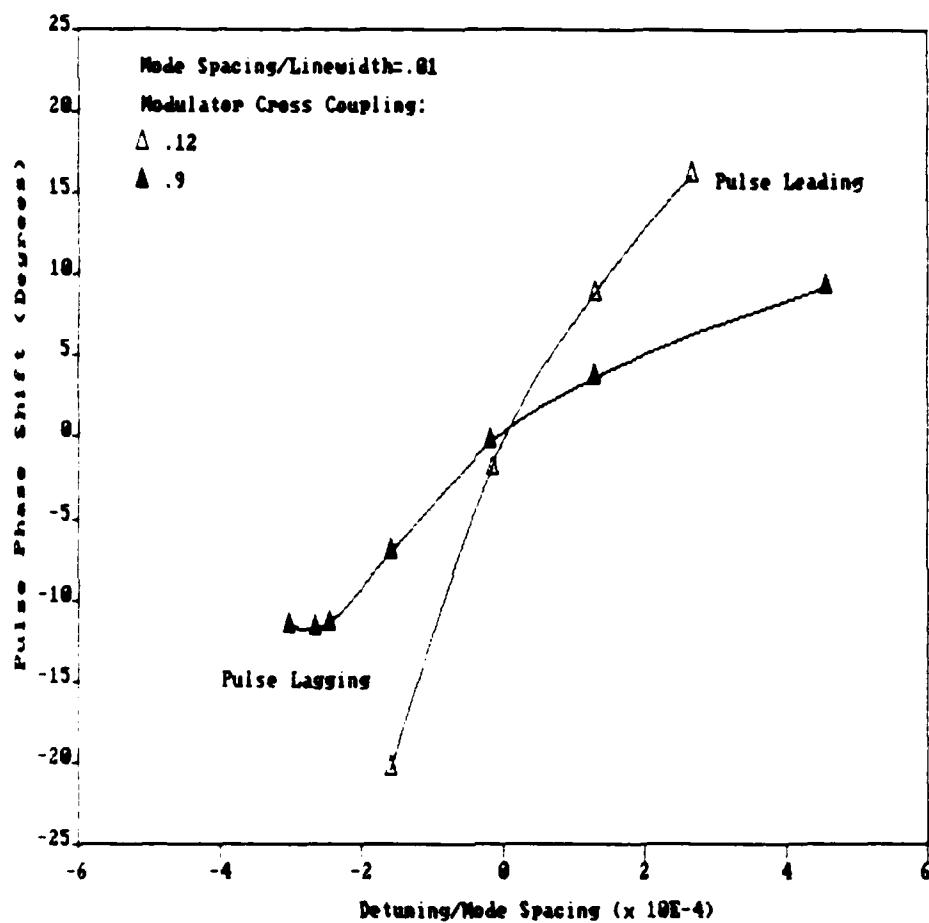


Figure 7. Phase shift of pulse versus normalized modulator detuning in a simulated Nd:YAG laser having a 15 GHz linewidth intracavity etalon.

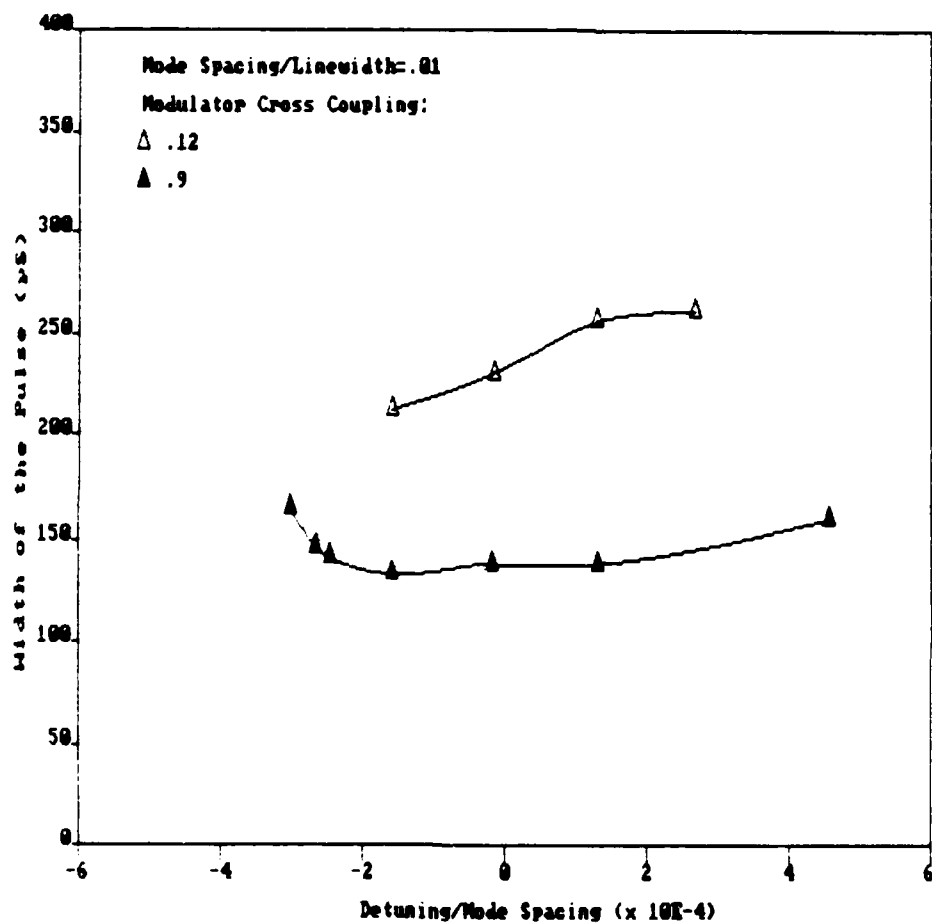


Figure 8. Width of pulse versus normalized modulator detuning in a simulated mode-locked Nd:YAG laser having a 15 GHz linewidth intracavity etalon.

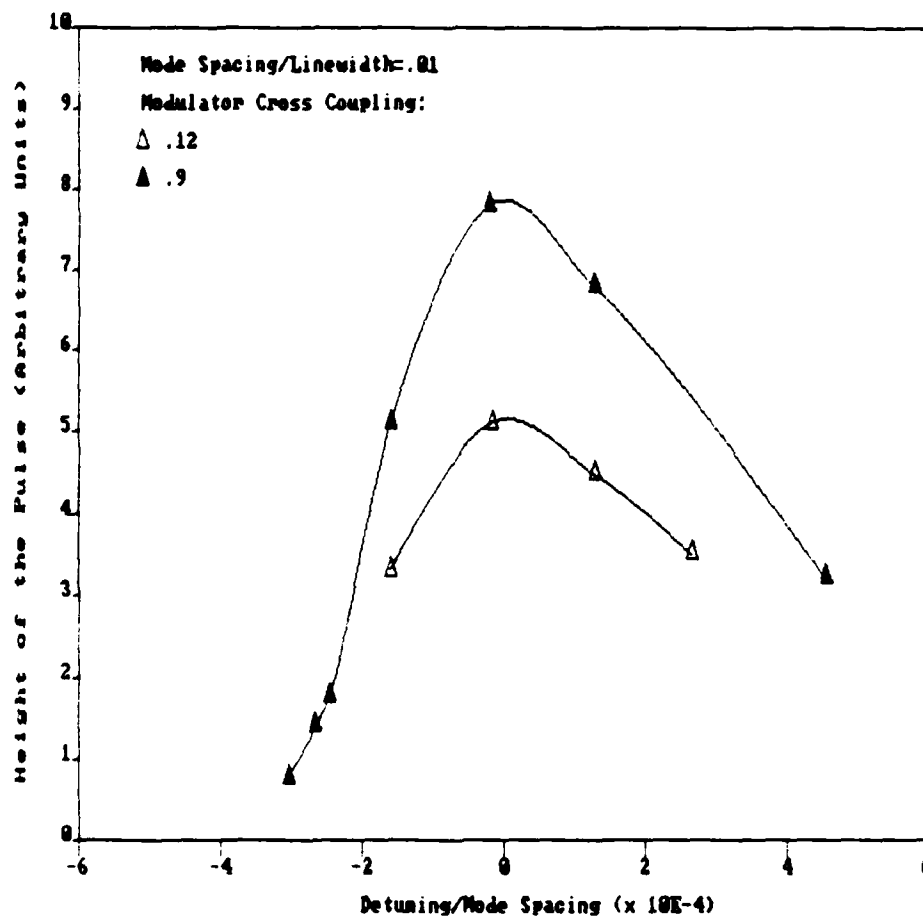


Figure 9. Pulse height versus normalized modulator detuning in a simulated mode-locked Nd:YAG laser having a 15 GHz linewidth intracavity etalon.

the right range based on the various statements in the literature. Figures 10, 11, and 12 show the results of this simulation. The computer runs were quite stable in this case requiring less computer time to reach steady state. The phase shifts were greater, as in the homogeneous-etalon cases, and somewhat larger detunings (normalized) were tolerated as in the latter homogeneous-etalon case. Experimentally, as will be seen in Section V following, phase shifts larger than this were observed and steady-state operation was possible at larger detunings. In fact, it was difficult experimentally to observe unstable operation in the inhomogeneous case.

3. General Conclusions Regarding the Simulations

The following general statements are seen very clearly from the results presented. For the internally loss modulated laser, whether inhomogeneously or homogeneously broadened, there is a zero detuning point where the output pulse has no phase shift relative to the modulator drive frequency. Changing the modulator frequency from this value causes a shift in the output pulse phase. This shift is less for greater loss modulation amplitude. Also with increasing modulation the pulse becomes more peaked and more narrow. The sharpest, narrowest pulses occur when the modulator is driven at the zero detuning frequency. This is the desired performance in order for the stabilization scheme that was the goal of this work to function. The confirmation of the predicted Nd:YAG behavior was one of the main goals of the research.

One fundamental question was whether the desired operation depended upon the center mode being exactly at the line-center of the medium. Computer runs with a shift of the center mode from line-center showed

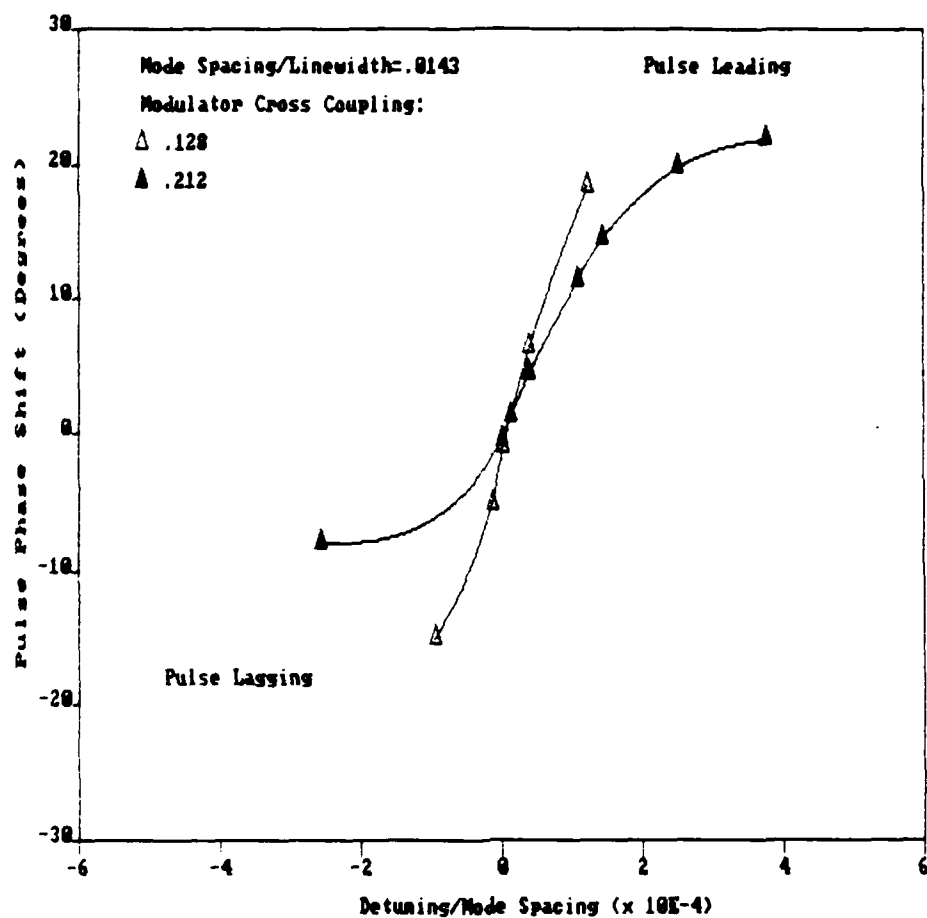


Figure 10. Phase shift of pulse versus normalized modulator detuning in a simulated mode-locked Argon laser.

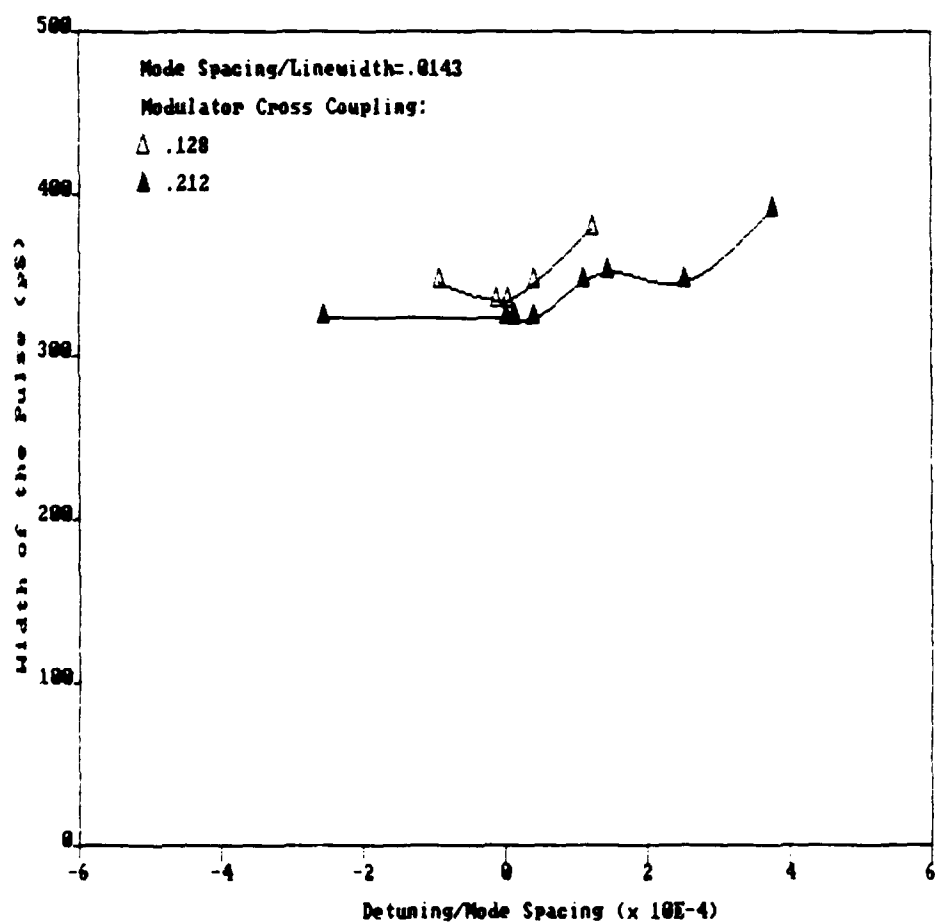


Figure 11. Width of pulse versus normalized modulator detuning in a simulated mode-locked Argon laser.

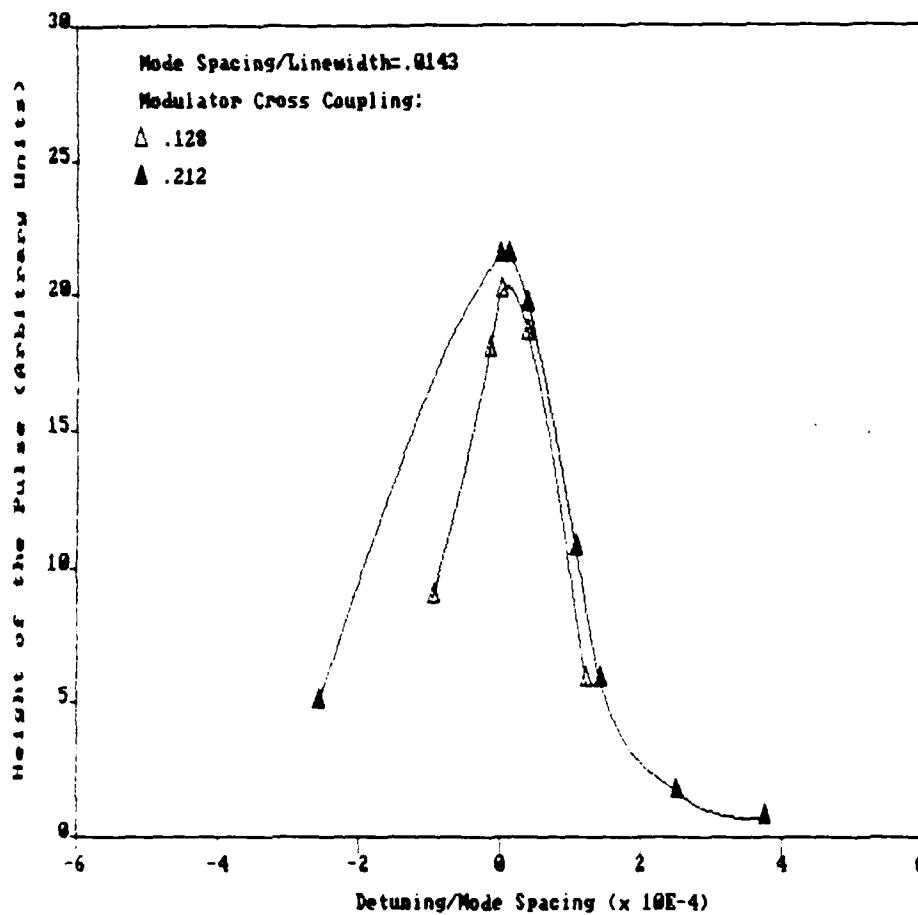


Figure 12. Pulse height versus normalized modulator detuning in a simulated mode-locked Argon laser.

that there was no observable change in the desired behavior.

The computer simulation was quite satisfactory and proved to be invaluable in the rest of the research effort.

V. EXPERIMENTAL WORK

The laser used in the experimental work was a Spectra-Physics Inc. Model 170 cw Argon laser operated at 4880\AA . The nominal length was $L = 2.09\text{ m}$ giving a longitudinal mode spacing of 71.7 MHz . For mode locking the laser an IntraAction corp. acousto-optic mode-locker Model ML-35C was used. It had been constructed by the manufacturer to have an acoustic center frequency of $35.8 \pm 0.02\text{ MHz}$. Additional details on the laser and mode-locker are given in Appendix C and Appendix D respectively. The mode-locker operated in the usual acoustic standing-wave mode in which the effective loss modulation frequency is twice the acoustic drive frequency. Also the mode-locker had to be oriented at the Bragg diffraction angle, necessitating an adjustable holder so that fine tuning adjustments of the mode-locker orientation relative to the laser beam could be made.

A. THE DISCRIMINANT

In studying the basic mode-locked performance of the laser a tunable RF source was used to drive a power amplifier which fed the mode locker. Mode locking was obtained at a modulator drive center frequency of 35.578 MHz . Then the RF source was detuned from the center frequency to observe the phase shift of the pulses relative to the modulator drive signal. The resulting discriminant, shown in Figure 13, meant that a stabilization scheme would be possible. This result was not new for an

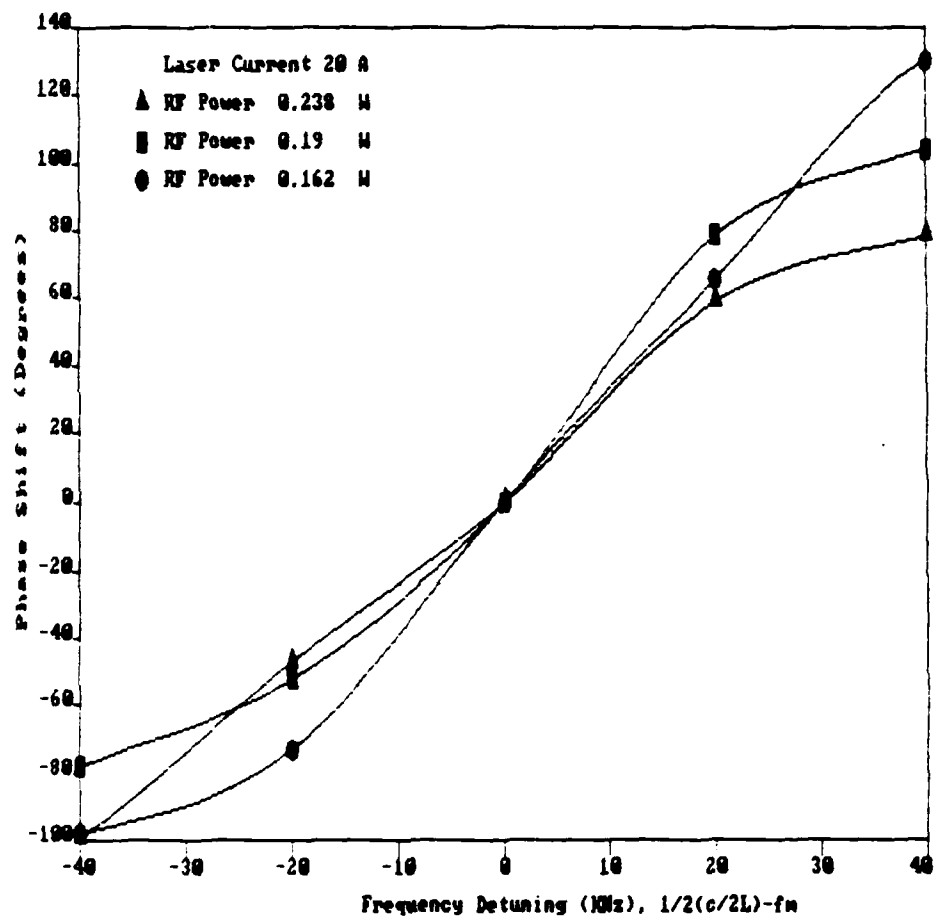


Figure 13. Measured phase shift of pulse versus detuning of modulator in a mode-locked Argon laser.

Argon laser, which is mainly inhomogeneously broadened, but meant simply that the system was performing as expected and that the planned approach could be continued.

B. THE STABILIZATION CIRCUIT

When one has a discriminant such as that shown in Figure 13, the stabilization scheme becomes fairly straight forward and simple. The operation of the system, shown in the block diagram of Figure 14, can be explained as follows. The standard phase locked loop (PLL) integrated circuit (IC) consists of a voltage controlled oscillator (VCO) and a phase comparator which produces an error voltage proportional to the phase and frequency difference between the output of the VCO and the input signal to the IC. This error voltage is applied to the control terminal of the VCO so that its output is synchronized with the input signal. The input to the PLL is taken from the envelope of the pulsed laser output as detected by the ultra-fast-response photo diode (Hamamatsu S1188) and amplified by a differential video amplifier (LM 733). The output of the amplifier, which consists of only the fundamental component or first beat note of the laser pulse envelope since it is bandwidth limited, is then fed to a digital frequency divider IC (74S175D Flip-Flop). The phase comparator of the phase locked loop IC (XR215) compares the frequency and phase of the output of the frequency divider to that of the VCO and locks the output frequency of the VCO to the frequency divider output. By adjusting the complete system loop phase appropriately, this locking can be made to occur at zero detuning of the modulator where the shift in phase of the pulse is zero. One simple way to adjust the system phase is to slightly detune the 35.8 MHz power amplifier. Figures 15 and 16 show the schematic

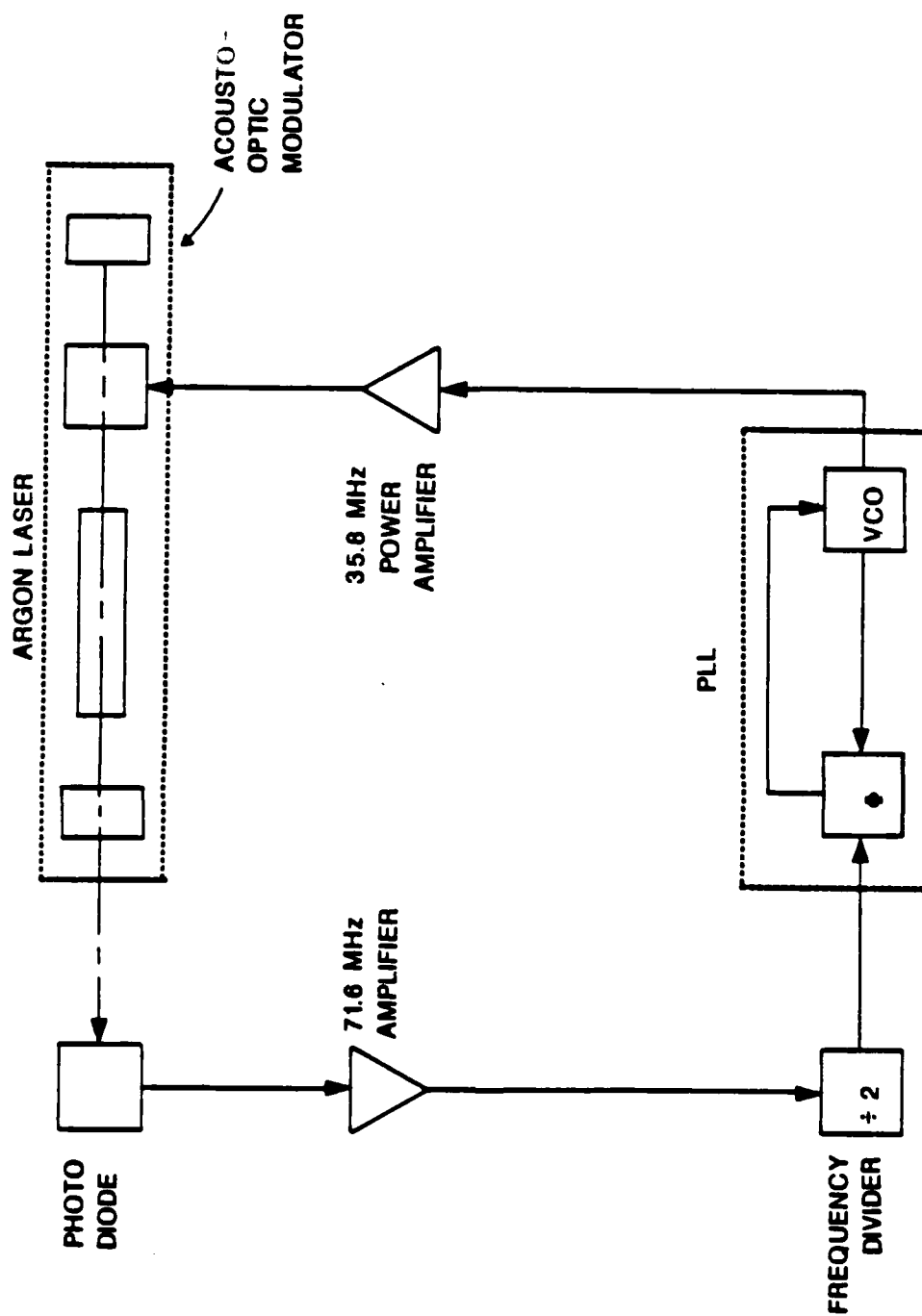


Figure 14. Block diagram of stabilization circuit for a mode-locked Argon laser.

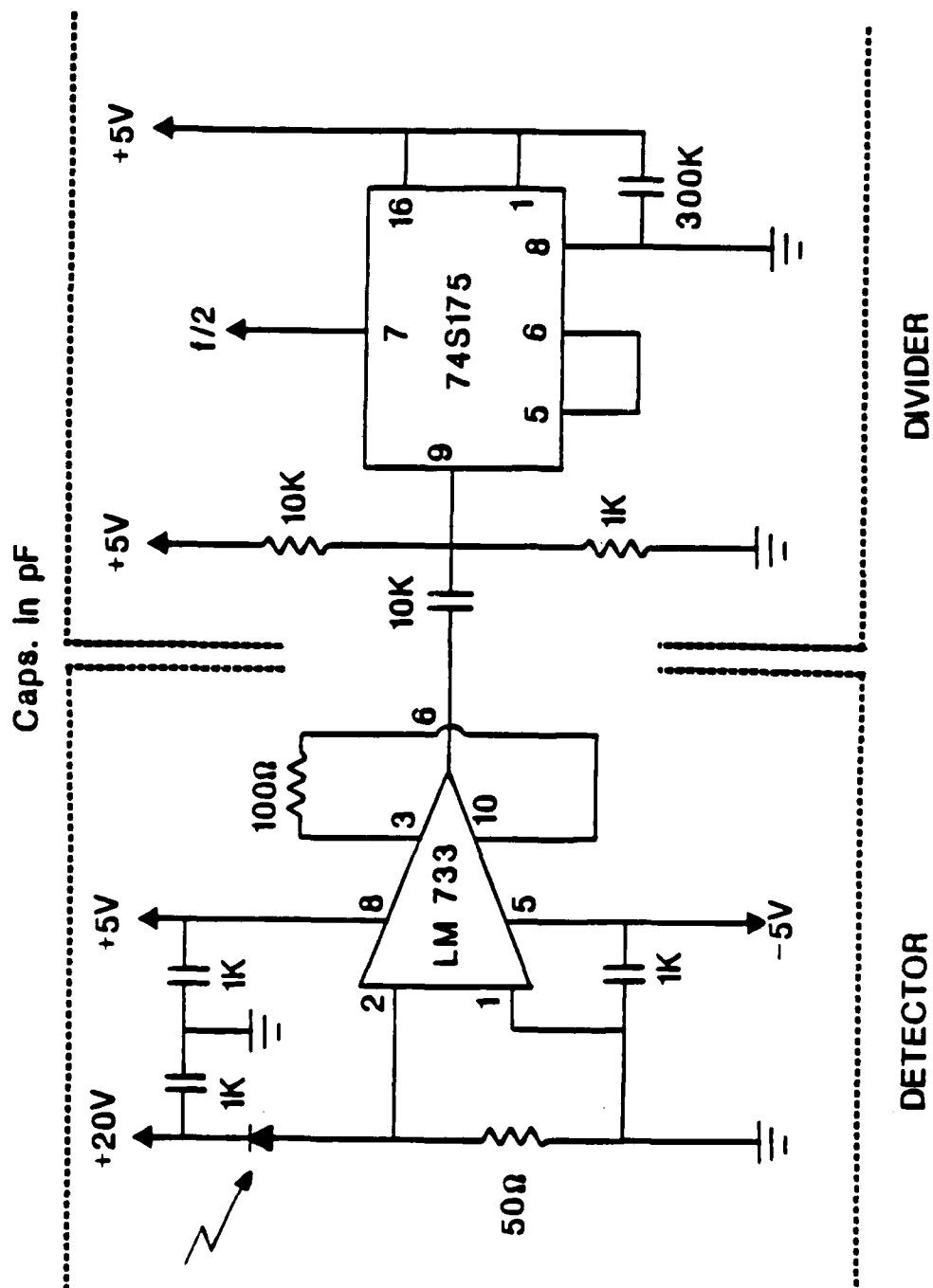


Figure 15. Schematic diagram of the detector amplifier and frequency divider.

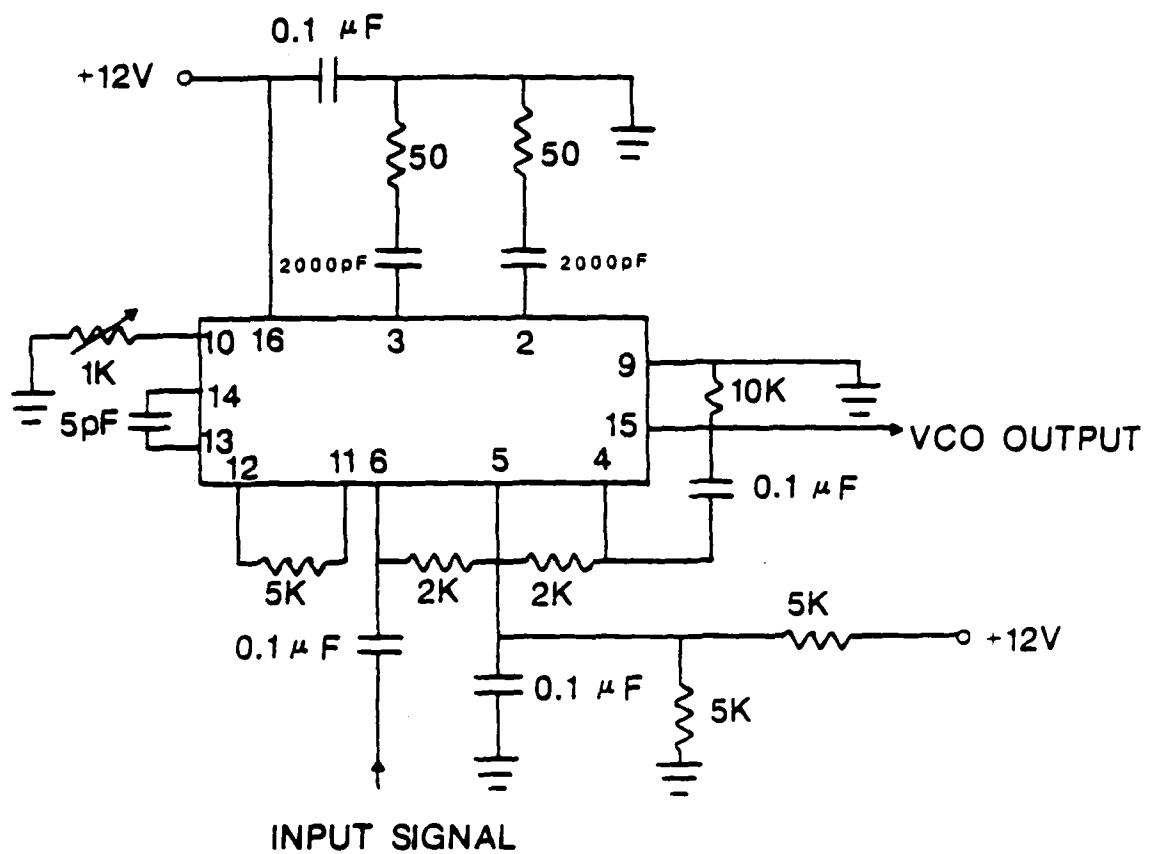


Figure 16. Schematic diagram of the phase locked loop (PLL).

diagrams of the detector amplifier/frequency divider and the PLL, respectively. Once the system phase is adjusted as noted, the "zero phase" point of operation is maintained by the feedback as parameters such as the laser cavity length (and hence the mode spacing) change. The "zero phase" operating point corresponds to optimum performance conditions.¹⁸

C. CHECKING SYSTEM PERFORMANCE

In checking the system performance various data had to be taken without breaking the feedback loop. A second photo diode detector was placed off the main beam axis, sampling the laser output from a beam splitter as shown in Figure 17. The laser output after passing through a variable attenuator A1 was sampled by the beam splitter A2. The transmitted beam, after passing through the variable attenuator A3 was focused on to the photo diode D1. The detected signal was then amplified and fed onto the frequency divider circuit. The beam reflected off of the beam splitter, after passing through the attenuator A4, was focused on to the second photo diode D2 for measurement purposes. Figure 18 shows the circuit diagram of detector D2. The variable attenuators A3 and A4 were inserted in the system to control the intensities of the transmitted and reflected beams independently, in order to add flexibility in preventing the photo diodes from becoming saturated.

The loop was broken at the input to the PLL and an external generator output substituted for the output from the frequency divider (Figure 17). The PLL output voltage and resulting mode-locked laser output were observed as the power level input to the PLL was varied. The results, shown in Figures 19 and 20, show that there is a

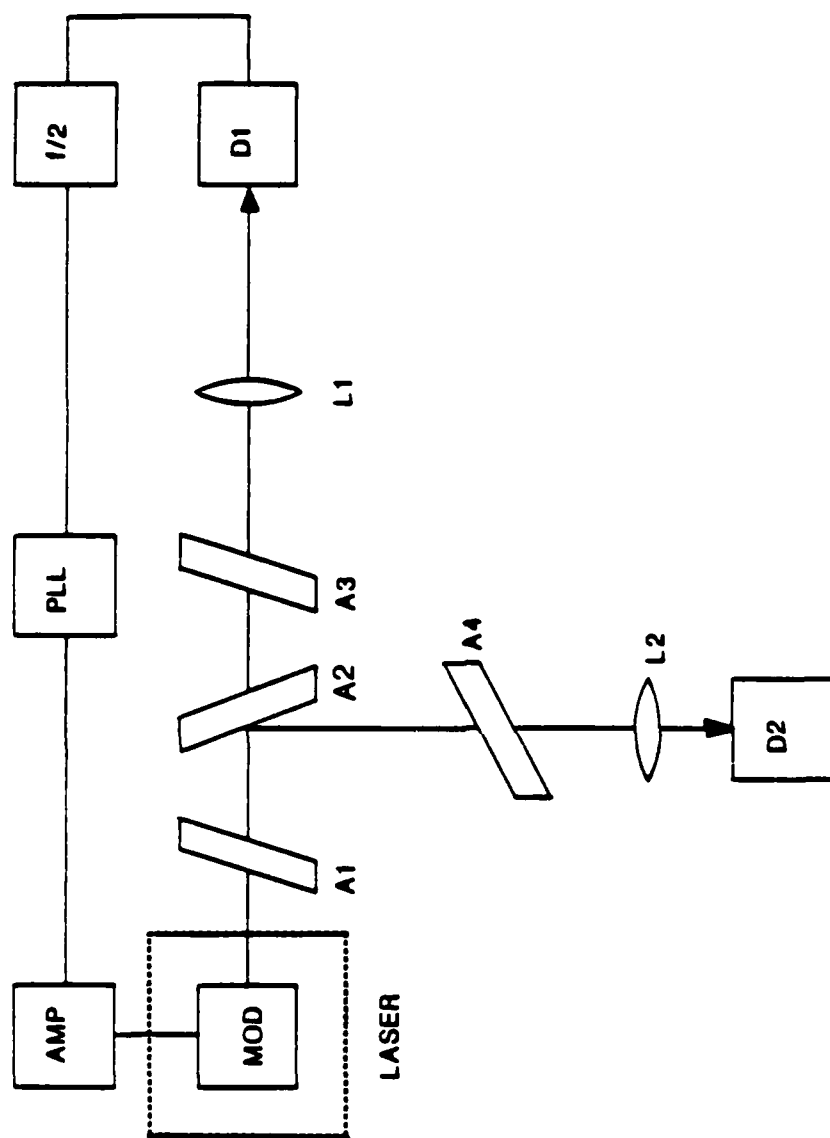


Figure 17. Block diagram of test arrangement.

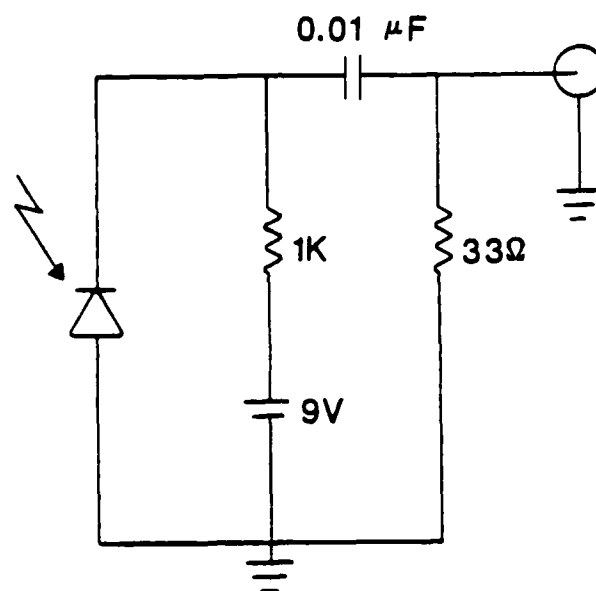


Figure 18. Circuit diagram of detector D2.

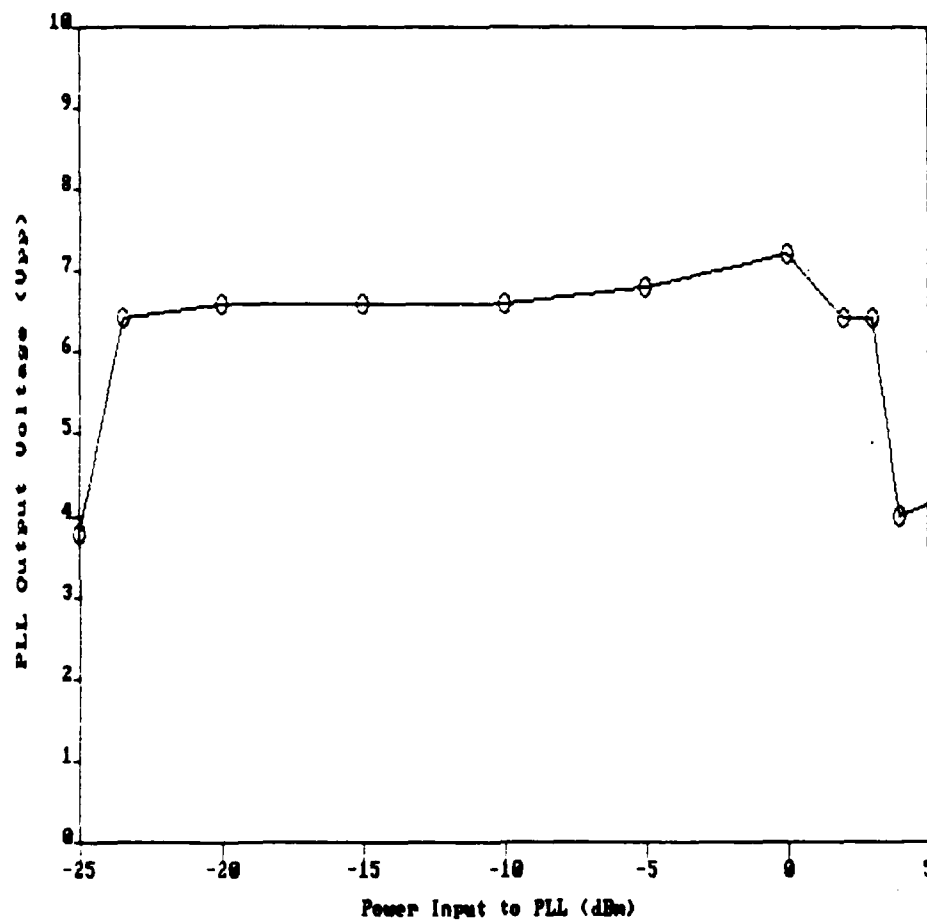


Figure 19. Phase locked loop output when fed directly by a signal generator.

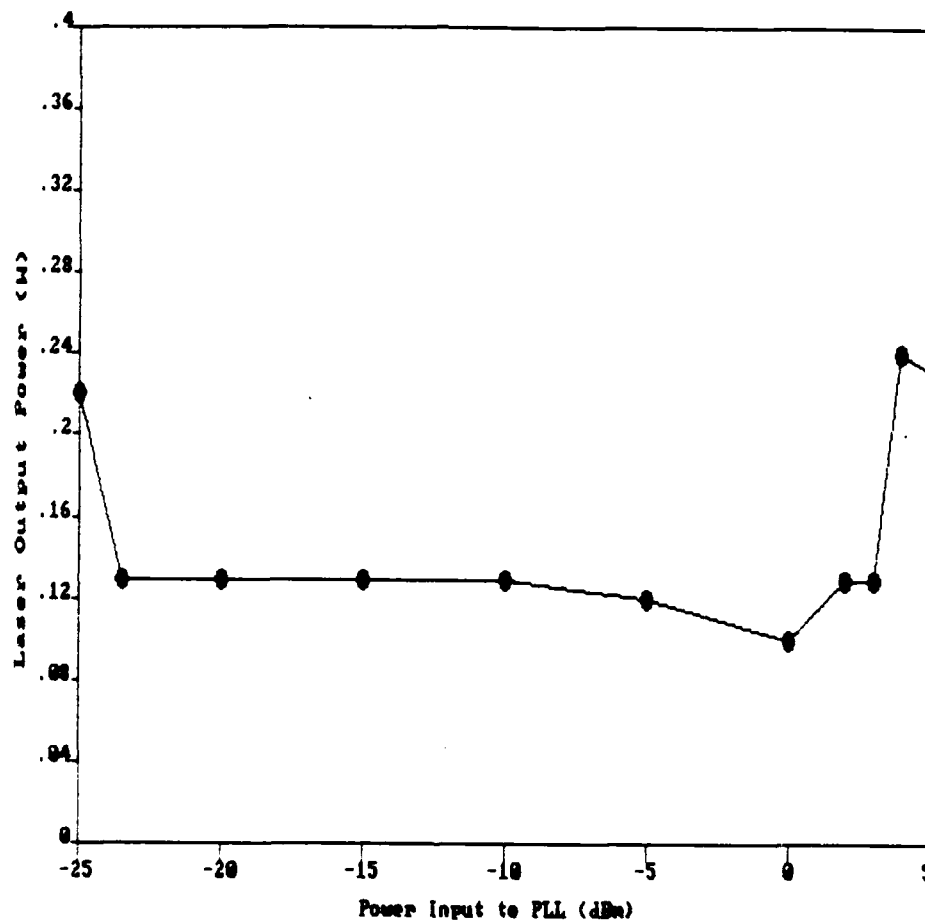


Figure 20. Laser mode-locked average output power when phase locked loop was fed directly by a signal generator.

considerable range of input to the PLL (almost 30dB) over which the PLL performs satisfactorily. Figures 21 and 22 show the pulse shape and beat note spectrum in the stabilized mode-locked condition. The shortest duration pulses observed were 1.8 nS.

D. EFFECTS OF CAVITY LENGTH VARIATION

Perhaps the ultimate test of the system is whether or not it controls the modulator drive frequency so that it tracks the mode spacing frequency as cavity length varies.

The laser used had no convenient means of varying cavity length directly. However, one can vary the optical cavity length by inserting a dielectric slab into the cavity and rotating it away from the position perpendicular to the laser beam. This can work well and changes in effective cavity length can be obtained so long as the resultant beam offset doesn't cause too much deterioration in performance due to misalignment.

A quartz slab or etalon 1.2 cm thick was inserted in the cavity and rotated $\pm 10^\circ$ from normal. The change in cavity length as the etalon is rotated from normal has a theoretical variation in the mode spacing frequency as shown in Figure 23. With the complete loop in operation, the experimental change in mode spacing (i.e., fundamental beat note) was measured as the etalon was rotated and the data points were plotted also in Figure 23. The asymmetry in the data points and their deviation from the theoretical curve can be explained as due to the wedging of the etalon (wedging was detected by observing the reflected spots from its front and back surfaces using a He-Ne laser).

Other performance parameters of the system were studied as the effective length of the cavity was varied by use of the etalon. As

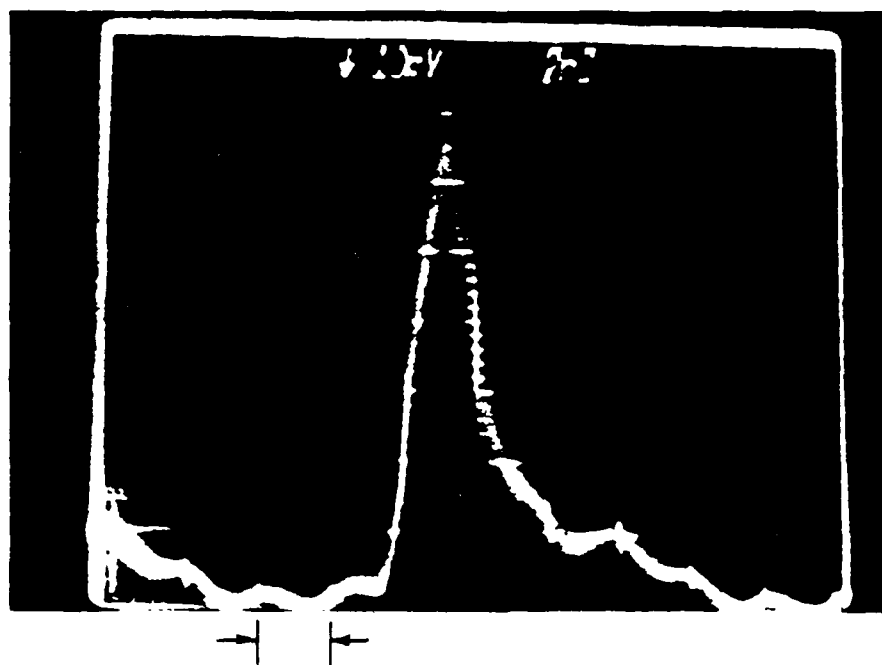


Figure 21. Mode locked pulse from Argon
laser: 2nS/Division.

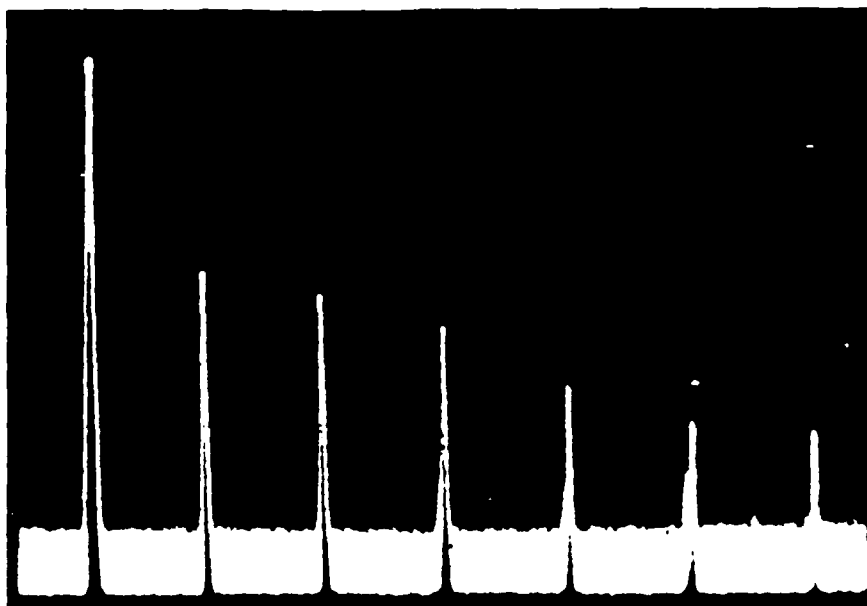


Figure 22. Beat notes in output of mode-locked Argon laser: 50 MHz/Division.

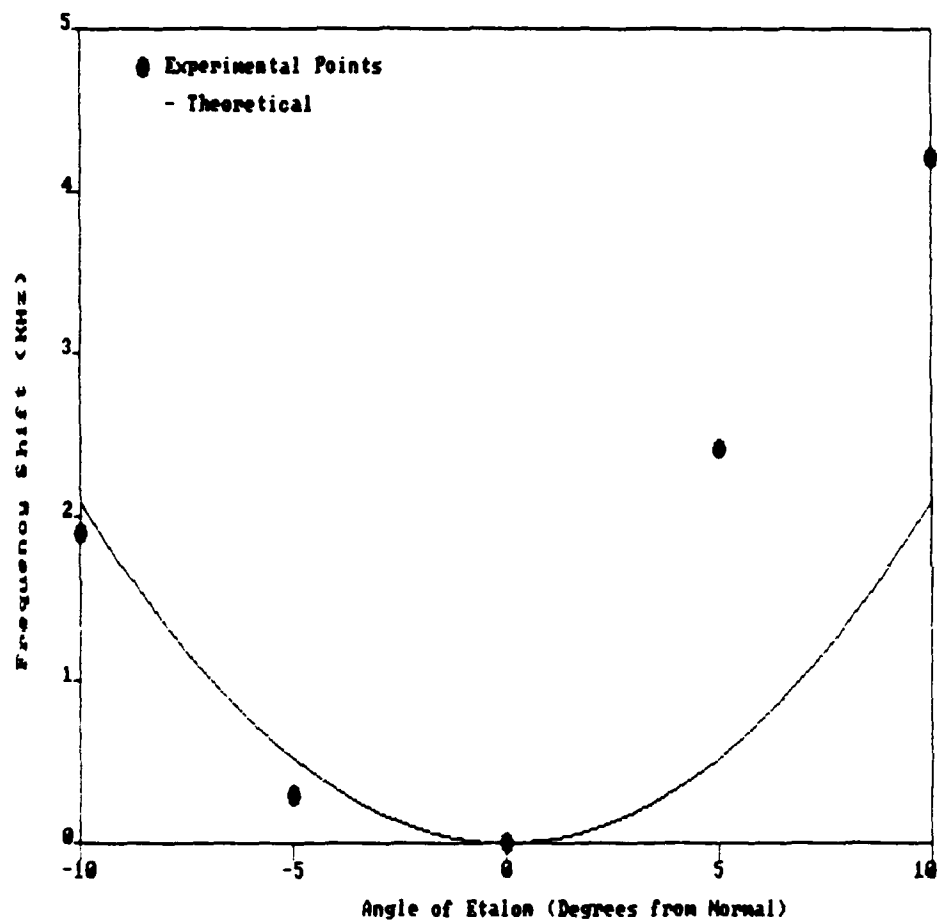


Figure 23. Change in laser mode spacing and mode-locked pulse repetition rate with rotation of etalon in an Argon laser.

shown in Figure 24, the stabilization loop kept the effective modulation frequency near optimum even as the cavity length was varied, resulting in a broad range where the pulse phase shift was minimal. The effect of the cavity length variation on the laser output power was also observed, as shown in Figure 25, and indicated a range over which the power output was relatively unaffected by length changes, also indicating that optimum mode locking was maintained.

E. CLOSED LOOP DRIFT

Although the purpose of the feedback system was not to hold the mode-locking frequency constant but instead to vary the modulator frequency to accomodate changes in the mode spacing frequency, it was thought desirable to observe the absolute stability. The frequency variations of the VCO output with loop open (the inherent changes in the VCO frequency) and loop closed (the change due to drift in mode spacing) were measured versus time. Shown plotted in Figure 26 are the results observed over a period of 30 minutes.

A drift of 37 KHz was observed when the loop was open, indicating that the VCO itself had a tendency to drift as the ambient temperature varied. The overall drift was reduced to 1.55 KHz when the loop was closed and that variation presumably was due to changes in cavity length.

For comparison, the wide variation of the frequency of the first beat note (having a nominal value of 71.7 MHz) of the free running laser is shown in Figure 27. These data were recorded using the high speed photo diode followed by a video amplifier as in Figure 15. Frequency was measured with a counter in all cases.

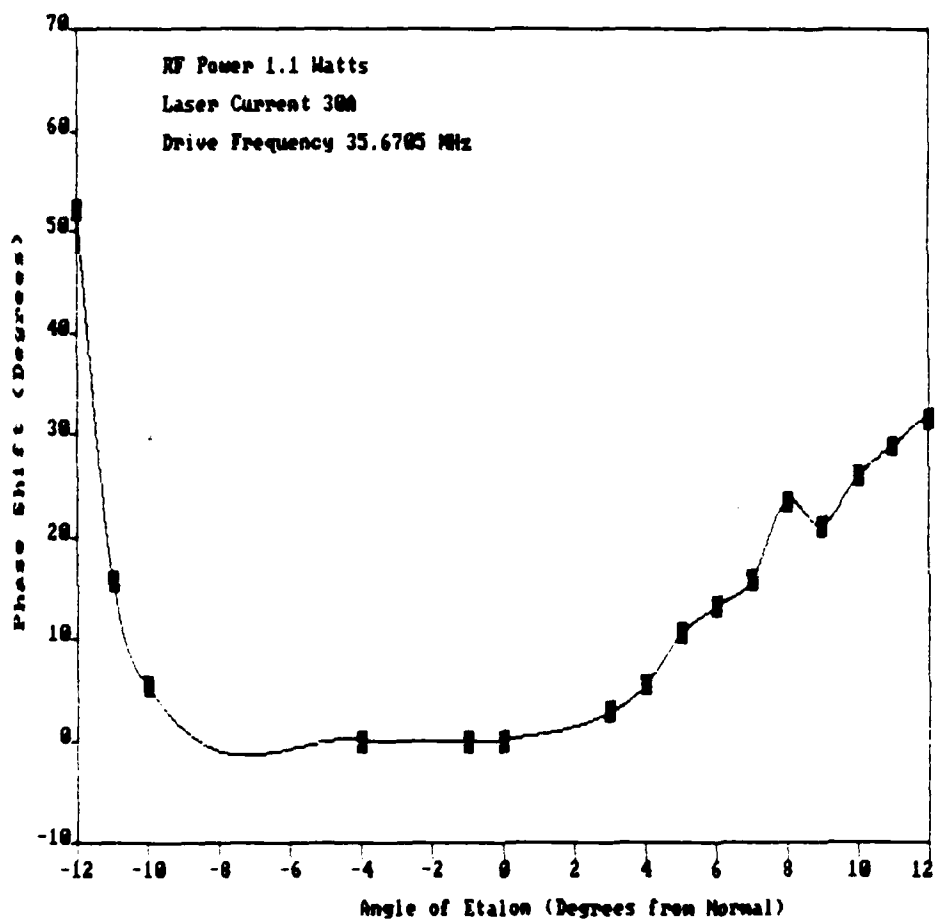


Figure 24. Phase shift of mode-locked pulse from optimum as intracavity etalon is rotated.

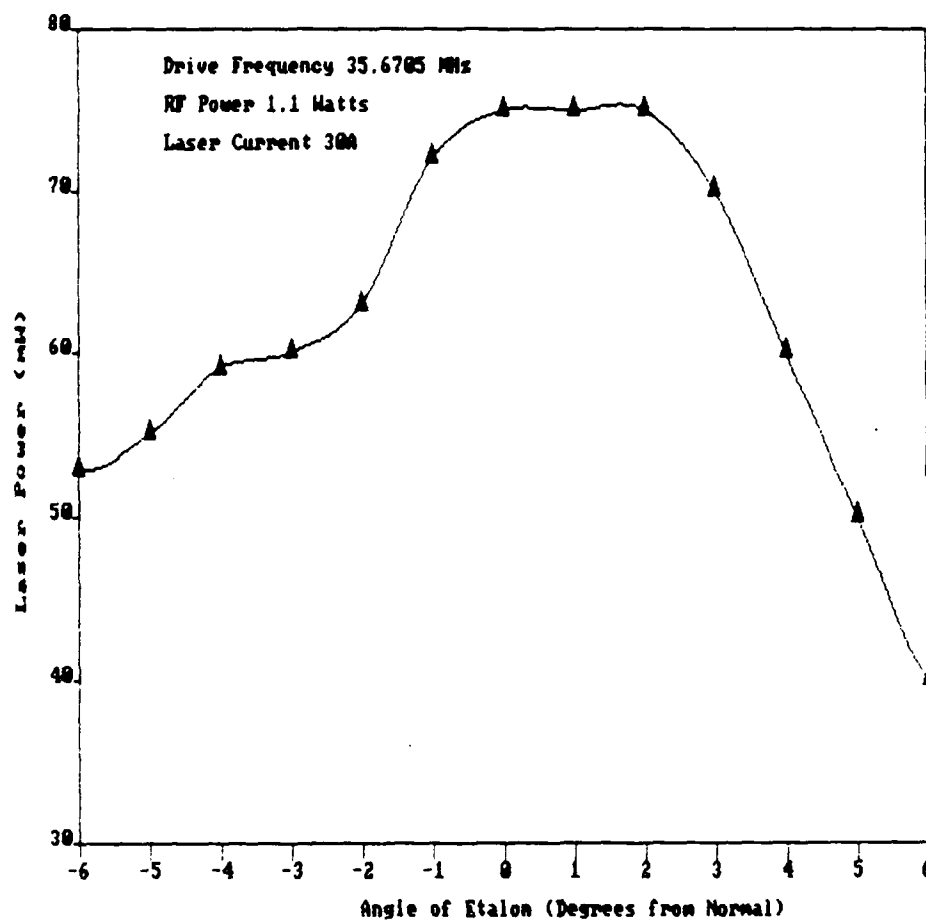


Figure 25. Variation in mode-locked laser power with rotation of intracavity etalon.

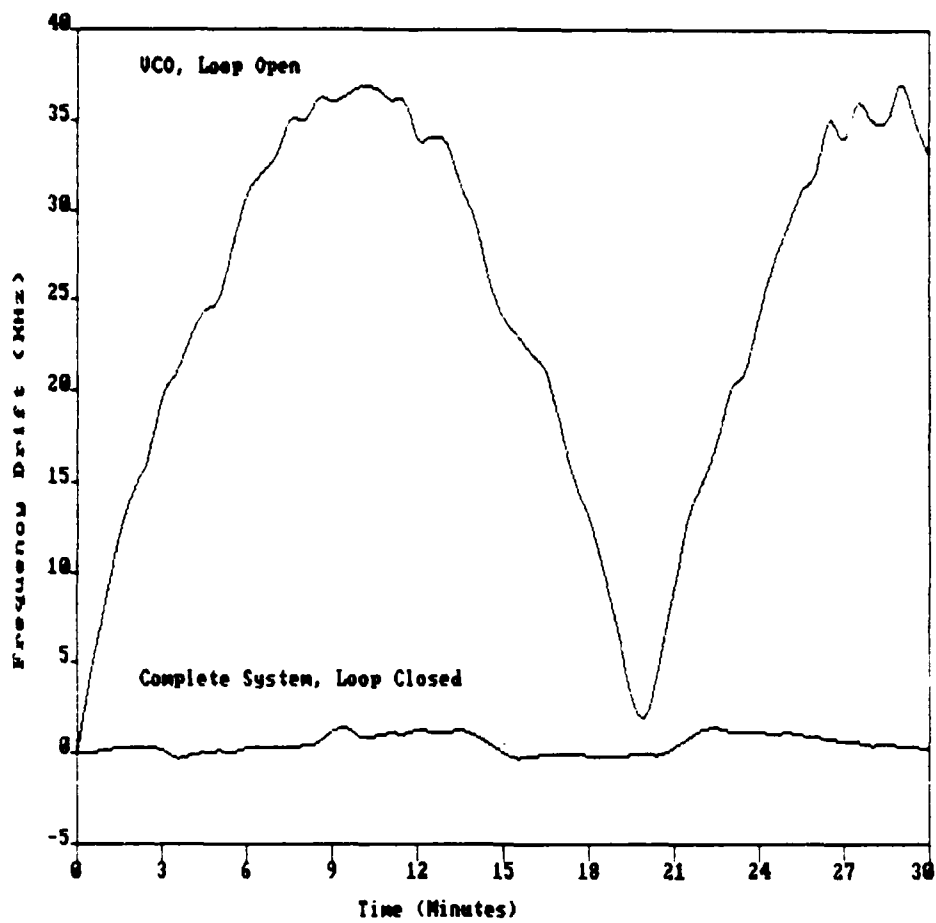


Figure 26. Frequency drift of VCO output with time, both with loop open and with loop closed.

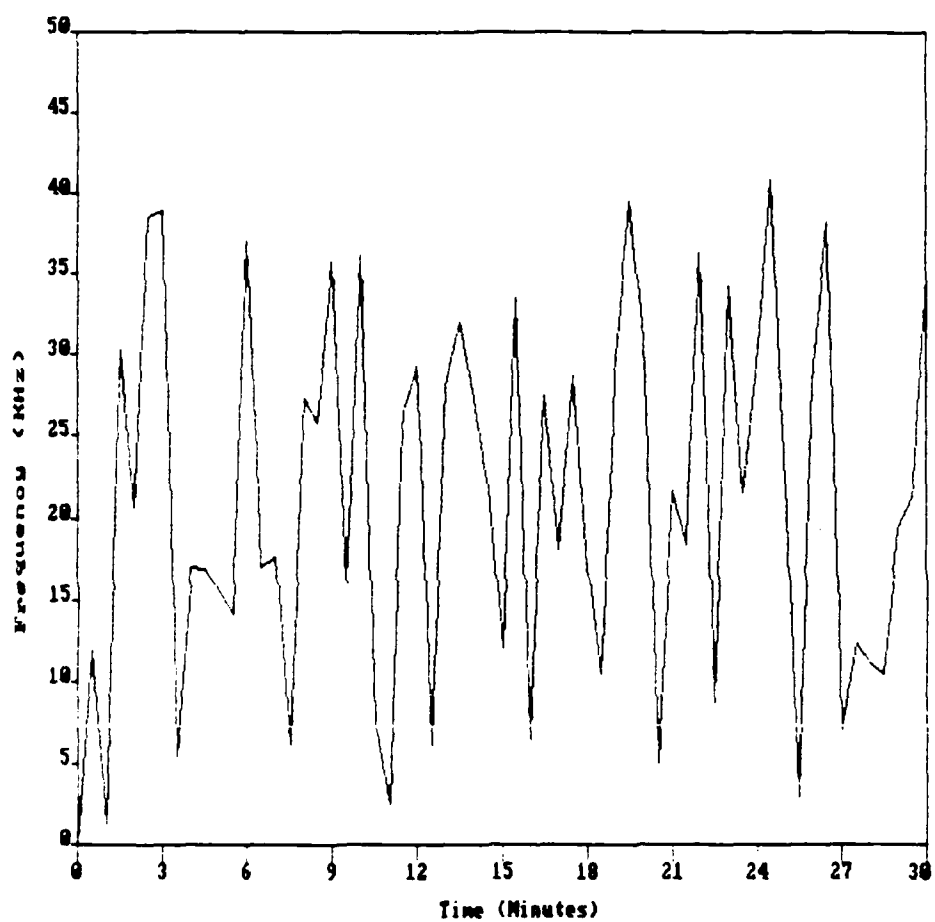


Figure 27. Variation in frequency of first beat note in a free running Argon laser.

VI. CONCLUSIONS

The objectives of the research have been met. A computer simulation of a loss-modulated, mode-locked homogeneously broadened laser has shown that a discriminant exists for stabilization of the laser in a scheme whereby the modulation frequency would be locked to the laser $c/2L$ frequency. The significance of the various parameters was shown by this simulation.

A computer simulation of a loss-modulated mode-locked inhomogeneously broadened laser was used in guiding experimental work in stabilizing such a laser. A stabilization technique, based on the shift of the phase of the pulse, was implemented with an Argon laser and shown to operate as hoped. The frequency of the modulator was locked to the laser $c/2L$ frequency and stable operation was obtained even though the laser operating conditions drifted with time.

VII. CONFERENCE PRESENTATIONS

One conference presentation has been made on the research described in this report and another has been accepted for presentation. They are as follows:

O. P. McDuff, A. Atashi, S. C. Jain, and J. Taboada, "Feedback Stabilization of an Actively Mode Locked Laser," presented at the Eighth International Conference on Lasers and Applications, LASERS '85, Las Vegas, Nevada, December 2-6, 1985. To be published in conference proceedings.

O. P. McDuff, D. T. Scott, and J. Taboada, "A Computer Simulation of a Feedback- Stabilized Actively Mode-Locked Laser," to be presented at IEEE SOUTHEASTCON '86, Richmond, Virginia, March 23-26, 1986. To be published in conference proceedings.

VIII. REFERENCES

1. L. E. Hargrove, R. L. Fork and M. A. Pollack, "Locking of He-Ne Laser Modes Induced by Synchronous Intracavity Modulation," Appl. Phys. Letters, Vol. 5, pp. 4-5, July 1964.
2. J. Taboada and W. D. Gibbons, "Retinal Tissue Damage Induced by Single Ultrashort 1060 nm Laser Light Pulses," Applied Optics, Vol. 17, pp. 2871-2873, Sept. 1978.
3. W. T. Ham, Jr., H. A. Mueller, A. I. Goldman, B. E. Newman, L. M. Holland and T. Kuwabara, "Ocular Hazard from Picosecond Pulses of Nd:YAG Laser Radiation," Science, Vol. 185, pp. 362-363, July 1984.
4. R. L. Fork, B. I. Greene and C. V. Shank, "Generation of Optical Pulses Shorter than 0.1 psec by Colliding Pulse Mode Locking," Appl. Phys. Letters, Vol. 38, pp. 671-672, May 1981.
5. A. E. Siegman, "An Antiresonant Ring Interferometer for Coupled Laser Cavities, Laser Output Coupling, Mode Locking, and Cavity Dumping," IEEE J. Quantum Electronics, Vol. QE-9, pp. 247-250, Feb. 1973.
6. H. Vanherzeele, J. L. Van Eck and A. E. Siegman, "Colliding Pulse Mode Locking of a Nd:YAG Laser with an Antiresonant Ring Structure," Applied Optics, Vol. 20, pp. 3484-3486, Oct. 1981.
7. M. A. Lewis and J. T. Knudtson, "Active-Passive Mode-Locked Nd:YAG Oscillator," Applied Optics, Vol. 21, pp. 2897-2900, Aug. 1982.
(This paper has a number of references to active-passive systems.)
8. O. P. McDuff, "Techniques for Ultra-Short Pulses in Nd:YAG Lasers," Final Report for 1984 USAF-SCEEE Summer Faculty Research Program, September 1984.
9. H. Nkatsuka, D. Grischkowsky, and A. C. Balant, "Non-linear, Picosecond-Pulse Propagation through Optical Fibers with Positive Group Velocity Dispersion," Phys. Rev. Lett., Vol. 47, pp. 910-913, September 1981.
10. C. V. Shank, R. L. Fork, R. Yen, and R. H. Stolen, "Compression of Femtosecond Optical Pulses," Applied Phys. Lett., Vol. 40, pp. 761-763, May 1982.
11. W. H. Glenn, M. J. Brienza, and A. J. DeMaria, Appl. Phys. Lett., Vol. 12, p. 54, 1968.
12. B. H. Soffer and J. W. Liun, J. Appl. Phys., Vol. 39, p. 5859, 1968.
13. J. M. Harris, R. W. Chrisman, and F. E. Lytle, "Pulse Generation in a cw Dye Laser by Mode-Locked Synchronous Pumping," Appl. Phys. Lett., Vol. 26, pp. 16-18, January 1975.

14. See, for example, advertising brochure for Spectra Physics series 3000 Nd:YAG lasers.
15. O. Svelto, "Techniques of Solid-State Lasers," Chapter C2 of Laser Handbook, Vol. 2, F. T. Arecchi and E. O. Schulz-Dubois, eds., North Holland Publishing Co., Amsterdam, 1972.
16. O. P. McDuff, "Techniques of Gas Lasers," Chapter C5 of Laser Handbook, Vol. 2, F. T. Arecchi and E. O. Schulz-Dubois, eds., North Holland Publishing Co., Amsterdam, 1972.
17. M. H. Crowell, "Characteristics of Mode-Coupled Lasers," IEEE J. Quant. Electr., Vol. QE-1, pp. 12-20, April 1965.
18. O. P. McDuff and S. E. Harris, "Nonlinear Theory of the Internally Loss Modulated Laser," IEEE J. Quant. Electronics, Vol. QE-3, pp. 101-111, March 1967.
19. S. E. Harris and O. P. McDuff, "Theory of FM Laser Oscillation," IEEE J. Quant. Electr., Vol. QE-1, pp. 245-262, Sept. 1965.
20. O. P. McDuff, Mode Coupling in Lasers, Ph.D. Dissertation at Stanford University, August 1966.
21. L. M. Osterink and J. D. Foster, "A Mode-Locked Nd:YAG laser," J. Appl. Phys., Vol. 39, pp. 4163-4165, August 1968.
22. D. J. Kuizenga and A. E. Seigman, "FM and AM Mode Locking of the Homogeneous Laser - Part I: Theory," IEEE J. Quant. Electr., Vol. QE-6, pp. 694-708, Nov. 1970.
23. W. E. Lamb, Jr., "Theory of an Optical Maser," Phys. Rev. 134, A1429-A1450 (June 1964).
24. B. D. Fried and S. D. Conte, The Plasma Dispersion Function (Hilbert Transform of the Gaussian) (New York, Academic Press, 1961).
25. R. H. Pantell and H. E. Putoff, Fundamentals of Quantum Electronics, John Wiley & Sons, New York, 1969.
26. H. A. Haus, "Modelocking of Semiconductor Laser Diodes," Jap. J. Appl. Phys., vol. 20, pp. 1007-1020, June 1981.
27. Laboratory Notebook of O. P. McDuff, USAF-UES 1985 Summer Faculty Research Program.
28. O. P. McDuff, "Active Mode-Locking Techniques for Ultra-Short Pulses in Nd:YAG Lasers," Final Report for USAF-UES 1985 Summer Faculty Research Program, September 1985.

APPENDIX A

DEVELOPMENT OF THE COMPUTER SOLUTION

A. PROBLEM DEFINITION

The mode-locked laser can be modeled as a system of coupled differential equations characterizing the modes oscillating within the cavity, as discussed in Section IV. Each mode is thought of as an optical signal having a definite magnitude and phase, and there is a differential equation for each of these. As is evident from equations (2) and (3), each oscillating mode depends heavily upon the modes adjacent to it; therefore, the solution must include a complete set of equations covering all the modes that may be oscillating. This can become a computation intensive problem, since some lasers may have hundreds of modes oscillating at any particular time.

B. SCALING THE EQUATIONS

It was convenient to scale (2) and (3) so that the number sizes would be easier to work with and in addition so that a given computer run could be interpreted as representing more than one set of physical parameters.

The time scale was changed by letting

$$t = T_o \tau \quad (27)$$

to give scaled equations

$$\begin{aligned} \frac{dE_n}{d\tau} = & -T_o \Delta F \alpha_n E_n + T_o \Delta F G_n E_n - T_o \Delta F \alpha_a E_n \\ & - T_o \Delta F \alpha_c [E_{n+1} \cos(\phi_{n+1} - \phi_n) - E_{n-1} \sin(\phi_n - \phi_{n-1})] \end{aligned} \quad (28)$$

$$\begin{aligned} \frac{d\phi_n}{d\tau} = & n \Delta \nu T_o - T_o \Delta F \psi_n \\ & - \frac{1}{E_n} T_o \Delta F \alpha_c [E_{n+1} \sin(\phi_{n+1} - \phi_n) - E_{n-1} \sin(\phi_n - \phi_{n-1})] \end{aligned} \quad (29)$$

where

$$\Delta F = \frac{c}{2L} \quad (30)$$

To further emphasize the normalized nature of the equations, definitions and new labels were taken as follows

$$\begin{aligned} A &= T_o \Delta F \alpha_n \\ D/2 &= T_o \Delta F \alpha_c \\ D &= T_o \Delta F \alpha_a \\ F &= \Delta \nu T_o \\ X_n &= E_n \\ Y_n &= \phi_n \end{aligned} \quad (31)$$

so that (28) and (29) become

$$\begin{aligned} \dot{X}_n &= -AX_n + \frac{B_n}{SAT} X_n - DX_n \\ &\quad - \frac{D}{2} [X_{n+1} \cos(Y_{n+1} - Y_n) + X_{n-1} \cos(Y_n - Y_{n-1})] \end{aligned} \quad (32)$$

$$\begin{aligned} \dot{Y}_n &= nF - \frac{EN_n}{SAT} \\ &\quad - \frac{1}{X_n} \frac{D}{2} [X_{n+1} \sin(Y_{n+1} - Y_n) - X_{n-1} \sin(Y_n - Y_{n-1})] \end{aligned} \quad (33)$$

The equations for the $\frac{B_n}{SAT}$ and $\frac{EN_n}{SAT}$ terms, saturated gain and mode pulling respectively, depend on whether homogeneous or inhomogeneous broadening apply. The equations of Section IV are used to obtain the appropriate forms.

1) Homogeneous Broadening

In this case the line shape is Lorentzian and (23) gives

$$B_n = \frac{B_o}{[2(n+\Delta n) \frac{\Delta \Omega}{\Delta \nu_L}]^2 + 1} \quad (34)$$

where

$$B_o = T_o \Delta F g_o, \quad (35)$$

and gives

$$SAT = 1 + \frac{C}{B_o} \sum_m X_m^2 B_m. \quad (36)$$

The term Δn is the shift of the zeroth mode from line center, as a fraction of mode spacing. The term $\Delta\Omega/\Delta\nu_L$ is the ratio of mode spacing to the Lorentzian line width.

Equation (24) gives for the homogeneous mode pulling

$$\frac{EN_n}{SAT} = \frac{B_n 2(n+\Delta n) \frac{\Delta\Omega}{\Delta\nu_L}}{SAT}, \quad (37)$$

where the function SAT is as given by (36).

2) Inhomogeneous Broadening

In this case the line shape is that of the plasma dispersion function as discussed in Section IV, and (15) and (16) give

$$B_n = B_o \frac{Z_1\left(\frac{\nu_n - \nu_o}{Ku}\right)}{Z_1(0)}, \quad (38)$$

where B_o is as defined in (35) above, and give

$$SAT = \sqrt{1 + CX_n^2}. \quad (39)$$

Equation (17) gives for the inhomogeneous mode pulling

$$EN_n = B_o \frac{Z_r\left(\frac{\nu_n - \nu_o}{Ku}\right)}{Z_1(0)} \quad (40)$$

and in this case the effects of saturation upon mode pulling are neglected.

C. SELECTION OF SCALED PARAMETERS

Using the scaled parameters, one can make the program behave similarly regardless of the actual physical parameters. For example the value of $B_o - A$ determines the start-up transient and has a strong effect

on how rapidly steady state is reached. By choosing $B_0 - A$ approximately the same each time, similar performance of the computer program can be obtained for each set of runs.

For a given laser the following procedure has been found to be useful. The value of ΔF depends on the length of the laser cavity and thus is known. The value of A can be chosen based on experience with previous runs. This is related to the known single pass loss by (31) and the value of T_0 thus is determined. The value of B_0 is determined then from the known unsaturated single pass power gain g_0 and (31), or else from the estimated number of modes having a net gain and using (34) or (38). In the inhomogeneous case, this will be the number of free-running modes. The value of D is selected depending on what value of average modulator loss one wants to study and by direct scaling from the value of A (see (31)). The value of F is selected depending on what detuning one wishes to study and using (31). Zero effective detuning occurs when the nF term in (33) just cancels out the linear portion (versus frequency) of the dispersion term EN_n/SAT in (33). One could also define "zero detuning" as the value of F that gives a pulse that occurs exactly at $\phi_m = \pi$ radians as discussed in Section IV. Initial values of the mode amplitudes and phases can be chosen similar to those of the expected solution in order to reduce the computer time necessary to reach steady state. From the known linewidth of the laser medium and the known ΔF , one knows the value of $\Delta\Omega/\Delta\nu_L$ (homogeneous case) or $\Delta\Omega/Ku$ (inhomogeneous case). If an intracavity etalon is used, the line shape is Lorentzian and the effective linewidth is that of the etalon.²² The value of the center mode shift Δn is selected depending on the study one wishes to make. The saturation constant C merely sets the scale of the

mode amplitudes. It can be calculated to make the center mode without perturbation equal to any desired value, such as 10, and then all other modes and hence the pulse peak amplitude can be expressed relative to this center mode amplitude. Another possibility is to express all the amplitudes in terms of the free-running power which results from the choice of C. In the inhomogeneous case, all modes having B_n greater than A will have non-zero free running values. In the homogeneous case (as idealized here) only the center mode will have a non-zero value (it will quench all the rest of the modes).

Once a given set of input parameters $\Delta\Omega/\Delta\nu_L$, A, B_0 , C, D, F and type of saturation are selected, the computer run can be interpreted in alternate ways (i.e. as alternate "lasers") since it is normalized. The way these input parameters are printed out in the program is shown later in subsection G, following. Suppose that a set of the parameters has been used in a run; then, the following interpretation procedure could be used.

$$(i) \text{ Select } \Delta F \text{ (hence } \Delta\Omega), \text{ giving } \Delta\nu_L \quad (41)$$

$$(ii) \text{ Assume an appropriate value of } \alpha_n \quad (42)$$

$$(iii) \text{ Calculate } g_0 = \frac{\alpha_n}{A} B_0 \quad (43)$$

$$(iv) \text{ Calculate } \alpha_a = \frac{\alpha_n}{A} D \quad (44)$$

$$(v) \text{ Calculate } \alpha_c = \frac{\alpha_a}{2} \quad (45)$$

$$(vi) \text{ Calculate } \frac{\Delta\nu}{\Delta\Omega} = \frac{\alpha_n}{2\pi A} F \quad (46)$$

In (vi), zero detuning can be defined by subtracting from F a value as discussed in the above paragraph.

(vii) Calculate the free running mode amplitudes for normalization purposes:

$$\text{inhomogeneous} \quad X_n = \sqrt{\frac{1}{C} \left[\left(\frac{B_n}{A} \right)^2 - 1 \right]} \quad (47)$$

$$\text{homogeneous} \quad X_0 = \sqrt{\frac{1}{C} \left(\frac{B_0}{A} - 1 \right)} \quad (48)$$

(viii) From the plotted pulse (plotted versus $v_m t$), calculate the pulse width and its phase shift in terms of the modulator cycle.

D. SOLUTION METHOD

The program uses a fourth order Runge-Kutta method for the solution of the system of first order nonlinear differential equations. An optional error control routine is incorporated.

1) Runge-Kutta

The Runge-Kutta differential equation solution is a hybrid method that evaluates several points on each subinterval of the function. The constant coefficients are determined by forcing agreement with the highest order Taylor series possible. This improves over the pure Taylor or Euler methods since it reduces the complexity of the derivatives which must be found. The tradeoff is that the function values must be calculated several more times; twice for second order, four times for fourth order, etc.

For the assumptions:

$$y'_n = f(x, y)$$

$$y(x_0) = y_0$$

The resulting formula and constants for the method are:

$$y_{n+1} = y_n + (1/6)(k_1 + 2k_2 + 2k_3 + k_4)$$

$$k_1 = hf(x_n, y_n)$$

$$k_2 = hf(x_n + h/2, y_n + k_1/2)$$

$$k_3 = hf(x_n + h/2, y_n + k_2/2)$$

$$k_4 = hf(x_n + h, y_n + k_3)$$

For a system of differential equations, say 1 to n, this formula is logically extended to include all the equations as valid function variables or arguments.

2) Parameters

Program variables providing control over the Runge-Kutta solution are:

- N - The total number of equations.
- TEST - The limit for the independent variable t, i.e., where to stop the solution.
- T2 - The starting value (t0) for t.
- H - The initial increment size.
- Q - Results are printed every Q steps.
- Z - An error check is made every Z steps, if this option is enabled.
- EXPT - The approximate number of correct decimal places to match at each step of the error check.
- SKIP - Skip the error check flag: 1=yes, skip; 0=no.

In the program the equations are slightly altered and appear as below:

```
C
      CALL FUNCT(TINP,VAR,F)
      DO 20 I=1,N
        K(I,1)=H*F(I)
        VAR(I)=X(I,2)+0.5*K(I,1)
20    CONTINUE
      TINP = T2 + 0.5*H
      CALL FUNCT(TINP,VAR,F)
      DO 259 I=1,N
        K(I,2)=H*F(I)
        VAR(I)=X(I,2) + 0.5*K(I,2)
259  CONTINUE
      CALL FUNCT(TINP,VAR,F)
      DO 30 I=1,N
        K(I,3)=H*F(I)
        VAR(I)=X(I,2) + K(I,3)
```

```

30  CONTINUE
    TINP=T2+H
    CALL FUNCT(TINP,VAR,F)
    DO 35 I=1,N
        K(I,4)=H*F(I)
        X(I,3)=X(I,2)+0.166667
        &      *(K(I,1)+2.0*(K(I,2)+K(I,3)+K(I,4)))
35  CONTINUE

```

C

An autostop feature of the program allows the program to stop before the specified time limit if the solution has reached "steady state." Steady state was defined as a repetition of the current values of the magnitudes to three decimal places for five successive print increments (notice the print increment is different from the Runge-Kutta step increment). This definition may be changed by some slight code modification as described later.

A plotting option was also added to the program. This option computes the beat pattern due to all the modes, giving the output pulse envelope. The equation used for this computation is (26) which is derived from the summation of a number of sinusoidal waves. In program form, from subroutine PLOTTER, this becomes:

```

      DO 50 I=1,MAXP
        DO 30 L=1,NO
          DO 30 M=1,NO
            P(I)=P(I)+X(L)*X(M)
            &      *DCOS((L-M)*THETA*X(NO+L)-X(NO+M))
30      CONTINUE
        P(I)=DABS(P(I)/2)
        LP(I)=DLOG(P(I))
        THETA=THETA+PINC
50  CONTINUE

```

The plotting control variables are described below:

IPLOT - 1 means to plot, 0 not to plot.
 PINC - The increment used between plotted points.
 IPSHRT- 0 is to print 80 column output,
 1 is to use 132 column output.
 BTHETA- The beginning plot value.
 ETHETA- The ending plot value.

Note that only 200 points can be plotted, and if more than this limit is specified (by the combination of PINC and BTHETA and ETHETA), then only the first 200 will be plotted.

Under normal conditions (IPLOT=1) the program will plot the pulse as it appears at the last iteration before the solution stops. However a feature was added to allow more than the last iteration's pulse to be plotted. IPLOT can be set equal to an integer, say n, greater than 1 to force consecutive plotting of n iterations. This enhancement allows examination of the pulse shape at different times and is convenient in the event that a steady state is not reached.

E. COMPUTER VERSION OF EQUATIONS

Within the program, one array, X(I), is used to hold both the magnitude and the phase values during computation. A problem arises with the equations since each mode depends on those next to it and computer arrays are not infinite; thus, special consideration must be given to the first and last element. For the end modes, special versions of the equations were developed, which treated the next (nonexistent) mode as if it were negligible.

1) Amplitude Equations

The equations for F(1) and F(NO) are the specially modified first and last modes. The general equation shown, F(I), is placed in a loop to compute all other modes considered. They are presented below.

$$F(1) = -A*T1 + B(1)*T1/SAT(NO,C,B0,B,X) \\ \& \quad -D*(X(2)*DCOS(T2))/2 - D*T1$$

$$F(I) = -A*T1 + B(I)*T1/SAT(NO,C,B0,B,X) \\ \& \quad - D*(X(I+1)*DCOS(T2) + X(I-1)*DCOS(T3))/2 \\ \& \quad - D*T1$$

$$F(NO) = -A*T1 + B(NO)*T1/SAT(NO,C,B0,B,X) \\ \& \quad - D*T1 - D*(X(NO-1)*DCOS(T2))/2$$

Where the temporary variables T1, T2, and T3 are used to conserve execution time (by preventing unnecessary array indexing) and are defined as:

```

T1=X(1)
T2=X(NO+2) - X(NO+1)

T1= X(I)
T2= X(NO+I+1) - X(NO+I)
T3= X(NO+I) - X(NO+I-1)

T1=X(NO)
T2=X(N) - X(N-1)

```

2) Phase Equations

Since the phase values are stored below the magnitude values in the array, the indices for them are added to the number of modes, NO. The equations are presented below,

```

F(NO+1)= -EN(1)/SAT(NO,C,B0,B,X)
&      + NN(1)*FF - (D/T1/2)*(X(2)*DSIN(T2))

F(NO+I) = -EN(I)/SAT(NO,C,B0,B,X)
&      + NN(I)*FF - (D/T1/2)*(X(I+1)*DSIN(T2)
&      - X(I-1)*DSIN(T3))

F(N) = -EN(NO)/SAT(NO,C,B0,B,X)
&      +NN(NO)*FF - (D/T1/2)*(-X(NO-1)*DSIN(T1))

```

Where the temporary variables T1, T2, and T3 are as defined for the amplitude equations.

3) Saturation Effects

In the above equations the function called SAT can be changed to accomodate either homogeneous or inhomogeneous saturation. The two methods are presented below. Note that inhomogeneous saturation of a mode X has no dependence on the other modes, whereas homogeneous saturation equations do show dependence (i.e. when one mode begins to saturate, it has an effect on all modes).

a. Homogeneous Saturation

```
SUM=0
DO 20 J=1,NO
  T1 = X(J)
  SUM=SUM+T1*T1*B(J)
20 CONTINUE
SAT=1 + C/BO * SUM
```

b. Inhomogeneous Saturation

```
T1=X(1)
SAT=DSQRT( 1 + C*T1*T1 )
```

F. CUSTOMIZING THE PROGRAM

1) Modulation

The program can easily be modified for either loss or frequency modulation. This only involves changing the subroutine FUNCT, which contains the differential equations. Actually, there are only a few items to be changed, such as numerical signs and cosines to sines, or vice versa.

2) Saturation

The saturation types for the equations is also easily changed. The equation computing the saturation for each mode, SAT, has been placed in a separate function. This can be modified with FORTRAN statements to give any saturation desired, those shown in this report or any other forms. However, consideration must be given to where in the equations this saturation has effect. Notice that the program is currently coded for SAT to be used in the denominator. Care should be used so that the desired value is not actually inverted when rewriting SAT (see the examples in the previous section). The SAT expression appears in different terms depending on the different types of saturations.

3) Number of Modes

Since the solution method used has no upper limit imposed for the

maximum number of equations, the limit is arrived at by other factors. The most important is the sizes of the arrays used to hold the calculated values. This is, in turn, determined by the size of memory or disk storage available on the machine. Another factor which might be considered is the time (or expense) that will be taken by using more and more modes. This could become a very serious practical limitation.

Since all the modes are interdependent, all the equations are kept in one array. The magnitudes are kept in the top half and the phases are kept in the lower half. Several variables are used to keep track of the number of modes considered by the program. They are outlined below.

NMAX - The number of modes to one side of center.

NO - The total number of modes= $2*NMAX+1$

N - Total number of equations= $2*NO$,
phase and magnitude.

Some of the arrays must be long enough to hold all N values (such as arrays X, F, NUM, DEN, etc.). Other arrays are only concerned with either magnitude or phase. In this case, it would be the number of modes, NO, that is important. Some of these arrays are XW, YW, XDOT, YDOT, etc.

4) Autostop Feature

The essential lines concerning the autostop feature are listed here. The feature considers all calculated mode magnitudes over the last five print increments. The array SSTEEST contains the number of time increments in the past that the value of the magnitude has been the same, within the limits of 3 decimal places. If this is less than five, then the solution continues. If not, then the program branches to 126 to print out the results, i.e. it has been steady state for five print increments of time.

```

      IF(J.GT.1) THEN
        DO 42 I=1,NO
          IF(XW(J-1,I).LE.XW(J,I)+.0001.AND.
&          XW(J=1,I).GE.XW(J,I)-.0001) THEN
            SSTEEST(I)=SSTEEST(I)+1
          ELSE
            SSTEEST(I)=0
          ENDIF
        42 CONTINUE
      ENDIF
      DO 43 I=1,NO
        IF(SSTEEST(I).LE.5) GOTO 44
      43 CONTINUE
      GOTO 126

```

5) Multiple Plot Options

To add the multiple plot option, the lines below were altered to the form given here (currently implemented only in the LMLASERI program, since some array indices must be reordered for correct calling of the subroutine).

```

      IF(IPLOT.NE.0) THEN
        JS=J - IPLOT + 1
        DO 1304 I=JS,J
          WRITE(IOUT,*)
&          'THE FOLLOWING PLOT IS FOR TIME T=',TI(I)
          CALL PLOTTER(XW(1,I),YW(1,I))
      1304 CONTINUE
      ENDIF

```

G. THE PROGRAM OUTPUT

A listing of the complete program for the homogeneously broadened case is included in Appendix B, together with a sample set of output data. The relationships between the equation symbols, program symbols, and the computer print-out labels are as in Table 1 on the next page. The mode amplitudes and phases X_n , Y_n and their derivatives \dot{X}_n , \dot{Y}_n are primarily printed to help one see what is happening. The plot of the pulse is the output of fundamental interest. Its phase shift depends on where the pulse peak falls relative to $v_m t = \pi$. Its width in seconds is equal to the half amplitude width in radians multiplied by $\frac{1}{2\pi}$ times the

modulator period, $2L/c$. Its peak amplitude can be compared to other runs and/or to the free running power.

TABLE 1

Relationship between Symbols

Symbol in Normalized
Equations (28) and (29)

Program Symbols

Print-out Label

A	A	A
C	C	C
D	D	LOSS
$\Delta\Omega/\Delta\nu_L$	MODESP	MODESP
F	FF	F
Δn	SPLINC	SHIFT
B_n	B(I)	B(N)
EN_n	EN(I)	E(N)
X_n	X(I)	X(#)
Y_n	X(NO+I)	Y(#)
$dX_n/d\tau$	F(I)	XDOT(#)
$dY_n/d\tau$	F(NO+I)	YDOT(#)
v_m^t	THETA	T
$W(\tau)$	P(I)	Y(T)

APPENDIX B

LISTING OF PROGRAM CODE AND SAMPLE OUTPUT DATA

FOR

HOMOGENEOUS SATURATION

[illegible]


```

C      SI=1                                LML01110
C      CALL TAPLAT(SI+SPL10,IC,SPLO,SPLV,  LML01120
C      &          SPES,SPLW,SPLZ,2,6(1))    LML01130
C      CONTINUE                             LML01140
C      DO 3 I=1,N0                           LML01150
C      SPLV(I)=R(I)                          LML01160
C      CONTINUE                             LML01170
C      CALL SETUPSPES,SPLV,IC,SPES,SPLW,SPLZ  LML01180
C      DO 3 I=1,N0                           LML01190
C      SI=1                                LML01200
C      CALL TAPLAT(SI+SPL10,IC,SPLO,SPLV,  LML01210
C      &          SPES,SPLW,SPLZ,2,6(1))    LML01220
C      CONTINUE                             LML01230
C      ENDOF                                LML01240
C      ... ECHO PRINT INITIAL DATA         LML01250
C      IF (NMAX.GT.0) THEN                  LML01270
C      WRITE(IOUT,100) IC,IC0,SPLO,FF,SCON,MCN,SPL10  LML01280
100    FORMAT('I=',I7.0,'X=',F7.0,'X=',F10.0,'X=',F7.0,  LML01290
C      'X=',F7.0,  LML01300
C      'X=',F10.0,'X=',F7.0,  LML01310
C      'X=',F10.0,'X=',F7.0,  LML01320
C      'X=',F7.0)  LML01330
C      WRITE(IOUT,101) (R(I), I=1,N0)       LML01340
101    FORMAT('R(I)=',F10.0/  LML01350
C      ' ',F10.0/  LML01360
C      ' ',F10.0)  LML01370
C      WRITE(IOUT,102) (S(I), I=1,N0)       LML01380
102    FORMAT('S(I)=',F10.0/  LML01390
C      ' ',F10.0/  LML01400
C      ' ',F10.0)  LML01410
C      ELSE  LML01420
C      WRITE(IOUT,103)  LML01430
C      IC,IC0,SPLO,  LML01440
C      FF,SCON,MCN,SPL10,  LML01450
C      MCN1,FF1,SCON1,SPLO1,  LML01460
103    FORMAT('IC=',I7.0,'X=',F7.0,'X=',F10.0,'X=',F7.0,  LML01470
C      'X=',F7.0,  LML01480
C      'X=',F10.0,'X=',F7.0,  LML01490
C      'X=',F10.0,'X=',F7.0,  LML01500
C      'X=',F7.0,  LML01510
C      'X=',F10.0,  LML01520
C      'X=',F7.0)  LML01530
C      ...  LML01540
C      WRITE(IOUT,104)  LML01550
104    FORMAT('SCON=',F10.0,'SPLO=',F10.0,  LML01560
C      'FF=',F10.0,  LML01570
C      'MCN=',F10.0,  LML01580
C      'MCN1=',F10.0,  LML01590
C      'FF1=',F10.0,  LML01600
C      'SCON1=',F10.0,  LML01610
C      'SPLO1=',F10.0,  LML01620
C      'MCN1=',F10.0,  LML01630
C      'FF1=',F10.0,  LML01640
C      'SCON1=',F10.0,  LML01650
C      'SPLO1=',F10.0,  LML01660
C      'MCN1=',F10.0,  LML01670
C      'FF1=',F10.0,  LML01680
C      'SCON1=',F10.0,  LML01690
C      'SPLO1=',F10.0,  LML01700
C      'MCN1=',F10.0,  LML01710
C      'FF1=',F10.0,  LML01720
C      'SCON1=',F10.0,  LML01730
C      'SPLO1=',F10.0,  LML01740
C      'MCN1=',F10.0,  LML01750
C      'FF1=',F10.0,  LML01760
C      'SCON1=',F10.0,  LML01770
C      'SPLO1=',F10.0,  LML01780
C      'MCN1=',F10.0,  LML01790
C      'FF1=',F10.0,  LML01800
C      'SCON1=',F10.0,  LML01810
C      'SPLO1=',F10.0,  LML01820
C      'MCN1=',F10.0,  LML01830
C      'FF1=',F10.0,  LML01840
C      'SCON1=',F10.0,  LML01850
C      'SPLO1=',F10.0,  LML01860
C      'MCN1=',F10.0,  LML01870
C      'FF1=',F10.0,  LML01880
C      'SCON1=',F10.0,  LML01890
C      'SPLO1=',F10.0,  LML01900
C      'MCN1=',F10.0,  LML01910
C      'FF1=',F10.0,  LML01920
C      'SCON1=',F10.0,  LML01930
C      'SPLO1=',F10.0,  LML01940
C      'MCN1=',F10.0,  LML01950
C      'FF1=',F10.0,  LML01960
C      'SCON1=',F10.0,  LML01970
C      'SPLO1=',F10.0,  LML01980
C      'MCN1=',F10.0,  LML01990

```

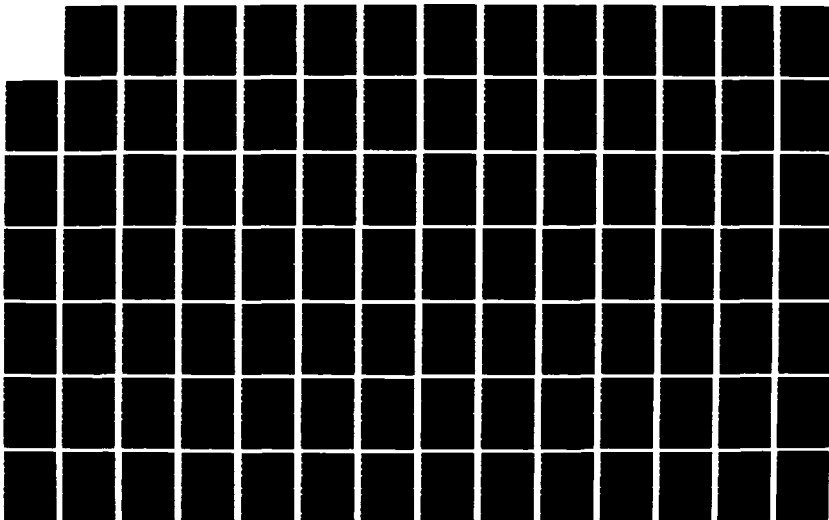
AD-A187 859

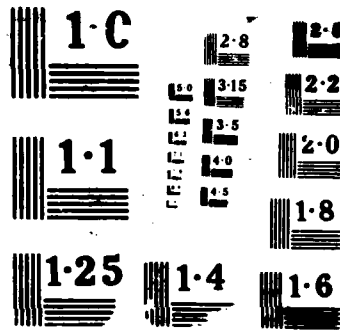
UNITED STATES AIR FORCE RESEARCH INITIATION PROGRAM
1984 RESEARCH REPORTS (U) SOUTHEASTERN CENTER FOR
ELECTRICAL ENGINEERING EDUCATION INC 5 W D PEELE
MAY 86 AFOSR-TR-87-1722 FF9620-82-C-0035 F/G 7/2

08/10

UNCLASSIFIED

NL





```

7  CONTINUE                                     LML01650
   CTR1 = 0                                     LML01670
   CTR2 = 0                                     LML01680
   CTR3 = 0                                     LML01690
   CTR4 = 0                                     LML01700
   PRT = 5015                                  LML01710
   J = 2                                        LML01720
C                                         LML01730
C ... ???                                     LML01740
C                                         LML01750
   U3 = 15.0 * (10.0 ** EXPT)                 LML01760
   U3 = 15.0 * (10.0 ** (EXPT-5))             LML01770
10  CONTINUE                                  LML01780
   WRITE(IOUT,*) 'GIVE ME THE KK.'           LML01790
   CALL FUNCT(T2,X(1,2),F)                     LML01800
   DO 20 I=1,N                                  LML01810
C       WRITE(IOUT,*) 'F(1,1) = ',F(1)         LML01820
       K(I,1)=F(1)                             LML01830
       VA(I)=X(1,2)+0.5*K(I,1)                 LML01840
20  CONTINUE                                  LML01850
   TINF = T2 + 0.5*H                           LML01860
   CALL FUNCT(TINF,VA,F)                       LML01870
   DO 25 I=1,N                                  LML01880
       K(I,2)=F(1)                             LML01890
       VA(I)=X(1,2) + 0.5*F(1,1)              LML01900
25  CONTINUE                                  LML01910
   CALL FUNCT(TINF,VA,F)                       LML01920
   DO 30 I=1,N                                  LML01930
       K(I,3)=F(1)                             LML01940
       VA(I)=X(1,2) + X(1,3)                  LML01950
30  CONTINUE                                  LML01960
   TINF=T2+H                                    LML01970
   CALL FUNCT(TINF,VA,F)                       LML01980
   DO 35 I=1,N                                  LML01990
       K(I,4)=F(1)                             LML02000
       X(I,5)=X(1,1)+0.15000007*(X(1,1)+2.0*(X(1,2)+K(I,3))+K(I,4)) LML02010
35  CONTINUE                                  LML02020
C                                         LML02030
   IF (CTR2-51.78) GOTO 200                    LML02040
   TS=T2+H                                       LML02050
C                                         LML02060
C ... NOW TEST TO SEE IF THE TIME VARIABLE HAS REACHED THE FIRST LML02070
C ... VALUE THAT IS TO BE PRINTED (A FUNCTION OF U3). LML02080
C                                         LML02090
   IF (TS+H.LT.PRT) GOTO 100                  LML02100
C                                         LML02110
C ... STORE VALUES TO BE PRINTED LML02120
C                                         LML02130
   TI(J)=TS                                     LML02140
   CALL FUNCT(TI,X(1,5),F)                     LML02150
   DO 40 I=1,N                                  LML02160
       X(J,I) = X(1,5)*F                        LML02170
       X(J,I)=F(1)                             LML02180
       Y(J,I) = F(1)+F(1,3)                   LML02190
       Y(J,I)=F(1+Y)                          LML02200

```

```

40 CONTINUE
C
C ... TEST TO SEE IF THE LAST 5 PRINT VALUES UNCHANGED, IF SO, STOP.
C
  IF(J,GT,1) THEN
    DO 42 I=1,5
      IF(X(J,I).EQ.X(J-1,I).AND.
      & X(J,I).GE.X(J,I)-.0001) THEN
        SSTEST(I)=SSTEST(I)+1
      ELSE
        SSTEST(I)=0
      ENDIF
    ENDIF
42 CONTINUE
    DO 43 I=1,5
      IF(SSTEST(I).EQ.0) GOTO 44
43 CONTINUE
    GOTO 100
C
44 J=J+1
    PRT=PRT+1
C
55 IF (3*PRT,GT,1) GOTO 100
    CTR4=CTR4+1
C* WRITE(10,1,*) 'AFTER 3*PRT=1? CTR4=1,CTR2,CTR3,CTR4
    IF (CTR4,GT,5) GOTO 100
    CTR4=CTR4+1
C* WRITE(10,1,*) 'AFTER 3*PRT=2? CTR4=1,CTR2,CTR3,CTR4
    IF (CTR4,GT,5) GOTO 100
C* WRITE(10,1,*) 'AFTER 3*PRT=3? CTR4=1,CTR2,CTR3,CTR4
C
C ... NOW DO THE CALCULATIONS
C
50 CTR3=CTR3+1
C* WRITE(10,1,*) 'AFTER CTR3=50,CTR3=1,CTR1,CTR2,CTR3,CTR4
  I=I2
  DO 45 I=1,4
    XP(I)=X(I,2)
    YP(I)=X(I,3)
    X(I,2)=X(I,1)
45 CONTINUE
    T2=T1
    TP=M
    N=2.0*N
    CTR2=1
C* WRITE(10,1,*) 'AFTER T2=10, AFTER CTR2=1'
    GOTO 10
C
209 CTR2=0
C* WRITE(10,1,*) 'AFTER CTR2=209,CTR3=1,CTR1,CTR2,CTR3,CTR4
    DO 46 I=1,4
      YP(I)=X(I,3)
46 CONTINUE
    DO 47 I=1,4
      IF (ABS(YP(I)).GT.(1.0E+(-7))*ABS(XP(I))) GOTO 309
47 CONTINUE

```

LML02210
 LML02220
 LML02230
 LML02240
 LML02250
 LML02260
 LML02270
 LML02280
 LML02290
 LML02300
 LML02310
 LML02320
 LML02330
 LML02340
 LML02350
 LML02360
 LML02370
 LML02380
 LML02390
 LML02400
 LML02410
 LML02420
 LML02430
 LML02440
 LML02450
 LML02460
 LML02470
 LML02480
 LML02490
 LML02500
 LML02510
 LML02520
 LML02530
 LML02540
 LML02550
 LML02560
 LML02570
 LML02580
 LML02590
 LML02600
 LML02610
 LML02620
 LML02630
 LML02640
 LML02650
 LML02660
 LML02670
 LML02680
 LML02690
 LML02700
 LML02710
 LML02720
 LML02730
 LML02740
 LML02750


```

C* WRITE(IOUT,*)'AFTER #47 LOOP, DEN(1),NUM(1)=',DEN(1),NUM(1)      LML02760
DO 49 I=1,N                                                         LML02770
  E(I)=DABS(1.0-NUM(I)/DEN(I))                                       LML02780
C                                                                     LML02790
22 CALL MAXMUM(F,N,EMAX,MAXM)                                         LML02800
C* WRITE(IOUT,*)'AFTER CALL TO MAXMUM'                               LML02810
  IF (DB.ST.EMAX) GOTO 49                                           LML02820
C* WRITE(IOUT,*)'AFTER IF (DB.ST.EMAX), DB,EMAX                     LML02830
  H=HP/2.0                                                           LML02840
  GOTO 509                                                           LML02850
C                                                                     LML02860
409 IF (LB.LB.EMAX) GOTO 249                                         LML02870
C* WRITE(IOUT,*)'AFTER LINE 409, LB,EMAX                             LML02880
  H=2.0*HP                                                           LML02890
C                                                                     LML02900
509 WRITE(IOUT,501) H                                                LML02910
501 FORMAT(' IN THE FOLLOWING CALCULATIONS H=',F10.3/)             LML02920
  IF (CTR.NE.1) GOTO 25                                             LML02930
C* WRITE(IOUT,*)'AFTER IF (CTR.NE.1) CTR5=',CTR1,CTR2,CTR3,CTR4    LML02940
C                                                                     LML02950
75 CTR3=0                                                            LML02960
  CTR4=0                                                            LML02970
  WRITE(IOUT,*) 'SOLUTION WAS RESTARTED USING NEW H'               LML02980
  WRITE(IOUT,*)                                                     LML02990
C* WRITE(IOUT,*) 'CTR=',CTR1,CTR2,CTR3,CTR4                       LML03000
  GOTO 25                                                            LML03010
C                                                                     LML03020
C                                                                     LML03030
309 DO 77 I=1,N                                                      LML03040
77 E(I)=DABS(NUM(I)-H*DEN(I))                                         LML03050
C* WRITE(IOUT,*)'AFTER LINE 309, DB,EMAX, H'                       LML03060
  GOTO 22                                                            LML03070
C                                                                     LML03080
249 H=HP                                                             LML03090
C* WRITE(IOUT,*)'AFTER LINE 249, H=',H                               LML03100
25 CTR1=0                                                            LML03110
C* WRITE(IOUT,*)'AFTER LINE 25, CTR5=',CTR1,CTR2,CTR3,CTR4         LML03120
  IF (CTR.EV.0) GOTO 15                                             LML03130
C* WRITE(IOUT,*)'AFTER IF (CTR.EV.0)'                               LML03140
  DO 79 I=1,N                                                        LML03150
    X(I,2) = X(I,1)                                                 LML03160
    X(I,3) = NUM(I)                                                 LML03170
79 CONTINUE                                                         LML03180
  T2=T                                                                LML03190
C                                                                     LML03200
C ... ERROR CHECK IS COMPLETELY. NOW PREPARE TO INTEGRATE NEXT STEP. LML03210
C                                                                     LML03220
125 DO 125 I=1,N                                                     LML03230
    X(I,1)=X(I,2)                                                   LML03240
    X(I,2)=X(I,3)                                                   LML03250
125 CONTINUE                                                         LML03260
  T1=T2                                                             LML03270
  T2=T3                                                             LML03280
C                                                                     LML03290
C ... NOW CHECK TO SEE IF THE TIME VARIABLE HAS REACHED THE LAST  LML03300

```

```

C ... VALUE TO BE PRINTED. IF NOT, GO OFF ANOTHER ROUND.
C
126 IF (T2.LE.TEST) GO TO 1)
SUM=0
JS=1
IF (J.GT.0) JS=J-5
DO 127 I=1,4
T1=X(I,3)
S04=SUM+T1*T1
127 CONTINUE
LC=(.25)*SUM*S04
RTS04=SQRT(S04)
DO 135 I=1,4
XSUM(I)=X(I,3)/RTS04
135 CONTINUE
J=J-1
IF (ISHORT.NE.1) THEN
WRITE(I,OT,50)
450 FORMAT('1',X,'T',X,'X(-5)',5X,'X(-4)',5X,'X(-3)',5X,'X(-2)',
5X,'X(-1)',5X,'X(1)',5X,'X(2)',5X,'X(3)',5X,'X(4)',
5X,'X(5)')
IF (IMAX.GT.0) THEN
WRITE(I,OT,50)(T(I), (X(I,3), I=6,10), 5=1,5)
500 FORMAT('5',F12.3,F12.3,F12.3,F12.3,F12.3)
WRITE(I,OT,50) SUM
550 FORMAT('7',50,'M 500000000 X(4) =',F15.3,/)
WRITE(I,OT,50) XSUM(I), I=6,10)
600 FORMAT(5X,F12.3,F12.3,F12.3,F12.3,F12.3)
WRITE(I,OT,50)
650 FORMAT('1',X,'T',X,'X(-10)',5X,'X(-9)',5X,'X(-8)',5X,
5X,'X(-7)',5X,'X(-6)',5X,'X(-5)',5X,'X(-4)',5X,'X(-3)',5X,'X(-2)',5X,
5X,'X(-1)',5X,'X(1)',5X,'X(2)',5X,'X(3)',5X,'X(4)',5X,'X(5)',5X,
5X,'X(6)',5X,'X(7)',5X,'X(8)',5X,'X(9)',5X,'X(10)')
WRITE(I,OT,70)(T(I), (X(I,3), I=1,5), (X(I,3), I=17,21), 5=1,5)
700 FORMAT('5',F12.3,F12.3,F12.3,F12.3,F12.3,10X,F10.3)
WRITE(I,OT,50) SUM
WRITE(I,OT,70) (XSUM(I), I=1,5), (XSUM(I), I=17,21)
750 FORMAT(5X,F12.3,F12.3,F12.3,F12.3,F12.3,10X,F10.3)
ELSE
WRITE(I,OT,50)(T(I), (X(I,3), I=1,10), 5=1,5)
WRITE(I,OT,50) SUM
WRITE(I,OT,50) XSUM(I), I=1,10)
ENDIF
DO 750 I=1,4
YH0=X(I,3)/F12
YFIX=YH0
YH0=(YH0-YFIX)*F12
YDEB(I-10)=57.2/57.0*YH0
700 CONTINUE
ELSE
C ... HERE, PREPARE FOR OFF-SCREEN OUTPUT.
DO 200 I=COUNT,JS,J,7
IEND=ICOUNT+5
IF (J.LT.IEND) IEND=J
WRITE(I,OT,F011V(I,3)) 5=ICOUNT,IEND)
DO 200 I=I,JS,7

```

LML03310
 LML03320
 LML03330
 LML03340
 LML03350
 LML03360
 LML03370
 LML03380
 LML03390
 LML03400
 LML03410
 LML03420
 LML03430
 LML03440
 LML03450
 LML03460
 LML03470
 LML03480
 LML03490
 LML03500
 LML03510
 LML03520
 LML03530
 LML03540
 LML03550
 LML03560
 LML03570
 LML03580
 LML03590
 LML03600
 LML03610
 LML03620
 LML03630
 LML03640
 LML03650
 LML03660
 LML03670
 LML03680
 LML03690
 LML03700
 LML03710
 LML03720
 LML03730
 LML03740
 LML03750
 LML03760
 LML03770
 LML03780
 LML03790
 LML03800
 LML03810
 LML03820
 LML03830
 LML03840
 LML03850

```

      WRITE(IOUT,753)
      INT(NH(I)), (XW(5,1), S=ICOUNT, IEND)
204  CONTINUE
      WRITE(IOUT,751) (TI(I), S=ICOUNT, ICOUNT+6)
      WRITE(IOUT,753)
      & (INT(NH(I)), (XW(5,1), S=ICOUNT, ICOUNT+6), I=NO, 2, -1)
751  FORMAT('1' I=:', /F10.3)
753  FORMAT(' X(', I2, '):', /F10.3)
205  CONTINUE
      ENDIF
C
C
      IF (ISPHOT.EQ.1) THEN
        WRITE(IOUT,800)
        & 800  FORMAT('1', 4X, 'T', 4X, 'Y(-5)', 5X, 'Y(-4)', 5X, 'Y(-3)', 5X, 'Y(-2)',
        & 5X, 'Y(-1)', 5X, 'Y(0)', 5X, 'Y(1)', 5X, 'Y(2)', 5X, 'Y(3)', 5X, 'Y(4)',
        & 5X, 'Y(5)')
        IF (NMAX.GT.5) THEN
          WRITE(IOUT,800) (TI(I), (YX(I,1), I=6, 10), S=1, J)
          WRITE(IOUT,800)
        & 850  FORMAT(/' PHASE ANGLES IN DEGREES ', /)
          WRITE(IOUT,800) (YDE(I), I=6, 10)
          WRITE(IOUT,800)
        & 900  FORMAT('1', 4X, 'T', 4X, 'Y(-10)', 5X, 'Y(-7)', 5X, 'Y(-3)', 5X,
        & 'Y(-7)', 5X, 'Y(-5)', 5X, 'Y(5)', 5X, 'Y(7)', 5X, 'Y(10)', 5X, 'Y(1)',
        & 5X, 'Y(10)')
          WRITE(IOUT,800) (TI(I), (YX(I,1), I=1, 5), (YX(I,1), I=17, 21), S=1, J)
          WRITE(IOUT,800)
          WRITE(IOUT,800) (YDE(I), I=1, 5), (YDE(I), I=17, 21)
        ELSE
          WRITE(IOUT,800) (TI(I), (YX(I,1), I=1, NO), S=1, J)
          WRITE(IOUT,800)
          WRITE(IOUT,800) (YDE(I), I=1, NO)
        ELSE
          WRITE(IOUT,800) (TI(I), (YX(I,1), I=1, NO), S=1, J)
          WRITE(IOUT,800)
          WRITE(IOUT,800) (YDE(I), I=1, NO)
        ENDIF
      ELSE
        HERE, N SPARE FILE SPARE IOUT.
        DO 211 ICOUNT=15, J, 7
          IEND=ICOUNT+6
          IF (J.GT.IEND) IEND=J
          WRITE(IOUT,915) (TI(I), S=ICOUNT, IEND)
          DO 211 I=NO, 2, -1
            WRITE(IOUT,915)
            & 211  WRITE(IOUT,915) (TI(I), (YX(I,1), S=ICOUNT, IEND)
          CONTINUE
          & 211  WRITE(IOUT,915) (TI(I), S=ICOUNT, ICOUNT+6)
          & 211  WRITE(IOUT,915)
          & 211  WRITE(IOUT,915) (TI(I), (YX(I,1), S=ICOUNT, ICOUNT+6), I=NO, 2, -1)
          & 211  FORMAT('1' I=:', /F10.3)
          & 211  FORMAT(' Y(', I2, '):', /F10.3)
          & 211  CONTINUE
          & 211  ENDIF
        CALL FUNCT(T2, X(1,1), Y)
        DO 212 I=1, NO
          DERIV(I)=XCT(I,1)-F(I)

```



```

5      5X,'YOUT(5)')
      IF(NMAX.UT.5) THEN
        WRITE(10UT,500)(T(I),,(YOUT(5,I),I=0,16),J=1,J)
        WRITE(10UT,575)
        WRITE(10UT,1000) (DO=1,IF(1),I=0,16,10+16)
        WRITE(10UT,1100)
1100    FORMAT('1',5X,'1',5X,'YOUT(-1)',2X,'YOUT(-9)',2X,'YOUT(-5)',
           5X,'YOUT(-7)',5X,
           5X,'YOUT(-3)',15X,'YOUT(1)',5X,
           5X,'YOUT(7)',5X,'YOUT(11)',5X,'YOUT(5)',
           5X,'YOUT(15)')
        WRITE(10UT,700)(T(I),,(YOUT(5,I),I=1,5),
           5X,'YOUT(17),I=17,21),J=1,J)
        WRITE(10UT,575)
        WRITE(10UT,750) (DO=1,IF(1),I=0,16,10+16),
           5X,'YOUT(17),I=17,21,10+21)
      ELSE
        WRITE(10UT,500)(T(I),,(YOUT(5,I),I=1,16),J=1,J)
        WRITE(10UT,575)
        WRITE(10UT,1000) (DO=1,IF(1),I=0,16,10)
      ENDIF
    ELSE
      HERE, HERE+1, HERE+5, HERE+10, HERE+15, HERE+20, HERE+25, HERE+30, HERE+35, HERE+40, HERE+45, HERE+50, HERE+55, HERE+60, HERE+65, HERE+70, HERE+75, HERE+80, HERE+85, HERE+90, HERE+95, HERE+100, HERE+105, HERE+110, HERE+115, HERE+120, HERE+125, HERE+130, HERE+135, HERE+140, HERE+145, HERE+150, HERE+155, HERE+160, HERE+165, HERE+170, HERE+175, HERE+180, HERE+185, HERE+190, HERE+195, HERE+200, HERE+205, HERE+210, HERE+215, HERE+220, HERE+225, HERE+230, HERE+235, HERE+240, HERE+245, HERE+250, HERE+255, HERE+260, HERE+265, HERE+270, HERE+275, HERE+280, HERE+285, HERE+290, HERE+295, HERE+300, HERE+305, HERE+310, HERE+315, HERE+320, HERE+325, HERE+330, HERE+335, HERE+340, HERE+345, HERE+350, HERE+355, HERE+360, HERE+365, HERE+370, HERE+375, HERE+380, HERE+385, HERE+390, HERE+395, HERE+400, HERE+405, HERE+410, HERE+415, HERE+420, HERE+425, HERE+430, HERE+435, HERE+440, HERE+445, HERE+450, HERE+455, HERE+460, HERE+465, HERE+470, HERE+475, HERE+480, HERE+485, HERE+490, HERE+495, HERE+500, HERE+505, HERE+510, HERE+515, HERE+520, HERE+525, HERE+530, HERE+535, HERE+540, HERE+545, HERE+550, HERE+555, HERE+560, HERE+565, HERE+570, HERE+575, HERE+580, HERE+585, HERE+590, HERE+595, HERE+600, HERE+605, HERE+610, HERE+615, HERE+620, HERE+625, HERE+630, HERE+635, HERE+640, HERE+645, HERE+650, HERE+655, HERE+660, HERE+665, HERE+670, HERE+675, HERE+680, HERE+685, HERE+690, HERE+695, HERE+700, HERE+705, HERE+710, HERE+715, HERE+720, HERE+725, HERE+730, HERE+735, HERE+740, HERE+745, HERE+750, HERE+755, HERE+760, HERE+765, HERE+770, HERE+775, HERE+780, HERE+785, HERE+790, HERE+795, HERE+800, HERE+805, HERE+810, HERE+815, HERE+820, HERE+825, HERE+830, HERE+835, HERE+840, HERE+845, HERE+850, HERE+855, HERE+860, HERE+865, HERE+870, HERE+875, HERE+880, HERE+885, HERE+890, HERE+895, HERE+900, HERE+905, HERE+910, HERE+915, HERE+920, HERE+925, HERE+930, HERE+935, HERE+940, HERE+945, HERE+950, HERE+955, HERE+960, HERE+965, HERE+970, HERE+975, HERE+980, HERE+985, HERE+990, HERE+995, HERE+1000, HERE+1005, HERE+1010, HERE+1015, HERE+1020, HERE+1025, HERE+1030, HERE+1035, HERE+1040, HERE+1045, HERE+1050, HERE+1055, HERE+1060, HERE+1065, HERE+1070, HERE+1075, HERE+1080, HERE+1085, HERE+1090, HERE+1095, HERE+1100, HERE+1105, HERE+1110, HERE+1115, HERE+1120, HERE+1125, HERE+1130, HERE+1135, HERE+1140, HERE+1145, HERE+1150, HERE+1155, HERE+1160, HERE+1165, HERE+1170, HERE+1175, HERE+1180, HERE+1185, HERE+1190, HERE+1195, HERE+1200, HERE+1205, HERE+1210, HERE+1215, HERE+1220, HERE+1225, HERE+1230, HERE+1235, HERE+1240, HERE+1245, HERE+1250, HERE+1255, HERE+1260, HERE+1265, HERE+1270, HERE+1275, HERE+1280, HERE+1285, HERE+1290, HERE+1295, HERE+1300, HERE+1305, HERE+1310, HERE+1315, HERE+1320, HERE+1325, HERE+1330, HERE+1335, HERE+1340, HERE+1345, HERE+1350, HERE+1355, HERE+1360, HERE+1365, HERE+1370, HERE+1375, HERE+1380, HERE+1385, HERE+1390, HERE+1395, HERE+1400, HERE+1405, HERE+1410, HERE+1415, HERE+1420, HERE+1425, HERE+1430, HERE+1435, HERE+1440, HERE+1445, HERE+1450, HERE+1455, HERE+1460, HERE+1465, HERE+1470, HERE+1475, HERE+1480, HERE+1485, HERE+1490, HERE+1495, HERE+1500, HERE+1505, HERE+1510, HERE+1515, HERE+1520, HERE+1525, HERE+1530, HERE+1535, HERE+1540, HERE+1545, HERE+1550, HERE+1555, HERE+1560, HERE+1565, HERE+1570, HERE+1575, HERE+1580, HERE+1585, HERE+1590, HERE+1595, HERE+1600, HERE+1605, HERE+1610, HERE+1615, HERE+1620, HERE+1625, HERE+1630, HERE+1635, HERE+1640, HERE+1645, HERE+1650, HERE+1655, HERE+1660, HERE+1665, HERE+1670, HERE+1675, HERE+1680, HERE+1685, HERE+1690, HERE+1695, HERE+1700, HERE+1705, HERE+1710, HERE+1715, HERE+1720, HERE+1725, HERE+1730, HERE+1735, HERE+1740, HERE+1745, HERE+1750, HERE+1755, HERE+1760, HERE+1765, HERE+1770, HERE+1775, HERE+1780, HERE+1785, HERE+1790, HERE+1795, HERE+1800, HERE+1805, HERE+1810, HERE+1815, HERE+1820, HERE+1825, HERE+1830, HERE+1835, HERE+1840, HERE+1845, HERE+1850, HERE+1855, HERE+1860, HERE+1865, HERE+1870, HERE+1875, HERE+1880, HERE+1885, HERE+1890, HERE+1895, HERE+1900, HERE+1905, HERE+1910, HERE+1915, HERE+1920, HERE+1925, HERE+1930, HERE+1935, HERE+1940, HERE+1945, HERE+1950, HERE+1955, HERE+1960, HERE+1965, HERE+1970, HERE+1975, HERE+1980, HERE+1985, HERE+1990, HERE+1995, HERE+2000, HERE+2005, HERE+2010, HERE+2015, HERE+2020, HERE+2025, HERE+2030, HERE+2035, HERE+2040, HERE+2045, HERE+2050, HERE+2055, HERE+2060, HERE+2065, HERE+2070, HERE+2075, HERE+2080, HERE+2085, HERE+2090, HERE+2095, HERE+2100, HERE+2105, HERE+2110, HERE+2115, HERE+2120, HERE+2125, HERE+2130, HERE+2135, HERE+2140, HERE+2145, HERE+2150, HERE+2155, HERE+2160, HERE+2165, HERE+2170, HERE+2175, HERE+2180, HERE+2185, HERE+2190, HERE+2195, HERE+2200, HERE+2205, HERE+2210, HERE+2215, HERE+2220, HERE+2225, HERE+2230, HERE+2235, HERE+2240, HERE+2245, HERE+2250, HERE+2255, HERE+2260, HERE+2265, HERE+2270, HERE+2275, HERE+2280, HERE+2285, HERE+2290, HERE+2295, HERE+2300, HERE+2305, HERE+2310, HERE+2315, HERE+2320, HERE+2325, HERE+2330, HERE+2335, HERE+2340, HERE+2345, HERE+2350, HERE+2355, HERE+2360, HERE+2365, HERE+2370, HERE+2375, HERE+2380, HERE+2385, HERE+2390, HERE+2395, HERE+2400, HERE+2405, HERE+2410, HERE+2415, HERE+2420, HERE+2425, HERE+2430, HERE+2435, HERE+2440, HERE+2445, HERE+2450, HERE+2455, HERE+2460, HERE+2465, HERE+2470, HERE+2475, HERE+2480, HERE+2485, HERE+2490, HERE+2495, HERE+2500, HERE+2505, HERE+2510, HERE+2515, HERE+2520, HERE+2525, HERE+2530, HERE+2535, HERE+2540, HERE+2545, HERE+2550, HERE+2555, HERE+2560, HERE+2565, HERE+2570, HERE+2575, HERE+2580, HERE+2585, HERE+2590, HERE+2595, HERE+2600, HERE+2605, HERE+2610, HERE+2615, HERE+2620, HERE+2625, HERE+2630, HERE+2635, HERE+2640, HERE+2645, HERE+2650, HERE+2655, HERE+2660, HERE+2665, HERE+2670, HERE+2675, HERE+2680, HERE+2685, HERE+2690, HERE+2695, HERE+2700, HERE+2705, HERE+2710, HERE+2715, HERE+2720, HERE+2725, HERE+2730, HERE+2735, HERE+2740, HERE+2745, HERE+2750, HERE+2755,
```

LML05510
 LML05520
 LML05530
 LML05540
 LML05550
 LML05560
 LML05570
 LML05580
 LML05590
 LML05600
 LML05610
 LML05620
 LML05630
 LML05640
 LML05650
 LML05660
 LML05670
 LML05680
 LML05690
 LML05700
 LML05710
 LML05720
 LML05730
 LML05740
 LML05750
 LML05760
 LML05770
 LML05780
 LML05790
 LML05800
 LML05810
 LML05820
 LML05830
 LML05840
 LML05850
 LML05860
 LML05870
 LML05880
 LML05890
 LML05900
 LML05910
 LML05920
 LML05930
 LML05940
 LML05950
 LML05960
 LML05970
 LML05980
 LML05990
 LML06000
 LML06010
 LML06020
 LML06030
 LML06040
 LML06050

100

51.87

[illegible]

```

      IF (X.LT.0(1)) GO TO 30
      DO 10 J=1,N1
      IF (X.LT.0(J+1)) GO TO 20
10    CONTINUE
      I=N1
      GO TO 30
20    I=J
      DX=X-0(I)
      IF (LINCOS.NE.1) GO TO 30
      LINEAR INTERPOLATION
      DU=0(I+1)-0(I)
      IF (DU.NE.0.) GO TO 40
      Y=.5*(V(I+1)+V(I))
      RETURN
40    Y=V(I)+((V(I+1)-V(I))/DU)*(X-0(I)+0(I))
      WRITE (JOUT,*) 'EXIT 1,1,0(I),LINCOS',X,I,0(I),LINCOS
      RETURN
      HERMITE CONTINUED INTERPOLATION
50    Y=V(I)+DX*(S(I)+DX*(M(I)+DX*(B(I))))
      WRITE (JOUT,*) 'EXIT 2,1,0(I),LINCOS',X,I,0(I),LINCOS
      RETURN
      END
C===== SETUP
      SUBROUTINE SETUP(N,N1,N2,N3,N4)
      C
      C   DETERMINE SLOPES AND COEFFICIENTS FOR
      C   PIECEWISE CONTINUOUS LINEAR
      C
      DOUBLE PRECISION
      S(1),S2,S1,S(2),V(1),S(1),C(1),Z(1)
      N1=N-1
      C
      C   GET SLOPES AT POINTS AND A WEIGHTED AVERAGE OF END SLOPES
      DO 10 I=2,N1
      S2=0(I+1)-0(I)
      S1=0(I)-0(I-1)
      S(I)=(S1*(V(I+1)-V(I))/C1+S2*(V(I)-V(I-1))/C1)/(S1+S2)
10    CONTINUE
      C
      C   FIND SLOPES TO MAKE V(I) EQUAL ZERO AT FIRST AND LAST POINTS
      S(1)=1.5*(V(2)-V(1))/C(1)-.5*S(2)
      S(N)=1.5*(V(N)-V(N-1))/C(N)-.5*S(N-1)
      C
      C   DETERMINE COEFFICIENTS NEEDED FOR CUBIC INTERPOLATION
      DO 20 I=1,N1
      S1=0(I+1)-0(I)
      S2=(V(I+1)-V(I))/C1
      Z(I)=(S(I+1)+S(I)-1.5*S1)/(S1+S1)
      M(I)=(S1-S(I))/S1-L(I)+1
20    CONTINUE
      RETURN
      END

```


X(11):	0.209	0.209	0.209	0.209	0.209
X(12):	0.253	0.253	0.253	0.253	0.253
X(13):	0.304	0.304	0.304	0.304	0.304
X(14):	0.361	0.361	0.361	0.361	0.361
X(15):	0.425	0.425	0.425	0.425	0.425
X(16):	0.497	0.497	0.497	0.497	0.497
X(17):	0.575	0.575	0.575	0.575	0.575
X(18):	0.661	0.661	0.661	0.661	0.661
X(19):	0.752	0.752	0.752	0.752	0.752
X(20):	0.847	0.847	0.847	0.847	0.847
X(21):	0.946	0.946	0.946	0.946	0.946
X(22):	1.047	1.047	1.047	1.047	1.047
X(23):	1.147	1.147	1.147	1.147	1.147
X(24):	1.245	1.245	1.245	1.245	1.245
X(25):	1.339	1.339	1.339	1.339	1.339
X(26):	1.426	1.426	1.426	1.426	1.426
X(27):	1.505	1.505	1.505	1.505	1.505
X(28):	1.572	1.572	1.572	1.572	1.572
X(29):	1.625	1.625	1.625	1.625	1.625
X(30):	1.667	1.667	1.667	1.667	1.667
X(31):	1.699	1.699	1.699	1.699	1.699
X(32):	1.721	1.721	1.721	1.721	1.721
X(33):	1.733	1.733	1.733	1.733	1.733
X(34):	1.735	1.735	1.735	1.735	1.735
X(35):	1.726	1.726	1.726	1.726	1.726
X(36):	1.705	1.705	1.705	1.705	1.705
X(37):	1.672	1.672	1.672	1.672	1.672
X(38):	1.625	1.625	1.625	1.625	1.625
X(39):	1.567	1.567	1.567	1.567	1.567
X(40):	1.497	1.497	1.497	1.497	1.497
X(41):	1.415	1.415	1.415	1.415	1.415
X(42):	1.320	1.320	1.320	1.320	1.320
X(43):	1.212	1.212	1.212	1.212	1.212
X(44):	1.090	1.090	1.090	1.090	1.090
X(45):	0.953	0.953	0.953	0.953	0.953
X(46):	0.801	0.801	0.801	0.801	0.801
X(47):	0.634	0.634	0.634	0.634	0.634
X(48):	0.453	0.453	0.453	0.453	0.453
X(49):	0.258	0.258	0.258	0.258	0.258
X(50):	0.050	0.050	0.050	0.050	0.050
X(51):	-0.171	-0.171	-0.171	-0.171	-0.171
X(52):	-0.336	-0.336	-0.336	-0.336	-0.336
X(53):	-0.534	-0.534	-0.534	-0.534	-0.534
X(54):	-0.765	-0.765	-0.765	-0.765	-0.765
X(55):	-1.028	-1.028	-1.028	-1.028	-1.028
X(56):	-1.322	-1.322	-1.322	-1.322	-1.322
X(57):	-1.646	-1.646	-1.646	-1.646	-1.646
X(58):	-2.000	-2.000	-2.000	-2.000	-2.000
X(59):	-2.393	-2.393	-2.393	-2.393	-2.393
X(60):	-2.825	-2.825	-2.825	-2.825	-2.825
X(61):	-3.296	-3.296	-3.296	-3.296	-3.296
X(62):	-3.806	-3.806	-3.806	-3.806	-3.806
X(63):	-4.355	-4.355	-4.355	-4.355	-4.355
X(64):	-4.944	-4.944	-4.944	-4.944	-4.944
X(65):	-5.573	-5.573	-5.573	-5.573	-5.573
X(66):	-6.243	-6.243	-6.243	-6.243	-6.243
X(67):	-6.954	-6.954	-6.954	-6.954	-6.954
X(68):	-7.706	-7.706	-7.706	-7.706	-7.706
X(69):	-8.500	-8.500	-8.500	-8.500	-8.500
X(70):	-9.336	-9.336	-9.336	-9.336	-9.336
X(71):	-10.215	-10.215	-10.215	-10.215	-10.215
X(72):	-11.137	-11.137	-11.137	-11.137	-11.137
X(73):	-12.103	-12.103	-12.103	-12.103	-12.103
X(74):	-13.114	-13.114	-13.114	-13.114	-13.114
X(75):	-14.171	-14.171	-14.171	-14.171	-14.171
X(76):	-15.274	-15.274	-15.274	-15.274	-15.274
X(77):	-16.424	-16.424	-16.424	-16.424	-16.424
X(78):	-17.622	-17.622	-17.622	-17.622	-17.622
X(79):	-18.869	-18.869	-18.869	-18.869	-18.869
X(80):	-20.166	-20.166	-20.166	-20.166	-20.166
X(81):	-21.514	-21.514	-21.514	-21.514	-21.514
X(82):	-22.914	-22.914	-22.914	-22.914	-22.914
X(83):	-24.367	-24.367	-24.367	-24.367	-24.367
X(84):	-25.874	-25.874	-25.874	-25.874	-25.874
X(85):	-27.437	-27.437	-27.437	-27.437	-27.437
X(86):	-29.057	-29.057	-29.057	-29.057	-29.057
X(87):	-30.735	-30.735	-30.735	-30.735	-30.735
X(88):	-32.472	-32.472	-32.472	-32.472	-32.472
X(89):	-34.269	-34.269	-34.269	-34.269	-34.269
X(90):	-36.127	-36.127	-36.127	-36.127	-36.127
X(91):	-38.047	-38.047	-38.047	-38.047	-38.047
X(92):	-40.030	-40.030	-40.030	-40.030	-40.030
X(93):	-42.077	-42.077	-42.077	-42.077	-42.077
X(94):	-44.189	-44.189	-44.189	-44.189	-44.189
X(95):	-46.367	-46.367	-46.367	-46.367	-46.367
X(96):	-48.612	-48.612	-48.612	-48.612	-48.612
X(97):	-50.925	-50.925	-50.925	-50.925	-50.925
X(98):	-53.308	-53.308	-53.308	-53.308	-53.308
X(99):	-55.762	-55.762	-55.762	-55.762	-55.762
X(100):	-58.289	-58.289	-58.289	-58.289	-58.289
X(101):	-60.890	-60.890	-60.890	-60.890	-60.890
X(102):	-63.566	-63.566	-63.566	-63.566	-63.566
X(103):	-66.318	-66.318	-66.318	-66.318	-66.318
X(104):	-69.147	-69.147	-69.147	-69.147	-69.147
X(105):	-72.054	-72.054	-72.054	-72.054	-72.054
X(106):	-75.040	-75.040	-75.040	-75.040	-75.040
X(107):	-78.106	-78.106	-78.106	-78.106	-78.106
X(108):	-81.254	-81.254	-81.254	-81.254	-81.254
X(109):	-84.485	-84.485	-84.485	-84.485	-84.485
X(110):	-87.800	-87.800	-87.800	-87.800	-87.800
X(111):	-91.200	-91.200	-91.200	-91.200	-91.200
X(112):	-94.686	-94.686	-94.686	-94.686	-94.686
X(113):	-98.260	-98.260	-98.260	-98.260	-98.260
X(114):	-101.923	-101.923	-101.923	-101.923	-101.923
X(115):	-105.677	-105.677	-105.677	-105.677	-105.677
X(116):	-109.523	-109.523	-109.523	-109.523	-109.523
X(117):	-113.463	-113.463	-113.463	-113.463	-113.463
X(118):	-117.498	-117.498	-117.498	-117.498	-117.498
X(119):	-121.629	-121.629	-121.629	-121.629	-121.629
X(120):	-125.858	-125.858	-125.858	-125.858	-125.858
X(121):	-130.186	-130.186	-130.186	-130.186	-130.186
X(122):	-134.615	-134.615	-134.615	-134.615	-134.615
X(123):	-139.147	-139.147	-139.147	-139.147	-139.147
X(124):	-143.784	-143.784	-143.784	-143.784	-143.784
X(125):	-148.528	-148.528	-148.528	-148.528	-148.528
X(126):	-153.381	-153.381	-153.381	-153.381	-153.381
X(127):	-158.345	-158.345	-158.345	-158.345	-158.345
X(128):	-163.421	-163.421	-163.421	-163.421	-163.421
X(129):	-168.611	-168.611	-168.611	-168.611	-168.611
X(130):	-173.916	-173.916	-173.916	-173.916	-173.916
X(131):	-179.338	-179.338	-179.338	-179.338	-179.338
X(132):	-184.879	-184.879	-184.879	-184.879	-184.879
X(133):	-190.541	-190.541	-190.541	-190.541	-190.541
X(134):	-196.326	-196.326	-196.326	-196.326	-196.326
X(135):	-202.236	-202.236	-202.236	-202.236	-202.236
X(136):	-208.273	-208.273	-208.273	-208.273	-208.273
X(137):	-214.439	-214.439	-214.439	-214.439	-214.439
X(138):	-220.736	-220.736	-220.736	-220.736	-220.736
X(139):	-227.166	-227.166	-227.166	-227.166	-227.166
X(140):	-233.731	-233.731	-233.731	-233.731	-233.731
X(141):	-240.433	-240.433	-240.433	-240.433	-240.433
X(142):	-247.275	-247.275	-247.275	-247.275	-247.275
X(143):	-254.259	-254.259	-254.259	-254.259	-254.259
X(144):	-261.388	-261.388	-261.388	-261.388	-261.388
X(145):	-268.664	-268.664	-268.664	-268.664	-268.664
X(146):	-276.089	-276.089	-276.089	-276.089	-276.089
X(147):	-283.666	-283.666	-283.666	-283.666	-283.666
X(148):	-291.397	-291.397	-291.397	-291.397	-291.397
X(149):	-299.285	-299.285	-299.285	-299.285	-299.285
X(150):	-307.332	-307.332	-307.332	-307.332	-307.332
X(151):	-315.541	-315.541	-315.541	-315.541	-315.541
X(152):	-323.914	-323.914	-323.914	-323.914	-323.914
X(153):	-332.454	-332.454	-332.454	-332.454	-332.454
X(154):	-341.164	-341.164	-341.164	-341.164	-341.164
X(155):	-350.047	-350.047	-350.047	-350.047	-350.047
X(156):	-359.106	-359.106	-359.106	-359.106	-359.106
X(157):	-368.344	-368.344	-368.344	-368.344	-368.344
X(158):	-377.764	-377.764	-377.764	-377.764	-377.764
X(159):	-387.369	-387.369	-387.369	-387.369	-387.369
X(160):	-397.163	-397.163	-397.163	-397.163	-397.163
X(161):	-407.149	-407.149	-407.149	-407.149	-407.149
X(162):	-417.330	-417.330	-417.330	-417.330	-417.330
X(163):	-427.709	-427.709	-427.709	-427.709	-427.709
X(164):	-438.289	-438.289	-438.289	-438.289	-438.289
X(165):	-449.074	-449.074	-449.074	-449.074	-449.074
X(166):	-459.968	-459.968	-459.968	-459.968	-459.968
X(167):	-471.075	-471.075	-471.075	-471.075	-471.075
X(168):	-482.399	-482.399	-482.399	-482.399	-482.399
X(169):	-493.944	-493.944	-493.944	-493.944	-493.944
X(170):	-505.714	-505.714	-505.714	-505.714	-505.714
X(171):	-517.713	-517.713	-517.713	-517.713	-517.713
X(172):	-529.945	-529.945	-529.945	-529.945	-529.945
X(173):	-542.414	-542.414	-542.414	-542.414	-542.414
X(174):	-555.124	-555.124	-555.124	-555.124	-555.124
X(175):	-568.079	-568.079	-568.079	-568.079	-568.079
X(176):	-581.284	-581.284	-581.284	-581.284	-581.284
X(177):	-594.743	-594.743	-594.743	-594.743	-594.743
X(178):	-608.460	-608.460	-608.460	-608.460	-608.460
X(179):	-622.439	-622.439	-622.439	-622.439	-622.439
X(180):	-636.684	-636.684	-636.684	-636.684	-636.684
X(181):	-651.199	-651.199	-651.199	-651.199	-651.199
X(182):	-665.989	-665.989	-665.989	-665.989	-665.989
X(183):	-681.059	-681.059	-681.059	-681.059	-681.059
X(184):	-696.414	-696.414	-696.414	-696.414	-696.414
X(185):	-712.059	-712.059	-712.059	-712.059	-712.059
X(186):	-727.999	-727.999	-727.999	-727.999	-727.999
X					

THE

51.94

X(1)(*):	-0.000	-0.000	0.000	0.000	0.000
Y(1)(*):	0.000	0.000	-0.000	-0.000	-0.000
Z(1)(*):	0.000	0.000	-0.000	-0.000	-0.000
1 T=	00.000	00.000	70.000	72.000	74.000
Y(1)(40):	-0.000	-0.000	-0.000	-0.000	-0.000
Y(1)(39):	-0.000	-0.000	-0.000	-0.000	-0.000
Y(1)(38):	-0.000	-0.000	-0.000	-0.000	-0.000
Y(1)(37):	-0.000	-0.000	-0.000	-0.000	-0.000
Y(1)(36):	-0.000	-0.000	-0.000	-0.000	-0.000
Y(1)(35):	-0.000	-0.000	-0.000	-0.000	-0.000
Y(1)(34):	-0.000	-0.000	-0.000	-0.000	-0.000
Y(1)(33):	-0.000	-0.000	-0.000	-0.000	-0.000
Y(1)(32):	-0.000	-0.000	-0.000	-0.000	-0.000
Y(1)(31):	-0.000	-0.000	-0.000	-0.000	-0.000
Y(1)(30):	-0.000	-0.000	-0.000	-0.000	-0.000
Y(1)(29):	-0.000	-0.000	-0.000	-0.000	-0.000
Y(1)(28):	-0.000	-0.000	-0.000	-0.000	-0.000
Y(1)(27):	-0.000	-0.000	-0.000	-0.000	-0.000
Y(1)(26):	-0.000	-0.000	-0.000	-0.000	-0.000
Y(1)(25):	-0.000	-0.000	-0.000	-0.000	-0.000
Y(1)(24):	-0.000	-0.000	-0.000	-0.000	-0.000
Y(1)(23):	-0.000	-0.000	-0.000	-0.000	-0.000
Y(1)(22):	-0.000	-0.000	-0.000	-0.000	-0.000
Y(1)(21):	-0.000	-0.000	-0.000	-0.000	-0.000
Y(1)(20):	-0.000	-0.000	-0.000	-0.000	-0.000
Y(1)(19):	-0.000	-0.000	-0.000	-0.000	-0.000
Y(1)(18):	-0.000	-0.000	-0.000	-0.000	-0.000
Y(1)(17):	-0.000	-0.000	-0.000	-0.000	-0.000
Y(1)(16):	-0.000	-0.000	-0.000	-0.000	-0.000
Y(1)(15):	-0.000	-0.000	-0.000	-0.000	-0.000
Y(1)(14):	-0.000	-0.000	-0.000	-0.000	-0.000
Y(1)(13):	-0.000	-0.000	-0.000	-0.000	-0.000
Y(1)(12):	-0.000	-0.000	-0.000	-0.000	-0.000
Y(1)(11):	-0.000	-0.000	-0.000	-0.000	-0.000
Y(1)(10):	-0.000	-0.000	-0.000	-0.000	-0.000
Y(1)(9):	-0.000	-0.000	-0.000	-0.000	-0.000
Y(1)(8):	-0.000	-0.000	-0.000	-0.000	-0.000
Y(1)(7):	-0.000	-0.000	-0.000	-0.000	-0.000
Y(1)(6):	-0.000	-0.000	-0.000	-0.000	-0.000
Y(1)(5):	-0.000	-0.000	-0.000	-0.000	-0.000
Y(1)(4):	-0.000	-0.000	-0.000	-0.000	-0.000
Y(1)(3):	-0.000	-0.000	-0.000	-0.000	-0.000
Y(1)(2):	-0.000	-0.000	-0.000	-0.000	-0.000
Y(1)(1):	-0.000	-0.000	-0.000	-0.000	-0.000
Y(1)(0):	-0.000	-0.000	-0.000	-0.000	-0.000
Y(1)(-1):	-0.000	-0.000	-0.000	-0.000	-0.000
Y(1)(-2):	-0.000	-0.000	-0.000	-0.000	-0.000
Y(1)(-3):	-0.000	-0.000	-0.000	-0.000	-0.000
Y(1)(-4):	-0.000	-0.000	-0.000	-0.000	-0.000
Y(1)(-5):	-0.000	-0.000	-0.000	-0.000	-0.000
Y(1)(-6):	-0.000	-0.000	-0.000	-0.000	-0.000
Y(1)(-7):	-0.000	-0.000	-0.000	-0.000	-0.000
Y(1)(-8):	-0.000	-0.000	-0.000	-0.000	-0.000
Y(1)(-9):	-0.000	-0.000	-0.000	-0.000	-0.000
Y(1)(-10):	-0.000	-0.000	-0.000	-0.000	-0.000

[illegible]

APPENDIX C

LASER CHARACTERISTICS

Spectra Physics Model 170 cw Argon

Laser Diameter.....1.6 mm
Beam Divergence.....0.6MR @ 514.5 nm
Resonator Configuration....High Conductivity, welded head shield and low
expansion quartz rods
Cavity Length.....2.09 Meters (nominal)
Longitudinal Mode Spacing (c/2L).....71.7 MHz
Noise @ 514.5 nm.....Approximately 1% RMS
Long term output power stability..... $\pm 0.5\%$
Input power.....460 $\pm 8\%$, 3-phase, 60A/line
Operating Wavelength (tunable with a prism).....4880 Å

APPENDIX D

MODE-LOCKER SPECIFICATIONS

IntraAction Corp. Model ML-35C

Wavelength.....4880 Å, with high power AR V-coat
Acoustic Center Frequency.....35.8 MHz \pm 0.02 MHz
Acoustic Mode Spacing.....460 KHz \pm 10 KHz
RF Bandwidth..... \pm 15% of center frequency
Active Optical Aperture.....3 mm x 5 mm
Diffraction Efficiency.....50%
Drive Power (water cooled).....5 watts
Temperature Tuning.....+ 7 KHz/°C
Static Optical Insertion Loss.....0.3% or less
Window Description.....1° wedge

1984-85 USAF-SCEEE SUMMER FACULTY RESEARCH PROGRAM

Sponsored by the

AIR FORCE OFFICE OF SCIENTIFIC RESEARCH

Conducted by the

SOUTHEASTERN CENTER FOR ELECTRICAL ENGINEERING EDUCATION

FINAL REPORT

RAMAN SPECTROSCOPY OF CAROTENOIDS
AND OTHER MOLECULES IN UNSTIMULATED AND
STIMULATED, CULTURED Y-1 MOUSE ADRENAL TUMOR CELLS

Prepared by:	Dr. James J. Mrotek
Academic Rank:	Associate Professor
Department, School and University:	Department of Physiology School of Medicine Meharry Medical College
Research Location:	Department of Physiology School of Medicine Meharry Medical College Nashville, Tennessee
USAF Research:	Dr. John Taboada Neurosciences Branch Clinical Sciences Division School of Aerospace Medicine Brooks AFB, Texas
Date:	January 5, 1985
Contract No:	F49620-82-C-0035

RAMAN SPECTROSCOPY OF CAROTENOIDS
AND OTHER MOLECULES IN UNSTIMULATED AND
STIMULATED, CULTURED Y-1 MOUSE ADRENAL TUMOR CELLS

by

James J. Mrotek

ABSTRACT

Y-1 mouse adrenal tumor cells and HEP-2, a human neoplastic, respiratory tract, fibroblast cell line were experimental tissues to be used in studies funded by this grant. Experiments to clarify the involvement of cell surface activity and mitosis in Raman activity were to be conducted. Although we were able to obtain a lens with sufficient enlargement capabilities and we purchased an illuminator with sufficient intensity to provide adequate contrast, sufficient funds to purchase a sensitive videocamera and videotape recorder capable of time-lapse operation were not available.

Laser effects on physiological parameters such as steroidogenesis, remain to be determined. We proposed carrying out these experiments at Brooks AFB, however, Dr. Taboada has not completed renovation of the Raman spectrometer; he has been having difficulty resilvering mirrors.

Carotenoids in Y-1 cell extracts were to be identified using high pressure liquid chromatography (HPLC). Although cells were incubated with carotene, stimulated with ACTH, and extracted, HPLC could not be performed. A special column is required for this type of chromatography; after we completed extraction in June 1985, we could not purchase this column because we exhausted our budget. The paper work indicating we had received the remaining \$3000 of our \$12,000 grant was not received until the second week of November. We have ordered the column and are awaiting its arrival to complete our experiments.

Studies using a Coulter counter set to count particles within various size ranges showed that: (a) only a relatively small number of cell fragments (< 10 microns in diameter) were associated with HEP-2 and Y-1 cell suspensions; (b) since relatively few HEP-2 and Y-1 cell counts were recorded in the 15-25 micron range, this suggests that there were few cell clumps; (c) maximum counts were observed in the 10-13 micron range for HEP-2 cells; and (d) Y-1 cells diameters appeared to be less uniform because maximum numbers were detected in a 10 to 15 micron range (with slightly more cells measured in the 13-15 micron range).

Acknowledgement

Acknowledgement is made of the School of Aerospace Medicine, Brooks Air Force Base, Texas, the Air Force Systems Command, the Air Force Office of Scientific Research and the Southeastern Center for Electrical Engineering Education for the opportunity to continue investigations funded from the summer of 1983 to the present. Project supervision was by Dr. John Taboada, Neurosciences Branch of the Clinical Sciences Division. This project could not be conducted without the approval of Dr. Wolf and the enthusiastic support of Dr. Bryce Hartman. Special mention must be made of the previous consideration and courtesy of the Epidemiology Division administration, particularly Dr. Jerry Schmidt and Sgt Dwight Saunier. Without the continuing cooperation, technical assistance, tissue culture facilities and supplies from Dr. Vee Davison and the members of her virology laboratory, Jim Disponet, Cliff Miller, Sgt. Donna Norris and Airman Richard Green, our work could not have progressed to this report. At Meharry Medical College, mention must be made of the assistance of the Dean of the School of Medicine, Dr. Walter Leavell, and Physiology Department Chairman, Dr. James Townsel, without the special allowances made by these individuals this work would not have been possible. Special mention must be made of Mr. George Williams in the Meharry Grants Office, since 1983 he has consistently gone beyond job requirements to ensure smooth handling of our purchase requisitions; even after a requisition has left his hands I can call on him to check on status and expedite clearances.

RAMAN SPECTROSCOPY OF CAROTENOIDS
AND OTHER MOLECULES IN UNSTIMULATED AND
STIMULATED, CULTURED Y-1 MOUSE ADRENAL TUMOR CELLS

by

James J. Mrotek

I. INTRODUCTION

THEORETICAL BACKGROUND FOR RAMAN SPECTROSCOPICAL STUDIES:

Because a molecule interacts with the incident photons with which it is irradiated, a small number of photons of shorter (anti-Stokes) or longer (Stokes) wavelengths than those of the original incident light will be scattered by the molecule during the irradiation. Laser-Raman spectroscopy is performed by scanning a range of wavelengths immediately preceding, and succeeding, the wavelength of the incident photons to detect photons scattered by the irradiated molecules. In theory, a given molecule will produce only a limited number of specific spectra.

PROJECT HISTORY

Through the use of USAF School of Aerospace Medicine lab director's funds and support, Dr. John Taboada, working in the Clinical Sciences Division of the School of Aerospace Medicine, developed a research program and experimental facility to investigate the laser-Raman spectroscopy of molecules in living systems. Dr. Taboada's studies of molecules and cells using Raman spectroscopy is intended to provide semi- or non-invasive diagnostic techniques for clinical testing, improving clinical diagnosis of Air Force personnel and monitoring the suitability of Air Force personnel to perform their tasks.

The promise of laser Raman spectrometry in carrying out this intent is evident from existing literature (1-4) and from preliminary published and unpublished experiments conducted by Dr. Taboada and me (5). Since the summer of 1983, Dr. Taboada and I were involved in developing several aspects of the laser Raman technique. The object of my summer 1983 collaboration with Dr. Taboada was to determine whether cultured normal and neoplastic mammalian and human cell types produced Raman spectra and whether these spectra were modified by exogenous stimulants. Since I was familiar with properties of the Y-1 mouse adrenal tumor cell line and its special culture conditions, we began the studies with these cells. Cultured steroid producing cells can be used for

studying the internal and external conditions affecting steroid production, and Raman spectra, because the intracellular molecules and steps involved in steroidogenesis are relatively well defined.

RESEARCH BACKGROUND AND PROPOSED EXPERIMENTS

From 1983 through the present, the author of this final report was funded by: two AFOSR/SCEEE RISE grants, a contract from the AFOSR/Utah Consortium for Biotechnology Research, and two SCEEE summer research fellowships. Each of these grants and fellowships contributed to the development of procedures designed to insure that laser Raman data acquisition from living mammalian cells would be valid. The RISE proposals provided funds for supplies, technicians, and equipment with which methods for preparing and examining cell samples in the Raman spectrometer could be optimized. The Utah consortium contract provided funds for equipment to be used to rapidly and accurately determine cell numbers, to determine division cycle times of the cultured cells being examined by spectrometry and to develop methods for examining purified molecules that are characteristic of cultured adrenal cells. Although these methods and the equipment were used to acquire additional Raman data during the 1984 AFOSR/SCEEE summer research fellowship, certain questions remained unanswered; these were the subject of the investigations conducted using 1984-85 RISE grant funds.

II. RESULTS

In this report the previous findings obtained using a mouse adrenal tumor cell line, Y-1, and a human neoplastic, respiratory tract, fibroblast cell line, HEP-2, are summarized; remaining questions still needing investigation for that particular facet of our work are then indicated; the experimental protocols used to investigate that question are described; and the results are then presented.

1. I initially proposed in the 1983 RISE application that the use of cell suspensions for Raman spectroscopy could be avoided if cells grown on coverslips were inverted over a wellled microscope slide containing HBSS. This proposal proved to be impractical because it necessitated focusing the incident laser beam within a single cell. An alternative method suggested by Dr. Taboada involved "tunneling" the laser beam into the edge of a microscope slide to which cells were attached, the beam caroms from surface to surface down the slide and stokes and anti-stokes wavelengths emitted from contacted cells on the slide surface are scanned by the photon detector. Determining practicality of Dr. Taboada's "tunneling" procedure must still be tried. Cells grown in steri-

lized microscope slide wells will be covered and positioned in the laser beam. Special slide holders with adjusting micrometers were required to allow us to introduce the beam into the slide end. These holders were to be fabricated at Brooks AFB. To date, I have not received information regarding their status.

TABLE I
COULTER COUNTER SIZING OF HEP-2 AND Y-1 CELLS

HEP-2					
<u>RUN</u>	<u>7-10</u>	<u>10-13*</u>	<u>13-15</u>	<u>15-20</u>	<u>20-25</u>
1	1.67	16.25**	10.01	9.92	0.33
2	3.14	15.89	11.54	11.91	1.69
3	1.42	15.92	8.97	10.52	0.87
4	1.01	17.22	9.21	9.99	0.99

Y-1					
<u>RUN</u>	<u>7-10</u>	<u>10-13</u>	<u>13-15</u>	<u>15-20</u>	<u>20-25</u>
1	3.76	11.89	13.88	4.79	1.01
2	1.12	8.39	10.58	2.12	0.21
3	1.10	12.89	12.32	3.51	0.89
4	2.43	9.35	13.18	4.80	1.23

* Counts for particles whose diameters (in microns) fall within this range. Space limitations prevent including standard errors of the mean; all counts were statistically valid.

** X 10⁻⁵ particles.

attempts were made using the Coulter counter purchased with Utah consortium funds to verify fragmentation and clumping results for HEP-2 cells, and extend this data to Y-1 cells. As understanding of counter operations improved, we also attempted to establish approximate cell diameters. By resetting the count discriminators to detect larger and larger particles after each count, we expected that fragment and clump counts, and cell size, could be inferred. Data concerning very small fragments and cell size was inconclusive. Further experiments were required to determine fragment counts and refine cell diameter ranges. Using the Coulter counter, these experiments confirmed existing data on Y-1 and HEP-2 cell fragment counts and refined cell diameter ranges (Table I). These studies conducted at Meharry Medical College using the previously purchased Coulter counter showed that: (a) only a relatively small number

of cell fragments (< 10 microns in diameter) were associated with HEP-2 and Y-1 cell suspensions; (b) since relatively few HEP-2 and Y-1 cell counts were recorded in the 15-25 micron range, this suggests that there were few cell clumps; (c) maximum counts were observed in the 10-13 micron range for HEP-2 cells; and (d) Y-1 cells diameters appeared to be less uniform because maximum numbers were detected in a 10 to 15 micron range (with slightly more cells measured in the 13-15 micron range).

3. Since beginning our studies, we have been concerned about long-term laser irradiation effects on a suspended cell. In previous studies beam effects on cell mortality were determined by counting live/dead cells before and after Raman spectrometry. These were negligible. Laser effects on physiological parameters such as steroidogenesis, remain to be determined. We proposed carrying out these experiments at Brooks AFB, however, Dr. Taboada has not completed renovation of the Raman spectrometer; he has been having difficulty resilvering mirrors. Control cells and cells exposed to various laser wavelengths during a standard scanning run were to be divided into two equal samples with each being incubated thirty minutes. One sample was to be incubated with 10 milliunits of ACTH, the other would serve as control. Since a laser tuned to the wavelengths associated with cytochrome emissions might have affected steroid production, we would have expected to observe reduced steroidogenesis if these experiments could have been completed.

4. To explain high levels of Raman spectral activity obtained from HEP-2 and Y-1 cells during my 1983 summer research fellowship, I suggested metabolic and cell surface activities as sources of these spectra and Dr. Taboada felt that mitosis might be an alternative source of this activity. To conduct these evaluations, time-lapse videotaping capabilities was needed for the inverted Nikon microscope which was obtained for me by the Utah consortium. Time-lapse videomicroscopy can establish both cycle time between mitoses and cell surface activity. Several factors (insufficient image magnification and illuminating intensity, and lack of a sensitive videocamera and a time-lapse videotape recorder) previously prevented us from obtaining data related to the above goal. Although we were able to obtain a lens with sufficient enlargement capabilities and we purchased an illuminator with sufficient intensity to provide adequate contrast, sufficient funds to purchase a sensitive videocamera and videotape recorder capable of time-lapse operation were not available. Experiments to clarify the involvement of cell surface activity and mitosis in Raman activity were therefore not conducted at Meharry Medical College.

5. Because differentiated cellular function depends on large concentrations of certain unique intracellular molecules, in previous experiments we obtained preliminary suggestions that characteristic Raman spectra are produced by intracellular HEP-2 or Y-1 molecules irradiated with a laser beam tuned to one of several wavelengths. Using 514 and 488 nm, data obtained from both cell lines was encouraging but inconclusive because of insufficient replication.

We also used ATP as one of the stimulants of 514 nm irradiated HEP-2 cells; this stimulant produced interesting effects on spectra when used in the summer of 1983 (5). Eventhough ATP was only used once this summer as a HEP-2 treatment, we were unable to repeat previous results for reasons that are unclear. We also used cAMP as a stimulant of 514 nm irradiated HEP-2 cells. Our use of cAMP as a stimulant resulted from information suggesting that dibutyryl cAMP was used to decrease the yield of Herpes-Simplex 1 virus particles released from inoculated HEP-2 cells (6). Although our cells were uninoculated, we used the precedence of this work to guide ours. In two replications, no repeat events were associated exclusively with cAMP; this was too few replicates to sustain any conclusions about this work. Although we intended to repeat each of these experiments several times more to obtain information about "signature" emissions by HEP-2 cells and about ATP and cAMP effects, lack of an operating laser Raman spectrometer prevented completion of these experiments. Similarly, the cytochrome response of HEP-2 cells to irradiation at 476.5 and 488 nm also needed to be investigated because literature studies indicated that HEP-2 cells irradiated with 6.5 mm radiowaves of 1 mW/cm² flux density reduced cytochrome oxidase and NAD- and NADP-diaphorase activities (7). Since radar effects on operating personnel is one concern of the Air Force, such a study might have proved to be a valuable tool in evaluating radar effects. Again, lack of an operating Raman system prevented us from conducting these studies.

6. In experiments conducted during the summer of 1984, two repeated emissions by intracellular molecules were obtained from two cAMP-treated Y-1 replicates irradiated with 514 nm. Whether these events result from cAMP treatment, or characteristic emissions of the Y-1 adrenal cell, was uncertain. Since control cells were only scanned once, these results were also inconclusive. All events associated with a single treatment component will continue to be inconclusive if they occur during scanning-time for another event because the present spectrophotometer is still not completely converted to detecting a large number of events simultaneously. In the 1984 experiments there were too few replicates to draw conclusions about "signature" molecules in Y-1 cells

irradiated at 514 nm. These experiments could not be repeated at Brooks AFB because the laser spectrometer is no longer operable nor have Raman spectrometer modifications permitting detection of a larger number of events in one scan been completed.

7. In the 1984 experiments we detected no repeated emissions by intracellular molecules in cAMP-treated Y-1 cells irradiated at 488 nm. Lack of replication of this cAMP treatment prevents conclusions from being drawn. As discussed previously, events that were noted only in controls may occur, but be missed, during scanning. In addition, the existing three replications of the experiment did not seem sufficient to draw conclusions about common cellular events, although it was interesting that a limited number of events common to both treatments were observed during those experiments. In particular, any events encompassing a range of 6 - 8 wave numbers might represent characteristic Y-1 cell molecular emissions after irradiation at 488 nm. More replication was required to verify those possibilities. Lack of a functioning laser Raman spectrometer prevented further replication of our observations during the period of this grant.

8. The 1984 experiments using Y-1 cells irradiated at 476.5 nm involved runs repeated on the same sample, runs on different samples, and a run on a sample pool of three different cell generations. Rigid criteria were established to judge events. These criteria included: the occurrence of only a few events per treatment category, the repetition of an event in at least 50% of the replicates, a relatively narrow range of wave numbers in an event, and the appearance of a given event in > 3 treatments. Because of the number of runs on these different Y-1 samples and the use of rigid judgements in designating valid events, emissions that were recorded in these experiments may be considered characteristic of the various control Y-1 cell treatment components at 476.5 nm.

Data obtained using these criteria suggested that relatively large concentrations of unique intracellular molecules can produce characteristic Raman signatures for a particular cell type. Detection of 476.5 nm-stimulated emissions appeared to be improved if a parallel polarizer was inserted between sample and detector to minimize background fluorescence.

Non-polarized emissions from controls appeared in a narrow event range in 50% of the replicates at three different wave numbers, $> 50\%$ of the polarized control cell emissions were associated with seven narrow range events, and only three events were narrow range in 44% of the control replicates regardless of polarity. In

response to cAMP stimulation, Y-1 cells seemed to produce few emissions, regardless of polarity, differing from those of control cells. However, a single non-polarized relatively narrow range emission recorded in the combined control/cAMP-treated cell data was replicated in 50% of the runs. Polarization improved stimulated event detection in the control/cAMP-treated cells; six relatively narrow range events were detected in 50% or more of the replicates. The relatively large number of replications available by pooling data from all treatment components revealed that sixteen relatively narrow range emissions occurred $\geq 50\%$ in three, or four, of the components; one of these (720-1-3-4-8-30) was replicated eleven out of fourteen times.

The 476.5 wavelength produced what appeared to be several characteristic Y-1 emissions at 480, 600, 900, 970, 1010, 1060, 1650, and 1750; these emissions are analogous to 476.5 nm irradiated carotenoid and heme protein emissions (8). Although two other wave numbers were also associated with these molecules (1330 and 1430), events at these wave numbers were cancelled by water scan background events. If water events at 1335 were disregarded, six out of fourteen events would be recorded. Similarly, 1418 and 1438 +5 water events cancelled three events centering around 1430. Carotenoids and cytochromes irradiated at 488 nm emit at wave numbers of 1040, 1300, and 1460 (8).

It must be noted that most mammalian cells in vivo and in vitro are unable to synthesize carotenoids and their derivatives; they are, however, able to absorb them from their nutrients (9). Vitamin A, a carotenoid, is stored in intracellular adrenocortical lipid droplets (10, 11). Rats deficient in vitamin A show reduced rates of glucocorticoid production, probably due to failure of deoxycorticosterone to be hydroxylated to the glucocorticoid, corticosterone (12, 13). The Eagle's minimum essential medium with Earle's salts used in culturing Y-1 adrenal cells did not contain carotenoids (Gibco catalog, Palo Alto, CA). Whether these molecules could be absorbed from the serums used in their maintenance was unknown until recently. Now information regarding the major constituents of serums is available; HyClone Laboratories (Logan, Utah) indicates that their fetal bovine and horse serums contain, respectively, a total of > 209 and 233 ng/100 g serum of these carotenoids: retinoic acid, retinyl palmitate, retinyl acetate, retinol and carotene. In the summer of 1984, there was some uncertainty that Y-1 cells could have absorbed carotenoids from their incubating medium because we used fetal bovine and horse serum from KC Biological (Lexina, Kansas). In our report we suggested that serums from different commercial sources should not differ; we have now consulted with KC Biologicals and confirmed that their serums do

contain a carotenoids. In 1984 we observed that adrenal cells contain large concentrations of various cytochromes, flavo- and heme proteins, including cytochromes a, a3, b, b5, c, c1, side-chain cleavage, 11 beta and 21 beta P-450s, P-420, adrenodoxin, flavoprotein and non-heme iron (14, 15). These iron-containing proteins are used in the synthesis of steroid hormones, or to provide energy-containing compounds for viability and steroid synthesis (16). Concentrations for a few bovine adrenal mitochondrion and microsome heme proteins represent a total of 151 nanomoles heme protein/mg protein may exist in a bovine adrenal cell. While similar figures do not exist for Y-1 adrenal cells, the bovine concentrations may be extrapolated using the conversion factor: 0.6 nanograms protein/mouse adrenal cell (17). In our experiments we routinely used 1.2 million cells; our sample, therefore, had approximately 108.7 total nanomoles heme protein. At the time of our 1984 proposal we suggested that Y-1 cells would be useful as models both for studying carotenoids and for examining laser Raman spectra associated with iron-containing compounds.

To further study phenomena identified during the 1984 summer experiments, techniques for enriching cellular carotenoids in Y-1 and HEP-2 cells were to be used to examine effects on signature spectra. Vitamin A or other carotenoids would be dissolved in organic solvents and dried onto Diatomaceous sands in order to provide large surface areas coated with the carotenoids. Diatomaceous sands would then be incubated with cell culture serums at 37° C for three hours, centrifuged to remove the sand, filter sterilized, then added to Eagles' minimum essential medium for incubation with HEP-2 or Y-1 cells. Following enriched, or non-enriched, cell stimulation with cAMP or ACTH, control and stimulated cells or their subcellular components were to be chloroform/methanol extracted and carotenoids in the extracts were to be identified using high pressure liquid chromatography (HPLC). Although cells were incubated using the above protocol and extracted, HPLC could not be performed. A special column is required for this type of chromatography; after we completed extraction and attempted to purchase this column in June 1985, we found that our budget, representing the first \$9000 sent to us by SCEEE, was exhausted. SCEEE did not provide the paper work indicating we had recieved the remaining \$3000 of our \$12,000 grant until the second week of November. We have ordered the column and are awaiting its arrival to complete our experiments.

Experiments to be conducted at Brooks AFB using cytochrome inhibitors which bind (aminogluthethimide, metapyrone or aniline) or poison (carbon monoxide or cyanide) cytochromes could not be completed because a spectrometer was not available.

For the same reason we could not investigate HEP-2 cell cytochrome response to irradiation at 476.5 and 488 nm even though literature studies indicated that these cells irradiated with 6.5 mm radiowaves of 1 mW/cm² flux density reduced cytochrome oxidase and NAD- and NADP-diaphorase activities (7). Since one of the Air Force concerns is for personnel exposed to radar, HEP-2 treated according to the preceding protocol might have provided valuable insight into this area.

REFERENCES

1. Webb, S.J., and Stoneham, M.E., "Resonances Between Ten To The Eleventh Power And Ten To The Twelfth Power Hz In Active Bacterial Cells As Seen By Laser Raman Spectroscopy," Physics Letters, Vol. 60A, pp. 267-268 (1977).
2. Davydov, A.S., "The Migration Of Energy And Electrons In Biological Systems," Biology And Quantum Mechanics, (Pergamon Press, Oxford, U.K., 1982), pp. 185-207.
3. Bilz, H., Buttner, H., and Froelich, H., "Electret Model For The Collective Behavior Of Biological Systems," Z. Naturforsch., Vol. 36B, pp. 208-212 (1981).
4. Webb, S.J., Lee, R., and Stoneham, M.E., "Possible Viral Involvement In Human Mammary Carcinoma: A Microwave and Laser-Raman Study," International Journal of Quantum Chemistry, Quantum Biology Symposium 4, (John Wiley and Sons, Inc., New York, 1977), pp. 277-284.
5. Taboada, J., and Mrotek, J., "Evidence for Davydov Solitons in the Anti-stokes Raman Spectra of Living HEP-2 and Y-1 Cancer Cells," Abstract presented to the annual American Physical Society meetings, San Antonio, Texas (1984).
6. Stanwick, T.L., Anderson, R.W., and Nahmias, A.J., "Interaction between cyclic nucleotides and herpes simplex viruses: productive infection", Infect. Immun., Vol. 18, pp. 342-347 (1977).
7. Zaliubovskaia, N.P., and Kiselev, R.I., "[Biological Oxidation in Cells Exposed to Microwaves in the Millimeter Range]", Tsitol. Genet., Vol. 12, pp. 1232-1236 (1978).
8. Yu, T., and Srivastava, U., "Raman Spectroscopy of Ferrocyclochromes and Carotenoids", J. Raman Spectro-

scopy, Vol. 9, pp. 166-175 (1980).

9. Willmer, J.S., and Laughland, D.H., "The Distribution of Radioactive Carbon in the Rat After the Administration of Randomly Labeled C14-beta Carotene", Cand. J. Biochem. Physiol., Vol. 35, pp. 819-826 (1957).
10. Popper, H., and Greenberg, R., "Visualization of Vitamin A in Rat Organs by Fluorescence Microscopy" Arch. Path., Vol. 32, pp.11-32 (1941).
11. Wallace, D.L., Plopper, C.G., Bucci, T.J., and Sauberlich, H.E., "Autoradiographic Localization of Vitamin A in the Adrenal Gland of Rats. Life Sciences, Vol. 17, pp. 1693-1698 (1975).
12. Lowe, J.S., Morton, R.A., and Harrison, R.G., "Aspects of Vitamin A Deficiency in Rats", Nature, Vol. 172, pp. 716-719 (1953).
13. Johnson, B.C., and Wolf, G., "The Function of Vitamin A in Carbohydrate Metabolism; Its Role in Adrenocorticoid Production", Vitamins and Hormones, Vol. 18, pp. 457-483 (1968).
14. Cooper, D.Y., Levin, S., Narasimhulu, S., Rosenthal, O., and Estabrook, R.W., "Mechanism of C-21 Hydroxylation of Steroid", Functions of the Adrenal Cortex, Vol. 2, pp. 897-941 (1968).
15. Purvis, J.L., Battu, R.G., and Peron, F.G., "Generation and Utilization of Reducing Power in the Conversion of 11-Deoxycorticosterone to Corticosterone in Rat Adrenal Mitochondria", Functions of the Adrenal Cortex, Vol. 2, pp. 1007-1055 (1968).
16. Hall, P. F., "Part IV. Mixed-function Oxidases Of The Adrenal Cortex. Properties Of Soluble Cytochrome P-450 From Bovine Adrenocortical Mitochondria," Annals Of The New York Academy Of Sciences, Vol. 212, pp. 195-207 (1973).
17. Mrotek, J.J., and Hall, P.F., "Response Of Adrenal Tumor Cells To Adrenocorticotropin: Site Of Inhibition By Cytochalasin B," Biochemistry, Vol. 16, pp. 3177-3181 (1977).

MILITARY FAMILY STRESS AND JOB PERFORMANCE

SUBMITTED BY: Lena Wright Myers

ACADEMIC
RANK: Professor

DEPARTMENT AND
UNIVERSITY: Department of Sociology
Jackson State University
Jackson, MS

DATE: July 31, 1985

CONTRACT NUMBER: F49620-82-C-0035

INTRODUCTION

This is a study of the relationship between family stress and job performance in the Air Force. There is an emphasis in this study that differentiates it from most previous studies of military family stress. That emphasis is upon the effects of family stress on work attitudes and behavior. Most of the previous research has focused on the influence of being in the military upon the family. One potentially important effect that does not appear to have been studied at all is the possible influence of family stress on occupational commitment and job involvement. Work and family are typically not separate and isolated arenas. Therefore, it seems reasonable to expect that marital stress would influence level of commitment to work and as a result, would affect occupational role performance and even the decision to stay on the job. This study includes an analysis of factors that affect self-investment in work of Air Force Personnel, including family related stress.

Stress in dual career families often results from the fact that, in order to stay together, one spouse must change jobs if the other's career requires movement from one geographic area to another. This is likely to be an especially difficult problem for military families because of the frequency of moves among posts. The purpose of this study is to examine the ways in which family stress generated

by the career problems of their wives influence the work orientation and job performance of Air Force Personnel.

The data for the research was secured by interviewing one hundred men in the Air Force from dual career families at Keesler Air Force Base in Biloxi, Mississippi. The names were randomly picked from a list of all married men at Keesler whose wives were employed at the time of the study. The interviews were done by appointment in a private office on the Base. The interviews were conducted by two professionally trained interviewers. A pretest of the interview schedule was conducted with 10 male Air Force Personnel at Keesler.

Information was collected in the interviews regarding level of stress resulting from dual career families which was the independent variable. The interview schedule also included measures of self-investment in work and self-perceived occupational role performance which were the dependent variables. There were also variables which the researcher assumed might influence the relationship between family stress and the hypothesized work-related outcomes of such stress. Examples were age, career stage, military occupational speciality, and stress tolerance. A major focus of this report is upon the way in which the nature and level of one's job influences the relationship between family stress and job performance.

This research was sponsored by the United States Office of Scientific Research and subcontracted by the Southeastern Center for Electrical Engineering (SCEEE) and Jackson State University. The proposal was developed while the researcher served as a 1984 Summer Faculty Research Fellow.

CHARACTERISTICS OF THE SAMPLE

The largest proportion of the sample, eighty-four percent, entered the Air Force as basic enlistees. Only 13 of the sample entered the Air Force as commissioned officers; 3 were First Lieutenants and 13 were Second Lieutenants. Our sample had been in the Air Force an average of 15 years with a range from 3 to 30 years. The age ranged from 21 to 52 years. The highest rank among the persons interviewed was a Colonel and the lowest a Staff Sergeant.

TABLE 1
RESPONDENTS' EDUCATION

Education	No.	%
High School	25	25.0
Some College	40	40.0
College Degree	21	21.0
Masters Degree	4	4.0
Post Masters	7	7.0
Ph.D.	1	1.0
M.D.	2	2.0
Total.	100	100.00

Table 1 gives the breakdown of the educational level of the sample. The categories, "1 year of college," "2 years of college," and "3 years of college" were collapsed into one category - "some college." This was the largest category with 40 respondents having this amount of education. Twenty-five respondents were high school graduates; 21 were college graduates; 4 had obtained a masters degree; 7 had post master training; 1 had a Ph.D. and there were 2 medical doctors included in the sample.

The respondents were asked to list their specific job titles as given to them by the Air Force. The result of this probe was a listing of 30 different job levels. For analytical purpose, the 30 job levels were collapsed into 2 levels: one was a managerial and professional level and the other a clerical and technical level.

Job titles include:

1. Instructor
2. Micro-biologist
3. Chief of Computer Maintenance
4. Supervisor Work Center
5. Public Affairs Specialists
6. Inspector General
7. Lab Technician
8. Computer Technician
9. Airmen Performance Reporter
10. Satellite Communication Technician
11. Director of Information Systems Doctrine Office
12. Deputy Base Commander
13. Staff Radiation Physist
14. Executive Officer
15. Operation Officer (Communication)
16. Chief of Security (Police)
17. Legal Service Technician
18. Discharge Case Worker
19. Personnel System
20. Documentation Clerk
21. Transportation Specialist
22. Flight Supervisor
23. Administrative Specialist
24. Air Traffic Controller
25. Computer Operator
26. Chief of Training Evaluation Division
27. Assignment Clerk
28. Documentation Clerk

EDUCATION AND EMPLOYMENT OF WIVES

The following Table shows the level of education obtained by the respondents wives. Most of the wives had at least a high school education, 25 percent had some college, 11 percent had a college degree, 16 percent had a masters degree, and 4 percent had some post graduate education.

TABLE 2
EDUCATIONAL LEVEL OF WIVES

Education	No.	%
Less than High School	8	8
High School	36	36
Some College	25	25
College Degree	11	11
Master Degree.	16	16
Post Masters	4	4
Total	100	100

Table 3 shows the types of jobs held by the wives of the men interviewed. Table 3 shows the majority of the wives were employed as clerical, 20 percent as teachers, 19 percent nurses, 7 percent social workers, 13 percent in private business, and 6 percent were factory workers. The respondents were asked if their wives' present job was the one she had most of the time and 94 percent said that it was. They were also asked if they thought that the job presently held by their wife was one she planned to stay in until she retired and 56 percent answered affirmatively.

TABLE 3
EMPLOYMENT OF WIVES

Job	No.	%
Private Business	13	13
Clerical	35	35
Teacher	20	20
Nurse	19	19
Social Worker	7	7
Factory Worker	6	6
Total	100	100

Because we are concerned with family stress resulting from the wife's work experience , the level of job satisfaction of the wife is an important variable. The resources available for the study did not permit interviewing both husbands and wives so the only information we have is the husband's report of his perception of his wife's job satisfaction. This may not be a major shortcoming since the focus of the study is on family stress and it is unlikely that a level of dissatisfaction sufficient to generate such stress would go unnoticed by the husband. The following table shows the level of job satisfaction of wives as perceived by the respondents in this study.

TABLE 4
WIVES' JOB SATISFACTION AS PERCEIVED BY HUSBAND

Level of Satisfaction	No.	%
Very Satisfied	43	46
Somewhat Satisfied	27	29
Neither Satisfied nor dissatisfied	9	9
Somewhat dissatisfied	6	6
Very Dissatisfied	9	10
Total	94	100

The respondents were also asked whether they thought that moving from one base to another made it difficult for their wives to find jobs. Sixty-two percent answered "yes" to this question. Table 5 shows the response to a follow-up question asking how often this problem was experienced. It is clear from these data that a substantial proportion of wives is dual career — Air Force families have problems of this kind.

TABLE 5
REPORTED DIFFICULTY OF WIVES FINDING JOBS

Frequency of Occurrence of Difficulty	No.	%
Always	28	28
Most of the Time	22	22
Sometimes	11	11
Hardly Ever	10	10
Not Applicable	29	29
Totals	100	100

EFFECTS OF FAMILY STRESS ON JOB PERFORMANCES

A series of questions were asked that were intended to find out if the respondents saw any effect of family stress on how well they performed their jobs. The questionnaire items were in the form of statements with which the respondents were asked to agree or disagree. The responses to these items show that many of the Air force Personnel are aware of problems of this sort. Table 6 reports these data.

TABLE 6
FAMILY STRESS AND JOB PERFORMANCE

Items	Strongly Agree		Agree		Neither Agree nor Disagree		Disagree		Strongly Disagree		Totals	
	No.	%	No.	%	No.	%	No.	%	No.	%	No.	%
"Worrying about things at home sometimes keep me from doing as good a job as I could"	7	7	27	27	13	13	42	42	11	11	100	100
"I often think about problems at home when I am at work"	1	1	17	17	27	27	41	41	14	14	100	100
"My wife is happy that I am in the Air Force." . .	25	25	37	37	21	21	15	15	2	2	100	100
"The necessity to move frequently from one base to another causes tension between my wife and me." . .	5	5	31	31	14	14	30	30	20	20	100	100
"My job often interferes with my family life." .	1	1	19	19	21	21	39	39	20	20	100	100

Additional evidence regarding a potential influence of family stress on job performance is provided by data collected on self investment in work. Self investment in work refers to the level of commitment to work based on the effect of work on one's self esteem. Evidence from previous research indicates that there is a wide range in the extent to which occupational achievement affects self-esteem. It seems reasonable to expect a relationship between level of commitment to work and level of job performance: persons with a high level of self investment in work should have higher levels of occupational achievement. If family stress affects self investment in work, it may also affect job performance. The following table reports the relationship between an item measuring family stress and one measuring self investment in work.

TABLE 7
FAMILY STRESS AND WORK COMMITMENT

Work Commitment Item: "The most important things that happen to me involve my job."	Family Stress: "I often think about problems at home when I am at work."				Totals	
	Agree		Disagree			
	No.	%	No.	%	No.	%
Agree	18	64.3	8	11.4	26	26.5
Disagree	10	35.7	62	38.6	72	73.5
Totals	28	100.0	70	100.0	98	100.0

$\chi^2 = 28.37$ $df = 1$ $\alpha = .05$

The data in Table 7 indicate a statistically significant relationship between family stress and commitment to work. This relationship merits further study in subsequent analyses of the data from this research project and in future projects.

Because we have data regarding both family stress and perceived job performance, it is also possible to analyze the relationship between measures of these two variables. This relationship is examined in Table 8.

TABLE 8
FAMILY STRESS AND JOB PERFORMANCE

Family Stress Item: "I Often think about Problems at home when I am at work."	Job Performance Item: "The Person I work for is very satisfied with my work performance."				Totals	
	Agree		Disagree			
	No.	%	No.	%	No.	%
Agree	14	32.6	53	93.0	67	67.0
Disagree	29	67.4	4	7.0	33	33.0
Totals	43	100.0	57	100.0	100	100.0

$$\chi^2 = 40.47 \quad df = 1 \quad r = .05$$

According to the data in Table 8, there is a statistically significant relationship between family stress and perceived job performance. This finding in conjunction with the other data reported above suggests that further analysis of this relationship would be fruitful. Additional analyses of data from the present study which bear on this relationship are planned.

EFFECTS OF JOB LEVEL

In the process of analyzing data from this study, an interesting and unexpected finding was obtained. There appears to be a systematic difference in the major variables with which we are concerned depending upon, the level and nature of the respondent's job in the Air Force. When responses of persons in managerial and professional jobs are compared with those of persons in clerical and technical jobs, differences appear in both potential for family stress and in perceived job performance. This classification corresponds to some extent with the rank of the respondents and rank may also account for some of the findings.

TABLE 9
FREQUENCY OF WIFE'S DIFFICULTY IN FINDING EMPLOYMENT

Job Levels	Hardly Ever		Somewhat		Most of the Time		Always	
	No.	%	No.	%	No.	%	No.	%
Managerial and Professional	4	40	9	82	8	36	10	36
Clerical and Technical	6	60	2	18	14	64	18	64
Totals	10	100	11	100	22	100	28	100

N = 71 $\chi^2 = 10.43$ df = 3 P < .02 No Response = 29

Data in Table 9 show that for wives of those respondents in managerial and professional positions, 40 percent hardly ever experienced difficulty in finding employment; 32 percent sometimes experienced this difficulty; 36 percent reported difficulty "most of the time," and 10 percent reported that they always experienced difficulty in securing employment on the new base. Among clerical and technical personnel, however, a higher proportion of their wives experienced difficulty in finding employment after relocation. When respondents' job level was run against how frequently the wife experienced difficulty in finding employment, a significance relationship was shown. The majority of the wives overall, 50, experienced difficulty in finding employment most or all of the time.

TABLE 10
WIVES SATISFACTION WITH PRESENT JOB

Job Level	Wives' Satisfaction with Present Job									
	Very Satisfied		Somewhat Satisfied		Neither		Somewhat Dissatisfied		Dissatisfied	
	No.	%	No.	%	No.	%	No.	%	No.	%
Managerial and Professional	23	53	14	52	7	78	2	33	1	11
Clerical and Technical	20	47	13	48	2	22	4	64	8	39
Totals	43	100	27	100	9	100	6	100	9	100

N = 94 $\chi^2 = 9.76$ df = 4 P < .05

In analyzing the variable, wife's satisfaction with present job, it was found that overall, 43 women were very satisfied with their present jobs, while 27 were reported by their husbands as being somewhat satisfied. Twenty-four wives were reported as being indifferent or dissatisfied with their present jobs. There was a statistically significant relationship between job level and wives' satisfaction with present job. Wives of Air Force personnel in managerial and professional positions were more satisfied than were the wives of the personnel in other positions.

TABLE 11
LACK OF PROMOTION DUE TO JOB PERFORMANCE

Job Level	"Because of problems with how I do my job, I may not be promoted as soon as I would like."							
	Agree		Neither Agree Nor Disagree		Disagree		Strongly Disagree	
	No.	%	No.	%	No.	%	No.	%
Managerial and Professional	2	20	7	43	28	51	12	63
Clerical and Technical	8	80	9	57	27	49	7	37
Totals	10	100	16	100	55	100	19	100

$$N = 99 \quad \chi^2 = 11.53 \quad df = 3 \quad P < .01$$

Lack of promotion due to job performance was a variable examined in this research. This was measured through the use of a scale with responses ranging from strongly agree to strongly disagree with a statement saying, "Because of problem with how I do my job, I may not be promoted as soon as I would like". On the management and professional level, 2 persons agreed that a lack of promotion was due to job performance, while 7, 28, and 12 were indifferent, disagreed,

and strongly disagreed, respectively. Eighty percent of those respondents in clerical and technical positions agreed that job performance was one reason for not being promoted, while 57 percent neither agreed or disagreed, 49 percent disagreed and 37 percent strongly disagreed.

There was a strong relationship between the variables. Those respondents in clerical and technical positions agreed more so than the personnel in managerial and professional positions that they were not promoted because of job performance. On the other hand, managers and professionals disagreed, more so than others, that lack of promotion was due to job performance.

TABLE 12
RATING OF JOB PERFORMANCE AS BETTER THAN AVERAGE

Job Level	"I am probably better than average on my job"									
	Strongly Agree		Agree		Neither Agree Nor Disagree		Disagree		Strongly Disagree	
	No.	%	No.	%	No.	%	No.	%	No.	%
Managerial and Professional	21	65	17	33	7	78	2	50	2	50
Clerical and Technical	11	35	34	67	2	22	2	50	2	50
Totals	32	100	51	100	9	100	-	100	-	100

N = 100 $\chi^2 = 11.53$ df = 4 P < .05

Among managerial and professional respondents 21 strongly agreed that their performance on the job was better than average, 17 agreed, 7 were indifferent, 2 disagreed, and 2 strongly disagreed. However, 11 clerical and technical personnel strongly agreed that their job performance was better than average, and only 2 strongly disagreed.

The relationship between job level and respondents rating their job performance as being better than average was found to be significant. The pattern of this relationship, however, is not altogether clear. There are substantial differences between the proportion persons in the two job levels who "strongly agree" and who "agree" with the assertion that their performance is better than average but the differences are in opposite directions on the two response categories. Additional research may be required to explain the nature of this relationship.

TABLE 13
SUPERVISORS' SATISFACTION WITH JOB PERFORMANCE

Job Level	The person I work for is very satisfied with my job performance									
	Strongly Agree		Agree		Neither Agree Nor Disagree		Disagree		Strongly Disagree	
	No.	%	No.	%	No.	%	No.	%	No.	%
Managerial and Professional	20	54	22	43	0	0	5	83	2	100
Clerical and Technical	17	46	29	57	4	100	1	17	0	0
Totals	37	100	51	100	4	100	6	100	2	100

N = 100

$\chi^2 = 9.33$

df = 4

P < .05

Supervisor's satisfaction with job performance was looked at in reference to the respondents' view of this variable. On the managerial and professional level, it was strongly agreed by 20 (54 percent) of these persons that their supervisors were satisfied with their job performance, while 17 (46 percent) strongly agreed in the clerical and technical positions. The level of disagreement, however, on both levels was low: the respondents at both levels felt that their supervisors approved of their job performance. This relationship was found to be significant at less than the .05 level but the nature of the relationship is not clear. The managerial and professional personnel appear to have stronger opinions about the views of their supervisors with a higher percentage at both ends of the range on the variable. This is the pattern that would be expected among persons with higher self investment in work.

TABLE 14

PERFORMANCE LEVEL BETTER THAN OTHERS

Job Level	"I think I do my job better than most others with whom I work."									
	Strongly Agree		Agree		Neither Agree Nor Disagree		Disagree		Strongly Disagree	
	No.	%	No.	%	No.	%	No.	%	No.	%
Managerial and Professional	20	57	15	43	10	50	3	33	1	100
Clerical and Technical	15	43	20	57	10	50	6	64	0	0
Totals	35	100	35	100	20	100	9	97	1	100

N = 100 $\chi^2 = 3.38$ df = 4 P > .05

Respondents were asked if their job performance on base was better than others. Table 14 is a compilation of those responses. The relationships between job level and the perception that one's job performance level is better than others is not statistically significant. The general pattern in the distribution of responses is similar to the preceding table: most of the respondents report that they are performing well on the job.

TABLE 15
EFFECTS OF PROBLEMS AT HOME OR WORK

Job Level	"Worrying about things at home sometimes keeps me from doing as good a job as I could."									
	Strongly Agree		Agree		Neither Agree Nor Disagree		Disagree		Strongly Disagree	
	No.	%	No.	%	No.	%	No.	%	No.	%
Managerial and Professional	0	-	13	48	7	54	19	45	10	90
Clerical and Technical	7	100	14	52	6	46	23	56	1	10
Totals	7	100	27	100	13	100	42	100	11	100

N = 100 $\chi^2 = 14.82$ df = 4 P < .01

It was also assumed in this research that worrying about problems at home might hamper one's work. Data in Table 15 show that at the managerial and professional level, no one strongly agreed that this was a problem, while 10 of the respondents strongly disagreed. Seven of the clerical and technical personnel strongly agreed and only 1 strongly disagreed.

A significant relationship exists between respondents' job level and a lowering of job performance as a result of worrying about problems at home.

TABLE 16

GEOGRAPHIC MOBILITY AS A SOURCE OF FRICTION BETWEEN
FAMILY MEMBERS

Job Level	"The necessity to move frequently from one base to another causes tension between my wife and me."									
	Strongly Agree		Agree		Neither Agree Nor Disagree		Disagree		Strongly Disagree	
	No.	%	No.	%	No.	%	No.	%	No.	%
Managerial and Professional	2	40	13	45	2	14	18	60	12	60
Clerical and Technical	3	60	16	55	12	36	12	20	8	40
Totals	5	100	29	100	14	100	30	100	20	100

$N = 98$ $\chi^2 = 11.61$ $df = 4$ $P < .05$

A possible cause of stress at home with wife and family was frequent moving. Of the total sample, over one third said that frequent moves produced stress at home. This appears to be a somewhat greater problem for clerical and technical personnel than for managerial and professional personnel. A higher proportion of the former group than the latter agreed that this was a problem while managers and professionals tended to disagree more often. This relationship was statistically significant at less than the .05 level.

SUMMARY AND CONCLUSIONS

Previous research on dual career families indicates that frequent geographic mobility required by one spouse's career creates problems for the other spouse that produce family stress. There is also research evidence showing that family stress may affect performance on the job. This study contributes to this body of research by examining the relationship between family stress and job performance among Air Force personnel, whose frequent moves among bases is especially likely to create stress in dual career families.

The data show that one-half of the respondents say that their wives were only somewhat satisfied or, in some measure, dissatisfied with their jobs. Also, a substantial majority of the respondents reported that their wives had problems finding jobs as a result of the necessity of moving from one base to another. It is clear that these respondents recognize that a problem exists in this area. The effect of family stress on job performance was also apparent in the results of this study.

One of the major findings of this study is that the problems related to frequent geographic mobility, family stress, and job performance are not evenly distributed across different military ranks and types of jobs. Personnel in lower ranking clerical and technical positions appear to have more difficulty of this

type than do personnel in higher ranking managerial and professional positions. Wives of the clerical and technical respondents have more difficulty finding jobs and report less satisfaction with their present jobs. In addition the respondents in clerical and technical positions more often said that problems at home affected their job performance and that geographic mobility was a source of family stress. Air Force personnel in this category also saw a closer link between job performance and lack of promotion.

These results indicate a promising direction for future research. Studies following up on the project should be designed to add information about who is or is not affected by family stress related to frequent geographic mobility and should provide a more detailed explanation for these differences. Research of this type would be useful in pinpointing the persons whose work attitudes and behavior are most likely to be affected by family stress and would be helpful in designing programs to help relieve these problems.

UNITED STATES AIR FORCE SURVEY

Hello, my name is

I am working on a survey being done by Jackson State University and a grant from the United States Air Force. We are interviewing men in the Air Force from dual-career families, that is, where both husbands and wives are employed. You are one of the people here at Keesler who have been selected to be interviewed. Your name was picked from a list of all married persons at Keesler. It will not take much of your time. Your answers will be strictly confidential and, in fact, your name will not be put on the answer sheet.

Lena Wright Myers, Ph.D.
Professor of Sociology

1. How long have you been in the Air Force? _____
2. At what rank did you enter the Air Force? _____
3. How long have you been in your present rank? _____
4. Do you plan to stay in the Air Force until you retire?
____ Yes (1)
____ No (2)
5. If yes, is there anything that might make you change your mind?
____ Yes (1)
____ No (2)
 - a. If yes, what? _____
 - b. If no, why are you leaving? _____
 - c. What do you plan to do when you leave? _____
6. At what Base were you before you came here? _____
 - a. How long were you there? _____
 - b. Where were you before you went to that Base? _____
 - c. How long were you there? _____

[Note to Interviewer: Skip temporary duty assignments of 6 months or less in duration. Obtain history of moves for past _____ years]

Now we would like some information about your job in the Air Force. What is your present job? (GET SPECIFIC TITLE)

7. a. _____
(Job Title not Rank)
- b. What do you do on the job? What are some of your duties?

- c. How long have you been in that job? (GET YEAR AT WHICH CONTINUOUS EMPLOYMENT ON THIS JOB BEGAN)

Year,

3. Now we would like to find out about the jobs of members of your family. What was your father's occupation at the time you left high school?

a. _____
(Job Title)

b. Was that the kind of job he did most of his life? (Check One)

(1) _____ Yes (Go to Question 9)

(2) _____ No

c. If no, what kind of job did he have most of the time?

(Job Title)

9. Was your mother employed at the time you left high school? (Check one)

(1) _____ Yes (Go to Question b)

(2) _____ No

a. If yes, what kind of job did she have?

(Job Title)

b. If no, was she ever employed full-time?

(1) _____ Yes

(2) _____ No

c. If yes, what kind of job did she have most of the time she was employed?

(Job Title)

d. If no, (Go to Question 10)

10. MARRIED

a. Is your wife employed?

___ Yes (1) What kind of job does she have?

___ No (2) _____
(Job Title)

b. Is that the kind of job she has most of the time?

___ Yes (1) (Go to 11)

___ No (2) What kind of job does she have most of the time?

(Job Title)

11. Does she plan to stay in this kind of job until she retires?

___ Yes (1)

___ No (2)

12. Does moving from one base to another make it difficult for her to find a job?

___ Yes (1)

___ No (2)

12a. If Yes, how often

___ Always

___ Most of the time

___ Sometimes

___ Hardly ever

13. How satisfied would you say she is with her present job? (Check one)

___ Very satisfied

___ Somewhat satisfied

___ Neither Satisfied nor
dissatisfied

___ Somewhat dissatisfied

___ Very dissatisfied

14. Did your wife have jobs before now?

___ Yes (1)

___ No (2)

a. If yes, what kind of job? _____

b. How long on each job? _____

(GET SPECIFIC JOB TITLES and period of time on each)

15. How do you think she felt about having to move from one job to another?

16. Have there been times when you were away from your wife for a long time because of your job with the Air Force?(Check one)

 Yes (1) How long?
 No (2) (Go to 17)

- 16a. What prevented your family from going with you?

- b. Which of those times prevented your wife from going with you?

Here is a card with a scale from 1 to 10 on it. The scale represents the range in the extent to which success or failure at work affects how we feel about ourselves. It is NOT a measure of HOW we feel about ourselves? It is, instead, a measure of how much our WORK AFFECTS how we feel about ourselves. For some people, success at work is the only thing that counts, while for others it does not make any difference at all. A person for whom work is the most important thing in life and who would have to be successful at work in order to think well of himself would be at the extreme left end of this scale. (POINT) The other end (POINT) of the scale would represent a person who regards other things as being more important than work and who does not need to succeed at work in order to feel that he is a success. Is the meaning of the scale clear? (If Yes, Go to a. If No, Repeat Instructions)

17. a. What point on this scale (MOVE FINGER BACK AND FORTH ALONG SCALE) show the importance of work to how you feel about yourself?
 b. At what point would you say you were five years ago?
 c. How do you think you will feel five years from now?

(NOTE: If interviewee was not employed five years ago, write "NA" in b. If interviewee does not intend to be employed five years from now write "NA" in c.)

Now on this same card I would like for you to tell me where you think your wife falls on the scale. You may not know for sure but please make a guess about how she feels about her work. Interviewer should repeat instructions, if necessary.

13. ___a. What point in this scale (MOVE FINGER BACK AND FORTH ALONE SCALE) show the importance of work to how she feels about herself?
- ___b. At what point do you think she was five years ago?
- ___c. At what point do you think she will be five years from now?

19. Do you plan to keep the job you have now for the rest of your career in the Air Force?

___Yes (1)

___No (2)

If no, why will you make this change? _____

20. Would you say the job you have now in the Air Force is the best of any of the jobs you ever had?

___Yes (1) (Go to b)

___No (2)

a. If no, what job was better? _____
(Job Title)

b. What made it better? _____

21. What would have to happen to you to feel that you are more successful at work? PROBE: Anything else?

22. How certain do you feel about your chances of being promoted during the next year or two? Would you say you were: (Check One)

☐ Very Certain ☐ Uncertain
☐ Certain ☐ Very uncertain
☐ Somewhat certain

23. How important is it to you to be promoted? Would you say it was: (Read and Check)

☐ Very important ☐ Slightly important
☐ Somewhat important ☐ Not at all important

24. In general, would you say you have already achieved most of the goals you set for yourself in your work life or are there still things you feel it is important for you to accomplish? How satisfied are you with what you have accomplished? Would you say you are: (Read and Check one)

☐ Very satisfied ☐ Dissatisfied
☐ Satisfied ☐ Very dissatisfied

Now, we would like to know how much you agree or disagree with some statements about work. Please try to think about your responses as though you were giving them to yourself rather than to me or anyone else.

Here is a card with numbered responses ranging from strongly agree to strongly disagree. I will read the statement and you tell me which number on the card represents your responses. While all of the statements are somewhat similar, each contains something different. Please think about the statements carefully before responding (Put Checks in Spaces)

	1	2	3	4	5
	Strongly		Neither		Strongly
	Agree	Agree	Agree nor	Disagree	Disagree
			Disagree		
25. The major satisfaction in my life comes from my job	<input type="checkbox"/>	<input type="checkbox"/>	<input type="checkbox"/>	<input type="checkbox"/>	<input type="checkbox"/>
26. Doing my job well increases my feeling of self esteem	<input type="checkbox"/>	<input type="checkbox"/>	<input type="checkbox"/>	<input type="checkbox"/>	<input type="checkbox"/>
27. I am very much involved personally in my work	<input type="checkbox"/>	<input type="checkbox"/>	<input type="checkbox"/>	<input type="checkbox"/>	<input type="checkbox"/>

	1	2	3	4	5
	Strongly Agree	Agree	Neither Agree nor Disagree	Disagree	Strongly Disagree
28. The type of work I do is important to me when I think about how successful I am in life	—	—	—	—	—
29. The most important things that happen to me involve my job.	—	—	—	—	—
30. I think members of my family feel proud when they tell people what I do for a living	—	—	—	—	—
31. I live, eat and breathe my job	—	—	—	—	—
32. When I do my work well, it gives me a feeling of accomplishment.	—	—	—	—	—
33. Most things in life are more important than work	—	—	—	—	—
34. I feel a great sense of personal satisfaction when I do my job well.	—	—	—	—	—
35. I'm really a perfectionist about my work.	—	—	—	—	—
36. When I make a mistake or do something badly at work, it sometimes bothers me for days.	—	—	—	—	—
37. If I could not do my job well, I would feel that I was a failure as a person.	—	—	—	—	—

	1	2	3	4	5
	Strongly Agree	Agree	Neither Agree nor Disagree	Disagree	Strongly Disagree
38. When I perform my job well, it contributes to my personal growth and development	—	—	—	—	—
39. I feel depressed when I fail at something connected with my job.	—	—	—	—	—
a. I think I do my job better than most others with whom I work.	—	—	—	—	—
b. The person I work for is very satisfied with my job performance.	—	—	—	—	—
c. Worrying about things at home sometimes keep me from doing as good a job as I could.	—	—	—	—	—
d. Because of problems with how I do my job, I may not be promoted as soon as I would like.	—	—	—	—	—
e. I often think about problems at home when I am at work.	—	—	—	—	—

	1	2	3	4	5
	Strongly Agree	Agree	Neither Agree Nor Disagree	Disagree	Strongly Disagree
f. My wife is happy that I am in the Air Force.	_____	_____	_____	_____	_____
g. I am probably better than average on my job	_____	_____	_____	_____	_____
h. The necessity to move frequently from one Base to another causes tension between my wife and me.	_____	_____	_____	_____	_____
i. It seems to me I am not doing my job as well as I used to.	_____	_____	_____	_____	_____
j. My job often inter- feres with my family life.	_____	_____	_____	_____	_____

10. Now we would like some information about who does chores in your household. I will read a list of chores and I would like you to tell me whether each one is done entirely by you, mostly by you, entirely by your wife, mostly by your wife, or more or less equally by you and your wife. If the chore is done mostly by someone other than you or your wife, please tell me who does it. Here is a card with possible responses on it. Who in your house does this:

a b c d e o NA

- (1) Cooking?
- (2) Paying the bills?
- (3) Shopping for food?
- (4) Shopping for household goods?
- (5) Repairing things that get broken?
- (6) Emptying the garbage?
- (7) Cleaning the house?
- (8) Washing the windows?
- (9) Mowing the lawn?

a b c d e o NA

- (10) Washing the dishes?
- (11) Taking care of a child
when he or she is sick?
- (12) Washing the clothes?

41. Now, I have a few more questions about some possible everyday life experiences.

	(1) Never	(2) Sometimes	(3) Frequently	(4) Always
1. Do you try to do as much as possible in the least amount of time?	—	—	—	—
2. Do you become impatient with delays or interruptions?	—	—	—	—
3. Do you always have to win at games to enjoy yourself?	—	—	—	—
4. Do you find yourself speeding up the car to beat the red light?	—	—	—	—
5. Are you unlikely to ask for or indicate you need help with a problem?	—	—	—	—
6. Do you constantly seek the respect and admiration of others?	—	—	—	—
7. Are you overly critical of the way others do their work?	—	—	—	—
8. Do you have the habit of looking at your watch or clock often?	—	—	—	—
9. Do you constantly strive to better your position and achievements?	—	—	—	—
10. Do you spread yourself "too thin" in terms of your time?	—	—	—	—
11. Do you have the habit of doing more than one thing at a time?	—	—	—	—
12. Do you frequently get angry or irritable?	—	—	—	—

	1) Never	(2) Sometimes	(3) Frequently	(4) Always
13. Do you have little time for hobbies or time by yourself?	—	—	—	—
14. Do you have a tendency to talk quickly or hasten conversations?	—	—	—	—
15. Do you consider yourself hard-driving?	—	—	—	—
16. Do your friends or relatives consider you hard-driving?	—	—	—	—
17. Do you have a tendency to get involved in multiple projects?	—	—	—	—
18. Do you have a lot of deadlines in your work?	—	—	—	—
19. Do you feel vaguely uncomfortable if you relax and do nothing during leisure?	—	—	—	—
20. Do you take on too many responsibilities?	—	—	—	—

Now, to finish up, we need a little more information about you.

42. How old were you on your last birthday? (WRITE IN YEARS) _____
(Years)

43. How many years of school did you have? (CIRCLE)
6 7 8 9 10 11 12 1 2 3 4 M. A. Ph. D.

44. Have you had any additional job training?

(1) ___ Yes

(2) ___ No (Go to 46.)

If Yes, What sort of training was it? _____

How long did it last? _____

45. How many years of school did your wife have? (CIRCLE)

6 7 8 9 10 11 12 / 1 2 3 4 M.A. Ph.D.

46. Have she had any additional job training?

(1) Yes

(2) No (Go to 48)

If yes, What sort of training was it? _____

How long did it last? _____

If any college training, what was her major? _____

47. Do you have any children? (Check one)

(1) Yes

(2) No

If yes,

a. What are their ages? (Record Below)

b. Which ones, if any, are still in school? (IF IN SCHOOL) What year are they in school? (RECORD BELOW)

AGE

YEAR IN SCHOOL

RESEARCH INITIATION PROGRAM

Sponsored by the

AIR FORCE OFFICE OF SCIENTIFIC RESEARCH

Conducted by the

SOUTHEASTERN CENTER FOR ELECTRICAL ENGINEERING EDUCATION

FINAL REPORT

EVALUATION & VALIDATION of

Ada* PROGRAMMING SUPPORT ENVIRONMENTS

Prepared by: Mike Burlakoff, Assistant Professor
Department & University: Computer Science Department
Southwest Missouri State University
Springfield, Mo., 65804
Research Period: January 7 through June 28, 1985
Contract: F49620-82-C-0035
Date of Report: July 5, 1985

*Ada is a Registered Trademark of the US Government (AJPO)

ACKNOWLEDGEMENTS

This work is sponsored by the Air Force Office of Scientific Research (AFOSR) under the Research Initiation Grant Program. The program is administered by the Southeastern Center for Electrical Engineering Education (SCEEE) under contract F49620-82-C-0035. This research was also supported through cost share by Southwest Missouri State University (SMSU). Therefore, the author wishes to thank Dr. Bruno Schmidt, Computer Science Department Head and the SMSU administration for their support.

The work was completed by participating as a member of the Evaluation & Validation (E&V) team. The E&V task is sponsored by the Ada Joint Program Office (AJPO) and is conducted by the Air Force Avionics Laboratory (AFWAL/AAAF). The team is headed by Ms. Virginia Castor.

ABSTRACT

The research consisted of contributions as a member of the Evaluation & Validation (E&V) Team for Ada Programming Support Environments (APSEs).

Following are the major activities: An Assessment of Availability of E&V Tools and Aids was developed. Much of the other work included review of on-going E&V and related E&V projects technical material. Following the reviews, comments and recommendations were prepared. The primary areas of review were the following: Joint Services Software Engineering Environment Operational Concept Document; Life Cycle Software Engineering Environment Taxonomy; the E&V Tools and Aids Document; Guidelines for the Evaluation of Technical Proposals from the Ada Prospective; and sections of the E&V Requirements Document.

Research Initiation Program, Final Report, Evaluation & Validation
of Ada Programming Support Environments, Mike Burlakoff, July 5, 1985

I. BACKGROUND OF Ada and the E&V TASK.

In 1975 the Department of Defense (DoD) High Order Language Working Group was formed with the goal of establishing a single high order language for use in DoD systems (in particular, in Embedded Computer Systems). Following establishment of technical requirements and international competition, the Ada language as currently defined in (2) was selected. One of the major goals of Ada is to reduce the rapidly increasing costs of software development and maintenance in military systems.

Early in the development process it was realized that the acceptance and benefits derived from a common language could be increased substantially by the development of an integrated system of software development and maintenance tools. The requirements for such an Ada Programming Support Environment (APSE) were stated in the STONEMAN (1) document. STONEMAN identifies the APSE as support for "the development and maintenance of Ada application software throughout its life cycle." (3)

In June 1983 the Ada Joint Program Office (AJPO) proposed the formation of the E&V Task and a tri-service APSE E&V Team, with the Air Force designated as the lead service. In October 1983 the Air Force officially accepted responsibility as the lead service on the E&V Task. The purpose of the E&V team is to develop the techniques and tools which will provide a capability to perform assessment of APSEs and to determine conformance of APSEs to applicable standards. As E&V technology is developed, it will be made available to the community for use by DoD components, industry, and academia as deemed appropriate by the respective organizations. (3)

II. OBJECTIVES.

The objectives of the effort were to participate in the on-going work of the E&V team and to contribute to that activity. The E&V team consists of four working groups, where each group is responsible for a particular area of E&V. The major area of participation during this period was with the Requirements Working Group (REQWG). The REQWG is responsible for: 1) Life-cycle E&V issues, 2) Definition of E&V requirements, 3) Analysis of E&V requirements, 4) Identifying issues which may impact development of E&V technology and 5) Providing recommendations for development/acquisition of E&V tools/aids. (3)

III. ACTIVITIES/RESULTS.

Following are the major activities and results:

1. Development of Assessment of Availability of E&V Tools & Aids Report. (8)

This work was developed independently and then reviewed by several members of the E&V team during the June 1985 E&V quarterly meeting. A copy of the report is attached.

2. Review of Joint Services Software Engineering Environment (JSSEE) Operational Concept Document (OCD). (6)

The Software Technology for Adaptable Reliable Systems (STARS) project of the Office of the Secretary of Defense is proposing the development of a common software environment for mission critical systems for DoD use in the 1990's. The OCD described the way JSSEE will appear to the users, and the way that the users will interact with the JSSEE installation.

Following is a summary of the comments as a result of review of the OCD:

1) A background section giving the history and background of JSSEE would have been useful. Also, the scope of the document was much broader than given in the introduction. The purpose of the document seemed unclear.

2) The relationship of JSSEE to Ada and STONEMAN was unclear.

3) Some of the OCD specifications relating to matters such as responsiveness, metrics, installation support, etc. were questionable and poorly defined.

4) The information regarding Configuration Management and Support was lacking in detail in regards to responsibilities, etc.

Following review of the JSSEE OCD, it occurred to the author that beginning development of a JSSEE was being proposed. Following the development, the use of JSSEE would be required in DoD in the 1990's time period. The author strongly disagrees with this concept for the following reasons: 1) Past experience has shown that purposeful development of large software environments generally results in such large, inefficient software systems, that they are not acceptable by the users, and 2) because of the rapid technological advances in the computer sciences area, it seems that the DoD should not be bound to the use of a mid-80's planned environment. Rather, the DoD should keep abreast of the latest computer hardware/software technology and implement appropriate technological advances. A message to this effect was sent by the author to the JSSEE STARS project office.

3. Review of Life-Cycle Software Engineering Environment (SEE) Taxonomy Report. (5)

This report presents a taxonomy of tool features for a life-cycle software engineering environment. The purpose of the taxonomy is to classify tool features and functions in an organized manner.

Following are some to the uses of the taxonomy: Listing desirable features and functions of specific tools, providing a means of comparison of tools and environment features and functions and for determining conformance of a tool or environment to original requirements specifications.

The major recommendation for this report was that an expanded explanation of the application of the taxonomy to specific tools was needed. The document was unclear in a number of areas. It was felt that the taxonomy could be useful to a wider audience if the examples were clarified and expanded. A number of recommendations in this regard were made.

4. Review of Tools and Aids Requirements Document. (7)

The Tools and Aids Requirements document describes the implementation of the technology required to evaluate and validate components of an APSE. This particular version was a first draft.

The document seemed to be well done. Comments were minor and no technical changes were recommended.

5. Review of Ada Proposal Guidelines. (4)

This report provides a set of guidelines for use in the assessment of technical proposals that are submitted in response to a Request for Proposal which specifies the use of Ada.

Recommendations were provided for a possible approach for the development of these guidelines. It was recommended that the guidelines be divided into four categories: 1) Compiler, 2) Ada Support Tools, 3) Ada Programming Design Language (PDL) and 4) Personnel. Examples of items to be evaluated under each category were then presented. Following development of the report referenced in (4), review and comments were provided. In general the comments were minor, and no major technical changes were proposed. It was felt that the version was well written and complete.

6. Miscellaneous.

Review and recommendation of several other E&V documents was completed. Among these were draft Sections 4 and 5 of the E&V Requirements Documents. Section 4 is titled: Required APSE Evaluations and Validations and Section 5 is: Quality Guidance for E&V Technology.

IV. SUMMARY AND RECOMMENDATIONS.

The E&V team is composed of members from government, industry and academia. Most of the members are volunteers who freely donate a great deal of time to the many E&V activities. The members are to be commended for their work and contributions to the advancement of technology in this important area of software engineering.

In the author's opinion, there have been several notable E&V achievements. These are listed below. Also given, are recommendations for areas of continued E&V team emphasis.

Achievements

1) Development of technology on techniques and methods for evaluating APSEs and the associated support software tools. This includes techniques such as component/attribute lists and questionnaire evaluations for software components.

2) Providing visibility and awareness on the importance of E&V through appropriate meetings, workshops and published technical documents. (For example, see (9)).

Recommendations for E&V Emphasis

1) Apply the developed E&V technology to specific APSEs, and support tools. These applications would be an aid in evaluating the effectiveness of the E&V technology itself, and serve to show areas that require modification or improvement.

2) Continue emphasis on the development of the Ada Compiler Evaluation Capability (ACEC). The ACEC should be a valuable E&V product which aids in determining the quality of Ada compilers.

3) Continue the theoretical development of E&V technology. Consider a comprehensive study of past E&V accomplishments and applications of currently developed technology as mentioned in 1) above. Then update the E&V plan to reflect the results of the study.

(Attachment 1)

Assessment of Availability of Evaluation & Validation Tools & Aids,
Mike Burlakoff, June 14, 1985

I. INTRODUCTION.

The Evaluation & Validation (E&V) availability assessment is presented to assist managers and software developers in determining the availability of evaluation and validation tools and techniques for a particular APSE or APSE support software tool. The question that should be answered by applying this assessment is: "If I decide to use this support software tool, what is the availability of E&V tools/aids which I can apply to assess the quality of this support software tool?"

This assessment may be applied in several different ways:

- (1) As a guide to determine the types of E&V capabilities that are available. Note that the use of this assessment requires knowledge of the existing E&V tools/aids for this support tool.
- (2) Prior to tool development, managers may use the assessment to direct that certain (or all) E&V capabilities be developed during the system development.
- (3) Several tools with similiar functional capabilities may be rated in terms of E&V availability. A comparison of the final ratings between the tools may then be made.

II. APPLYING THE ASSESSMENT

The assessment is grouped into four categories:

- (1) Evaluation.
- (2) Validation.
- (3) Formal Qualification Tests.
- (4) User tests.

These categories were chosen because they represent the most useful E&V techniques for determining the quality of a tool or the techniques that may be used to assess the quality.

The categories and the assessment criteria are listed below. Under each category is an explanation of the category, followed by the Guidance Criteria and the Ratings.

The evaluator may wish to simply assign a score to each category and then sum and average the scores. If desired, a weight may be given to certain of the categories. This would depend on the tool being evaluated. For example, it is expected that certain basic tools would not be required to have a formal validation suite of tests developed. In this case a weight of 0 for this category may be appropriate.

III. AVAILABILITY ASSESSMENT.

A. EVALUATION: AVAILABILITY/QUALITY.

Evaluation generally measures capabilities such as performance, efficiency, optimizations, options and capacities. The existence and quality of documentation are evaluated. Configuration management and control and maintenance procedures and supportability are also included in the evaluation process. Typical evaluators are: Requirements and specifications lists, guidelines, procedures and methods, metrics, benchmarks, tests and test suites, questionnaires, decision aids, monitored experiments, and test management systems. This assessment should determine whether quality evaluation criteria exists and whether it has been applied to this or similiar tools.

GUIDANCE CRITERIA

RATING

- | | |
|--|--------------------|
| 1. No evaluaters exist and none are planned. | Very Low (0) _____ |
| 2. No evaluaters exist, but they may be easiliy developed. Plans exist to develop evaluaters. | Low (1) _____ |
| 3. Evaluaters exist. The quality is acceptable. | Good (2) _____ |
| 4. Quality formal evaluaters are available and have been applied to similiar tools of this type. | High (3) _____ |
| 5. Quality formal evaluaters are available and have been successfully applied to this tool. | Very High(4) _____ |

B. VALIDATION: AVAILABILITY/QUALITY.

Validation of a tool involves a set of formal tests to establish conformance with a standard or specification. The primary example of tool validation is the Ada Compiler Validation Capability (ACVC). The ACVC is used to measure conformance of Ada compilers to the Ada Language Standard (ANSI/MIL-STD-1815A). This assessment should determine whether a quality validation capability exists, and whether it has been applied to this or similar tools. Note that a validation capability implies the existence of a standard for the tool. The assessment should not penalize a tool for non-availability of a validation capability if no standard exists.

GUIDANCE CRITERIA

RATING

- | | |
|--|-------------------|
| 1. No validation capability exists and none is planned. | Very Low (0)_____ |
| 2. No validation capability exists, but plans exist to develop a validation suite. | Low (1)_____ |
| 3. A validation capability exists. It has not been applied to similar tools. | Good (2)_____ |
| 4. A validation capability exists. It has been applied to similar tools. | High (3)_____ |
| 5. Formal validation exists. This tool has been successfully validated. | Very High(4)_____ |

C. FORMAL QUALIFICATION TESTS: AVAILABILITY/QUALITY.

Formal Qualification Tests (FQT) are generally developed by the vendor as part of the software development project. They are termed "formal" since in many cases, they are written to satisfy system requirements and/or a formal test plan. These may be used by the vendor or customer prior to software delivery to demonstrate that the system meets requirements and specifications. Included in this category would be tests developed by a separate organization such as a Independent Validation/Verification (IV&V) Team. This assessment should determine whether FQT tests exist, have been successfully executed, and are well documented on use and expected results.

GUIDANCE CRITERIA

RATING

- | | |
|--|-------------------|
| 1. No FQT tests exist. | Very Low (0)_____ |
| 2. Some FQT tests exist. Their use or results are not documented. | Low (1)_____ |
| 3. FQT tests exist. They demonstrate that the system meets specifications and requirements. However, their use and expected results are not documented. | Good (2)_____ |
| 4. FQT tests exist and have been successfully executed by the vendor. Documentation on the use of the tests and results is available. | High (3)_____ |
| 5. FQT tests exist and have been successfully executed by the vendor. The tests have shown that the system meets specifications and requirements. Documentation on the use and results of the tests is complete. | Very High(4)_____ |

D. USER TESTS: AVAILABILITY/QUALITY.

User tests are generally informally developed by the vendor or user. While validation and FQT tests determine formal compliance with specifications and requirements, user tests may verify specific functions and capabilities of interest to a user (or vendor). Examples of users tests could be: 1) Verification of a response to a error situation; 2) checking the size/speed efficiency of all or parts of a system; and 3) An example program that is furnished by the vendor to the user to determine that the system executes upon initial delivery. This assessment should determine the existence of quality user tests, whether they have been successfully executed, and if any documentation exists on the use and expected results.

GUIDANCE CRITERIA

RATING

- | | |
|---|-------------------|
| 1. No user tests exist. | Very Low (0)_____ |
| 2. No user tests exist. Plans exist to develop some tests. | Low (1)_____ |
| 3. User tests exist. They have been executed by the vendor. Little information is available on the use or results of the tests. | Good (2)_____ |
| 4. User tests exist from both the vendor and user. Information exists on their use and results. | High (3)_____ |
| 5. User tests exist from both the vendor and user. They have been successfully executed. Documentation exists on their use and results. | Very High(4)_____ |

REFERENCES

1. DoD. "Stoneman". Requirements for Ada Programming Support Environments. Feb 80.
2. DoD. Ada Programming Language, ANSI/MIL-STD-1815A. 22 Jan 83.
3. V.L. Castor. Evaluation & Validation (E&V) Plan. Version 2.0. 31 Dec 84.
4. V.L. Castor. Guidelines for the Evaluation of Technical Proposals From the Ada Perspective. 8 Apr 85.
5. E.S. Kean, F.S. Lamonic. A Taxonomy of Tool Features for a Life Cycle Software Engineering Environment. 8 Apr 85.
6. STARS Joint Service Team. Joint Service Software Engineering Environment Operational Concept Document. 15 Nov 84.
7. B. Fritz. Tools and Aids Requirements Document (Draft). 21 Mar 85.
8. D.B. Baker. Ada Decision Matrix. 23 Mar 84.
9. V.L. Castor, Evaluation & Validation (E&V) Team Public Report, Volume I. 30 Nov 84.

USAF-SCEEE RESEARCH INITIATION
IN SCIENCE PROGRAM (RISE)

Sponsored by the
AIR FORCE OFFICE OF SCIENTIFIC RESEARCH

Conducted by the
SOUTHEASTERN CENTER FOR ELECTRICAL ENGINEERING EDUCATION

FINAL REPORT

KINETICS OF HOMOGENEOUS GAS PHASE OXIDATION OF
HYDRAZINE IN AIR

Investigator:	Dr. Datta V. Naik
Academic Rank:	Associate Professor
Department & University:	Department of Chemistry Monmouth College, New Jersey
Research Location:	Monmouth College, New Jersey
Contract No.:	84RIP57

KINETICS OF HOMOGENEOUS GAS PHASE OXIDATION
OF HYDRAZINE IN AIR

ABSTRACT

The kinetics of oxidation of hydrazine in dry air has been studied in a 190-liter pillow-shaped Teflon[®] chamber as a function of the Teflon surface-to-air volume (S/V) ratio. The rate of hydrazine air oxidation in the chamber at room temperature is found to increase linearly with increasing S/V. Extrapolation of the reaction rate to zero S/V yields a rate constant of 0.012 (half-life of 58 hours) for the homogeneous gas phase oxidation of hydrazine in dry air in absence of an active surface.

ACKNOWLEDGEMENT

The author thanks the Southeastern Center for Electrical Engineering Education (SCEEE), the Air Force Office of the Scientific Research and Monmouth College for providing him with the opportunity and funding to work on this project.

The author is grateful to Dr. Daniel A. Stone, Tyndall Air Force Base, Florida, for suggesting this area of research, and for his collaboration and guidance. The assistance of Mr. Daniel Vasquez and Ms. Deborah Vaughn, chemistry students at Monmouth, in this project is appreciated.

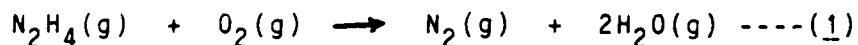
KINETICS OF HOMOGENEOUS GAS PHASE OXIDATION OF HYDRAZINE IN AIR

I. INTRODUCTION:

Hydrazine (N_2H_4) is an important member of the family of high energy fuels widely used by the United States Air Force and Space Transportation System. For example, hydrazine as a 70% solution in water is used as a propellant for the emergency power unit (EPU) of the F-16 fighter plane. A 50-50 blend of N_2H_4 and unsymmetrical dimethyl-hydrazine (UDMH), known as Aerozine-50, is used as a fuel for the Titan missile. Hydrazine and monomethylhydrazine(MMH) are used in the Space Shuttle as propellants for the thrusters and for the auxillary power units.

Hydrazine and its derivatives are highly toxic. The recommended maximum exposure to hydrazine propellants is extremely low. NIOSH recommends 30 ppb for hydrazine. The widespread usage of hydrazine with its documented toxicity (1,2) to humans and other organisms makes it necessary to characterize the processes which control the fate of hydrazine in the environment. In view of the problems associated with spills and vapor releases which occur during handling, storage and transport of hydrazine, it is important to understand the kinetics of air oxidation of hydrazine.

Previous work in this area by Stone (3), using glass reaction chambers (30 ml-55 liter) had established that the hydrazine oxidation in air proceeds by the main reaction:



The production of small amounts of ammonia during the oxidation was also reported and was attributed to heterogeneous side reactions.

The rate of hydrazine air oxidation was found to be strongly dependent upon the reaction-cell geometry, surface composition of the cell, and its surface to volume ratio.

Stone's experiments involved small glass reaction chambers with high surface to volume ratios (minimum 0.3 cm). Actual air oxidation of hydrazine in ambient atmosphere is expected to encounter a surface to volume ratio of $9 \times 10^{-6} \text{ cm}^{-1}$ (4). Stone's kinetic study has been extended by Pitts and co-workers (5,6) at the Statewide Air Pollution Research Center (SAPRC) of the University of California at Riverside using experimental conditions approaching those of the ambient atmosphere.

The SAPRC experiments were conducted using 3800-liter and 6400-liter Teflon[®] reaction chambers with significantly lower surface-to-volume ratios. Teflon[®] was chosen because of its expected inertness in these processes. Unfortunately, only a limited number of kinetic runs were made and the reported values for the half-life (τ) of the hydrazine decay in air showed considerable scatter. Nevertheless, the data still agreed with the trends in the rate of hydrazine air-oxidation reported earlier. The half-life obtained in the 6400-liter reaction chamber was longer than that obtained in the 3400-liter chamber indicating the faster reaction rate with larger surface-to-volume ratio even for a Teflon surface. The half-life obtained with wet air was lower than that with dry air. The accelerated decay of the hydrazines in wet air had been observed before by Stone (7).

The SAPRC study of hydrazine decay in air was extended by Naik and Stone (8) using a 320-liter Teflon reaction chamber (interfaced with an FT-IR spectrometer) to obtain reliable and systematic kinetic

data for the hydrazine oxidation in air. The study was conducted at the Environics Laboratory of the Air Force Engineering and Services Center, Tyndall AFB, Florida, under the Summer Faculty Research Program (SFRP) of the Air Force Office of Scientific Research (AFOSR). This work demonstrated that reproducible data can be obtained for the kinetics of hydrazine decay in air using the 320-liter chamber. Essential characteristics of the chamber included its inherent Teflon surface of about 3.5 m and a surface-to-volume ratio of approximately 10.9 m^{-1} (ignoring the surfaces associated with multi-reflection infrared optics and other hardware inside the chamber).

The major conclusions of the study by Naik and Stone (8) were:

1. Hydrazine decay in dry, purified air in the chamber has an average half-life of 12.6 hours.
2. The reaction rate increases significantly with increases in the humidity of the air.
3. The reaction rate is strongly influenced by the type of surface, and surface-to-volume (S/V) ratio.
4. Among the types of surfaces introduced to the chamber (Teflon, Cu, Al, stainless steel, painted surface), copper affects the reaction rate the most.
5. The Teflon surface not only is not inert but in fact has a significant catalytic effect on the air oxidation of hydrazine.

One of the important conclusions from all the previous studies on the kinetics of hydrazine decay in air has been that the heterogeneous hydrazine-air reaction on the exposed surfaces in the chambers plays a dominant role. Of particular relevance to the present study is the fact that even Teflon surfaces have a significant accelerating effect on the reaction.

Hydrazine vapors released directly to the atmosphere will encounter no significant surface area compared to the vast volume of the air in the atmosphere. The fate of hydrazine in air under such conditions will be primarily due to the homogeneous gas phase reaction, and the maximum half-life of hydrazine (slowest reaction rate) in the atmosphere will be determined by the rate constant for the homogeneous oxidation of hydrazine in dry air. The present study was undertaken to estimate this rate constant for the homogeneous reaction.

II. OBJECTIVES:

The objective of the project was to estimate the rate constant for the homogeneous gas phase oxidation of hydrazine in dry air.

III. EXPERIMENTAL

1. APPROACH:

The overall rate constant observed for the air oxidation of hydrazine in presence of a surface may arise from two identifiable kinetic processes:

- a) the homogeneous gas phase reaction, and
- b) the heterogeneous reaction involving the surface.

The observed reaction rate can be expressed as equation 2 which assumes that each of these processes is pseudo-first order in hydrazine concentration, and that the heterogeneous reaction rate is directly proportional to S/V ratio.

Observed Rate = Heterogeneous Rate + Homogeneous Rate

$$R_{obs} = k_{het} (S/V) [N_2H_4] + k_{hom} [N_2H_4] \text{ -----(2)}$$

where k_{het} = rate constant for the heterogeneous reaction, and
 k_{hom} = rate constant for the homogeneous reaction.

Rearranging equation 2 gives,

$$R_{\text{obs}} = [k_{\text{het}} (S/V) + k_{\text{hom}}] [N_2H_4] \text{ -----(3)}$$

For a given kinetic experiment, S/V will be a constant and therefore,

$$R_{\text{obs}} = k_{\text{obs}} [N_2H_4] \text{ -----(4)}$$

where k_{obs} = observed rate constant

$$k_{\text{obs}} = k_{\text{het}} (S/V) + k_{\text{hom}} \text{ -----(5)}$$

Equation 5 predicts that a plot of k_{obs} versus S/V ratios should be a straight line with a slope equal to heterogeneous rate constant (k_{het}) and the intercept (at zero S/V) will be the homogeneous rate constant (k_{hom}).

Alternatively, a direct determination of the homogeneous rate constant (k_{hom}) in the laboratory will require either use of a huge Teflon reaction chamber with negligible S/V or the use of a chamber made up of a material completely inert to the hydrazine-air system. Since neither of these approaches seems practical, the indirect determination of the homogeneous rate constant by the extrapolation technique was used in this work.

2. MATERIALS:

Anhydrous hydrazine (fuel grade, 98+ percent purity) was obtained from Rocky Mountain Arsenal and was used for the kinetic experiments as received. Air (breathing quality) tanks were supplied by Seaboard Welding - a local welding supplier. Hydrochloric acid, hydrazine sulfate and paradimethylaminobenzaldehyde (PDABA) were obtained from Fisher Scientific, NJ.

The colorimetric reagent, PDABA, was purified by recrystallization from ethanol. Hydrazine sulfate was used in preparing the colorimetric standard curve for hydrazine.

3. PROCEDURE:

The kinetic experiments were conducted in a chamber constructed of DuPont/FEP (50 micron) Teflon[®] film having a fully-inflated volume of about 190 liters (Figure 1). The chamber was equipped with an inlet port for the introduction of dry air and hydrazine, an exhaust port for the purging operation in-between kinetic runs, and an air sampling port. The Teflon[®] surface area inside the chamber was kept constant and it was calculated from measurements of the inside dimensions of the chamber. Variation in the S/V ratio was achieved by changing the chamber volume which was controlled by the extent of chamber inflation. The volume of the chamber for each kinetic experiment was calculated from the size of the inflated chamber.

The hydrazine sample was introduced into the chamber (partially filled with dry air) by the injection of the desired volume (usually 40-50 microliters) of N_2H_4 into the injection bulb (pre-warmed to 60° - 70°C). The hydrazine vapors were then flushed into the chamber by using dry air until the chamber was inflated to the desired size.

The dry air used in this study was obtained from an air tank (initially at 2500 psi). Before reaching the chamber the air was passed through a drying tube and a hydrocarbon filter to yield air with relative humidity of 5-8 percent. The temperature and humidity of air inside the chamber was measured by using Vaisala Digital Humidity and Temperature Indicator model HMI-31 and model HMP-31UT Relative Humidity and Temperature Probe.

Leak integrity of the chamber was monitored by observing change in the size of the inflated chamber. Initially, the chamber leaked significantly which was found to be due to cracks

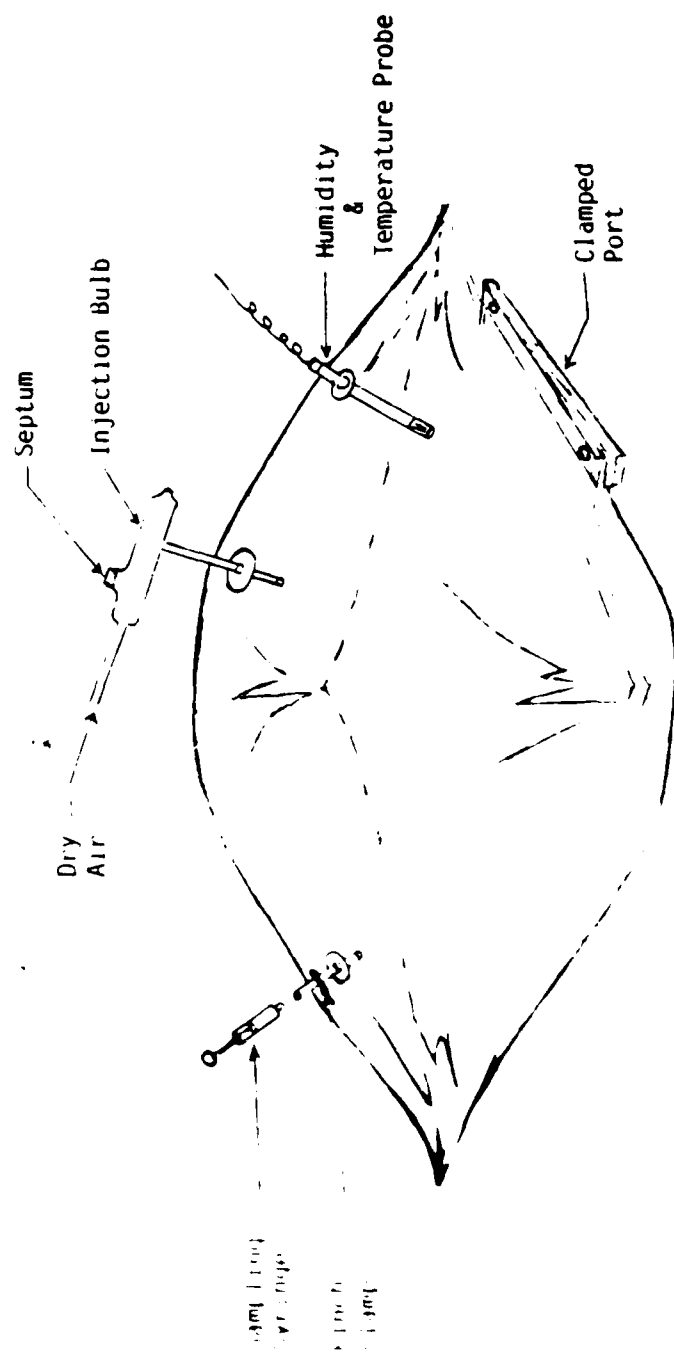


Figure 1 Teflon[®] reaction chamber.

NO-A187 859

UNITED STATES AIR FORCE RESEARCH INITIATION PROGRAM

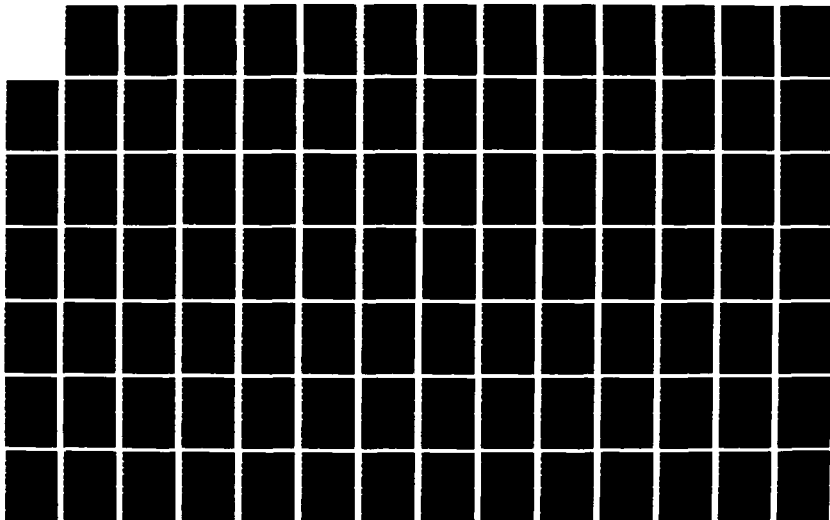
89/10

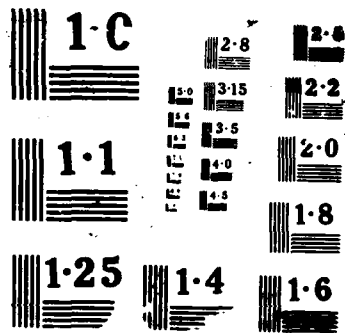
1984 RESEARCH REPORTS (U) SOUTHEASTERN CENTER FOR
ELECTRICAL ENGINEERING EDUCATION INC S M D PEELE

UNCLASSIFIED

MAY 86 AFOSR-TR-87-1722 FF9628-82-C-0035 F/G 7/2

NL





at the seams. The leak was stopped when all the seams were sealed and strengthened with Mylar[®] adhesive tape. Even with all the sealing the size of the inflated chamber decreased noticeably over a 24 hour period. Therefore, most of the kinetic runs were performed over a six hour period during which there was no significant change in chamber size. The loss of air from the chamber over extended period was thought to be due to permeability of Teflon[®] to air.

The Teflon[®] chamber was found to be definitely permeable to water vapor. The relative humidity of chamber air with no hydrazine increased slowly with time when the humidity outside the chamber was high (see Table 1). No effort was made to control the humidity, except to start the kinetic experiments with dry air (relative humidity, 5-8%).

The concentration-time profile of hydrazine in the chamber in a kinetic run was followed by using the colorimetric method of Watt and Chrisp (9) to determine the hydrazine concentration. The actual analysis involved the withdrawing of 2.0 ml of an air sample from the chamber with a 10.0 ml gas syringe without the needle. It was found that the steel needle absorbed substantial amounts of hydrazine which interfered with the determination of hydrazine level in sampled air. Therefore the sample port was fitted with a tygon tubing one end of which extended inside the chamber and the outside end attached to the cannula of the syringe. In between sampling operation the tubing was closed with a pinch-clamp. Following the withdrawal of the air sample, 1.0 ml of the colorimetric reagent, p-dimethylamino-benzaldehyde, was taken in the same syringe. The syringe contents

TABLE 1

CHANGE IN PERCENT RELATIVE HUMIDITY OF AIR INSIDE THE REACTION
CHAMBER WITH TIME.

Humidity outside the chamber: 77-79%

Temperature: 25-26°C

Time, Hours	% R. Humidity
0	5.5
0.75	6.5
1.60	7.8
2.25	8.7
2.92	9.2
3.41	9.6
3.80	10.1
5.25	10.7

were shaken to allow reaction of hydrazine with the reagent to produce p-dimethylaminobenzaldehyde which has a maximum absorbance at 460 nm. The absorbance measurements were made with a Perkin Elmer Lambda-3 spectrophotometer, and using a 1 ml cuvet with 1 cm path length.

All the kinetic runs were made with an initial hydrazine concentration in the range of 150-400 ppm which falls within the sensitivity limits of the analytical method. Hydrazine analyses were made at periodic intervals during each kinetic run, and from the first order kinetic plot ($\ln [N_2H_4]$ vs time) the observed rate constant, k_{obs} , were determined ($k_{obs} = -\text{slope}$). Whenever possible, the k_{obs} were determined in triplicate for a given S/V ratio. Kinetic runs were made with four different S/V ratios.

IV. RESULTS AND DISCUSSION.

The observed rate constant and the corresponding half lives for different Teflon[®] surface to air volume (S/V) ratios are listed in Table 2. The data shows dependence of the hydrazine-air reaction rate on the S/V ratio as was observed in the earlier study (8). The half-life for air-oxidation of hydrazine in the fully inflated chamber of volume 180 liters ($S/V = 13.9 \text{ m}^{-1}$) was found to be 7.2 hrs. which compares with the half-life of 12.6 hrs. for the same reaction in a larger 350 liter Teflon chamber ($S/V = 10.9 \text{ m}^{-1}$) used in the previous study (8). A representative kinetic run is illustrated in Figure 2.

TABLE 2

OBSERVED RATE CONSTANTS, K_{obs} , FOR AIR OXIDATION OF HYDRAZINE¹

Teflon Surface Area S (m^2)	Air Volume V (m^3)	S/V m^{-1}	Avg. ² K_{obs}	Avg. ² τ , hrs.
2.50	0.180	13.9	0.091	7.6
2.50	0.152	16.4	0.113	6.1
2.50	0.115	21.7	0.134	5.2
2.50	0.100	25.0	0.161	4.3

¹All kinetic runs were made at room temperature, 24-28° C.

²Average of at least three kinetic runs

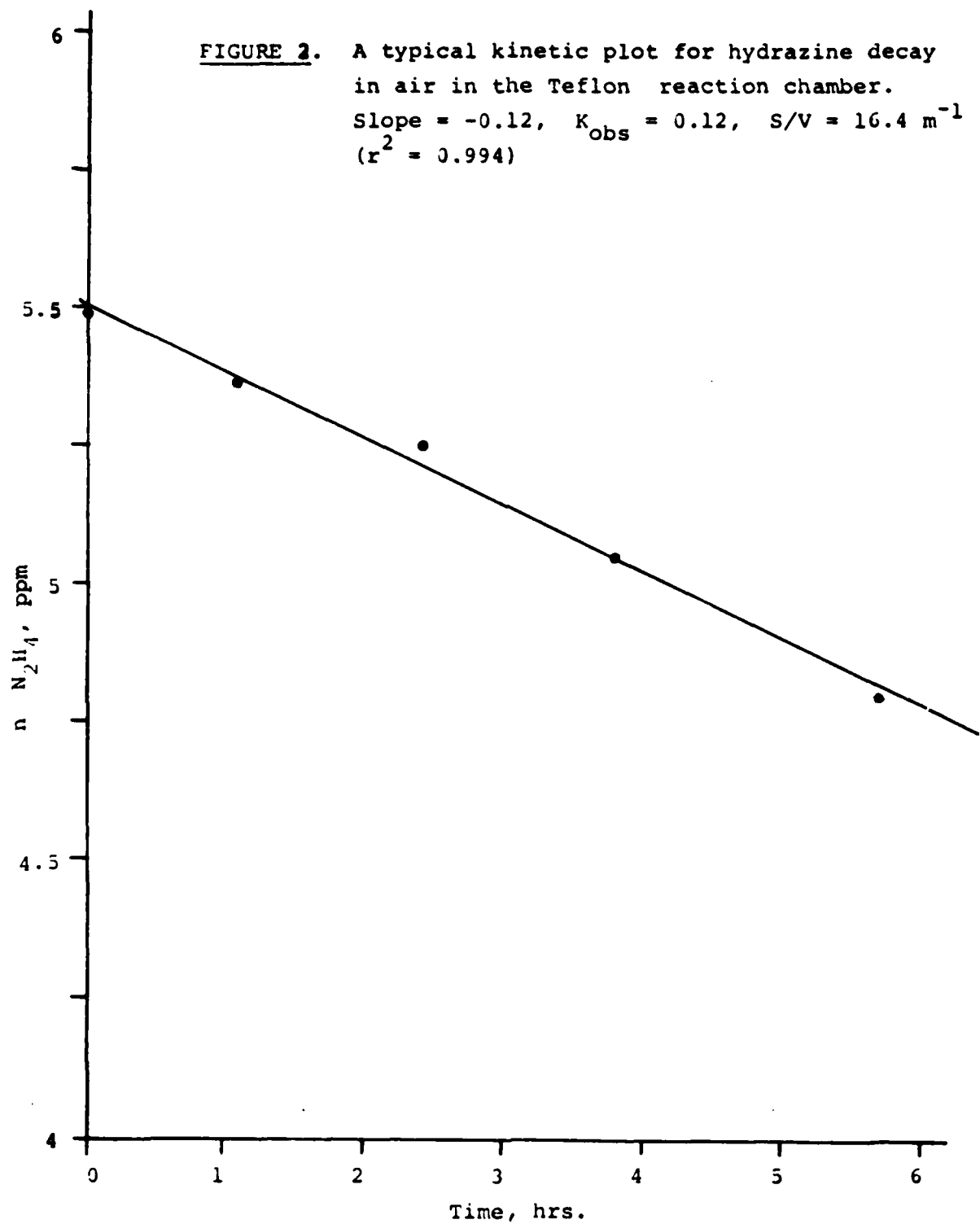
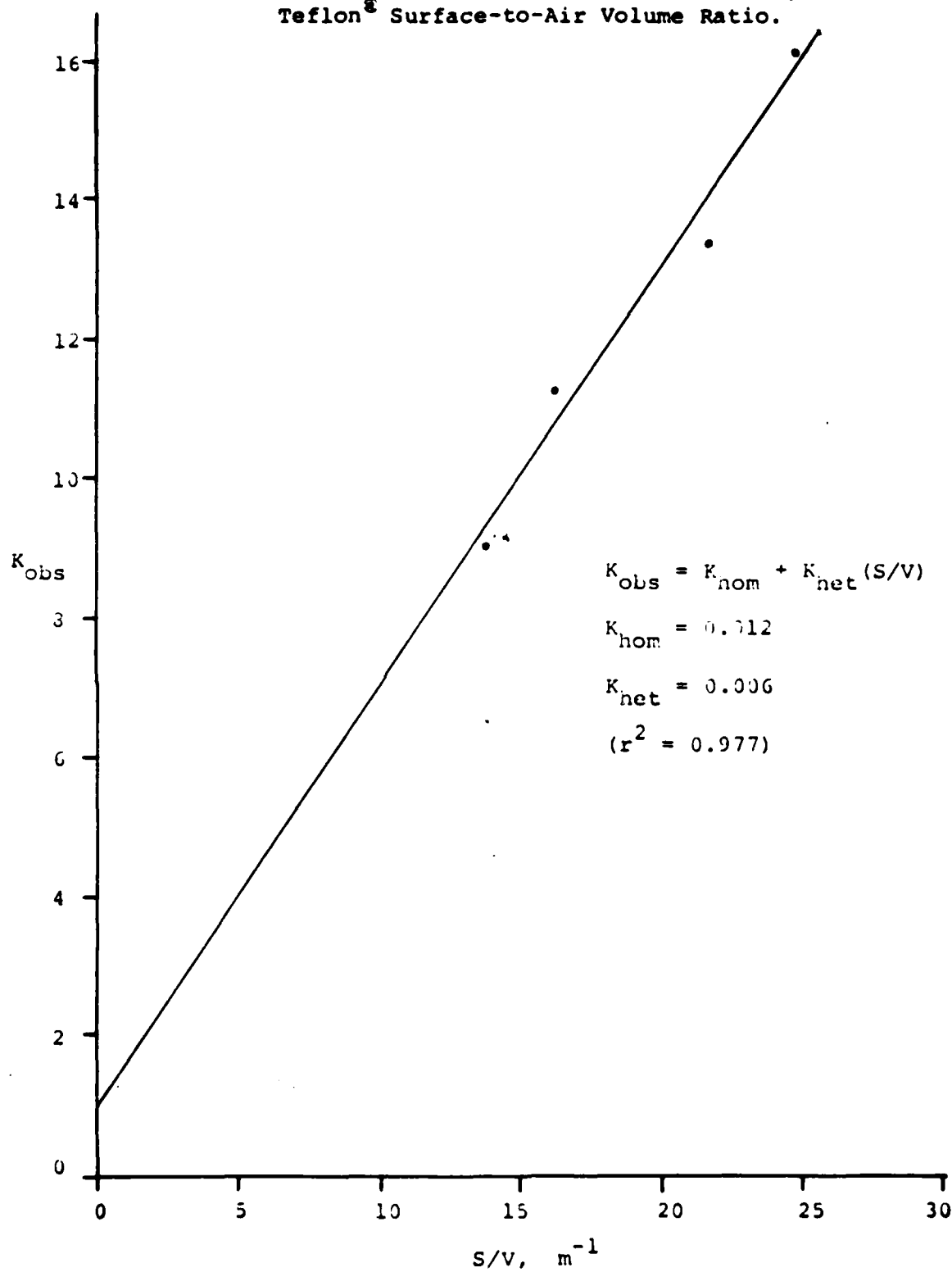


FIGURE 3. Plot of Observed Rate Constants, K_{obs} , versus Teflon[®] Surface-to-Air Volume Ratio.



The rate of air oxidation of hydrazine is observed to increase with increasing S/V ratio. A plot of k_{obs} versus S/V ratios (Figure 3) approximates a straight line as predicted by equation 5. The slope of this line, which corresponds to heterogeneous rate constant for the surface reactivity is 0.0059 ($\tau = 117$ hrs.) per S/V of m^{-1} . Extrapolation of the line to zero S/V yields a k_{obs} value of 0.012. Thus, at zero S/V, the half-life of air oxidation of hydrazine can be estimated as 58 hours.

The results of this work show that:

- a) Teflon[®] surface is not inert to the air oxidation of hydrazine.
- b) Teflon[®] (50 μm) film is permeable to moisture, and probably also allows permeation of air and hydrazine.
- c) In absence of any active surface, air oxidation of hydrazine is very slow.
- d) Hydrazine vapors released to atmosphere (which has very low surface to volume ratio) will have a long half-life, estimated at 58 hours.

V. RECOMMENDATIONS

The present study suggests a need to investigate the air oxidation of hydrazine in a reaction chamber made out of an inert, non-permeable material. No material is presently available which is both non-permeable to air, moisture and hydrazine, and which would have an inert surface with respect to the hydrazine oxidation. Therefore, finding or designing such a material should precede

any further kinetic study of the reaction. In addition, a systematic study should be conducted to study the effect of moisture on the air oxidation of hydrazine.

REFERENCES

1. Aerospace Medical Research Laboratory. Proceedings of the Fourth Annual Conference on Environmental Toxicology, NTIS AD-781, Paper Laboratory, December 1973.
2. International Agency for Research on Cancer. Evaluation of Carcinogenic Risk of Chemicals to Man., Lyon, Vol. 4. International Agency for Research on Cancer, 1974.
3. Stone, D.A., The Autoxidation of Hydrazine Vapor. Report No. CEEDO-TR-78-17, Tyndall AFB, Florida: Air Force Syst. Command, Civ. Environ. Eng. Dev. Off., January 1978.
4. The National Research Council, Ozone and other Photochemical Oxidants, National Academy of Sciences, Washington DC, 1977, p. 66.
5. Pitts, J.N. Jr., Tuazon, E.C., Carter, W.P.L., Winer, A.M., Harris, G.W., Atkinson, R., and Graham, R.A., Atmospheric Chemistry of Hydrazines: Gas Phase Kinetics and Mechanistic Studies. Final Report ESL-TR-80-39. Tyndall AFB, Florida: Air Force Eng. Services Ctr., August 1980.
6. Tuazon, E.C., Carter, W.P., Brown, R.V., Atkinson, R., Winer, A.M., and Pitts, J.N. Jr., Atmospheric Reaction Mechanisms of Amine Fuels. Final Report ESL-TR-82-17. Tyndall AFB, Florida: Air Force Eng. Services Ctr., March 1984.
7. Stone, D.A., The Vapor Phase Autoxidation of Unsymmetrical Dimethylhydrazine and 50-Percent Unsymmetrical Dimethylhydrazine-50-Percent Hydrazine Mixtures. Report No. ESL-TR-80-21. Tyndall AFB, Florida: Air Force Eng. Services Ctr., April 1980.
8. Naik, D.V., and Stone, D.A., Air Oxidation of Hydrazine - A Kinetic Study. Final Report, 1984 USAF-SCEEE Summer Faculty Research Program, Tyndall AFB, Fl.
9. Watt, G.W., and Chrisp, J.D., "A Spectrophotometric Method for the Determination of Hydrazine", Anal. Chem., Vol. 24, pp. 2006-2010, 1952.

SOFTWARE CORRECTIONS AND EXTENSIONS FOR AN
INTEGRATED PARTICLE SIZING SYSTEM

Arthur M. Sterling and Keith S. Watson

Department of Chemical Engineering
Louisiana State University
Baton Rouge, Louisiana 70803

March, 1986

FINAL REPORT

December, 1984 - November, 1985

PREFACE

This work was conducted at the Department of Chemical Engineering, Louisiana State University, Baton Rouge, Louisiana, 70803, under Subcontract No. 84 RIP 58 with the Southeastern Center for Electrical Engineering Education, Inc., as a part of contract No. F49620-82-C-0035 with the United States Air Force.

Work on this contract was performed between 1 December 1984 and 31 November 1985. Dr. Warren D. Peele was the Contracting Officer, and Captain Paul Kerch, USAF Engineering and Services Laboratory (AFESC/RD), Tyndall AFB, Florida, was the Scientific Contract Monitor.

This work was closely coordinated with related work being carried out by the UCI Combustion Laboratory, Mechanical Engineering, University of California, Irvine, 92717. The individuals who participated were Dr. G.S. Samuelsen, Craig P. Wood, and B. Alexander.

SECTION I

INTRODUCTION

A. BACKGROUND

The Environics Division of the Air Force Engineering and Service Center at Tyndall Air Force Base, Florida, deals with environmental problems arising from Air Force operations. Included are the problems associated with soot emission from gas-turbine combustors.

Since 1978, the Environmental Sciences Branch of the Environics Division has conducted and supported research on the use of fuel additives to reduce sooting. As part of this program, a micro-processor controlled, laser-based instrument for non-invasive measurements of soot particle size in laboratory flames was developed at the UCI Combustion Laboratory, Department of Mechanical Engineering, University of California, Irvine, through a subcontract with Spectron Development Laboratories, Inc., Costa Mesa, California. A copy of this instrument, the Integrated Particle Sizing System, was installed in the Tyndall laboratory in 1982.

As a 1984 USAF-SCEEE Summer Faculty Fellow, one of us (AMS) had the opportunity to evaluate this instrument. Several problems were identified relating to the quantitative results that can be obtained:

- there is a broadening of the measured size distribution for monodisperse particles on the order of one-half the dynamic range of the instrument.
- the software that controls data acquisition, analysis, and display had problems that reduced the efficiency of instrument operation.
- there was no documentation of the software, which limits the feasibility of software correction and extension. The goal of this work was to address the problems associated with the software, and to correct and extend the software wherever possible.

B. PRINCIPLE OF THE INTEGRATED PARTICLE SIZING SYSTEM (IPSS)

The IPSS contains two different techniques for particle size measurements. One, for particles larger than 3 μm , is based on the visibility method, and will not be discussed here. The other is based on the ratio of the intensity

of light scattered by a particle at two different forward angles, the so-called intensity-ratio technique. This ratio is measured for individual particles, and sorted into a discrete distribution (histogram). The distribution of intensity ratios is then related to the particle size distribution through light-scattering theory.

C. SPECIFIC SOFTWARE PROBLEMS AND PROPOSED SOLUTIONS

1. Software Tables

In processing the measured intensity ratios, three tables are used to convert the ratio histogram to a size histogram. One table contains the value of the ratio corresponding to each bin of the histogram. A second table contains the corresponding particle size for each bin of the histogram. A third table contains the corresponding width of the particle size range for each bin of the histogram.

The correspondence between the ratio, the particle size, and the bin width, however, does not agree with the theoretical calculations carried out by Spectron Development Laboratories (SDL). Since it was unknown whether it was the theoretical calculations or the implementation of the tables that was in error, we proposed to recalculate the values starting with first principles. As we show below, this required a detailed knowledge of the optics, the electronics, and the software components of the system.

A fourth table is needed to convert the size distribution to a distribution of correct number density. The values in this table contain a correction for the probe volume size for each bin in the histogram. The probe volume correction tables were not implemented, i.e., each entry in the table contained the value of unity. We proposed to develop a method to implement the probe volume correction tables. Although we have essentially completed this development, its implementation requires information on the optics of the IPPS that is currently unavailable.

2. CRT and Hardcopy Display

There are minor problems associated with the assembly language programs that produce CRT and hardcopy plots of the intensity ratio and size distributions.

In the CRT display of the intensity ratio histogram, one line (or several lines) appears to contain twice the measured count at the expense of a

neighboring bin. It was unknown whether this was a problem with the sorting routine or a problem with the control of line widths in the display routine.

Also, the hardcopy of the intensity ratio distribution does not contain annotation, and the page control results in plots being out of synchronization with the page size, i.e. plots are often printed over the top of the paper perforations.

The particle size distribution routine has three problems. First, it is improperly scaled. Second, hardcopy plots cannot be printed. Third, when the particle size distribution routine is executed, the effective rate for subsequent data collection is reduced to approximately ten percent of the previous rate.

We proposed to correct these problems. As we show below, this was accomplished by correcting the assembly language software and restructuring the BASIC language software.

D. SOFTWARE EXTENSIONS

The electronic components of the IPSS have the capability to collect values of either: 1) the intensity ratio, or 2) the intensity from either of the two angles. However, the software supports only the collection of ratios. We proposed to extend the software to implement the collection of single channel intensity data and to display and plot the single channel intensity distributions.

F. OVERVIEW OF REPORT

We begin by presenting a brief overview of the optical and electronic components of the system. Wherever possible, we provide a mathematical model of the system behavior.

We then discuss the modifications of the assembly language and BASIC language programs which we have implemented to solve the program problems discussed above.

The basis for correction of the software tables is then documented, and the corrected tables, are presented and compared to the previous tables.

Finally, we describe a simulation program we have developed to model the operation of the IPSS. This simulation program can eventually be used to obtain probe volume corrections for any specified system parameters and to develop improved calibration procedures.

SECTION II

HARDWARE COMPONENTS OF THE INTEGRATED PARTICLE SIZE SYSTEM (IPSS)

A. OVERVIEW

The hardware components of the Integrated Particle Sizing System that relate to particle sizing by intensity ratioing are briefly described below. These components include a laser, the transmitting and collecting optics, amplifiers, signal-processing electronics, and the computer interface. The computer software, which collects and processes the data, is described in Section III. Details of the IPSS components can be found in the operator's manuals (References 1 through 5).

B. OPTICAL COMPONENTS

1. Laser

The radiation source for the system is a Lexel, Model 95-2, cw Argon laser. The laser is operated in a multiline, TEM_{00} mode, the dominant longitudinal modes being at 514.5 nm and 488.0 nm; the 488.0 nm line is used for intensity ratioing. The beam is polarized in the vertical plane.

The manufacturers specifications indicate a guaranteed output of 2.5 W in the multiline mode. The guaranteed power for the 488.0 nm line is 800 mW, or 32 percent of the total power. The $1/e^2$ beam diameter and beam divergence for the 514.5 nm line is given as 1.3 mm and 0.6 mrad respectively. The corresponding values for the 488.0 nm line will be approximately 97 percent of these values or 1.27 mm and 0.58 mrad, respectively.

The output power is selected and maintained by control of the current through the plasma tube. This provides about $\pm 3\%$ amplitude power stability over a 1-hour operating time. The laser is normally operated at about 21 amperes. Higher current levels have been reported to result in a transition to the TEM_{01} first order donut mode. The relationship between the current and the power at 488.0 nm is unknown, so the nominal operating power of the 488.0 nm beam is also unknown.

2. Transmission Optics

The principal components of the transmission optics are a dispersion prism, a beam expander, a focussing lens, and mirrors to guide the beam. The arrangement of these components is shown in Figure 1.

The dispersion prism separates the 488.0 nm (blue) beam used for intensity ratioing from the 514.5 nm (green) beam. The beam is expanded by a photographic telephoto lens and then focussed by an 500 mm lens (see Figure 1). The waist of the focussed beam defines the sample point of the instrument.

3. Collection Optics

Light scattered by particles passing through the beam waist is collected by two lens systems in the horizontal planes of the waist and at two different forward angles from the incident beam axis. In the IPSS at the Tyndall laboratory, the lenses are at 20 degrees (small angle) and 40 degrees (large angle) off axis in the forward direction, as shown in Figure 1.

Each lens system consists of two identical 300 mm, f/4 lenses contained in a cylindrical enclosure. The system is positioned so the sample point of the instrument coincides with the focal point of the first lens. Thus the scattered light collected by the first lens is collimated and then refocussed by the second lens upon a pinhole aperture. The light passing through the pinhole impinges upon the cathode of a photomultiplier tube.

Pinhole apertures of different sizes are mounted on a pinhole rotator. A particular size is selected by rotating the mount so that the desired size is positioned at the entrance to the PM tube.

The combination of each of the two collection lenses and their PM tube pinhole aperture defines two more waists at the sample point. The intersection of the laser beam waist with the two waists defined by the collection lens-PMT aperture systems determines the effective sample volume of the instrument. Roughly, the sample volume can be viewed as the volume formed by the intersection of three cylinders: 1) a cylinder aligned with the laser beam axis with a diameter equal to the diameter of the beam waist; 2) a cylinder aligned with the optical axis of the small angle collection lenses with a diameter equal to the diameter of its PMT pinhole aperture; and 3) a cylinder aligned with the optical axis of the large angle collection lenses

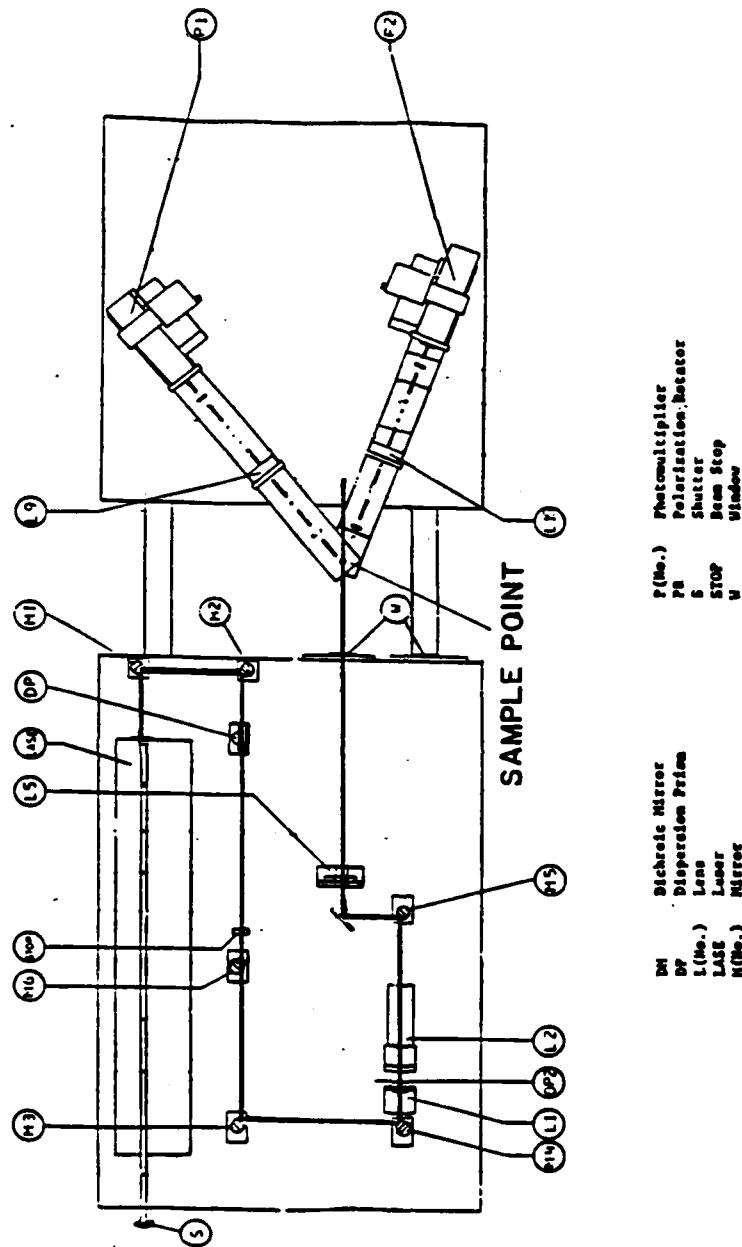


Figure 1. Schematic Diagram of IPPS Optics for Intensity Ratio Measurements.
Adapted from Reference 1.

with a diameter equal to its PMT pinhole aperture. The characteristics of the sample volume are discussed in more detail in Section VI.

When a particle passes through the sample volume, it scatters the laser light. Each lens system collects a portion of this light and focuses the collected light on its PMT pinhole aperture. Thus a pulse of light will be seen by each PM tube for each particle passing through the sample volume.

4. Comments on Optical Components

Several features of the optical system preclude detailed quantitative analysis of the IPPS. The beam expander used in the system allows an expansion of approximately 1.7x to 8.3x, depending on the effective focal length setting of the zoom lens. Since the raw beam diameter is known only approximately, and since the exact correspondence between focal length setting and beam expansion is unknown, the diameter of the expanded beam can, at best, be known only approximately. As discussed in Section VI, this leads to a large uncertainty in the diameter of the focussed beam at its waist.

Furthermore, mirror 5 (see Figure 1) is too small to accommodate the beam at its greatest expansion. Since the diameter of the beam waist varies inversely with the diameter of the beam being focussed, this implies that the smallest sampling volume cannot be used.

C. ELECTRONIC COMPONENTS

The electronic components: 1) convert the scattered light collected by the optical system to analog electrical signals; 2) process these signals; 3) convert the processed signals to digital form, and 4) transfer the digital data to a computer. The components consist of photo multiplier tubes (PMT's) and their associated power supplies; a dual-channel, logarithmic amplifier; a ratio processor; an interface; and a customized Apple II microcomputer.

1. Photomultiplier tubes

The detectors for the IPSS are RCA 8575 photomultiplier tubes. The PM tubes are powered by Bertran Associates (BA), model PMT-20A/N (Option 3) high voltage power supplies. These supplies provide 0-2kV at 2mA d.c.

The PMT's utilize a photosensitive cathode and a number of additional electrodes called dynodes to achieve high sensitivity together with rapid response time. Light striking the cathode excites electrons in the photo-

sensitive material. A number of these electrons (proportional to the intensity of the incident light) are sufficiently excited to "break free" of the cathode. The dynodes are arranged in a series of increasing potentials; as electrons from the cathode or a preceding dynode strike the next dynode, an even greater number are emitted to the next stage. The output current thus depends on two factors; 1) the incident light intensity, and 2) the PMT supply voltage. This dependence can be represented as

$$i = (F)(C)(10^{kE}) \quad (1)$$

where: E = supply voltage

F = radiant flux striking the cathode

and C and k are constants associated with a particular PMT.

2. Log Amplifier

The dual-channel logarithmic amplifier (LA-1000) converts the current pulses from the PMT into positive voltage pulses. For pulse widths as small as 10 μ s the amplifier is rated for current amplitudes as small as 1 nA (10^{-9} amp); for pulse widths as small as 2 μ s, it is rated for amplitudes as small as 1 μ A (10^{-6} amp). Since line capacitance affects amplifier response, two short wires should be used to connect the PMTs to the amplifier.

The output of the log amplifier is related to the input as

$$V = 2 \log(i/i_0) \quad (2)$$

where i_0 is a reference current generated by the log amplifier and is of the order 10^{-8} amp.

The relationship between the output voltage of the log amp and the radiant flux of scattered light at the PMT cathode is obtained by combining equations 1 and 2. That is

$$V = 2 \log (FC 10^{kE}/i_0) \quad (3)$$

The radiant flux, F , will be equal to the power of the light, P , passing through the pinhole aperture divided by the sensitive area of the cathode, A , i.e.

$$F = P/A \quad (4)$$

Substitution into equation (3) and expanding the logarithmic term yields

$$V = 2[\kappa + kE + \log P] \quad (5)$$

where

$$\kappa = \log (C/Ai_o)$$

is a constant characteristic for each PMT - log amp combination.

As can be seen from equation (5), the output voltage should be directly proportional to the PMT supply voltage and to the log of the scattered power collected by the lens.

This relationship was tested by placing a scatter (a microscope cover slip) at the sample point of the instrument and measuring the output of the two channels of the log amplifier as the PMT supply voltage was changed. The results, Figure 2, show that the relationship holds approximately at sufficiently high supply voltages. The slope of the curves provides estimates for the gain k of the PMT's.

3. Ratio Processor

The ratio processor (RP-1001) utilizes analog circuitry to process the signals from the log amps. The processed signal is then digitized. In addition, TTL circuitry is used to control the processing-conversion process. A simplified schematic of the ratio processor is given in Figure 3; a complete schematic is available in Reference 2.

a. Signal Processing

The signals from the log amplifiers (Channel A is from the large angle and Channel B from the small angle) are fed to buffer amplifiers with unit gain. Each channel then feeds into a peak-detect-and-hold circuit.

The output of the B channel peak detector is fed to an inverting amplifier (A3) with variable gain (0.95-1.05x) and variable DC offset. The gain and offset are adjusted by trim resistors mounted on the circuit boards. Thus the output of amplifier A3 is equal to the negative of the peak voltage derived from channel B.

The output of amplifier A3, $-V_{BP}$, and the output of the channel A peak detector, V_{AP} , are fed to an inverting summing amplifier (A4) with a gain of five. Thus the output of amplifier A4 is equal to $5(V_{BP} - V_{AP})$. From equation (5) we see that the voltage to be digitized is equal to

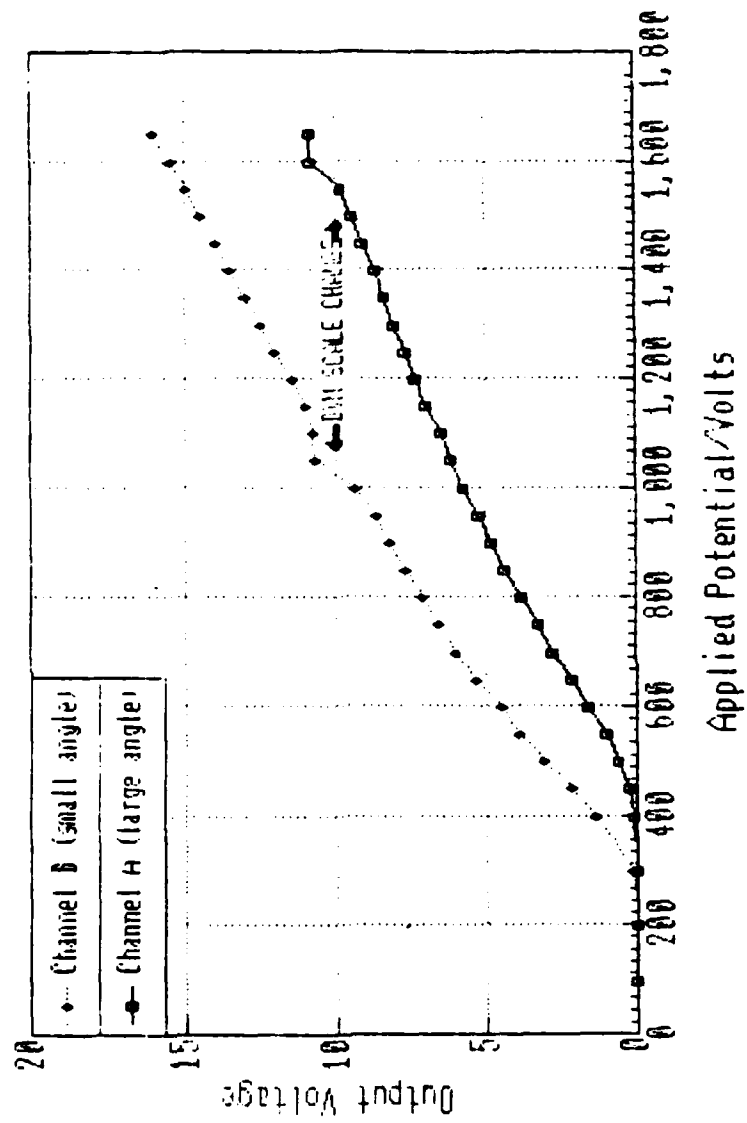
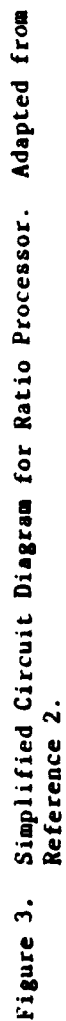


Figure 2. Effect of high voltage supply to photomultiplier tubes on output of log amplifiers at constant luminous flux.



$$5(V_{BP} - V_{AP}) = 10 \log \left(\frac{P_B}{P_A} \right) + D \quad (6)$$

where $D = 10 [(\kappa_B - \kappa_A) + (k_B E_B - k_A E_A)]$

One can show that proper calibration of the instrument results in the value of D being zero.

The ratio processor validation logic identifies valid signals (see below) as those for which $V_{AP} \geq 4.0$ volts and $V_{BP} \leq 10.0$ volts. Thus the output of amplifier A4 will vary from 0 to 30 volts. However, the conversion of this signal to digital form is limited to the range 0 to 10 volts. Thus, with D equal to zero, we see from equation (6) that

$$0 \leq 10 \log (P_B/P_A) \leq 10$$

or

$$0 \leq \log (P_B/P_A) \leq 1$$

or

$$0.1 \leq (P_A/P_B) \leq 1.0 \quad (7)$$

The ratio (P_A/P_B) is the "intensity ratio", which is related to particle size. Equation (7) indicates that "valid" values of the intensity ratio will fall between 0.1 and 1.0.

c. Analog to Digital Conversion

The analog-to-digital conversion of the output of amplifier A4 is performed by a Burr-Brown ADC82AG. The ADC82 (the AG suffix indicates a ceramic package) is a self-contained unit including internal clock, reference, and comparator. An identical converter is used to digitize the output of either the A or B channel peak detector (see Figure 2).

The accuracy of a successive approximation A/D converter is affected by quantization, gain, offset, linearity, differential linearity, and power supply sensitivity errors.

All successive approximation A/D converters have a quantization error of $\pm \frac{1}{2}$ LSB (least significant bit); the ADC82 is an eight bit converter

digitizing a ten volt range so the quantization error is approximately ± 20 mV. The gain and offset errors are factory trimmed to $\pm 0.05\%$ of full scale for the 0 to 10V range; no external adjustment is necessary to obtain accuracy of ± 1 LSB (39mV). The linearity error is the deviation of an actual bit transition from the ideal transition value; differential linearity error is the deviation in the "width" of each code (the difference between two transitions). Burr-Brown specifies linearity errors of a maximum of $\frac{1}{2}$ LSB (20 mV).

Only seven bits of the 8 bit ratio data word are actually transferred to the microcomputer. The least significant bit provides room for a validity check bit. A zero level indicates valid data. As mentioned above data are deemed valid when the input signal meets three criteria: the B input level is less than 10 V, the A input is greater than a specified minimum, and the width of the A input signal is greater than a specified minimum. For high speed operation the minimum voltage is set to +4 V and the minimum width is 2 μ s; for low speed/wide dynamic range operation the minimum voltage is set to +2 V and the minimum width is 10 μ s.

The 4.0 V validation criteria and the 2 μ s width criteria can be adjusted by trim potentiometers on the circuit board. Signal tracing on the Tyndall processor showed these values to be set at approximately 3.85 V and 2.25 μ s.

The two ADC82s drive two Schottky tri-state drivers; additionally the ADC82 for the ratio data drives the ratio display on the RD-1001 panel. The outputs from the two drivers are connected to a common data bus. Since each driver is enabled independently, care should be taken to insure both drivers are not simultaneously enabled; this would cause permanent damage to the drivers. The drivers and the ratio display are not shown on Figure 2.

Of particular interest is the transfer function of the A/D converters, i.e. how they convert the analog voltage to digital values. For the ADC82 converters used in the ratio processor, the following specifications are given by Burr-Brown. The least significant bit has a value of $10 \text{ V} / 2^8 = 39.06 \text{ mV}$. The transition values are

MSB	LSB
000..000	+10V - $3/2$ LSB
011..111	+ 5V
111..110	+0V + $1/2$ LSB

where 0 indicates the transition bit. The bit code designation is complementary straight binary. These specifications indicate that the transition voltages will occur as

111..111	→ 111..110	→ 10.53 mV
111..110	→ 111..101	→ 58.59 mV
111..101	→ 111..100	→ 97.65 mV
.		
000..011	→ 000..010	→ 9.89285V
000..010	→ 000..001	→ 9.93165V
000..001	→ 000..000	→ 9.97075V

As will be shown in Section IV, this transfer function is needed for the correction of the software tables.

d. Timing and Control Logic

The threshold detector generates the THD (threshold detect) timing pulse. This pulse rises when the signal on channel A exceeds 1.5 volts and falls when the signal on channel A drops below 1.0 volts. The rising edge of the THD pulse raises the PDE (peak detector enable) signal. Thus the PDE signal is only generated when the input from channel A rises from less than 1.0 volts to greater than 1.5 volts, providing the system with a degree of protection from background noise.

The threshold level can be modified from the nominal 1.5 volts by a 10-turn pot on the rear of the ratio processor case. Normal operation requires this potentiometer to be set to 0.0. Also, one should not confuse the threshold level with the 4.0 V validation level.

The rising edge of the PDE signal lowers the PDD (peak detector dump) signal, which allows the capacitors in the peak detector to charge. The voltage across each capacitor increases as the signal voltage increases, but owing to the presence of the diode in the peak detector circuit, the capacitor can not discharge as the signal falls. The voltage across the capacitor remains at the peak voltage encountered during the signal pulse.

A one volt fall in the channel A signal causes the NSD (negative slope detect) signal to be raised by the negative slope detector. The rising

edge of the NSD signal in turn lowers the PDE signal "locking in" the current peak voltages. The assertion of NSD also causes a 1 μ s assertion of the ACC (analog-to-digital convert command) signal. The falling edge of the ACC pulse initiates the digitization of the selected single channel and the analog difference between the two peaks (see below). The use of the falling edge of the ACC allows the analog voltages to stabilize before digitization. During analog-to-digital conversion, the ADCS (analog-to-digital status) signal is high; the conversion takes approximately 2.8 μ s.

The falling edge of the ADCS signal (indicating digitization is complete) initiates three signals: PDD (peak detector dump), DF (data flag), and RES (reset). The PDD signal discharges the capacitors in the peak detector circuits. The DF signal is sent to the interface in the Apple II microcomputer to indicate that digital data are available. The RES clears the timing and log circuitry for the next signal. The length of the PF and RES signals is 1 μ s unless an external hold signal is received from the Apple II interface. The hold signal allows digital data to be maintained until data transfer is complete.

4. Interface

There are nine output lines from the RP-1001 to the Apple II; the lines consist of eight data lines and the data flag. There are four input lines to the RP-1001; these lines consist of the two enables for the digital buffers/drivers (to select raw data or ratio data), the channel select (to choose which single channel gets digitized), and the processing hold signal.

A Rockwell 6552 VIA (versatile interface adapter) interfaces the lines from the RP-1001 to the 6502-based microcomputer. The 6552 is mounted on an interface board residing in the Apple II's seventh expansion slot. The 6552 incorporates internal timers, data latches, software configured peripheral control lines, and interrupt generation in a single package. The 6552 is memory mapped into the microcomputer's address space; the 6552 is controlled by read/write operations to specific memory addresses. The interface board also includes a CD4050 buffer/converter and a 74LS04 inverter.

The 6552 operates in handshake mode. One peripheral line serves as a valid data strobe (CA1), and another passes back the handshake output (CA2). Signals on the 8 data lines are ignored until an active transition on CA1. During this transition, the data present is latched into the A register;

simultaneously the 6552 handshakes (tells the sending device it received the data strobe) by bringing CA2 high. CA2 is subsequently held high until the microcomputer performs a read/write operation on the A register. The output from CA2 passes through an inverter generating the processing hold signal; the RP-1001 is held until the current data word is read from the A register.

SECTION III

SOFTWARE: STRUCTURE, MODIFICATIONS, AND EXTENSIONS

The ratio processing software uses 6502 assembly language, BASIC, and DOS (Disk Operating System) to drive an environment composed of an Apple II, two disk drives, a printer, and the RP-1001 interface (the Rockwell 6552 VIA). The software tasks include data collection, processing and storage/retrieval.

A. DATA COLLECTION

Data collection is a high-speed task necessitating assembly language routines. These routines do the following:

- 1) initialize the 6552,
- 2) set-up the tables,
- 3) draw the histogram outline,
- 4) turn on clocking,
- 5) collect data,
- 6) turn off clocking,
- 7) convert data, and
- 8) put RP-1001 in hold state.

The 6552 initialization consists of setting the peripheral A port for use as an input latch with handshake in on CA1 and handshake out on CA2 (see II.C.4), setting the timers to generate an interrupt every 1/500 second, and setting the NMI (non-maskable interrupt) vector to point to the address of the clock count increment routine.

The number of counts are stored in two tables, TBM and TBL; TBM contains the most significant byte and TBL contains the least. Each time a data word is received, the corresponding byte in TBL is decremented; when the byte is decremented to zero a point is plotted on the screen, TBM is decremented, and TBL is reloaded with the scale factor. The larger the scale factor, the more times a data word has to be received to produce an increase in the histogram line. When the TBM is decremented to zero, data acquisition stops. The table set-up routine simply stores 99 in the TBM (corresponding to a maximum of 99 points to plot in a vertical line to the top of the histogram) and the scale factor in the TBL entries.

The outline drawing routine draws lines between a series of points stored as absolute x and y screen coordinates. These coordinates are "bloaded" (loaded at a specific address from a binary file) from either "TICTBL" or "TICTBLDR"; the former holds the pattern for the ratio histogram (log scale) and the latter for the size histogram (linear scale). The data acquisition, replot, and size calculation functions utilize this routine.

The clocking is enabled by writing the appropriate value to the control register on the 6552; it is in turn disabled by writing a new value to the register (the control register is located at an offset 31 bytes above the slot address, the timer start value is \$C0, and the stop value is \$40).

The data acquisition loop is represented by the flow chart shown in Figure 4. The data acquisition loop continues until a key is pressed, a bin is "full" (the corresponding line in the histogram has reached the top), or the sample limit is reached. If a key is pressed, a return from subroutine operation transfers control back to the calling procedure. If a bin becomes full the transfer of control uses the fact that the return addresses for subroutines calls can be removed from the stack. For example, say routine "A" calls routine "B" which in turn calls routine "C"; when "C" finishes, (with a return command) control transfers back to "B". If for some reason the programmer desires control to pass back to "A" on completion of "C" (and the programmer knows the routines are always called in that sequence), the programmer can have "C" remove the return address to "B" from the stack, and thus when the return in "C" executes, control passes to routine "A" directly. In this way control is passed from the graphing subroutine (called by the data acquisition loop) directly back to the routine that called the data acquisition loop routine whenever a bin becomes "full". In a similar manner, the valid count increment routine returns control to the routine calling the data acquisition routine when the valid count becomes equal to the sample limit.

Upon completion of data acquisition, the TOTAL counter holds the total of data words received. The VALID counter holds the total of data words with a zero validity (valid signals) that get plotted. The INVALID counter holds the total of data words with a zero validity bit that do not get plotted -- generally the first and last bins. The difference between the total count and the sum of the invalid and valid counts ($TOTAL - (VALID + INVALID)$) equals the total of data words received with an invalid status bit (a 1). The TBM table

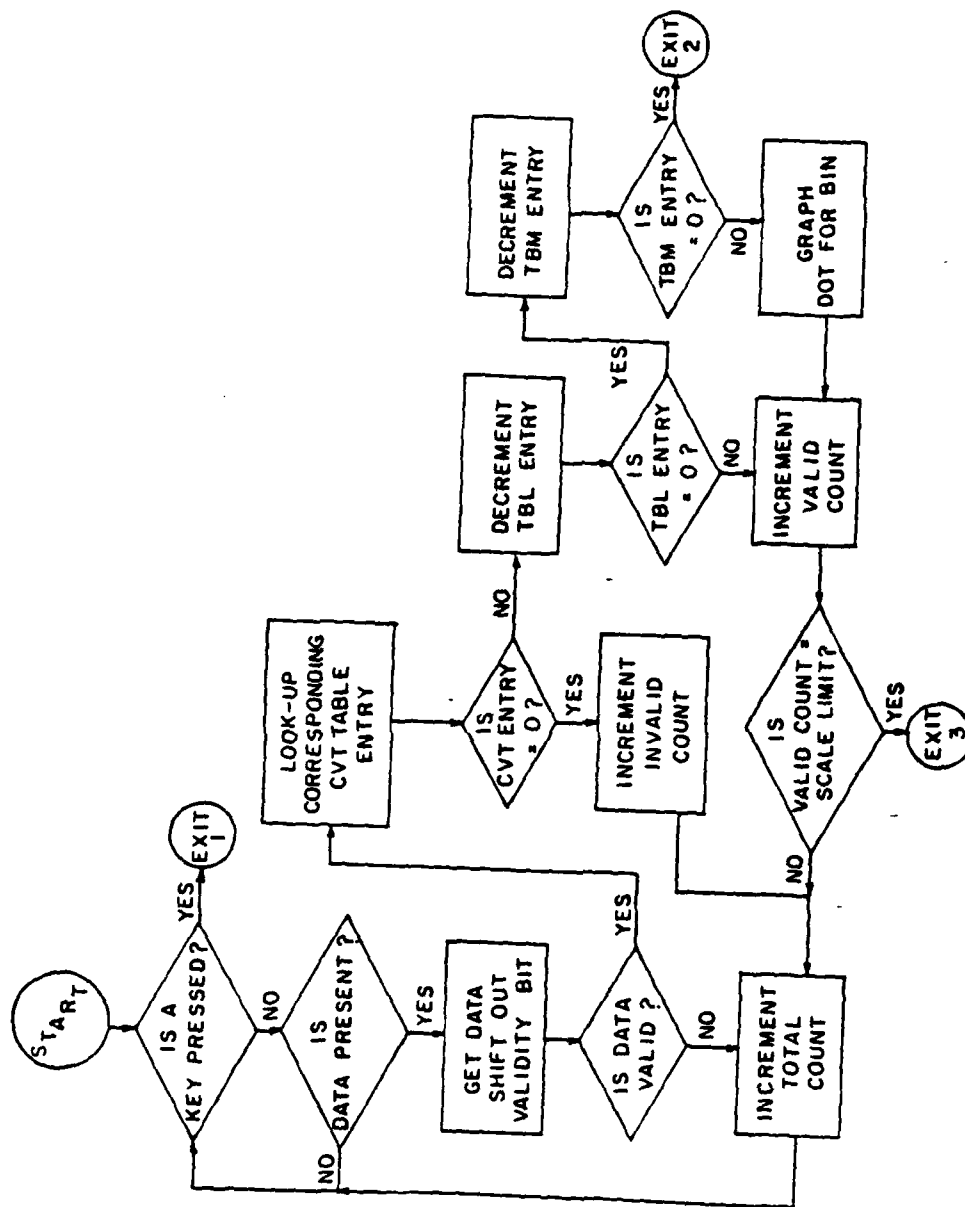


Figure 4. Data Acquisition Flow Chart

entries hold 99 less the number of times the corresponding TBL tables were decremented to zero. So the total count in each bin equals: $(99 - \text{TBM}[x]) * \text{SCALE} + (15 - \text{TBL}[x])$, where x corresponds to the bin number.

The convert routine translates the table data into regular 16 bit unsigned integers so that the total count in each bin equals $(\text{TBM}[x] * 256) + \text{TBL}[x]$.

The ratio processor is put into a hold state by placing the CA2 line of the 6552 manually to a high state; this is accomplished by leaving handshake mode when a \$ED is loaded into the peripheral control register of the 6552.

B. BASIC LANGUAGE DATA PROCESSING

1. Program Description

The program MAIN is written in Applesoft BASIC; the interpreter is ROM based. The program interfaces the assembly data collection routines for the user, performs size calculations, and takes care of data storage/ retrieval/ display. Different versions of the program exist due to on-site modifications; the following described features may not be in all versions. A basic description of program functions will be given first, and a more detailed analysis of the program structure will follow.

The following commands were implemented:

- "?" - Displays listing (partial) of valid commands.
- "N" - Acquire data under old run number.
- "O" - Acquire data under new run number.
- "C" - Change entries for data processing.
- "D" - Display listings of particle size and count.
- "P" - Print ratio histogram and listing of particle size and count.
- "F" - File data on diskette in Drive 2.
- "L" - Load data from diskette in Drive 2.
- "R" - Replot data (either loaded or acquired) normalized.
- "S" - Compile size histogram.
- "Z" - Input settings to label printouts (size, laser power, HV1/HV2).
- "X" - Input settings to label printouts (radial).
- "Y" - Input settings to label printouts (velocity).
- "K" - Input settings to label printouts (knobs).

"A" - Input settings to label printouts (axial).

"E" - Input settings to label printouts (EQ ratio).

The "?" command will display a list of commands and corresponding functions; only nine commands are listed ("O", "C", "N", "D", "P", "F", "L", "R", "S"). The other commands are not part of the basic system; they are extra additions that appear in many versions.

The "N" and "O" commands perform data collection. The "N" command prompts the user for a "run" name; the "O" command uses the previous "run" name. The concatenation of the series name and the run name is used to label the particular set of data when stored on disk. These commands invoke the assembly languages routines described earlier.

The "C" command is used to change processing parameters. Current parameters are listed in numbered order, and the user then is queried for the number of the item to change. Descriptive information used to label data includes the date, the series, and a user comment line. The ratio plotting parameters include the sample limit, the scale factor, and the print level. The sample limit determines the upper limit (in powers of 10) of the VALID count. The scale factor determines the number of data words received in a bin before another dot is plotted. The print level determines the minimum bin count for a bin to appear in the data listings; in other words, if fewer than "print level" data words are received in a bin then that bin is skipped during data listings for the "P", "D", and "S" commands. The data reduction tables are used to convert ratio information to size information. These tables are stored in text files on disk one and are dependent on the collection angles and the refractive index of the particles being measured.

The "D", "P", and "S" are used to display/print information concerning the size and count information. The "P" and "D" commands produce the same information, but the "P" command produces a hardcopy of the data and the ratio histogram. The information produced by "D" or "P" consists of a listing of the ratio, size, and count for each bin. The "S" command creates a size histogram, computes statistical information (linear mean, volume mean, standard deviation) for the distribution, and lists the same information given by the "P" and "D" commands.

The "F" and "L" commands store and retrieve data. The "F" command stores the current data under its series and run names. The "L" command prompts the user for a series name and a run name then loads the appropriate

data. Additionally the "L" command gains access to a routine called AUTODUMP, an addition available in many versions. This routine allows the user to specify a single series and a list of runs in that series to be processed as a group. Histograms of each run, normalized to the run with the highest count in a single bin, are produced to allow comparison in scale of different runs.

The "R" command replots the current data normalized to the bin with the highest count.

The "X", "V", "K", "A" and "E" commands are used to help the user create a meaningful comment line for the data description entries described under command "C".

2. Program Layout

The version of "main" as described above is approximately 12k (actually 12489 bytes) of source code. The code begins at \$4000 (16384). The positioning of the code at this location allows the size of the program not to interfere with the use of high resolution graphics.

The program is a monolithic entity without a great deal of formal structure. In particular, the addition of the AUTODUMP routine severely complicates control flow in an attempt to make use of existing code. In all there are over 85 "goto" instructions imbedded in the code; since major restructuring of this code was part of the LSU project, only a superficial description of the various segments is included here. The description of program functions by program line number is given in Table 1. A listing of the version from which Table 1 was derived is included in Appendix A.

C. THE RATIO PROCESSING SOFTWARE SYSTEM

The operational software resides in files on disk 1. Disk 2 is used only for storage of collected data. Disk 1 contains the ratio processing software, the data reduction tables, and miscellaneous utility programs.

The system is a "turn-key" system (i.e. it boots up in a running state). This is due to the one line program "HELLO" which simply causes the text file "M" to be executed. When a text file executes, each line of text is treated as if it were typed in at the keyboard. "M" configures the Applesoft interpreter to load and execute MAIN at \$4000; "MAIN" is the primary software module; it in turn loads the assembly routines. The assembly routines (actually their machine language counterparts) are contained in "ASM1.0";

TABLE 1. DESCRIPTION OF PROGRAM FUNCTIONS BY LINE NUMBER

<u>Line(s)</u>	<u>Functions</u>
3	Sets the top of memory to allow loading of assembler routines.
400 - 480	Reads the time, valid, invalid and total count values from the screen memory.
900 - 940	Reads the ratio bin counts from the tables created by the assembler routines.
1000 - 1026	Sets-up assembler routines in memory.
1040 - 1060	Allocates and initialize variables.
1061 - 1064	Sets data reduction defaults and loads them.
1065 - 1998	Data reduction table loading routines
2000 - 2180	Displays current values for "C" command.
3000 - 3220	Edits values for "C" command.
4000 - 4200	Main executive loop; command line interpreter.
4400 - 4510	"?" code; command descriptions.
5000 - 5040	Sets new run number.
5050 - 5150	Acquires ratio data; initializes counters and calls assembler routines.
6000 - 6270	"D" and "P" command code; produces listing of counts and sizes.
6500 - 6520	Extra AUTODUMP code to utilize 6000 - 6270
7000 - 7300	"F" command code; files current data.
8000 - 8150	"L" command code; loads data from files.
8200 - 8260	AUTODUMP query; transfers control to AUTODUMP routine.
8300 - 8430	Extra AUTODUMP code to utilizes 8000 - 8150
9000 - 9110	"R" command code; creates normalized ratio histogram.
9500 - 9520	Extra AUTODUMP code to utilize 9000 - 9110
10000 - 10250	"S" command code; produces size histogram.
10270 - 10420	"S" command code; produces statistical data.
10430 - 10740	"S" command code; produces data listings.
11000 - 12120	Produces comment line and toggles scale factor between 1 and 5.
15000 - 16050	AUTODUMP list editing and main execution loop.

additionally these routines require "INTVECT" (interrupt vector), "TICTBL" (ratio histogram outline), "TICTBLDR" (size histogram outline), and "CVT" (the table used to convert bin numbers to screen positions). The assembly language software is positioned at \$8800. The space between the assembly language software and the end of the source code is used for Applesoft variable allocation.

The data reduction tables (bin center and bin width) follow a simple naming convention. The first two letters denote the table type. Appended to the type is the collection angle pair ($5/2 = 50^\circ$ and 20° , etc.). Finally the particle type (implying the refraction index) and laser wavelength are added (BC 4/2/LTX/488 = bin center table for 40° and 20° collection angles, latex particles, and 488.0 nm laser light).

The utilities include a data reduction table generator (GENTABLES), a program to create "M" (CREATE M), a program to check data reduction table contents (SNOOP IN TABLES), a program to determine assembly language load positions (ADDRESS FINDER FOR BLOAD), and assorted programs from the Apple DOS system master disk. The only way to access this software is to abnormally terminate the ratio processing software (Cntrl-RESET does the trick) and then perform a CATALOG to determine what is available.

D. PROGRAM MODIFICATIONS AND EXTENSIONS

There are several errors in the version of the ratio processor software described above. Correction of many of these errors was simple; correction and extension of the software as a whole created some unforeseen problems.

The two primary errors of concern were the irregularities in the plotting of the ratio histogram and the drop in data collection rates after executing the routine to calculate particle sizes. The primary extensions involved variable scaling in the size histogram, the ability to hardcopy the size histogram, and the ability to collect and display histograms for single channel data.

1. Plotting Irregularities

The plotting irregularities were due to the bit mask used when calling the ROM based routine to draw a dot for a bin. The mask used was \$FF (all 1's). This mask had a side effect when used with a monochrome display; the size of a dot plotted was dependent on whether or not it was in a screen

position next to a plotted dot. This anomaly is based upon the image generation hardware used in the Apple to support color displays; the details of such hardware are intricate and beyond scope of this report. The correction involved changing the high resolution plotting color mask to \$7F.

2. Drop in Data Rate

The drop in the data rates was due to an oversight in interfacing the assembly language routine that drew the outline of the histogram and the BASIC language size histogram routine. The size routine would load the file containing the vector list of the outline, "poke" the start point into the assembly code, and call the assembly routines. Unfortunately the "poke" address was incorrect; the "poke" actually overwrote an RTS (return from subroutine) opcode and thereby dramatically increased the size of the data acquisition loop (instead of returning at the end of the routine with the RTS the program wandered through memory until it happened to hit another one). The correction of this "poke" eliminated the problem entirely.

3. Extensions

The extensions proved to be more problematic. The software was not structured and the methods used to utilize the assembly routines involved modifying the actual machine language instructions via the BASIC "poke" command. Changing the assembly language meant recalculation of all the addresses in the BASIC code. Modifying the BASIC was even more difficult because of space limitations in memory. The monitor program, the Applesoft interpreter (executes the BASIC), DOS (disk operating system) and its attendant buffers, text screen memory, high resolution memory, assembly language code and tables, and the BASIC source code are all co-resident. With all that in the 64K machine at once, there isn't much room for expansion.

a. Memory Usage

The first step was more efficient use of memory. The BASIC source had been loaded at \$4000 to avoid collision with the high resolution graphics page, and the assembly had been loaded in between the BASIC source and DOS. The space between the start of the high resolution page and the low end of memory where BASIC source is normally loaded had been wasted; the assembly language was re-positioned at \$1000 thereby gaining 4K of space for BASIC extensions.

b. Modularization

The next step was modularization of the BASIC code to facilitate software extension and maintenance. Unconditional branching was eliminated as the primary execution flow control mechanism; functions were grouped in separated line number sequences and invoked through the "gosub-return" mechanism. This allowed simplification of control and eliminated duplication (code to produce the particle size and count information for the "D" and "P" commands was identical to code performing the same function for the "S" command).

c. Variable Scaling

The assembly language routine to draw the histogram outline is fast (relative to performing the same operation in BASIC) and compact; unfortunately the process of "bloading" the vector files is extremely time consuming relative to the time to generate the outline from BASIC commands, and the 256 bytes necessary for the table is greater than the corresponding BASIC code space requirements. To implement variable scaling, to reduce the potential for an error like the one that caused data rate reductions, and to simplify the code, the task of drawing the outline was moved to the BASIC source.

Variable scaling is easily achieved once the outlines are produced dynamically from BASIC code. Lines are drawn between screen positions specified by coordinate pairs; the origin is the upper left screen position with the first coordinate increasing as one moves right and the second coordinate increasing as one move down. If a size histogram of particle from size M to size N ($M < N$) is desired and I is the number of hash marks to be linearly spaced between M and N, then the size corresponding to each i^{th} hash mark between M and N is given by:

$$\text{Size} = M + \frac{(i)(N - M)}{I + 1}$$

Likewise, the screen positions for the high marks are computed by:

$$X = A + \frac{i(B - A)}{I + 1}$$

where X is the horizontal position of the hash mark, and A and B are the

horizontal positions of the first and last hash marks respectfully. Thus to find the horizontal position for a bin size of P between M and N:

$$\text{Position} = A + \frac{(B - A)(P - M)}{(N - M)}$$

d. Size Distribution Hardcopy

The extension to produce a hardcopy of the size histogram involved copying the procedure used for the ratio histogram; the reason for the lack of success by personnel working at Tyndall on this item was the fact that control codes imbedded in the ratio histogram routine did not print in the listing and were thus overlooked.

e. Single Channel Collection

The last extension involved altering the way the 6552 VIA interface was initialized to enable the raw data digital buffer instead of the ratio data digital buffer. Additionally the raw data word is eight bits wide and contains no validity bit so the code in the data acquisition loop to check the validity bit was removed. The resultant code is stored in the file "ASM1.1". The selection of raw or ratio histogram is accomplished with the "M" command; the selection of large or small angle data for raw data digitization is accomplished through the "A" command.

E. REVISED STRUCTURE

To guarantee clarity, maintainability, and extensibility the following structure guidelines were adopted.

1. The code to process a command starts at line number that is a multiple of 1000.
2. Command code is invoked with the GOSUB primitive and control is returned with the RETURN primitive.
3. Offline processing tasks (tasks not involving the necessity of data collection) reside in separate program files invoked with the RUN command; control is returned with "RUN MAIN".
4. Invisible characters are not imbedded in source code; they are replaced by the use of the CHR\$ primitive.

5. The file MAINDOC contains the program MAIN with in-line documentation (unfortunately addition of in-line documentation to MAIN itself would increase its size beyond space limititious).
6. All available commands are listed by the "?" command.

Observance of these guidelines will simplify future programming tasks.

SECTION IV

SCATTERING CALCULATIONS

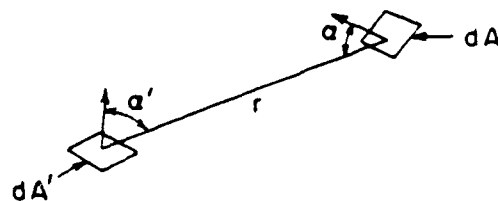
A. OVERVIEW

The Integrated Particle Sizing System belongs to a class of instruments collectively known as single particle counters. As such, its concept is based on the theory for scattering of a plane, linearly-polarized light wave by a single, homogeneous, isotropic sphere of arbitrary size and refractive index. This theory, valid in regions far removed from the scatterer (the far-field zone), was first formulated by Mie in 1908.

We review below the results of the Mie theory that are needed to calculate the theoretical response of the IPSS to a scatterer. The details leading to these results are available elsewhere (References 6 through 9).

B. RADIATION INTENSITY

To understand the principle of the IPSS, we must consider how to specify the amount of energy associated with the light scattered from a particle that is collected by a lens located some distance away. Consider an element of area dA' that emits electromagnetic radiation, which impinges on an area dA on a receiver at a distance r . The two elements of area have normals forming the angles α' and α with the line joining them, as shown below.



The amount of energy received by dA is measured in joules. The rate at which energy is received by dA is the power dP measured in watts. The power

per unit surface area normal to the direction of r received by dA is called the intensity^a (W/m^2), i.e.

$$I = \frac{dP}{dA \cos \alpha} = \frac{dP}{dA_n} \quad (8)$$

The solid angle $d\omega$ subtended by dA_n as viewed from dA is

$$d\omega = dA_n / r^2$$

so the intensity can also be written as

$$I = dP / r^2 d\omega$$

Since we will be interested in the radiation power passing through dA , we can then write

$$dP = I dA_n = r^2 I d\omega \quad (9)$$

It will be convenient to describe the spatial dependence of the intensity of scattered radiation in terms of a spherical coordinate system as shown in Figure 5. It will be assumed that the incident radiation is linearly polarized, with the electric field vector aligned with the x axis, and that a particle is located at the origin. We will be interested in calculating the intensity at a point r, θ, ϕ that results from scattering of the incident radiation by the particle.

The plane that contains both the direction of propagation of the incident wave (the z axis) and the direction of observation (the position vector \vec{r}) is called the scattering plane. The distance from the scatterer to the point of observation is r , the scattering angle is θ , and the angle between the scattering plane and the plane of polarization of the incident radiation is ϕ . We will then seek expressions for $I(r, \theta, \phi)$ from which we can calculate

$$dP(r, \theta, \phi) = I(r, \theta, \phi) dA_n = I(r, \theta, \phi) r^2 d\omega \quad (10)$$

^aIn current practice (Reference 10), the quantity defined by equation (8) is called the irradiance and given the symbol E , and the symbol I is used for the term radiant intensity defined by $dP/d\omega$. Thus the intensity defined here is equal to the radiant intensity multiplied by r^2 . The use of intensity as defined by equation (8), however, is so firmly entrenched in the literature on light scattering, we will use it here to avoid confusion.

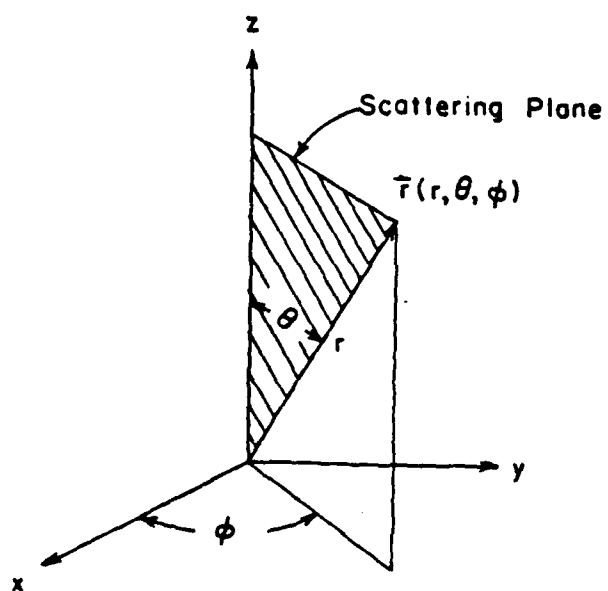


Figure 5. Definition of Coordinate System and Scattering Plane used for Scattering Calculations.

C. MIE THEORY

The Mie theory follows from a rigorous solution to the Maxwell equations and their associated boundary conditions for the radiation field resulting from the scattering of a linearly-polarized plane wave by a homogeneous, isotropic sphere of arbitrary size and refractive index. The solution takes the form of an infinite series, the terms of which include the product of an associated Legendre polynomial, with argument $\cos\theta$, and a spherical Bessel function with argument kr where k is the wave number $2\pi/\lambda$, λ being the wave length of the radiation. The coefficients in the series are evaluated in terms of the size parameters $\chi = \pi d/\lambda$, where d is the particle diameter. Finally, the series is multiplied by a circular function (\sin or \cos) whose argument is the angle ϕ that characterizes the polarization of the incident radiation.

For regions far removed from the scatterer, the series can be simplified by taking asymptotic values of the Bessel functions for large r ; the series then involves only Legendre polynomials. The result is that the radiation field can be completely specified in terms of known functions of the wave length λ , refractive index m , the dimensionless particle size χ , and the position in the field prescribed by the coordinates (r, θ, ϕ) .

In particular, the intensity of the scattered radiation can be expressed as

$$I(I_0, \lambda, r, \chi, m, \theta, \phi) = \frac{\lambda^2 I_0}{4\pi^2 r^2} \{i_1(\chi, m, \theta) \sin^2 \phi + i_2(\chi, m, \theta) \cos^2 \phi\} \quad (11)$$

where $i_1(\chi, m, \theta)$ and $i_2(\chi, m, \theta)$ are intensity functions, defined such that the product of i_1 or i_2 with $\lambda^2 I_0 / 4\pi^2 r^2$ is the component of the scattered intensity polarized perpendicular and parallel to the scattering planes, respectively. The incident radiant intensity is I_0 , and the distance from the scatterer is r . The intensity functions i_1 and i_2 are related to the amplitude functions S_1 and S_2 as

$$i_1(\chi, m, \theta) = |S_1(\chi, m, \theta)|^2 \quad (12)$$

and

$$i_2(\chi, m, \theta) = |S_2(\chi, m, \theta)|^2 \quad (13)$$

where we have adopted the notation of van de Hulst (Reference 6). Henceforth, the dependence on χ and m will not be written explicitly, i.e. we will write

$$I(r, \theta, \phi) = \frac{\lambda^2 I_0}{4\pi^2 r^2} \{i_1(\theta) \sin^2 \phi + i_2(\theta) \cos^2 \phi\} \quad (14)$$

D. EVALUATION OF THE INTENSITY FUNCTIONS

A number of computer programs are available for the calculation of the intensity functions i_1 and i_2 (see for example, References 8, 11, and 12). The program used here was written by D.M. Ogden (Reference 12).

The computer program requires as input parameters the size parameter, the wavelength of the incident radiation, the refractive index of the surrounding media, the real and imaginary part of the complex refractive index, and the scattering angle θ . The pertinent output parameters are the intensity functions $i_1(\theta)$ and $i_2(\theta)$.

E. CALCULATIONS OF COLLECTED LIGHT POWER

We are interested in the power of the light scattered by a particle that is collected by a lens of a given diameter and focal length and with a given geometric orientation with respect to the scatterer.

Consider, for example, the geometric configuration shown in Figure 6. The normal to the center of the circle lies in the y-z plane and forms an angle θ_0 with the z axis. It is assumed that a plane wave propagating in the z direction, whose electric field vector oscillates in the x-z plane, impinges on a scatterer at the origin. The distance from the scatterer to the center of the circle is f . The position of the circle is characterized by the coordinates of its center: f , θ_0 , and ϕ_0 . For the case shown, $\phi_0 = \pi/2$.

We can locate an elemental area dA on the surface of the circle with the polar coordinates r and β . The distance from the origin to dA is s , and the outward normal to dA forms an angle α with the line from the origin to dA along s . The location of dA is established by its coordinates (s, θ, ϕ) .

The power of the scattered light collected by dA is, from equation (9),

$$dP = I(s, \theta, \phi) s^2 dw$$

where dw , the solid angle subtended by dA , is given by

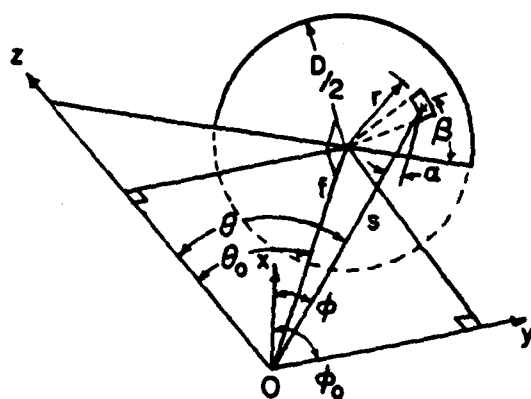


Figure 6. Geometric Construction for Calculation the Scattering Angles and Scattering Distance.

$$dw = \frac{(dA) \cos \alpha}{s^2}$$

Thus

$$dP = I(s, \theta, \phi) \cos \alpha \, dA$$

It can be seen from Figure 6 that

$$\cos \alpha = f/s$$

so

$$dP = \frac{I(s, \theta, \phi) f \, r \, dr \, d\beta}{s} \quad (15)$$

To complete the derivation, we must relate s , θ , and ϕ to r , β , f , θ_0 and ϕ_0 . Those relations can be obtained as follows. If we let

$$a = f \sin \theta_0 + r \cos \beta \cos \theta_0 \quad (16a)$$

$$b = r \sin \beta \quad (16b)$$

$$c = (a^2 + b^2)^{1/2} \quad (16c)$$

then

$$s = (r^2 + f^2)^{1/2} \quad (16d)$$

$$\theta = \sin^{-1} (c/s) \quad (16e)$$

$$\phi = \sin^{-1} (a/c) \quad (16f)$$

Thus for any position on the circle given by r and β , the parameters s , θ , and ϕ can be obtained, and the power collected by dA becomes

$$dP = \frac{\lambda^2 I_0}{4\pi^2 s^3} \{i_1(\theta) \sin^2 \phi + i_2(\theta) \cos^2 \phi\} f r \, dr \, d\beta$$

where $i_1(\theta)$ and $i_2(\theta)$ are obtained from the Mie code.

An example of this calculation is shown in Figure 7 for a latex particle, of size parameter 4.2, irradiated with linearly polarized radiation of wavelengths 0.488 μm . The scattered light intensity is calculated over the surface of a 300 mm diameter lens located 75 mm from the particle (an f-number of 4). The optical axis of the lens is given by $\theta_0 = 20$ degrees and $\phi_0 = \pi/2$. The power is normalized by its maximum value and the iso-power contours are

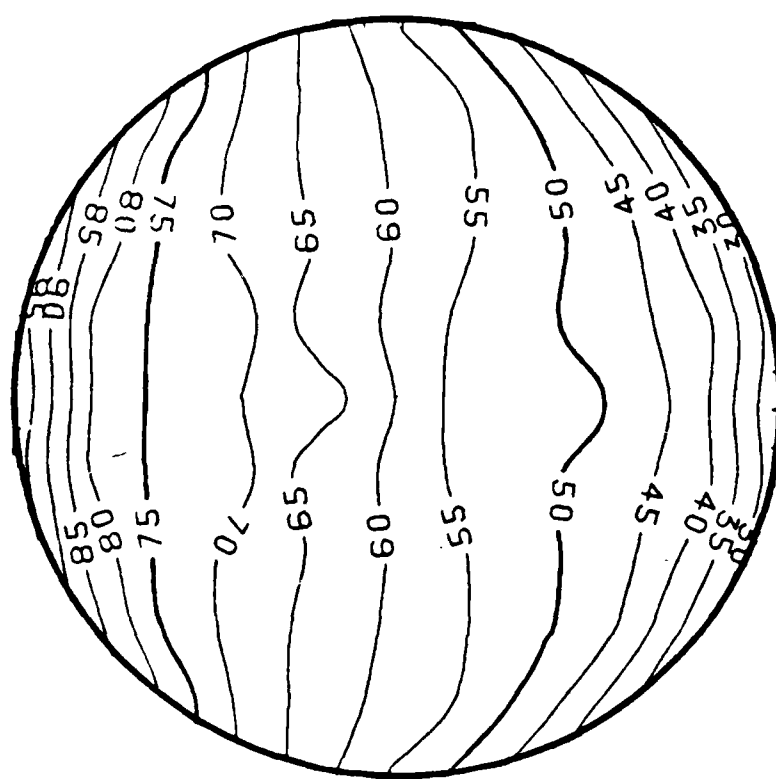


Figure 7. Intensity Contours Over an $f/4$ Lens.

shown. As can be seen, there is substantial variation in the power over the surface of the lens. This indicates that for accurate calculations, the power of the scattered radiation must be integrated over the collection surface, i.e. we must take

$$P = \frac{\lambda^2 I_0}{4\pi^2} \int_0^{2\pi} \int_0^R \left\{ \frac{i_1(\theta)\sin^2\phi + i_2(\theta)\cos^2\phi}{s^3} \right\} r dr d\beta \quad (17)$$

F. NUMERICAL INTEGRATION

It is more convenient if we cast equations (16) and (17) in a slightly different form by dividing the power by the incident intensity and using dimensionless length variables normalized by the lens radius. Then

$$C_{sp} = P/I_0$$

and

$$F = \frac{f}{D} = \frac{f}{2R}$$

where C_{sp} is the partial scattering cross section of the lens and F is the lens f-number. In dimensionless form, we have

$$C_{sp} = \frac{F \lambda^2}{2\pi^2} \int_0^{2\pi} \int_0^1 \left\{ \frac{i_1(\theta)\sin^2\phi + i_2(\theta)\cos^2\phi}{s^3} \right\} \rho d\rho d\beta \quad (18)$$

where

$$\begin{aligned} \rho &= \frac{r}{R} \\ s &= \frac{s}{R} = (\rho^2 + 4F^2)^{\frac{1}{2}} \\ A &= \frac{a}{R} = 2F\sin\theta_0 + \rho\cos\beta\cos\theta_0 \\ B &= \frac{b}{R} = \rho\sin\beta \\ C &= \frac{c}{R} = (A^2 + B^2)^{\frac{1}{2}} \\ \theta &= \sin^{-1} \left(\frac{C}{S} \right) \\ \phi &= \sin^{-1} \left(\frac{A}{C} \right) \end{aligned} \quad (19)$$

The radius of the circle is then divided into M segments, as shown in Figure 8 (where $M = 4$), with $M + 1$ nodes at $0, 1/M, \dots, 1$. The area of the circle about node 0 is

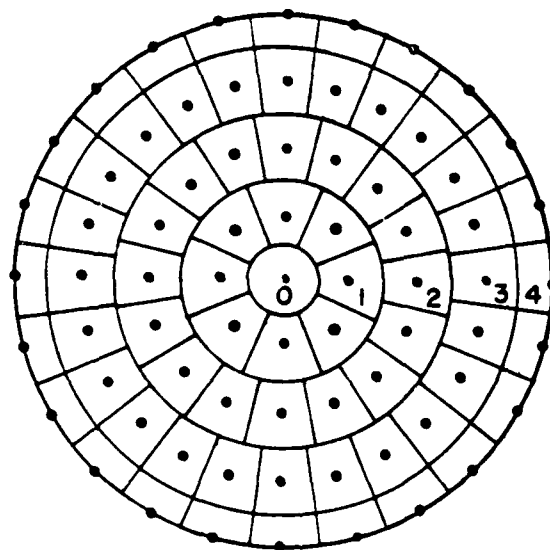


Figure 8. Scheme for Subdivision of Lens Surface.

$$A_0 = \pi \left(\frac{1}{2M} \right)^2 = \frac{\pi}{4M^2}$$

If the annulus containing node 1 is subdivided into K segments of angle $\Delta\beta_1$, the area of a sector about node 1 is then

$$A_1 = \left[\left(\frac{3}{2M} \right)^2 - \left(\frac{1}{2M} \right)^2 \right] \frac{1}{K} = 2/KM^2$$

Equating A_1 to A_0 we obtain $K = 8$ so that $\Delta\beta = 2\pi/8 = \pi/4$

In a like manner, we can obtain a similar expression for the value of $\Delta\beta$ in any annulus such that the defined sector area is equal to A_0 . The general result for $\Delta\beta$ in the annulus about node j is

$$\Delta\beta_j = \pi/4_j; j = 1, 2, \dots, M-1$$

Since the width of the ring about node M is one-half the width of the other rings, a segment with $\Delta\beta_M = \Delta\beta_{M-1}$ will give an area equal to $A_0 [(4M-1)/8(M-1)]$ which is about equal to $A_0/2$ for large M.

In this manner the circle is divided into $(4)(M+2)(M-1) + 1$ sectors. The numerical integration then takes the form

$$C_{sp} = \frac{F\lambda^2}{2\pi^2} \left\{ [G(\theta_0, \phi_0) + \sum_{j=1}^{M-1} \sum_{k=1}^{8j} G(\theta_{jk}, \phi_{jk})] \frac{\pi}{4M^2} \right. \\ \left. + \left[\sum_{k=1}^{8(M-1)} G(\theta_{Mk}, \phi_{Mk}) \right] \frac{\pi(4M-1)}{4M^2(M-1)} \right\} \quad (20)$$

along with

$$\begin{aligned} \rho_k &= k/M \\ S_k &= (\rho_k^2 + 4F^2)^{\frac{1}{2}} \\ \beta_j &= (j-1)\pi/8j \\ A_{jk} &= 2F\sin\theta_0 + \rho_k \cos\beta_j \cos\theta_0 \\ B_{jk} &= \rho_k \sin\beta_j \\ C_{jk} &= (A_{jk}^2 + B_{jk}^2)^{\frac{1}{2}} \\ \theta_{jk} &= \sin^{-1}(C_{jk}/S_{jk}) \\ \phi_{jk} &= \sin^{-1}(A_{jk}/C_{jk}) \end{aligned} \quad (21)$$

and

$$G(\theta_{jk}, \phi_{jk}) = i_1(\theta_{jk}) \sin^2 \phi_{jk} + i_2(\theta_{jk}) \cos^2 \phi_{jk} \quad (22)$$

A FORTRAN program has been written to carry out these calculations. Input to the program consists of the particle diameter, the particle refractive index (in general complex), the refractive index of the ambient media, the wave length of the radiation, the lens f-number, and the angles θ_0 and ϕ_0 . The main program calls a subroutine INTG2 which does the integration and returns the partial scattering cross section for the lens. INTG2, in turn, calls two subroutines. One of them is MIE, which returns the intensity functions. The other, ANGLES, require as input F, ρ , β , θ_0 , and ϕ_0 . It returns the variables S, θ , ϕ defined by equations (21).

G. INTENSITY RATIOS

The numerical integration described above was used to calculate the ratio of the power of the radiation scattered by a particle and collected by f/4 lenses at two different angles θ_0 , i.e. the intensity ratio. For both lenses, we have taken $\phi = \pi/2$.

As can be seen from equation (17), the intensity ratio is

$$\frac{P(\theta_1)}{P(\theta_2)} = \frac{C_{sp}(\theta_1)I_0}{C_{sp}(\theta_2)I_0} = \frac{C_{sp}(\theta_1)}{C_{sp}(\theta_2)} = R(\theta_1, \theta_2)$$

where θ_1 is the large angle and θ_2 is the small angle formed by the lens axes with the axis of the incident beam. As can be seen, the incident intensity cancels. This, of course, is the motivation for using the ratio technique.

Our preliminary trials showed that there was essentially no change in the calculated intensity ratio when $M > 4$. Thus for all further calculations we have used this value.

To test the adequacy of the Mie scattering calculations, we have computed the intensity ratio as a function of particle size for scattering at 20° and 40°. The particle refractive index was 1.56 - 0.0i. These calculations were then compared to calculations carried out by Dr. Paul Bonczyk at United Technology Research Center, for the same scattering angles and particle refractive index. The comparison is shown in Figure 9. As can be seen, the computations are in excellent agreement. This indicates that the Mie code used in this work is sufficiently accurate.

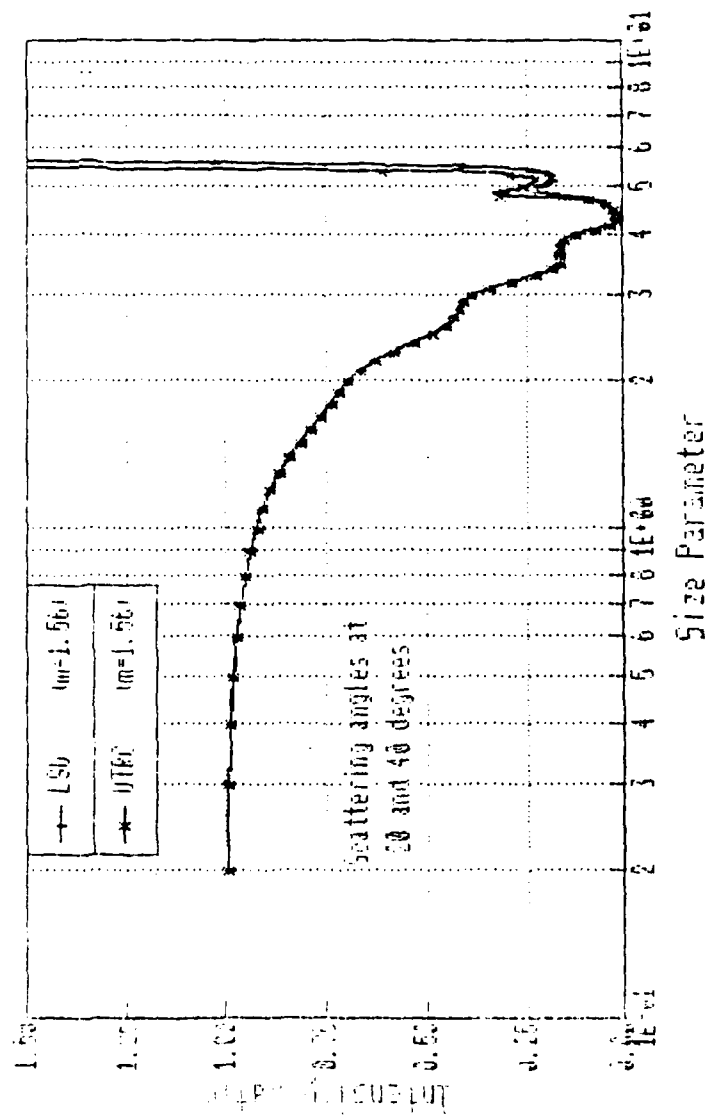


Figure 9. Validation of Intensity Ratios.

SECTION V

CORRECTION OF SOFTWARE TABLES

A. OVERVIEW

We have described in the previous section the theory by which the intensity ratio R can be calculated for a given angle pair, particle size, and particle refractive index. The measurement problem is the reverse, i.e. given a value R for a particular angle pair and particle refractive index, one must find the particle size.

The measurement problem is illustrated in Figure 10. The Mie theory provides the function $R(\chi, m, \theta_1, \theta_2)$; the measurement demands the function $\chi(R, m, \theta_1, \theta_2)$. This latter function cannot be calculated directly-- it must be obtained by numerical inversion of $R(\chi, m, \theta_1, \theta_2)$.

Furthermore, as described in Sections II and III, the quantity digitized by the ratio processor is the value of $10\log(1/R)$ with 7 bit resolution over the range 0 to 10 volts, and that this data word is truncated to 6 bits by the software. This means that each of the $2^6 = 64$ possible values of the 6 bit digital data words represent a range of ratios, and for each ratio range there is a corresponding range of sizes, as shown in Figure 10.

The inversion problem involves two steps:

- 1) determine the range and mean for the values of the ratios represented by each of the 64 data words. These values depend only on the characteristics of the analog - digital converter.
- 2) for each angle pair - refractive index combination, determine the mid point (bin center) and range (bin width) of the corresponding size from the calculated $R(\chi, m, \theta_1, \theta_2)$.

Having then measured the intensity ratios and sorted the measured values into a discrete distribution, the corresponding discrete size distribution and its statistical properties can be obtained from the bin center and bin width tables.

B. INVERSE OF RATIOS TABLE

The values in the inverse of ratios table are determined by the particular transfer function of the analog to digital converters, as discussed in Section II. Using the transfer function given in the specification sheet for the Burr-Brown converters, we have calculated the voltage ranges and the

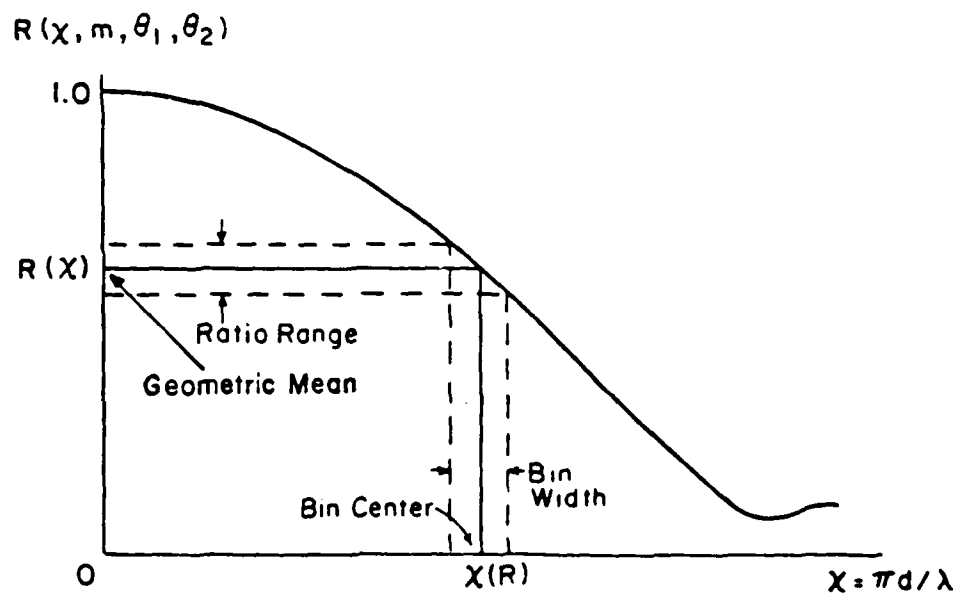


Figure 10. Relationship Between Measured Ratios and Calculated Particle Sizes.

corresponding ratio ranges for the 128 possible, 7-bit data words. These values, shown in Table 2 differ from those listed in Table 2, Reference 2. The difference owes to a different transfer function; SDI assumed that the transition voltages occurred at integral multiples of $10.0/256 = 0.03906$ rather than at the transition values given in the Burr-Brown specifications.

From the values in Table 2, the mid-points of the voltage ranges corresponding to each of the 64, 6-bit data words were obtained. The mid-point of a voltage range is related to the mean of the corresponding ratio range as follows. Since the voltage converted is

$$V = 10\log(1/R)$$

the range of voltages represented by the 6-bit data word is

$$10\log(1/R_1) \leq V \leq 10\log(1/R_2)$$

Thus the mid-point (the arithmetic mean) of the voltage range is

$$\bar{V} = 5\log(1/R_1 R_2) = 10\log(1/\bar{R})$$

or

$$\bar{R} = (R_1 R_2)^{1/2}$$

Thus the mid-point of the voltage range corresponds to the geometric mean of the ratio range.

The geometric means of the ratio range, for each of the 6-bit data words comprise the INV OF RATIOS table. This table is used to relate a measured ratio to a corresponding particle size and size range as described below. The corrected values of the INV OF RATIOS table are given in Table 3, where they are compared to the original values provided by SDL. As mentioned above, the differences owe to a correction of the transfer function for the ADC.

The effect of the revised ADC transfer function on the relation between bin number and the corresponding particle size is illustrated in Figure 11, where we have used the intensity ratios calculated by SDL for 60/20 ratioing with latex particles, and we have applied the two transfer functions to these data. As can be seen, the difference is small at large particle sizes, but at small particle sizes (where the slope of the ratio-size curve approaches unity) the difference is about 100 percent.

TABLE 2. CORRECTED DATA WORD - SIGNAL RATIO VALUES.

DATA WORD	RATIO RANGE	DATA WORD	RATIO RANGE
0	0.9866 - 1.0000	32	0.5649 - 0.5751
1	0.9690 - 0.9866	33	0.5548 - 0.5649
2	0.9517 - 0.9690	34	0.5449 - 0.5548
3	0.9348 - 0.9517	35	0.5352 - 0.5449
4	0.9181 - 0.9348	36	0.5256 - 0.5352
5	0.9017 - 0.9181	37	0.5163 - 0.5256
6	0.8857 - 0.9017	38	0.5071 - 0.5163
7	0.8699 - 0.8857	39	0.4980 - 0.5071
8	0.8544 - 0.8699	40	0.4891 - 0.4980
9	0.8391 - 0.8544	41	0.4804 - 0.4891
10	0.8242 - 0.8391	42	0.4719 - 0.4804
11	0.8095 - 0.8242	43	0.4635 - 0.4719
12	0.7950 - 0.8095	44	0.4552 - 0.4635
13	0.7809 - 0.7950	45	0.4471 - 0.4552
14	0.7669 - 0.7809	46	0.4391 - 0.4471
15	0.7533 - 0.7669	47	0.4313 - 0.4391
16	0.7398 - 0.7533	48	0.4236 - 0.4313
17	0.7266 - 0.7398	49	0.4160 - 0.4236
18	0.7137 - 0.7266	50	0.4086 - 0.4160
19	0.7010 - 0.7137	51	0.4013 - 0.4086
20	0.6885 - 0.7010	52	0.3942 - 0.4013
21	0.6762 - 0.6885	53	0.3871 - 0.3942
22	0.6641 - 0.6762	54	0.3802 - 0.3871
23	0.6523 - 0.6641	55	0.3735 - 0.3802
24	0.6407 - 0.6523	56	0.3668 - 0.3735
25	0.6292 - 0.6407	57	0.3603 - 0.3668
26	0.6180 - 0.6292	58	0.3538 - 0.3603
27	0.6070 - 0.6180	59	0.3475 - 0.3538
28	0.5962 - 0.6070	60	0.3413 - 0.3475
29	0.5856 - 0.5962	61	0.3353 - 0.3413
30	0.5751 - 0.5856	62	0.3293 - 0.3353
31	0.5649 - 0.5751	63	0.3234 - 0.3293

TABLE 2. CORRECTED DATA WORD - SIGNAL RATIO VALUE (CONCLUDED).

DATA WORD	RATIO RANGE	DATA WORD	RATIO RANGE
64	0.3120 - 0.3176	96	0.1786 - 0.1819
65	0.3064 - 0.3120	97	0.1754 - 0.1786
66	0.3010 - 0.3064	98	0.1723 - 0.1754
67	0.2956 - 0.3010	99	0.1692 - 0.1723
68	0.2903 - 0.2956	100	0.1662 - 0.1692
69	0.2851 - 0.2903	101	0.1633 - 0.1662
70	0.2801 - 0.2851	102	0.1603 - 0.1633
71	0.2751 - 0.2801	103	0.1575 - 0.1603
72	0.2702 - 0.2751	104	0.1547 - 0.1575
73	0.2653 - 0.2702	105	0.1519 - 0.1547
74	0.2606 - 0.2653	106	0.1492 - 0.1519
75	0.2560 - 0.2606	107	0.1465 - 0.1492
76	0.2514 - 0.2560	108	0.1439 - 0.1465
77	0.2469 - 0.2514	109	0.1414 - 0.1439
78	0.2425 - 0.2469	110	0.1388 - 0.1414
79	0.2382 - 0.2425	111	0.1364 - 0.1388
80	0.2339 - 0.2382	112	0.1339 - 0.1364
81	0.2298 - 0.2339	113	0.1316 - 0.1339
82	0.2257 - 0.2298	114	0.1292 - 0.1316
83	0.2217 - 0.2257	115	0.1269 - 0.1292
84	0.2177 - 0.2217	116	0.1246 - 0.1269
85	0.2138 - 0.2177	117	0.1224 - 0.1246
86	0.2100 - 0.2138	118	0.1202 - 0.1224
87	0.2063 - 0.2100	119	0.1181 - 0.1202
88	0.2026 - 0.2063	120	0.1160 - 0.1181
89	0.1990 - 0.2026	121	0.1139 - 0.1160
90	0.1954 - 0.1990	122	0.1119 - 0.1139
91	0.1919 - 0.1954	123	0.1099 - 0.1119
92	0.1885 - 0.1919	124	0.1079 - 0.1099
93	0.1852 - 0.1885	125	0.1060 - 0.1079
94	0.1819 - 0.1852	126	0.1041 - 0.1060
95	0.1786 - 0.1819	127	0.0010 - 0.1041

TABLE 3. CORRECTED VALUES OF THE INV OF RATIOS TABLE.

<u>BIN #</u>	<u>LSU VALUE</u>	<u>SDL VALUE</u>	<u>BIN #</u>	<u>LSU VALUE</u>	<u>SDL VALUE</u>
1	0.9517	0.9475	33	0.3010	0.2996
2	0.9181	0.9140	34	0.2903	0.2890
3	0.8857	0.8817	35	0.2801	0.2788
4	0.8544	0.8505	36	0.2702	0.2690
5	0.8242	0.8205	37	0.2606	0.2595
6	0.7950	0.7915	38	0.2514	0.2503
7	0.7670	0.7635	39	0.2425	0.2414
8	0.7398	0.7365	40	0.2340	0.2329
9	0.7137	0.7105	41	0.2257	0.2247
10	0.6885	0.6854	42	0.2177	0.2167
11	0.6641	0.6612	43	0.2100	0.2091
12	0.6407	0.6378	44	0.2026	0.2017
13	0.6180	0.6153	45	0.1954	0.1946
14	0.5962	0.5935	46	0.1885	0.1877
15	0.5751	0.5725	47	0.1819	0.1811
16	0.5548	0.5523	48	0.1754	0.1747
17	0.5352	0.5328	49	0.1692	0.1685
18	0.5163	0.5140	50	0.1633	0.1625
19	0.4980	0.4958	51	0.1575	0.1568
20	0.4804	0.4783	52	0.1519	0.1513
21	0.4635	0.4614	53	0.1466	0.1459
22	0.4471	0.4451	54	0.1414	0.1407
23	0.4313	0.4294	55	0.1364	0.1358
24	0.4161	0.4142	56	0.1316	0.1310
25	0.4013	0.3995	57	0.1269	0.1263
26	0.3872	0.3854	58	0.1224	0.1219
27	0.3735	0.3718	59	0.1181	0.1176
28	0.3603	0.3587	60	0.1139	0.1134
29	0.3475	0.3460	61	0.1099	0.1094
30	0.3353	0.3338	62	0.1060	0.1055
31	0.3234	0.3220	63	0.1020	0.1018
32	0.3120	0.3106			

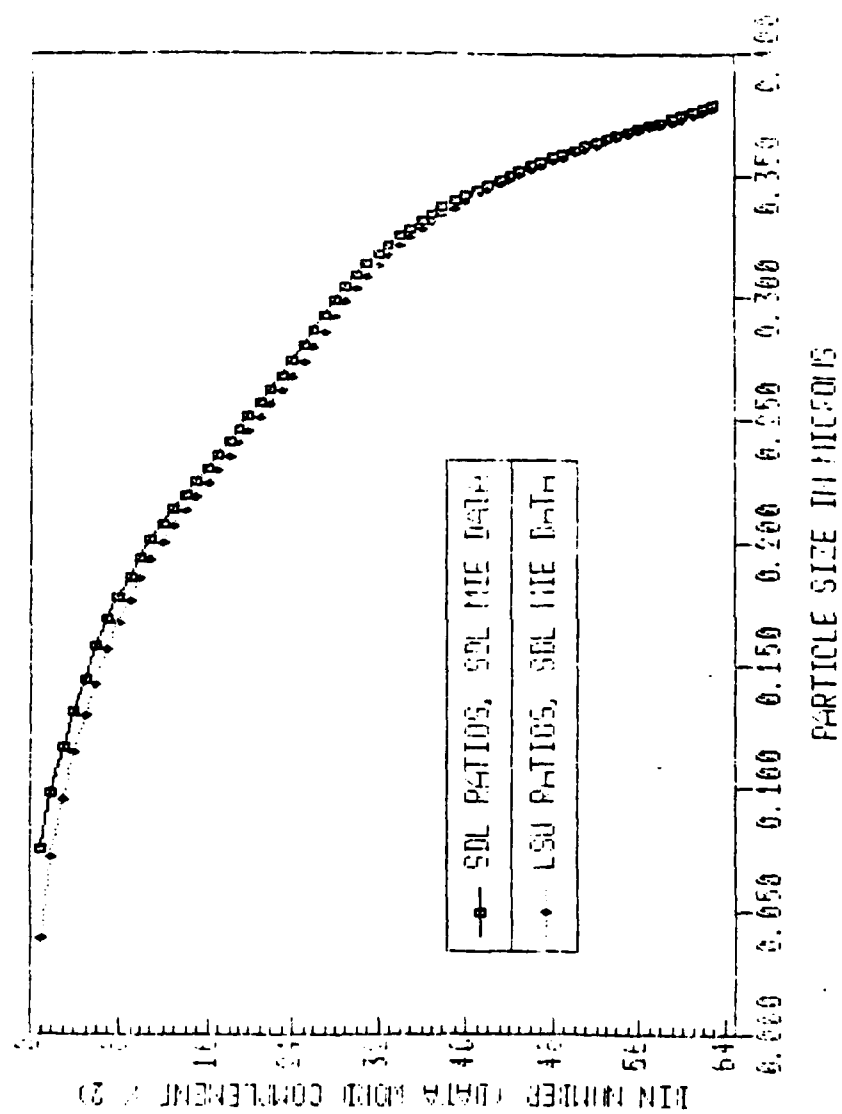


Figure 11. Effect of ADC Transfer Function on Measured Ratio-Size Relationship.

Note that only 63 of the 64 possible values are listed in Table 3. As described in Section III, the ratio range corresponding to data words 0 and 1 in Table 1 are not used, i.e. ratios in the range 0.9690 to 1.0000 are not processed.

C. BIN CENTER AND BIN WIDTH TABLES

The bin center and bin width tables for each angle pair - refractive index combination were constructed as follows:

- 1) The upper and lower limits on the particle size corresponding to ratios of slightly less than 1.0 and 0.1 were determined using the Mie theory code.
- 2) This size range was divided into 600 increments and the intensity ratio was calculated for each of these 600 sizes.
- 3) The size corresponding to the ratio at the geometric mean and at the transition points for each of the 64 ratio intervals was then found by linear interpolation from the 600 values calculated in step 2.
- 4) The bin center values were identified with the interpolated size at the geometric mean of the ratio range.
- 5) The bin width values were identified with the difference between the interpolated sizes at the upper and lower transition points of the ratio.

This procedure is straightforward provided the function $R(\chi)$ is well-behaved, i.e. if the variation in $R(\chi)$ with χ is monotonic. If there are local maxima and minima in the function $R(\chi)$, however, the inversion process leads to multivaluedness of $\chi(R)$, and one is faced with the problem of how to deal with this multivaluedness.

This problem, which only occurred in inverting ratio functions for latex particles, is illustrated in Figure 12. Within the ratio range R_1 to R_2 , there are two possible values of χ at the local maximum and minimum, and three possible values elsewhere. It is clear that the inversion problem is indeterminate -- the measurement cannot provide unique values for the size in the ratio range $R_1 \leq R \leq R_2$.

To eliminate the multivaluedness of χ for these situations, the function $R(\chi)$ was simply assumed to vary linearly between R_2 and R_1 as shown in Figure 13.

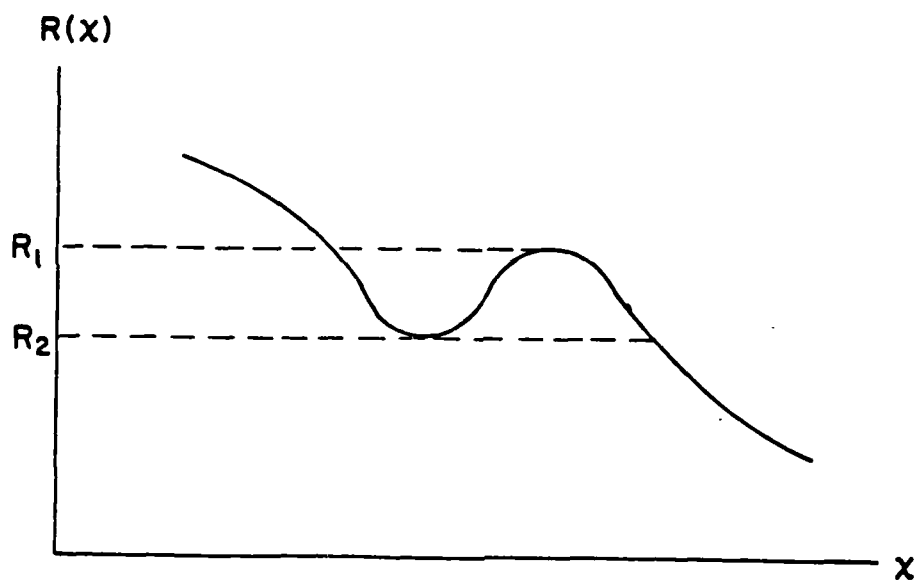


Figure 12. Ambiguities in the Inversion of Function with Local Maxima and Minima.

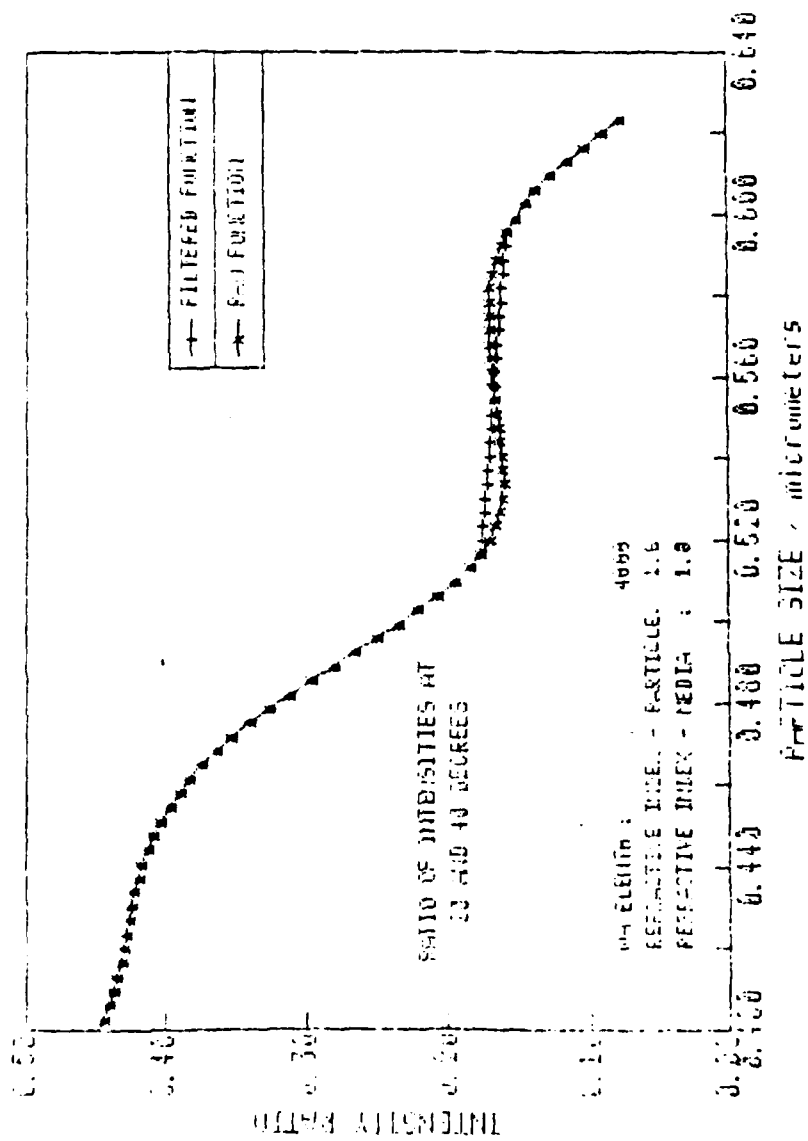


Figure 13. Resolution of Size Ambiguity

The problem with the bin center tables supplied with the software is illustrated in Figure 14, where we compare the calculated relationship between the intensity ratio and size with the corresponding values given in a bin center table. The particular case is for 40/20 ratioing with latex particles. Since there is very little difference between our calculated values and the values calculated by SDL, and the effect of the ADC transfer function is small except at small particle sizes, the error must owe to the implementation of the inversion process carried out by SDL.

The corrected bin center and bin width tables for 40/20, 50/20, and 60/20 ratioing with latex ($m = 1.60$) and soot ($m = 1.57 - 9.56i$) are given in Tables 4 through 6. The corrected values are compared to the previous values in Figures 15 through 26.

A FORTRAN program to calculate the bin center and bin width tables for any angle pair, lens f-number, and particle refractive index has been provided to the Tyndall laboratory. Figures 14 through 25 were obtained using this program.

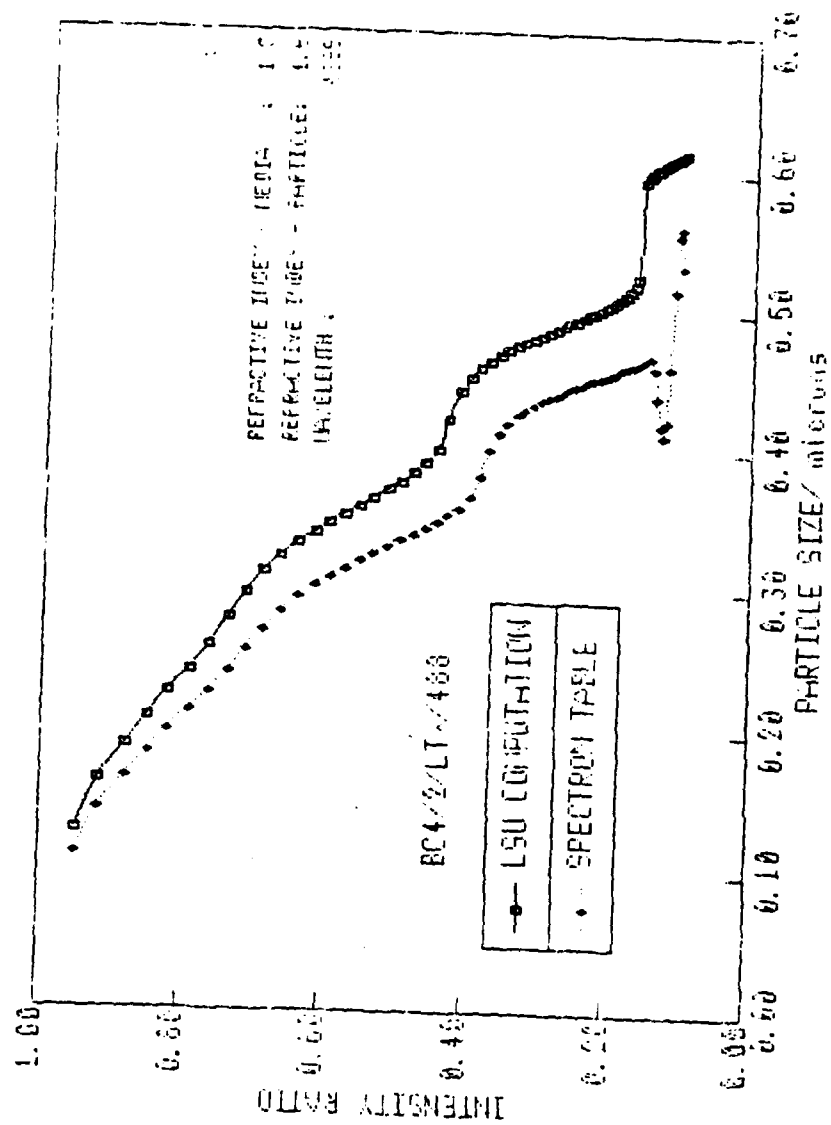


Figure 14. Disparity Between the Calculated Relationship of Intensity Ratio to Particle Size and the Implementation of this Relationship in the Bin Center Table.

TABLE 4. CORRECTED VALUES OF THE BIN CENTER AND BIN WIDTH TABLE FOR 40/20 RATIOING.

BIN #	LATEX		SOOT	
	BIN CENTER	BIN WIDTH	BIN CENTER	BIN WIDTH
1	0.12242	0.04583	0.12220	0.04231
2	0.15999	0.03146	0.15629	0.02884
3	0.18683	0.02342	0.18164	0.02295
4	0.20768	0.01899	0.20276	0.01968
5	0.22540	0.01695	0.22124	0.01746
6	0.24203	0.01674	0.23780	0.01576
7	0.25931	0.01819	0.25286	0.01443
8	0.27851	0.01975	0.26670	0.01336
9	0.29771	0.01750	0.27966	0.01258
10	0.31306	0.01335	0.29191	0.01196
11	0.32477	0.01042	0.30361	0.01146
12	0.33418	0.00860	0.31485	0.01103
13	0.34213	0.00743	0.32568	0.01064
14	0.34914	0.00666	0.33614	0.01027
15	0.35552	0.00615	0.34623	0.00990
16	0.36150	0.00586	0.35595	0.00954
17	0.36728	0.00575	0.36531	0.00918
18	0.37305	0.00585	0.37430	0.00883
19	0.37904	0.00623	0.38298	0.00852
20	0.38562	0.00712	0.39135	0.00823
21	0.39357	0.00930	0.39944	0.00797
22	0.40540	0.01752	0.40729	0.00774
23	0.43128	0.02512	0.41493	0.00754
24	0.44782	0.01144	0.42237	0.00736
25	0.45670	0.00735	0.42964	0.00719
26	0.46302	0.00557	0.43676	0.00705
27	0.46802	0.00454	0.44374	0.00691
28	0.47219	0.00388	0.45059	0.00678
29	0.47582	0.00341	0.45731	0.00666
30	0.47905	0.00307	0.46390	0.00653
31	0.48197	0.00281	0.47037	0.00641
32	0.48467	0.00261	0.47672	0.00629
33	0.48719	0.00245	0.48295	0.00617
34	0.48958	0.00233	0.48906	0.00604
35	0.49186	0.00224	0.49505	0.00593
36	0.49406	0.00217	0.50092	0.00582
37	0.49621	0.00213	0.50668	0.00571
38	0.49833	0.00211	0.51234	0.00560
39	0.50044	0.00211	0.51789	0.00550
40	0.50255	0.00213	0.52334	0.00541
41	0.50471	0.00219	0.52870	0.00532
42	0.50695	0.00228	0.53398	0.00523
43	0.50930	0.00244	0.53917	0.00516
44	0.51184	0.00267	0.54429	0.00508
45	0.51467	0.00306	0.54933	0.00501
46	0.51803	0.01160	0.55432	0.00495
47	0.54836	0.04063	0.55924	0.00489
48	0.58826	0.02718	0.56410	0.00484
49	0.59775	0.00387	0.56891	0.00478
50	0.60113	0.00301	0.57367	0.00473
51	0.60386	0.00251	0.57838	0.00469
52	0.60617	0.00215	0.58305	0.00464
53	0.60820	0.00191	0.58767	0.00460
54	0.61000	0.00172	0.59225	0.00456
55	0.61164	0.00157	0.59678	0.00452
56	0.61316	0.00146	0.60128	0.00448
57	0.61456	0.00136	0.60575	0.00444
58	0.61588	0.00128	0.61017	0.00441
59	0.61713	0.00122	0.61456	0.00438
60	0.61831	0.00116	0.61892	0.00434
61	0.61945	0.00111	0.62325	0.00432
62	0.62054	0.00107	0.62755	0.00429
63	0.62165	0.00116	0.63209	0.00480

TABLE 5. CORRECTED VALUES OF THE BIN CENTER AND BIN WIDTH TABLES FOR 50/20 RATIOING.

BIN #	LATEX		SOOT	
	BIN CENTER	BIN WIDTH	BIN CENTER	BIN WIDTH
1	0.09286	0.03510	0.09444	0.03420
2	0.12285	0.02626	0.12261	0.02411
3	0.14620	0.02094	0.14377	0.01893
4	0.16509	0.01707	0.16097	0.01578
5	0.18065	0.01434	0.17563	0.01381
6	0.19390	0.01234	0.18870	0.01242
7	0.20548	0.01094	0.20057	0.01139
8	0.21590	0.01001	0.21154	0.01057
9	0.22559	0.00945	0.22175	0.00989
10	0.23488	0.00920	0.23133	0.00929
11	0.24407	0.00927	0.24035	0.00877
12	0.25349	0.00964	0.24888	0.00831
13	0.26343	0.01028	0.25699	0.00791
14	0.27405	0.01094	0.26470	0.00755
15	0.28518	0.01107	0.27211	0.00727
16	0.29594	0.01023	0.27925	0.00701
17	0.30551	0.00886	0.28614	0.00678
18	0.31369	0.00755	0.29282	0.00658
19	0.32068	0.00650	0.29931	0.00641
20	0.32675	0.00569	0.30564	0.00625
21	0.33211	0.00507	0.31181	0.00610
22	0.33692	0.00458	0.31784	0.00597
23	0.34129	0.00419	0.32374	0.00584
24	0.34533	0.00389	0.32952	0.00571
25	0.34908	0.00363	0.33517	0.00559
26	0.35261	0.00343	0.34069	0.00547
27	0.35595	0.00327	0.34610	0.00535
28	0.35915	0.00313	0.35138	0.00523
29	0.36223	0.00303	0.35655	0.00511
30	0.36522	0.00296	0.36160	0.00499
31	0.36815	0.00291	0.36653	0.00488
32	0.37104	0.00288	0.37135	0.00476
33	0.37392	0.00289	0.37606	0.00466
34	0.37682	0.00293	0.38066	0.00455
35	0.37978	0.00300	0.38516	0.00445
36	0.38284	0.00313	0.38957	0.00436
37	0.38606	0.00332	0.39389	0.00427
38	0.38951	0.00363	0.39812	0.00419
39	0.39335	0.00411	0.40226	0.00411
40	0.39782	0.00495	0.40633	0.00403
41	0.40344	0.00665	0.41033	0.00396
42	0.41179	0.01139	0.41426	0.00390
43	0.42766	0.01746	0.41813	0.00384
44	0.44187	0.01043	0.42194	0.00378
45	0.45000	0.00671	0.42569	0.00372
46	0.45575	0.00506	0.42939	0.00367
47	0.46027	0.00411	0.43303	0.00362
48	0.46404	0.00348	0.43663	0.00358
49	0.46728	0.00303	0.44019	0.00353
50	0.47013	0.00270	0.44370	0.00349
51	0.47269	0.00243	0.44717	0.00345
52	0.47501	0.00222	0.45060	0.00341
53	0.47714	0.00205	0.45399	0.00337
54	0.47911	0.00190	0.45734	0.00333
55	0.48095	0.00177	0.46065	0.00330
56	0.48267	0.00167	0.46393	0.00326
57	0.48429	0.00158	0.46717	0.00323
58	0.48582	0.00149	0.47038	0.00319
59	0.48728	0.00142	0.47355	0.00316
60	0.48867	0.00136	0.47670	0.00312
61	0.49000	0.00131	0.47980	0.00309
62	0.49128	0.00126	0.48288	0.00306
63	0.49259	0.00136	0.48611	0.00301

TABLE 6. CORRECTED VALUES OF THE BIN CENTER AND BIN WIDTH TABLES FOR 60/20 RATIOING.

BIN #	LATEX		SOOT	
	BIN CENTER	BIN WIDTH	BIN CENTER	BIN WIDTH
1	0.07603	0.02863	0.07772	0.02850
2	0.10038	0.02179	0.10166	0.02077
3	0.12008	0.01802	0.12008	0.01658
4	0.13668	0.01536	0.13518	0.01388
5	0.15094	0.01328	0.14805	0.01202
6	0.16333	0.01159	0.15934	0.01063
7	0.17415	0.01018	0.16943	0.00966
8	0.18378	0.00911	0.17868	0.00889
9	0.19243	0.00822	0.18724	0.00828
10	0.20028	0.00752	0.19526	0.00778
11	0.20751	0.00697	0.20282	0.00736
12	0.21425	0.00654	0.20999	0.00699
13	0.22061	0.00622	0.21681	0.00667
14	0.22671	0.00600	0.22333	0.00638
15	0.23263	0.00586	0.22957	0.00611
16	0.23844	0.00580	0.23556	0.00586
17	0.24424	0.00582	0.24131	0.00564
18	0.25010	0.00592	0.24684	0.00543
19	0.25610	0.00610	0.25217	0.00524
20	0.26232	0.00636	0.25733	0.00507
21	0.26883	0.00666	0.26232	0.00490
22	0.27564	0.00694	0.26714	0.00477
23	0.28268	0.00709	0.27184	0.00463
24	0.28975	0.00698	0.27641	0.00451
25	0.29658	0.00661	0.28087	0.00440
26	0.30294	0.00608	0.28522	0.00430
27	0.30873	0.00550	0.28947	0.00421
28	0.31395	0.00496	0.29363	0.00412
29	0.31867	0.00449	0.29771	0.00404
30	0.32294	0.00408	0.30171	0.00396
31	0.32684	0.00374	0.30563	0.00389
32	0.33043	0.00344	0.30949	0.00382
33	0.33374	0.00320	0.31328	0.00376
34	0.33682	0.00298	0.31701	0.00370
35	0.33971	0.00279	0.32068	0.00364
36	0.34242	0.00263	0.32430	0.00358
37	0.34498	0.00249	0.32785	0.00353
38	0.34741	0.00237	0.33136	0.00347
39	0.34972	0.00226	0.33480	0.00342
40	0.35192	0.00216	0.33820	0.00337
41	0.35403	0.00207	0.34154	0.00332
42	0.35606	0.00199	0.34483	0.00326
43	0.35802	0.00192	0.34807	0.00321
44	0.35991	0.00186	0.35126	0.00316
45	0.36175	0.00181	0.35440	0.00311
46	0.36353	0.00176	0.35749	0.00306
47	0.36526	0.00172	0.36053	0.00302
48	0.36696	0.00168	0.36352	0.00297
49	0.36862	0.00164	0.36646	0.00292
50	0.37025	0.00162	0.36936	0.00287
51	0.37185	0.00159	0.37221	0.00283
52	0.37344	0.00158	0.37502	0.00278
53	0.37501	0.00156	0.37778	0.00274
54	0.37657	0.00155	0.38050	0.00270
55	0.37812	0.00155	0.38318	0.00266
56	0.37966	0.00155	0.38581	0.00262
57	0.38122	0.00156	0.38841	0.00258
58	0.38278	0.00157	0.39097	0.00254
59	0.38436	0.00159	0.39350	0.00251
60	0.38596	0.00162	0.39599	0.00247
61	0.38760	0.00165	0.39844	0.00244
62	0.38927	0.00170	0.40086	0.00241
63	0.39112	0.00199	0.40340	0.00267

COMPARISON OF SPECIFIC AND LSU
BIN CENTER TABLES
PC472 LIX 188

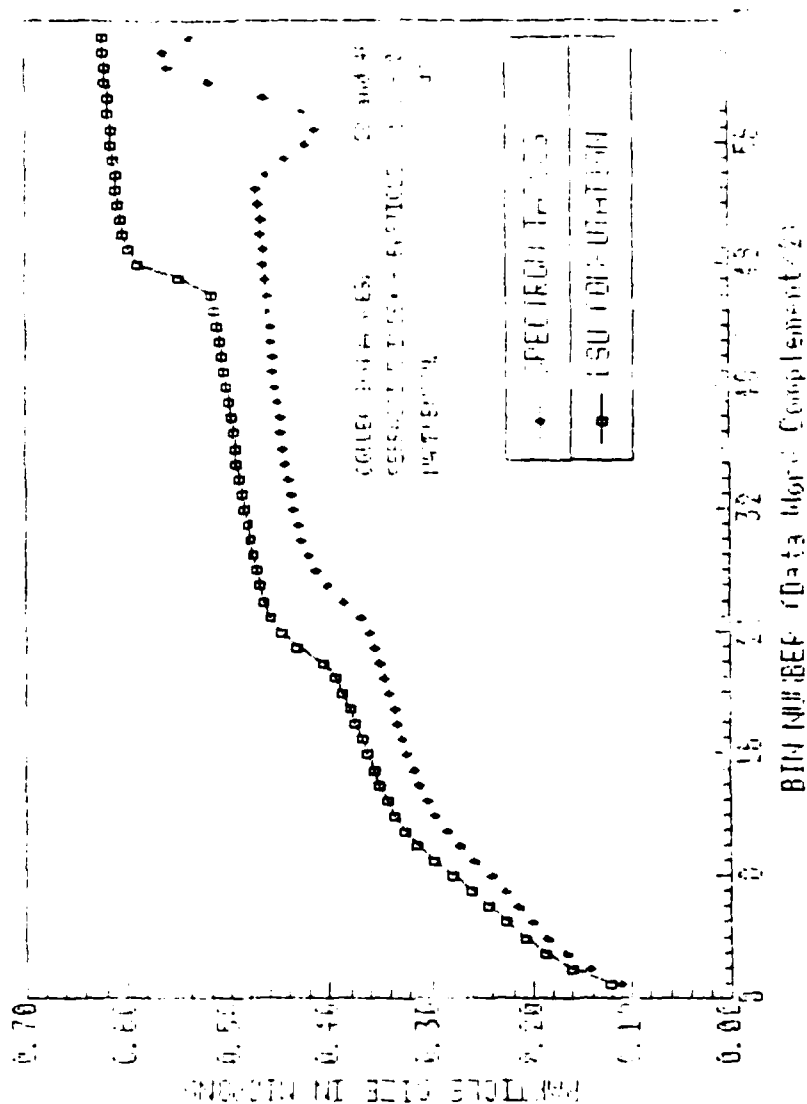


Figure 15. Correction of Bin Center Tables for 40/20 Ratioing with Latex Particles.

COMPARISON OF SPECTROM & LSU
BIN WIDTH TABLES
BW4/2/LTX 488

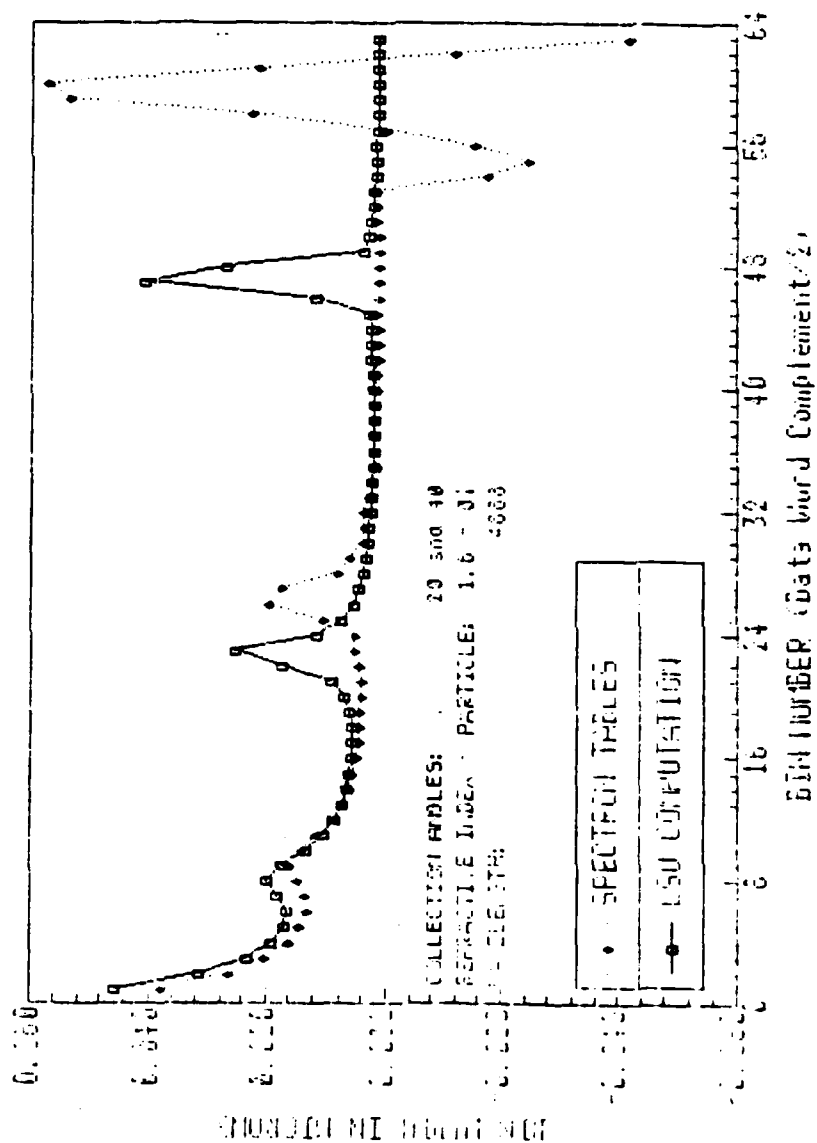


Figure 16. Correction of Bin Width Tables for 40/20 Ratioing with Latex Particles.

COMPARISON OF SPECTRON & LCU BIN CENTER TABLES SL-4 2 5001 488

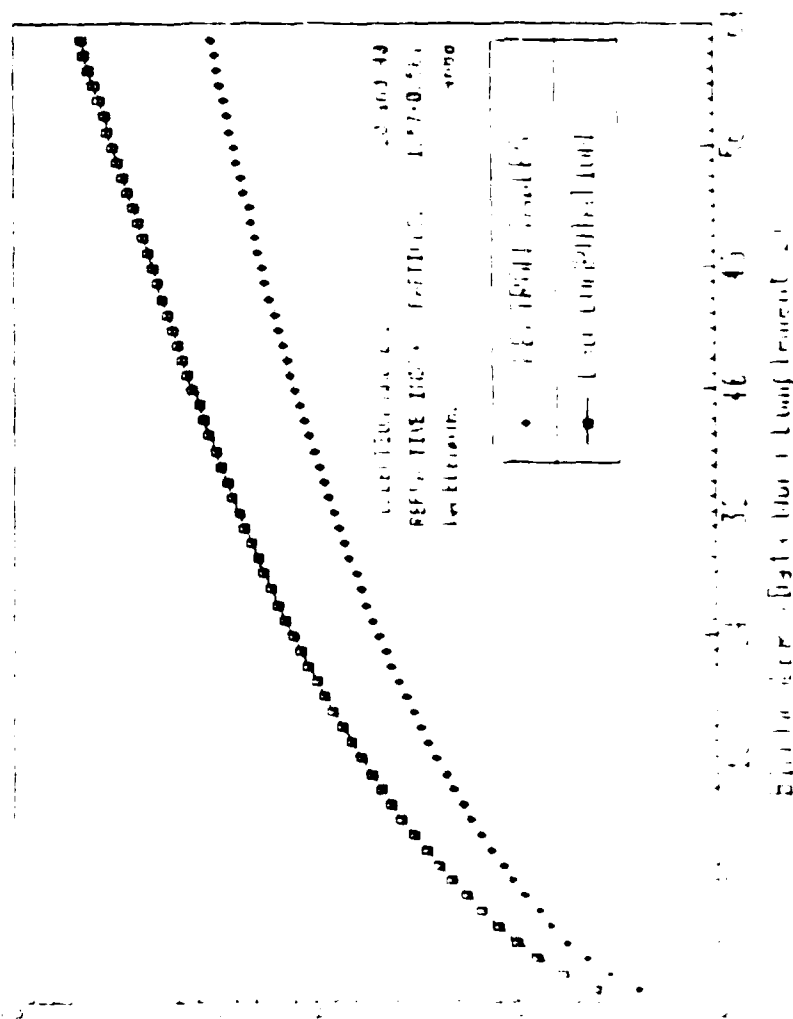


Figure 17 - Correction of Bin Center Tables for 40/20 Ratioing with Soot Particles

100% of light at 400 nm
 100% of light at 400 nm
 100% of light at 400 nm

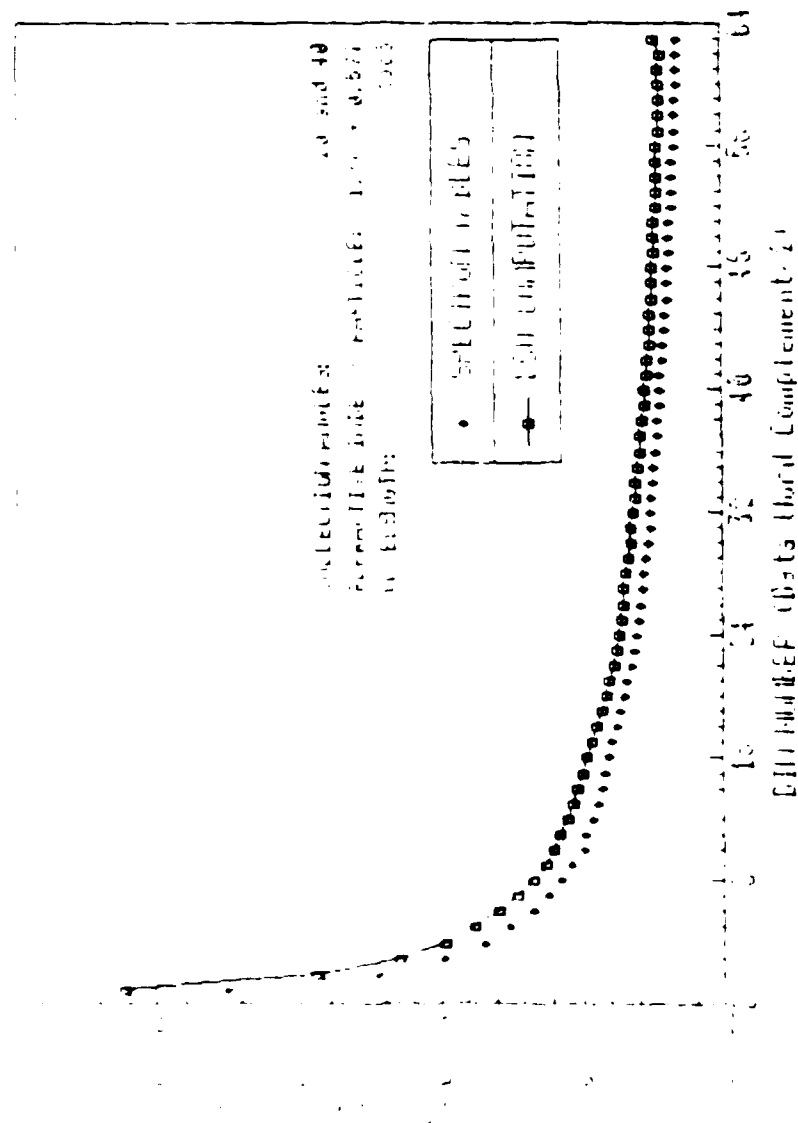


Figure 18. Correction of Bin Width Tables for 40/20 Ratioing with Soot Particles.

COMPARISON OF SPECTRON & LSU
BIN CENTER TABLES
BC572/LTX/468

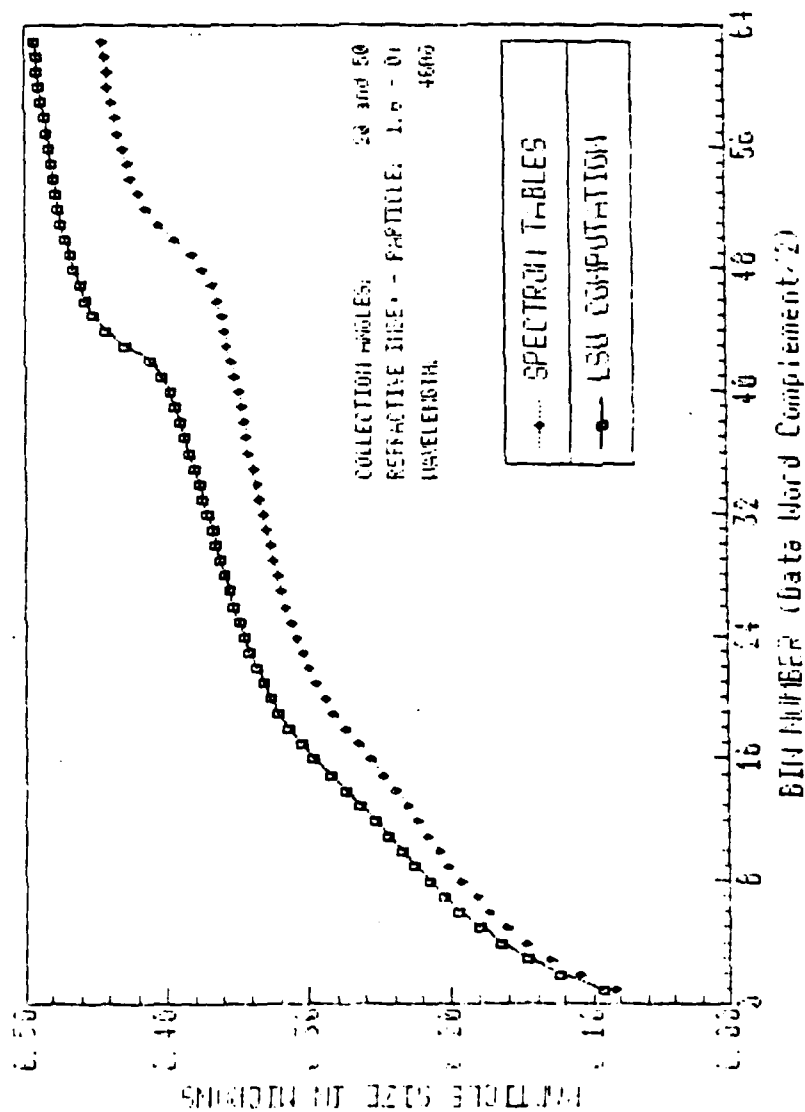


Figure 19. Correction of Bin Center Tables for 50/20 Ratioing with Latex Particles.

COMPARISON OF SPECTROM & LSU BIN WIDTH TABLES BW5/2/LTX/488

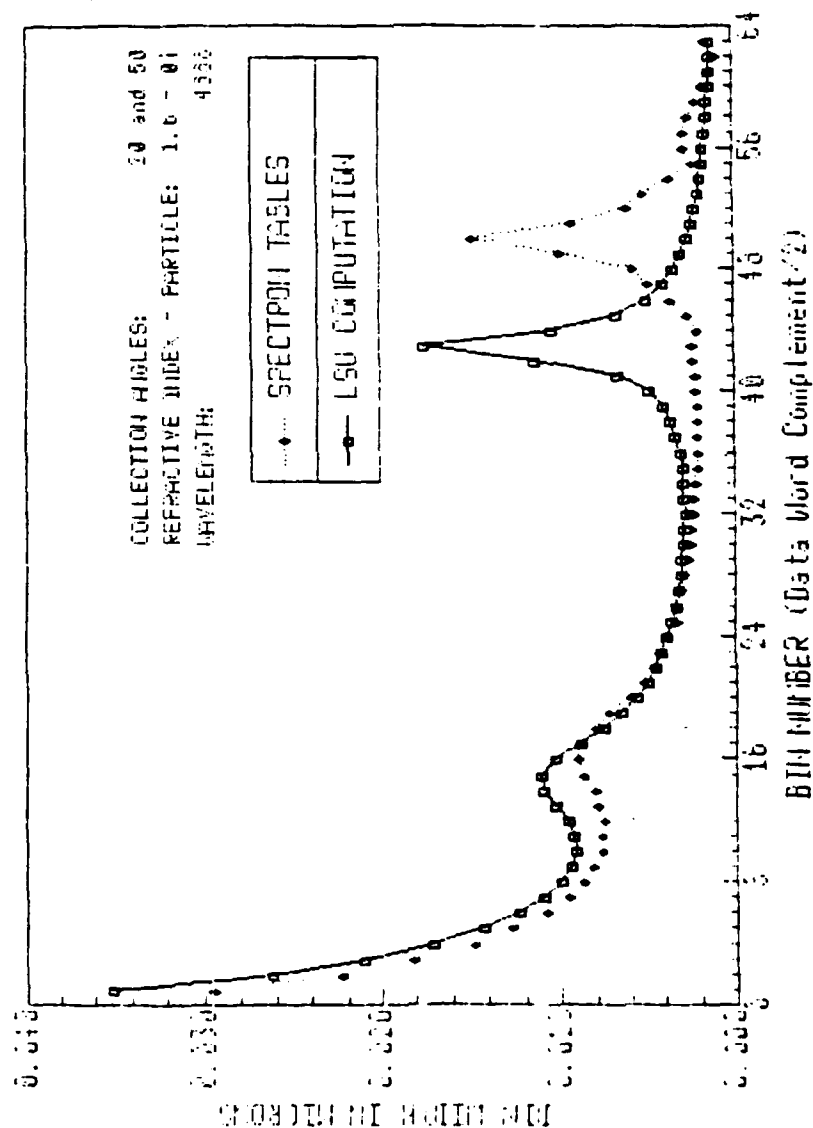


Figure 20. Correction of Bin Width Tables for 50/20 Ratioing with Latex Particles.

COMPARISON OF SPECTRON & LSU
BIN CENTER TABLES
BC5 2 5007488

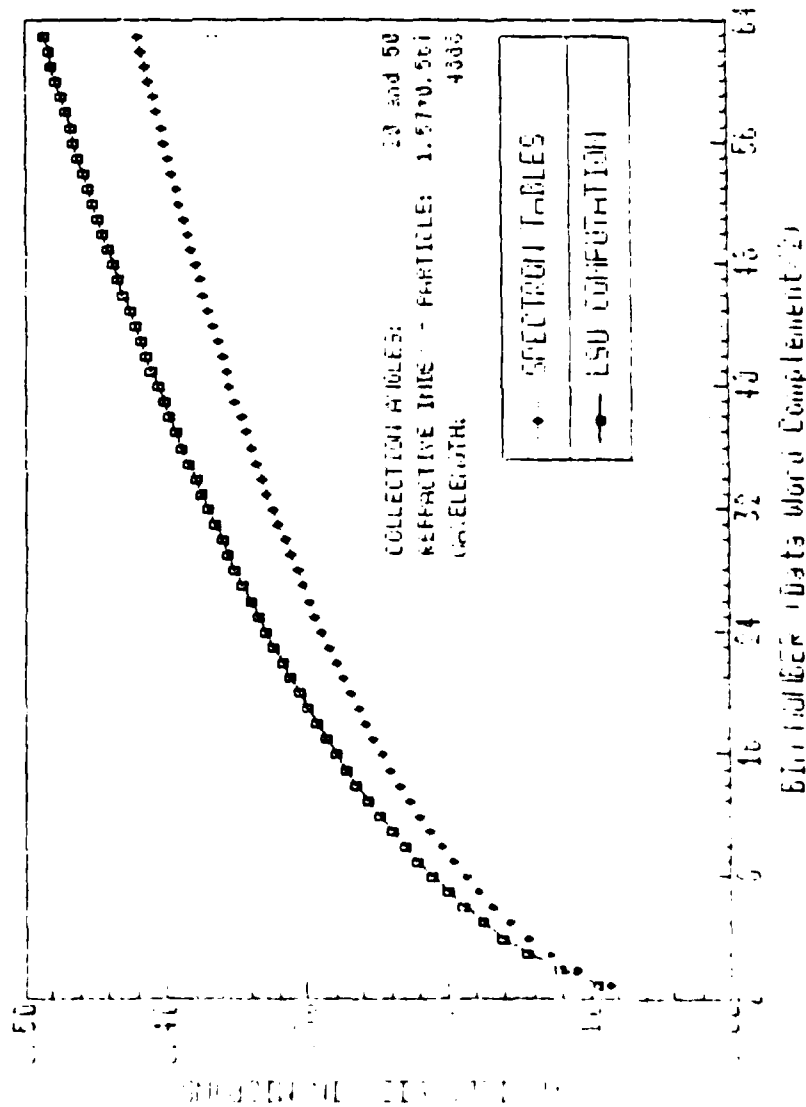


Figure 21. Correction of Bin Center Tables for 50/20 Ratioing with Soot Particles.

COMPARISON OF SPECTRON & LSU
BIN WIDTH TABLES
BW5/2/SOOT/488

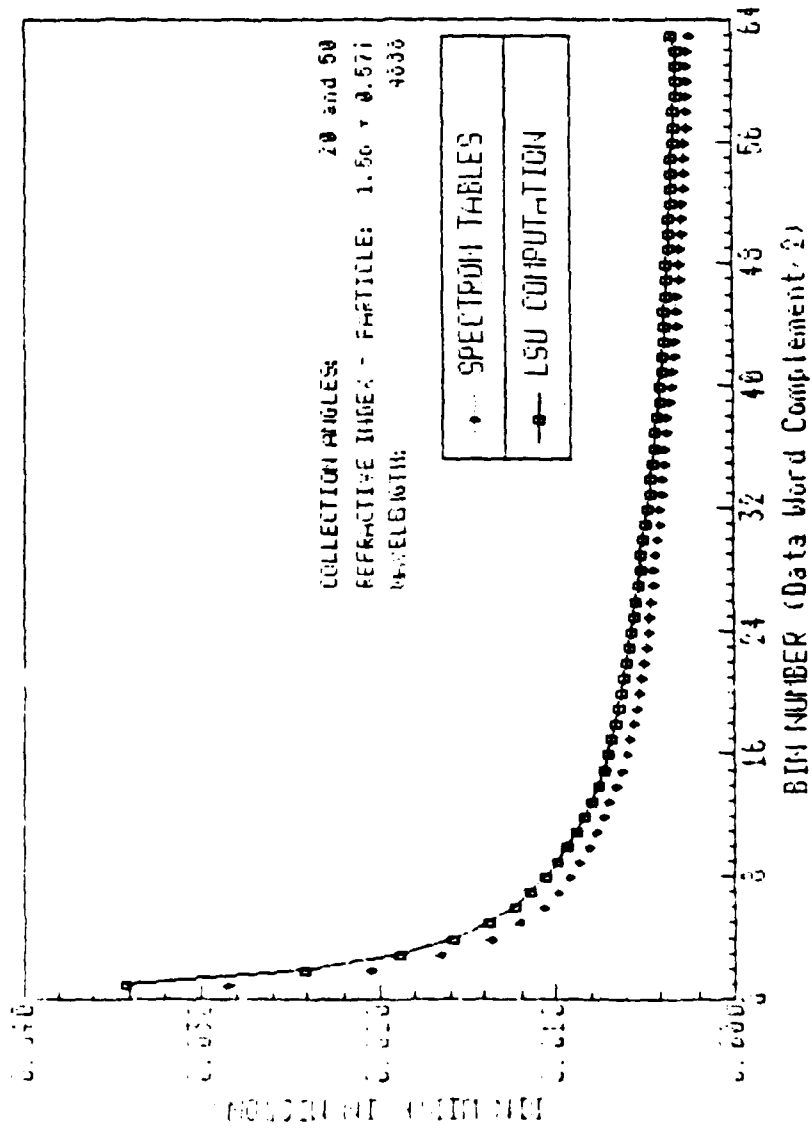


Figure 22. Correction of Bin Width Tables for 50/20 Ratioing with Soot Particles.

COMPARISON OF SPECTRON & LSU BIN CENTER TABLES EUGENE L. LIX 1988

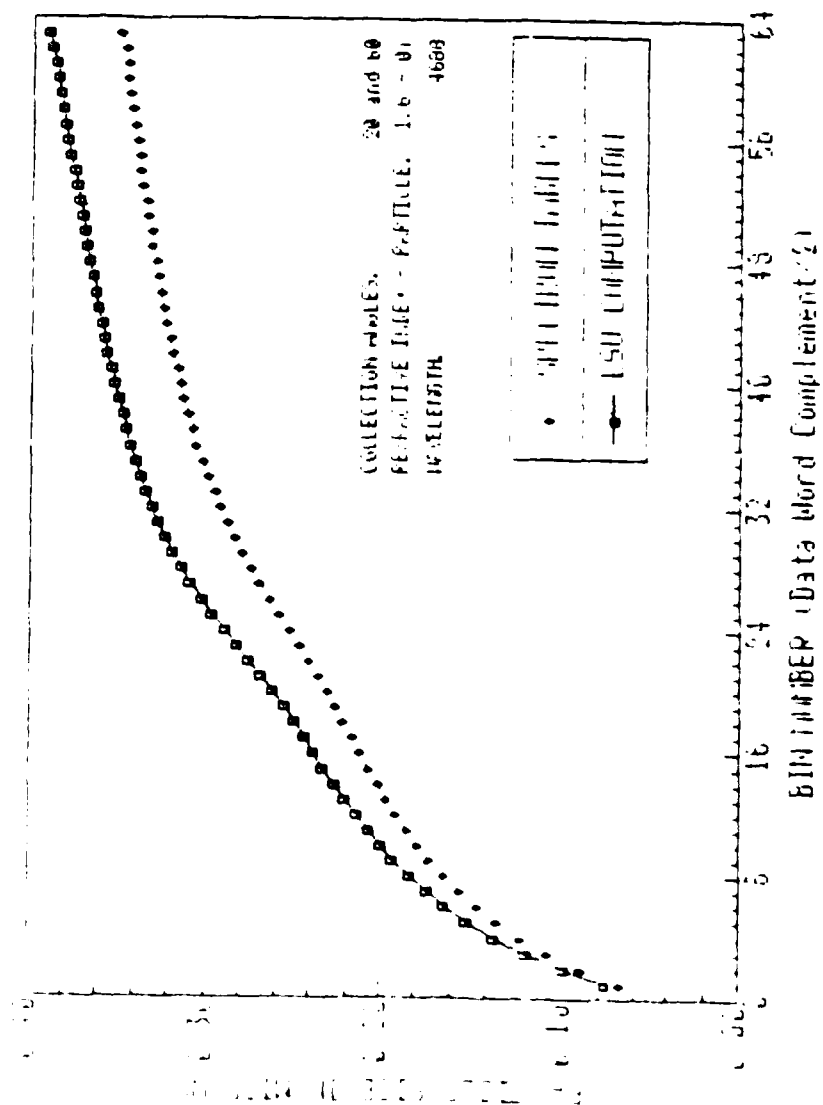


Figure 23. Correction of Bin Center Tables for 60/20 Ratioing with Latex Particles.

COMPARISON OF SPECTRON & LSU
BIN WIDTH TABLES
BUB 24LT7433

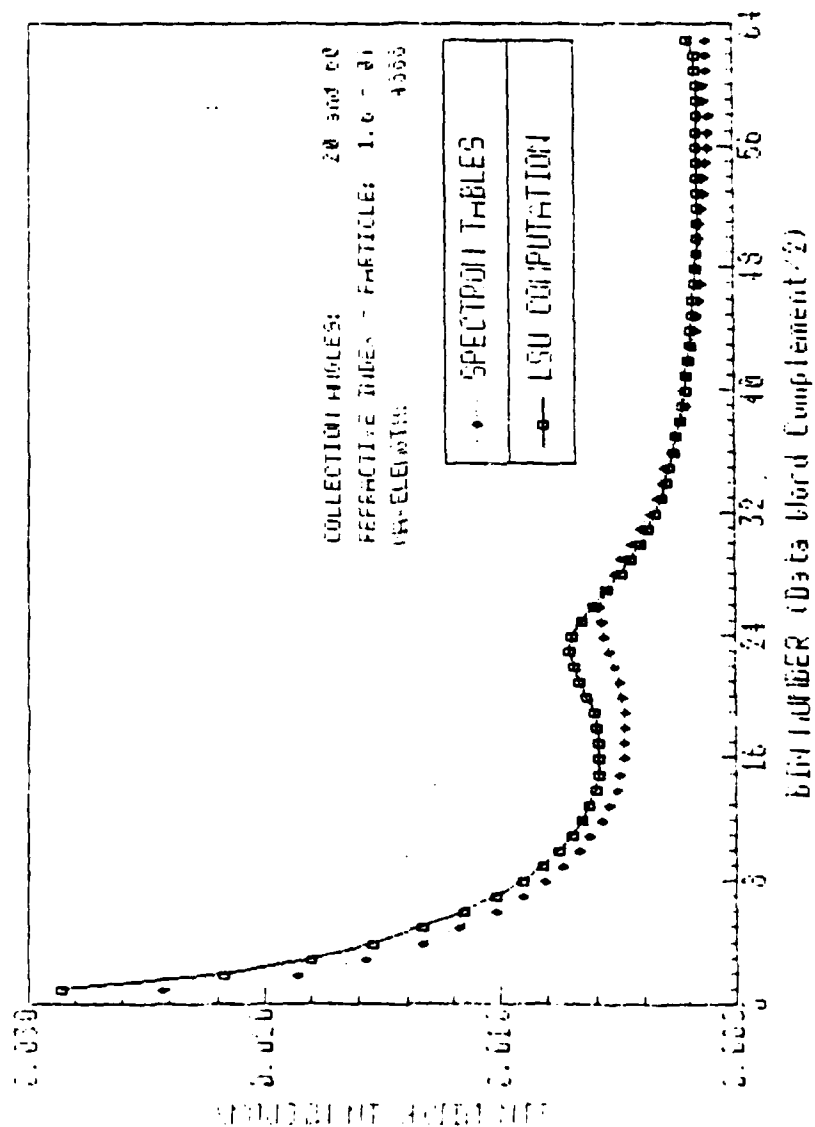


Figure 24. Correction of Bin Width Tables for 60/20 Ratioing with Latex Particles.

COMPARISON OF SPECTROM & LSU
BIN CENTER TABLES
BC6.2 (SOOT) 468

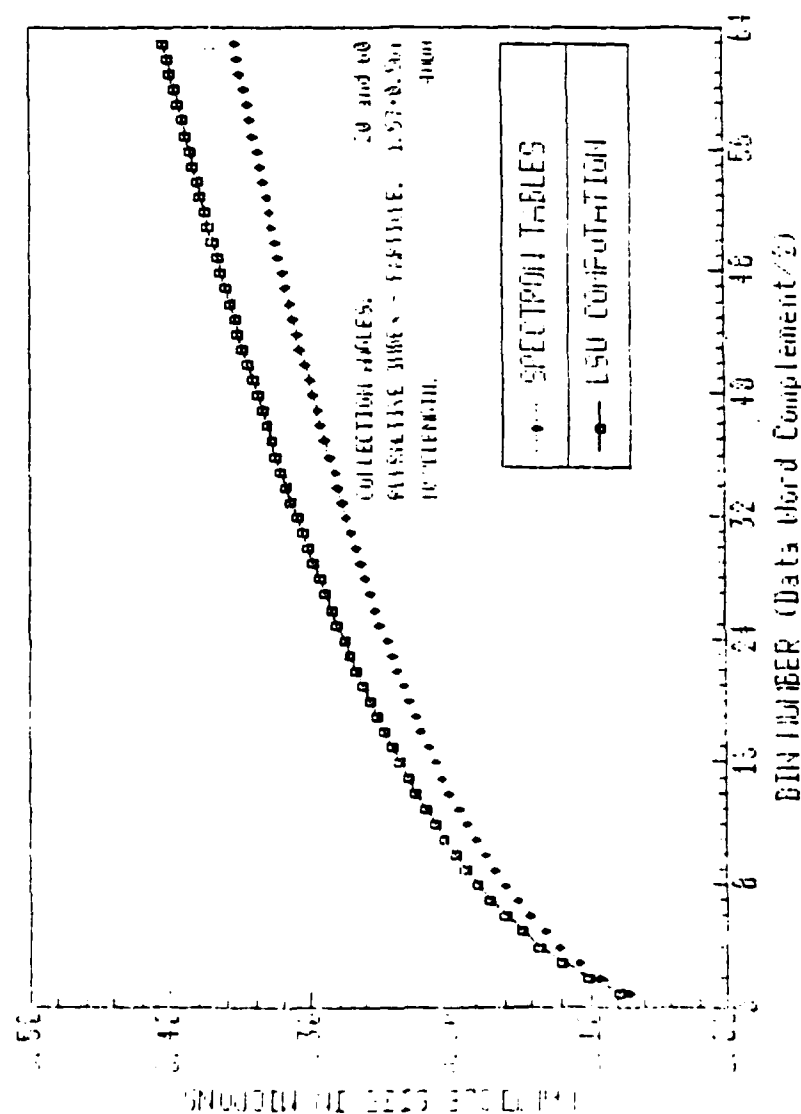


Figure 25. Correction of Bin Center Tables for 60/20 Ratioing with Soot Particles.

COMPARISON OF SPECTROM & LSU
BIN WIDTH TABLES
BW 16/2/SOOT/488

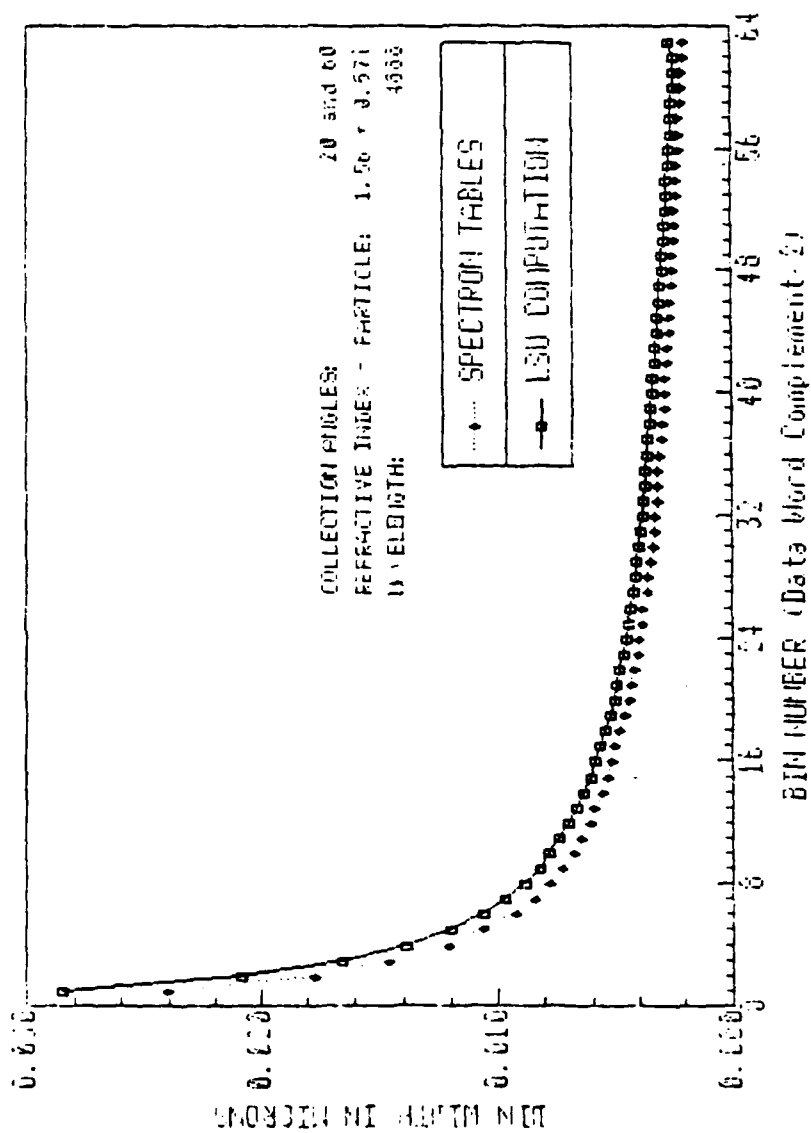


Figure 26. Correction of Bin Width Tables for 60/20 Ratioing with Soot Particles.

SECTION VI

PROGRESS ON PROBE VOLUME CORRECTIONS

A. OVERVIEW

In addition to local particle size distributions, the particle number density is an important parameter for characterizing a sooting flame. That is, one desires to know local values of the number of particles per unit volume. A difficulty arises in obtaining this parameter from the intensity ratio data because the effective sampling volume varies with particle size.

The particular relationships between particle size and sampling volume depend on:

- 1) the variation of incident light intensity in the sample space,
- 2) the scattering characteristics of the particles,
- 3) the apertures of the collection optics, and
- 4) the data validation criteria of the signal processor.

We have discussed the second and the fourth of these dependencies in the previous sections, although we have yet to show how they relate to sample volume. We will do this qualitatively below, after first describing an appropriate model for the distribution of the incident intensity in the sample space. We will then show how the optical aperture (the entrance pupil) of the collection optics also varies with position within the sample space. Finally, we will describe a computer simulation of the intensity ratioing technique that can eventually be used to obtain probe volume corrections.

B. INCIDENT INTENSITY DISTRIBUTION

The distribution of radiation intensity near the waist of a focused laser beam is given by

$$\frac{I(r,z)}{I(0,0)} = \frac{1}{[1 + (\frac{z\lambda}{\pi w_0})^2]^{\frac{1}{2}}} \exp \left[- \frac{2r^2}{w_0^2 [1 + (\frac{z\lambda}{\pi w_0})^2]^{\frac{1}{2}}} \right] \quad (23)$$

where z is the distance along the beam axis (measured from the beam waist), r is the transverse distance from the beam axis, w_0 is the beam waist radius (the distance from the beam axis where the intensity falls to $1/e^2$ the value at the axis), and λ is the wavelength.

The beam waist diameter depends on the diameter of the original beam that is being focussed. As above, we also mean the diameter at the $1/e^2$ level, as we will through this discussion. Approximately,

$$w_0 = \frac{4 \lambda f}{\pi d_b} \quad (24)$$

where f is the focal length of the focussing lens and d_b is the diameter of the original beam. For a discussion on approximate nature of this relation see References 13 and 14.

In principle, given the original beam diameter, the focal length of the focussing lens, and the laser beam power, one can completely describe the spatial variation of the beam intensity at and about the beam waist. As pointed out in Section II.B.4, however, neither the original beam diameter or the beam power is known for the system under investigation. Nevertheless, equations (23) and (24) are needed for the further developments described below.

C. DATA VALIDATION CRITERIA AND SCATTERING CHARACTERISTICS

The effect of data validation criteria on the sample volume is easily described as follows. Consider a particle of a particular size d_{min} passing through the exact midpoint of the beam waist. As shown by equation (23), the incident intensity on the particle is $I(0,0) = I_0$. Let the high voltage supply to the large angle PMT be adjusted so that the maximum voltage of the resulting pulse from the log amp is 4.0 V, i.e. the minimum voltage criteria.

Now suppose that the particle passes through the waist at some point removed from the exact center. As seen from equation (23), the incident intensity is less than I_0 , and we would expect the intensity of the scattered light also to be less than when the particle passes through the center. That is, the maximum value of the resulting voltage pulse will be less than 4.0 V -- the signal will be identified as invalid and it will not be processed. Thus the effective sampling volume for a particle of d_{min} approaches zero.

A similar reduction in the peak voltage generated by a particle larger than d_{min} will also occur. But it must be displaced a finite distance from the center of the waist before the peak voltage falls below 4.0 V. One could in principle, trace out the locus of positions away from the center of the beam waist where the peak voltage falls to 4.0 V. This would define the effective sampling volume for this particle.

One can imagine an exceptional case for a particle of size d_{\min} , where the effective volume is greater than zero. Suppose its directional scattering characteristics are such that the amount of light scattered and collected by the large angle lens increases because of a different scattering angle at its off-center position. If this increase, at least, compensates for the reduction in incident intensity, the voltage pulse will have a maximum equal to or greater than 4.0 V when it passes through the off-center location, and the sample volume will therefore be greater than zero. Thus the sample volume can be effected by both the intensity variations in the sample space and the scattering characteristics of the particle.

D. ENTRANCE PUPIL

The sampling volume can also be affected by variations in the effective aperture (entrance pupil) of the collection optics. We describe below a simple case to show how the entrance pupil varies with the relative position of the particle in the collection optics geometry. We then treat this effect quantitatively.

1. Single Collection System

Consider a single collection optics system consisting of a matched pair of lenses of focal length f and diameter d_2 , and a pinhole aperture of diameter d_1 located at one of the focal points of the two lenses, as shown in Figure 27. We have shown the pair of matched lenses as a single lens in this figure. Now consider a point source of light at some arbitrary position $(x, 0, z)$, where the origin of the coordinate system is located at the focal point f . What is the open aperture for the collection of the emitted light through the lens and the pinhole aperture?

An application of geometric optics provides the answer by the following two steps (refer to Figure 27):

1. project the pinhole aperture from the image space into the object space. This projection will result in the image of the pinhole being centered about the z -axis in the x - y plane at the focal point f , i.e. at $z = 0$.
2. project the pinhole image through the point $(x, 0, z)$ onto the x - y plane of the lens. The entrance pupil will be the intersection of the projected aperture of the pinhole (with radius R_1 centered at

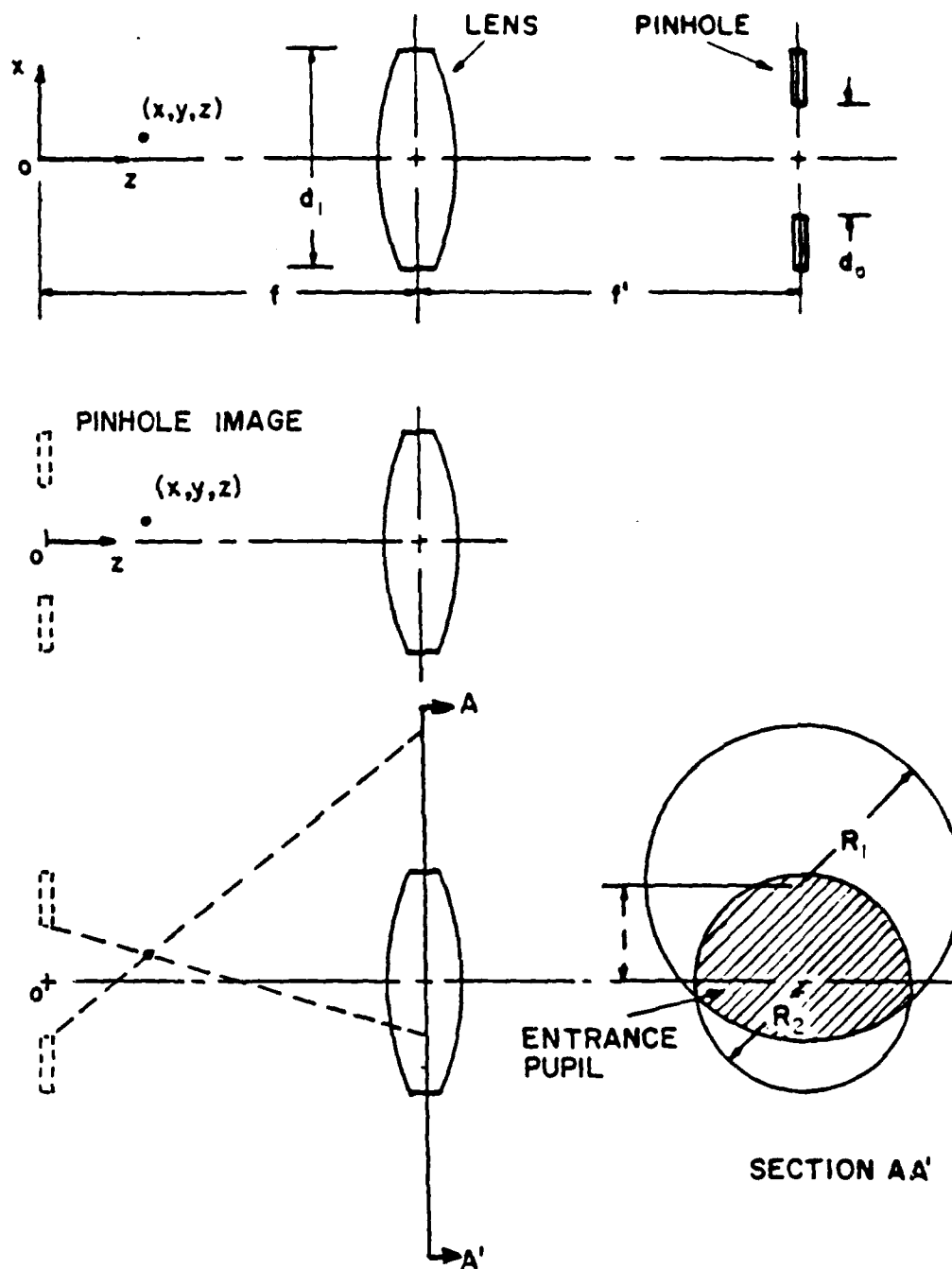
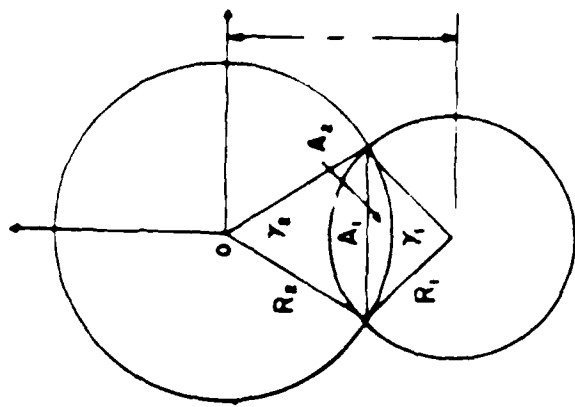


Figure 27. Construction of the Entrance Pupil for a Lens-Pinhole Optical System.



r = distance of particle from z axis

\bar{r}_1 = distance of centroid of A_1 from z axis

\bar{r}_2 = distance of centroid of A_2 from z axis

\bar{r} = distance of centroid of from z -axis

constraint on K_1 and K_2

$$K_1 + K_2 = 0$$

constraint on l

$$K_1 + K_2 = l^2 + Y_1^2 + Y_2^2$$

constraint on A_1 and A_2

$$A_1 + A_2 = A$$

constraint on r

$$r^2 = Y_1^2 + Y_2^2$$

constraint on \bar{r}_1 and \bar{r}_2

$$\bar{r}_1 + \bar{r}_2 = \bar{r}$$

constraint on \bar{r}

$$\bar{r}^2 = Y_1^2 + Y_2^2$$

constraint on \bar{r}_1 and \bar{r}_2

$$\bar{r}_1^2 + \bar{r}_2^2 = \bar{r}^2$$

constraint on \bar{r}_1 and \bar{r}_2

$$\bar{r}_1^2 + \bar{r}_2^2 = \bar{r}^2$$

constraint on \bar{r}_1 and \bar{r}_2

$$\bar{r}_1^2 + \bar{r}_2^2 = \bar{r}^2$$

constraint on \bar{r}_1 and \bar{r}_2

$$\bar{r}_1^2 + \bar{r}_2^2 = \bar{r}^2$$

constraint on \bar{r}_1 and \bar{r}_2

$$\bar{r}_1^2 + \bar{r}_2^2 = \bar{r}^2$$

constraint on \bar{r}_1 and \bar{r}_2

$$\bar{r}_1^2 + \bar{r}_2^2 = \bar{r}^2$$

Figure 28. Construction of Entrance Pupil Area and Centroid

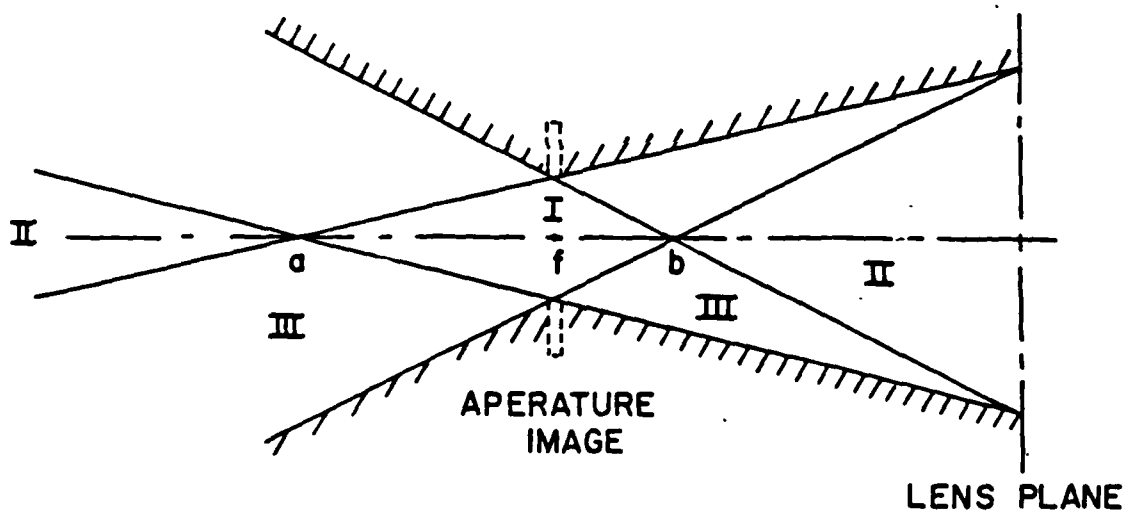


Figure 29. Schematic Representation of the Object Space for a Single Lens-Pinhole Optical System.

θ_1 with the laser beam axis, and θ_2 is taken as $\pi/2$. This construction provides the polar coordinates θ and $r = \bar{r}$ of the centroid of the entrance pupil on the collection lens surface. The origin of the polar coordinate system is at the point where a line from the particle location (x, y, z) drawn parallel to the z axis intercepts the x - y plane of the collection lens. The scattering angles θ and ϕ can then be calculated as described in Section III F, i.e. equations (16) with f replaced by $f-z$ and r replaced by $r + \bar{r}$. The angle beta is given by $\tan^{-1}(-x/-y)$.

2. Dual Collection System

For a collection system with two lens-pinhole combinations aligned at angles θ_1 and θ_2 to the beam axis, the entrance pupil for each of them can be determined as described above. We show schematically in Figure 31 the characteristics for a $40^\circ/20^\circ$ system.

Consider the system response for a very small particle ($x < 0.1$) for which the intensity of the scattered light is spatially uniform. The intensity ratio for this particle will be 1.0 at all collection angles. If the particle passes through region I, in which the entrance pupils for both collection systems are determined by the lens apertures, the measured ratio will be 1.0. A particle passing through region II, however, will result in a measured ratio less than 1.0. This owes to a reduction in the entrance pupil of the large angle collection system while the entrance pupil to the narrow angle collection system remains limited by its lens aperture. Thus the power of the light collected by the large angle system will be reduced (because of a smaller entrance pupil) while the power collected by the small angle system will be unaffected. The degree of reduction depends on the particular position in regions II through which the particle passes; near the outer edge the ratio will go to zero.

The opposite occurs in regions III -- the power collected by the narrow angle system is reduced while that collected by the large angle system remains the same. Thus the measured ratio will be greater than 1.0. In the overlapping regions, both entrance pupils are reduced and the measured ratio may fall between zero and infinity depending on the position of the particle within these regions.

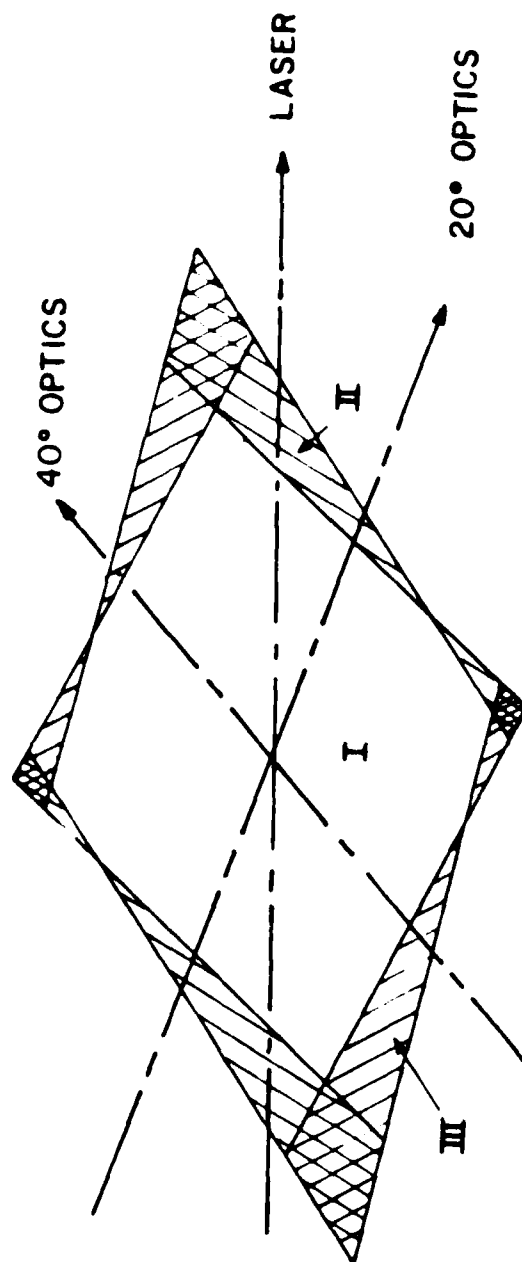


Figure 31. Schematic Representation of the Object Space for a Dual Lens-Pinhole Optical System.

E SIMULATION OF THE IPSS SYSTEM

In order to study the effects discussed above on intensity ratio measurements we have written a FORTRAN program to simulate the IPSS. The simulation program is constructed as follows:

- 1) An xyz coordinate system is established at the center of the focussed laser beam waist (the sample point). The x-axis is aligned with the electric field vector of the laser and the z axis is coincident with the axis of the laser. The beam intensity at the origin is set to an arbitrary value I_0 , and the beam waist diameter is set to an arbitrary value w_0 .
- 2) Two optical collection systems are established at arbitrary angles θ_{0A} and θ_{0B} with the optical axis in the y-z plane, i.e. $\phi_{0A} = \phi_{0B} = \pi/2$. A coordinate system $x_A y_A z_A$ and $x_B y_B z_B$ is established for the two optical systems with the origins at the origin of the xyz system, and x_A and x_B aligned with x. Angle A is the large angle and B is the small angle.
- 3) A particle of arbitrary size and refractive index is passed through the sample space along any arbitrary trajectory, although a trajectory parallel to either the x or the y axis is most meaningful. The coordinates of the particle in the $x_A y_A z_A$ and $x_B y_B z_B$ system are obtained by simple coordinate transformations, i.e.
$$\begin{aligned}x_1 &= x \\y_1 &= y \cos\theta_{01} - z \sin\theta_{01} \\z_1 &= y \sin\theta_{01} + z \cos\theta_{01}\end{aligned}\quad i = A, B$$
- 4) The entrance pupil areas, and the scattering angles and scattering distances to the enhanced pupil centroids are then calculated for each of the two collection systems as described above.
- 5) The incident intensity at the particle position is calculated from equation (23).

- 6) With the incident beam intensity, particle size and refractive index, entrance pupils, and scattering parameters known, the power at the scattered light is calculated for each optical system by equation (17). Rather than integrating over the entrance pupil, however, the power dP at the centroid is simply multiplied by the area of the entrance pupil.
- 7) The outputs of the dual channel log amplifier V_A and V_B are calculated from equation (5). This required prior "calibration". The constants k_A and k_B were obtained from Figure 2 and the value of κ_1 was obtained from typical Tyndall laboratory results, i.e. when the small angle PMT voltage supply is set to $V_B = 1512$ V, $0.364 \mu\text{m}$ latex particles provide output voltages pulses with peak values ranging up to 8.72 V. The program was run for this particle size located at the origin of the xyz system and the power collected by the narrow angle lens system P_B was calculated. Setting $V_A = 8.72$ V in equation (5) and solving for the κ_A provides its value. In a similar manner, the constant κ_B was determined. With the large angle PMT high voltage set to 1435 V, the measured intensity ratio for a $0.364 \mu\text{m}$ latex particle is 0.425 . From equations (5) and (6).

$$V_A = V_B - 2 \log \left(\frac{1}{R} \right) = 2 [\kappa_A + \kappa_A E_A + \log P_A]$$

P_A was calculated as above and κ_A was then determined.

- 8) The data validation criteria are then applied. For valid signals, ($V_A \geq 4.0$ V, $V_B \leq 10.0$ V), the intensity ratio is then calculated and sorted into a 64 bin histogram.

We have not yet tested this simulation program extensively. Our initial results, however, indicate that the entrance pupil - data validation effects do not cause a broadening of the intensity ratio distribution, as was found by Hirleman (Reference 15) for a narrow-angle, slit aperature system. It was this possibility that was one of the motivations for developing the simulation.

E. PROBE VOLUME CORRECTION

Because of the complex dependencies of the sample volume on intensity distributions, beam waist diameter, entrance pupils and the like, an analytical evaluation of the probe volume corrections is unlikely. They can, however, be determined with the system simulation. This can be done as follows for a system with given collection angles, lens F-numbers, pinhole diameters, and beam waist diameter:

- 1) particles of refractive index m , with sizes equal to the bin centers for the particular angle pair, can be "measured" with the simulation program at points on a grid in the y - z or x - z plane of the sample volume.
- 2) At each grid point, the output voltage from the large angle channel of the log amp can be calculated.
- 3) The 4.0 V contour in the plane can then be determined with standard contour routines.

The area enclosed by the 4.0 V contour will be the desired probe volume "size".

For probe volume corrections of any reasonable accuracy, an accurate value for the beam waist diameter will be needed. As mentioned in Section II, this value is presently unknown for the Tyndall system.

SECTION VII

CONCLUSIONS AND RECOMMENDATIONS

A. CONCLUSIONS

The following objective have been accomplished

- 1) The software for the IPPS has been modified to:
 - correct the CRT display of ratio histograms
 - correct the CRT display of valid-invalid data counts
 - correct the data acquisition rate reduction after using the particle size distribution routine
 - correct the line and page control on hard-copy output
- 2) The software has been extended to:
 - allow variable scaling for particle size distributions
 - annotate hard copy plots
 - implement single-channel data acquisition
 - calculate, display, store, and print single channel voltage distributions
- 3) The INV OF RATIO table has been corrected.
- 4) The bin center and bin width tables have been corrected for 40/20, 50/20, and 60/20 ratioing with latex and soot.
- 5) A FORTRAN program to calculate bin center and bin width tables, for any angle pair, lens f-numbers, and any particle refractive index, has been written and provided to the Tyndall laboratory.
- 6) Substantial progress has been made on correcting probe volume correction tables. This progress is represented by a FORTRAN program to simulate the operation of the IPSS for intensity ratio measurements. It was not possible, however, to calculate the probe volume corrections without additional detailed information on the configuration of the Tyndall version of the IPPS.

B. RECOMMENDATIONS

In order to implement the probe volume correction work, and to provide additional quantitative information on the IPSS characteristics, the following steps are recommended.

- 1) The power of the 488 μm beam should be measured as a function of laser current.
- 2) The beam diameter ($1/e^2$) should be measured as a function of the focal length setting of the beam expander.
- 3) For a given scatterer, say a microscope cover slip, the A and B channel output of the log amplifier should be measured as a function of laser current at nominal operating levels of the photomultiplier high-voltage power supplies.

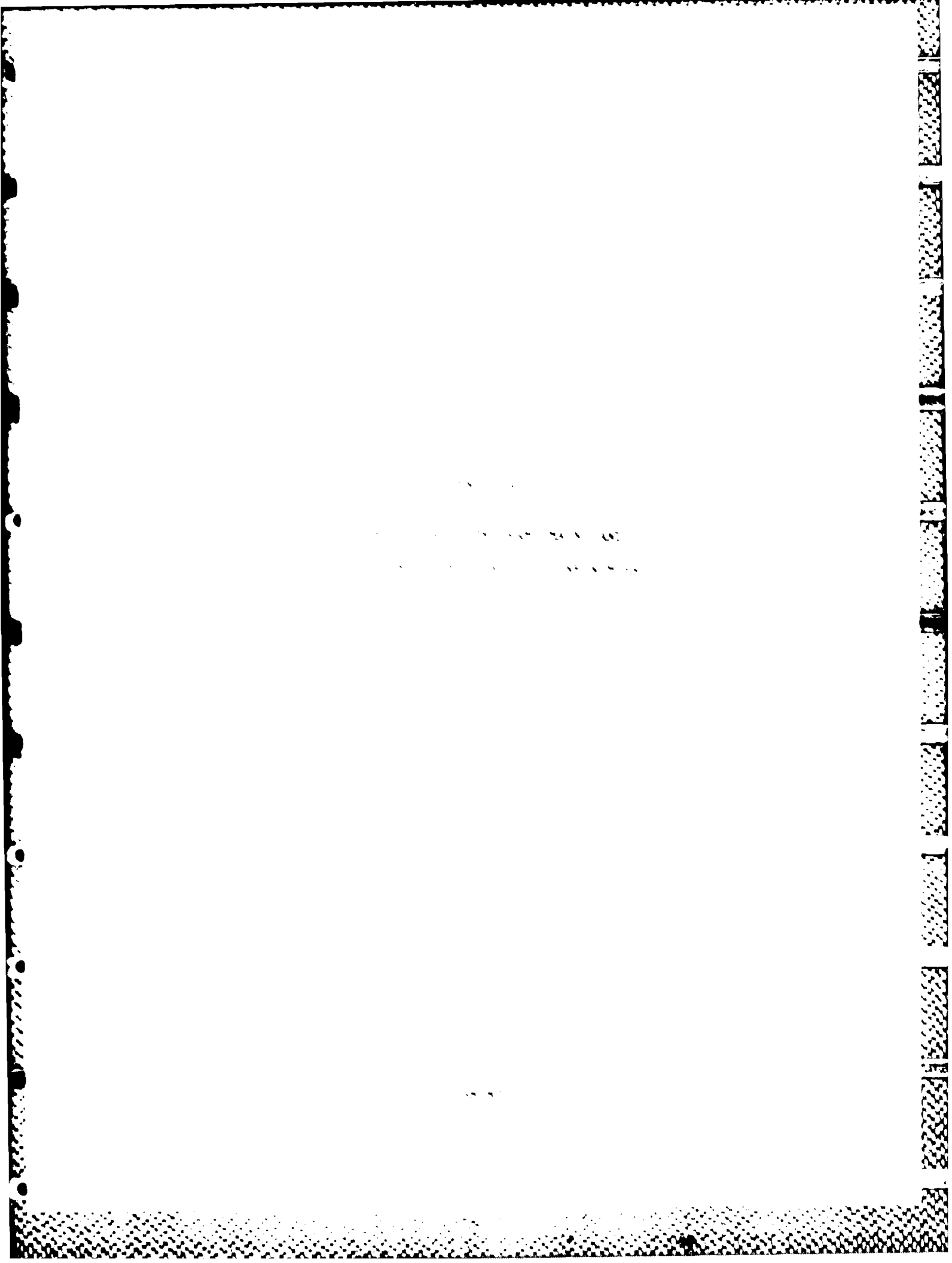
The first two of these tasks will provide information about the incident intensity distribution of the beam waist (the sample point) necessary to implement the probe volume corrections. The third will provide information to completely characterize the PMT responses.

When this information is available, it is further recommended that the simulation program be used to

- 4) Calculate the narrow voltage distribution for latex particle sizes and pinhole diameters routinely used in calibration. A comparison of measured narrow-angle voltage distributions (at various settings of the narrow-angle PMT power supply) with the calculated distribution will provide a much improved method for instrument calibration.
- 5) Calculate the probe volume corrections for routinely used expanded beam diameters and pinhole diameters.

REFERENCES

1. Integrated Particle Sizing System, Operator's Manual, Spectron Model 100, IPSS-100, Spectron Development Laboratories, Costa Mesa, California, 1981.
2. Ratioing Processor RP-1000, Operator's Manual, Spectron Development Laboratories, Costa Mesa, California, 1981.
3. Visibility Processor VP-1000, Operator's Manual, Spectron Development Laboratories, Costa Mesa, California, 1981.
4. Data Management System DMS-100, Operator's Manual, Spectron Development Laboratories, Costa Mesa, California, 1981.
5. High Voltage Supply HVS-100, Operator's Manual, Spectron Development Laboratories, Costa Mesa, California, 1981.
6. van de Hulst, H. C., Light Scattering by Small Particles, John Wiley & Sons, New York, 1957.
7. Kerker, Milton, The Scattering of Light, Academic Press, New York, 1969.
8. Doren, Craig F., and Huttman, Donald R., Absorption and Scattering of Light by Small Particles, John Wiley & Sons, New York, 1974.
9. Born, Max, and Wolf, Emil, Principles of Optics, Pergamon Press, New York, 1959.
10. Quantities, Units, and Symbols, The Royal Society, London, 1974.
11. Dave, J.V., Subroutines for Computing the Parameters of the Scattered Magnetic Radiation Scattered by a Sphere, IBM Scientific Center, Report No. 320-3237, Palo Alto, California, 1968.
12. Ogden, D.M., Scattering Amplitude Functions for a Dual Beam LAM, Department of Mechanical Engineering, Washington State University, TR Report 78-21, Pullman, Washington, 10 July 1978.
13. Herman, R.M., Prado, John, and Wiggins, T.A., Diffraction and Processing of Gaussian Beams, Applied Optics, vol. 24, pp. 1040-1045, 1 May 1985.
14. Hirleman, E.D., and Stevenson, W.H., Intensity Distribution Properties of a Gaussian Laser Beam Focus, Applied Optics, vol. 15, pp. 1440-1441, 1 November 1976.
15. Hirleman, E.D., and Moon, H.K., Response Characteristics of the Multiple-Ratio Single-Particle Counter, Journal of Colloid and Interface Science, vol. 87, May 1982.



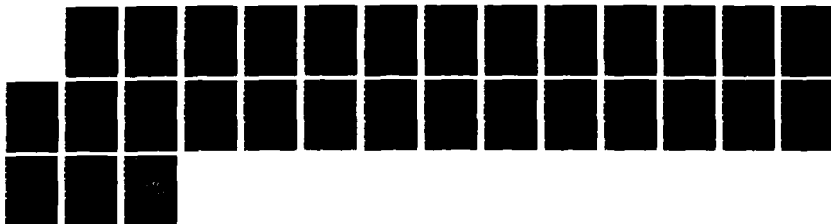
AD-A187 859

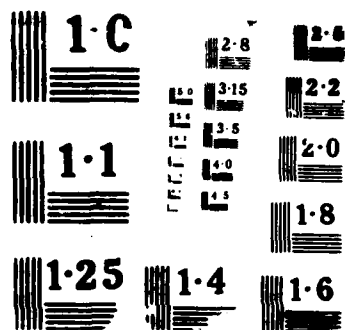
UNITED STATES AIR FORCE RESEARCH INITIATION PROGRAM
1984 RESEARCH REPORTS (U) SOUTHEASTERN CENTER FOR
ELECTRICAL ENGINEERING EDUCATION INC S W D PEELE
MAY 86 AFOSR-TR-87-1722 FF9620-82-C-0035 F/G 7/2

10/10

UNCLASSIFIED

ML





3L18T

```

0 REM
2 TEXT : HOME : VTAB 10: MTAB 15: PRINT "LOADING..."
3 NIMES: 34800: GOTO 1000
400 A = 10:B = 100:C = 1000:D = 10000:E = 100000:F = 174:B = 1000000
410 VA = (PEEK (11895) - F) + (A * (PEEK (11884) - F)) + (B * (PEEK (11883)
      - F)) + (C * (PEEK (11882) - F)) + (D * (PEEK (11881) - F)) + (E *
      (PEEK (11880) - F))
420 IV = (PEEK (2013) - F) + (A * (PEEK (2012) - F)) + (B * (PEEK (2011)
      - F)) + (C * (PEEK (2010) - F)) + (D * (PEEK (2009) - F)) + (E *
      (PEEK (2008) - F))
430 TB = (PEEK (2038) - F) + (A * (PEEK (2037) - F)) + (B * (PEEK (2036)
      - F)) + (C * (PEEK (2035) - F)) + (D * (PEEK (2034) - F)) + (E *
      (PEEK (2033) - F)) + (B * (PEEK (2032) - F))
440 A = PEEK (1903):B = PEEK (1904):C = PEEK (1907):D = PEEK (1909):E =
      PEEK (1910)
470 TI = (100 * (A - F)) + (10 * (B - F)) + (C - F) + (1 * (D - F)) + (1 *
      (E - F))
480 RETURN
900 FOR I = 0 TO 43
910 RA1(I) = PEEK (37159 + I * 3) + 254 * PEEK (37415 + I * 3)
920 NEXT
930 DA = 1
940 RETURN
999 PRINT

```

```

1000 DA = "": PRINT D91"BLDADASH1.0,D1"
1010 PRINT D91"BLDQCTICM,D1"
1020 PRINT D91"BLDQCVT,D1"
1025 PRINT D91"BLDADINTVECT,D1"
1026 POKE 28472,B8: POKE 28473,G4: CALL 28472
1040 DIM RA2(43),MCN(43),PCN(43),PB2(43),KAR(43)
1045 DIM BINM(42),RT(43),RT(43),BC(43),WT(43),MC(43),CT(43)
1047 DIM RUN(75),SE(175)
1050 M10 = "": SIZE IN BIN
1051 K20 = "RATIO MICRONS COUNT RATIO MICRONS COUNT"
1052 M10 = "LISTING OF RAW COUNTS"
1053 M10 = "LISTING OF REDUCED COUNT RATE"
1054 B10 = "1.0 .8 .6 .4 .2 .1 RATIO"
1055 B20 = "MIN MID MAX SIZE"
1060 BL = "518F = 51PL = 5"
1061 X89 = "DIRECT1"
1062 BC9 = "BC4/2/LTX/489"
1063 B49 = "BMA/2/LTX/489"
1064 BOSUB 1100: BOSUB 1130: BOSUB 1170
1065 REM --
1070 POKE -14544,237: REM RATEPCR,ED
1080 PRINT D91"OPEN INV OF RATIOS,D1": PRINT D91"READING OF RATIOS"
1082 FOR I = 0 TO 42: INPUT RC(I): NEXT
1084 PRINT D91"CLOSEINV OF RATIOS"
1084 GOTO 2000
1100 EN9 = 189:N = 1: ONERR GOTO 1300
1105 PRINT D91"OPEN",X89",D1": PRINT D91"READ",J189
1110 FOR I = 0 TO 42: INPUT KAR(I): NEXT
1120 PRINT D91"CLOSE",X89
1125 RETURN
1130 EN9 = BC9:N = 2: ONERR GOTO 1300
1135 PRINT D91"OPEN",BC9",D1": PRINT D91"READ",JBC9
1140 FOR I = 0 TO 42: INPUT BC(I): NEXT
1150 PRINT D91"CLOSE",JBC9
1160 RETURN
1170 EN9 = BM9:N = 3: ONERR GOTO 1300
1175 PRINT D91"OPEN",BM9",D1": PRINT D91"READ",JBM9
1180 FOR I = 0 TO 42: INPUT BINM(I): NEXT
1190 PRINT D91"CLOSE",JBM9
1200 RETURN
1300 POKE 214,0:ER = PEEK (222)
1310 IF ER < > 5 THEN TEXT : HOME : VTAB 10: MTAB 13: PRINT "DISK I/O E
      RROR": GOTO 4000
1320 PRINT D91"CLOSE",JEN9
1330 PRINT D91"DELETE",JEN9
1340 IF N = 1 THEN X89 = " "
1350 IF N = 2 THEN BC9 = " "
1360 IF N = 3 THEN BM9 = " "
1398 GOTO 2000
1999 PRINT

```

```

2000 REM
2040 TEXT : HOME : PRINT " NP 1001 HISTOGRAM GENERATOR"
2043 PRINT
2050 PRINT "1 DATE: "IDAG
2060 PRINT "2 SERIES: "ISEG1" RUN: "JRM
2070 PRINT "3 COMMENT: "ICOM
2080 PRINT : INVERSE
2090 PRINT " RATIO PLOTTING PARAMETERS "
2100 NORMAL : PRINT
2110 PRINT "4 SAMPLE LIMIT: 10-"JBL
2120 PRINT "5 SCALE FACTOR: "JBF
2130 PRINT "6 PRINT LEVEL: "JPL
2140 PRINT : INVERSE
2150 PRINT " DATA REDUCTION TABLES "
2160 PRINT "7 CROSS SECTION TABLE: "JX8
2170 PRINT "8 BIN CENTER TABLE: "JBC
2180 PRINT "9 BIN WIDTH TABLE: "JBM
2199 GOTO 3000
2999 PRINT

```

```

3000 VTAB 21: MTAB 1: PRINT "ENTER NO. OF ITEM TO CHANGE AND NEW DATA"
3005 IF C9 = "10" GOTO 4000
3010 VTAB 22: MTAB 1: INPUT "ITEM NO.7 "IC9
3020 C = INT ( VAL (C9))
3030 IF C < 0 OR C > 9 THEN PRINT "": GOTO 4000
3040 IF C = 0 GOTO 4000
3050 VTAB 22: MTAB 15: INPUT "NEW DATA? "IN9
3070 ON C GOSUB 3080,3100,3120,3140,3160,3180,3190,3210
3075 GOTO 2040
3080 IF LEN (N9) > 32 THEN PRINT "": GOTO 3050
3090 DA9 = N9: RETURN
3100 IF LEN (N9) > 10 THEN PRINT "": GOTO 3050
3110 SE9 = N9: RETURN
3120 IF LEN (N9) > 94 THEN PRINT "": GOTO 2000
3130 CD9 = N9: RETURN
3140 IF VAL (N9) < 1 OR VAL (N9) > 4 THEN PRINT "": GOTO 3050
3150 BL = VAL (N9): RETURN
3160 IF VAL (N9) < 1 OR VAL (N9) > 200 THEN PRINT "": GOTO 3050
3162 BF = VAL (N9): RETURN
3168 IF VAL (N9) < 0 OR VAL (N9) > 1000 THEN PRINT "": GOTO 3050
3169 PL = VAL (N9): RETURN
3170 IF LEN (N9) > 18 THEN PRINT "": GOTO 2000
3175 IS9 = N9
3180 GOSUB 1100: RETURN
3190 IF LEN (N9) > 20 THEN PRINT "": GOTO 2000
3195 BC9 = N9
3200 GOSUB 1130: RETURN
3210 IF LEN (N9) > 20 THEN PRINT "": GOTO 2000
3215 BM9 = N9
3220 GOSUB 1170: RETURN
3999 PRINT

```

```

**** ACQUIRE OLD OR NEW ****
5000 TEXT : HOME : VTAB 5
5010 PRINT "DATE: "JDAE: PRINT
5020 PRINT "SERIES: "ISE: PRINT
5030 PRINT "LAST RUN NUMBER: "IRU: PRINT
5040 INPUT "NEW RUN NUMBER? "IRU
5050 TEXT : HOME : VTAB 21: HTAB 1: PRINT 810
5060 VTAB 22: HTAB 1: PRINT 820
5070 VTAB 23: HTAB 3: PRINT "VALID 000000": HTAB 24: PRINT "SECONDS 000.
00"
5080 VTAB 24: HTAB 1: PRINT "INVALID 000000":
5081 HTAB 16: PRINT RUN:
5082 HTAB 27: PRINT "TOTAL 0000000":
5100 POKE 214, 6 - BL: POKE 215, SF
5105 POKE 34810, 34
5110 CALL 34814
5120 AD = 1
5130 803UB 400
5140 803UB 900
5150 HF = 1: GOTO 4010
5999 PRINT "

```

```

": REM CTRL-L
4000 VTAB 23: PRINT "
4010 VTAB 24: HTAB 16: PRINT "COMMAND?": GET C0
4015 PRINT C0
4020 IF C0 = "7" GOTO 4400
4030 IF C0 = "C" GOTO 2040
4040 IF C0 = "N" GOTO 5050
4050 IF C0 = "D" GOTO 5050
4060 IF C0 = "P" OR C0 = "P" THEN 4000
4080 IF C0 = "F" GOTO 7000
4090 IF C0 = "L" GOTO 8000
4100 IF C0 = "R" GOTO 9000
4110 IF C0 = "S" GOTO 10000
4115 IF C0 = "Z" GOTO 11000
4116 IF C0 = "I" GOTO 11200
4117 IF C0 = "V" GOTO 11300
4118 IF C0 = "T" GOTO 12000
4119 IF C0 = "K" GOTO 12100
4120 IF C0 = "A" GOTO 12110
4121 IF C0 = "E" GOTO 12120
4200 PRINT "": GOTO 4010
4400 TEXT : HOME : VTAB 5
4410 PRINT "C-CHANGE ENTRIES": PRINT
4420 PRINT "N-ACQUIRE DATA UNDER NEW RUN NUMBER": PRINT
4430 PRINT "O-ACQUIRE DATA UNDER OLD RUN NUMBER": PRINT
4440 PRINT "D-DISPLAY LISTINGS OF SIZE": PRINT
4450 PRINT "P-PRINT HISTOGRAM AND LISTING OF SIZE": PRINT
4460 PRINT "F-FILE DATA ON DISKETTE IN DRIVE 2": PRINT
4470 PRINT "L-LOAD DATA FROM DISKETTE IN DRIVE 2": PRINT
4480 PRINT "R-RELOT RATIO HISTOGRAM": PRINT
4490 PRINT "S-CALCULATE AND PLOT SIZE INFORMATION": PRINT
4510 GOTO 4010
4999 PRINT "

```

```

***** DISPLAY OR PRINT *****
4000 IF NF = 0 THEN TEXT : HOME : VTAB 10: PRINT "PRINT FUNCTION MUST BE
PRECEDED BY DATA": PRINT TAB(5): "ACQUISITION OR REPEAT FUNCTIONS-
4002 IF NF = 0 THEN GOTO 4000
4004 IF C0 = "P" THEN PR = 1
4006 PRINT : IF C0 = "D" THEN 4010
4008 PRINT D0: "PR02"
4010 PRINT ""
4012 TEXT : HOME
4014 HTAB 3: PRINT "DATE: "IDAT
4016 HTAB 3: PRINT "SERIES: "ISE01
4020 HTAB 3: PRINT "COMMENT: "IC00
4046 PRINT
4050 N = 0: RW = 0
4060 FOR I = 0 TO 42
4070 IF RAB(I) > N THEN N = RAB(I)
4080 RW = RW + RAB(I)
4090 NEXT
4100 HTAB 3: PRINT "MAX RAW COUNT = "IN
4110 HTAB 3: PRINT "TOTAL RAW COUNT = "IRW
4112 HTAB 3: PRINT "SAMPLE TIME: "ITI: "SECONDS"
4115 PRINT : PRINT N00: PRINT : PRINT N10: PRINT N20: PRINT
4120 J = 0
4122 FOR I = 0 TO 42
4124 IF RAB(I) < PL THEN 4129
4126 BT(J) = MC(I): RT(J) = RAB(I): CT(J) = RC(I): J = J + 1
4129 NEXT I
4130 J = J - 1
4132 J = INT (J - 1) / 2)
4134 FOR I = 0 TO J
4136 PRINT CT(I): TAB( 8): INT (BT(I) * 100) / 100: TAB( 15): RT(I):
4138 IF J > 1 & 1 > J THEN GOTO 4142
4140 PRINT TAB( 21): CT(I + J + 1): TAB( 28): INT (BT(I + J + 1) * 100) /
100: TAB( 33): RT(I + J + 1)
4141 NEXT
4142 IF PR = 0 THEN 4159
4143 IF J < 16 THEN FOR I = 1 TO 16 - J: PRINT : NEXT I
4144 IF J > 16 THEN J = J - 16: FOR I = 1 TO 32 - J: PRINT : NEXT I
4146 PRINT C00 (25): "00"
4150 PRINT TAB( 20): "GRAPH OF NORMALIZED RAW COUNTS VERSUS": PRINT TAB(
20): "LOGRITHMIC INTENSITY RATIO FROM 1 TO 1"
4159 IF PR = 0 THEN PRINT : HTAB 1: VTAB 24: PRINT "PRINT? (Y/N)": GET
C0: IF C0 = "Y" THEN C0 = "P": GOTO 4000: GOTO 4010
4161 FOR I = 1 TO 13: PRINT : NEXT I
4163 PRINT C00 (125): "4044"
4167 PRINT C00 (125): "504"
4170 PRINT D0: "PR40"
4200 IF ZC = 1 THEN 4300
4370 GOTO 4010
4499

4500 REM -----> P-----
4510 C0 = "L"
4520 GOTO 4020
4999 PRINT

```

```

8000 OVER 8000 7200
8001 IF ZC = 0 THEN 8205: REM -----
8003 S8 = S8
8004 IF ZC = 1 THEN 8310
8010 TEXT : HOME :06 = --: PRINT : PRINT D81-CATALOG,02-
8020 INPUT "SERIES ?" :S8
8030 IF S8 = "2" AND ZC = 1 THEN 8000 8300
8031 IF S8 = "1" THEN S8 = S8: 8000 4000
8037 IF ZC = 1 THEN 8400: REM -----
8040 INPUT "RUN ?" :RUS
8050 PRINT : PRINT D81-OPEN SERIES "ISE91" RUN "IRUS",D2-
8060 PRINT D81-READ SERIES "ISE91" RUN "IRUS
8070 INPUT D81: INPUT C8: INPUT T1: INPUT IV
8080 FOR I = 0 TO 42: INPUT RAX(I): NEXT
8091 PRINT D81-CLOSE: REM "IRUS
8100 VA = 0: FOR I = 0 TO 42: VA = VA + RAX(I): NEXT
8110 YS = VA + IV
8130 DA = 1
8140 POKE 214,0
8150 GOTO 9000
8199

8200 REM -----PROMPT FOR A.D.-----
8204 IF ZC = 1 THEN 8250
8205 ZC = 0
8210 GOSUB 14000
8220 INPUT "AUTO DUMP (Y/N)?" :Z8
8230 HOME
8240 IF Z8 = "Y" THEN 15000
8250 C8 = "L"
8260 GOTO 8005
8300 REM -----S8 > L-----
8310 S8 = S8(ZP)
8320 GOTO 8030
8400 REM -----RUS > L-----
8410 RUS = RUS(ZP)
8420 ZP = ZP + 1
8430 GOTO 8030
8500 REM -----STOP A.D.-----
8510 ZC = 0: GOTO 2040
8999 PRINT "

```

```

9000 TEXT : HOME : POKE 34810,34: CALL 35280
9010 VTAB 21: HTAB 1: PRINT G18
9020 VTAB 22: HTAB 10: PRINT "SERIES: "ISE91" RUN: "IRUS
9030 VTAB 23: HTAB 3: PRINT "VALID "IVAI: HTAB 26: PRINT "SECONDS "IT1:
9040 VTAB 24: HTAB 1: PRINT "INVALID "IVL: HTAB 27: PRINT "TOTAL "IT6:
9050 N = 0
9055 FOR I = 0 TO 42
9060 IF RAX(I) > N THEN N = RAX(I)
9065 NEXT
9070 FOR I = 0 TO 43
9080 IF RAX(I) = 0 THEN 9100
9090 HPLOT (I * 3) + 41,155 TO (I * 3) + 41,155 - INT ((RAX(I) - 1) / N
) * 152)
9100 NEXT
9104 HF = 1
9105 IF ZC = 1 THEN 9500
9110 HF = 1: GOTO 4010
9499

9500 REM -----PXL-----
9510 C8 = "p"
9520 GOTO 4020
9999 PRINT "

```

```

10330 B3 = B3 + V * X ^ 3
10340 NEXT
10350 B4 = B3 / B2
10360 B1 = B1 / NW
10370 B2 = (B2 / NW) ^ .5
10380 B3 = B3 / NW ^ .33333
10390 FOR I = 0 TO 42
10400 SD = SD + (NCN(I) * (BC(I) - B1) ^ 2)
10410 NEXT
10420 SD = (SD / NW) ^ .5
10430 PRINT : PRINT : PRINT TAB( 5) "DISPLAY OR PRINT DA
TA? (D/P)"; GET C$
10440 IF C$ < > "P" THEN GOTO 10460
10450 PR = 1: PRINT : PRINT D$ "PR#2"
10460 TEXT = NONE : HTAB 5: PRINT DAS: PRINT TAB( 5) "SERIES: "ISEE: PRINT
TAB( 5) "PRUN: "IRUN
10470 TAB 5: "PRINT TAB( 5) IC06
10481 IF PR = 0 THEN GOTO 10490
10482 PRINT "GRAPH OF NORMALIZED REDUCED COUNTS"
10484 PRINT "VERSUS SIZE FROM 0 TO 3 MICRONS IN"
10485 PRINT TAB( 13) ".5 MICRON STEPS"
10486 PRINT
10490 HTAB 5: PRINT "MAX RAW COUNT="; TAB( 18) INT (N * 10) / 10
10500 HTAB 5: PRINT "TOTAL RAW COUNT="; IRM
10510 HTAB 5: PRINT "TOTAL REDUCED COUNT="; INT (NW * 10) / 10
10520 HTAB 5: PRINT "LINEAR MEAN DIA: " TAB( 20) INT (B1 * 100) / 100;
MICRONS"
10530 HTAB 5: PRINT "SURFACE MEAN DIA: " TAB( 20) INT (B2 * 100) / 100;
MICRONS"
10540 HTAB 5: PRINT "VOLUME MEAN DIA: " TAB( 20) INT (B3 * 100) / 100;
MICRONS"
10550 HTAB 5: PRINT "BAUTER MEAN DIA: " TAB( 20) INT (B4 * 100) / 100;
MICRONS"
10560 HTAB 5: PRINT "STANDARD DEVIATION: " TAB( 20) INT (SD * 100) / 10
0; " MICRONS"
10570 HTAB 5: PRINT "SAMPLE TIME: " TAB( 18) "11" SECONDS"
10580 PRINT : PRINT H$; PRINT
10590 PRINT "SIZE IN REDUCED BIN SIZE IN REDUCED BIN"
10595 PRINT "MICRONS COUNT WIDTH MICRONS COUNT WIDTH"
10596 PRINT
10600 J = 0: I = 0
10610 IF I = 42 THEN GOTO 10630
10620 IF INT (RAX(I) / TAB(I)) < PL THEN I = I + 1: GOTO 10610
10630 BT(J) = BC(I) : RT(J) = INT (RAX(I) / TAB(I)) : WT(J) = SINW(I) : J = J +
1
10640 I = I + 1: GOTO 10610
10650 JL = J - 1
10660 J = INT ((J - 1) / 2)
10670 FOR I = 0 TO J
10680 PRINT = " TAB( 18) (I) * 100) / 100; TAB( 9) : RT(I) TAB( 16) INT (W
T(I) * 1000) / 1000)
10690 IF (J + I + 1) > JL THEN GOTO 10710
PRINT TAB( 22) INT (BT(I) + J + 1) * 100) / 100; TAB( 29) : RT(I + J
+ 1) TAB( 36) INT (WT(I + J + 1) * 1000) / 1000
NEXT I
10700 IF PR = 0 THEN PRINT : PRINT "PRINT? (Y/N)"; GET C$; IF C$ = "Y"
THEN GOTO 10450
10720 IF PR = 1 THEN PR = 0: PRINT : PRINT : PRINT : PRINT : PRINT : PRINT
: PRINT : PRINT D$ "PR#0"
10730 PRINT : PRINT D$ "BLADICTACTL.D1"; GOTO 4010

```



```

15000 REM -----A.D. LIST PROMPT-----
15010 ZC = 1:ZN = 0:ZP = 1
15020 SE9 = "/"
15100 REM -----LOOP TARGET-----
15110 Z09 = SE9
15120 GOSUB 14000
15130 VTAB 20: PRINT "*** TO EXIT INPUT LOOP ENTER X AS-"
15131 VTAB 21: PRINT "SERIES & PRESS RETURN TWICE-"
15133 VTAB 3: HTAB 10
15140 PRINT "FILE NUMBER "I2P: PRINT
15150 INPUT "SERIES="ISE9
15160 INPUT "RUN 9 ="IRU9
15170 IF SE9 = "/" THEN 15190
15180 GOTO 15270
15190 REM
15210 SE9 = Z09
15220 GOSUB 14000
15230 HTAB 10: PRINT "FILE NUMBER "I2P: PRINT
15240 PRINT "SERIES="ISE9
15250 PRINT "RUN 9 ="IRU9
15260 FOR I = 0 TO 200: ZD = 0: NEXT I
15270 HOME
15280 SE9(I2P) = SE9
15290 RU9(I2P) = RU9
15300 ZN = ZP
15310 IF ZP = 74 THEN 15400
15320 IF SE9 = "1" THEN 15500
15330 ZP = ZP + 1
15340 GOTO 15100
15400 REM
15410 SE9(75) = "1":ZP = 75:ZN = 75
15430 PRINT ""
15450 GOTO 15500
15499

15500 REM -----A.D. COMMANDS-----
15510 GOSUB 14000
15511 VTAB 14
15520 PRINT "RETURN-RESUME LIST INPUT-"
15521 PRINT "D -START DATA DUMP-"
15522 PRINT "L -LIST THE LIST-"
15523 PRINT "E -EDIT LIST-"
15524 PRINT "C -CLEAR LIST-"
15540 VTAB 9: INPUT "A.D.COMMAND?"I2Z9
15550 IF I2Z9 = "L" THEN 15600
15551 IF I2Z9 = "C" THEN 15700
15552 IF I2Z9 = "E" THEN 15800
15553 IF I2Z9 = "D" THEN 15900
15590 GOTO 15100
15599

```

```

10740 GOTO 4010
11000 REM -----UCI COMMENT-----
11005 Z49 = "CENTER"
11006 Z59 = ""
11007 Z69 = "0.276 - 249
11010 HOME: TEXT: VTAB 10
11020 INPUT "SIZE="I219
11030 INPUT "W1/W2="I229
11040 INPUT "LASER POWER="I239
11100 C09 = "D" + Z19
11103 C09 = C09 + " W=" + Z29
11110 C09 = C09 + " LASER=" + Z39
11120 C09 = C09 + " R=" + Z49
11123 C09 = C09 + " A1=" + Z49
11124 C09 = C09 + " ED/R=" + Z79
11130 C09 = C09 + " U=" + Z59
11149 C9 = "10"
11150 GOTO 2040
11200 HOME: TEXT: VTAB 5: PRINT "PREVIOUS R="I249
11210 VTAB 12: INPUT "RADIAL="I249: GOTO 11100
11300 HOME: VTAB 12: INPUT "VELOCITY="I259: GOTO 11100
12000 IF SF = 5 THEN 12050
12010 IF SF = 1 THEN SF = 5
12020 GOTO 12049
12030 SF = 1
12049 C9 = "10"
12050 GOTO 2040
12100 HOME: VTAB 12: INPUT "KNOB SETTINGS="I229: GOTO 11100
12110 HOME: VTAB 12: INPUT "AXIAL="I249: GOTO 11100
12120 HOME: VTAB 12: INPUT "ED RATIO="I279: GOTO 11100
14999

```

```

13400 REM -----LIST LIST-----
13410 GOSUB 14000
13412 INPUT "PRINT LIST?"1229
13414 IF 229 < > "Y" THEN 13418
13416 PRG 2
13418 GOSUB 14000
13420 IF 229 = 0 THEN 13470
13422 PRINT TAB(10);"SERIES"1
13423 PRINT TAB(30);"RUN 0"1
13424 PRINT : PRINT
13426 FOR 22 = 1 TO 22
13428 PRINT 221
13430 PRINT TAB(10);55(22)1
13432 PRINT TAB(30);RUB(22)1
13434 PRINT
13436 NEXT 22
13438 PRG 0
13440 PRINT : PRINT
13442 INPUT "PRESS RETURN"1229
13444 GOTO 13500
13446 PRINT "FILE EMPTY"
13448 GOTO 13444
13450

```

```

13700 REM -----CLEAR LIST-----
13710 ZP = 1
13720 ZN = 0
13730 GOTO 15500
15800 REM -----EDIT LIST-----
15810 GOSUB 14000
15820 ZD = ZP
15830 INPUT "ENTRY NUMBER="12P
15840 INPUT "SERIES="1559(1P)
15850 INPUT "RUN 0 ="1RUI12P)
15860 ZP = ZD
15870 PRINT : INPUT "MORE ?"1229
15880 IF 229 = "Y" THEN 15310
15890 GOTO 15400
15900 REM -----START A.D.-----
15910 ZP = 1
15920 C0 = "L"
15925 VTAB 24: PRINT "ALIGN PAPER TO TOP OF FORM"1
15930 GOTO 4020
14000 REM -----A.D. PAGE-----
14010 TEXT : HOME
14020 HTAB 12
14030 PRINT " AUTO DUMP"
14040 PRINT : PRINT
14050 RETURN
24444

```

J
J&XREF

A 400, 410, 420, 430, 440, 470
AD 3120
B 400, 410, 420, 430, 440, 470
BCS 1062, 1130, 1133, 1150, 1330, 2160, 3193
BCI 1043, 1140, 6126, 10190, 10300, 10400, 10430
BIC 1043, 1180, 10100, 10630
BMS 1063, 1170, 1173, 1190, 1340, 2170, 3213
C 400, 410, 420, 430, 440, 470, 3020, 3030, 3040, 3070
CS 3003, 3010, 3020, 4010, 4013, 4020, 4030, 4040, 4050, 4060, 4080, 4090, 4100, 4110, 4113, 4116, 4117, 4118, 4119, 4120, 4121, 6004, 6003, 6139, 6310, 8230, 9310, 10230, 10430, 10440, 10710, 11149, 12049, 13920
COS 2070, 3130, 6020, 7070, 8070, 10470, 11100, 11103, 11110, 11120, 11123, 11126, 11130
CTI 1043, 6126, 6136, 6140
D 400, 410, 420, 430, 440, 470
DS 1000, 1010, 1020, 1023, 1080, 1084, 1103, 1120, 1133, 1130, 1173, 1190, 1320, 1330, 6004, 6170, 7030, 7060, 7090, 7240, 7250, 8010, 8050, 8060, 8090, 8091, 10007, 10008, 10244, 10450, 10720, 10730
DA 930, 8130, 10000
DAS 2030, 3090, 3010, 6013, 7070, 8070, 10440
E 400, 410, 420, 430, 440, 470
ENS 1100, 1130, 1170, 1320, 1330
ER 1300, 1310, 7200, 7210, 7213, 7220
F 400, 410, 420, 430, 470
S 400, 430
S1S 1034, 5030, 9010
S2S 1033, 3040
M1S 1030, 6113
M2S 1031, 6113
HF 5130, 6000, 6002, 9104, 9110, 10243
HRS 1022, 6113
HSS 1033, 10380
I 900, 910, 1082, 1110, 1140, 1180, 6040, 6070, 6080, 6122, 6124, 6126, 6129, 6134, 6136, 6138, 6140, 6143, 6144, 6161, 7080, 8080, 8100, 9033, 9040, 9070, 9080, 9090, 10040, 10050, 10060, 10080, 10100, 10130, 10140, 10150, 10170, 10180, 10190, 10213, 10220, 10290, 10300, 10390, 10400, 10400, 10610, 10620, 10630, 10640, 10670, 10680, 10690, 10700, 13240
IV 420, 7070, 8070, 8110, 9040
J 6120, 6126, 6130, 6132, 6134, 6138, 6140, 6143, 6144, 10400, 10430, 10450, 10460, 10470, 10490, 10700
JL 6130, 6138, 10450, 10490
LS 10071, 10072, 10073, 10074, 10222, 10223
M 10030, 10140, 10180
N 1100, 1130, 1170, 1340, 1350, 1360, 6030, 6070, 6100, 9030, 9060, 9090, 10030, 10050, 10490
NS 3030, 3080, 3090, 3100, 3110, 3120, 3130, 3140, 3150, 3160, 3162, 3168, 3169, 3170, 3173, 3190, 3193, 3210, 3213
NCI 1040, 10100, 10140, 10150, 10180, 10300, 10400
NN 10030, 10150, 10340, 10370, 10380, 10420, 10510
PCI 1040, 10180, 10220
PL 1040, 2123, 3169, 6124, 10420
PR 6004, 6142, 6139, 10450, 10481, 10710, 10720
PSI 1040, 10190, 10220
Q 10002, 10007, 10008, 10010, 10011, 10012, 10013, 10071, 10072, 10073, 10074, 10223, 10224

QS 10002, 10003, 10244
 RAX 910, 1040, 4070, 4080, 4124, 4124, 7080, 8080, 8100, 9040, 9080, 9090, 100
 SO, 10040, 10100, 10420, 10430
 RC 1043, 1082, 4124
 RT 1043, 4124, 4134, 4140, 10430, 10480, 10700
 RU 13850
 RUS 2040, 3030, 3040, 3081, 4014, 7030, 7040, 7090, 7230, 7240, 7230, 8040, 80
 30, 8040, 8090, 8410, 9020, 10440, 13140, 13230, 13290
 RUS 1047, 8410, 13290, 13434
 RW 4030, 4080, 4110, 10030, 10040, 10300
 S1 10280, 10310, 10340, 10400, 10320
 S2 10280, 10320, 10330, 10370, 10330
 S3 10280, 10330, 10330, 10380, 10340
 S4 10330, 10330
 SD 10280, 10400, 10420, 10340
 SES 2040, 3110, 3020, 4014, 7030, 7040, 7090, 7230, 7240, 7230, 8003, 8020, 80
 30, 8031, 8050, 8040, 8090, 8310, 9020, 10440, 13020, 13110, 13130, 13170, 13210
 , 13240, 13280, 13320
 SES 1047, 8310, 13280, 13410, 13434, 13840
 SF 1040, 2120, 3142, 3100, 12000, 12010, 12030
 SL 1040, 2110, 3130, 3100
 SS 7240, 8003, 8031
 ST 1043, 4124, 4134, 4140, 10430, 10480, 10700
 T9 7290, 7293
 TI 470, 4112, 7070, 8070, 9030, 10370
 TS 430, 8110, 9040
 UB 10071, 10072, 10073, 10074, 10222
 VA 410, 8100, 8110, 9030
 WT 1043, 10430, 10480, 10700
 X 10220, 10221, 10222, 10223, 10224, 10230, 10300, 10310, 10320, 10330, 1388
 O
 XA 1040, 1110, 10100, 10420, 10430
 X8 1041, 1100, 1103, 1120, 1340, 2130, 3173
 Y 10220, 10223, 10230, 10300, 10310, 10320, 10330
 Z1 11020, 11100
 Z2 11030, 11103, 12100
 Z3 11040, 11110
 Z4 11003, 11120, 11200, 11210
 Z5 11004, 11130, 11300
 Z6 11007, 11123, 12110
 Z7 11007, 11124, 12120
 ZC 4200, 7233, 8001, 8004, 8030, 8037, 8204, 8205, 8310, 9103, 13010
 ZD 13240
 ZI 13430, 13432, 13434, 13434, 13440
 ZN 13010, 13300, 13410, 13420, 13430, 13720
 ZO 13820, 13840
 ZOS 13110, 13210
 ZP 7233, 8310, 8410, 8420, 13010, 13140, 13230, 13280, 13290, 13300, 13310, 1
 3330, 13410, 13710, 13820, 13830, 13840, 13850, 13860, 13910
 ZS 8220, 8240, 13340, 13350, 13351, 13352, 13353, 13412, 13414, 13444, 13870,
 13880

APPENDIX B

LISTING OF NEW BASIC PROGRAM "MAIN" AND
VARIABLE CROSS-REFERENCE BY LINE NUMBER

318T

```

10 REM LBU RATIO PROCESSOR 18 OCT 83
20 TEXT : HOME : VTAB 10: HTAB 15: PRINT "LOADING..."
100 D0 = C#00 (4)
120 PRINT D0;"BLDADCT,D1"
130 PRINT D0;"BLDADCT,D1"
140 POK 28672,80: POK 28673,96: CALL 28672
150 REM
200 DIM RAX(63),MCN(63),PCN(63),PBZ(63),KAR(63)
205 DIM BIN(62),BT(63),RT(63),BC(63),MT(63),RC(63),CT(63)
210 DIM RUB(75),SE6(75)
214 M08 = "NORMALIZED COUNTS VERSUS SIZE IN MICRONS"
215 M10 = "SIZE IN BIN"
220 M20 = "RATIO MICRONS COUNT RATIO MICRONS COUNT"
225 M30 = "LISTING OF RAW COUNTS"
230 M36 = "LISTING OF REDUCED COUNT RATE"
235 B10 = "1.0 .8 .6 .4 .2 .1 RATIO"
240 B20 = "MIN MID MAX SIZE"
245 BL = 5:SF = 3:PL = 3:DA = 0:RA = 233:BI = 201:SA = 0:LA = 255
250 REM CNTRL L

```

```

300 PRINT D0;"OPEN INV OF RATIOS,D1": PRINT D0;"READING OF RATIOS"
310 FOR I = 0 TO 62: INPUT RC(I): NEXT
320 PRINT D0;"CLOSE INV OF RATIOS"
400 X0 = "ISECTI"
410 B0BUB 2700
420 BC8 = "BC4/2/LTX/489"
430 B0BUB 2750
440 B46 = "BM4/2/LTX/489"
450 B0BUB 2800
500 B0BUB 2000
600 B0BUB 8000
610 REM CNTRL L

```

```

700 VTAB 24: NTAB 14: PRINT "COMMAND?": GET C$
705 PRINT C$
710 IF C$ = "-" THEN GOSUB 1000
715 IF C$ = "C" THEN GOSUB 2000
720 IF C$ = "N" THEN GOSUB 3000
725 IF C$ = "O" THEN GOSUB 4000
730 IF C$ = "P" THEN GOSUB 5000
735 IF C$ = "L" THEN GOSUB 6000
740 IF C$ = "R" THEN GOSUB 7000
745 IF C$ = "H" THEN GOSUB 8000
750 IF C$ = "A" THEN GOSUB 9000
755 IF C$ = "B" THEN PRINT : PRINT D$ "RUN AUTODUMP.D1"
760 IF DA = 0 THEN TEXT : HOME : VTAB 10: PRINT "NO DATA AVAILABLE": GOTO 700
765 IF MOD = "8" AND (C$ = "D" OR C$ = "P" OR C$ = "8") THEN HOME : PRINT
      "RAW DATA MODE SELECTED, SIZE PROCESSING UNAVAILABLE!": PRINT : PRINT
      : GOTO 785
770 IF C$ = "S" THEN GOSUB 760
775 IF C$ = "P" THEN GOSUB 11000
780 IF C$ = "D" THEN GOSUB 12000
785 PRINT " ": GOTO 700
790 REM CTRL L

1000 TEXT : HOME : VTAB 5
1010 PRINT "C-CHANGE ENTRIES": PRINT
1020 PRINT "N-SELECT RATIO OR SINGLE CHANNEL MODE": PRINT
1030 PRINT "A-SELECT LARGE OR SMALL ANGLE CHANNEL": PRINT
1040 PRINT "N-Acquire DATA UNDER NEW RUN NUMBER": PRINT
1050 PRINT "O-DISPLAY LISTINGS OF SIZE": PRINT
1060 PRINT "P-PRINT HISTOGRAM AND LISTING OF SIZE": PRINT
1070 PRINT "F-FILE DATA ON DISKETTE IN DRIVE 2": PRINT
1080 PRINT "L-LOAD DATA FROM DISKETTE IN DRIVE 2": PRINT
1090 PRINT "R-REPEAT RATIO HISTOGRAM": PRINT
1100 PRINT "B-CALCULATE AND PLOT SIZE INFORMATION": PRINT
1110 PRINT "B-PERFORM AUTO DUMP BATCH PROCESSING"
1120 RETURN
1130 REM CTRL L

```

```

2000 TEXT : HOME : PRINT " RP 1001 HISTOGRAM GENERATOR"
2001 PRINT "1 DATE: "IDAT
2010 PRINT "2 SERIES: "IES91" RUN: "IRUN
2020 PRINT "3 COMMENT: "ICOM
2030 PRINT : INVERSE
2040 PRINT "4 RATIO PLOTTING PARAMETERS "
2050 NORMAL : PRINT
2060 PRINT "4 SAMPLE LIMIT: 10""1BL
2070 PRINT "5 SCALE FACTOR: "1SF
2080 PRINT "6 PRINT LEVEL: "1PL
2090 PRINT : INVERSE
2100 PRINT " DATA REDUCTION TABLES "
2110 NORMAL : PRINT
2120 PRINT "7 CROSS SECTION TABLE: "1X86
2130 PRINT "8 BIN CENTER TABLE: "1BC6
2140 PRINT "9 BIN WIDTH TABLE: "1BW6
2150 VTAB 21: HTAB 1: PRINT "ENTER NO. OF ITEM TO CHANGE AND NEW DATA"
2160 VTAB 22: HTAB 1: INPUT "ITEM NO.7 "IQ6
2170 Q = INT ( VAL (IQ6))
2180 IF Q > 0 AND Q < 10 THEN VTAB 22: HTAB 15: INPUT "NEW DATA7 "IN6: ON
2190 GOSUB 2400,2420,2440,2460,2480,2500,2520,2530,2580: GOTO 2000
2200 RETURN
2210 REM
2220 REM
2400 IF LEN (IN6) > 32 THEN RETURN
2410 DA6 = IN6: RETURN
2420 IF LEN (IN6) > 10 THEN RETURN
2430 SE6 = IN6: RETURN
2440 IF LEN (IN6) > 94 THEN RETURN
2450 CO6 = IN6: RETURN
2460 IF VAL (IN6) < 1 OR VAL (IN6) > 6 THEN RETURN
2470 BL = VAL (IN6): RETURN
2480 IF VAL (IN6) < 1 OR VAL (IN6) > 200 THEN RETURN
2490 SF = VAL (IN6): RETURN
2500 IF VAL (IN6) < 0 OR VAL (IN6) > 1000 THEN RETURN
2510 PL = VAL (IN6): RETURN
2520 IF LEN (IN6) > 18 THEN RETURN
2530 IS6 = IN6
2540 GOSUB 2700: RETURN
2550 IF LEN (IN6) > 20 THEN RETURN
2560 SC6 = IN6
2570 GOSUB 2750: RETURN
2580 IF LEN (IN6) > 20 THEN RETURN
2590 BW6 = IN6
2600 GOSUB 2800: RETURN
2610 REM CTRL L

```



```

3000 TEXT : HOME : VTAB 5
3010 PRINT "DATE: "DATE: PRINT
3020 PRINT "SERIES: "SERIES: PRINT
3030 PRINT "LAST RUN NUMBER: "IRUN: PRINT
3040 INPUT "NEW RUN NUMBER? "IRUN
3050 GOSUB 4000
3060 RETURN
3070 REM
3080 REM
3090 REM
4000 TEXT : HOME : VTAB 21: HTAB 1: PRINT 810
4010 VTAB 22: HTAB 1: PRINT 820
4020 VTAB 23: HTAB 3: PRINT "VALID 000000": HTAB 24: PRINT "SECONDS 000.
00":
4030 VTAB 24: HTAB 1: PRINT "INVALID 000000":
4040 HTAB 14: PRINT RUN1
4050 HTAB 27: PRINT "TOTAL 00000000":
4060 POKE 214,6 - SL: POKE 215,SF
4070 GOSUB 4200
4080 CALL 4100
4090 GOSUB 4600
4100 GOSUB 4600
4110 DA = 1: RETURN
4120 REM
4130 REM
4200 HGR : HCOLOR= 3: HPLOT 33,3 TO 227,3 TO 227,154 TO 33,154 TO 33,3
4210 RETURN
4400 FOR I = 0 TO 43
4410 RAX(I) = PEEK (4900 + I * 3) + 254 * PEEK (5154 + I * 3)
4420 NEXT
4430 RETURN
4440 REM
4450 REM
4460 A = 10:B = 100:C = 1000:D = 10000:E = 100000:F = 174:G = 1000000
4470 VA = (PEEK (1883) - F) + (A * (PEEK (1884) - F)) + (B * (PEEK (188
3) - F)) + (C * (PEEK (1882) - F)) + (D * (PEEK (1881) - F)) + (E *
(PEEK (1880) - F))
4480 IV = (PEEK (2013) - F) + (A * (PEEK (2012) - F)) + (B * (PEEK (201
1) - F)) + (C * (PEEK (2010) - F)) + (D * (PEEK (2009) - F)) + (E *
(PEEK (2008) - F))
4490 TB = (PEEK (2038) - F) + (A * (PEEK (2037) - F)) + (B * (PEEK (203
4) - F)) + (C * (PEEK (2035) - F)) + (D * (PEEK (2034) - F)) + (E *
(PEEK (2033) - F)) + (B * (PEEK (2032) - F))
4500 A = PEEK (1903):B = PEEK (1904):C = PEEK (1907):D = PEEK (1909):E
= PEEK (1910)
4510 T1 = 1100 * (A - F) + 110 * (B - F) + (C - F) + (.1 * (D - F)) + (.
01 * (E - F))
4560 RETURN
4570 REM CNTRL L

```

```

5000 QMERR GOTO 5500
5010 TEXT : HOME : VTAB 10: HTAB 15: PRINT "FILING DATA..."
5020 PRINT : PRINT D01"OPEN SERIES "ISE01" RUN "IRUN",D2"
5030 PRINT D01"WRITE SERIES "ISE01" RUN "IRUN
5040 PRINT D01"PRINT D01: PRINT T1: PRINT IV
5050 FOR I = 0 TO 42: PRINT RAX(I): NEXT
5060 PRINT : PRINT D01"CLOSE SERIES "ISE01" RUN "IRUN
5070 POKE 214,0: RETURN
5080 REM
5090 REM
5100 REM
5110 ER = PEEK (222)
5120 TEXT : HOME
5130 IF ER = 5 OR ER = 6 THEN GOTO 5560
5140 IF ER = 14 THEN GOTO 5620
5150 IF ER = 9 THEN GOTO 5390
5160 VTAB 10: HTAB 10: PRINT "DISK I/O ERROR ON": PRINT : HTAB 11: PRINT
ISE01" "IRUN: PRINT
5170 POKE 214,0
5180 RETURN
5190 PRINT : PRINT D01"DELETE SERIES "ISE01" RUN "IRUN: PRINT **: GOTO 60
00
5290 PRINT : PRINT D01"DELETESERIES "ISE01" RUN "IRUN
5300 VTAB 10: HTAB 10: PRINT "DATA DISKETTE FULL": PRINT : HTAB 7: PRINT
"REPLACE WITH NEW DISKETTE"
5310 GOTO 5640
5320 T9 = PEEK (218) + PEEK (219) + 254
5330 VTAB 10: HTAB 7: PRINT "SYNTAX ERROR AT LINE "I79
5340 POKE 214,0: RETURN
5350 REM CNTRL L

```

```

4000 REM
4010 TEXT : HOME : D0 = "": PRINT D0:"CATALOG,D2"
4020 INPUT "SERIES ? " : I$E0
4030 INPUT "RUN ? " : I$R0
4040 PRINT : PRINT D0:"OPEN SERIES " : I$E0 : " RUN " : I$R0 : ".D2"
4050 PRINT D0:"READ SERIES " : I$E0 : " RUN " : I$R0
4060 INPUT D0:" INPUT C08: INPUT T1: INPUT IV
4070 FOR I = 0 TO 42: INPUT RAX(I): NEXT
4080 PRINT : PRINT D0:"CLOSE SERIES " : I$E0 : " RUN " : I$R0
4090 PRINT D0:"CLOSE"
4100 VA = 0: FOR I = 0 TO 42: VA = VA + RAX(I): NEXT
4110 TB = VA + IV
4120 DA = I
4130 POKE 216,0
4140 GOSUB 7000
4150 RETURN
4160 REM CNTRL L

```

```

7000 TEXT : HOME : GOSUB 4200
7010 VTAB 21: HTAB 1: PRINT B19
7020 VTAB 22: HTAB 3: PRINT "SERIES: " : I$E0 : " RUN: " : I$R0
7030 VTAB 23: HTAB 3: PRINT "VALID " : I$V1 : " HTAB 24: PRINT "SECONDS " : I$T1
7040 VTAB 24: HTAB 1: PRINT "INVALID " : I$V1 : " HTAB 27: PRINT "TOTAL " : I$TB
7050 N = 0
7060 FOR I = 0 TO 43
7070 IF RAX(I) > N THEN N = RAX(I)
7080 NEXT
7090 FOR I = 0 TO 43
7100 IF RAX(I) = 0 THEN 7120
7110 HPLOT (I * 3) + 34,155 TO (I * 3) + 34,155 - INT (RAX(I) * 132 / N)
7120 NEXT
7130 DA = I: RETURN
7140 REM CNTRL L

```

```

8000 TEXT : HOME : VTAB 10
8010 PRINT "SELECT DESIRED COLL": "SECTION MODE BY": PRINT "ENTERING AN
      "R" FOR RATIO D": "ATA OR": PRINT "AN "B" FOR "R SI": "MLE "I": "CHANNEL
      DATA.": PRINT : INPUT "MODE? (R/S)": "MODE
8015 IF (MOD < > "B") AND (MOD < > "S") THEN 8000
8020 IF MOD = "R" THEN PRINT "R" THEN 8000
8030 IF MOD = "S" THEN PRINT "S" THEN 8000
8040 RETURN
8050 REM
8060 REM
9000 TEXT : HOME : VTAB 10
9010 PRINT "SELECT SMALL OR LARGE ANGLE SENSOR": PRINT "FOR": "SINGLE
      CHANNEL COLLECTION BY": PRINT "ENTERING AN "S" FOR SMALL ANGLE DATA":
      PRINT "OR AN "L" FOR LARGE ANGLE DATA.": PRINT : INPUT "CHANNEL? (S/
      L)": "100
9015 IF (OS < > "S") AND (OS < > "L") THEN 9000
9020 IF OS = "S" THEN POKE 4097,SA
9030 IF OS = "L" THEN POKE 4097,LA
9040 RETURN
9050 REM CTRL L

```

```

10005 PRINT "PLEASE ENTER A NUM": "BER FOR THE SMALLEST": PRINT "PARTICLE
      SIZE TO BE DISPLAYED": INPUT "JML
10010 IF JML < 0 GOTO 740
10015 PRINT "PLEASE ENTER A NUM": "BER FOR THE LARGEST": PRINT "PARTICLE
      SIZE TO BE DISPLAYED": INPUT "JMH
10025 MH = INT (MH * 100 * .5) / 100: JML = INT (JML * 100 * .5) / 100
10030 IF JML > MH GOTO 740
10035 GOSUB 10900
10045 OS = "
10050 FOR I = 0 TO 4: OS = STR$ ((I / 4) * (MH - JML) + JML) / 100
10055 IF J < 3 THEN OS = OS + "0": J = 3
10060 IF J > 3 THEN OS = OS + "0"
10065 IF I = 4 THEN OS = OS + "
10070 OS = OS + OS + "
10075 VTAB 21: PRINT OS
10085 PRINT "H08
10100 N = 0: MN = 0: M = 0: RM = 0
10105 FOR I = 0 TO 42
10110 IF RAX(I) > N THEN N = RAX(I)
10115 RM = RM + RAX(I)
10120 NEXT I
10125 FOR I = 0 TO 42
10130 MN(I) = INT (RAX(I) / (XAR(I) * BMM(I)))
10135 NEXT I
10140 FOR I = 0 TO 42
10145 IF M < MN(I) THEN M = MN(I)
10150 MN = MN + MN(I)
10155 NEXT I
10200 FOR I = 0 TO 42
10205 PCN(I) = 154 - (MN(I) / M) * 153
10210 PRZ(I) = INT ((PC(I) - ML) * 180 / (MH - ML))
10215 NEXT I
10220 FOR I = 0 TO 42
10225 X = 40 + PRZ(I): Y = PCN(I)
10235 IF Y > 154 THEN GOTO 10250
10240 IF X < 40 OR X > 220 GOTO 10250
10245 PLOT X,154 TO X,Y
10250 NEXT I
10260 REM CTRL L

```



```

11020 PRINT D01"PR02"
11030 PRINT
11520 IF J < 16 THEN FOR I = 1 TO 16 - J: PRINT : NEXT I
11530 IF J > 16 THEN J = J - 16: FOR I = 1 TO 35 - J: PRINT : NEXT I
11540 PRINT CHR(23); "80"
11550 PRINT TAB(20); "GRAPH OF NORMALIZED RAW COUNTS VERSUS": PRINT TAB(
20); "LOGRITHMIC INTENSITY RATIO FROM 1 TO .1"
11560 FOR I = 1 TO 13: PRINT : NEXT I
11570 PRINT CHR(12)
11580 PRINT D01"PR00"
11590 RETURN
11600 REM CNTRL L

12005 TEXT : MOVE
12010 MTAB 5: PRINT "DATE: "IDAT
12020 MTAB 5: PRINT "SERIES: "ISER1"
12030 MTAB 5: PRINT "COMMENT: "ICOM
12040 PRINT
12050 N = 0: RM = 0
12060 FOR I = 0 TO 42
12070 IF MAX(I) > N THEN N = MAX(I)
12080 RM = RM + MAX(I)
12090 NEXT I
12100 MTAB 5: PRINT "MAX RAW COUNT = "IN
12110 MTAB 5: PRINT "TOTAL RAW COUNT = "IRM
12120 MTAB 5: PRINT "SAMPLE TIME: "ITI;" SECONDS"
12130 PRINT : PRINT NRG: PRINT : PRINT H16: PRINT H29: PRINT
12140 J = 0
12150 FOR I = 0 TO 42
12160 IF MAX(I) < PL THEN 12180
12170 ST(J) = BC(I):RT(J) = MAX(I):CT(J) = RC(I):J = J + 1
12180 NEXT I
12190 JL = J - 1
12200 J = INT ((J - 1) / 2)
12210 FOR I = 0 TO J
12220 PRINT CT(I): TAB( 8): INT (ST(I) * 100) / 100: TAB( 15): RT(I):
12230 IF J + 1 + 1 > JL THEN GOTO 11500
12240 PRINT TAB( 21): CT(I) + J + 1: TAB( 28): INT (ST(I + J + 1) * 100) /
100: TAB( 35): RT(I + J + 1)
12250 NEXT I
12260 RETURN
12270 REM CNTRL L

```

J
J&JREP

A 4400, 4410, 4420, 4430, 4440, 4450, 10920
B 4400, 4410, 4420, 4430, 4440, 4450
BCS 420, 2075, 2540, 2750, 2760, 2780, 2910
BCI 205, 2770, 10210, 10420, 10470, 10595, 12170
BIC 205, 2820, 10130, 10595
BMS 440, 2080, 2590, 2800, 2810, 2830, 2920
C 4400, 4410, 4420, 4430, 4440, 4450
CS 700, 705, 710, 715, 720, 725, 730, 735, 740, 745, 750, 755, 765, 770, 775,
780
CDS 2020, 2480, 3040, 4040, 10505, 12030
CTI 205, 12170, 12220, 12240
D 4400, 4410, 4420, 4430, 4440, 4450
DS 100, 120, 130, 300, 320, 755, 2710, 2730, 2760, 2780, 2810, 2830, 2880, 28
90, 3020, 3030, 3040, 3580, 3590, 6010, 6040, 6050, 6080, 6090, 8020, 8030, 1030
S, 10445, 11020, 11580
DA 245, 760, 4110, 6120, 7130
DAS 2010, 2410, 3010, 3040, 4040, 10500, 12010
E 4400, 4410, 4420, 4430, 4440, 4450
EWS 2700, 2750, 2800, 2880, 2890
ER 2840, 2870, 3300, 3320, 3330, 3340
F 4400, 4410, 4420, 4430, 4450
G 4400, 4430
G1S 235, 4000, 7010
G2S 240, 4010
HOS 214, 10085, 10310
HIS 215, 12130
H2S 220, 12130
HRS 225, 12130
HSS 230, 10840
I 310, 2720, 2770, 2820, 4400, 4410, 3050, 6070, 6100, 7040, 7070, 7090, 710
0, 7110, 10050, 10045, 10070, 10105, 10110, 10115, 10125, 10130, 10140, 10145, 1
0150, 10200, 10205, 10210, 10220, 10225, 10400, 10415, 10420, 10445, 10470, 1058
0, 10585, 10590, 10595, 10400, 10415, 10420, 10425, 10430, 10910, 10920, 11520,
11530, 11540, 12040, 12070, 12080, 12130, 12140, 12170, 12180, 12210, 12220, 122
30, 12240
IV 4420, 3040, 4040, 6110, 7040
J 10050, 10055, 10060, 10580, 10595, 10605, 10610, 10615, 10625, 10630, 1132
0, 11530, 12140, 12170, 12190, 12200, 12210, 12230, 12240
JL 10405, 10425, 12190, 12230
LA 245, 9030
M 10100, 10145, 10205
MOS 765, 8010, 8015, 8020, 8030
N 2700, 2750, 2800, 2900, 2910, 2920, 7050, 7070, 7110, 10100, 10110, 10515,
12050, 12070, 12100
NS 2100, 2400, 2410, 2420, 2430, 2440, 2450, 2460, 2470, 2480, 2490, 2500, 25
10, 2520, 2530, 2550, 2560, 2580, 2590
NCI 200, 10130, 10145, 10150, 10205, 10420, 10470
NW 10100, 10130, 10430, 10455, 10460, 10480, 10525
PCI 200, 10205, 10225
PL 245, 2050, 2510, 10590, 12160
PSI 200, 10210, 10225
S 2095, 2100
SS 2090, 2095, 9010, 9015, 9020, 9030, 10050, 10055, 10060, 10070, 10300, 103
05, 10310
GLS 10045, 10045, 10070, 10075, 10310

RA 243
 RAXI 200, 4410, 3050, 6070, 6100, 7070, 7100, 7110, 10110, 10113, 10130, 10390,
 10393, 12070, 12080, 12160, 12170
 RC 205, 310, 12170
 RT 205, 10393, 10420, 10430, 12170, 12220, 12240
 RUS 2013, 3030, 3040, 4040, 5020, 5030, 5040, 5330, 5380, 5390, 6030, 6040, 60
 50, 6080, 7020, 10300, 12020
 RUS 210
 RW 10100, 10113, 10320, 12030, 12080, 12110
 S1 10410, 10423, 10430, 10470, 10530
 S2 10410, 10430, 10443, 10433, 10533
 S3 10410, 10433, 10443, 10440, 10540
 S4 10443, 10543
 SA 243, 9020
 SD 10410, 10470, 10480, 10530
 SES 2013, 2430, 3020, 3020, 3030, 3040, 3330, 3380, 3390, 6020, 6040, 6050, 60
 80, 7020, 10300, 12020
 SES 210
 SF 243, 2043, 2490, 4040
 S1 243
 SL 243, 2040, 2470, 4040
 ST 205, 10393, 10420, 10430, 12170, 12220, 12240
 T9 5420, 5430
 TI 4430, 5040, 6040, 7030, 10333, 12120
 TE 4430, 6110, 7040
 VA 4410, 6100, 6110, 7030
 WM 10013, 10023, 10030, 10050, 10210
 WL 10005, 10010, 10023, 10030, 10050, 10210
 WT 205, 10393, 10420, 10430
 X 10223, 10240, 10243, 10420, 10423, 10430, 10433
 XA 200, 2720, 10130, 10390, 10393
 XSB 400, 2070, 2330, 2700, 2710, 2730, 2900
 Y 10223, 10233, 10243, 10420, 10423, 10430, 10433

3

APPENDIX C

LISTINGS OF ASSEMBLER SOURCE CODE

FOR "ASM1.0" AND "ASM1.1"

IL

```

1 *****
2 * RP 16-3000 SERIES ASSEMBLY CODE
3 *
4 *
5 * FOR RP-1001
6 *
7 * TAKEN FROM SPECTRON SOURCE
8 *
9 * L.S.U. CHEMICAL ENGINEERING
10 *
11 * EDITED BY K. MATSON
12 *
13 * RATIO DATA VERSION
14 *****
15 *
16 * DMS 91000
17 *
18 * APPLE EQUATES
19 *
20 * COLOR EQU 97F
21 * HCOLOR EQU 9E4
22 * INIT EQU 9F3E2
23 * POSI EQU 9F411
24 * PLOT EQU 9F457
25 * DRAW EQU 9F53A
26 *
27 * I/O EQUATES
28 *
29 * EQU 9C700
30 * RATDRA EQU 10*011
31 * RATDRA EQU 10*013
32 * TIMER1 EQU 10*014
33 * RATACR EQU 10*018
34 * RATPCR EQU 10*01C
35 * RATIFR EQU 10*01D
36 * RATTEM EQU 10*01E
37 *
38 * GENERAL EQUATES
39 *
40 * MHI EQU 93FB
41 * INTVECT EQU 9F9
42 * DATA EQU 91400
43 * DRTB EQU 91401
44 * DRTC EQU 91402
45 * TINS EQU 9771
46 *
47 * GENERAL REGISTERS
48 *
49 * TEMP EQU 9CE
50 * AUTO EQU 9E3
51 * ASTR EQU 9D4
52 * SCL EQU 9D7
53 * RAT10 EQU 9EF
54 * DATEMP EQU 9ED

```

```

55 *
56 *
57 *
58 * TBL EQU 91800
59 * TBL EQU 91300
60 * TM EQU 91400
61 * CVT EQU 91500
62 *
63 *
64 *
65 *
66 *
67 * DRIVER
68 *
69 *
70 * ENTRY: CALLED FROM BASIC
71 * ASTR MUST HAVE 4 MINUS
72 * SAMPLE EXPINENT.
73 * SCL MUST HAVE SCALE
74 * FACTOR.
75 *
76 * GSES MUST HAVE 1 AXIS
77 * LBS OF PMTR TO BEGIN-
78 * NING OF GRAPH.
79 *
80 * CALL SUBS
81 * SET HOLD HI AFTER DATA
82 *
83 * CALLS: INITIAP
84 * TICK
85 * CLKN
86 * DATAD
87 * CLKOFF
88 * CONV
89 *
90 * EXIT: RATIO DATA PASSED IN
91 * HISTOGRAM TABLE
92 * COUNTERS PASSED IN
93 * REGISTERS
94 *
95 * DRIVE JBR INITIAP
96 * JBR SETTBL
97 * JBR CLKN
98 * JBR DATAD
99 * JBR CLKOFF
100 * JBR CONV
101 * STA RATPCR SET HOLD HI
102 *
103 * RTB
104 * END DRIVER
105 *
106 *
107 *
108 * INIT
109 *
110 * INITIAP LDA 9643
111 * STA RATPCR
112 * LDA 96E9 SET CTRL LINES

```

```

113 STA RATPCR
114 LDA 90
115 STA RATDRA DATA DIR IN
116 LDA 98CE TIMER COUNT
117 STA TIMER1
118 LDA 98C7
119 STA TIMER1+1
120 LDA 984C
121 STA MHI
122 LDA INTVECT
123 STA MHI+1
124 LDA INTVECT+1
125 STA MHI+2
126 LDA 987
127 STA TEMP+1
128 LDA RATIRA CLEAR FLAG
129 LDA 9C010 CLEAR KEY
130 RTB
131 *
132 *
133 *
134 * SETTBL
135 *
136 *
137 *
138 * SETTBL LDX 90
139 * LDA 9899 PNE LOAD M88
140 * STA TBL,X STORE IN TABLE
141 * LDA SCL LOAD SCALE
142 * STA TBL,X STORE IN TABLE
143 * INI LOAD
144 * RTB
145 *
146 *
147 * TIME
148 *
149 *
150 *
151 * INTR PMA
152 * TPA
153 * PMA
154 * TPA
155 * PMA
156 * JBR INCT INCREMENT TIME
157 * LDA TIMER1
158 * PLA
159 * TPA
160 * PLA
161 * TPA
162 * PLA
163 * RTI
164 *
165 * INCT CLC
166 * LDA 984B
167 * ADC TINS+5 ADD TO SCREEN
168 * BCS CARI BRANCH IF CARRY
169 * SEC
170 * SBC 9844 READJUST

```

171	STA TIME+5	230	ADC (TEMP),Y ADD TO SCRN	290	
172	RTS	231	BCS OVFL	291	
173		232	SEC	292	DATAG1 LDA RATIFR LOAD FLAG
174		233	BEC 8846	293	AND 8802
175	CAR1	234	STA (TEMP),Y	294	BNE INDATA DATA FLAG CX
176	STA TIME+5	235	RTS	295	JMP DATAG
177	LDA 8846	236		296	
178	ADC TIME+4	237		297	
179	BCS CAR2	238	OVFL	298	INDATA LDA RATIFR GET DATA
180		239		299	LBR
181	SEC 8846	240		300	BCC 8000
182	STA TIME+4	241		301	LDA 8807 POINT TO INVALD
183	RTS	242		302	STA TEMP
184		243		303	LDA 0
185		244		304	STA AUTO NO AUTO STOP
186	CAR2	245		305	JSR INCC
187	STA TIME+4	246		306	JMP DATAG
188	LDA 8846	247		307	LBR
189	ADC TIME+2	248		308	EDR 88FF
190	BCS CAR3	249		309	STA RATIO
191	SEC	250		310	JSR BRAP
192	SEC 8846	251		311	JMP DATAG
193	STA TIME+2	252		312	
194	RTS	253		313	
195		254		314	
196		255	CLKN	315	CONV
197	CAR3	256		316	
198	STA TIME+2	257		317	
199	LDA 8846	258		318	
200	ADC TIME+1	259	CLKN	319	CONV
201	BCS CAR4	260		320	CON1
202	SEC	261		321	LDA 80
203	SEC 8846	262		322	LDA 80L LOAD SCALE
204	STA TIME+1	263		323	BSC TBL,X SUB FROM DATA
205	RTS	264		324	STA TBL,X STORE IT
206		265	CLKOFF	325	SEC
207		266		326	LDA 8899 SET PRELOAD
208	CAR4	267		327	BSC TBL,X SUB FROM DATA
209	STA TIME+1	268		328	STA TBL,X TEMP TABLE
210	LDA 8846	269	CLKOFF	329	LDA 80
211	ADC TIME	270		330	STA TBL,X
212	BCS CAR5	271		331	INI
213	SEC	272		332	BNE CON1 LOOP TIL 0
214	SEC 8846	273		333	
215	STA TIME	274		334	CON3
216	RTS	275	DATAG	335	CON2
217		276		336	LDA TBL,X
218		277		337	ADC TBL,X ADD MSB
219	CAR5	278		338	STA TBL,X SAVE IT
220	STA TIME	279	DATAG LDA 88FO PNT TO TOTAL	339	LDA 80
221	RTS	280		340	ADC TBL,X ADD CARRY
222		281		341	STA TBL,X
223		282		342	DEV
224	INCC	283		343	BNE CON2 LOOP FOR ALL
225		284		344	INI
226		285		345	BNE CON3
227	INCC	286	DATAG BIT 8C000 KEY?	346	RTS
228	CLC	287	BPL DATAG1 BRANCH IF NOT	347	
229	LDA 8847	288	LDA 8C010 CLR KEY	348	
		289	RTS	349	

```

350 * GRAF
351 *
352 *
353 *
354 GRAF
355 LDY RATIO
356 LDY CMT, Y
357 BEQ BAD
358 DEC TBL, X
359 BNE ICNT
360 LDA BCL
361 STA TBL, X
362 DEC TBL, X
363 BNE NOROF
364 INC TBL, X
365 LDA #1
366 STA TBL, X
367 BNE ENDO
368 *
369 *
370 CLC
371 LDA TBL, X
372 ADC #903
373 LDY #0
374 JBR PLOT
375 *
376 ICNT
377 STA TEMP
378 LDA ASTA
379 STA AUTO
380 JBR INCC
381 LDA #900
382 STA TEMP
383 LDA #0
384 STA AUTO
385 JBR INCC
386 RTB
387 *
388 *
389 ENDO
390 PLA
391 PLA
392 RTB
393 *
394 *
395 BAD
396 STA TEMP
397 LDA #0
398 STA AUTO
399 JBR INCC
400 LDA #900
401 STA TEMP
402 LDA #0
403 STA AUTO
404 JBR INCC
405 RTB
406 *
407 *

```

```

GET RATIO
CMT THR TBL
BRNCH IF BAD
DEC LSR
SKIP MSB INC7
LOAD SCALE
RELQAD
DEC MSB
OVFL
BRNCH ALWAYS
LOAD PNTR
ADD OFFSET
PLOT IT
PMT TO VALID
LOAD AUTO STOP
NO AUTO STOP
CLR KEYBOARD
PMT TO INVALID
NO AUTO STP
PMT TO TOTAL
NO AUTO STP

```

```

1 .....
2 *
3 * RP 18-3000 SERIES ASSEMBLY CODE
4 *
5 * FOR RP-1001
6 *
7 * TAKEN FROM SPECTRON SOURCE
8 *
9 * L.S.U. CHEMICAL ENGINEERING
10 *
11 * EDITED BY K. WATSON
12 *
13 * RAW DATA COLLECTION VERSION
14 * .....

15 * ORB 01000
16 *
17 * APPLE EQUATES
18 *
19 *
20 COLOR EQU 07F
21 HCOLOR EQU 0E4
22 INIT EQU 0F3E2
23 POSI EQU 0F411
24 PLOT EQU 0F457
25 DRAW EQU 0F53A
26 *
27 * I/O EQUATES
28 *
29 IO EQU 0C700
30 RATORB EQU 10-010
31 RATORDB EQU 10-012
32 RATIRA EQU 10-011
33 RATORDBA EQU 10-013
34 TITER1 EQU 10-014
35 RATORA EQU 10-018
36 RATORC EQU 10-01C
37 RATORF EQU 10-01D
38 RATTEN EQU 10-01E
39 *
40 * GENERAL EQUATES
41 *
42 NMI EQU 0318
43 INIVECT EQU 0F4
44 ANGLE EQU 01A03
45 DATA EQU 01A00
46 DRTB EQU 01A01
47 DRTC EQU 01A02
48 TIPS EQU 0771
49 *
50 * GENERAL REGISTERS
51 *
52 TEMP EQU 0CE
53 AUTO EQU 0E3
54 ABTR EQU 00A
55 SCL EQU 007

56 RATIO EQU 0EF
57 DRTMP EQU 0EB
58 *
59 *
60 *
61 TBLT EQU 01800
62 TBL EQU 01300
63 TBM EQU 01400
64 CVT EQU 01500
65 *
66 *
67 *
68 *
69 *
70 * DRIVER
71 *
72 * ENTRY: CALLED FROM BASIC
73 * ABTR MUST HAVE A MINUS
74 * SAMPLE EXPONENT.
75 * SCL MUST HAVE SCALE
76 * FACTOR.
77 *
78 *
79 *
80 *
81 *
82 *
83 *
84 *
85 *
86 *
87 *
88 *
89 *
90 *
91 *
92 *
93 *
94 *
95 *
96 * .....
97 DRIVE JBR INITMP
98 JBR SETTBL
99 JBR CLKON
100 JBR DATAQ
101 JBR CLKOFF
102 JBR CONW
103 LDA 00ED
104 STA RATORC SET HOLD HI
105
106 *
107 * END DRIVER
108 *
109 * .....
110 *
111 * INIT
112 *
113 INITMP LDA 0043

114 STA RATORC
115 LDA 00CY SELECT RAW DATA

116 STA RATORC
117 LDA 00FF
118 STA RATORDB
119 LDA ANGLE
120 STA RATORB
121 LDA 00
122 STA RATORDBA
123 LDA 00CE
124 STA TITER1
125 LDA 00C7
126 STA TITER1+1
127 LDA 004C
128 STA NMI
129 LDA INIVECT
130 STA NMI+1
131 LDA INIVECT+1
132 STA NMI+2
133 LDA 007
134 STA TEMP+1
135 LDA RATIRA
136 LDA 00C10
137 RTS

138 *
139 *
140 *
141 *
142 *
143 *
144 *
145 SETTBL LDN 00
146 LDA 0099 PRE LOAD NBS
147 STA TBM, X STORE IN TABLE
148 LDA SCL LOAD SCALE
149 STA TBL, X STORE IN TABLE
150 INX
151 RNE LOAD
152 RTS
153 *
154 *
155 * TIME
156 *
157 *
158 INTR
159
160 PHA
161 TBA
162 PHA
163 TXA
164 PHA
165 JBR INCT INCREMENT TIME
166 LDA TITER1
167 PLA
168 TAX
169 PLA
170 TAY
171 RTI
172 INCT CLC

```

173	LDA 8948		231 • INCC		291 •	RTB
174	ADC TMS+5	ADD TO SCREEN	232 •		292 •	
175	BCS CAR1	BRANCH IF CARRY	233 •		293 •	
176	SEC		234 INCC	LDY 86	294 DATA1	LDA RATIFR LOAD FLAG
177	SBC 8944	READJUST	235 INCC	CLC	295 AND 8902	AND 8902
178	STA TMS+5		236	LDA 8947	296 BNE INDATA	DATA FLAG CX
179	RTB	RETURN	237	ADC (TEMP),Y	297 JMP DATAG	
180 •			238	BCS OVFL	298 •	
181 •			239	SEC	299 •	
182 CAR1	LDA 8980		240	SBC 8946	300 INDATA	LDA RATINA GET DATA
183	STA TMS+5		241	RTB	301 LBR	
184	LDA 8946	LOAD ADD NUM	242 •		302 LBR	
185	ADC TMS+4		243 •		303 EDR 84FF	
186	BCS CAR2	BRANCH IF CARRY	244 •		304 STA RATIO	
187	SEC		245 OVFL	LDA 8980	305 JBR GRAF	JMP DATAG
188	SBC 8944	READJUST	246	STA (TEMP),Y	306 •	
189	STA TMS+4		247	DEV	307 •	
190	RTB		248	CPY AUTO	308 •	
191 •			249	BNE ICC	309 •	CONV
192 •			250 •		310 •	
193 CAR2	LDA 8980		251 •	LDA 8981	311 •	
194	STA TMS+4		252	STA (TEMP),Y	312 •	
195	LDA 8946		253	PLA	313 •	
196	ADC TMS+2		254	PLA	314 CONV	
197	BCS CAR3		255	PLA	315 CON1	
198	SEC		256	PLA	316	LDA SCL
199	SBC 8946		257	RTB	317	SCL LOAD SCALE
200	STA TMS+2		258		318	SBC TBL,X SUB FROM DATA
201	RTB		259 •		319	STA TBL,X STORE IT
202 •			260 •		320	LDA 8999
203 •			261 •	CLKON	321	GET PRELAD
204 CAR3	LDA 8980		262 •		322	SBC TBL,X SUB FROM DATA
205	STA TMS+2		263 •		323	STA TBL,X TEMP TABLE
206	LDA 8946		264 •		324	LDA 80
207	ADC TMS+1		265 •		325	STA TBL,X
208	BCS CAR4		266 CLKON	LDA 89C0	326	INX
209	SEC		267	STA RATTEN	327 •	BNE CON1
210	SBC 8944		268	RTB	328 •	LOOP TIL 0
211	STA TMS+1		269 •		329 CON3	
212 •			270 •		330 CON2	
213 •			271 •	CLKOFF	331	LDY SCL
214 •			272 •		332	GET SCALE FACTOR
215 CAR4	LDA 8980		273 •		333	CLC
216	STA TMS+1		274 •		334	ADD MSB SCLL
217	LDA 8946		275 •		335	LDA TBL,X
218	ADC TMS		276 CLKOFF	LDA 8940	336	ADC TBL,X ADD MSB
219	BCS CAR5		277	STA RATTEN	337	STA TBL,X SAVE IT
220	SEC		278	RTB	338	LDA 80
221	SBC 8944		279 •		339	ADC TBL,X ADD CARRY
222	STA TMS		280 •		340	STA TBL,X
223 •			281 •	DATAG	341	DEV
224 •			282 •		342 •	DECA SCALE
225 •			283 •		343 •	BNE CON2
226 CAR5	LDA 8980		284 •		344 •	LOOP FOR ALL
227	STA TMS		285 •		345 •	BNE CON3
228	RTB		286 •		346 •	RTB
229 •			287 •		347 •	
230 •			288 DATAG	BIT 80000 KEY7	348 •	LDY RATIO
			289	SPL DATA1 BRANCH IF NOT	349	GET RATIO
			290	LDA 8C010 CLR KEY	350	LDX CVT,Y
						CONV TBL

351	REQ BAD	BRANCH IF BAD
352	DEC TBL, X	DEC LBB
353	BNE ICNT	SKIP MBS INC?
354	LDA SCL	LOAD SCALE
355	STA TBL, X	RELOAD
356	DEC TBL, X	DEC MBS
357	BNE MROF	OVFL
358	INC TBL, X	
359	LDA 01	
360	STA TBL, X	
361	BNE END0	BRANCH ALWAYS
362		
363		
364	MROF	
365	CLC	LOAD PNTR
366	LDA TBL, X	ADD OFFSET
367	ADC 0003	
368	LDV 00	PLOT IT
369	JBR PLOT	
370		
371	LDA 0057	PNT TO VALID
372	STA TEMP	
373	LDA ABTR	LOAD AUTO STOP
374	STA AUTO	
375	JBR INCC	
376	LDA 00F0	
377	STA TEMP	
378	LDA 0	
379	STA AUTO	NO AUTO STOP
380	JBR INCC	
381	RTB	
382		
383		
384	LDA 0C010	CLR KEYBOARD
385	PLA	
386	PLA	
387	RTB	
388		
389		
390	REQ BAD	PNT TO INVALID
391	STA TEMP	
392	LDA 0	
393	STA AUTO	NO AUTO STP
394	JBR INCC	
395	LDA 00F0	PNT TO TOTAL
396	STA TEMP	
397	LDA 0	
398	STA AUTO	NO AUTO STP
399	JBR INCC	
400	RTB	
401		
402		
403		

END

DATE

FILMED

3-88

DTIC